SWELLING BEHAVIOUR OF UNSATURATED EXPANSIVE CLAYS

by

S. WILLIAMS BSc

Thesis presented in fulfilment of the requirement

for the degree of Doctor of Philosophy

Council for National Academic Awards, London.

Sponsoring Establishment
Department of Civil Engineering and Building
The Polytechnic of Wales, U.K.

Collaborating Establishment
Department of Civil Engineering
University of Aston, Birmingham.

April 1988

To My Dear Mother and Father

LIST OF CONTENTS

CERTIFICATION OF RESEARCH

This is to certify that, except when specific reference to other investigations is made, the work described in this thesis isthe result of the investigations of the candidate.

S. Williams

S.Williams

(Candidate)

April 1988

(Date)

G.O. Rowlands

(Director of Studies)

April 1988

(Date)

B.S. Bhogal

(Supervisor)

April 1988

(Date)

DECLARATION

This is to certify that neither this thesis, nor any part of it, has been presented, or is being currently submitted, in candidature for any degree at any other Academic Institution.

S. Williams

S. WILLIAMS

(Candidate)

ACKNOWLEDGEMENTS

The Author wishes to express his gratitude to Mr. G.O. Rowlands his Director of Studies, and Mr. B.S. Bhogal his Supervisor, for their constant help and encouragement.

He is also grateful to Mr. R.D. McMurray, the Head of Department of Civil Engineering and Building for his support and the use of departmental facilities.

The assistance of the technical staff at the Departments of Civil Engineering and Building and Mechanical Engineering in connection with the manufacture and modification of equipment is gratefully acknowledged, as are the useful discussions with Mr. S. Ackerley (Imperial College) and Mr. F. Evans (E.L.E. International) regarding equipment design.

The use of facilities in the Departments of Science, Chemistry and Mathematics at various times throughout the project is also very much appreciated.

The financial assistance of the Science Engineering Research Council is gratefully acknowledged.

The advice of Dr. R. Kettle (University of Aston) on various aspects is appreciated.

Finally, the author is appreciative of Mrs. M.W. Ellis for her perseverance in typing this difficult script.

SUMMARY

SWELLING BEHAVIOUR OF UNSATURATED EXPANSIVE CLAYS

by

S. WILLIAMS BSc.

This thesis examines two available approaches for predicting the swelling behaviour of unsaturated expansive clays:

(i) simplified empirical relationships for rapidly identifying swelling soils and

(ii) a more accurate prediction method suitable for design purposes and based upon experimentally measured swell moduli.

The work was prompted by the absence of a universally accepted procedure for use with these soils.

The initial (and shorter) phase of the work uses published swell data to assess available empirical swell prediction methods and also determine the relative significance of soil parameters used for this purpose.

The work suggests that potentially expansive soils can be identified and classified, and the national or regional soil classification systems may be easily amended to allow for this.

The results indicated :

(i) the swell prediction methods are suitable for indicating the degree of swell behaviour only, and methods for actually quantifying volume change are usually limited to localised application

(ii) in situ suction correlated closely with swell for available data, therefore it is suggested that the suction-swell relationship be derived for numerous soils in order to assess the possibility of using it as a stand-alone indicator.

The second and most significant phase of the work involved an assessment of Fredlund's constitutive model approach for unsaturated soils when applied to the swell prediction of expansive clays. This required considerable equipment development for measuring volume changes and controlling the stresses of the soil, air and water phases. In addition, two conventional consolidometers (oedometers) were linked to a chart recorder to facilitate continuous data acquisition.

An experimental programme of three test series was then instigated to provide data by which Fredlund's theory could be assessed; these included Null tests to assess the validity of the chosen stress state variables, Volume change (uniqueness tests) to evaluate Fredlund's constitutive equations and finally, Consolidometer swell tests to further evaluate the constitutive equations and assess an established soils laboratory test for swell prediction purposes.

The results showed :

(i) in general, Fredlund's constitutive model approach is suitable for predicting volume changes in unsaturated expansive clays of a liquid limit range typically found in the field (up to 142%).

(ii) despite equipment limitations, equal changes of the stress components (σ, U_a and U_w) produced negligible volume changes, thereby confirming the stress state variables.

(iii) both the stress control and consolidometer tests indicated reasonable agreement between measured and predicted swell values, thus confirming the suitability of Fredlund's constitutive model approach to expansive unsaturated clays.

(iv) the theory makes no provision for (a) discontinuous phases in soils found at saturation levels below 25% and above 80-85% and (b) the non elastic behaviour of unsaturated soils following a reversal in stress change.

Fredlund's theory should therefore be further studied for soils composed of discontinuous phases and the effects of stress reversals upon volume change. The development of a full triaxial testing system is recommended.

CHAPTER 1

INTRODUCTION

1.1 DISTRIBUTION

Although the constructional difficulties associated with moisture related volume changes in London clay were documented as long ago as 1841 by Bartholomew, it was not until the 1930s that engineers in the United States isolated expansion in partially saturated clays as a major contributor to constructional damage; consequently, soils exhibiting considerable swell upon wetting (such as Montmorillonite rich clays) were termed expansive.

Shrink-swell problems have long been known to occur in arid/tropical environments due to the 'thirst' of the soils and their subsequent ability to absorb water. Thus, other problem areas were identified in similar regions over the world as ideas and technology spread.

Today, it is recognised that by far the largest part of the earth's (land) surface is covered with partially saturated soils; expansive soil 'hot spots' have been identified over the entire globe (Fig. 1.1). This map constitutes the known areas; however, it is expected that as the development of unused land progresses, so other problem areas will be identified.

The problem of expansive soils is not a major one within the UK, this being due to the consistently mild but damp climate. In consequence, despite there being a large area of potentially expansive/shrinkable soils (fig. 1.2), the majority of these remain saturated and hence quite stable; even where soils are partially saturated, the seasonal moisture variation is small, and limited to shallow depths.

Despite on-going UK research in this field since the late 1940s, there was a general lack of awareness of the potential problem until the recent drought periods of 1976 and 1984. During these summers, the ground in the South East dried to unprecedented depths causing considerable shrink-swell related damage to the foundations of many residential structures.

The damage at this time was primarily related to the climatic variation; however, extensive studies by the Building Research Establishment have shown that the influence of vegetation (especially tree roots) may also induce significant volume changes within the soil.

The planting of new trees close to existing structures may lead to moisture losses and cause shrinkage problems; on the other hand, removal of trees from an existing site will cause the local moisture level to rise to its equilibrium value thereby inducing expansion.

1.2 MAGNITUDE OF THE PROBLEM

The magnitude of the expansive soil problem is difficult to quantify since much of the damage is slight and is therefore not reported.

In the United States, recent surveys indicated that the annual financial loss incurred due to problems directly related to expansive soils, exceeded $8 billion.

The UK problem is much smaller than this. However, the 1976 drought resulted in £30m of insurance claims alone. The 1984 drought is thought to have been worse, although the increasing numbers of insurance claims were partly due to a greater public awareness of the problem.

1.3 TYPES OF DAMAGE

The presence of expansive soils can and inevitably will cause problems for most types of structures (eg shallow foundations, hydraulic structures etc.). The type of damage is closely related type of structure and is typically as follows :

lightly loaded structures : will commonly exhibit cracking to their walls and floors.

hydraulic structures : such as canal linings, reservoir linings, swimming pool walls and floors are particularly prone to swelling and cracking. Although initial damage may be due to either constructional defects or swelling of soils, any effects will subsequently be magnified by the leakage of water into the surrounding soil.

flexible highway and runway pavements : although cracking can be accommodated, extreme uneveneness may render them unusable.

soil backfills : may upon the absorption of water, subject the retaining structure to considerable increased pressure with consequent displacement and damage.

slope stability : must also be carefully considered since the shear strength of swelling soils can reduce considerably upon wetting.

Close attention must be paid to any tension cracks which develop since these will provide access channels for the water, thereby further weakening the soil at an already likely slip plane.

1.4 THE VOLUME CHANGE PROCESS

All soils have an equilibrium moisture content dictated by gravity acting against the forces holding water in the soil. This moisture content may vary and in turn induce volume change; total volume change is directly related to the moisture content ie. an increase in moisture content will result in an increased volume change and vice versa.

It is important to note that not all unsaturated clays are 'expansive' in nature and that some soils under certain loading conditions will exhibit a collapse phenomena upon wetting. In addition, although expansive soils will always exhibit a high shrinkage characteristic, shrinkable soils will not always exhibit expansive tendencies.

For the purpose of this project therefore, an expansive soil is considered to be one which exhibits noticeable swelling following only a slight increase in moisture content.

1.5 PREVIOUS DEVELOPMENTS

In an effort to consolidate their knowledge of the behaviour of expansive unsaturated clays, investigators have conducted extensive studies into two areas:

(a) to evaluate the pertinent factors that influence swelling and
(b) to develop methods of analysis for predicting volumetric behaviour

The first area of research has been aimed to provide practical methods for assessing the degree of expansiveness of different soils; these studies have tended to be empirical in nature eg. classification systems. However, none of the proposed methods have yet been incorporated into any national soil classification system.

The second area of research encompasses the theoretical and technological aspects associated with soils. The classical laws of soil mechanics have been well developed and successfully applied for over fifty years in saturated soils. However, the state of soil mechanics as applied to unsaturated swelling soils has made little progress since the 1960s.

1.6 SCOPE OF THE WORK

On the basis of the current state of soil science therefore, there is a clear need for a sound theoretical analysis to enable the engineer to assess the potential volume change problem associated with expansive soils.

The underlying aim of this project has therefore been to develop a suitable method for predicting the expansive behaviour of soils. It is, however, appreciated that a total solution to this problem is beyond the means of any single work.

The scope of the work is indicated in Figure 1.3.

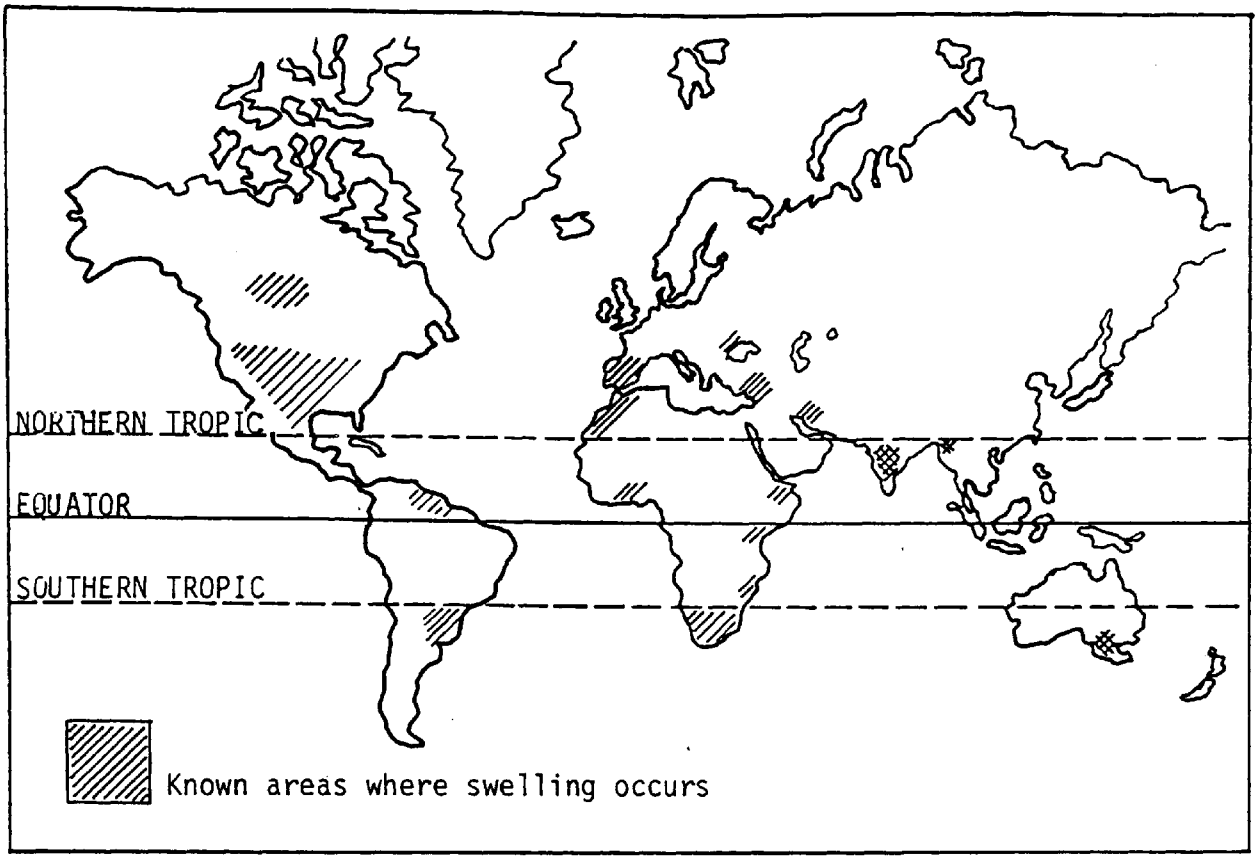

FIGURE 1.1

WORLD DISTRIBUTION OF
SWELLING SOILS

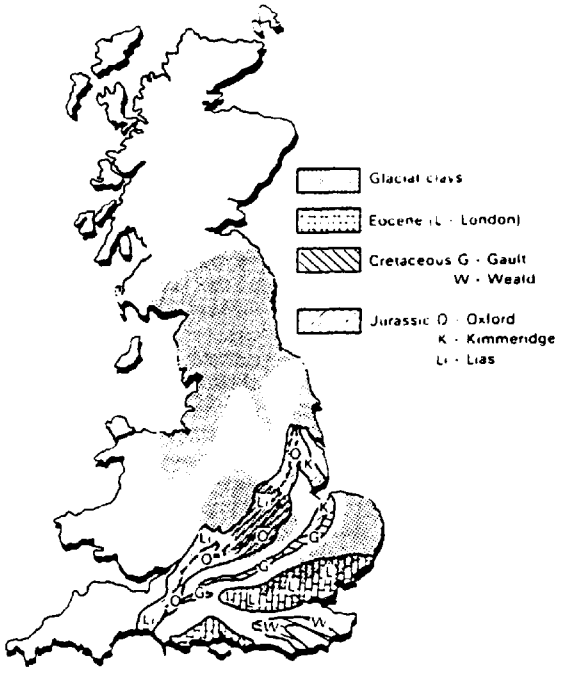

(a) Distribution of stiff clays

Clay type	Group	Plasticity index: %	Clay size fraction: %	Volume change potential
Gault	A	68	69	Very high
Gault	A	60	59	Very high
Kimmeridge	A	53	67	High/very high
London	A	52	60	High
Weald	A	43	62	High
Oxford	A	41	56	High
London	A	28	65	Medium/high
Glacial till (Garston, Herts)	B	28	41	Medium
Glacial till (Redcar, Yorks)	B	23	43	Medium
Glacial till (Cowden, Humberside)	B	20	40	Medium
Glacial till (Tyneside)	B	17	30	Low/medium
Glacial till (Glasgow)	B	15	20	Low

(b) Examples of volume change potential of some stiff clay deposits.

FIGURE 1.2

SWELL / SHRINK SUSCEPTIBLE
SOILS IN THE UK.

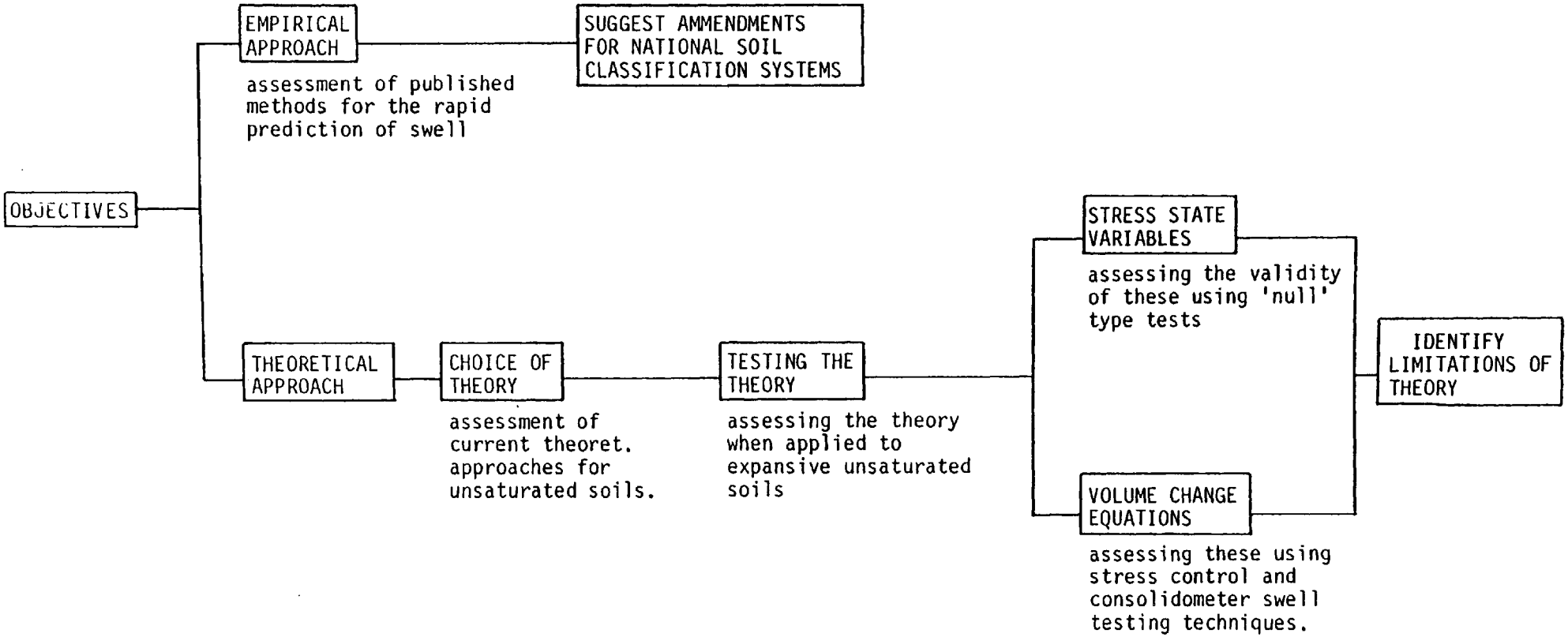

FIGURE 1.3

SCOPE OF THESIS

CHAPTER 2

THE NATURE OF EXPANSIVE CLAYS

2.1 INTRODUCTION

The practical difficulties associated with expansive clays are discussed in the previous chapter. They primarily occur as a result of :

(a) the substantial increase in volume when the clay is unrestrained

(b) the development of swell pressure if the clay is totally or partially confined.

These expansive properties may be described under two broad headings :

1. Expansive Character : this describes the ability of the clay constituents to expand .

It is related to the clay mineral composition, past and present loading history and the natural and imposed aqueous environments.

Volume change may also be due to chemical processes acting on certain non-clay minerals which result in the formation of new minerals of lower density.

2. Expansive Behaviour : this is the actual volume change exhibited by a clay under specific conditions (in situ or laboratory). It is related to the interactions of various intrinsic and extrinsic factors of varying degrees of intensity, acting alone or together upon the system.

The aim of this chapter therefore, is to examine the nature of expansive clays on the basis of these two headings. Emphasis is placed upon the behaviour of Kaolinite and Montmorillonite clay minerals, since these are subsequently employed to produce synthetic clay mixtures .

In considering mixtures of the above clay minerals, Dumbleton and West (1966) and Seed et al (1962) indicate that the liquid limit, plastic index and swell behaviour are not linearly related to the Montmorillonite content . These observations must be corroborated for the materials available to this project ; this will provide a better understanding of the clay minerals employed and assist in the choice of suitable test mixture proportions .

Expansive Character .

2.2 Mineralogical and Chemical Structure of the Clay

2.2.1 Basic structural units

The swelling mechanism of expansive clay may be described in terms of mineralogical and chemical structure. Only a brief description is given here to enable the explanation of various basic phenomena. The reader is referred to Grim (1953) for a fuller coverage. All clay minerals are colloidal - sized crystals that appear like tiny plates or flakes. These flakes consist of crystal sheets which have a repeating atomic structure. In fact, there are only two fundamental crystal sheets, comprising the tetrahedral or silica and the octahedral or alumina units .

The silica unit is composed of four oxygen atoms which take the form

of a tetrahedron containing a silicon atom at its centre. These individual tetrahedra combine to form sheets (fig. 2.1(b)). The oxygen atoms at the base of the tetrahedra lie in one plane and each one is shared by two tetrahedra. In the plane of the silicon, the apex of the tetrahedron consists of a hydroxyl ion, such that the silicon layer lies between a layer of hydroxyls above (at the apex) and a layer of oxygen below (at the tetrahedron base). The silicon plane can be symbolised as figure 2.1(c). representing the oxygen basal layer and the hydroxyl apex layer.

The alumina unit (fig. 2.2(a)) is made up of six hydroxyl ions which take the form of an octahedron with an atom of aluminium ions (gibbsite) or magnesium ions (brucite) between two dense layers of hydroxyls which are arranged in an octahedral pattern. Several such units may combine to form sheets as in figure 2.2(b). A single sheet may be schematically represented as in figure 2.2(c).

The above units combine in nature in several configurations to form the clay minerals. The four predominant types are :

2.2.2 Kaolinite - made up of gibbsite sheets (with aluminium atoms at their centres) joined to silica sheets through the unbalanced oxygen atoms at the apexes of the silicas, (i.e. the apexes of the silica layer and one layer of the gibbsite form a combined layer).

This structure may be symbolised as in figure 2.3(a) Kaolinite consists of many such layers, one on top of the other as figure 2.3(b).

In the common plane between the sheets, the oxygen ions of the silica and hydroxyl ions of the gibbsite are held together, it appears, by hydrogen bond forces. This type of bond is fairly strong, it being extremely difficult to separate the layers, and as a result

Kaolinite is relatively stable and water is unable to penetrate between the layers. Kaolinite consequently shows relatively little swell on wetting.

2.2.3 Halloysite - this clay mineral is similar in its basic structure to that of Kaolinite, with the difference that the bond between the individual units is due to a molecular layer of water. If this water is removed (e.g. by drying) this mineral behaves differently from Kaolinite. Consequently, soil containing halloysite will change its properties drastically if it is dried sufficiently to drive off the molecular water layer, since this process is irreversible.

2.2.4 Montmorillonite - this is the most common of all the clay minerals in expansive clay soils and is the most important due to its high swelling properties. Its basic structure is made up of a gibbsite sheet between two silica sheets, and may be symbolised as in figure 2.4(a).

The gibbsite layer may include atoms of aluminium, iron, magnesium or a combination of these. In addition, the silicon atoms of the tetrahedra may interchange with aluminium atoms.

These structural changes are called isomorphous changes, and result in a net negative charge on the clay mineral. Cations which are in the soil water (e.g. Na^{+}, Ca^{++}, K^{+} etc.) are attracted to the negatively charged clay plates, and exist in a continuous state of interchange.

The basic montmorillonite units are stacked such that the cations interact (figure 2.4(b)).The bond between the individual montmorillonite units is relatively weak and dependent on the type of exchangeable cations, so that water is easily able to penetrate between the sheets and cause their separation and subsequent swelling. It follows that montmorillonite is extremely expansive.

This expansivity decreases as the adsorbed cation changes in the following order : Sodium (most active), lithium, potassium, calcium, magnesium and hydroxyl (least active).

Thus , lime , gypsum and cement may be used to stabilise soil by replacing the active sodium ions with less active calcium ions.

Normally, montmorillonite exists as extremely small particles with dimensions of the order of a few Angstrom units.

2.2.5 Illite - the basic structure is similar to that of montmorillonite, but there is a pronounced replacement of aluminium ions by silicon ions. This results in a larger net negative charge than in the case of montmorillonite. However, a significant proportion of this negative charge is balanced by adsorbed non-exchangeable potasium ions, which bond the basic illite unit (ref. fig. 2.5). It follows that the illite units are more strongly bound and therefore swell much less than montmorillonite.

2.3 Clay Mineral - Water Interaction

2.3.1 An overview

Clay particles are always hydrated i.e. surrounded by layers of water molecules called 'adsorbed water'. The properties of clays (plasticity, compaction etc.) are greatly influenced by the thickness of these water layers as are the engineering characteristics. The properties of the water are discussed later.

The clay particles have an overall negative charge and attract positively charged ions (exchangeable cations) from the salts in the pore water until the charge deficiency is balanced. The hydration capacity of the exchangeable cations/adsorbed ions increases with decreasing ionic radius. Common ions in increasing order of ionic radii are Na^{+}, Ca^{++} and K^{+}.

The initial deficiency is equal to the cation exchange capacity, and noted as being influenced by : particle size, temperature, availability and concentration of ions in solution, clay mineral structure, isomorphic substitutions, and soil water pH value.

The exchangeable cations are not all held in a layer at the clay surface, but are present at some average distance from the surface. Although the negatively charged surface attracts the positively charged ions, the high concentrations of ions at the surface causes many to diffuse away. The overall balance of Coulomb electrical energy and thermal diffusion results in a diffuse layer of cations - often termed the double diffuse layer.

2.3.2 Clay particle charge

The electrical charges exhibited by clay mineral grains are caused by the following :

(a) change deficiencies due to ionic substitution within lattice

(b) broken bonds at grain edges

(c) imperfection

(d) the polar nature of ions exposed at clay particle surfaces

The last cause (d), includes the negative electrical charge of oxygen in the silicon tetrahedral layer and a positive charge due to the hydroxyl portion in the aluminium octahedral layer. Little imperfections and broken bonds may produce either a positive or negative charge.

The magnitude and location of these electrical charges are different for the various clay minerals and are fundamental in explaining the ability of some minerals to imbibe significantly more water than others.

2.3.3 Clay mineral associated water

Water associated with clay minerals exists as three types :

(a) Hydroxyl or bound water - this water forms part of the octahedral layer and cannot be removed by heating at temperatures below $400^{o}C$ for most clay minerals.

(b) Interlayer water - this is double layer water which occurs between surfaces in some clays. It is gradually removed by heating up to 150^{o}-$200^{o}C$.

(c) Pore water - this water occurs in the open space between grains and also constitutes the more tightly bound double layer water on grain surfaces. This water is essentially removed by drying at room temperature and completely removed at heating at approximately 100°C.

The clay minerals which exhibit appreciable expansion or shrinkage are called expansive clay minerals and include montmorillonite, vermiculite, chlorite and mixed layer combinations of these minerals with each other or with other clay minerals. Halloysite, (the tubular hydrous member of the Kaolinite family)and illite, do not generally exhibit volume change to the same extent as montmorillonite, vermiculite or chlorite, and are termed non-swelling minerals.

Table 2.1 lists some representative free swell data for the more common clay minerals. The distinctions between swelling and non-swelling clays and between interlayer and pore water are illustrated in figures 2.6(a) and 2.6(b).

The clay particles are represented in the deflocculated state. The double layer water adsorbed between clay layers in expandable clays and the water adsorbed on the surfaces of other clays possess properties which are somewhat different from those of the water in the pore spaces .

The double layer water exhibits a certain degree of crystallinity which is not a property of pore water. The crystallinity is

greatest adjacent to the clay mineral itself and decreases outward from the mineral surface.

The thickness of the orientated water layer is difficult to determine due to there being no sharp division between it, and the free water .

Yong and Warkentin (1966) indicate that the first two or three layers of water molecules are bonded to the surface, and that adsorbed water properties are exhibited out to approximately 15A from the surface. Overall, the thickness appears to be dependent on the nature of the clay mineral and type of cation present .

Montmorillonite exhibits larger thicknesses of orientated water than other clay minerals. The cations which enhance the orientation, are those whose hydrated or non hydrated size can be accommodated within the structure for example sodium lithium fits, whereas calcium and magnesium do not.

2.4 Microscale Mechanisms (Clay Particle Interaction)

Snethen et al (1975) indicate six primary mechanisms that influence the ' expansive' characteristics of expansive clay (table 2.3). these should not be confused with the physical factors that influence the magnitude and rate of volume change (ref.Section 2.2) .

However, it is inferred that the major portion of volume change is attributable to: osmotic repulsion, clay particle attraction, cation hydration and capillary imbibition.

The influences of these four major mechanisms are frequently combined and termed the total soil suction (Snethen , 1979) .

2.5 Consistency Limits

2.5.1 Introduction

The many aspects which contribute to expansive character are summarised in the preceding sections. A desirable practical application of these is their use for predicting the engineering behaviour of clays - and in particular expansion characteristics. Unfortunately, most of the properties cannot be directly measured and those that can, require complex, expensive apparatus.

For many years however, the consistency limits (liquid , plastic and shrinkage indices) have proved to be effective empirical methods of evaluating soil behaviour . They can be explained in - terms of the basic processes noted earlier, and linked by experimental evidence to swell behaviour .

2.5.3 Definitions

The Atterberg limits were developed by a Swedish agricultural scientist Atterberg (1911) to define several limits of consistency of behaviour by means of simple laboratory tests. These tests were :

(1) Upper limit of viscous flow
(2) Liquid limit - lower limit of viscous flow
(3) Sticky limit - where clay loses its adhesion - to a metal blade
(4) Cohesion limit - where grains cease to cohere to each other
(5) Plastic limit - lower limit of plastic state
(6) Shrinkage limit - lower limit of volume change .

He was the first to realise that the plasticity of clays could be defined in terms of the upper and lower limits, i.e. the liquid and plastic limits. He also defined the plasticity index as the range of moisture content where the soil is plastic and suggested that this could be used for soil classification .

2.5 Consistency Limits

2.5.1 Introduction

The many aspects which contribute to expansive character are summarised in the preceding sections. A desirable practical application of these is their use for predicting the engineering behaviour of clays - and in particular expansion characteristics. Unfortunately, most of the properties cannot be directly measured and those that can, require complex, expensive apparatus.

For many years however, the consistency limits (liquid , plastic and shrinkage indices) have proved to be effective empirical methods of evaluating soil behaviour . They can be explained in - terms of the basic processes noted earlier, and linked by experimental evidence to swell behaviour .

2.5.3 Definitions

The Atterberg limits were developed by a Swedish agricultural scientist Atterberg (1911) to define several limits of consistency of behaviour by means of simple laboratory tests. These tests were :

(1) Upper limit of viscous flow
(2) Liquid limit - lower limit of viscous flow
(3) Sticky limit - where clay loses its adhesion - to a metal blade
(4) Cohesion limit - where grains cease to cohere to each other
(5) Plastic limit - lower limit of plastic state
(6) Shrinkage limit - lower limit of volume change .

He was the first to realise that the plasticity of clays could be defined in terms of the upper and lower limits, i.e. the liquid and plastic limits. He also defined the plasticity index as the range of moisture content where the soil is plastic and suggested that this could be used for soil classification .

Later on, Terzaghi and Casagrande standardised the Atterberg limit tests so that they could be readily used for soil classification for engineering purposes. In present geotechnical engineering practice it is only the liquid limit, the plastic limit and sometimes the shrinkage limit that are used. The sticky and cohesion limits appear to be more useful in ceramics and agriculture .

The following paragraphs discuss each of the above limits in greater detail with special reference to their relevance to swelling behaviour .

2.5.3 Liquid limit .

When the moisture content of a clay is increased above the plastic limit , a point is reached Where it possesses no cohesion and begins to flow as a fluid. The moisture content at this stage is termed the liquid limit .

The variation of the liquid limit is much greater than that of the plastic limit. The exchangeable cations, salt concentration and hence interparticle forces, have a more prominent role in its determination.

The liquid limit is reached, when the distances between the particles are such that the interactive forces become sufficiently weak to allow an easy relative movement between them .

In expansive clays such as montmorillonite, the dominant interparticle force is repulsion (resulting from water layer interaction) . The magnitude of this force and hence liquid limit , determines the inter particle spacing and is inversely proportional to the salt concentration .

Seed (1962) defines the liquid limit as the moisture content at which the net attractive force within the clay (i.e. clay - water

attraction) is reduced to a value producing an approximately constant shear strength value .

Consequently, the larger attractive intensity (CEC), or surface area, then the larger will be the spacing required to maintain a constant shear strength value and thus the greater the liquid limit.

By similar reasoning it follows that for a constant moisture content, the shear strength will increase with increasing cation exchange capacity and vice versa . It would appear therefore that the shear strength is indicative of the swell potential .

To the authors knowledge, the use of shear strength as a swell indicator has received little previous attention. Although this aspect is considered outside the scope of this project, its potential for swell indication is noted, and further research is recommended .

The literature indicates some differences of opinion regarding the exact value of shear strengh of a soil at liquid limit ; numerous writers propose such values e.g. Seed(1962) - 2.45 KN/M^2 , Medhat and Whyte (1984) - 1.6 KN/M^2. However, the latter value appears to have undergone a more rigorous preferred evaluation.

On a more fundamental basis, the liquid limit may be considered as the moisture content at which a specimen will exhibit a specific shear strength and volume change . A higher liquid limit therefore indicates an increased potential for swelling, since the specimen must absorb more water (and swell more) to exhibit the same shear strength.

In conclusion, both the liquid limit and expansion properties (i.e. swell and swell pressure) are closely related to the inter-particle repulsion forces ; it is therefore not surprising that the liquid limit is widely employed as an indicator of swell potential.

2.5.4 Plastic limit

"A plastic soil is defined as that in which the cohesion between units or particles is sufficiently low to allow movement, yet sufficiently high to allow the particles to maintain the new moulded position." (Yong and Warkentin, 1966).

The plastic limit is widely acknowledged as varying much less than the liquid limit. It increases as the surface area of the clay increases but not in direct proportion e.g. the surface area of montmorillonite is 40 times that of Kaolinite, but the plastic limit is only 2-3 times as large.

The plastic limit cannot therefore be related simply to the thickness of the water layers around the clay particles.

As in the case of liquid limit, Medhat and Whyte (1984) contend that all soils at their plastic limit will exhibit a constant shear strength value.

There is some contention as to the precise value of this shear strength, and they chose 110 kN/m^2 , since it represents a state about mid-way into the stiff consistency range for clays (75-150 kN/m^2).

In conclusion, the variation of plastic limit between different clay types is considerably less than that of the liquid limit. Its decreased sensitivity renders it less suitable for the indication of swell, and this is reflected in its limited use in this role throughout the literature.

2.5.5 Plasticity index

The plastic or plasticity index is the range of moisture content over which a clay is plastic and is inversely related to the size of the particles. It is equal to the difference between the liquid and plastic limits.

Grim (1953) indicates that the plasticity index of a clay mineral increases considerably with increasing cation exchange capacity (CEC) thus making it a good indicator of potential swell. The plasticity index of a low CEC clay is raised dramatically by the addition of only a small amount of a high CEC clay. This increase is due primarily to the large change in liquid limit, since as previously indicated, the plastic limit remains fairly constant.

2.5.6 Shrinkage limit

The shrinkage limit is that moisture content of a soil below which no further volume change will occur. Shrinkage arises from the pressure difference across the curved air-water interfaces of the voids at the specimen boundary. It occurs as a result of the evaporation of water from the pores.

As water evaporates from a saturated specimen, a curved interface is formed in the voids. The resulting pressure difference causes water to be drawn from within the specimen, and thus creates an equal decrease in total volume. This form of shrinkage will continue so long as the pressure deficiency exceeds the clay particle repulsive forces.

Eventually, a condition is reached where particle interaction restricts shrinkage, and further increments of water removal are partly replaced by air. This point, which is termed the shrinkage limit is not usually so sharply defined, nor does the lower end of the shrinkage curve (as in figure 2.7) always lie on the axis. This latter aspect is due to the tightly held adsorbed surface water being more difficult to drive off than the pore water; consequently, considerable adsorbed water may remain long after the free pore water has evaporated. In the case of montmorillonite, a large amount of water is tightly held so that a pronounced departure from the curve would be expected.

The shrinkage limit is also dependent upon the arrangement of particles and clay mineral type. A more random particle arrangement increases the shrinkage limit and a more parallel arrangement decreases it.

The shrinkage limit also increases slightly with increasing cation exchange capacity. Overall however, the variation in shrinkage limit between soil types is limited. However, this has not deterred other researchers from using it as an indicator of potential swell.

2.6 Clay Mineral Mixture Behaviour - Experimental Study

2.6.1 Introduction

One method of obtaining test materials of suitable expansion characteristics is through the use of synthetically constituted clay mineral mixtures. This has been undertaken in this project,

where Kaolinite (China clay) and sodium montmorillonite (Wyoming-Bentonite) have been mixed in different proportions to provide a range materials with different expansive properties . Full details of these minerals are given in appendix B .

The properties and behaviour of single minerals are discussed in the previous sections . However, there is very little information regarding the behaviour of synthetically constituted clay mineral mixtures . The main references include Seed et.al. (1964) , Dumbleton and West (1966) and a review by Rowlands (1984) . Unfortunately, the findings of Seed et. al. (1964) are of limited value to this study, since they do not provide data . The references indicate that theinfluence of varying montmorillonite content will not necessarily be proportional to the swell behaviour or soil properties . Therefore, since synthetic mixtures of Kaolinite and montmorillonite are to be used for the study of expanding clays, it is desirable that the relative contribution of each constituent mineral towards this behaviour beassessed.

This is undertaken by producing trial batches of the proposed mixtures , and conducting Atterberg limits and preliminary consolidometer swell tests; the latter tests are subsequently used in the analysis of Fredlunds theory (chapter 8)

These results are supplemented with compatible data by Dumbleton and West (1966) .

2.6.2 Experimental programme

Sythetic mechanical mixtures of Kaolin and Montmorillonite were prepared to the proportions listed below and their liquid

limits, plastic limits and swell properties determined .

Percent content by mass	
Sodium Montmorillonite (Wyoming Bentonite)	Kaolinite (China Clay)
* 0	100
* 10	90
* 20	80
25	75
* 30	70
50	50
75	25
100	0

Only the mixtures denoted '*' are subsequently employed for the main testing programe since those containing greater than 30% montmorillonite possess plasticity and expansion characteristics well outside those expected in the field .

2.6.3 Presentation of results

The results are presented graphically by plotting the measured properties (described above) against the Montmorillonite content . The following aspects are examined .

(a) data plotted on the Casagrande's plasticity chart

(b) relationship between liquid limit / plastic index and the bentonite (montmorillonite) content

(c) relationship between swell characteristics (swell pressure, void ratio change, compressibility and the liquid and plastic limits .

2.6.4 Comments

(a) plasticity data

The author's data - when plotted on Casagrande's plasticity chart lies on a near straight line inclined at 45^{o} (figure 2.8). This intersects the U line (upper limit of most soils) where the liquid limit equals 200% and the montmorillonite content equals 30%. from the same figure, it appears that the plasticity data after Sherif et al (1982), Nayak and Christensen (1974) and Jawed (unpublished) is compatible with that obtained by the author .

The authors plasticity line or 'signature' obtained from the clay mineral combinations is particularly similar to those indicated by Holtz and KovaKs (1981) for various types (exact positioning will depend upon the minerals employed) . Although natural soils (i.e. not synthetically produced mixtures) plot below the U line, Sherif et.al. (1982) indicate that high sodium montmorillonite content synthetically produced mixtures will plot above the U line .

The precise liquid limit/plastic limit values for high swell minerals must be treated with caution due to their thixotropic character .

Thixotropic clays take considerable time to equilibrate following a moisture increase , and will in turn cause the liquid limit to apparently vary with time unless testing is conducted on a specific time scale .

(b) Effects of montmorillonite proportions upon the liquid limit

Grim (1962) indicates that the mere presence of sodium montmorillonite (however small) with another clay mineral will ensure that the nature of the exchangeable cation becomes a significant controlling factor.

Dumbleton and West (1966) (in contradiction to this) indicate that the addition of up to 25% montmorillonite to Kaolinite has little or no effect upon the liquid and plastic limits. Above this, the resultant changes in liquid limit and plastic index for an increase in mineral content are noted as approximately linear, following Casagrande's 'A' line.

The author notes that the liquid limit for the montmorillonite used by Dumbleton and West (1966) is less than 150%, which suggests a lower swell type mineral such as calcium-montmorillonite. The influence of this mineral upon the liquid limit would be considerably smaller than that used by the author.

The author notes that the addition of even a small amount of sodium montmorillonite to Kaolinite (refer fig 2.8 and 2.9) considerably influences the liquid limit of a mineral mixture (100% Kaolinite + 0% montmorillonite : LL = 47% ; 90% Kaolinite + 10% montmorillonite : LL = 82%).

Results by Nayak and Christensen (1973) and Sherif et al (1982) confirm that synthetic mineral mixtures employing sodium montmorillonite exhibit similar plasticity characteristics even when mixed

with inert minerals other than Kaolinite (e.g. quartz sand and or grundite).

It is noted from figure 2.9 that the rate of increase of both liquid limit and plasticity index increases with increasing Wyoming bentonite (sodium montmorillonite) content. The increase in liquid limit/plasticity index is clearly some definite function of the mineral content. This also appears to be the case for results after Dumbleton and West (1966) (although the influence of calcium montmorillonite used is less pronounced).

(c) Swell characteristics

All swell characteristics are noted as increasing with increasing montmorillonite content .

The void ratio change versus mineral content plot (figure 2.10) is approximately linear up to 50% montmorillonite content. Little usable data is available for higher contents since such mixtures have a very long equilibration time, in addition the large swell exhibited exceed the measuring capacity of the equipment. In general however, the swell appears to tend to a maximum value before 100% montmoillonite content is reached.

An earlier series of tests conducted by the author on an expansive soil indicates that the swell pressure in an oedometer (consolidometer)

specimen comes to equilibrium essentially within 48 hours (refer fig.2.11 moisture). This seems conservative in comparison with observation by Sherif et al (1982), who note the swell pressure as equilibrating after 24 hours for a range of mixes. The author's results (fig. 2.12) indicate that the swell pressure increases in the form of an S-shaped function with increasing montmorillonite content. The behaviour can be summarised as in Table 2.4.

The swell and compressibility index versus montmorillonite content plots (figure 2.13) do not indicate clear relationships. Trends are observable, but the spread of data prevent the determination of precise relationships. The general observation is that the indices increase with increasing montmorillonite content.

2.6.5 Conclusions

1. The author's data for synthetic soil mixtures plot as a straight line 'signature' on Casagrande's plasticity chart. The linearity of this is considered as indicative of the experimental consistency.

2. Repeated experimentation by the author indicates that the synthetically constituted clay mixtures plot above the U line (upper limit) on Casagrande's plasticity chart.

3. The plots of liquid limit and plastic index against the montmorillonite content exhibit definite relationships. The gradients of both liquid limit and plastic limit with montmorillonite content appears to increase for higher montmorillonite contents.
   This is confirmed by data from Dumbleton and West (1966).

4. All swell characteristics generally increase with increasing montmorillonite content.
   The void ratio change increases linearly up to 50% montmorillonite content then tends towards a maximum value for 100% montmorillonite content.
   The swell pressure tends to a constant value for lower and higher montmorillonite contents (i.e. < 20% and > 55% respectively).

5. The compressibility and swell indices (i.e. the volume changes resulting from loading and unloading respectively) gradually increase with montmorillonite content. The scatter of data points prevents the determination of firm relationships.

6. All the above observations are influenced by the initial density, moisture content and loading conditions.

7. The good relationship between either the liquid limit or plastic index or percent swell or swell pressure and the bentonite content verifies that the plastic index and/or liquid limit should be considered for use as a basis for prediction purposes.

EXPANSIVE BEHAVIOUR

2.7 INTRODUCTION

This describes the actual volume change behaviour exhibited by expansive clays following a change of moisture content under laboratory or field conditions.

The behaviour is determined by certain physical properties which combine and/or interrelate.

Snethen et al (1975) proposes a two-fold categorisation of those physical properties: (1) intrinsic properties: which contribute to or influence the actual volume change (in situ or laboratory materials) and (2) environmental conditions i.e. extrinsic factors : which enhance the probability and magnitude of expansivity (particularly in situ materials).

The following section discusses the physical properties in terms of the above mentioned combinations and interrelationships. The intrinsic physical properties are discussed in some detail due to their relevance to this project whereas the environmental conditions are covered only briefly.

2.8 INTRINSIC PROPERTIES

(a) Soil composition

This includes the type and amount of clay minerals within the soil and their size and specific areas. The mineral composition determines the clay's potential for swelling.

The size of the clay mineral particles (in expansive materials) affects volume change by controlling the development of double layer water on the particle periphery. Small particle sizes result in large effective surface areas which permit considerable double layer water thicknesses and hence swelling.

Clay particle size, although not an independent parameter, is often characteristic of specific clay minerals.

(b) Dry density

This is an important factor in determining the magnitude of expansive behaviour - since the swell or swelling pressure increases with increasing dry density for constant moisture content.

Higher densities usually result in closer particle spacing thus causing greater double layer water interaction. This in turn results in higher repulsive osmotic forces and consequently greater volume change.

This is the case for both remoulded and undisturbed soils.

Seed and Chan (1959) note that dry density interrelates with the soil fabric by influencing inter-particle arrangement. They demonstrate experimentally that for a given compactive effort, the particle orientation increases with moisture content. (Figure 2.14).

(c) Soil fabric

The definition for soil fabric adopted in this thesis is that proposed by Seed and Chan (1959) and is assumed to refer to the arrangements and orientation of the constituent particles.

The type of clay mineral arrangement will also partly influence the direction and magnitude of volume change.

Clay mineral platelets are difficult to observe, but generally occur in either agglomerated (independent groups) or non-agglomerated (uniform fabric, no discernible groups) forms.

(d) Pore water properties

Volume change in expansive soils is attributable to the availability and variation of soil water quantity. It therefore follows that the water properties will significantly influence soil behaviour. As previously discussed in Section 2.3, the volume change in expansive soils is primarily due to the hydration of clay minerals. The degree of hydration is influenced by the amount and type of ions adsorbed on the clay particles and in the pore fluids. In addition, the volume change tends to be inversely related to the cation concentration (quantity of soluble salts) i.e. high cation concentration in the pore fluid (of similar types to those in the soil) reduce volume change and vice versa.

(e) Permeability

The permeability is extremely influential in the time rate of volume change. It is a function of the initial moisture content, dry density and soil fabric. For compacted soils, the permeability is greater at the lower moisture contents and dry densities and decreases to a near constant value at around optimum moisture content (OMC).

Minimum permeability occurs at the OMC and maximum dry density because of the close particle spacing and resulting fewer voids for

moisture movement.

Permeability is enhanced with in situ soils by the presence of discontinuities since they provide possible avenues for the introduction of moisture.

(f) Properties pertaining to expansive rocks and shales

The volume change exhibited by in situ (sedimentary) materials is further influenced by soil structure, cementation and diagenetic effects.

Soil structure refers to the macroscopic features/discontinuities contributing to the non homogeneity of materials.

Cementation includes the presence or non-presence of mineral cements and subsequent bonding action upon clay particles.

The diagenetic effects are the long term physical and chemical changes in the soil resulting from overburden and groundwater influence.

(g) Confinement, temperature and time

These are not intrinsic properties as defined in the opening paragraph. However, they do influence the role of the 'true' intrinsic properties in determining the amount and rate of volume change in both laboratory and in situ conditions.

The degree of confinement will determine the amount of swell and or swell pressure exerted on the foundation. An increase in confinement (or overburden) will increase the observed swell pressure and decrease the swell.

Krazynski (1973) indicates that temperature effects are limited to influencing the viscosity and specific gravity of the adsorbed water However localised temperature gradients can induce the migration of water from warmer to cooler regions .

The time is an interrelated'property' , where the period between initial wetting of the soil to the first indications of swell behaviour is a function of the soil permeability and availability of water .

2.9 ENVIRONMENTAL CONDITION

Environmental conditions significantly influence the swell behaviour of soils, and, but for the cases of constant conditions such as desert or permafrost, may vary considerably between sites.

The main factors influenced by environmental conditions are represented in figure 2.15 and listed below :

(a) Soil profile : this includes the thicknesses of expansive Soil layers . The thicker the layer, the more swell will be exhibited .

(b) depth of desiccation : thickness of the permanently moisture deficient soil layer .
The lateral variation in moisture content will also influence swell behaviour .

(c) Seasonal moisture variation : depth to which soil moisture is affected by seasonal climatic variations .

(d) Vegetation : long term growth or rapid removal will probably alter the soil moisture content , thus causing soil volume change .

(e) surface drainage: poor surface drainage, whether natural or man made leads to moisture accumulation resulting in probable volume change.

(f) modes of moisture transfer: includes gravitation, capillarity and thermal gradient influences.

(g) sources of water: the sources are numerous e.g. rainfall, groundwater table, irrigation, faulty sewerage/water supplies etc.

TABLE 2.1

TYPICAL VALUES OF FREE SWELL FOR COMMON CLAY MINERALS

Clay Mineral	Free Swell*(%)
Sodium Montmorillonite	1400-2000
Calcium Montmorillonite	45-145
Vermiculite**	--
Chlorite**	--
Illite	60-120
Kaolinite	5-60
Halloysite	70
Mixed layer type+	

* Test data based on swell in water of 10cc of dried,crushed material passing No. 30 sieve and retained on the No.50 sieve.

**Free swell is variable and dependent on size and crystallinity.

+ Free swell is variable and dependent on amount of expandable clay minerals present.

TABLE 2.2

CATION EXCHANGE CAPACITIES OF CLAY MINERALS

Clay Mineral	CEC Milliequivalents per 100g
Kaolinite	3-15
Halloysite, 2 H_2O	5-10
Montorillonite	80-150
Illite	10-40
Vermiculite	100-150
Chlorite	10-40

TABLE 2.3

Natural Microscale Mechanisms Causing Volume Change in Expansive Soils

Mechanism	Explanation	Influence on Volume Change
Osmotic repulsion	Pressure gradients developed in the double-layer water due to variations in the ionic concentration in the double layer. The greatest concentration occurs near the clay particle and decreases outward to the boundary of the double layer	The double-layer boundary acts as an osmotic membrane when exposed to an external source of free water; that is, it tries to draw the water into the double layer to reduce the ionic concentration. The result is an increase in the double-layer water volume and the development of repulsive forces between interacting double layers. The net result is an increase in the volume of the soil mass
Clay particle attraction	Clay particles possess a net negative charge on their surfaces and edges which result in attractive forces for various cations and in particular for dipolar molecules such as water. This makes up the major "holding" force for the double-layer water	In an effort to satisfy the charge imbalance, the volume of water in the double layer will continue to increase until a volume change of the soil mass occurs
Cation hydration	The physical hydration of cations substituted into or attached to the clay particle	As the cations hydrate, their ionic radii increase, resulting in a net volume change of the soil mass
London-van der Waal forces	Secondary valence forces arising from the interlocking of electrical fields of molecule associated with movements of electrons in their orbits. The phenomenon frequents molecules in which the electron shells are not completely filled	The interlocking of electrical fields causes a charge imbalance which creates an attractive force for molecules such as water
Capillary imbibition	Movement of water into a mass of clay particles resulting from surface tension effects of water and air mixtures in the pores of the clay mass. Compressive forces are applied to the clay particles by the menisci of the water in the pores	As free water becomes available to the clay mass, the pore water menisci begin to enlarge and the compressive forces are relaxed. The capillary film will enlarge and result in a volume change or supply water for one of the other mechanisms
Elastic relaxation	A readjustment of clay particles due to some change in the diagenetic factors	Volume change results from particle reorientation and/or changes in soil structure due to changes in the diagenetic factors

TABLE 2.4

INFLUENCE OF BENTONITE CONTENT UPON SWELL PRESSURE

Montmorillonite Content by mass. (%)	Influence upon Swell Pressure
≤ 20	least effect
20-50	greatest effect
≥ 55	reduced rate of effect

FIGURE 2.1

BASIC STRUCTURAL UNITS IN THE SILICA SHEET

(a) BASIC UNIT

(b) SHEET

(c) SYMBOLISED SILICA PLANE

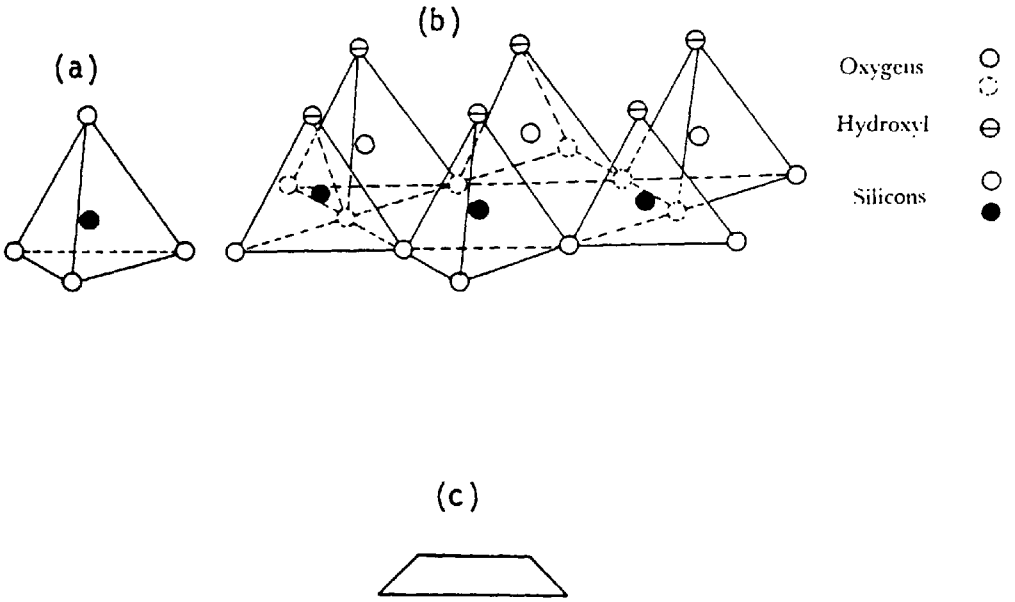

FIGURE 2.2

BASIC STRUCTURAL UNITS IN THE ALUMINA SHEET

(a) BASIC UNIT

(b) SHEET

(c) SYMBOLISED ALUMINA UNIT

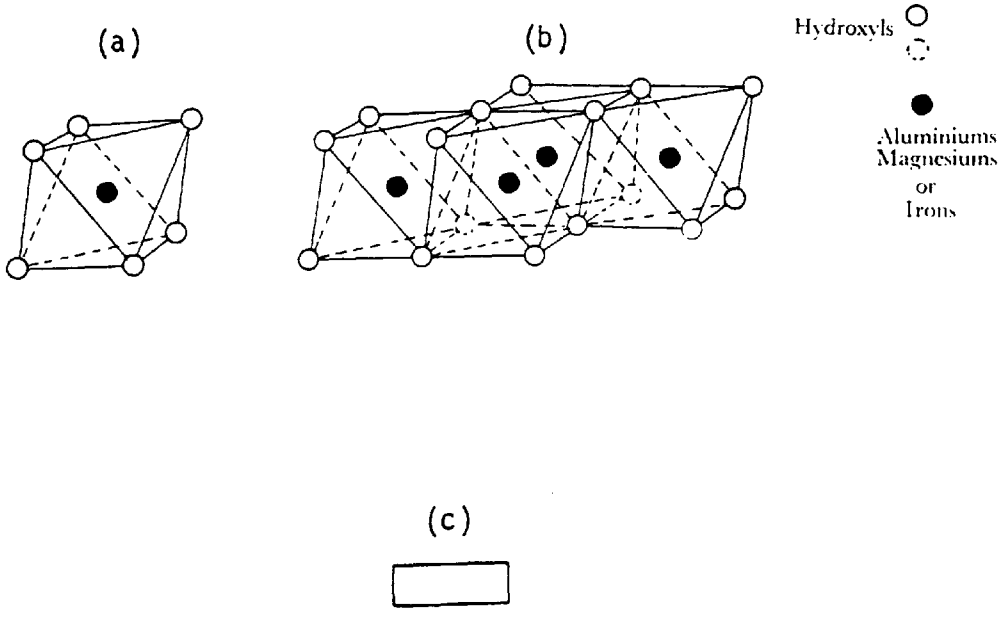

FIGURE 2.3

SYMBOLISED KAOLINITE STRUCTURE

(a) BASIC STRUCTURE

(b) STACKED UNITS

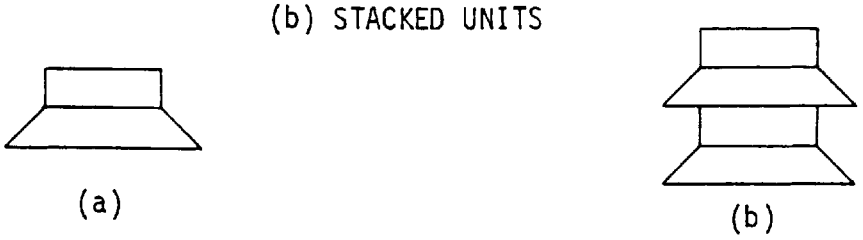

(a) (b)

FIGURE 2.4

SYMBOLISED MONTMORILLONITE STRUCTURE

(a) BASIC STRUCTURAL UNIT

(b) STACKED UNITS INTERACTING

(a) (b)

FIGURE 2.5

INTERACTION OF ILLITE UNITS

non exchangeable potassium ions resulting in stronger bonds between montmorillonite units.

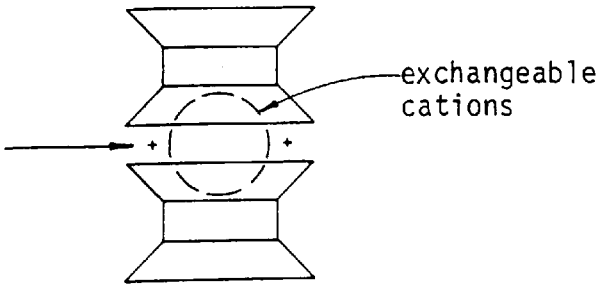

FIGURE 2.6

DEFLOCULATED CLAY MINERAL ASSOCIATIONS

(a) SHOWING SURFACE WATER (ILLITE)

(b) SHOWING SURFACE AND INTERLAYER WATER (MONTMORILLONITE)

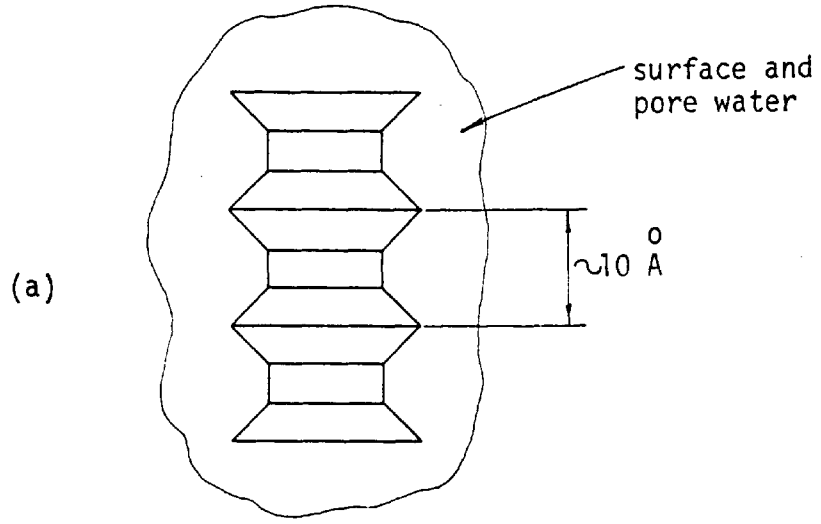

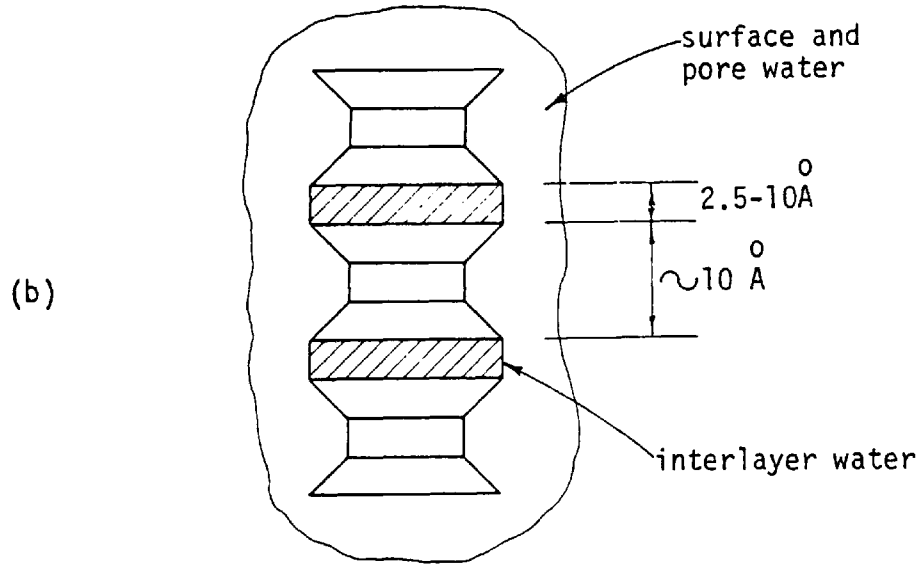

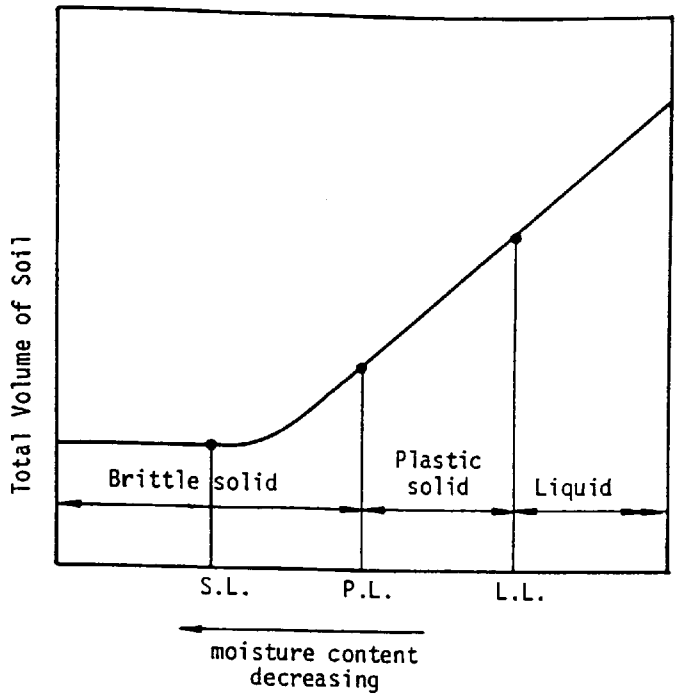

FIGURE 2.7

THE VARIATION OF TOTAL VOLUME WITH MOISTURE CONTENT.

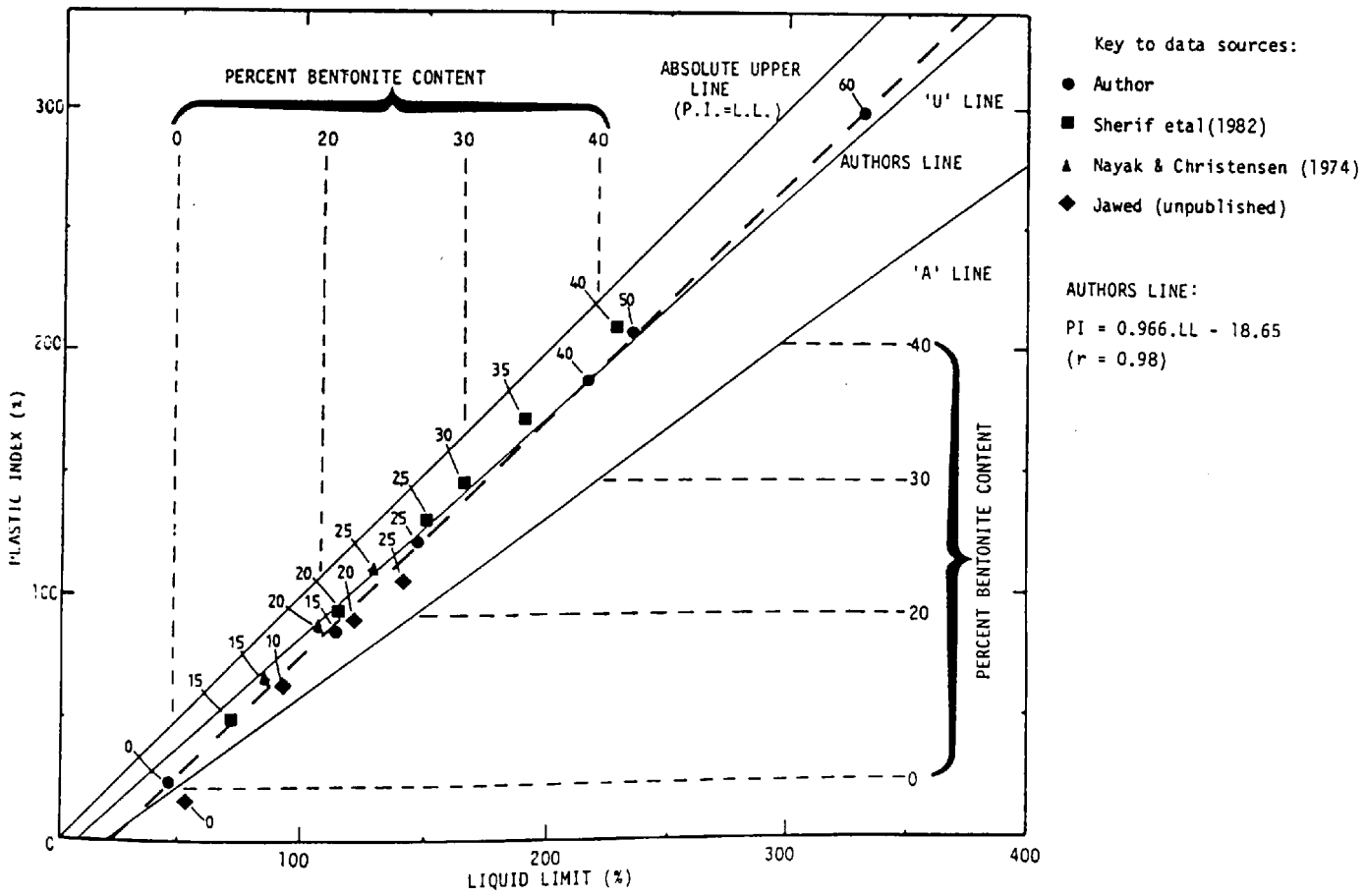

FIGURE 2.8

THE INFLUENCE OF BENTONITE CONTENT UPON PLASTIC INDEX AND LIQUID LIMIT. (CASAGRANDES PLASTICITY CHART)

FIGURE 2.9

THE INFLUENCE OF CLAY MINERAL PROPORTIONS UPON THE LIQUID LIMIT AND PLASTIC INDEX.

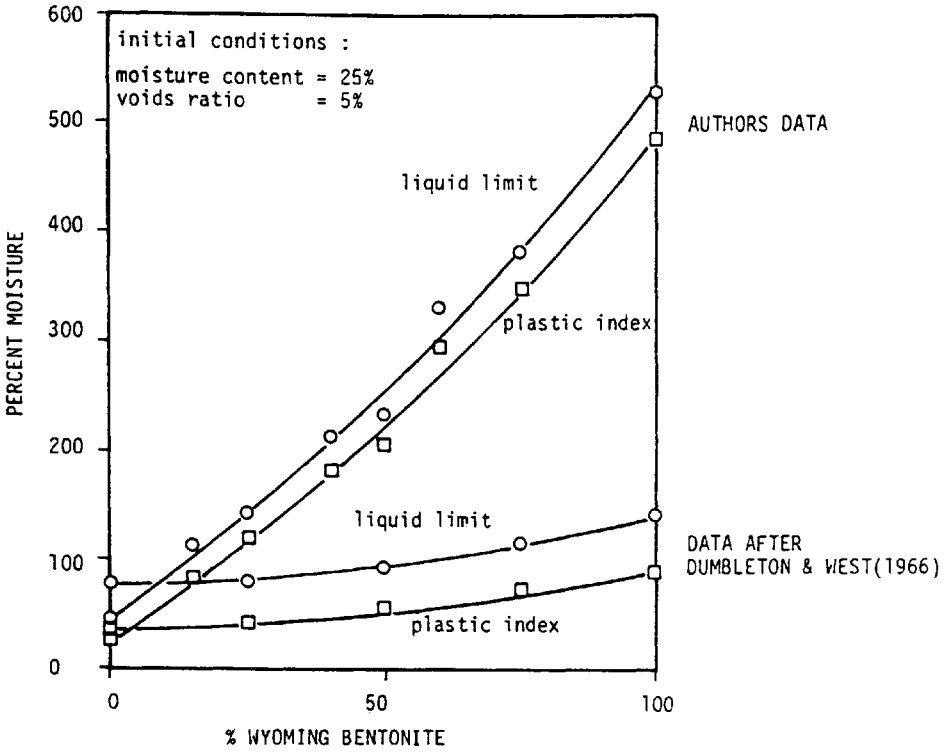

FIGURE 2.10

THE INFLUENCE OF CLAY MINERAL PROPORTIONS UPON THE VOLUME CHANGE CHARACTERISTICS.

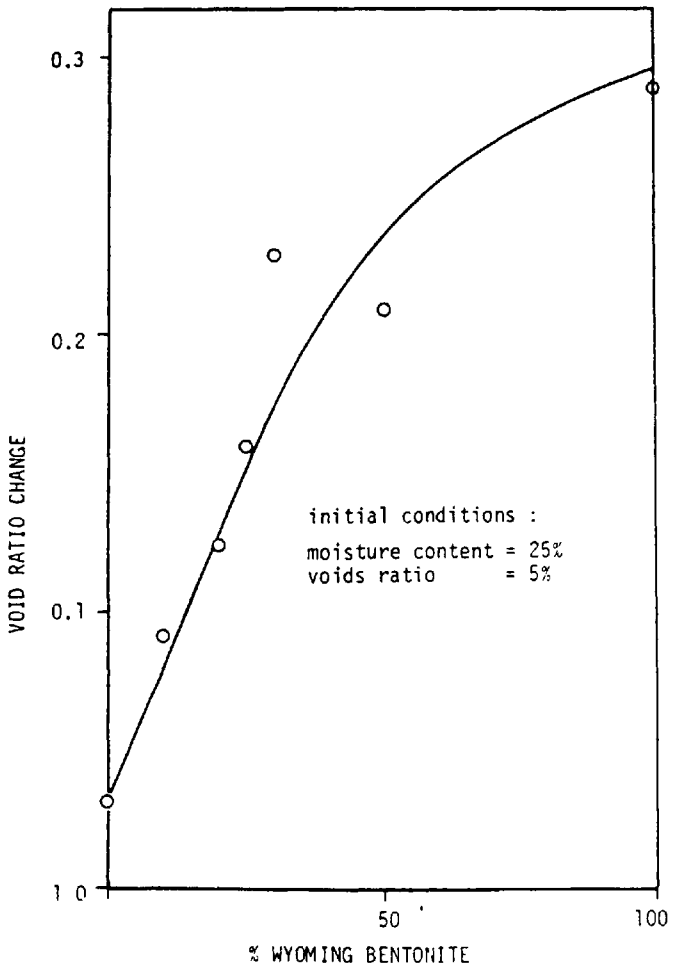

FIGURE 2.11

DEVELOPMENT OF SWELL PRESSURE

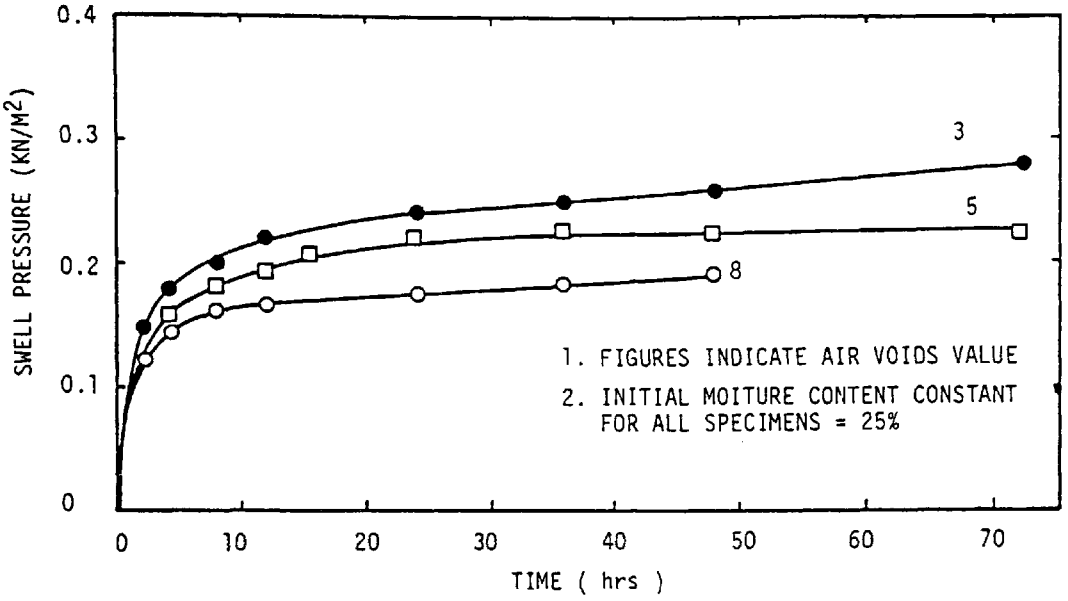

FIGURE 2.12

THE INFLUENCE OF CLAY MINERAL PROPORTIONS UPON THE SWELL PRESSURE CHARACTERISTICS.

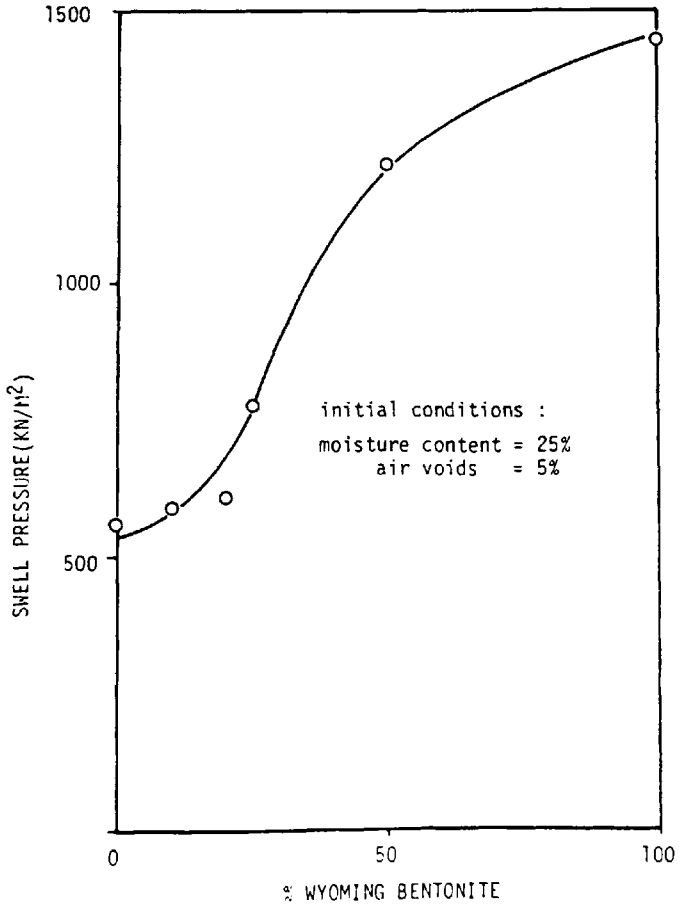

FIGURE 2.13

THE INFLUENCE OF CLAY MINERAL PROPORTIONS UPON THE SWELL AND COMPRESSIBILITY INDICIES.

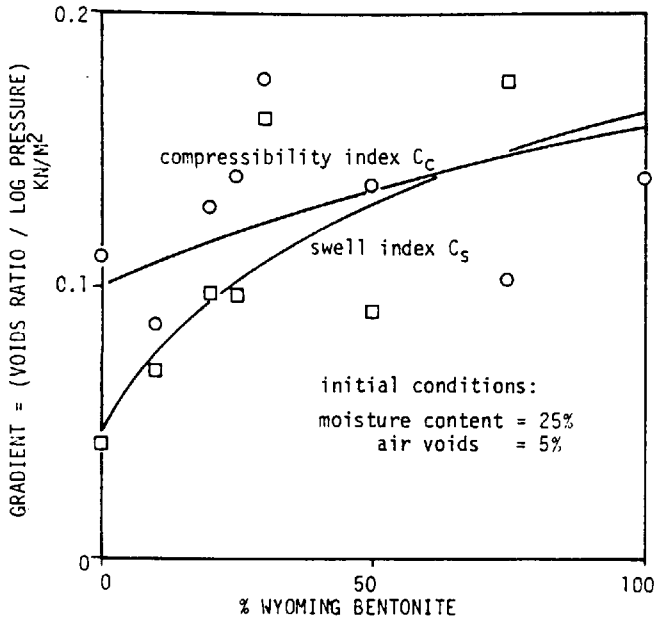

FIGURE 2.14

MOULDING WATER CONTENT VERSUS DRY DENSITY AND PARTICLE ORIENTATION FOR COMPACTED KAOLINITE SPECIMENS (SEED AND CHAN,1959)

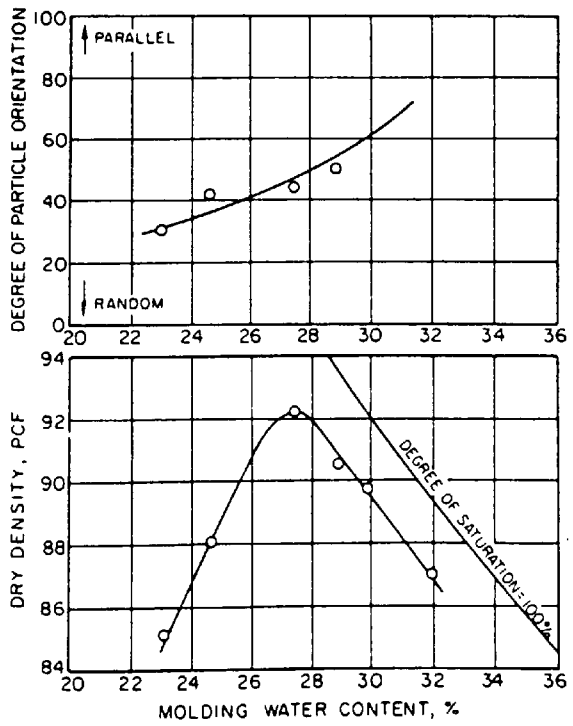

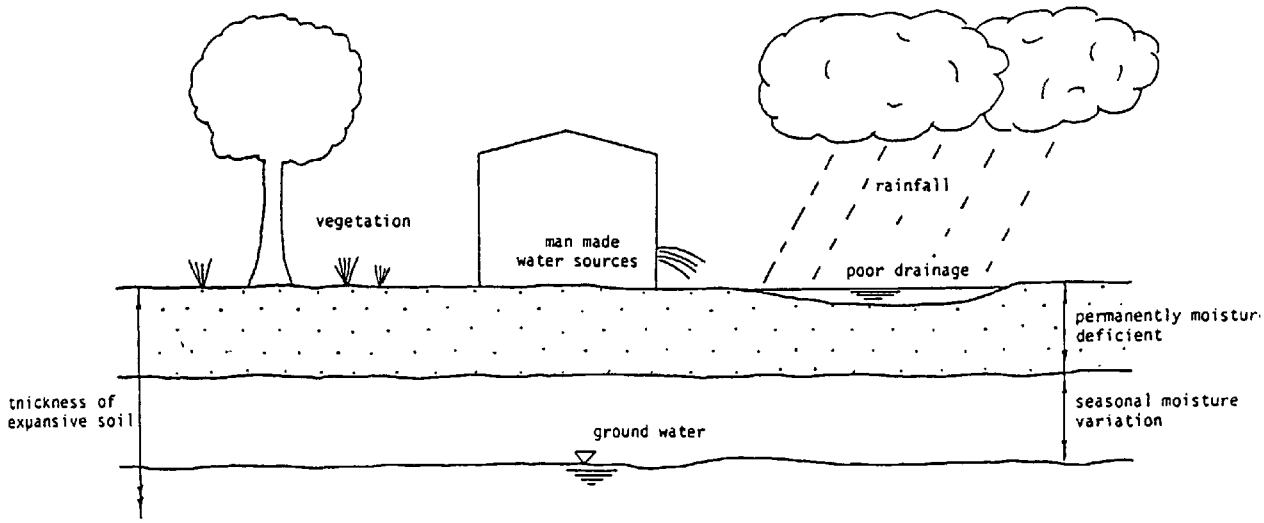

FIGURE 2.15

ENVIRONMENTAL FACTORS
AFFECTING VOLUME CHANGE

CHAPTER 3

METHODS FOR THE IDENTIFICATION AND CLASSIFICATION OF EXPANSIVE CLAYS

3.1 INTRODUCTION

The purpose of an identification/classification technique for swelling soils is to characterise the potential volume change behaviour of suspected problem materials. A review of the literature indicates a large amount of research in this field over the last twenty years, with development tending towards the use of consistency limits and/or particle size as a basis for swell prediction. In addition, very few of these techniques have been accepted into the national soil classification systems due largely to their limited geographic application.

The aim of this chapter therefore, is to evaluate several of the published swell prediction techniques and to examine how a similar system might be incorporated into a main standard national soil classification system. The chapter is divided into three sections : Initially, the published swell prediction testing techniques are examined - recommendations being made as to their reliability.

The variability of data quality is noted and several aspects investigated including testing procedures and definitions of potential swell.

In the second section, a statistical analysis of several data sources is made in an attempt to determine the order of soil parameter significance and to assess whether there are any important soil parameters not presently being employed for swell prediction. Statistical equations are also derived to describe the swell of each data source.

The final section examines the main Engineering Soil Classification systems and discusses their application to the volume change behaviour of soils (in particular swell prediction).

The main conclusions of the preceding sections are summarised and the application of the most suitable swell prediction method to the BSCS and AASHTO systems outlined.

3.2 AN EVALUATION OF SWELL CLASSIFICATION SYSTEMS FOR EXPANSIVE CLAY SOILS

3.2.1 Objectives

The aim of this section is to evaluate several published swell classification systems used to predict the potential volume change of a suspected swelling soil.

Two aspects of the systems are evaluated :

(i) ability to qualitatively and quantitatively predict swell and

(ii) applicability to undisturbed and remolded specimens.

These systems are used to forewarn the engineer of a soils ability to swell; they are applied at the outset of site investigations and should

(a) be easy to understand and implement

(b) provide a consistent criteria for predicting swelling behaviour for as wide a range of soils as possible

(c) indicate whether any further detailed measurement of swell is necessary

A study of the literature indicates a trend towards a more comprehensive definition of potential swell. In particular, Snethen (1979) suggests that swelling soils should be considered in terms of the initial specimen conditions and include moisture content, dry density, fabric, structure, stress conditions, states of confinement and finally the water regime.

Clearly, such a detailed description is necessary to make very accurate predictions; however, the measurement of all these factors appears unwieldy for rapid preliminary evaluation purposes.

The majority of available identification methods can be categorised into five groups (Snethen, 1979) :

(a) soil composition group
(b) physical indicator group
(c) physicochemical group
(d) index property group
(e) soil classification group

Examination of these indicates that the soil composition, physicochemical and physical indicator groups are unsuitable for routine use due to their specialised nature.

However, the index property group (which include liquid, plastic and shrinkage limits, linear shrinkage and free swell) are considered to be suitable due to (a) the ease with which the properties can be measured and (b) the good correlations noted in the literature between some index values and swell potential.

The soil classification group is often interrelated with the index property group and therefore also considered suitable for rapid identification purposes.

In consequence, published methods from both of these groups will be assessed in the following sections.

3.2.2 Published Swell Prediction Systems

A number of empirical approaches based on the use of index properties such as Atterberg limits, linear shrinkage, free swell and also clay content,

have been developed as an aid to the identification of soil swelling characteristics.

In most instances, the indices are correlated with field data, and used individually or combined to predict the swelling characteristics of the soil.

The result is several single and multi-property categorisation of the relative magnitudes of potential volume change.

The categorisation may be either Quantitative, Qualitative - or both. Quantitative predictions yield actual values of swell (i.e.change in specimen height expressed as a percentage of the original height), whereas qualitative predictions designate the degree of anticipated swell only.

The following review is sectioned to reflect the two main divisions within the published index property based methods, namely those based upon Atterberg limits only and those based upon a combination of Atterberg limits and clay content.

3.2.2.1 Systems primarily based upon Atterberg limits and clay content

(a) Individual Research

The majority of simplified swell prediction methods have been developed since the late 1950s.

Most have incorporated the plasticity index and clay content, however only a few consider the shrinkage index and/or initial specimen conditions.

The developments are largely individually directed and uncoordinated. In consequence, the main research is discussed in chronological order. Holtz (1959) correlates observed swell with colloid content, plasticity index and shrinkage limit (Table 3.1) using regional data from the S.W. United States.

Seed (1962)'s extensive investigation on synthetically prepared compacted soils indicates that the swelling potential of a swelling clay mineral is related to its activity and clay content where

$$S = K.(A^{2.44}).(C^{3.44}) \qquad (3.1)$$

K = constant (related to the clay type)

S = swell (percentage of the original specimen height)

In the same paper, Seed presents a second simplified equation based upon plasticity index along where :

$$S = (K)(m)(P.I.^{2.44}) \qquad (3.2)$$

m = empirical constant = 60 (natural soils) = 100 (synthetic soils)

The second equation is graphically presented in figures 3.1(a) and 3.1(b).

Van der Merwe (1964) modifies the activity chart originally proposed by Williams (1958) to account for swelling behaviour. The chart (figure 3.2) plots plasticity index against clay content and can be used to qualitatively predict swell behaviour. He also relates probable percentage swell to the qualitative swell categories, although these are apparently limited in application to the regions from which the data was derived (S. Africa).

Ranganatham and Satyanarayana (1969) test four naturally occurring Indian soils and relate swelling potential to swell activity and clay content or shrinkage index; such that :

$$S = m.(S.I^{2.67}) \qquad (3.3)$$

swell activity = (shrinkage Index)÷(clay content)

m = constant (= 41.13 for natural soils)

SI = shrinkage index = $W_L - W_{SL}$

However, the authors claim an accuracy of only ± 34% which evidently limits its application. (Ref. figure 3.3 for graphical representation).

Nayak and Christensen (1971) claim to consider the double diffuse layer of clays when relating anticipated swell behaviour to clay content, plasticity index and initial moisture content.

Relationships are presented for several synthetic soil mixtures in addition to natural soils :

Kaolinite and bentonite mixtures

$$\text{swell pressure (psi)} = (6.982 \times 10^{-2})(PI)^{1.92} \cdot \frac{C^2}{w_i^2} + 9.119 \qquad (3.4)$$

$$\text{swell (\%)} = (4.494 \times 10^{-3})(PI)^{1.74} \cdot \frac{C}{w_i} + 14.722 \qquad (3.5)$$

All soils (a range of synthetic mixtures)

$$\text{swell pressure (psi)} = (3.582 \times 10^{-2})(PI)^{1.12} \cdot \frac{C^2}{w_i^2} + 3.791 \qquad (3.6)$$

$$\text{swell (\%)} = (2.29 \times 10^{-2})(PI)^{1.45} \cdot \frac{C}{w_i} + 6.38 \qquad (3.7)$$

C = clay content (%)

PI = plasticity index (%)

w_i = initial moisture content (%)

The graphical relationship for all soils is given in figure 3.4(Plasticity).

B.R.E. Digest No. 240/I (1980) examines the difficulties with low rise buildings on shrinkable clay soils and presents an empirical classification system based on plastic index and clay content for predicting

the potential shrinkage or swell of a suspect soil.

The swell categories are derived from several (unquoted) data sources, and the reader is warned that the system provides only a general indicator.

(b) National standard Soil Classification Systems

The following systems predict swelling behaviour upon the basis of clay content and Atterberg limits. Although these are discussed in detail in Sections 3.4.22 and 3.4.45, they are briefly described below for continuity.

Civil Aeronautics Administration (CAA) Classification System (1945)

This system employs grain size distribution and plasticity data for classifying all types of soil (ref. Table 3.27). Ranges of grain size and plasticity are established and a group number allocated to each soil category.

The system gives more attention to volume change and frost action than previous codes.

The percentage volume change is predicted following inundation of the soil (at field moisture content) with water. This is not considered satisfactory since the field moisture and soil types will vary considerably from site to site.

Unified Soil Classification System (USCS), 1953

Developed originally by the U.S. Army Engineers, the system is now widely employed for roads, airfields, embankments and foundations. The system classifies soil by allocating a soil group symbol which is dependent upon grain size distribution and plasticity limits. The soil groups are related to specific soil behaviour such as volume change characteristics,

permeability, strength and other factors of engineering significance. (Ref. Table 3.34).

Swell behaviour is described qualitatively, however, the only categories allocated are medium and high swelling - which the author considers insufficient.

Extended Casagrandes Soil Classification System, (1964)

This is very similar to the USCS, and again predicts the engineering behaviour of soils on the basis of grain size distribution and plasticity characteristics. In addition, the drinage characteristics and probable dry densities are also predicted.

Swell behaviour is broadly categorised as either medium or high ranges only - the exact boundaries slightly differing from the USCS. (Ref. Table 3.35).

3.2.2.2 Systemsprimarily based upon Atterberg limits

These systems have also been developed since the late 1950s. Although the majority continue to utilise the liquid limit value for making swell predictions, recent developments have tended to introduce in situ measurementsin order to increase their practical value.

Altmeyer (1955) presents a system to predict swell based upon shrinkage limits and linear shrinkage. Unlike the earlier system by Holtz, the colloid content is not considered, apparently to reduce equipment requirements.

Raman (1967) predicts swell in terms of plasticity index and shrinkage index (ref. Fig. 3.5). However, his relationships only relate to soils

up to a liquid limit of 66%, and are therefore of limited use with regard to high plasticity expansive soils.

Anderson and Thomsen (1969) propose a swell prediction method involving the plastic index alone. They acknowledge however that the method is probably limited for use with the highly plastic Alberta clays. As with the previous methods, the system is based on limited data. Refer to Table 3.7 for swell categories.

Komornik and David (1969) develop a relationship by multiple linear regression between measured swell pressure and liquid limit, initial moisture content and dry density. Correlations are based on undisturbed soil test specimens (although the base data is not quoted).

The relationship for swell pressure is of the form

$$\text{Log } P_s = 2.132 + 0.0208.W_L + 0.000665\ \gamma d - 0.0269\ W_i \qquad (3.8)$$

where

P_s = swell pressure (Kg/m^2) ; γd = dry density (Kg/m^3)

W_L = liquid limit ; w_i = initial moisture content

Vijayvergiya and Ghazzaly (1973) review some of the previous works and note that most swell predictions are derived from remoulded soil specimens. They then present a series of relationships correlated from undisturbed soil data in an effort to increase practical application. The relationships are as follows :

$$\text{Log } S = \frac{1}{12}\ (0.4.W_L - W_i + 5.5) \qquad (3.9)$$

$$\text{Log } S = \frac{1}{19.5}\ (\gamma d + 0.65\ W_L - 130.5) \qquad (3.10)$$

S = percentage swell ; γd = dry density (pcf)

and

$$\text{Log } P = \frac{1}{12} (0.4\ W_L - W_i - 0.4) \qquad (3.11)$$

$$\text{Log } P = \frac{1}{19.5} (\gamma d + 0.65\ W_L - 139.5) \qquad (3.12)$$

P = swell pressure (psi) ; W_i = initial moisture content (%)

W_L = liquid limit (%)

The authors claim that these relationships work very well and exhibit coefficients of determination in excess of 0.7; they are subsequently used as the basis of a swell prediction system (Table 3.8). However, it is noted that Vijayvergiya and Ghazzaly's specimens exhibited liquid limits not greater than 77%, and were obtained primarily from one region (SW.USA), in consequence, application of the relationships is limited by these restrictions.

Dakshanamurthy and Raman (1973) initially estimate the degree of swell upon the basis of liquid limits, plasticity index and shrinkage index. However, they subsequently noted that the swell behaviour could be equally predicted upon the basis of liquid limit only. Their second presentation as adapted to Casagrande's chart is displayed in figure 3.7; as a result of its similarity to the British (BSCS) and American (USCS) classification charts, its potential for amending these systems will be considered later.

The author presents a modification of Casagrande's chart, which may be used to predict percentage values of swell upon the basis of liquid limit. (Figure 3.8). However, the statistically derived swell ranges are limited in applicability due to the localised nature of the data catchment area.

It must be noted that consideration of swell data from varying climatic regions and different soils does not yield meaningful correlation.

In consequence this aspect has not been pursued further.

3.2.2.3 Swell classification systems for evaluation

The following systems have been chosen as representative of available swell prediction methods, and will now be assessed in conjunction with published data.

Based on Atterberg limits only	:	Holtz (1956) Dakshanamurthy and Raman (1973) S. Williams (1983)(unpublished) Vijayvergiya and Ghazzaly (1973) Ranganatham and Satyanarayana (1965) Raman (1967)
Atterberg limits and clay content	:	Holtz (1956) Seed et al (1962) Nayak and Christensen (1970) Van der Merwe (1964) Building Research Establishment (1980) Civil Aeronautics Administration (1946) Unified soil classification system (1953) Extended Casagrande's soil classification system (1954)

3.2.3 Selection of Data

3.2.3.1 Definitions of potential swell

Despite the availability of swell related data, much of the information is incompatible due to a variation in recorded parameters, omission of equipment details and variation in the definition of potential swell.

The latter variation exerts a critical influence over the measured swell values; the main published variations(also summarised in Table 3.10) are :

1. Gil (1969)

"The vertical swell of a laterally confined specimen under a 1psi surcharge,

following an increase in moisture content from field moisture level to 100% saturation - the specimen having first been subjected to the in situ overburden". Few sources of data are available in this format.

2. Seed et al (1962); Ranganatham and Satyanarayana (1965); Komornik and Livneh (1969); Anderson and Thomsen (1969)

"The vertical swell of a laterally confined specimen at maximum dry density and optimum moisture content under 1 psi surcharge, following inundation with water and subsequent saturation".

Few data sources are available in the above format.

3. Ladd and Lamb (1961); Vijayvergiya and Ghazzaly (1973); Salas and Serratosa (1957)

"The vertical potential swell of a laterally confined specimen from natural moisture conditions to saturation, under a 1 psi surcharge". This definition is widely employed with undisturbed and remoulded specimens. The prediction of swell can be inconsistent however, since the natural moisture content of a specimen may vary considerably from site to site.

There exists a good quantity of data in this format.

4. Snethen (1979)

"The vertical potential swell from natural moisture condition to saturation under actual overburden stresses. Specimens are initially at field conditions".

Snethen proposes this definition as a means of quantifying the likely in situ swell. It is considered inappropriate for general identification purposes since it applies varying conditions of loading to the specimen, and thus fails to determine the true relative swell potentials of various soils.

5. Holtz (1959)

"The vertical swell of an undisturbed specimen from air dried to saturation

under a 1 psi overburden".

The initial moisture level is not quoted, but is presumably equal to the lowest field moisture content. Although few data sources are available in this format, it is useful since the measured swell equals the maximum swell likely to be observed. This is therefore a consistent means of assessing swell.

3.2.3.2 Selection of potential swell definition

The choice of definition depends upon the overall requirements of the system and for the purpose of this study, whether sufficient data is available in the required format to make a meaningful correlation.

The definition after Holtz (1959) is preferred because :

(i) swelling tests conducted at the suggested lowest field moisture content will indicate the maximum likely extent of the problem.

(ii) the test is applicable to undisturbed and remoulded specimens.

However, only limited data is available in this format , and in consequence, a similar definition after Ladd and Lambe (1961) is chosen as an alternative.

This defines potential swell as commencing from the natural moisture content, which will not necessarily provide a good basis for comparing different localities. However, this was finally accepted since the data used in the study was primarily obtained from dry-arid climates, hence the soils will exhibit the major portion of their swell potential.

3.2.4 Assessment of swell classification systems

Qualitative system

3.2.4.1 Swell categories

Qualitative swell prediction systems assign a probable degree of swell upon the basis of the parameters discussed earlier.

The swell categories found in the literature are either arbitrarily established (i.e. no establishing criteria stated), or based upon statistically derived ranges of percent volume change.

Arbitrarily established systems include Raman (1967), BRE (1980), R&S (1965), USCS (1953), V&G (1973) and VDM (1964) (refer Table 3.10).

The statistically derived swell-category systems (ref. Table 3.11) include; Holtz (1957); Seed (1962); Altmeyer (1961); Anderson and Thomsen (1969) and Vijayvergiya and Ghazzaly (1973).

It is noted that the categories presented by Altmeyer, Anderson and V&G were derived using soils of relatively low swell potential; in consequence, predictions by their methods will tend to be too low.

The ranges proposed by Holtz and Seed on the other hand cover a larger range of swell and are therefore considered to be more widely applicable. Notably, Holtz proposes that soils exhibiting <10% expansion be classed low swelling. The author considers this misleading since a 10% swell rated soil can cause considerable damage to construction placed upon it.

The author therefore proposes modifications to Holtz' swell categories (Table 3.11), and his method is again applied to the data sources for assessment.

3.2.4.2 Criteria for comparison of systems

In order to compare the chosen systems it is necessary to select a base system or 'yardstick' by which the performance of the others can be assessed. (This does not necessarily imply that the chosen system is superior to the others, however the choice of a method based on parameters

of acknowledged significance should at least give an indication of any trends in behaviour).

It is noted that almost all of the reviewed swell prediction methods are either wholly or partly-based upon the liquid limit or plastic index; this is presumably due to the good plasticity-swell correlation generally indicated on a regional basis.

The system after Dakshanamurthy and Raman (1973) also uses liquid limit values for predicting the degree of swell and applies swell ranges to Casagrande's plasticity chart; this is therefore considered to be suitably representative of the available systems, and will be used as the reference system.

For the purpose of comparing qualitative predictions of swell behaviour, it is necessary to assign a rating value to each predicted swell category (i.e. low, medium, high and very high swell).

These categories are assigned a value of one (1) unit each. If for example the reference method predicts a medium swell, and the system being assessed predicts a very high swell, then the latter degree of swell is considered to be (+2) two units greater.

With this in mind, the general procedure for assessing the prediction method is therefore as follows :

(a) The reference degree of swell is determined for each specimen in the first data set.

(b) The degree of swell is then predicted for all specimens of the first data set using each prediction method in turn.

(c) The deviation between the 'predicted' and 'reference' degrees of swell is determined for each prediction method (as indicated above).

(d) The average deviation for each prediction method is determined.

(e) The above procedure is subsequently repeated for each data source.

The assessments of qualitative methods are presented in tabular (Tables 3.13 and 3.16) and graphical (figures 3.9 to 3.12) form.

3.2.4.3 Results : comments

Ladd and Lambe's Data

The swell prediction systems by Holtz, Raman, R&S and BRE exhibit the smallest errors (Table 3.13), with a maximum deviation between predicted and reference values, of 0.2 units. This is clearly indicated on the graphical display (fig. 3.9).

The largest deviations resulted from VDM's and V&G's systems - at times exceeding 1.5 units.

Holtz' (Undisturbed Soil) Data

All the examined systems yield accurate predictions, with a maximum deviation of -0.5 units being recorded.

R&S' system is the most accurate, with an average deviation of 0.024 units. These results are very good considering the varying origins of source data (Ref. Fig. 3.11 and Table 3.15).

The absence of an upper 'extra high' (EH) category in many systems results in such soils being under categorized with respect to swell potential.

Holtz (Remoulded Soil) Data

As with the undisturbed data, R&S' system yields the most accurate predictions, followed by Holtz then VDM. Virtually all predictions exhibit

a maximum deviation of 0.6 units, with the exception of V&G (γd and LL) at -1.3 units deviation (Refer Table 3.14). Both the USCS and extended Casagrande's system underpredict swell for high plasticity soils - (as indicated in the graphical presentation Fig. 3.10).

Snethen's (Undisturbed Soil) Data

Holtz and R&S' systems jointly exhibit the best predictions, with deviation not exceeding 0.15 units. The remaining systems predict swell behaviour with deviations not exceeding -0.65 units (Table 3.16); the only exception to this being VDM's system, with an average deviation of -1.65 units.

The underprediction of swell for very high plasticity soils is again noted, and attributed to a lack of an 'extra high' swell category in several of the prediction methods.

3.2.4.4 Results : conclusions

1. The following overall order of significance was determined for the top swell prediction methods: (i) Holtz (1957), (ii) Ranganatham and Satyanarayana (1965), (iii) Building Research Establishment (1980) and (iv) Raman (1967). These predict swell upon the basis of the following parameters.

   Holtz : colloid content, plastic index; shrinkage index

   R&S : shrinkage index

   BRE : plasticity index; clay fraction

   Raman : plasticity index, shrinkage index

2. On the basis of the data therefore, those prediction methods using plasticity index, shrinkage index and clay content exhibit the closest relationship with the reference system.

The significance of individual soil parameters is discussed in the next section.

2. The magnitude of deviation is clearly different for each data set, and this is attributed to the regional character of the specimens.
3. Soil classification systems such as the extended Casagrande's and USCS systems underpredict swell potential for the very high swelling soils. This is attributed to the absence of an 'extra high' swell category, which causes such soils to be designated 'very high swell' only.
4. It is suggested that the Building Research Establishment method is the most desirable of the four indicated in conclusion No. 1 since it does not base swell prediction upon shrinkage index.
   Although the other three methods, do use the shrinkage index value, it is generally accepted that the low variation of shrinkage index between widely varying soil types, makes it unsuitable for use as a swell indicator.

Quantitative systems

3.2.4.5 Criteria for Assessment of Prediction

These systems quantify swell, and express it as a percentage of the original specimen height.

The swell has been defined in Section 3.2.3.4, and the data by Holtz (undisturbed and remoulded) and Ladd and Lambe is compatible with this.

The prediction methods are assessed by comparing the resulting predicted swell values with the experimentally measured volume changes

from the data, such that

$$\text{percentage difference} = \frac{(\text{actual swell} \sim \text{predicted swell})}{\text{actual swell}} \times 100$$

The differences are calculated for all samples, and then averaged for each prediction method; this average difference is subsequently used as a basis for assessment.

3.2.4.6 Results : comments

Holtz (Remoulded Soil) Data

The majority of methods grossly overpredict swell using this data source. The system after V&G (γd and LL) and Seed yield the lowest differences between measured and predicted values of -33% and +43% respectively. The other systems grossly overpredict swell - differences ranging from 137% to 844% (Ref. Table 3.17). The graphical presentation of predictions (Fig. 3.13) clearly indicates the random nature of results.

Holtz (Undisturbed Soil) Data

The swell predictions do not correspond to the measured values for all prediction methods when using this data.

The best predictions are obtained using both of V&G's systems, nevertheless, they still deviate from the corresponding measured values by 100 percent. The differences are even greater for the other prediction methods.

Ladd and Lambe (Remoulded Data)

The swell prediction methods after CAA, Holtz and R&S yield the most accurate predictions, with average differences of +3, +7 and +17% respectively.

The remaining methods underpredict swell between -53% and -87% (average differences). The underpredictions are attributed to the low moisture content and hence high swelling of Ladd and Lambe's specimens.

The swell is underpredicted because, the empirical relationships used in the various methods are derived from soils at a higher moisture content and hence lower swell potential.

The graphical presentation of this data (Fig. 3.15) indicates an approximately linear relationship between measured and predicted values which are specific to each data source.

3.2.4.7 Results : conclusion

None of the examined quantitative swell prediction methods are sufficiently reliable for general application to all soils. The empirical relationships used in each method are evidently derived from regional data, and must therefore be applied on that basis only if meaningful predictions are to be made.

3.3 STATISTICAL ANALYSIS OF SWELL RELATED DATA

3.3.1 Basis for Statistical Analysis

Section 3.2 has highlighted (a) the variety of soil parameters employed in the prediction of swell behaviour and (b) the non-applicability of swell indication systems to all data sets (and therefore all geographical locations). It is therefore the aim of this section to further investigate these aspects by determining

(a) the order of significance of the more commonly used swell indicator parameters and also, highlight any other swell indicative parameters not currently employed in the reviewed systems.

(b) the relationships between swell behaviour and soil parameters.

(c) the differences between relationships based on data from several sources.

A stepwise regression analysis is chosen as the basis for examining the above points since this procedure yields the order of variable significance and also the linear relationships between the chosen variables.

The author recognises that the swell relationships might well be non linear, however, those obtained by stepwise linear regression are considered suitable for making an initial comparison. If the relationships from different sets of data and therefore different areas are similar, thereby conflicting earlier observations, then the data will be re-examined for higher order relationships.

3.3.2 Details of Statistical Analysis

3.3.2.1 Statistical Computer Package (STATPACK)

Statpack is an integrated interactive package for the statistical analysis of data-controlled from a terminal. It permits the user to issue simple commands for data analysis and will prompt him for necessary information. Data input may be from terminal, disk, magnetic tape or data bank. Input consists of observations each containing a value for every variable - these being defined by a number or alphabetic names of not more than five characters.

Options exist for evaluating data with missing values. It is also possible to restrict the data to only those observations where a certain set of circumstances occur.

3.3.2.2 Step-Regression

Statpack has twenty four commands covering most aspects of statistical analysis. However, for the purpose of this study the command 'Step Regression' is employed.

'Stepwise regression' as with other commands is actually a subroutine within the overall package and initially requires the identification of independent and dependent variables. The program then determines the most significant independent variable and conducts a regression analysis using it alone.

The second-most significant independent variable is then determined and another regression calculated employing this variable in addition to the first.

This procedure is repeated until all independent variables have been so analysed.

The stepwise regression therefore, not only determines the order of independent variable significance, but also yields the full relationships between the chosen variables.

3.3.2.3 Definition of Coefficients Resulting from Step-Regression

Coefficient of Determination (COD)

is a measure of the mutual relationship between variables (dependent and independent).

In this instance there is one dependent and four or more independent variables.

The coefficient varies between 0 and 1 ; 0 indicating no correlation, 1 indicating total correlation, i.e. the higher the value the more reliable the relationship.

Dependent variable

is that to which the whole expression relates. It is dependent upon all the other variables.

Independent variables

the derived statistical relationships are composed of one or more independent variables which are related (by the use of coefficients) to the Dependent variable.

3.3.3 Data

The variation in data quality is discussed in Section 3.2.3.1 and outlined in Table 3.10; bearing this in mind therefore, the following data sources are considered suitable for assessing the order of parameter significance : Holtz (1959), Ladd and Lambe (1961), Seed et al (1962), Nayak and Christensen (1971), Vijayvergiya and Ghazzaly (1973), Dakshanamurthy and Raman (1973), Snethen (1979).

3.3.4 Objectives

The objective is to alternately consider percentage swell and swell pressure values as the dependent variable of a regression analysis on the published swell related data. The other parameters are taken as independent variables, and examined in two groups :

(a) Liquid limit, plasticity index, initial moisture content and dry unit weight only (4 variables) i.e. as employed in swell simplified ID methods.

(b) Consideration of all available parameters (multiple variables) including those in (a).

A complete listing of the variables used and associated abbreviations is given in Table 3.21.

3.3.5 Key points of the regression analysis

1. The following orders of variable significance are noted for the examined data when employing four independent variables only :

(a) Percent swell: Liquid limit, Plastic index, Initial moisture content, Dry density.

(b) Swell pressure: Liquid limit, Initial moisture content, Plastic index, Dry density.

2. A general order of significance cannot be ascertained when considering multiple independent variables since each data source consists of a different combination of variables. However, the liquid limit, plastic index, clay content and suction parameter appear to consistently relate to swell behaviour, their relative order of significance depending upon which data source is employed.

3. The regression analysis has encompassed as many variables as are available from the published data. The 'regular' variables used by several other authors for swell prediction are confirmed as being significant, especially liquid limit, plastic index and clay content.

   The regression analysis of Snethen (1979) comprehensive data indicates that suction, is strongly related to the percent swell and swell pressure exhibited by a soil. The relationship between swell pressure and suction has a COD of 0.83 a value far in excess of that exhibited by any other single parameter.

   The implementation of suction as a method of swell identification requires ideally that the swell suction relationship be demonstrated as being unique for all soils.

To achieve this, it would be necessary to show that a specific soil suction would relate to a constant swell irrespective of the soil type. To the author's knowledge this has not previously been demonstrated.

4. The shrinkage index, shrinkage ratio and linear shrinkage are noted as consistently not correlating with swell behaviour.

5. The coefficient of determination of the swell and swell pressure relationships are consistently higher :

(a) by considering a greater number of independent variables

(b) when derived on the basis of remoulded instead of undisturbed specimens (this is considered due to the greater initial consistency of specimens).

6. The relationships for percent swell yield slightly higher COD's than those for swell pressure. This could be attributed to inconsistencies within the experimental data (the one dimensional testing equipment deforms during swell pressure testing thus yielding inconsistently low swell pressure values). The published data with the exception of Snethen (1979) apparently makes no allowance for this potential error source).

7. Relationships obtained by linear regression vary considerably depending upon the data source. Ref. Table 3.23 for relationships using four independent variables only. It appears that for them to work, such relationships should be employed under conditions (soil type, environment etc.) similar to those from which the original samples were taken.

8. It is noted that employing the logarithm of the dependent variables has little or no effect upon the order of independent variable significance and associated COD's.

3.4 NATIONAL SOIL CLASSIFICATION SYSTEMS FOR PREDICTING SWELL

3.4.1 Introduction

The underlying reason for soil classification systems is the need to improve communications between engineers and contractors regarding site conditions.

Various systems are observed in the literature which classify soils in order to assign them descriptive names or symbols. Such systems are designed to group soils according to the physical characteristics of their particles or according to the performance they exhibit when subjected to certain tests or conditions of service.

These systems include :

(a) visual inspection/simple identification tests

(b) textural classification (based on grain size distribution)

(c) classification based on consistency limits

These are discussed below with respect to swell prediction.

3.4.1.1 Visual inspection/simple identification tests

These include such tests as :

(i) visual examination of coarse grained fraction

(ii) dilatancy/shaking tests

(iii) dry strength

(iv) plasticity

(v) colour and odour

(vi) treatment with acid and finally

(vii) the shine test

The above tests permit an estimation of the role of the constituent fraction in a composite natural soil and facilitate a broad classification.

Such a system is proposed by the United States Bureau of Reclamation and provides comprehensive and detailed information in every respect. However, it does not make any allowance for swell behaviour.

A possible addition to these types of systems would be free-swell test (Holtz and Gibbs, 1956) which could provide an easily implemented indicator of swell potential. This test involves initially measuring the volume of a dried and crushed soil in a burette, its inundation with water and finally the measurement of its subsequent swell. However, the author notes the test's unreliability for use with extremely high plasticity soil (liquid limit > 150%), when difficulty is encountered in thoroughly wetting the specimen - thus yielding a less than maximum swell value.

3.4.1.2 Textural Classification (based on grain size distribution)

This approach classifies mixed grained soils as either gravel, sand, fine sand or silt - depending upon the predominant grain size. Kezdi (1974), indicates that this will only work provided the grain size distribution curve approximates to the normal probability curve. Several classification standards have incorporated this approach. For instance, United States Bureau of Reclamation (1974) (ref. Fig. 3.16) proposes a triangular classification chart, it being based on the division of soils into three principal fractions - sand-silt and clay. The sum percentage of these components is 100%.

These systems classify the soils on the basis of grain size distribution only. Since the swelling behaviour is recognised as depending

not only upon the clay quantity, but also upon the clay type (Seed et al, 1962), then these systems are considered of limited value for swell prediction purposes.

3.4.1.3 Soil classification based on consistency limits

Casagrande (1936) demonstrates the potentially wide variation in physical properties for soils of identical grain size distribution. He proposes that the classification of cohesive soils be based upon consistency limits (liquid limit, plastic index and plastic limit) since these are much more significant with respect to the behaviour of clay soils.

Casagrande (1932) presents the plasticity chart (Fig. 3.17) plotting the plastic index against the liquid limit. Each soil is thus represented as a point on the chart which is divided into six regions, each representing certain soil groups.

Three regions lie above and three below the empirically evolved 'A line' - this being defined by the equation :

$$\text{Plastic index} = 0.73\ (\text{liquid limit} - 20)$$

Silts and organic clays generally fall below the 'A' line. Kezdi (1974) and others indicate that soil specimens taken from the same stratum usually - when plotted - form a straight line approximately parallel to the 'A' line. The position of such a line permits important conclusions concerning the behaviour of soil (refer Table 3.25).

The author has attempted to predict swell on the basis of these lines. A large source of swell data is grouped according to the exhibited swell.

Each range of points are then subjected to a linear regression analysis, thus yielding a series of near parallel lines. These lines vary in gradient between the A and U lines (Fig. 3.18) but become closer spaced as the percent swell increases. The system is not considered of sufficient accuracy since the close proximity of the higher value swell lines will result in a wide variation of swell prediction for soils of only slightly differing plasticity characterisation.

Casagrande's plasticity chart is incorporated into the British and American soil classification systems. These are very similar in many respects and represent an attempt to unify the activity of soil mechanics institutions and establish a uniform presentation for technical writings.

A few of the systems presented in the literature have made some attempt at the prediction of volumetric soil behaviour (usually compressibility). However, these are extremely limited in their application to swelling soils (as will be shown later).

3.4.1.4 Classification systems to be assessed

It therefore appears that the textural soil classification systems are not particularly suited for making swell predictions.

This is not to say that the clay content as described in the textural classification systems has no relevance to swell behaviour, indeed, Sections 3.2 and 3.3 indicate the significance of clay content with respect to swell prediction, but when considered in combination with liquid limit and/or plastic index. Therefore, efforts will now be directed towards an assessment of systems utilising a combination of consistency limits and grain size distribution for the purpose of predicting swell.

The two main systems of this type to be evaluated are the PRA/AASHTO system devised for airfield and road construction, and the British and American soil classification systems employed in the construction industry. The following section will

(a) assess the systems for application to swelling soils and

(b) suggest amendments for the systems to enable swell prediction.

3.4.2 The Public Roads Administration System (Allen 1945) (AASHTO)

3.4.2.1 Description

The PRA system is an identification system intended to indicate the behaviour of materials used as a highway subgrade. It has received widespread use, and forms the basis of several other classification systems including: the revised PRA system; Civil Aeronautics Administration system and, most recently, the American Association of State Highway and Transportation Officials (AASHTO) and the Federal Highways system. At present it is most widely known as the AASHTO system and it is this version that will be examined.

AASHTO has seven basic soil groups designated A1-A7 (ref. Table 3.26) the soil being categorised according to performance characteristics: A1 being the best and A7 the worst. The A8 group is reserved for peat and highly organic soils.

Material quality within the basic soil groups is further indicated by an additional number or letter designation according to the results of sieve analysis and the Atterberg limits tests.

The first soil group encountered that matches the test data being the correct classification. The plasticity chart shown in Fig. 3.19 aids

classification and may be used in place of Table 3.26. The influence of the amount of fine material and plasticity is accounted for by including a parenthesised number (group index) to supplement the basic group symbol.

As with the group symbols, an increasing figure indicates decreasing quality of material. The group index is determined from a fixed relationship or, from a more recently proposed nomogram (Fig. 3.20) by adding two partial indices (based on the liquid limit and plastic index).

3.4.2.2 Developments of the PRA System that Predict Swell

(a) Civil Aeronautics Administration Classification System (1946)

The earlier CAA system incorporates a provision for swell prediction (Table 3.27) the reliability of which is examined in the first section of this chapter (Tables 3.17-3.19). In general the results indicate that the system will not consistently quantify swell and although predictions using Ladd and Lambe (1961) data indicate a low average error the overall spread of data is considerable (errors between 50 and -57%). The system is therefore considered inadequate for swell prediction.

(b) Public Roads Administration (PRA) System (1945) and AASHTO

The revised PRA system allocates a general rating to the soil for subgrade use. Although the rating can be indicative of engineering behaviour, it makes no specific allowance for swell susceptibility.

The AASHTO system classifies clay soils (in terms of their liquid limit, plastic index and percentage of clay sized particles present) as a group index. Although the system notes that an increase in group index will represent a lower grade engineering material, no relationship is indicated between the group index and swelling potential. To the author's knowledge, this aspect has also not been discussed in the literature.

This aspect requires investigation since a relationship between the group index and swelling potential would permit the use of AASHTO for swell prediction with minimum alteration.

3.4.2.3 Data

Upon the basis of discussions in Section 3.2.3, the following data sources are chosen as suitable for use with the AASHTO system : Ladd and Lambe (1961); Seed et al (1962); Ranganatham and Satyanarayana (1973), Nayak and Christensen (1973); Holtz (1957) - remoulded and undisturbed soils.

3.4.2.4 Plotting the Data (ref. figs 3.21 and 3.22 "indicies")

The results are plotted : AASHTO group index versus percent swell (fig. 3.21) and swell pressure (fig.3.22) in an effort to rapidly observe interrelationships.

A best fit line is then fitted through each set of points (indicated on the same figures) and the associated equations listed in Table 3.28.

3.4.2.5 Group Index vs. percent swell

The group index relates very well to percentage swell, although the exact relationship varies between data sources (fig. 3.21).

A linear regression through each set of data indicates a consistent increase in AASHTO group index with percent swell (the only exception being Holtz' remoulded soil data).

The results also indicate that the remoulded specimens exhibit a greater swell than the field specimens; this is attributed to an aligning of the clay platelets during the recompaction process, which in turn increases the swell of the soil (Chapter 2).

3.4.2.6 Group Index vs. swell pressure

The group index is also plotted against swell pressure (fig. 3.22) although the relationship is less convincing than that with the percentage swell.

The slopes of the regression lines through the data sets differ, and do not indicate a clear trend with regard to either remoulded or in situ soil data.

3.4.2.7 Relating swell behaviour to the Group Index

(a) Quantitative

The percentage swell - AASHTO group index relationship varies according to the data source, and also to the soil specimen type (i.e. whether remoulded or undisturbed).

Previous observations indicate that the remoulded specimens will generally swell more than the undisturbed ones, in consequence, it is suggested that the mean remoulded relationship be used to predict swell (fig. 3.21), which will at least given an 'upper bound' swell prediction.

The following relationship is proposed :

percent swell = 1.901. (Group Index)

(refer also Tables 3.30(a) and 3.30(b)).

The proposed relationship is applied to the data sources used in Section 3.2.3; it is then assessed by comparing the resulting swell predictions with the published experimentally measured values.

The results indicate that the swell is grossly over predicted in general (up to 880%!), and less successful than the other methods; in consequence, its use is not currently recommended.

(b) Qualitative predictions

To the author's knowledge, the group index has not previously been employed to predict swell behaviour. In consequence it was necessary to assign swell categories to the group index with due regard to the earlier work relating swell to clay content and plasticity index.

The resulting prediction method (Table 3.32) is assessed by employing the procedure as detailed in Section 3.2.4.3. The predictions are unfavourable (Tables 3.30(a) and 3.30(b)) with results ranging from an under prediction of -1.33 units to an over prediction of +0.6 unit (according to the data source).

Subsequent adjustment of the group index swell ranges (Table 3.33) improve the predictions dramatically (Tables 3.31(a) and 3.31(b)).

The results vary between an under prediction of 0.72 to an over prediction of 0.65 categories. Although not a vast improvement on first inspection, these are the maximum differences, with most results being improved (i.e. more accurate predictions).

Further adjustments to the group index ranges have met with no success.

3.4.2.8 Summarising remarks

The AASHTO system classifies soils with reference to their suitability as highway subgrade material. This suitability is expressed quantitatively as a 'group index', and relates to the liquid limit, plasticity index and percent of clay-sized particles. No indication is given of any group index-swell interrelationship.

The author derives such relationships from published data, and the results (Tables 3.31 and 3.33) indicate that they may be used to qualitatively predict swell with some confidence.

The proposed relationships are more successful than most of the other published systems; predictions differ from the reference values (obtained using the reference method) by less than 0.2 swell categories (swell being described qualitatively as either low, medium, high or very high categories).

The author's findings are summarised in Table 3.33, where swell is qualitatively related to the group index; the findings are implemented by including a parenthesised abbreviation of the swell category to the right hand side of the AASHTO soil group categorisation thus : for a soil of the following properties: 85% passing No. 200 sieve, Liquid limit = 85% and plasticity index = 30% then the final designation would be

A - 7 - 5	(45)	(VH)
AASHTO GROUP	GROUP INDEX	SWELL CLASSIFICATION

3.4.3 British Soil Classification System (BSCS)

The BSCS is the primary soil classification system used in the UK and many other parts of the world; in consequence, its lack of provision for identifying and clasifying swelling soils will be investigated further.

3.4.3.1 Casagrande's Soil Classification System

The BSCS is originally derived from this system, which groups soils according to their behaviour for a variety of potential construction related uses.

Following Casagrande's original work (Casagrande, 1948) the system was subsequently modified by the U.S. Army Engineers to become the Unified Soil Classification System (USCS). Although originally intended for the classification of soils in road and airfield construction, it has since been modified for application to foundations and embankments.

An extended version of Casagrande's system was proposed by the Road Research Laboratory in 1954 and a similar system is now recommended for use in the British Code of Practice for Site Investigations : BS5930 : 1981 and termed the British Soil Classification System for engineering purposes (BSCS).

3.4.3.2 BSCS : implementation

The BSCS is employed in association with a detailed description of the soil. The description should include the soil group name, grading information, plasticity, colour, particle characteristics, soil fabric, type of bedding, nature of discontinuities and strength, and any in situ conditions not previously detailed.

3.4.3.3 BSCS : Basis for Classification

The classification is undertaken on the basis of grain size and plasticity information.

Grain size

The particle size is a fundamental property of a soil and significantly influences its behaviour. Groups are established and given the following

ranges and symbols :

(a)	Boulders	|B|	> 200mm
(b)	Cobbles	|C|	60-200mm
(c)	Gravel	|G|	2-60mm (20-60 coarse, 6-20 medium, 2-6 fine)
(d)	Sand	|S|	0.06-2.0mm (0.6-2 coarse; 0.2-0.6 medium; 0.06-0.2 fine)

Plasticity

The major groups indicated above are divided into subgroups on the basis of grading and plasticity of fine material. Granular soils are described as well graded (W) and poorly graded (P). The latter group is subdivided into uniform graded (P_u) and gap graded (P_g).

Silts and clays are subdivided according to their liquid limits into: low (LL < 30%); medium (LL = 30-50%); high (50-70%); very high (LL = 70-90%); extremely high (LL > 90), they being designated L, M, H, V and E respectively.

Each subgroup is given a combined symbol in which the latter describing the predominant size fraction is written first (e.g. GW = well graded gravels; CH = clay with high plasticity). The plasticity chart was introduced by Casagrande (1948), (Fig. 3.17) and modified slightly for incorporation into the BSCS (Fig. 3.23). Silt tends to plot below the A line and clays above. Any group containing significant quantities of organic material is referred to as organic, and the letter 'O' is the suffix to the group symbol.

3.4.3.4 Mixed soils

The system records boulder and cobble proportions separately. The coarse deposits may be described as follows :

Boulders

> 50% of the coarse material is of boulder size (> 200mm). It may be described cobbly-boulders - if boulders are an important secondary constituent. Mixtures of very coarse material and soil can be described by combining the terms for the coarse and soil constituents.

The classification can be made either by rapid assessment or full laboratory procedure. The group symbol should be bracketted (signifying lower accuracy) if a rapid assessment is employed.

3.4.3.5 Provision within the Casagrande-based Systems for Expansive Clays

(a) BSCS

The BSCS apparently makes no provision for swelling soils in its present form. However, soils are described in terms of their grain sized distribution and plasticity, thus presenting an opportunity to incorporate one of the previously discussed swell prediction methods.

(b) USCS/USBR

The original Unified soil classification system, as developed by the U.S. Army Engineers in 1953, categorises the probable expansion/compressibility characteristics in terms of the soil group symbols (ref. Table 3.34). This system is assessed along with other swell prediction methods in Section 3.2.

The results are presented in figures 3.9-3.12 and it can be seen that the swell is accurately predicted for medium high swelling soils, but under predicted for the 'very high' and 'extremely high' swelling categories.

The average differences between predicted and measured values are given in Table 3.20(b) and indicate that this system, although not yielding

consistent predictions in relation to other systems, in fact exhibits a maximum underprediction of 0.55 units only.

This system is not as consistent as some of those assessed in Section 3.2.

(c) Extended Casagrande's System - Road Research Laboratory (1954)

These proposals are an extended version of the USCS, but enhance the detail with which a soil is described by increasing the number of soil groups used. As with the USCS, the system predicts the probable degree of swell on the basis of the soil group (ref. Table 3.35). The system is also assessed in Section 3.2, the results being presented in Tables 3.13-3.16.

The result summary (Table 3.20(b)) indicates that this system generally yields more accurate predictions than the USCS, however, a maximum underprediction of 0.55 units is noted in one instance.

3.4.3.6 Choice of swell prediction system

1. None of the examined quantitative swell prediction systems are of sufficient reliability for engineering application. The majority of predictions made, exhibit an error in excess of 100% (ref. Table 3.20(a)). Thus the adoption of any quantitative relationship is not presently recommended.

2. The qualitative swell predictions are compared with those made on the basis of D&R proposals. The following systems are then noted as yielding the best predictions (in descending order of significance).

   Holtz (1957), Ranganathan and Satyanarayana (1965), Building Research Establishment (1980) and Raman (1967) (ref. Section 3.2) the maximum errors being calculated as -0.455 units. These are considered as being quite acceptable.

3. The above systems predict swell on the basis of the following parameters :

   Holtz : colloid content; plastic index; shrinkage index

   R&S : shrinkage index

   BRE : plasticity index; clay function

   Raman : plastic index; shrinkage index

   However, the author contends that use of the shrinkage index as a swell indicator is inadvisable because :

   (i) it is not routinely determined for the BSCS

   (ii) it exhibits only a small variation

   (iii) it does not correlate well (statistically) with swell behaviour (ref. Section 3.3).

   The use of shrinkage index as an indicator of swell is therefore not recommended, and it is suggested that the clay content and plasticity index be considered for this purpose.

4. In accordance with the above guidelines, the expedient method of swell prediction after BRE (1980) is presently recommended.

3.4.3.7 System for predicting swell

On the basis of the above points, the author proposes incorporating the shrink prediction method after BRE, 1980 (Table 3.4) into the BSCS as a means of predicting swell.

This is achieved by extending Casagrande's plasticity chart to account for clay content.

The horizontal axis then becomes dual purpose and represents both liquid limit and clay content (%). Swell is best predicted upon the basis of clay content and plasticity index values, however

an indication of the volume change behaviour can be obtained by knowing Atterberg limits only.

The swell potential is predicted qualitatively and expressed as a swell category - Low (L), medium (m), high (h) or very high (VH).

3.4.3.8 Incorporating swell prediction into the BSCS group symbol

It is proposed that the existing soil group and subgroup symbols be utilised as originally outlined in the BSCS. Supplementary 'swell' designations are added at the right hand side of the group and circled to increase visibility.

3.4.3.9 Example of use

Consider a sandy clay: plasticity index = 65%; clay content = 80%; liquid limit = 90% for the BSCS.

Then the classification will be

C V S (VH) ← VERY HIGH SWELL

MAINLY CLAY	VERY HIGH PLASTICITY	SECONDARY CONSTITUENT SAND

If the percent swell can be estimated using an oedometer swell type test, then the swell designation could be amended by incorporating this value into it like thus : CVS(VH:25).

3.4.3.10 Incorporating quantitative swell prediction into the BSCS.

This is not presently possible for general application because of the poor correlations between swell and the employed parameters.

However, where a large data source is available from the required locality, then swell relationships may be correlated and applied on a local basis only.

The predicted swell value may be incorporated into the BSCS soil description group as indicated above.

TABLE 3.1

SWELL CLASSIFICATION(HOLTZ,1959)

COLLOID CONTENT (%-1Mm)	PLASTIC INDEX (%)	SHRINKAGE LIMIT (%)	EXPANSION (%)	CATEGORY
≤15	≤18	≥15	≤10	LOW
13-23	15-28	10-16	10-20	MEDIUM
20-31	25-41	7-12	20-30	HIGH
≥28	≥35	≤11	≥30	V.HIGH

TABLE 3.2

SWELL CLASSIFICATION(SEED ETAL,1962)

POTENTIAL SWELL (%)	DEGREE OF EXPANSION
0-1.5	LOW
1.5-5	MEDIUM
5-25	HIGH
≥25	V.HIGH

TABLE 3.3

SWELL CLASSIFICATION(RANGANATHAM & SATYANARAYANA,1965)

SHRINKAGE INDEX (%)	POTENTIAL SWELL CATEGORY
≤20	LOW
20-30	MEDIUM
30-60	HIGH
≥60	V.HIGH

TABLE 3.4

SWELL CLASSIFICATION(B.R.E. ,1980)

PLASTIC INDEX (%)	CLAY FRACTION (%)	SHRINKAGE POTENTIAL
≥35	≥95	V.HIGH
22-48	60-95	HIGH
12-32	30-60	MEDIUM
≤18	≤30	LOW

TABLE 3.5

SWELL CLASSIFICATION(ALTMEYER,1955)

LINEAR SHRINKAGE (%)	SHRINKAGE LIMIT (%)	PROBABLE SWELL (%)	SWELL CATEGORY
≤5	≥12	≤0.5	NON CRITICAL
5-8	10-12	0.5-15	MARGINAL
≥8	≤10	≥1.5	CRITICAL

TABLE 3.6

SWELL CLASSIFICATION(RAMAN,1967)

PLASTIC INDEX (%)	SHRINKAGE INDEX (%)	DEGREE OF EXPANSION
≤12	≤15	LOW
12-23	15-30	MEDIUM
23-32	30-40	HIGH
≥32	40	V.HIGH

TABLE 3.7

SWELL CLASSIFICATION(ANDERSON & THOMSEN,1969)

PLASTIC INDEX (%)	POTENTIAL SWELL (%)	DEGREE OF EXPANSION
≤20	≤1.5	LOW
20-31	1.5-4	MEDIUM
31-39	4 -6	HIGH
≥39	≥6.0	VERY HIGH

TABLE 3.8

SWELL CLASSIFICATION(VIJAYVERGIYA & GHAZZALY,1973)

NATURAL MOISTURE CONTENT / LIQUID LIMIT	PROBABLE SWELL PRESSURE .(TSF)	PROBABLE SWELL (%)
≥0.5	≤0.3	≤1
0.37-0.35	0.3-1.25	1.0-4.0
0.25-0.37	1.25-3.0	4.0-10.0
≤0.25	≥3.0	≥10

TABLE 3.9

SWELL CLASSIFICATION(DAKSHANAMURTHY & RAMAN,1973)

LIQUID LIMIT (%)	POTENTIAL SWELL CATEGORY
0-20	NON SWELLING
20-35	LOW SWELLING
35-50	MEDIUM SWELLING
50-70	HIGH SWELLING
70-90	V.HIGH SWELLING
≥90	X.HIGH SWELLING

TABLE 3.10

SUMMARY OF PUBLISHED SWELL DATA SOURCES

AUTHORS	TEST DETAILS		depth (ft)	dry unit weight (pcf)	dry density (pcf)	initial moisture (%)	liquid limit (%)	plastic limit (%)	plastic index (%)	specific gravity	clay content(<200Mm) %	colloid content(<2Mm) %	shrinkage limit (%)	shrinkage ratio (%)	linear shrinkage (%)	free swell (%)	initial void ratio	initial saturation (%)	percent swell (%)	swell pressure (tsf)	percent volume change(%)	total suction (tsf)	A parameter	B parameter	∝parameter	optimum moisture (%)	activity	field moisture(%)	No of specimens undisturbed	No of specimens remolded
	SWELL TESTS	SWELL PRESSURE TESTS																											
SALAS & SERRATOSA (1957)	swell under 1psi surcharge, field moisture-saturation.	constant volume type test					●	●	●										●										6
HOLTZ (1957)	swell under 1psi surcharge, field moisture-saturation.	-			●	●	●	●	●	●		●	●			●		●	●	●	●							47	40
LADD & LAMBE (1961)	swell under 1psi surcharge, field moisture-saturation.	constant volume type test					●	●	●		●		●	●		●			●	●						●	●		10
SEED ETAL (1962)	swell under 1psi surcharge, maximum dry density, optimum moisture content	-					●	●	●		●		●						●							●			23
RING (1965)	four cycles of alternate -wetting & drying.	-			●		●	●	●	●	●		●	●	●										●				12
RANGANATHAM & SATYANARAYANA (1965)	swell under 1psi surcharge max. dry density & optimum moisture content.	-			●		●	●	●		●		●			●			●						●				4
RAMAN (1967)	-	-					●	●	●				●															20	
ANDERSON & THOMSEN (1969)	swell under 1psi surcharge	-					●	●	●										●										6
GIL (1969)	load to overburden, then allow to swell under 1psi-natural moisture to saturation.	-		●		●	●	●	●	●			●						●							●	●	11	
KOMORNIK & LIVNEH (1969)	swell under 1psi surcharge, max. dry density & optimum moisture content	-				●	●	●	●		●								●							●			5
KATTI,KULKARNI & FOTEDAR (1969)	free three dimensional swell,measured by displacing water.	-					●	●	●	●	●		●	●						●									6
NAYAK & CHRISTENSEN (1971)	swell under 1psi surcharge-max. dry density, optimum moisure content.	-				●	●	●	●		●		●						●	●						●			18
DAKSHANAMURTHY & RAMAN (1973)	-	-		●		●	●	●	●		●		●														●	84	
VIJAYVERGIYA & GHAZZALY (1973)	swell under 1psi surcharge, natural moisture content to saturation.	constant volume test type		●	●	●	●	●	●										●	●								265	
SNETHEN (1979)	swell under overburden	constant volume test type		●		●	●	●	●	●	●	●	●	●	●		●		●	●		●	●	●	●			20	
SHERIF (1982)	swell freely-zero load	-					●	●	●	●																			8

TABLE 3.11
SWELL CATAGORIES AND ASSOCIATED SWELL RANGES

HOLTZ(1959)		SEED ETAL(1962)		ALTMEYER(1961)		ANDERSON & THOMSEN(1969)		VIJAYVERGIYA & GHAZZALY(1973)		AUTHOR	
POTENTIAL EXPANSION (%)	SWELL CATEGORY	POTENTIAL EXPANSION (%)	SWELL CATEGORY	POTENTIAL EXPANSION (%)	SWELL CATEGORY	POTENTIAL EXPANSION (%)	SWELL CATEGORY	POTENTIAL EXPANSION (%)	SWELL CATEGORY	POTENTIAL EXPANSION (%)	SWELL CATEGORY
<10	LOW	0-1.5	LOW	<0.5	NON CRITICAL	<1.5	LOW	<1.0	LOW	0-1	LOW
10-20	MEDIUM	1.5-5	MEDIUM	0.5-1.5	MARGINAL	1.5-4	MEDIUM	1-4	MEDIUM	1-10	MEDIUM
20-30	HIGH	5-25	HIGH	>1.5	CRITICAL	4-6	HIGH	4-10	HIGH	10-25	HIGH
>30	V.HIGH	>25	V.HIGH			>6	V.HIGH	>10	V.HIGH	>25	V.HIGH

TABLE 3.12
LIST OF SYSTEM ABBREVIATIONS

	AUTHOR(S)	ABBREVIATION
1.	HOLTZ(1957) - REMOLDED DATA	HR
	UNDISTURBED DATA	HU
2.	SEED ETAL (1962)	SEED
3.	RANGANATHAM & SATYANARAYANA(1965)	R&S
4.	RAMAN (1967)	R
5.	DAKSHANAMURTHY & RAMAN (1973)	D&R
6.	VAN DER MERWE (1975)	VDM
7.	NAYAK & CHRISTENSEN (1971)	N&C
8.	BUILDING RESEARCH ESTABLISHMENT(1980)	BRE
9.	WILLIAMS (AUTHOR)	SW
10.	VIJAYVERGIYA & GHAZZALY (1973) (dry density,liquid limit)	V&G(Jd & LL)
11.	VIJAYVERGIYA & GHAZZALY (1973) (moisture content,liquid limit)	V&G (MC&LL)
12.	EXTENDED CASAGRANDES SYSTEM(1954)	EXTCAS
13.	UNIFIED SOIL CLASSIFICATION SYSTEM(1953)- USCS	USCS
14.	CIVIL AERONAUTICS ADMINISTRATION (1946) - CAA	CAA
15.	SNETHEN(1979) - REMOLDED DATA	SNR
	UNDISTURBED DATA	SNU

TABLE 3.13

EVALUATION OF QUALITATIVE SWELL PREDICTIONS USING DATA BY LADD & LAMBE (1961)

SPECIMEN NUMBER	SWELL PREDICTION SYSTEMS																					
	D&R (base)	USCS		SEED		R&S		V&G(MC & LL)		VDM		BRE		R		EXTCAS		HOLTZ		SW	
	Cat.	Cat.	Dev.	Cat.	Dev.	Cat.	Dev.	Cat.	Dev.	Cat.	Dev.	Cat.	Dev.	Cat.	Dev.	Cat.	Dev.	Cat.	Dev.	Cat.	Dev.
1	VH	H	-1	H	-2	VH	-1	L	-3	VH	0	VH	0	VH	-1	H	-1	VH	-1	VH	0
2	VH	H	-1	VH	0	H	-1	L	-3	H	-1	VH	0	VH	0	H	-1	VH	0	VH	0
3	H	H	0	H	0	H	0	L	-2	VH	1	VH	0	VH	1	H	0	VH	1	VH	1
4	H	H	0	H	0	H	0	L	-2	VH	1	VH	1	VH	1	H	0	VH	1	VH	1
5	H	H	0	H	0	-	-	L	-2	VH	1	H	0	-	-	H	0	-	-	-	-
6	H	H	0	H	0	H	0	L	-2	L	-2	H	0	H	0	H	0	H	0	VH	1
7	M	M	0	M	0	M	0	L	-1	M	0	M	0	M	0	H	1	M	0	H	1
8	L/M	M	0	L	-1	L	-1	L	-1	L	-1	M	0	M	0	H	1	M	0	H	1
9	L	M	1	L	0	L	0	L	0	L	0	L	0	L	0	H	2	L	0	M	1
10	L	M	1	L	0	L	0	L	0	L	0	L	0	L	0	H	2	L	0	M	1
AVERAGE DEVIATION			0		-0.3		-0.33		-1.5		-0.1		0.1		0.111		0.4		0.1		0.7
ORDER OF SIGNIFICANCE			1		6		7		10		4		3		5		8		2		9

TABLE 3.14

EVALUATION OF QUALITATIVE SWELL PREDICTIONS USING DATA BY HOLTZ(1959) - REMOLDED SOILS

SPECIMEN NUMBER	SWELL PREDICTION SYSTEMS																					
	D&R (base)	USCS		HOLTZ		SEED ETAL		R&S		R		V&G(Jd & LL)		V&G(MC & LL)		VDM		BRE		EXTCAS		SW	
	Cat.	Cat.	Dev.	Cat.	Dev.	Cat.	Dev.	Cat.	Dev.	Cat.	Dev.	Cat.	Dev.	Cat.	Dev.	Cat.	Dev.	Cat.	Dev.	Cat.	Dev.	Cat.	Dev.
1	EH	H	-2	VH	-1	-	-	VH	-1	VH	-1	VH	-1	VH	-1	-	-	-	-	H	-2	VH	-1
2	EH	H	-2	VH	-1	-	-	VH	-1	VH	-1	VH	-1	VH	-1	-	-	-	-	H	-2	VH	-1
3	EH	H	-2	VH	-1	-	-	VH	-1	VH	-1	VH	-1	VH	-1	-	-	-	-	H	-2	VH	-1
4	EH	H	-2	VH	-1	-	-	VH	-1	VH	-1	VH	-1	VH	-1	-	-	-	-	H	-2	VH	-1
5	M	M	0	M	0	M	0	M	0	M	0	M	0	M	0	H	1	M	0	M	0	H	1
6	M	M	0	H	1	-	-	H	1	H	1	L	-1	M	0	-	-	-	-	M	0	VH	2
7	H	H	0	M/H	0	-	-	H	0	VH	1	M	-1	M/H	0	-	-	-	-	H	0	H	0
8	H	H	0	M/H	0	-	-	H	0	VH	1	L	-2	H	0	-	-	-	-	H	0	H	0
9	H	H	0	M/H	0	-	-	H	0	VH	1	L	-2	H	0	-	-	-	-	H	0	H	0
10	H	H	0	M/L	-1	M	-1	H	0	VH	1	L	-2	M	-1	M	-1	M-H	0	H	0	M	-1
11	H	H	0	M/H	0	H	0	H	0	VH	1	M	-1	VH	1	H	0	H	0	H	0	H	0
12	H	H	0	M/H	0	H	0	H	0	VH	1	L	-2	L	-2	H	0	H	0	H	0	H	0
13	L	M	1	M	1	L	0	L	0	M	1	L	0	M	1	M	1	L	0	M	1	H	2
14	M	M	0	M	0	L	-1	M/H	0	M	0	M	0	M/H	0	M	0	L	-1	M	0	H	1
15	H	H	0	H/VH	1	M	-1	H	0	H	0	L	-2	M	-1	M/H	0	M	-1	H	0	VH	1
16	VH	H	-1	VH	0	H	-1	VH	0	VH	0	L	-2	M	-2	VH	0	H	-1	H	-1	VH	0
17	M/H	M	0	H	0	M	-1	H	0	H	0	H	0	VH	1	H	0	M	-1	H	0	VH	1
18	H	H	0	H	0	M	-1	H	0	H	0	L	-2	M	-1	H	0	M	-1	H	0	VH	1
19	H	M	-1	M	-1	M	-1	H	0	M/H	0	L	-2	M	-1	H	0	M	-1	H	0	H	0
20	VH	H	-1	VH	0	H	-1	VH	0	VH	0	L	-3	M	-2	VH	0	VH	0	H	-1	VH	0
21	H	H	0	H/VH	0	M	-1	H	0	H	0	M	-1	M	-1	H	0	M	-1	H	0	VH	1
22	H	H	0	H/VH	0	M	-1	H	0	H	0	L	-2	M	-1	H	0	M	-1	H	0	VH	1
23	H	H	0	M	-1	-	-	H	0	H	0	M	-1	VH	1	-	-	-	-	H	0	H	0
24	H	H	0	M	-1	-	-	H	0	H	0	M	-1	H	0	-	-	-	-	H	0	H	0
25	H	H	0	M	-1	-	-	H	0	H	0	M	-1	M	-1	-	-	-	-	H	0	H	0
26	M	M	0	M	0	M	0	H	1	H	1	M	0	VH	2	H	1	M	0	H	1	H	
27	H	H	0	H	0	-	-	H	0	H	2	L	-2	L	-2	-	-	-	-	H	0	M	1
28	M	M	0	M	0	-	-	H	1	M	0	L	-1	M	0	-	-	-	-	M	0	H	1
29	H	H	0	VH	1	-	-	VH	1	VH	1	M	-1	M	-1	-	-	-	-	H	1	VH	1
30	H	H	0	H	0	-	-	H	0	VH	1	M	-1	M	-1	-	-	-	-	H	0	VH	1
31	H	H	0	M	-1	M	-1	H	0	H	0	L	-2	M	-1	H	0	M	-1	H	0	H	0
32	M	M	0	M	0	-	-	H	1	H	1	L	-1	M	0	-	-	-	-	H	1	H	1
33	H	H	0	H	0	-	-	H	0	VH	1	L	-2	M	-1	-	-	-	-	H	0	VH	1
34	H	H	0	VH	1	H	0	H	0	VH	1	M	-1	M	-1	VH	0	H	0	H	0	VH	1
35	H	H	0	H	0	H	0	H	0	VH	1	M	-1	M	-1	VH	0	H	0	H	0	VH	1
36	VH	H	-1	VH	0	VH	0	VH	0	EH	1	M	-2	VH	0	VH	0	VH	0	H	-1	VH	0
37	VH	H	-1	VH	0	VH	0	VH	0	VH	0	M	-2	H/VH	0	VH	0	VH	0	H	-1	VH	0
38	VH	H	-1	VH	0	M	-2	VH	0	VH	0	M	-2	VH	0	VH	0	VH	0	H	-1	VH	0
39	H	H	0	M/H	0	-	-	H	0	H	0	M	-1	VH	1	H	-1	M	-1	H	0	H	0
40	H	H	0	H	0	M	-1	H	0	VH	1	M	-1	VH	1	-	-	-	-	H	0	VH	1
AVERAGE DEVIATION			-0.325		-0.125		-0.636		0.025		0.325		-1.3		-0.425		0.182		-0.455		-0.225		0.4
DEGREE OF SIGNIFICANCE			6		2		10		1		5		11		8		3		9		4		7

Cat. = predicted swell category -
L : low; M : medium; H : high; VH : very high; EH : extremely high

Dev. = deviation of predicted swell category from the base prediction-
onthe basis of a simple numbering system.
Each category is separated from the adjacent ones by a single unit i.e.
a prediction of VH compared with a base value of H is assumed to have a
deviation of +1

REFER TO TABLE 3.12 FOR KEY TO SYSTEM ABBREVIATIONS

THE ABOVE INFORMATION APPLIES TO TABLES 13-16

TABLE 3.15

EVALUATION OF QUALITATIVE SWELL PREDICTIONS USING DATA BY HOLTZ(1959) - UNDISTURBED SOILS

SPECIMEN NUMBER	SWELL PREDICTION SYSTEMS																							
	D&R(base) Cat.	USCS Cat.	USCS Dev.	HOLTZ Cat.	HOLTZ Dev.	SEED Cat.	SEED Dev.	R&S Cat.	R&S Dev.	R Cat.	R Dev.	V&G(Jd & LL) Cat.	V&G(Jd & LL) Dev.	V&G(MC & LL) Cat.	V&G(MC & LL) Dev.	VDM Cat.	VDM Dev.	BRE Cat.	BRE Dev.	EXTCAS Cat.	EXTCAS Dev.	SW Cat.	SW Dev.
1	EH	H	-2	VH	-1	*	*	VH	-1	EH	0	VH	-1	H/VH	-1	*	*	*	*	H	-2	VH	-1
2	EH	H	-2	VH	-1	*	*	VH	-1	EH	0	VH	-1	VH	-1	*	*	*	*	H	-2	VH	-1
3	VH	H	-1	VH	0	*	*	VH	0	EH	1	M	-1	M	-1	*	*	*	*	H	-1	VH	0
4	VH	H	-1	VH	0	VH	0	VH	0	VH	0	H	-1	H	-1	VH	0	VH	0	H	-1	VH	0
5	H	H	0	H	0	H	0	H	0	VH	1	H	0	H	0	VH	1	VH	1	H	0	VH	1
6	VH	H	-1	H	-1	H	-1	VH	0	VH	0	VH	0	H	-1	VH	0	VH	0	H	-1	VH	0
7	M	M	0	M/L	0	L	-1	M	0	M	0	M	0	M	0	M	0	M	0	M	0	M	0
8	M	M	0	M/L	0	L	-1	M	0	M	0	L	-1	L	-1	M	0	M	0	M	0	M	0
9	M/H	M	0	M	-1	M/H	0	H	0	H	0	L/M	-1	M	-1	H	0	M	-1	H	0	H	0
10	M	M	0	H	1	*	*	H	1	H	1	*	*	L/M	0	*	*	*	*	M	0	VH	2
11	L	M	1	L	0	*	*	L	0	L	0	*	*	L	0	*	*	*	*	M	1	M	1
12	M	M	0	M	0	*	*	*	*	*	*	M	2	M	0	*	*	*	*	M	0	H	1
13	M	M	0	M	0	*	*	H	1	H	1	M	2	M	0	*	*	*	*	M	0	H	1
14	M	M	0	*	*	*	*	*	*	*	*	M	1.5	M	0	*	*	*	*	M	0	*	*
15	L	M	1	L	0	L	0	L	0	M/L	1	L	0	M	1	L/M	1	L	0	M	1	M	1
16	L	M	1	L	0	L	0	L	0	L	0	L	0	M	1	L/M	1	L	0	M	1	M	1
17	M	M	0	L	-1	L	-1	L	-1	M	0	L	0.6	M	0	L	-1	L	-1	M	0	M	0
18	H	H	0	H/VH	0	*	*	H	0	H	0	M	-1	H	0	*	*	*	*	H	0	VH	1
19	H	H	0	H	0	*	*	H	0	H	0	M	-1	M	-1	*	*	*	*	H	0	VH	1
20	H	H	0	H	0	*	*	H	0	H	0	M	-1	H	0	*	*	*	*	H	0	VH	1
21	H	H	0	M	-1	*	*	H	0	H	0	M	-1	VH	1	*	*	*	*	H	0	H	0
22	M	H	1	M	0	*	*	H	1	M/H	1	M	0	H	1	*	*	*	*	H	1	H	1
23	M	H	1	M/L	0	*	*	H	1	M	0	M	0	H	1	*	*	*	*	H	1	M	0
24	M	M	0	M	0	*	*	M/H	0	M/H	0	L	-1	*	*	*	*	*	*	M	1	H	1
25	H	H	0	H	0	*	*	H	0	VH	1	M	-1	*	*	*	*	*	*	H	0	VH	1
26	M	M	0	M/L	0	*	*	M	0	M	0	VH	2	H	1	*	*	*	*	M	0	M	0
27	M	M	0	M	0	*	*	H	1	M/H	0	*	*	*	*	*	*	*	*	H	1	H	1
28	M	M	0	M	0	*	*	H	1	H	1	*	*	*	*	*	*	*	*	M	0	H	1
29	M/H	M	0	H	0	*	*	*	*	*	*	L	-1	L	-1	*	*	*	*	H	0	VH	1
30	EH	H	-2	VH	-1	VH	-1	VH	35	EH	0	VH	-1	VH	-1	VH	-1	VH	-1	H	-2	VH	-1
31	EH	H	-2	VH	-1	*	*	VH	-1	EH	0	VH	-1	VH	-1	*	*	*	*	H	-2	VH	-1
32	H	H	0	M/H	0	*	*	H	0	VH	1	*	*	*	*	*	*	*	*	H	0	H	0
33	EH	H	-2	VH	-1	*	*	*	*	*	*	VH	-1	VH	-1	*	*	*	*	H	-2	VH	-1
34	*	M	*	*	*	*	*	*	*	*	*	*	*	*	*	*	*	*	*	H	*	*	*
35	M	M	0	M	0	*	*	H	1	H	1	L	-1	H	1	*	*	*	*	H	1	H	1
36	M	M	0	L	-1	*	*	L	-1	M	0	M	0	M	0	*	*	*	*	M	0	M	0
37	H	H	0	M/H	0	H	0	H	0	VH	1	*	*	*	*	VH	1	VH	1	H	0	H	0
38	H	H	0	M/H	0	H	0	H	0	VH	1	*	*	*	*	VH	1	VH	1	H	0	H	0
39	M	M	0	M	0	M	0	M	0	M	0	*	*	*	*	M	0	L	-1	M	0	H	1
40	*	H	*	M	12.5	*	*	*	*	*	*	*	*	*	*	*	*	*	*	H	*	H	1
41	H	H	0	VH	1	H	0	H	0	VH	1	M	-1	H	-1	VH	1	VH	1	H	0	VH	1
42	H	H	0	H	0	H	0	H	0	VH	1	M	-1	M	-1	VH	1	H	0	H	0	VH	1
43	VH	H	-1	VH	0	VH	0	VH	0	VH	0	VH	0	H	-1	VH	0	H	-1	H	-1	VH	0
44	H	H	0	VH	1	H	0	H	0	VH	1	L	-2	L	-2	VH	1	H	0	H	0	VH	1
45	VH	H	-1	VH	0	VH	0	VH	0	VH	0	M	-1	M	-1	VH	0	VH	0	H	-1	VH	0
46	H	H	0	H	0	H	0	H	0	VH	1	H	0	H	0	VH	1	VH	1	H	0	VH	1
47	H	H	0	H	0	*	*	H	0	VH	1	M	-1	M	-1	*	*	*	*	H	0	VH	1
AVERAGE DEVIATION			-0.213		-0.152		-0.263		0.024		0.414		-0.59		-0.324		0.368		0		-0.149		0.38
ORDER OF SIGNIFICANCE			5		4		6		2		10		11		7		8		1		3		9

TABLE 3.16

EVALUATION OF QUALITATIVE SWELL PREDICTIONS USING DATA BY SNETHEN(1979)

SPECIMEN NUMBER	SWELL PREDICTION SYSTEMS																							
	D&R (base) Cat.	D&R (base) Dev.	USCS Cat.	USCS Dev.	HOLTZ Cat.	HOLTZ Dev.	SEED ETAL Cat.	SEED ETAL Dev.	R&S Cat.	R&S Dev.	R Cat.	R Dev.	V&G(Jd & LL) Cat.	V&G(Jd & LL) Dev.	V&G(MC & LL) Cat.	V&G(MC & LL) Dev.	VDM Cat.	VDM Dev.	BRE Cat.	BRE Dev.	EXTCAS Cat.	EXTCAS Dev.	SW Cat.	SW Dev.
1	EH		H	-2	VH	-1	VH	-1	VH	-1	VH	-1	H	-2	M	-3	VH	-1	VH	-1	H	-2	VH	-1
2	H		H	0	H	0	H	0	H	0	VH	1	M	-1	L	-2	L	-2	H	0	H	0	VH	1
3	EH		H	-2	VH	-1	VH	-1	VH	-1	VH	-1	M	-3	L	-4	H	-2	VH	-1	H	-2	VH	-1
4	H		H	0	H	0	H	0	H	0	VH	1	M	-1	L	-2	H	0	H	0	H	0	VH	1
5	VH		H	-1	VH	0	VH	0	VH	0	VH	0	H	-1	VH	0	H	-1	H/VH	0	H	-1	VH	0
6	M		M	0	H	1	H	1	M	0	M	0	H	1	M	0	L	-1	H	1	M	0	VH	2
7	M		M	0	H	1	H	1	M	0	M	0	H	1	M	0	L	-1	H/VH	2	M	0	VH	2
8	M		M	0	H	1	H	1	M	0	M	0	VH	2	M	0	L	-1	H	1	M	0	VH	2
9	M		M	0	M	0	H	1	M	0	H	1	M	0	VH	2	L	-1	H	1	M	0	H	1
10	VH		H	-1	VH	0	VH	0	VH	0	VH	0	H	-1	VH	0	L	-3	H	-1	H	-1	VH	0
11	M		M	0	H	1	H	1	M	0	M	0	M	0	H	1	L	-1	H/VH	2	M	0	VH	2
12	VH		H	-1	VH	0	VH	0	VH	0	VH	0	H	-1	VH	0	M	-2	VH	0	H	-1	VH	0
13	M		M	0	M	0	M	0	M	0	M	0	H	1	M	0	L	-1	H	1	M	0	H	1
14	H		H	0	M	-1	H	0	H	0	H	0	M	-1	L	-2	L	-2	H	0	H	0	H	0
15	H		H	0	VH	1	VH	1	H	0	VH	1	L	-2	L	-2	L	-2	H	0	H	0	VH	1
16	VH		M	-2	VH	0	VH	0	H	-1	VH	0	VH	0	VH	0	L	-3	VH	0	M	-2	VH	0
17	VH		H	-1	VH	0	VH	0	H	-1	VH	0	H	-1	H	-1	H	-1	H	-1	H	-1	VH	0
18	H		H	0	H	0	H	0	H	0	H	0	*	*	VH	1	L	-2	H	0	H	0	VH	1
19	H		H	0	VH	1	VH	1	H	0	VH	1	M	-1	VH	1	L	-2	H/VH	1	H	0	VH	1
20	VH		H	-1	VH	0	VH	0	H	0	VH	0	M	-2	M/L	-3	M	-2	H	-1	H	-1	VH	0
AVERAGE DEVIATION				-0.55		0.15		0.25		-0.2		0.15		-0.6		-0.65		-1.65		0.2		-0.55		0.65
ORDER OF SIGNIFICANCE				8		2		5		4		1		9		10		11		3		6		7

TABLE 3.17

EVALUATION OF QUANTITATIVE SWELL PREDICTIONS USING DATA BY HOLTZ(1959) - REMOLDED SOILS

SPECIMEN NUMBER	SWELL (%)	SWELL PREDICTION SYSTEMS															
		HOLTZ SWELL	HOLTZ ERR.	SEED ETAL SWELL	SEED ETAL ERR.	R&S SWELL	R&S ERR.	V&G(Jd + LL) SWELL	V&G(Jd + LL) ERR.	V&G(MC + LL) SWELL	V&G(MC + LL) ERR.	N&C SWELL	N&C ERR.	SW SWELL	SW ERR.	CAA SWELL	CAA ERR.
1	33	30+	-9	*	*	60+	82	20+	-39	30+	-9	*	*	25+	-24	60+	82
2	54	30+	-44	*	*	60+	11	20+	-63	30+	-44	*	*	25+	-54	60+	11
3	33	30+	-9	*	*	60+	82	20+	-39	30+	-9	*	*	25+	-24	60+	82
4	33	30+	-9	*	*	60+	82	20+	-39	30+	-9	*	*	25+	-24	60+	82
5	2	10-20	689	2	-16	7	268	2	5	4	84	11	476	2	5	20	953
6	3	20-30	635	*	*	20	474	1	-78	2	-56	*	*	8	135	20	488
7	4	20	456	*	*	28	678	2	-58	5	39	*	*	15	317	30	733
8	1	20	1900	*	*	29	2800	1	-30	6	480	*	*	15	93	30	2900
9	-2	20	1100	*	*	29	1550	1-	120	6	390	*	*	15	113	30	1600
10	2	10	400	4	75	36	1700	1-	-70	2	0	8	322	18	800	40	1900
11	12	20	70	12	3	42	259	3	-74	15	28	18	51	18	54	40	242
12	2	20	1011	12	567	42	2233	1-	-83	1-	-55	13	635	18	900	40	2122
13	6	10-20	154	1-	-83	1-	-49	1-	-86	4	-29	8	38	1-	83	10	69
14	8	10-20	95	1-	-87	8	4	2	-81	5	-35	8	10	1	87	20	160
15	13	30	2	4	-68	38	204	1-	-96	4	-65	12	-2	10	-20	30	140
16	22	30+	40	12	-44	77+	258	1	-94	3	-87	14	-34	18	-16	50	133
17	19	20-30	20	2	-89	26	35	6	-68	11	-43	11	-44	9	3	15	-22
18	7	20-30	252	4	-51	48	576	1-	-89	1	-80	10	39	13	83	30	323
19	3	10-20	400	2	-33	18	500	1-	-80	2	-30	9	197	8	167	30	900
20	10	30+	203	18	82	73	637	1-	-90	1	-86	13	34	22	122	50	405
21	9	30	237	4	-55	48	439	3	-72	3	-64	11	24	12	134	30	237
22	3	30	900	4	33	48	1500	1-	-83	3	6	10	238	12	300	30	900
23	14	10-20	11	*	*	27	100	3	-81	16	19	*	*	12	-11	30	122
24	12	10-20	29	*	*	27	133	3	-78	6	-48	*	*	12	3	30	159
25	2	10-20	733	*	*	27	1400	3	39	2	33	*	*	12	567	30	157
26	15	10-20	-31	*	*	11	-29	2	-86	12	-18	5	-65	11	-25	20	36
27	1	10	900	2	-86	36	3500	1-	-50	1-	-70	*	*	13	1200	30	2900
28	0.4	10-20	37	*	*	8	1900	1-	125	2	3500	*	*	5	1150	20	4900
29	*	30+	*	*	*	65	*	4	*	5	*	*	*	21	*	40	*
30	0.54	20-30	4539	*	*	34	6196	2	233	9	1493	*	*	14	2493	25	4530
31	5	10-20	2121	5	2	26	442	1-	-89	2	-69	11	124	12	1500	30	525
32	4	10-20	329	*	*	18	414	1-	-72	8	137	*	*	12	243	20	471
33	9	20-30	194	*	*	38	341	1-	-89	4	-48	*	*	15	77	40	371
34	6	30+	400	20	233	54	800	2	233	2	-73	17	175	20	233	40	567
35	5	20-30	363	8	48	31	474	4	-26	3	-33	12	118	13	144	30	456
36	7	30+	348	25+	273	69	929	5	-27	20+	199	27	299	23	243	50	646
37	5	30+	500	30+	500	80+	1500	5	-10	10	100	30	490	25+	400	60+	1100
38	7	30+	355	5	-24	80+	1112	3	-62	11	59	24	259	22	233	50	658
39	13	20	49	*	*	36	169	5	-66	12	-10	14	1-	12	-10	30	124
40	13	20-30	91	3	-77	40	205	4	-69	12	-8	*	*	14	7	30	129
AVERAGE ERROR			486		43		844		-38		137		161		299		828
ORDER OF SIGNIFICANCE			6		2		8		1		3		4		5		7

SWELL : Percent Swell = $\frac{\text{change in specimen height}}{\text{original specimen height}} \times 100$

ERR. : Percent Error = $\frac{(\text{actual swell} \frown \text{predicted swell})}{\text{actual swell}} \times 100$

AVERAGE ERROR (%) = $\frac{\text{total errors for all specimens}}{\text{total number of specimens}}$

\- sign after the error signifies 'less than'

\+ sign after the error signifies 'greater than'

* signifies correlation unobtainable

REFER TO TABLE 3.12 FOR KEY TO SYSTEM ABBREVIATIONS

THE ABOVE INFORMATION APPLIES TO TABLES 17-19

TABLE 3.18

EVALUATION OF QUANTITATIVE SWELL PREDICTIONS USING DATA BY HOLTZ(1959) - UNDISTURBED SOILS

SPECIMEN NUMBER	SWELL (%)	HOLTZ SWELL	HOLTZ ERR.	SEED ETAL SWELL	SEED ETAL ERR.	R&S SWELL	R&S ERR.	V&G(Jd + LL) SWELL	V&G(Jd + LL) ERR.	V&G(MC + LL) SWELL	V&G(MC + LL) ERR.	N&C SWELL	N&C ERR.	SW SWELL	SW ERR.	CAA SWELL	CAA ERR.
		SWELL PREDICTION SYSTEMS															
1	7	30+	329	*	*	35	400	18	157	10	429	*	*	25+	257	60+	757
2	15	30+	100	*	*	40+	167	20+	33	20+	33	*	*	25+	67	60+	300
3	3	30+	1100	*	*	26	9400	3	20	4	40	*	*	25+	-100	60+	2300
4	10	30+	213	35	263	22	129	6	-38	7	-32	22	132	27	160	60+	525
5	8	20-30	198	24	184	16	90	8	-11	6	-35	21	150	20	138	40	376
6	12	20-30	112	17	46	19	61	11	-7	9	-28	16	31	22	86	50	324
7	2	10	426	1	-29	7	242	2	-21	4	111	10	426	1	47	20	953
8	0	10	*	1-	*	8	*	1-	*	1-	*	8	*	2	*	20	*
9	1-	15	3650	3	700	12	2775	1	1500	2	300	10	2285	12	2900	20	4900
10	2	20-30	1289	*	*	12	550	*	*	1	-44	*	*	12	567	30	1567
11	0	10-	*	*	*	3	*	*	*	1	*	*	*	1-	*	10	*
12	4	10-20	481	*	*	*	*	2	-53	4	-12	*	*	3	-30	20	365
13	1	10-20	16	*	*	10	10	2	122	3	178	*	*	9	900	20	2122
14	1-	*	*	*	*	*	*	2	1500	3	400	*	*	1	67	20	3233
15	1	10-	10	1-	-72	5	456	1-	-44	3	244	11	1076	1-	11	10	1011
16	3	10-	300	1-	-89	3	28	1-	-80	5	80	8	206	1-	-60	10	300
17	3	10-	2703	1-	-88	5	74	1-	-78	2	-48	8	192	1	-60	20	641
18	2	32	1584	*	*	15	689	4	111	8	321	*	*	15	689	30	1479
19	6	20-30	297	*	*	13	106	2	-683	5	-22	*	*	12	90	30	376
20	7	20-30	242	*	*	13	71	3	-59	6	-25	*	*	7	-65	30	311
21	5	10-20	306	*	*	12	145	2	-694	11	124	*	*	12	145	30	512
22	5	10-20	200	*	*	11	110	2	-60	9	70	*	*	5	0	20	300
23	2	10	400	*	*	10	400	1	-45	8	300	*	*	7	250	20	900
24	*	10-20	*	*	*	9	*	1-	*	*	*	*	*	8	*	20	*
25	*	20-30	*	*	*	13	*	2	*	*	*	*	*	15	*	30	*
26	4	10-	1500	*	*	7	75	20+	400	6	37	*	*	1	-75	10	150
27	*	10-20	*	*	*	10	*	*	*	*	*	*	*	5	*	20	*
28	*	10-20	*	*	*	10	*	*	*	*	*	*	*	2	*	20	*
29	2	20-30	12	*	*	*	*	1-	-75	1-	25	*	*	11	450	30	1400
30	16	30+	83	608	3609	35+	213	20+	22	20+	22	121	737	25+	52	60+	266
31	26	30+	17	*	*	35+	137	20+	-22	20+	-22	*	*	25+	2	60+	134
32	*	20	*	*	*	15	*	*	*	*	*	*	*	7	*	40	*
33	*	30+	*	*	*	*	*	20+	*	20+	*	*	*	25+	*	60+	*
34	*	*	*	*	*	*	*	*	*	*	*	*	*	*	*	30	*
35	2	10-20	689	*	*	10	416	1-	321	8	321	*	*	12	532	20	953
36	1	10-	10	*	*	4	378	1	22	2	67	*	*	1	11	20	2122
37	*	20	*	10	*	16	*	*	*	*	*	*	*	17	*	40	*
38	*	20	*	12	*	15	*	*	*	*	*	*	*	18	*	40	*
39	*	10-20	*	2	*	6	*	*	*	*	*	*	*	1	*	20	*
40	13	10-20	20	*	*	*	*	*	*	*	*	*	*	*	*	20	60
41	2	30+	1400	21	940	17	750	3	25	2	0	16	718	18	500	40	1900
42	1	20-30	22	9	7	13	11	4	218	4	264	13	12	13	108	30	2627
43	3	30	934	28	861	20	576	20	589	6	89	22	657	22	659	50	1624
44	1-	30	10100	20	6700	16	5433	1-	267	1-	267	15	5047	17	5767	40	13400
45	5	30	567	35	678	21	356	1-	-81	4	-6	22	358	23	1400	50	1011
46	3	20-30	826	10	281	14	419	5	889	9	215	15	472	14	419	25	826
47	1	20-30	1823	*	*	15	1015	3	123	2	54	*	*	14	977	30	2202
AVERAGE ERROR			969		927		828		118		109		833		549		1492
ORDER OF SIGNIFICANCE			7		6		4		4		1		5		3		8

TABLE 3.19

EVALUATION OF QUANTITATIVE SWELL PREDICTIONS USING DATA BY LADD & LAMBE(1961)

SPECIMEN NUMBER	SWELL (%)	HOLTZ SWELL	HOLTZ ERR.	SEED ETAL SWELL	SEED ETAL ERR.	R&S SWELL	R&S ERR.	V&G(Jd + LL) SWELL	V&G(Jd + LL) ERR.	N&C SWELL	N&C ERR.	SW SWELL	SW ERR.	CAA SWELL	CAA ERR.
		SWELL PREDICTION SYSTEMS													
1	40	30+	-25	15	-62	76	90	1-	-99	11	-73	22	-45	60+	50
2	35	30+	-14	25	-28	48	37	1-	-99	14	-59	21	-40	50	43
3	36	30+	-17	14	-60	46	28	1-	-99	11	-69	19	-47	40	11
4	38	30+	-21	9	-70	40	5	1-	-99	10	-75	17	-55	40	6
5	30	*	*	10	-67	*	*	1-	-99	11	-62	15	-50	30	0
6	28	20-30	-11	11	-61	36	29	1-	-99	13	-52	12	-57	40	43
7	23	10-20	-35	2	-92	6	-74	1-	-99	8	-65	5	-78	20	-13
8	16	10-20	6	1	-94	2	-88	1-	-99	8	-49	1-	-94	10	-38
9	12	10-	-13	1-	-99	1	-91	1-	-99	7	-41	1	-91	5	-57
10	6	10-	66	1-	-99	1-	-92	1-	-99	6	7	1-	-83	5	-17
AVERAGE ERROR			-7.1		-73.8		-17.3		-87		-53.9		-64		3.11
ORDER OF SIGNIFICANCE			2		6		3		7		4		5		1

TABLE 3.20(a)

ASSESSED QUANTITATIVE TYPE SWELL PREDICTION SYSTEMS

ORDER OF SIGNIFICANCE	DATA SOURCES		
	HR	HU	L&L
1	V&G(Jd,LL) (-38)	V&G(MC,LL) (109)	CAA(3.11)
2	SEED(43)	V&G(Jd,LL) (118)	H(-7.1)
3	V&G(MC,LL) (137)	SW (549)	R&S(-17.3)
4	N&C(161)	R&S(828)	N&C(-53.85)
5	SW (299)	N&C(833)	SW (-64)
6	H(486)	SEED(927)	SEED(-73.8)
7	CAA(828)	H(969)	V&G(Jd,LL) (-87)
8	R&S(844)	CAA(1492)	-

Bracketed figures indicate the average errors of swell predictions(when compared with actual values)

TABLE 3.20(b)

ASSESSED QUALITATIVE-TYPE SWELL PREDICTION SYSTEMS

ORDER OF SIGNIFICANCE	DATA SOURCES			
	SNR	L&L	HR	HU
1	R(0.15)	USCS(0)	R&S(0.025)	BRE(0)
2	H(0.15)	H(0.1)	H(-0.125)	R&S(0.024)
3	BRE(0.2)	BRE(0.1)	VDM(0.182)	CAS(-0.149)
4	R&S(-0.2)	VDM(-0.1)	CAS(-0.225)	H(-0.152)
5	SEED(-0.25)	R(0.111)	R(0.325)	USCS(-0.213)
6	CAS(-0.55)	SEED(-0.3)	USCS(-0.325)	SEED(-0.263)
7	SW (0.65)	R&S(-0.33)	SW (0.4)	V&G(MC,LL) (-0.324)
8	USCS(-0.55)	CAS(0.4)	V&G(MC,LL) (-0.425)	VDM(0.368)
9	V&G(Jd,LL) (-0.6)	SW (0.7)	BRE(-0.455)	SW (0.38)
10	V&G(MC,LL) (-0.65)	V&G(MC,LL) (-1.5)	SEED(-0.636)	R(0.414)
11	VDM (-1.65)	-	V&G(-1.33)	V&G(Jd,LL) (-0.59)

Bracketed figures indicate the average deviation of -predictions from the base values(category deviation)

TABLE 3.21
LIST OF VARIABLE ABBREVIATIONS

	VARIABLE	ABBREVIATION
1.	index number	INDEX
2.	depth(ft)	DEPTH
3.	dry unit weight(pcf)	DUW
4.	Initial moisture content(%)	MC
5.	liquid limit (%)	LL
6.	plastic limit (%)	PL
7.	plastic index (%)	PI
8.	optimum moisture content(%)	OMC
9.	dry density (pcf)	DD
10.	specific gravity	SG
11.	clay content (-200Mm) %	CLAY
12.	colloid content (-2Mm) %	COL
13.	activity	A
14.	shrinkage limit (%)	SL
15.	shrinkage ratio	SR
16.	linear shrinkage (%)	LS
17.	void ratio	VOID
18.	free swell (%)	FRSW%
19.	volume change (%)	VLCH%
20.	degree of saturation (%)	SAT
21.	total suction undisturbed(tsf)	SCUND
22.	suction A parameter(undisturbed)	AUND
23.	suction B parameter(undisturbed)	BUND
24.	suction parameter(undisturbed)	ALUND
25.	total suction (remolded)	SCREM
26.	suction A parameter(remolded)	AREM
27.	suction B parameter(remolded)	BREM
28.	suction parameter(remolded)	ALREM

TABLE 3.22(a)
COEFFICIENTS OF DETERMINATION
(4 VARIABLES ONLY)

DATA SOURCE	DEPENDENT VARIABLES			
	SWELL PRESSURE	LOG SWELL PRESSURE	PERCENT SWELL	LOG PERCENT SWELL
HR	0.212	*	0.85	0.579
HU	0.0738	*	0.528	*
L&L	0.880	0.84	0.925	*
N&C	0.572	0.563	0.986	0.891
V&G	0.436	0.481	0.43	0.559
SNR	0.860	0.853	0.674	0.674
SNU		*	0.323	0.375

INDEPENDENT VARIABLES : liquid limit(%), plastic index(%),initial moisture content(%), dry density(pcf)

COEFFICIENT OF DETERMINATION : measure of actual relationship between dependent and independent variables.

TABLE 3.22(b)
COEFFICIENTS OF DETERMINATION
(MULTIPLE VARIABLES)

DATA SOURCE	DEPENDENT VARIABLES			
	SWELL PRESSURE	LOG SWELL PRESSURE	PERCENT SWELL	LOG PERCENT SWELL
HR	0.286	*	0.865	0.709
HU	0.299	*	0.547	*
L&L	0.968	0.882	0.960	*
SEED	*	*	0.917	0.861
N&C	0.822	0.823	0.993	0.934
SNR	0.955	0.957	0.959	0.980
SNU	*	*	0.565	0.904

TABLE 3.23

RELATIONSHIPS OBTAINED BY LINEAR REGRESSION ANALYSIS (4 VARIABLES ONLY)

DEPENDENT VARIABLE (tsf)	DATA SOURCE	COEFFICIENTS					COEFFICIENT OF DETERMINATION
		COEFFICIENT A	LIQUID LIMIT (B)	PLASTIC INDEX (C)	INITIAL MOISTURE (D)	DRY DENSITY (E)	
SWELL PRESSURE	V&G	-14.376	0.1578	-0.09707	-0.03251	0.1087	0.436
"	SNR	0.03748	-0.0001551	0.0001243	0.0004324	0.0007962	0.86
"	HU	0.6886	-.01348	0.00992	-0.0032	0.0491	0.0738
"	HR	-0.4132	0.1241	-0.0976	-0.1163	0.000527	0.212
LOG SWELL PRESSURE	V&G	-2.2644	0.03261	-0.007955	-0.03069	0.01842	0.481
"	SNR	-1.244	-0.0005123	0.000774	0.001795	0.003069	0.853
PERCENT SWELL	V&G	-21.70	0.2640	-0.05247	-0.2023	0.17	0.43
"	SNU	-1.1373	0.08051	0.01674	-0.03077	-0.02294	0.323
"	SNR	94.359	-0.2129	0.4617	-1.027	-0.7233	0.674
"	HU	1.5086	-0.1572	0.2759	-0.0891	0.1091	0.528
"	HR	-12.211	1.127	-0.7803	-0.9373	0.00345	0.85
LOG PERCENT SWELL	V&G	-4.3705	0.04965	-0.02717	-0.02388	0.03009	0.559
"	SNU	0.43271	0.03523	-0.005121	-0.03925	-0.01744	0.375
"	SNR	13.541	-0.04042	0.06493	-0.1355	-0.1033	0.674
"	HR	-0.1327	0.1182	-0.09335	-0.0988	0.0007814	0.579

1. RELATIONSHIPS OF THE FORM : DEPENDENT VARIABLE = A + B(LIQUID LIMIT) + C(PLASTIC INDEX) + D(MOISTURE CONTENT) + E(DRY DENSITY)

2. INDEPENDENT VARIABLES = LIQUID LIMIT, PLASTIC INDEX , INITIAL MOISTURE CONTENT , DRY DENSITY

TABLE 3.24(a)

ORDER OF VARIABLE SIGNIFICANCE (4 VARIABLES ONLY)

DATA SOURCE [3]	DEPENDENT VARIABLES			
	SWELL PRESSURE (tsf)	LOG SWELL PRESSURE(tsf)	PERCENT SWELL	LOG PERCENT SWELL
HR	LL MC PI DD	*	LL MC PI DD	LL MC PI DD
HU	MC DD LL PI	*	PI LL DD MC	*
L&L	LL MC PI -	LL MC PI -	LL MC PI -	*
N&C	PI MC LL -	PI MC LL -	PI MC LL -	PI MC LL -
V&G	DD LL PI MC	MC LL DD PI	DD LL MC PI	DD LL PI MC
SNR	DD MC LL PI	DD MC LL PI	LL DD MC PI	LL DD MC PI
SNU	*	*	LL PI DD MC	LL MC DD PI

1. INDEPENDENT VARIABLES SHOWN IN ORDER OF DECREASING SIGNIFICANCE
2. LL = LIQUID LIMIT ; MC = INITIAL MOISTURE CONTENT ; PI = PLASTIC LIMIT ; DD = DRY DENSITY
3. REFER TO TABLE 3.12 FOR KEY TO DATA SOURCE/AUTHOR ABBREVIATIONS
4. * INDICATES NO CORRELATION AVAILABLE

TABLE 3.24(b)

ORDER OF VARIABLE SIGNIFICANCE (MULTIPLE VARIABLES)

DATA SOURCE [1]	DEPENDENT VARIABLES			
	SWELL PRESSURE (tsf)	LOG SWELL PRESSURE (tsf)	PERCENT SWELL	LOG PERCENT SWELL
HU	LL,MC,COL,PI,SG,SAT,SL,DD	N.A.	LL,MC,PI,SAT,COL,SL,DD,SG	LL,MC,COL,PI,SG,SAT,SL,DD
HU	SAT,COL,PI,DD,SL,MC,LL,SG	N.A.	PI,LL,DD,MC,SG,SAT,COL,SL	N.A.
L&L	LL,SL,PI,CLAY,A,MC	LL,CLAY,SL,PI,MC,A,	LL,CLAY,A,LL,SL,	N.A.
N&C	PI,CLAY,SL,OMC,LL,MC	PI,CLAY,MC,OMC,LL,SL	PI,CLAY,LL,MC,OMC,SL	PI,CLAY,LL,OMC,MC,SL
SNR	DD,SCREM,SG,AREM,CLAY,ALREM,COL, SL,PI,LL,LS,MC,BREM,SR	DD,SCREM,SG,AREM,CLAY, ALREM,PI,SL,BREM,LS,MC, COL,LL,SR	SCREM,COL,SG,CLAY,LS,SR,MC, SL,AREM,ALREM,BREM,DD,LL,PI	LL,SR,LS,ALREM,PI,SG,SL,MC, DD,SCREM,CLAY,AREM,COL
SNU	N.A.	N.A.	COL,LL,SCUND,DD,VOID,SG,MC, BUND,LS,SR,SL,CLAY,AUND,PI, ALUND	LL,SCUND,AUND,LS,PI,ALUND, SG,MC,BUND,VOID,CLAY,SR, COL,DD,SL

1. REFER TO TABLE 3.12 FOR KEY TO DATA SOURCE/AUTHOR ABBREVIATIONS
2. REFER TO TABLE 3.21 FOR KEY TO INDEPENDENT VARIABLE ABBREVIATIONS
3. N.A. INDICATES NO CORRELATION OBTAINED

TABLE 3.25

OBSERVED SOIL BEHAVIOUR WITH VARYING PLASTICITY(AFTER CASAGRANDE)

SOIL CHARACTERISTICS	AT CONSTANT LIQUID LIMIT & INCREASING PLASTIC INDEX	AT CONSTANT PLASTIC INDEX & INCREASING LIQUID LIMIT
COMPRESSIBILITY	ABOUT THE SAME	INCREASES
PERMEABILITY	DECREASES	INCREASES
RATE OF VOLUME CHANGE	DECREASES	-
TOUGHNESS NEAR THE PLASTIC LIMIT	INCREASES	DECREASES
DRY STRENGTH	INCREASES	DECREASES

TABLE 3.26

AASHTO CLASSIFICATION FOR HIGHWAY SUBGRADE MATERIAL

General Classification	*Granular Materials (35 per cent or Less Passing No. 200 Sieve*)*							*Silt-Clay Materials (More than 35 per cent Passing No. 200 Sieve*)*			
Group Classification	A-1		A-3	A-2				A-4	A-5	A-6	A-7
	A-1-a	A-1-b		A-2-4	A-2-5	A-2-6	A-2-7				A-7-5 A-7-6
Sieve analysis, percentage passing: No. 10 sieve* No. 40 sieve No. 200 sieve	50 max. 30 max. 15 max.	50 max. 25 max.	51 min. 10 max.	35 max.	35 max.	35 max.	35 max.	36 min.	36 min.	36 min.	36 min.
Characteristics of fraction passing No. 40 sieve* Liquid limit, per cent Plasticity index, per cent	6 max.		N.P.	40 max. 10 max.	41 min. 10 max.	40 max. 11 min.	41 min. 11 min.	40 max. 10 max.	41 min. 10 max.	40 max. 11 min.	41 min. 11 min.[a]
Group index[b]	0		0	0		4 max.		8 max.	12 max.	16 max.	20 max.
Usual types of significant constituent materials	Stone fragments, gravel and sand		Fine sand	Silty or clayey gravel and sand				Silty soils		Clayey soils	
General rating as a subgrade	Excellent to good							Fair to poor			

Classification Procedure: With required test data available, proceed from left to right on above chart and correct group will be found by process of elimination. The first group from the left into which the test data will fit is the correct classification.

[a] Plasticity index of A-7-5 subgroup is equal to or less than liquid limit minus 30. Plasticity index of A-7-6 subgroup is greater than liquid limit minus 30.

[b] See group index formula Fig. 2-12 for method of calculation. Group index should be shown in parentheses after group symbol as: A-2-6 (3), A-4 (5), A-6 (12), A-7-5 (17), etc.

* Sieve sizes are American. Approximate British equivalents as follows

United States A.S.T.M. E.11-26	Great Britain B.S. 410
10	8
40	36
200	200

TABLE 3.27

CAA SOIL CLASSIFICATION SYSTEM

Soil	*Total Percentage of Aggregate Retained on No. 10 U.S. Sieve*	*Material Passing No. 10 U.S. Sieve*				*Material Passing No. 40 U.S. Sieve*		
		Coarse Sand Per cent	*Fine Sand Per cent*	*Silt Per cent*	*Clay Per cent*	*Liquid Limit Per cent*	*Plasticity Index Per cent*	*Volume Change at FME Per cent*
E-1	0-45	40-85	5-55	0-10	0-5	25-	0-6	0-6
		85+						
E-2	0-45	15-50	25-75	0-15	0-10	25-	0-6	0-6
		75+						
E-3a	0-45	0-25	50-100	0-15	0-10	25-	0-6	0-6
		75+						
E-3b	0-45	0-35	30-80	10-45	0-20	35-	0-10	0-10
		55+						
E-4	0-45	0-25	30-75	10-30	5-25	45-	5-15	5-15
		55+						
E-5	0-55	0-20	20-65	20-75	0-20	45-	0-10	0-15
		65-						
E-6	0-55	0-20	0-45	5-70	15-50	50-	10-30	10-30
		55-						
E-6 Loess	0-10	0-10	0-25	50-98	0-15	50-	0-30	5-30
		55-						
E-7	0-55	0-20	0-40	5-70	15-50	60-	15-40	20-40
		55-						
E-8a Micaceous and diatomaceous silt-clay	0-55	0-15	0-40	35-75	15-35	30-60	10-50	10-40
		55-						
E-8b	0-55	0-15	0-40	5-50	30+	70-	20-50	30-50
		55-						
E-9	0-55	0-10	0-45	5-50	30+	80-	30+	40-60
		55-						
E-10	0-55	0-10	0-45	30-80	30-	60+	0-25	
		55-						
E-11 Muck or peat	0-10	0-25	0-50	10-60	5-25	60-400	0-60	
		55						

TABLE 3.28

RELATIONSHIPS BETWEEN SWELL BEHAVIOUR AND THE AASHTO GROUP INDEX.

DATA SOURCE	SWELL BEHAVIOUR RELATIONSHIPS			
	PERCENT SWELL		SWELL PRESSURE(psi)	
	GRADIENT	Y-INTERCEPT	GRADIENT	Y-INTERCEPT
LADD & LAMBE (1961)	0.167	0.331	0.868	-0.1599
SEED ETAL (1962)	0.083	1.476	*	*
RANGANATHAM & SATYANARAYANA (1965)	0.55	-6.21	*	*
NAYAK & CHRISTENSEN (1971)	0.604	-1.658	0.925	-4.754
SNETHEN (1979)	1.96	27.8	*	*
HOLTZ(1959) -UNDISTURBED SPECIMENS	2.863	2.579	0.1058	9.153
HOLTZ (1959) REMOLDED SPECIMENS	-0.103	7.894	-0.047	8.586

TABLE 3.29(part 1)

EVALUATION OF QUANTITATIVE SWELL PREDICTIONS ON THE BASIS OF THE AASHTO GROUP INDEX

DATA SOURCES											
LADD & LAMBE (1961)				SEED ETAL (1962)				RANGANATHAM & SATYANARAYANA (1965)			
SPECIMEN NUMBER	GROUP INDEX	PERCENT SWELL	ERROR	SPECIMEN NUMBER	GROUP INDEX	PERCENT SWELL	ERROR	SPECIMEN NUMBER	GROUP INDEX	PERCENT SWELL	ERROR
1	8	14	64	1	0	0	-100	1	3	6	-60
2	30	57	-63	2	0	0	-100	2	0	0	-100
3	12	23	36	3	2	4	-92	3	1	2	-88
4	6	11	71	4	0	0	-100	4	6	11	-46
5	12	23	23	5	0	0	-100				
6	24	46	-64	6	6	11	-80				
7	1	2	91	7	0	0	-100				
8	.4	8	50	8	0	0	-100				
9	0	0	-100	9	0	0	-100				
10	0	0	-100	10	0	0	-100				
				11	0	0	-100				
				12	5	10	-68				
				13	0	0	-100				
				14	2	4	-33				
				15	6	11	-32				
				16	1	2	-60				
				17	5	10	-20				
				18	10	19	0				
				19	0	0	-100				
				20	4	8	70				
				21	9	17	113				
				22	0	0	-100				
				23	6	11	358				
AVERAGE ERROR			-80				-45				-74
ORDER OF SIGNIFICANCE			4				2				3

TABLE 3.29(part 2)

DATA SOURCES											
HOLTZ(1959) - UNDISTURBED DATA				HOLTZ(1959) - REMOLDED DATA				NAYAK & CHRISTENSEN (1971)			
SPECIMEN NUMBER	GROUP INDEX	PERCENT SWELL	ERROR	SPECIMEN NUMBER	GROUP INDEX	PERCENT SWELL	ERROR	SPECIMEN NUMBER	GROUP INDEX	PERCENT SWELL	ERROR
5	27	51	431	8	1	2	-47	1	2	4	-60
6	25	48	471	16	0	0	-100	2	6	11	-31
7	7	13	10	17	6	11	-6	3	14	27	7
9	1	2	5	18	0	0	-100	4	2	4	-49
10	0	0	0	19	0	0	-100	5	8	15	-7
11	2	4	900	20	5	10	-20	6	20	38	74
12	2	4	122	21	15	29	35	7	4	8	-25
13	0	0	0	22	1	2	-89	8	11	21	58
30	0	0	-100	23	3	6	-15	9	19	36	101
31	0	0	-100	24	2	4	33	10	4	8	-70
32	0	0	-100	25	8	15	52	11	13	25	-33
50	72	137	735	26	3	6	-33	12	27	51	9
62	5	10	0	38	1	2	*	13	3	6	-70
63	9	17	0	55	4	8	*	14	11	21	-24
64	0	0	0	66	16	30	1400	15	28	53	48
67	15	29	2536	68	24	46	587	16	6	11	-42
69	33	63	2072	70	34	65	1200	17	10	19	-19
71	14	27	8900	72	7	13	97	18	26	49	74
73	17	32	611	75	3	6	55				
74	17	32	1085								
AVERAGE ERROR			879				173				-3.3
ORDER OF SIGNIFICANCE			6				5				1

$$\text{PERCENT SWELL} = \frac{\text{change in specimen height}}{\text{original specimen height}} \times 100$$

$$\text{ERROR} = \frac{(\text{actual swell} \frown \text{predicted swell})}{\text{actual swell}} \times 100$$

$$\text{AVERAGE ERROR (\%)} = \frac{\text{total errors for all specimens}}{\text{total number of specimens}}$$

SPECIMEN NUMBER = specimen identification number allocated by the original author

REFER TO TABLE 3.12 FOR KEY TO DATA SOURCE ABBREVIATIONS

TABLE 3.30(part 1)

EVALUATION OF QUALITATIVE SWELL PREDICTIONS ON THE BASIS OF THE AASHTO GROUP INDEX(METHOD No 1)

DATA SOURCES											
LADD & LAMBE (1961)				SEED ETAL (1962)				RANGANATHAM & SATYANARAYANA (1965)			
SPECIMEN NUMBER	GROUP INDEX	SWELL CATEGORY	DEVIATION	SPECIMEN NUMBER	GROUP INDEX	SWELL CATEGORY	DEVIATION	SPECIMEN NUMBER	GROUP INDEX	SWELL CATEGORY	DEVIATION
1	8	M	-2	1	0	L	-1	1	3	L	-2
2	30	H	-2	2	0	L	-2	2	0	L	-1
3	12	H	0	3	2	L	-3	3	1	L	-2
4	6	M	-1	4	0	L	-1	4	6	M	-2
5	12	H	0	5	0	L	-2				
6	24	VH	1	6	6	M	-2				
7	1	L	-1	7	0	L	0				
8	4	L	0	8	0	L	0				
9	0	L	0	9	0	L	0				
10	0	L	0	10	0	L	0				
				11	0	L	0				
				12	5	L	-2				
				13	0	L	0				
				14	2	L	-1				
				15	6	M	0				
				16	1	L	0				
				17	5	L	-1				
				18	10	M	-1				
				19	0	L	0				
				20	4	L	-1				
				21	9	M	0				
				22	0	L	0				
				23	6	M	0				
AVERAGE ERROR			-0.5				-0.74				-1.75
ORDER OF SIGNIFICANCE			=1				3				6

TABLE 3.30(part 2)

DATA SOURCES															
NAYAK & CHRISTENSEN (1971)				SNETHEN (1979)				HOLTZ(1959) - UNDISTURBED DATA				HOLTZ(1959) - REMOLDED DATA			
SPECIMEN NUMBER	GROUP INDEX	SWELL CATEGORY	DEVIATION	SPECIMEN NUMBER	GROUP INDEX	SWELL CATEGORY	DEVIATION	SPECIMEN NUMBER	GROUP INDEX	SWELL CATEGORY	DEVIATION	SPECIMEN NUMBER	GROUP INDEX	SWELL CATEGORY	DEVIATION
1	2	L	-1	1	81	VH	-1	5	27	VH	0	8	1	L	-1
2	6	M	-1	2	36	VH	1	6	25	VH	1	16	0	L	-2
3	14	H	-1	3	68	VH	-1	7	7	M	-2	17	6	M	-1
4	2	L	-1	4	33	VH	1	9	1	L	-1	18	0	L	0
5	8	M	-1	5	35	VH	0	10	0	L	-1	19	0	L	-1
6	20	VH	0	6	11	M	0	11	2	L	-1	20	5	L	-2
7	4	L	-1	7	30	VH	2	12	2	L	-1	21	15	H	-1
8	11	M	-1	8	25	VH	2	13	0	L	0	22	1	L	-1
9	19	VH	1	9	10	M	0	30	0	L	0	23	3	L	-2
10	4	L	-3	10	24	VH	2	31	0	L	0	24	2	L	-2
11	13	H	-2	11	27	VH	2	32	0	L	-1	25	8	M	-2
12	27	VH	-1	12	58	VH	0	50	72	VH	-1	26	1	L	-2
13	3	L	-2	13	22	VH	2	62	5	L	-2	38	1	L	-1
14	11	M	-2	14	35	VH	1	63	9	M	-1	55	4	L	-2
15	28	VH	-1	15	44	VH	1	64	0	L	-1	66	16	M	*
16	6	M	-1	16	10	M	-2	67	15	H	0	68	24	VH	0
17	10	M	-2	17	31	VH	0	69	33	VH	0	70	34	VH	0
18	26	VH	0	18	25	VH	1	71	14	H	0	72	7	M	-2
				19	50	VH	1	73	17	VH	0	75	3	L	-2
				20	42	VH	0	74	17	VH	1				
AVERAGE ERROR			-1.11				0.6				-0.5				-1.33
ORDER OF SIGNIFICANCE			4				2				=1				5

KEY TO ABBREVIATIONS

CAT = predicted swell categories:
L : low ; M : medium ; H : high ; VH : very high ; EH : extremely high

DEV. = deviation of predicted swell category from the base prediction after Dakshanamurthy and Raman(1973)

SPECIMEN NUMBER = identification number allocated by the original author

REFER TO TABLE 3.12 FOR KEY TO DATA SOURCE ABBREVIATIONS

TABLE 3.31(part 1)

EVALUATION OF QUALITATIVE SWELL PREDICTIONS ON THE BASIS OF THE AASHTO GROUP INDEX(METHOD No 2)

DATA SOURCES											
LADD & LAMBE (1961)				SEED ETAL (1962)				RANGANATHAM & SATYANARAYANA (1965)			
SPECIMEN NUMBER	GROUP INDEX	SWELL CATEGORY	DEVIATION	SPECIMEN NUMBER	GROUP INDEX	SWELL CATEGORY	DEVIATION	SPECIMEN NUMBER	GROUP INDEX	SWELL CATEGORY	DEVIATION
1	8	H	-1	1	0	L	-1	1	3	M	-1
2	30	VH	0	2	0	L	-2	2	0	L	-1
3	12	H	0	3	2	M	-2	3	1	L	-2
4	6	H	0	4	0	L	-1	4	6	H	-1
5	12	H	0	5	0	L	-2				
6	24	VH	1	6	6	H	-1				
7	1	L	-1	7	0	L	0				
8	4	M	0	8	0	L	0				
9	0	L	0	9	0	L	0				
10	0	L	0	10	0	L	0				
				11	0	L	0				
				12	-2	H	0				
				13	0	L	0				
				14	-1	M	0				
				15	0	H	1				
				16	0	L	0				
				17	-1	M	0				
				18	-1	H	0				
				19	0	L	0				
				20	-1	M	0				
				21	0	H	1				
				22	0	L	0				
				23	0	H	0				
AVERAGE ERROR			-0.1				-0.26				-1.5
ORDER OF SIGNIFICANCE			2				3				7

TABLE 3.31(part2)

DATA SOURCES															
NAYAK & CHRISTENSEN (1971)				SNETHEN (1979)				HOLTZ (1959) - UNDISTURBED DATA				HOLTZ(1959) - REOLDED DATA			
SPECIMEN NUMBER	GROUP INDEX	SWELL CATEGORY	DEVIATION	SPECIMEN NUMBER	GROUP INDEX	SWELL CATEGORY	DEVIATION	SPECIMEN NUMBER	GROUP INDEX	SWELL CATEGORY	DEVIATION	SPECIMEN NUMBER	GROUP INDEX	SWELL CATEGORY	DEVIATION
1	2	M	0	1	81	VH	-1	5	27	VH	0	8	1	L	-1
2	6	H	0	2	36	VH	1	6	25	VH	1	16	0	L	-2
3	14	VH	0	3	68	VH	-1	7	7	M	2	17	6	H	0
4	2	M	0	4	33	VH	1	9	1	L	-1	18	0	L	0
5	8	H	0	5	35	VH	0	10	0	L	-1	19	0	L	-1
6	20	VH	0	6	11	H	1	11	2	M	0	20	5	H	0
7	4	M	0	7	30	VH	2	12	2	M	0	21	15	VH	0
8	11	H	0	8	25	VH	2	13	0	L	-1	22	1	L	-1
9	19	VH	1	9	10	H	1	30	0	L	0	23	3	M	-1
10	4	M	-2	10	24	VH	0	31	0	L	0	24	2	M	-1
11	13	VH	-1	11	27	VH	2	32	0	L	0	25	8	H	-1
12	27	VH	-1	12	58	VH	0	50	72	VH	0	26	3	M	-1
13	3	M	-1	13	22	VH	2	62	5	H	0	38	1	L	-1
14	11	H	-1	14	35	VH	1	63	9	H	0	55	4	M	-1
15	28	VH	-1	15	44	VH	1	64	0	L	-1	66	16	VH	*
16	6	H	0	16	10	H	-1	67	15	VH	1	68	24	VH	0
17	10	H	-1	17	31	VH	0	69	33	VH	0	70	34	VH	0
18	26	VH	0	18	25	VH	1	71	14	VH	1	72	7	H	-1
				19	50	VH	1	73	17	VH	0	75	3	M	-1
				20	42	VH	0	74	17	VH	0				
AVERAGE ERROR			-0.38				0.65				0.05				-0.72
ORDER OF SIGNIFICANCE			4				5				1				6

KEY TO ABBREVIATIONS

CAT = predicted swell categories:
L : low ; M : medium ; H : high ; VH : very high ; EH : extremely high

DEV. = deviation of predicted swell category from the case prediction after Dakshanamurthy and Raman(1973)

SPECIMEN NUMBER = identification number allocated by the original author

REFER TO TABLE 3.12 FOR KEY TO DATA SOURCE ABBREVIATIONS

TABLE 3.32

POTENTIAL SWELL ON THE BASIS OF AASHTO GROUP INDEX, METHOD No 1

GROUP INDEX	POTENTIAL SWELL
0-5.5	LOW
5.5-11.5	MEDIUM
11.5-16	HIGH
>16	VERY HIGH

TABLE 3.33

POTENTIAL SWELL ON THE BASIS OF AASHTO GROUP INDEX-METHOD no 2.

GROUP INDEX	PROBABLE DEGREE OF SWELL
0-1	LOW
1-5	MEDIUM
5-12	HIGH
>12	VERY HIGH

TABLE 3.34

UNIFIED SOIL CLASSIFICATION SYTEM(USCS) ENGINEERING USE CHART.

Major Divisions (1)	(2)	Letter* (3)	Name (4)	Value as Subgrade When Not Subject to Frost Action (5)	Potential Frost Action (6)	Compressibility and Expansion (7)	Drainage Characteristics (8)
COARSE-GRAINED SOILS	GRAVEL AND GRAVELLY SOILS	GW	Well-graded gravels or gravel-sand mixture, little or no fines	Excellent	None to very slight	Almost none	Excellent
		GP	Poorly graded gravels or gravel-sand mixtures little or no fines	Good to excellent	None to very slight	Almost none	Excellent
		GM d	Silty gravels, gravel-sand-silt mixtures	Good to excellent	Slight to medium	Very slight	Fair to poor
		GM u		Good	Slight to medium	Slight	Poor to practically impervious
		GC	Clayey gravels, gravel-sand clay mixtures	Good	Slight to medium	Slight	Poor to practically impervious
	SAND AND SANDY SOILS	SW	Well-graded sands or gravelly sands, little or no fines	Good	None to very slight	Almost none	Excellent
		SP	Poorly graded sands or gravelly sands, little or no fines	Fair to good	None to very slight	Almost none	Excellent
		SM d	Silty sands, sand-silt mixtures	Fair to good	Slight to high	Very slight	Fair to poor
		SM u		Fair	Slight to high	Slight to medium	Poor to practically impervious
		SC	Clayey sands, sand-clay mixtures	Poor to fair	Slight to high	Slight to medium	Poor to practically impervious
FINE-GRAINED SOILS	SILTS AND CLAYS LL IS LESS THAN 50	ML	Inorganic silts and very fine sands, rock flour, silty or clayey fine sands or clayey silts with slight plasticity	Poor to fair	Medium to very high	Slight to medium	Fair to poor
		CL	Inorganic clays of low to medium plasticity, gravelly clays, sandy clays, silty clays, lean clays	Poor to fair	Medium to high	Medium	Practically impervious
		OL	Organic silts and organic silt-clays of low plasticity	Poor	Medium to high	Medium to high	Poor
	SILTS AND CLAYS LL IS 50 OR GREATER	MH	Inorganic silts, micaceous or diatomaceous fine sandy or silty soils, elastic silts	Poor	Medium to very high	High	Fair to poor
		CH	Inorganic clays to high plasticity, fat clays	Poor to fair	Medium	High	Practically impervious
		OH	Organic clays of medium to high plasticity organic silts	Poor to very poor	Medium	High	Practically impervious
HIGHLY ORGANIC SOILS		Pt	Peat and other highly organic soils	Not suitable	Slight	Very high	Fair to poor

* (1) Subdivision of GM and SM groups is for road and airfield materials. Designation d applied to soils with LL = 25 and PI = 5. Designation u to others.

TABLE 3.35

EXTENDED CASAGRANDES SOIL CLASSIFICATION SYSTEM

Major Divisions		*Description and Field Identification*	*Subgroups*	*Group Symbol*	*Applicable Classification Tests (Carried out on Disturbed Samples)*	*Applicable Observations and Tests Relating to the Material in Place (or carried out on Undisturbed Samples)*	*Shrinkage or Swelling Properties*
COARSE-GRAINED SOILS	Boulders and cobbles	Soils consisting chiefly of boulders larger than 8 in. in diameter or cobbles between 8 in. and 3 in. identifiable by visual inspection.	Boulder gravels	—	Particle-size analysis	Dry density and relative compaction	Almost none
	Gravel and gravelly soils	Soils with an appreciable fraction between the 3 in. and No. 7 B.S. sieves. Generally easily identifiable by visual inspection. A medium to high dry strength indicates that some clay is present. A negligible dry strength indicates the absence of clay.	Well graded gravel-sand mixtures, little or no fines	G W	Particle-size analysis	Moisture content and voids ratio	Almost none
			Well graded gravel-sands with small clay content	G C	Particle-size analysis, liquid and plastic limits on binder	Cementation Durability of grains	Very slight
			Uniform gravel with little or no fines	G U	Particle-size analysis	Stratification and drainage characteristics	Almost none
			Poorly graded gravel-sand mixtures, little or no fines	G P	Particle-size analysis		Almost none
			Gravel-sand mixtures with excess of fines	G F	Particle-size analysis, liquid and plastic limits on binder if applicable	Groundwater conditions	Almost none to slight
	Sands and sandy soils	Soils with an appreciable fraction between the No. 7 and the No. 200 B.S. sieve. Majority of the particles can be distinguished by eye. Feel gritty when rubbed between the fingers. A medium to high dry strength indicates that some clay is present. A negligible dry strength indicates absence of clay.	Well graded sands and gravelly sands, little or no fines	S W	Particle-size analysis	Large-scale loading tests	Almost none
			Well graded sands with small clay content	S C	Particle-size analysis, liquid and plastic limits on binder	California bearing ratio tests, shear tests and other strength tests	Very slight
			Uniform sands, with little or no fines	S U	Particle-size analysis		Almost none
			Poorly graded sands, with little or no fines	S P	Particle-size analysis		Almost none
			Sands with excess of fines	S F	Particle-size analysis, liquid and plastic limits on binder if applicable		Almost none to medium
FINE-GRAINED SOILS Containing little or no coarse-grained material	Fine-grained soils having low plasticity (silts)	Soils with an appreciable fraction passing the No. 200 B.S. sieve, and with liquid limits less than 35. Not gritty between the fingers. Cannot be readily rolled into threads when moist. Exhibit dilatancy.	Silts (inorganic) rock flour, silty fine sands with slight plasticity	M L	Particle-size analysis, liquid and plastic limits if applicable	Dry density and relative compaction	Slight to medium
			Clayey silts (inorganic)	C L	Liquid and plastic limits		Medium
			Organic silts of low plasticity	O L	Liquid and plastic limits from natural conditions and after oven-drying	Moisture content and void ratio	Medium to high
	Fine-grained soils having medium plasticity	Soils with liquid limits between 35 and 50. Can be readily rolled into threads when moist. Do not exhibit dilatancy. Show some shrinkage on drying.	Silty clays (inorganic) and sandy clays	M I	Particle-size analysis, liquid and plastic limits if applicable	Stratification, fissures, etc.	Medium to high
			Clays (inorganic) of medium plasticity	C I	Liquid and plastic limits	Drainage and groundwater conditions	High
			Organic clays of medium plasticity	O I	Liquid and plastic limits from natural conditions and after oven-drying	Consolidation tests	High
	Fine-grained soils having high plasticity	Soils with liquid limits greater than 50. Can be readily rolled into threads when moist. Greasy to the touch. Show considerable shrinkage on drying. All highly compressible soils.	Highly compressible micaceous or diatomaceous soils	M H	Particle-size analysis, liquid and plastic limits if applicable	Large-scale loading tests	High
			Clays (inorganic) of high plasticity	C H	Liquid and plastic limits	California bearing ratio tests, shear tests and other strength tests	High
			Organic clays of high plasticity	O H	Liquid and plastic limits from natural conditions and after oven-drying		High
Fibrous organic soils with very high compressibility		Usually brown or black in colour. Very compressible. Easily identifiable visually.	Peat and other highly organic swamp soils	Pt	Moisture content	and consolidation tests	Very high

* These unit weights apply only to soils with specific gravities ranging between 2.65 and 2.75

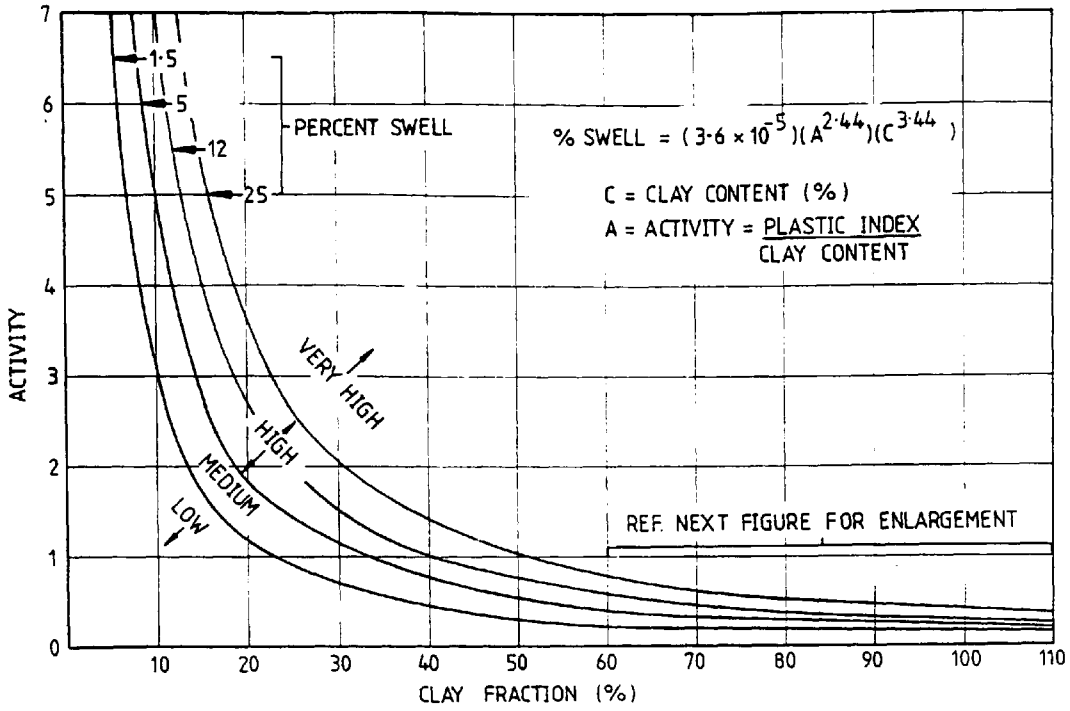

FIGURE 3.1(a)

SWELL POTENTIAL PREDICTION CHART
AFTER SEED ET AL.(1962) -
FULL RANGE.

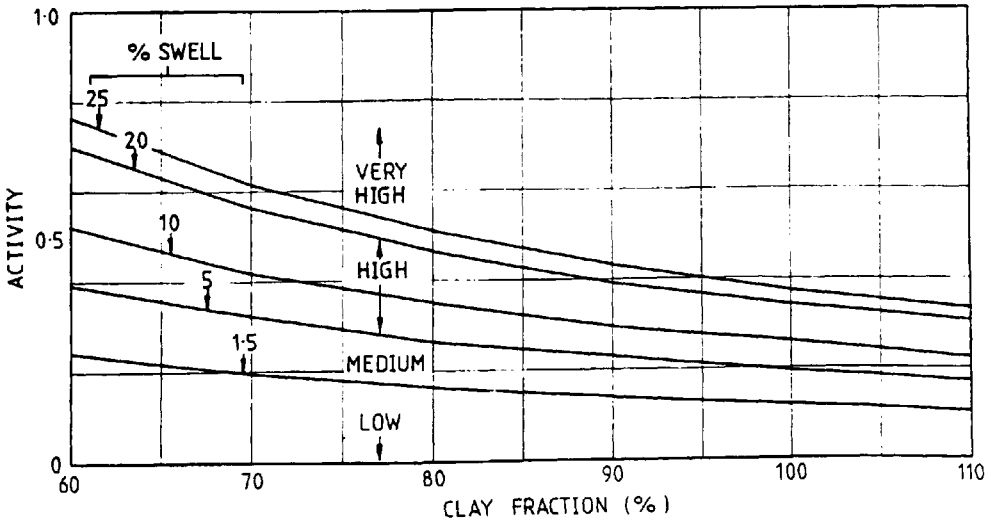

FIGURE 3.1(b)

SWELL POTENTIAL PREDICTION CHART
AFTER SEED ETAL.(1962) -
ENLARGED SECTION.

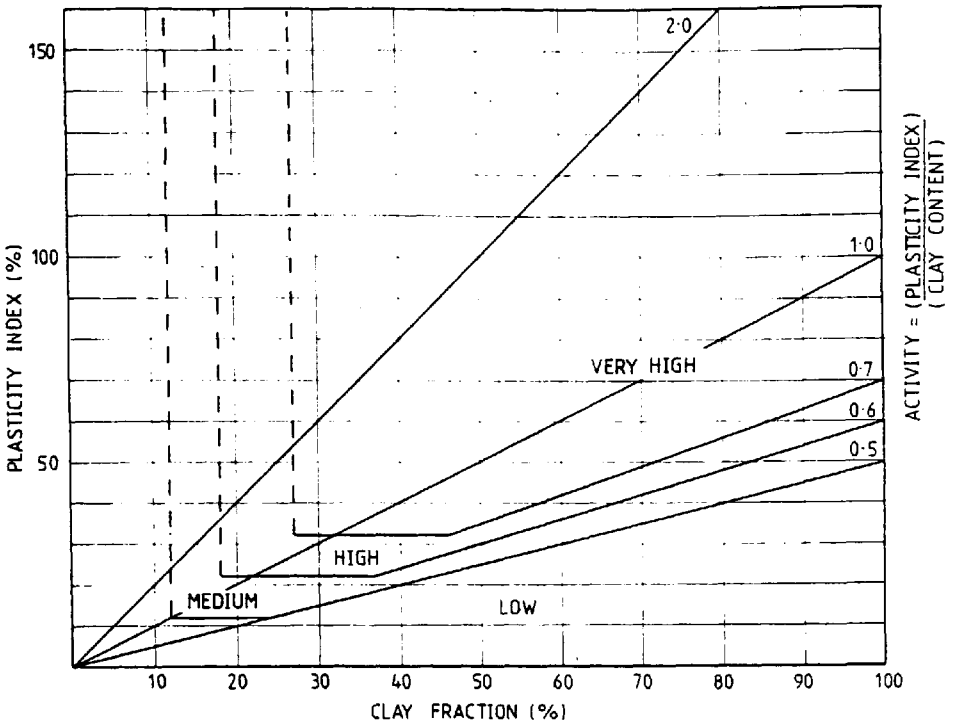

FIGURE 3.2

ACTIVITY CHART FOR SWELL PREDICTION
AFTER VAN DER MERWE (1975)

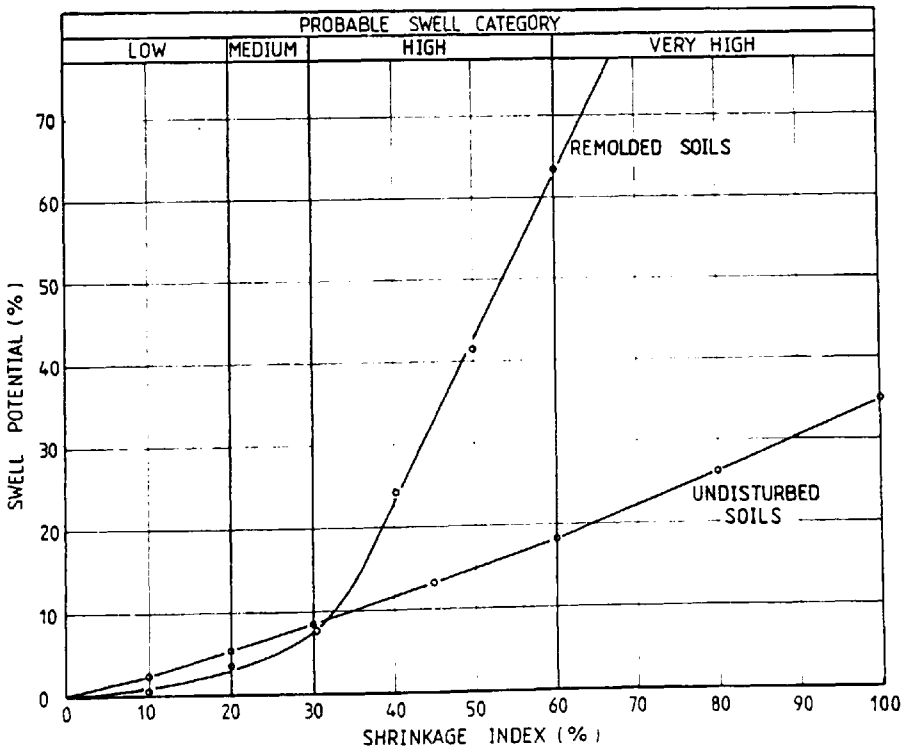

FIGURE 3.3

SWELL POTENTIAL PREDICTION CHART
AFTER RANGANATHAM & SATYANARAYANA(1965)

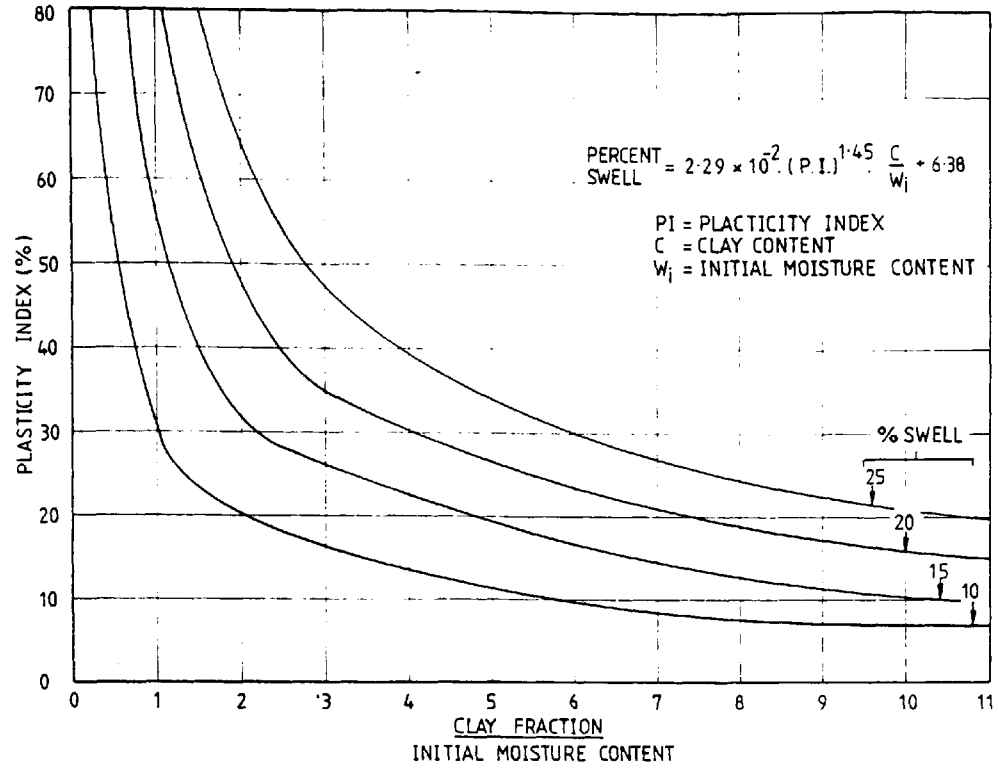

FIGURE 3.4

POTENTIAL SWELL PREDICTION CHART
AFTER NAYAK & CHRISTENSEN(1973)

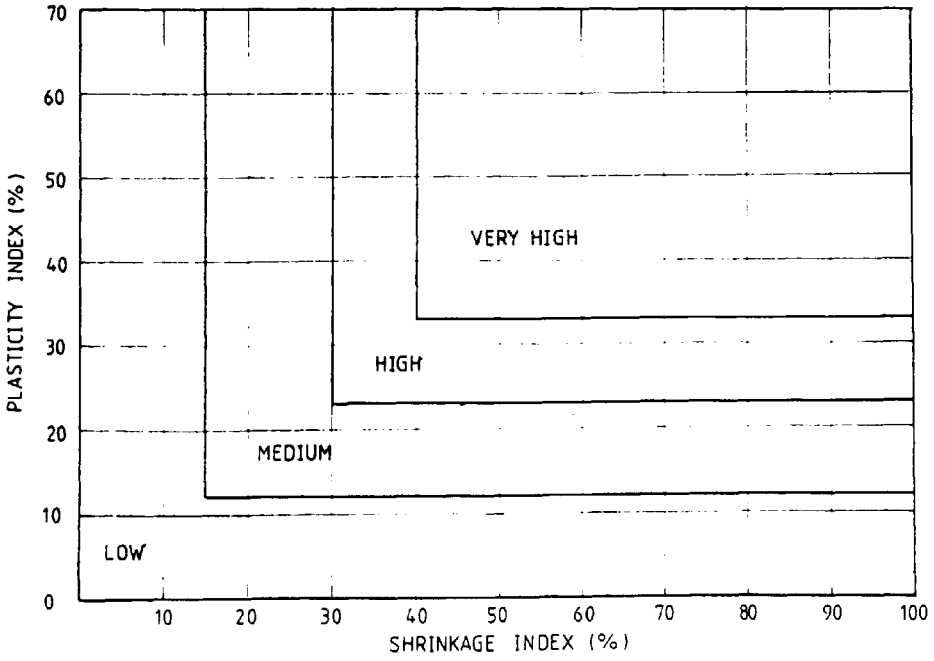

FIGURE 3.5

POTENTIAL SWELL PREDICTION CHART
AFTER RAMAN(1967)

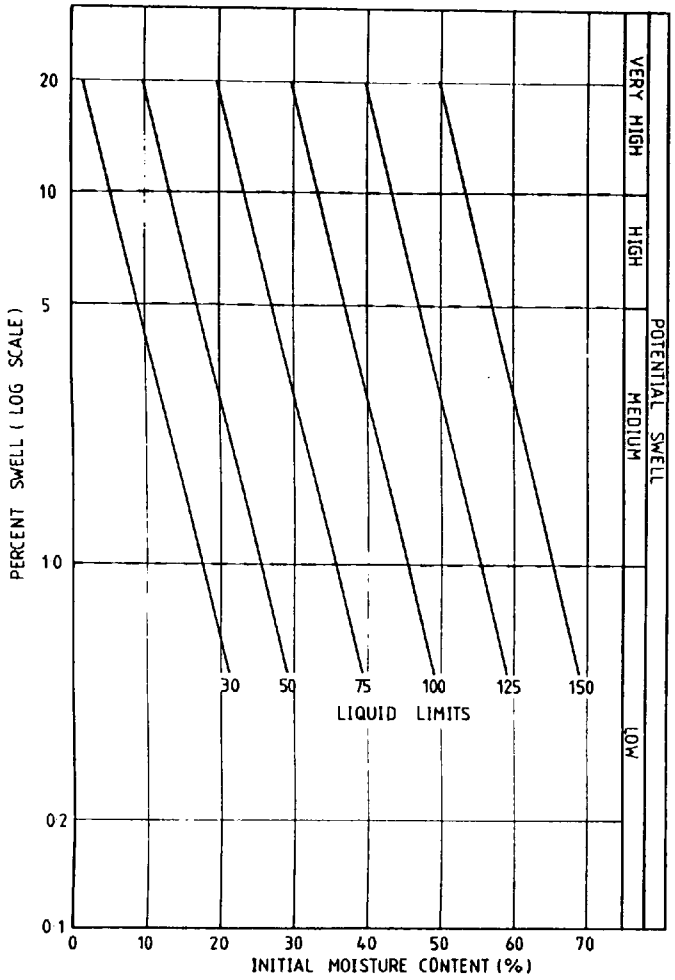

FIGURE 3.6(a)

POTENTIAL SWELL PREDICTION CHART
BASED ON INITIAL MOISTURE CONTENT
AFTER VIJAYVERGIYA & GHAZZALY(1973)

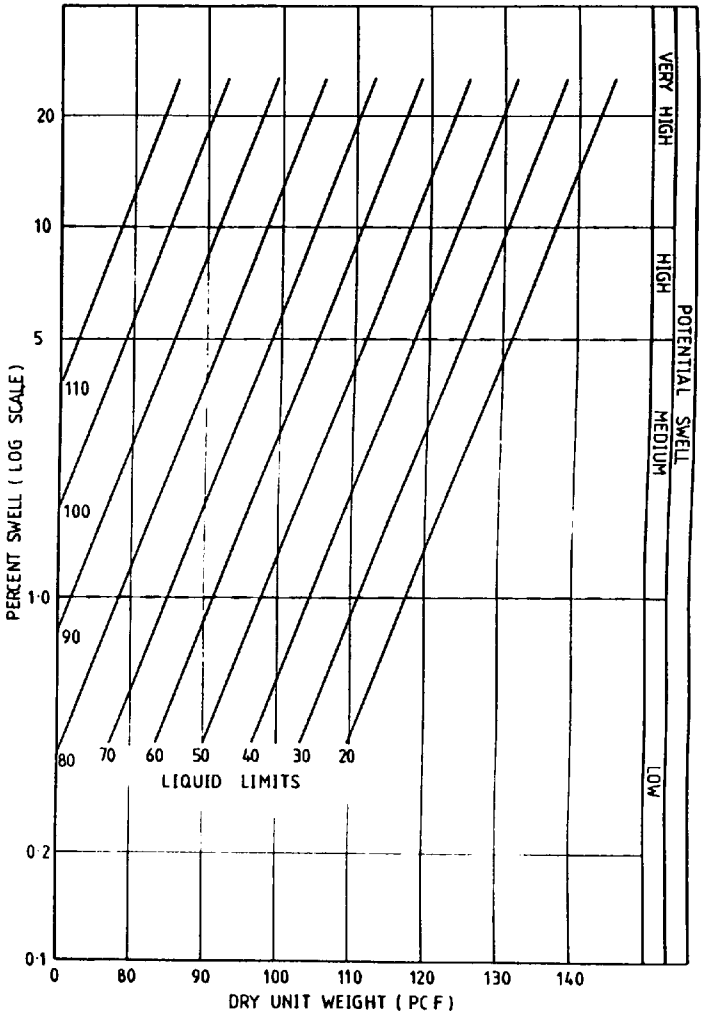

FIGURE 3.6(b)

POTENTIAL SWELL PREDICTION CHART
BASED ON INITIAL DRY UNIT WEIGHT
AFTER VIJAYVERGIYA & GHAZZALY(1973)

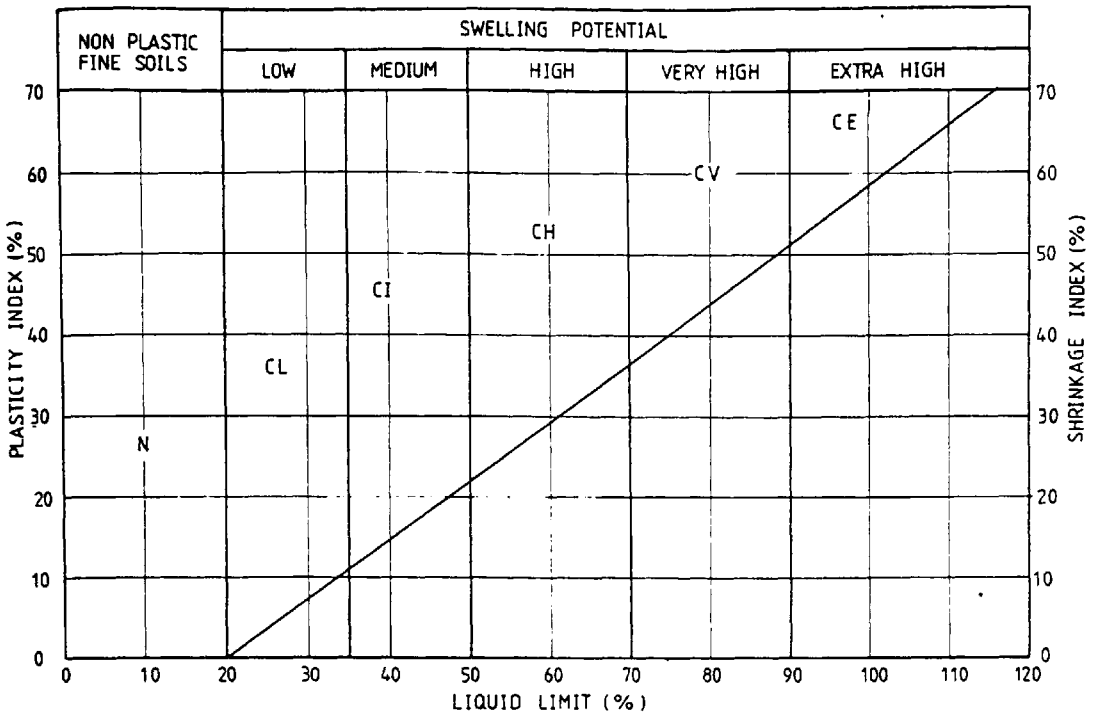

FIGURE 3.7

POTENTIAL SWELL PREDICTION CHART
AFTER DAKSHANAMURTHY & RAMAN(1973)

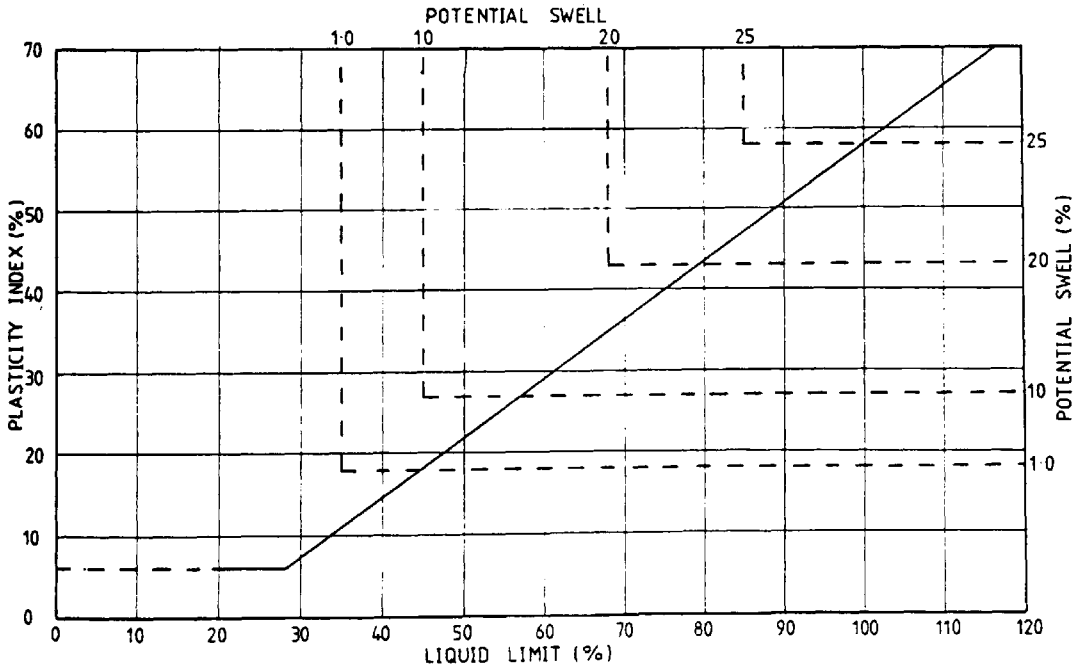

FIGURE 3.8

PROPOSED POTENTIAL SWELL PREDICTION CHART
BASED ON CASAGRANDES PLASTICITY CHART
- BY THE AUTHOR

KEY TO SWELL PREDICTION SYSTEMS:

1. HOLTZ
2. SEED ETAL
3. RANGANATHAM & SATYANARAYANA
4. RAMAN
5. VIJAYVERGIYA & GHAZZALY ($\gamma_d + W_l$)
6. VIJAYVERGIYA & GHAZZALY ($W_o + W_l$)
7. VAN DER MERWE
8. BUILDING RESEARCH ESTABLISHMENT
9. UNIFIED SOIL CLASSIFICATION SYSTEM
10. EXTENDED CASAGRANDES SYSTEM

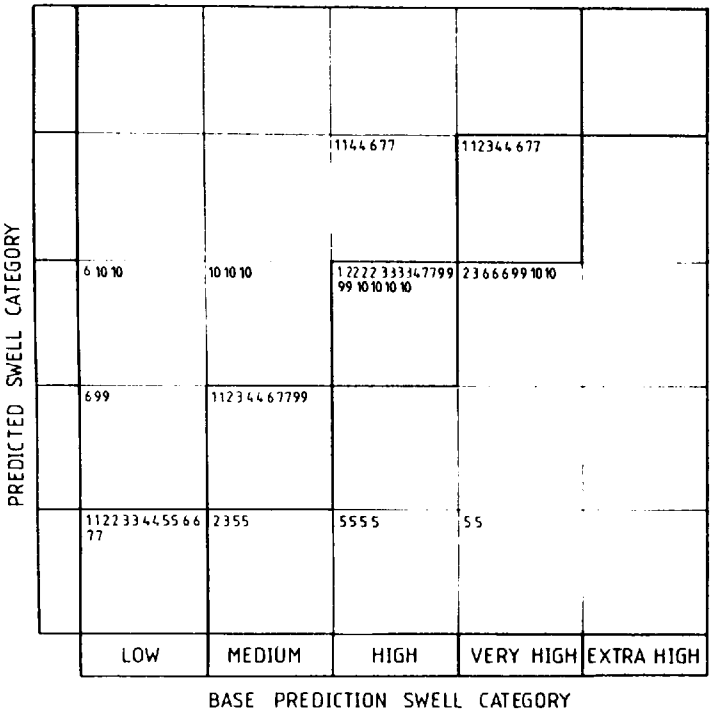

FIGURE 3.9

GRAPH COMPARING PREDICTED AGAINST BASE SWELL CATEGORIES.
DATA AFTER LADD & LAMBE(1961)

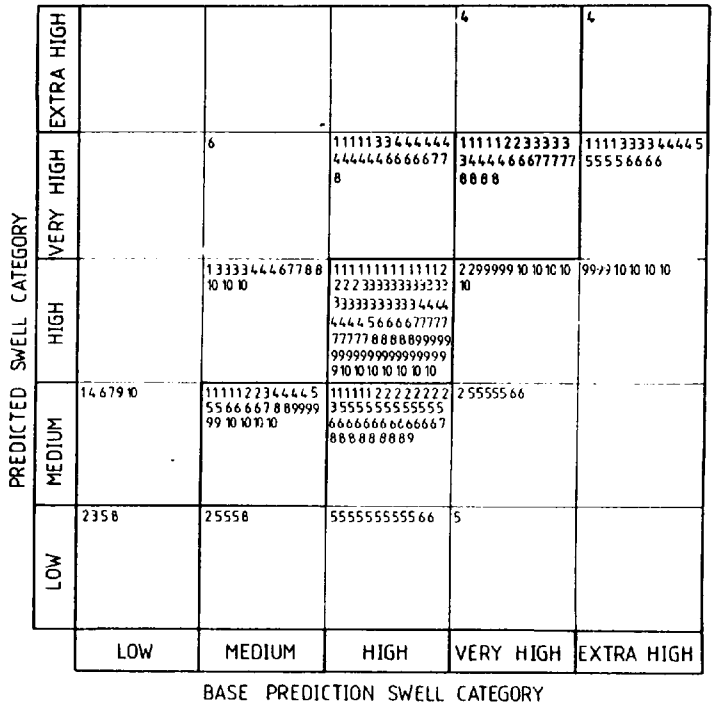

FIGURE 3.10

GRAPH COMPARING PREDICTED AGAINST BASE SWELL CATEGORIES.
DATA AFTER HOLTZ(1959)-REMOLDED SOILS

KEY TO SWELL PREDICTION SYSTEMS

1. HOLTZ
2. SEED ET AL
3. RANGANATHAM & SATYANARAYANA
4. RAMAN
5. VIJAYVERGIYA & GHAZZALY ($J_d + W_l$)
6. VIJAYVERGIYA & GHAZZALY ($W_o + W_l$)
7. VAN DER MERWE
8. BUILDING RESEARCH ESTABLISHMENT
9. UNIFIED SOIL CLASSIFICATION SYSTEM
10. EXTENDED CASAGRANDES SYSTEM

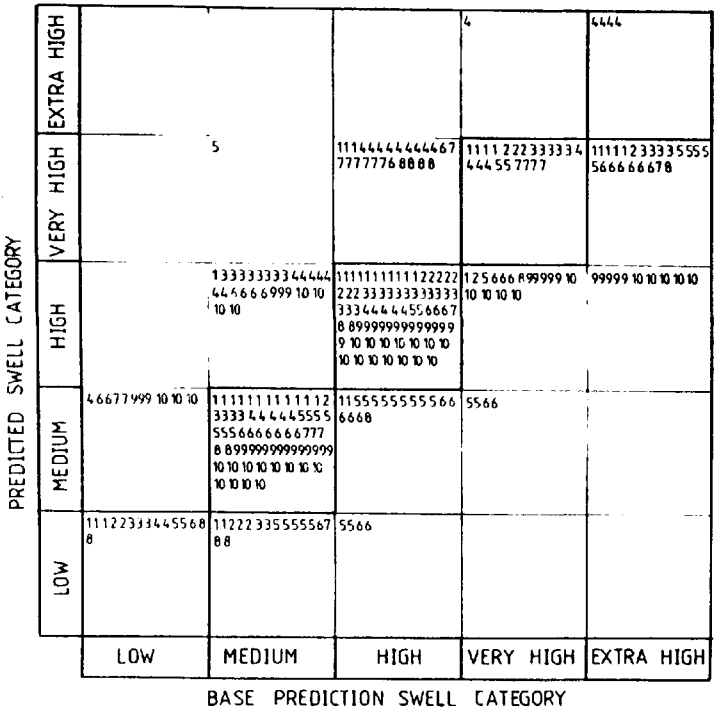

FIGURE 3.11

GRAPH COMPARING PREDICTED AGAINST BASE SWELL CATEGORIES. DATA AFTER HOLTZ(1959)-UNDISTURBED SOILS

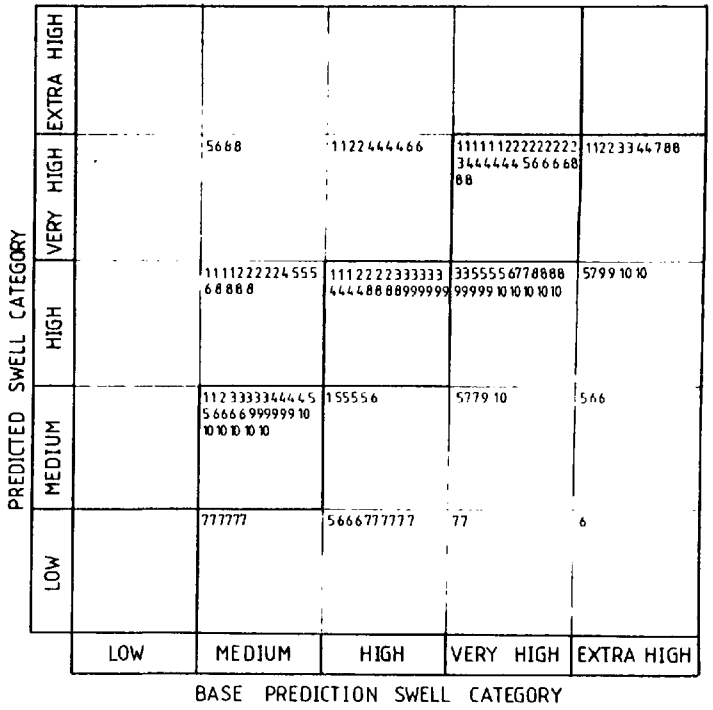

FIGURE 3.12

GRAPH COMPARING PREDICTED AGAINST BASE SWELL CATEGORIES. DATA AFTER SNETHEN(1979)

FIGURE 3.13

GRAPH COMPARING ACTUAL AGAINST
PREDICTED PERCENT SWELL.
DATA AFTER HOLTZ(1959)-REMOLDED SOILS

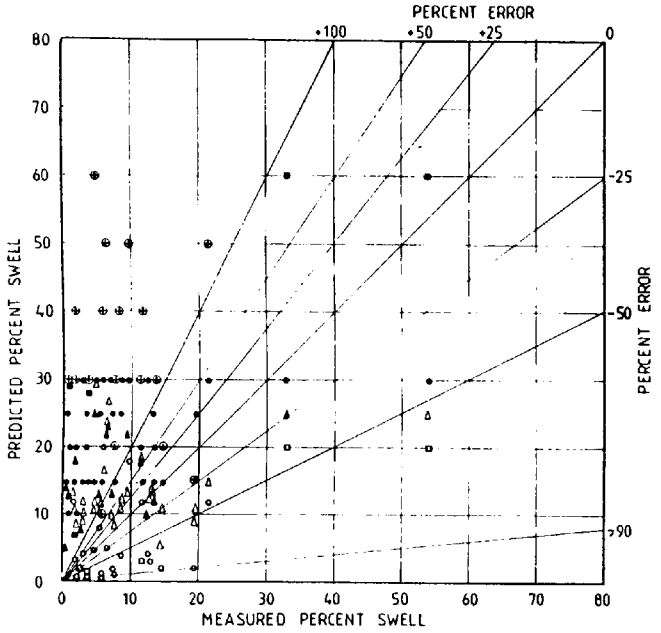

FIGURE 3.15

GRAPH COMPARING ACTUAL AGAINST
PREDICTED PERCENT SWELL.
DATA AFTER LADD & LAMBE(1961)

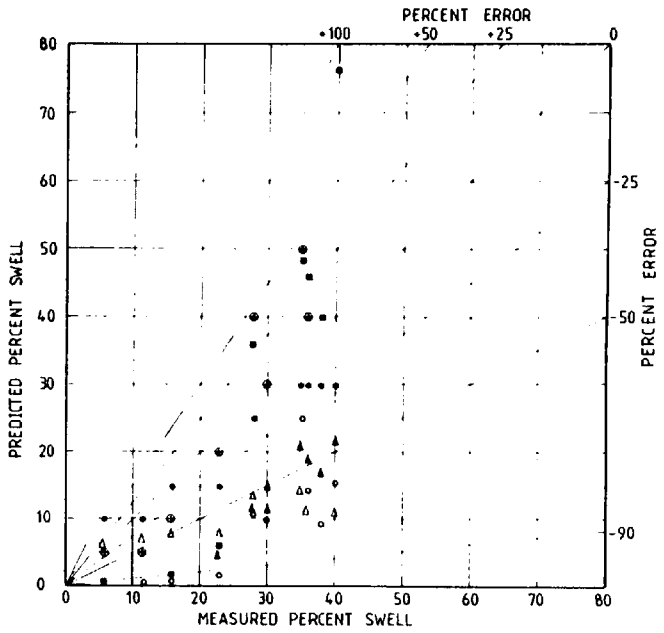

ADDITIONAL DETAILS

$$\text{PERCENT ERROR} = \left(\frac{\text{PREDICTED SWELL} \sim \text{MEASURED SWELL}}{\text{MEASURED SWELL}} \right)$$

KEY TO SWELL PREDICTION SYSTEMS

- • HOLTZ
- ○ SEED ET AL
- ▪ RANGANATHAM & SAYANARAYANA
- ▫ VIJAYVERGIYA & GHAZZALY (γ_d , W_i)
- ▲ WILLIAMS
- △ NAYAK & CHRISTENSEN
- ✱ CIVIL AVIATION AUTHORITY

FIGURE 3.14

GRAPH COMPARING ACTUAL AGAINST
PREDICTED PERCENT SWELL.
DATA AFTER HOLTZ(1959)-UNDISTURBED SOILS

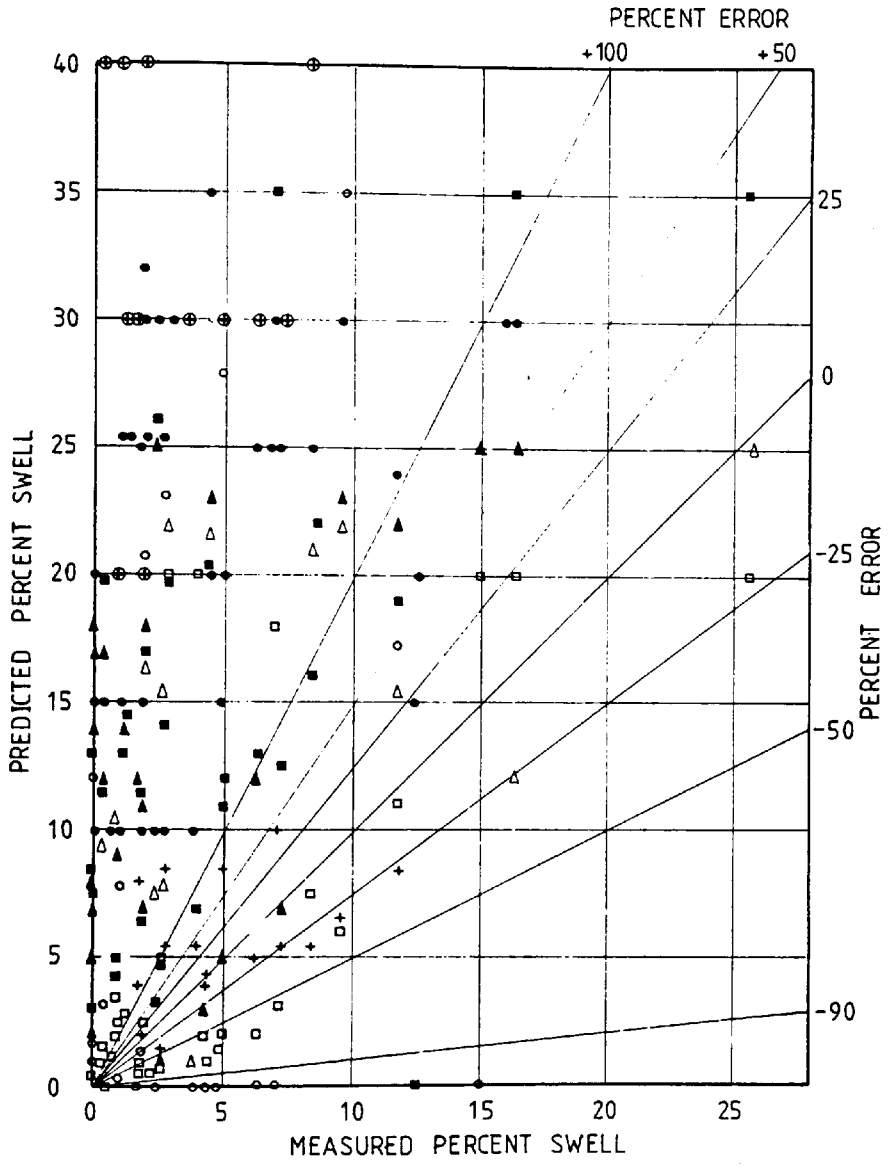

KEY TO SWELL PREDICTION SYSTEMS

- • HOLTZ
- ○ SEED ET AL
- ■ RANGANATHAM & SATYANARAYANA
- ▲ WILLIAMS
- □ VIJAYVERGIYA & GHAZZALY ($\gamma_d + W_l$)
- + VIJAYVERGIYA & GHAZZALY ($W_o + W_l$)
- ▲ NAYAK & CHRISTENSEN
- ⊕ CIVIL AVIATION AUTHORITY

$$\text{PERCENT ERROR} = \left(\frac{\text{PREDICTED SWELL} \frown \text{MEASURED SWELL}}{\text{MEASURED SWELL}} \right)$$

FIGURE 3.16

TRIANGULAR TEXTURAL CLASSIFICATION CHART
(a):PIETKOWSKI
(b):PUBLIC ROADS ADMINISTRATION

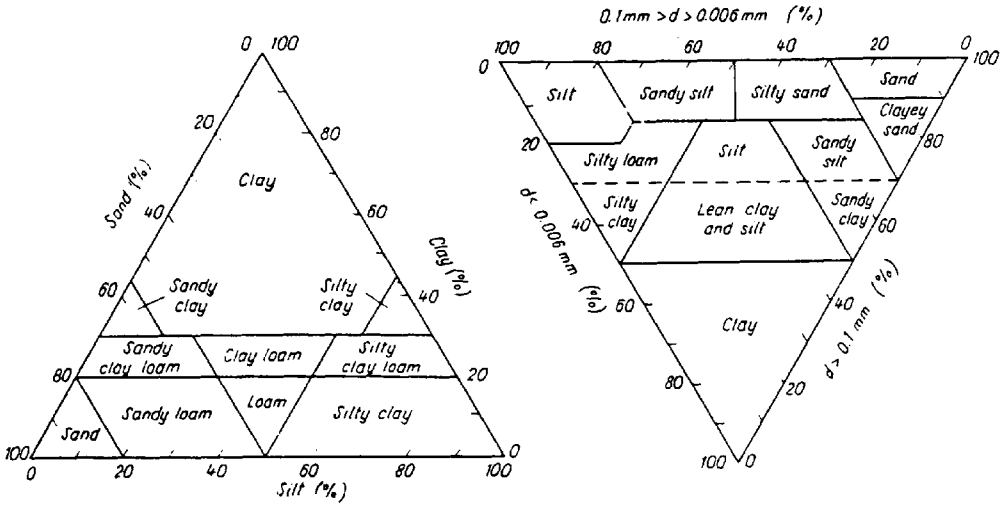

(a) (b)

FIGURE 3.17

CASAGRANDES PLASTICITY CHART

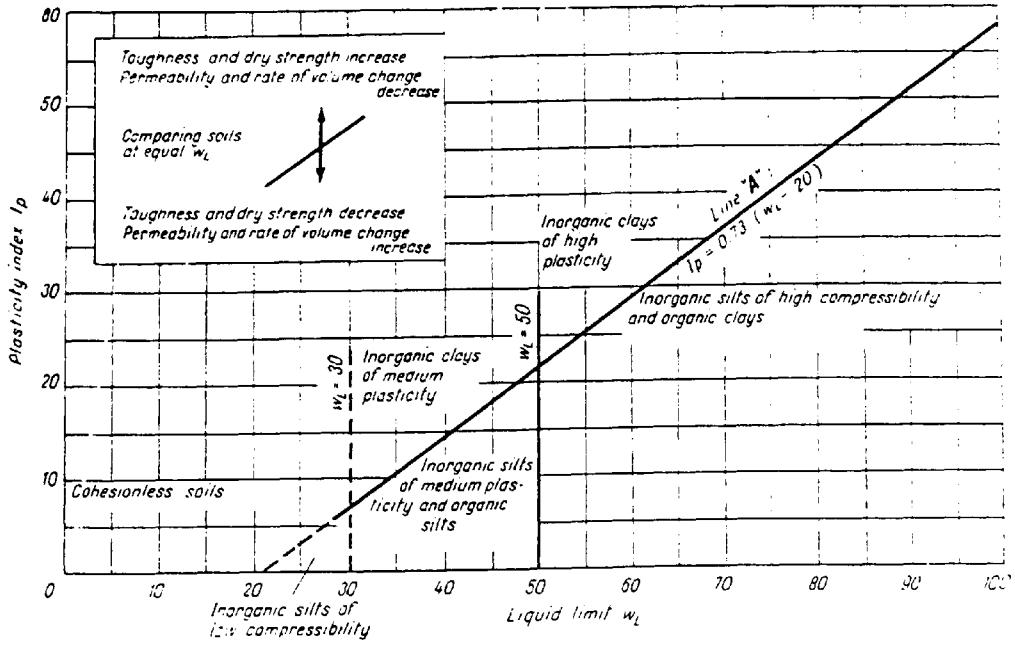

FIGURE 3.18

PROPOSED PLASTICITY CHART FOR
SWELL PREDICTION (AUTHOR)

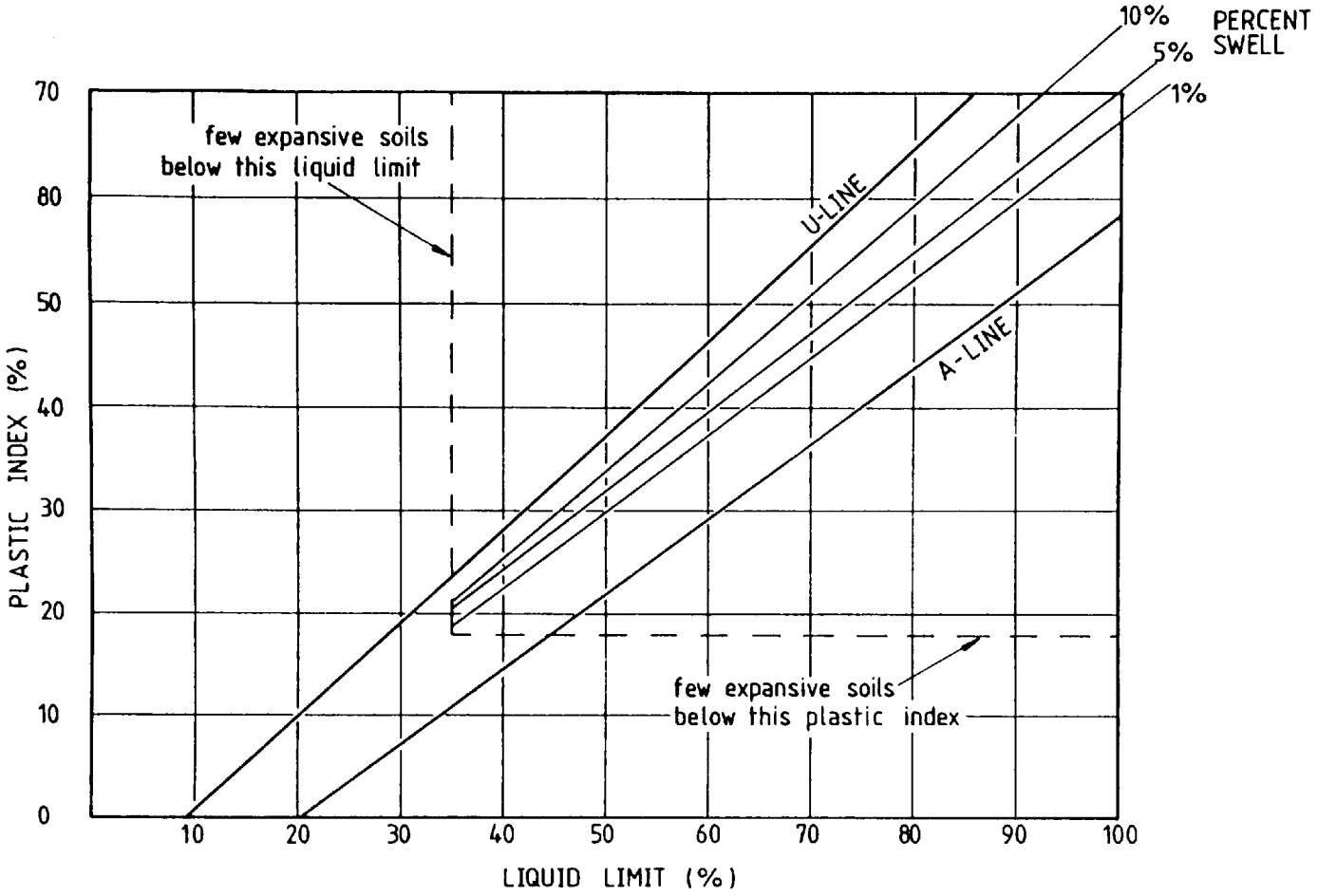

FIGURE 3.19

AASHTO PLASTICITY CHART

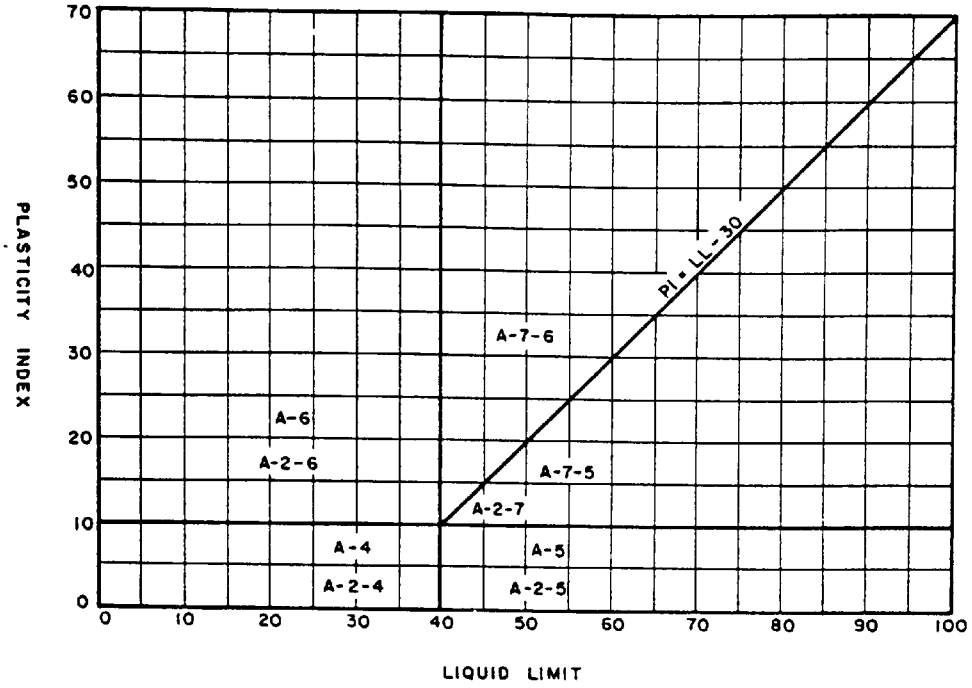

FIGURE 3.20

AASHTO GROUP INDEX CHART

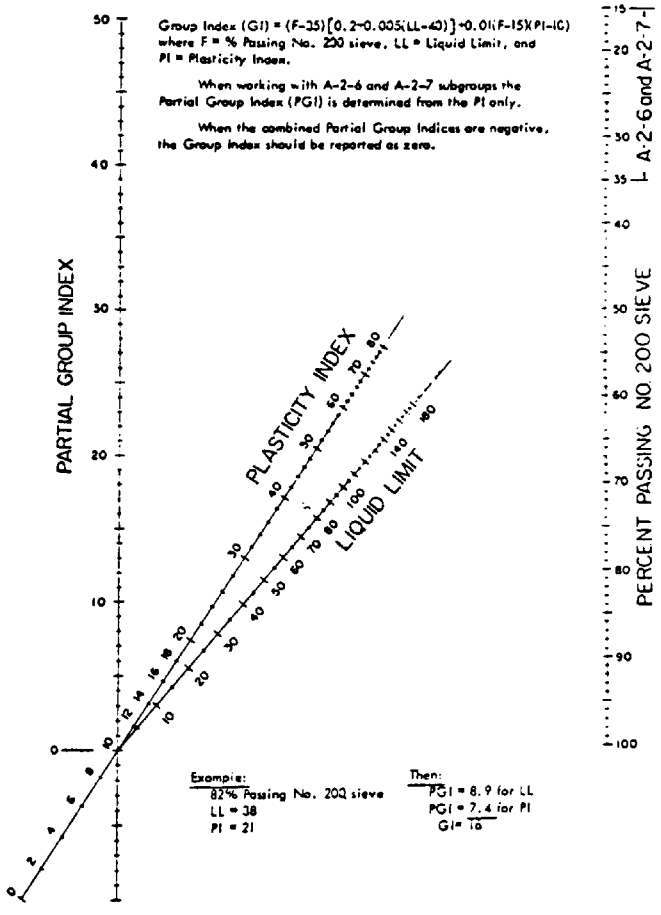

FIGURE 3.21

GRAPH COMPARING AASHTO GROUP INDICIES AGAINST PERCENT SWELL

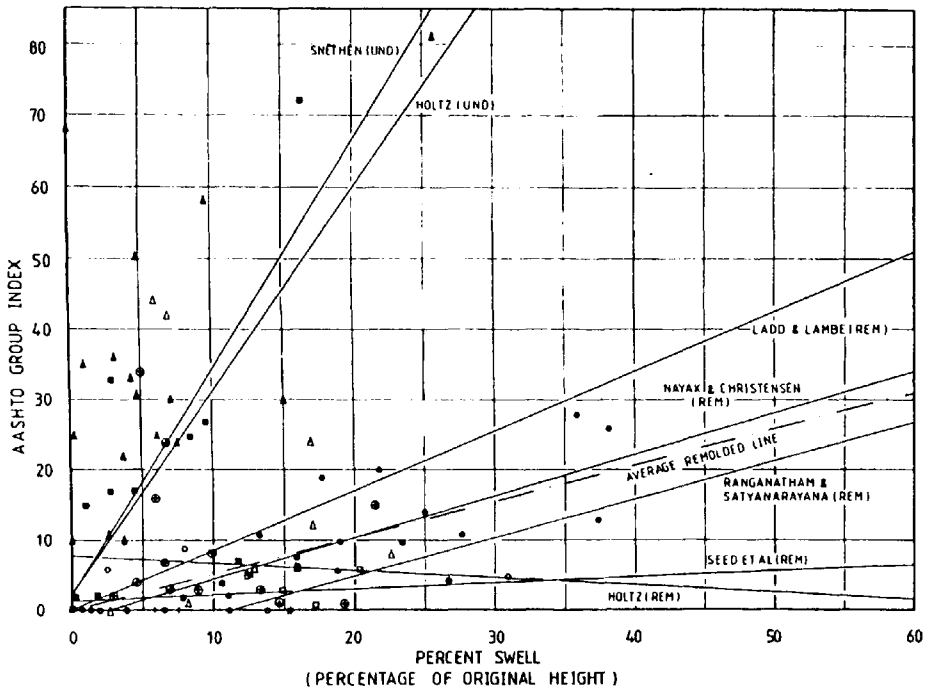

FIGURE 3.22

GRAPH COMPARING AASHTO GROUP INDICIES AGAINST SWELL PRESSURE

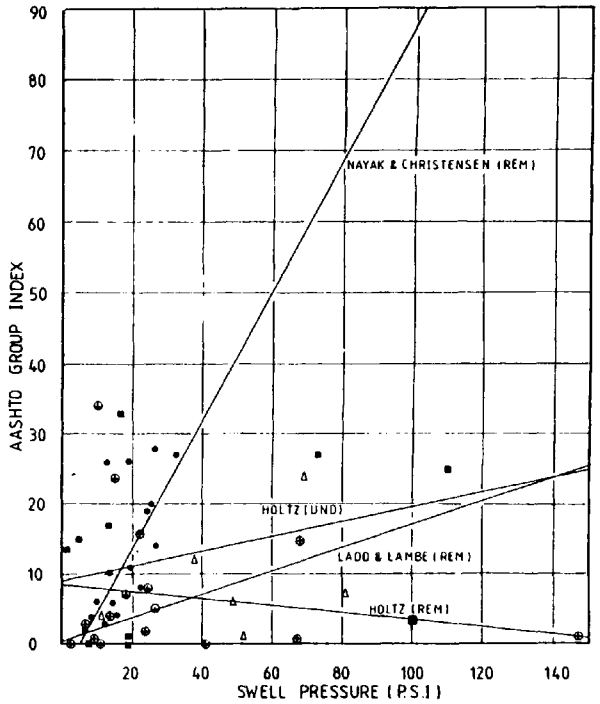

KEY TO DATA

- ▫ RANGANATHAM & SATYANARAYANA
- ○ SEED ET AL
- △ LADD & LAMBE
- ● HOLTZ REMOLDED (SOILS)
- ▪ HOLTZ (UNDISTURBED SOILS)
- • NAYAK & CHRISTENSEN
- ▲ SNETHEN (UNDISTURBED SOILS)

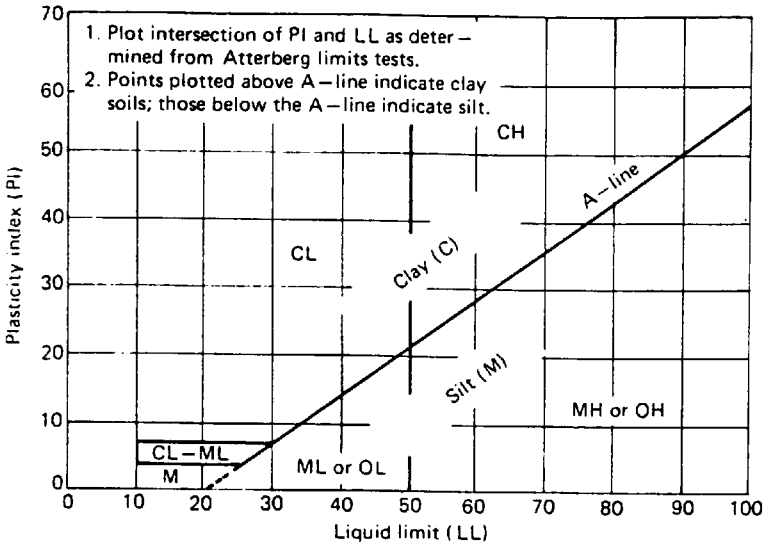

FIGURE 3.23

UNIFIED SOIL CLASSIFICATION SYSTEM
PLASTICITY CHART

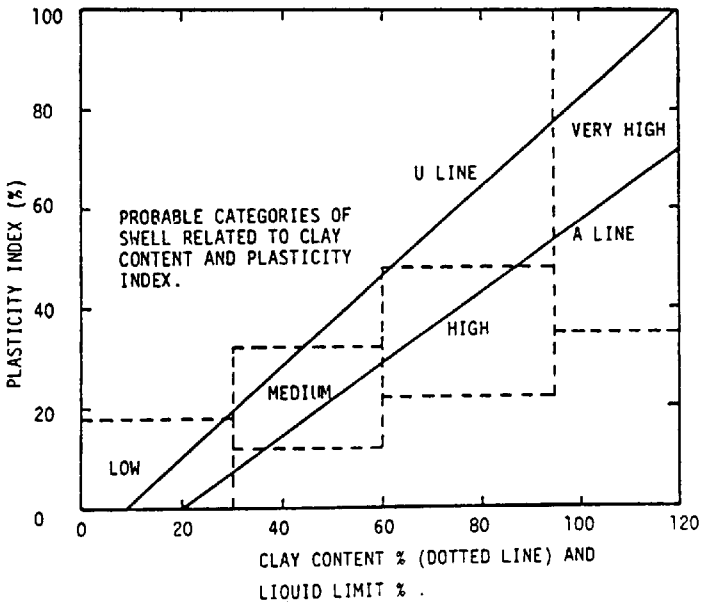

FIGURE 3.24

GRAPHICAL PRESENTATION OF THE B.R.E.
SWELL PREDICTION METHOD (author)

CHAPTER 4

A THEORY FOR DESCRIBING THE VOLUMETRIC BEHAVIOUR OF UNSATURATED SOILS

4.1 INTRODUCTION

4.1.1 Summary

The relationship between soil and water significantly affects the engineering behaviour of clay soils. It is therefore important to know how water is held in soils and how its influence can be measured, in order to understand volumetric behaviour.

This chapter summarises the various approaches developed for modelling soil behaviour and indicates the advantages of employing an 'effective stress' type approach even in unsaturated soils. Fredlund's theory is chosen as the most suitable, and its derivation quoted in some detail due to the relatively new approach of this work.

The theory is then critically appraised, and recommendations made of possible experimental verification and theoretical development.

4.1.2 Modelling soil-water behaviour

Three broad approaches are identified in the description of soil-water behaviour, these are the model, energy/ thermodynamic and electrical charge approaches.

The 'model approach' attempts to describe the geometry of the soil structure and can be employed to either determine the shape of the pore water films and amount of void air, or, relate the mechanical behaviour of the soil to the applied stresses. This follows logically from Terzaghi's effective stress principle.

The energy approach considers not the soil geometry but rather the total energy of the system and in particular, the energy with which water is held within a soil. Initially developed by Buckingham (1907) and subsequently modified by various agricultural scientists, the approach has been adopted by Croney et al, Aitchison and Jennings particularly in the field of unsaturated soils.

The electrical charge approach considers soil behaviour (in this case expansion) in terms of the attractive and repulsive electrical charges at interparticle level.

The prime causes are: 1. osmotic repulsion, 2. clay particle attraction and 3. cation hydration secondary forces resulting from VanderWaals forces, capillary imbibition and elastic relaxation (refer to Chapter 2 for fuller details).

4.1.3 Salient points

(a) The electrical charge approach is not presently suited for the general description of engineering soil behaviour. The difficulties resulting from an experimental and theoretical investigation are considered beyond the scope of this project.

(b) The energy/thermodynamic approach is receiving increased attention, particularly with regard to soil volume changes under in-situ conditions.

The present lack of theoretical development limits its engineering application, thus it is only considered of limited use to this project.

(c) The model approach appears to be the most suitable for application to unsaturated soils. The 'effective stress' method is widely accepted for prediction of the mechanical behaviour of saturated soil. Several modifications of this have been proposed for application to unsaturated soils but have met with limited success.

The model (or 'effective stress') approach will therefore be examined in greater detail.

4.2 THE ROLE OF EFFECTIVE STRESS AND STRESS STATE VARIABLES IN VOLUMETRIC SOIL BEHAVIOUR

4.2.1 Saturated soils

Terzaghi (1936) was the first to propose the effective stress principle. When a load is applied to a saturated soil it will be carried by the water in the soil voids (causing an increase in pore water pressure) or by the soil skeleton (grain-grain contact stresses) or be shared by both the water and soil skeleton.

The effect of load upon a soil depends upon the drainage conditions, and generally, the effective stress has been shown to be approximately equal to the intergranular stress and is given by equation (4.1).

i.e.

$$\sigma' = \sigma - u_w \qquad (4.1)$$

σ' = effective stress; σ = total stress; u_w = pore water pressure. The validity of the effective stress equation with regard to saturated soil behaviour is experimentally verified by Rendulic 1936; Bishop and Eldin 1950; Laughton 1955).

Bishop and Eldin (1950) suggest that shear strength behaviour is dependent upon intergranular contact area whereas volumetric change is not, and thus propose that the two mechanisms be treated separately.

Skempton (1960) presents a detailed analysis to support the effective stress concept with regard to saturated soils and reinforces Bishop and Eldin's separate treatment of volume change and shear strength change. His expressions are as follows :

$$\text{Shear strength} \quad \sigma' = \sigma - \left(1 - \frac{a \tan\psi}{\tan\phi'}\right) u_w \qquad (4.2)$$

σ'= effective stress; σ = total stress; a = area of contact; ψ = < intrinsic friction; ϕ' = angle of shearing resistance; u_w = pore water pressure.

$$\text{Volume change} \quad \Delta\sigma' = \Delta\sigma - \left(1 - \frac{C^s}{C^p}\right)\Delta u_w \qquad (4.3)$$

C^p = soil particle compressibility , C^s = soil structure compressibility.

The above compressibility equation is verified by Skempton (1961) and Nur and Byerlee (1972) who employ a constitutive equation of the general form :

$$-\left(\frac{\Delta V}{V}\right) = C^s \cdot \Delta\sigma' \qquad (4.4)$$

C^s = bulk compressibility of soil structure; $\Delta\sigma'$ = change in effective stress.

It is noted that this equation assumes that volume change is dependent upon only :

(a) one stress state variable

(b) soil structure compressibility

Fredlund notes from a study of the continuity requirement that volume change depends upon particle and soil structure deformations such that

$$\frac{\Delta V}{V} = \frac{\Delta V^s}{V} + \frac{\Delta V^p}{V} \qquad (4.4.1)$$

ΔV = total volume change ; ΔV^s = soil structure volume change

ΔV^p = soil particle volume change ; V = total volume.

Furthermore, Fredlund contends that the compression of soil structure is controlled by $(\sigma - u_w)$ and compression of the soil

particles by the all round pressure (u_w) . By writing the continuity requirement as a constitutive equation, he re-writes Skempton's equation into the form :

$$\frac{\Delta V}{V} = C^s \cdot (\Delta\sigma - \Delta u_w) + C^p \cdot \Delta u_w \qquad (4.5)$$

It can be seen that Skempton's equation (4.5) comprises of possibly two stress variables $(\sigma-u_w)$ and (u_w), which are linked together by soil properties C^s and C^p . His equations can be termed constitutive and are therefore quite different in character to those proposed by Terzaghi.

Jennings and Burland's (1962) interpretation of the effective stress concept (i.e. viewing effective stress as a stress state variable) is entirely consistent with Terzaghi's presentation.

Matyas and Radhakrishna (1968) define effective stress in two parts i.e.

(a) The change in volume and shear strength of a soil element caused by a change in its stress state are entirely due to the change in effective stresses. i.e. shear strength and void ratio are unique functions of effective stresses.

(b) The effective stress responsible for the mechanical effects in a soil element is uniquely determined by the total stress and pore pressure.

Although $\Delta\sigma'$ can cause a change in shear strength and volume, they need not necessarily be linked by a unique factor.

Other authors, e.g. Sridharan and Venkatappa (1973) retain Terzaghi's original definition of effective stress. Generally however, the literature indicates a deviation from Terzaghi's original proposition that pore pressure and total stress totally govern all deviations from equilibrium conditions.

4.2.2 Unsaturated soils

The importance of soil moisture deficiencies in relation to the mechanical behaviour of unsaturated soils is probably first noted by Croney et al at the TRRL in the early 1950's.

Alternatives or modifications to Terzaghi's effective stress equation for unsaturated soil are subsequently not proposed until the mid fifties.

Bishop (1955) proposes a tentative expression for effective stress in unsaturated soils :

$$\sigma' = \sigma - u_a + X(u_a - u_w) \qquad (4.6)$$

u_a = pore air pressure u_w = pore water pressure X = factor which depends upon degree of saturation, clay type, wetting or drying cycle; It varies from 0(dry clay) to 1(saturated clay).

Hilf (1956) in his presentation on 'Pore water pressure in compacted clays' indicates the importance of separating pore water and pore air pressure measurement in unsaturated soils. More importantly, he introduces the 'origin translation' (subsequently

termed axis translation) technique as a means of measuring moisture deficiencies greater than one atmosphere. This widely adopted technique is utilised in this project.

Lambe (1960) proposes a modified effective stress equation to account for electrochemical forces, but is unable to provide experimental verification due to the absence of a workable model, for measuring attractive/repulsive forces.

Several authors present expressions for effective stress in unsaturated soil to account for two pore media (air and water). All are summarised by Bishop in the pore pressure conference (London, 1960). Briefly these are :

CRONEY et al (1958) $\sigma' = \rho - \beta \cdot u_w$ (4.7)

where:

σ' = effective stress; ρ = total (normal); u_w = pore water pressure

β = bonding factor (approximate number of effective stress tension bonds contributing to shear strength).

AITCHISON (1960) $\sigma' = \sigma + \psi.\rho''$ (4.8)

where:

σ' = effective stress; σ = total stress; ρ'' = pore water pressure deficiency ($-u_w$) ; ψ = parameter varying from $0 \rightarrow 1$.

JENNINGS (1960) $\sigma' = \sigma + \beta \rho''$ (4.9)

where:

ρ'' = -ve pore water pressure; β = statistical factor similar to contact area - must be determined experimentally in each case.

Bishop concludes that expressions (4.6) to (4.9) are similar and that $\psi = \beta = p = X$ - equations (4.7) to (4.9) being instances of equation (4.6) with $u_a = 0$. (i.e. atmospheric). Bishop's equation (4.6) is adopted by the Conference.

Bishop and Donald (1961) control the total, air and water pressures in a series of shear tests on unsaturated silt and vary the stresses in such a way that the differences remain constant. Since the stress strain curve remains unaltered during testing, the effective stress is assumed to remain constant.

In discussing Bishop and Donald's results, Skempton (1961) claims that the formers' results verify Bishop's modified equation for use in unsaturated soils.

Jennings and Burland (1962) are among the first to criticise Bishop's equation. They tentatively conclude that the X parameter is limited in use to the following conditions:

(a) 60%+saturation in granular materials

(b) 90%+ saturation in clay soils

They also contend that collapse behaviour apparently disproves the validity of the effective stress principle (since soaking at constant volume should require an increase in total stress; instead, it requires a decrease in the case of Kaolinite specimens).

The authors and Coleman (1962) propose the portrayal of stresses with respect to air pressure in the analysis of unsaturated soils. (This is especially useful when relating to field conditions where the air pressure = atmospheric i.e. zero).

Coleman uses these relative pressures as independent stress variables in describing volumetric deformation.

Bishop and Blight (1963) note that variations in Bishop's suction term do not necessarily induce a change in effective stress and attribute this to the pore water surface tension acting over only a part of the soil particle surface area.

They conclude that volume change in unsaturated soil is highly dependent upon the stress components : $(\sigma - u_a)$ and $(u_a - u_w)$ as well as the effective stress history - although shear strength is less sensitive to such variations.

Aitchison (1965) and Blight (1969) note that the X parameter is a complex function of the processes to which the soil is subjected. Blight also contends that the collapse phenomena invalidates the effective stress principle.

Burland (1965) after questioning Bishop's equation, separates the forces acting on each particle into isotropic water stresses and the external load - induced shear. He explains collapse phenomena in terms of shear due to a decrease in normal stress.

Suction is defined by the review panel of the "Moisture Equilibria and Moisture Changes in Soils" Symposium, (Aitchison, 1965)

as consisting of two components : matrix and osmotic suction. These are defined as follows :

1. matrix suction

"The negative gauge pressure relative to the external gas pressure on the soil moisture, to which a solution identical in composition with the soil water must be subjected in order to be in equilibrium through a porous permeable wall with soil water".

2. Osmotic suction

"The negative gauge pressure to which a pool of pure water must be subjected in order to be in equilibrium through a semi permeable membrane (permeable to water only) with a pool containing a solution identical in composition with the water".

(these definitions are consistent with those cited by the International Society of Soil Science).

These definitions differ slightly from those presented at the 1961 Suction Conference where it is agreed that air pressure is an internal pressure. The 1969 conference however, defines air pressure as external.

Richards (1960) indicates that solute suction contributes significantly to the physical behaviour of unsaturated soils and proposes another effective stress equation :

$$\sigma' = \sigma - u_a + X_m (h_m + u_a) = X_s (h_s + u_a) \qquad (4.10)$$

where :

X_m = effective stress parameter for matrix suction

X_s = effective stress parameter for solute suction

h_m = matrix suction

h_s = solute suction

However, he does not provide an experimental verification.

Madedor (1967) considered that the stress component $(\sigma - u_a)$ and $(u_a - u_w)$ are best considered separately rather than in Bishop's form (equation (4.6)).

Aitchison (1967) examines Bishop's equation for unsaturated soils and concludes that "the individuality of X in relation to the other components of the equation mean that the effective stress law is no longer valid as a law, but merely a statement of principles . In practice, this results in a second conclusion: each parameter of effective stress σ and $(u_a - u_w)$ must be treated separately and be made to follow a defined stress path if the correct value of X is to function within a statement such as Bishop's equation".

"To put it another way: the complexity of the X term forces us to define a unique stress path for terms σ and $(u_a - u_w)$ in order that a correct effective stress value is obtained. Having achieved this, there is no need to attempt to quantify the X term - thus the complexity of the X term is irrelevant once we uncouple the two parameters in unsaturated soils".

Matyas and Radhakrishna (1968) introduce the concept of state and state parameter to help express relationships between stress and

deformation. They also introduce a three dimensional representation relating $(\sigma - u_a)$ and $(u_a - u_w)$ to either e or Sr . The surface or 'state surface' can be represented by an equation to describe volumetric change on the basis of stress change. Volumetric strains are shown to be predictable providing hystersis does not occur.

They conclude that the behaviour of unsaturated soils cannot be predicted on the behaviour of one variable only.

Barden, Madedor and Sides (1969) used separate control of $(\sigma - u_a)$ and $(u_a - u_w)$ to monitor volumetric changes in unsaturated soils. In applying volume change to the equations originally proposed by Coleman (1962) , they note that the nonlinear nature of the measured parameter implies that the equations are applicable to the current stress situation only. They also note the effect of hysteresis upon accurate volume change predictions.

Sridharan and Vankatappa (1973) note that volume change behaviour in clays is controlled by shearing resistance at inter-particle level and the double layer repulsive forces. A modified version of Lambe's equation is proposed. However, they conclude that there is no means (at their time of writing) to quantitatively measure repulsive and attractive particle forces. As far as the author is aware this is still the case.

Brackley (1971) examines Bishop's equation for effective stress experimentally and concludes that the principle is apparently invalidated for unsaturated soils. He proposes that unsaturated

volumetric behaviour be considered in terms of $(\sigma - u_a)$ and $(u_a - u_w)$ although he does not verify this experimentally.

Fredlund (1973) presents a general theory for modelling volume changes in unsaturated soils. Although his work is largely based upon the developments outlined above, he considers unsaturated soils as consisting of four separate phases,namely : soil,air water and an air-water interphase (contractile skin).
He contends that the contractile skin is the principal conductor of suction throughout the soil mass, and therefore incorporates it in his analysis of an unsaturated soil element.

However, so far as volume-weight relationships are concerned, the contractile skin may be ignored since the weight is negligible and may be considered as part of the water.

The equilibrium equations are written for each of the above phases in terms of measurable quantities. On the basis of these equations, the independent variables required to describe the stress state of an unsaturated soil are identified as : $(\sigma - u_a)$,$(\sigma - u_w)$ and $(u_a - u_w)$, any two of which may be used to describe the soil stress state. These variables are confirmed for the clay mineral Kaolinite only.

Suitable constitutive relationships are proposed from a semi empirical stand point, which combine the stress and deformation state variables, (based upon Biot, 1941, and Coleman, 1962).

The soil structure constitutive relation is obtained by inspecting incremental relations for a linear elastic-isotropic material. It can also be written to account for non-linear properties such that the normal strain in the x direction i.e.

$$\varepsilon = \frac{1}{\nu} \frac{\partial V}{\partial(\sigma - u_w)} \cdot d(\sigma - u_w) + \frac{1}{\nu} \cdot \frac{\partial V}{\partial(u_a - u_w)} \cdot (u_a - u_w) \qquad (4.11)$$

where V = unit volume

$\frac{1}{\nu} = \frac{\partial V}{\partial(\sigma - u_w)}$ = compressibility of soil structure when $d(u_a - u_w)$ is zero

$\frac{1}{\nu} \frac{\partial V}{\partial(u_a - u_w)}$ = compressibility of soil structure when $d(\sigma - u_w)$ is zero.

This may be re-written in terms of other combinations of stress state variable - all variations of which may be plotted graphically (Fig. E17(a)).

By considering the logarithm of the horizontal axes, linear relationships are obtained, the coefficient of which may be determined experimentally. This linear relationship is of the following form :

$$\Delta e = C_t \cdot \log \frac{(\sigma - u_a)}{(\sigma - u_a)_o} f + C_m \cdot \log \frac{(u_a - u_w)}{(u_a - u_w)_o} f \qquad (4.12)$$

where :

Δe = change in void ratio

C_t = volume change modulus w.r.t. total stress

The soil structure/void ratio constitutive relationship is insufficient to completely describe the change in state of an

unsaturated soil; either the air or water phase constitutive relations must also be formulated. However, because of the compressible nature of the air phase, the water phase relationship is chosen and this describes the water volume present in the referential soil element.

Assuming that the water is virtually incompressible, a constitutive relationship is formulated semi empirically on the basis of a linear combination of the state variables. As with the soil structure relationship, it may be written to account for non linear soil properties.

Therefore :

$$\Theta_w = \frac{1}{\nu} \frac{\partial V_w}{\partial(\sigma - u_w)} \cdot d(\sigma - u_w) + \frac{1}{\nu} \cdot \frac{\partial V_w}{\partial(u_a - u_w)} \cdot d(u_a - u_w) \qquad (4.13)$$

where

V_w = volume of water in element

$\frac{1}{\nu} \frac{\partial V_w}{\partial(\sigma - u_w)}$ = slope of the water volume versus $(\sigma - u_w)$ plot when $d(u_a - u_w)$ is zero

$\frac{1}{\nu} \frac{\partial V_w}{\partial(u_a - u_w)}$ = slope of water volume versus $(u_a - u_w)$ plot when $d(\sigma - u_w)$ is zero

This equation may be re-written for the other combinations of stress-strain variables (refer Fig. E17(b)).

These plots may be linearised by considering the logarithm of the horizontal axes and expressed by the relationship

$$\Delta w = D_t . \log \frac{(\sigma - u_a)}{(\sigma - u_a)_o} F + D_m . \log \frac{(U_a - U_w) f}{(U_a - U_w)_o} \qquad (4.14)$$

where

D_t = compressibility index with respect to total stress

Dm = compressibility index with respect to matrix suction

The change in air phase volume within the element can be written as the difference between the soil structure and water elemental volume change.

Fredlund claims the above relationships are unique provided that the volume changes are monotonic (i.e. no reversals in stress change.)

The above constitutive relationships are tested experimentally by measuring the volume changes resulting from stress changes in two orthogonal directions and comparing predicted and measured volume changes resulting from a stress change in a third direction. This is termed uniqueness testing and to the authors knowledge is only fully conducted upon low swell Kaolinite specimens (although a very limited number of tests are conducted upon the low-medium plasticity Devon silt). Thus the theory is validated for use with low swelling clay only (plasticity not exceeding 58%).

The practical application of the above testing techniques is difficult due to the complex nature of the equipment required. The literature indicates a simplified adaptation of the theory to the one dimensional oedometer test, namely Fredlund et al (1980, 1983) and Hamberg and Nelson (1984). These utilise the resulting data for the purpose of in situ ground heave prediction.

The two techniques are essentially different; Fredlund: a constant volume swell pressure type test and Hamberg and Nelson : their own "controlled strain test". Since the former is more widely employed to obtain compressibility and swell data it is presently considered more suitable for evaluating the unsaturated soil theory. Fredlund etal claim to verify the test by comparing insitu swell measurements with swell test data obtained from undisturbed soil specimens. This is undertaken with low-medium plasticity Regina clay only (LL = 64%).

4.2.3 Summarising Remarks

1. Terzaghi's effective stress principle

With regard to effective stress in saturated soils, the literature indicates that Terzaghi's effective stress $(\sigma - u_w)$, does not govern all soil behaviour.
For example, Skempton (1961) notes that the varying influences of soil structure and soil particle compressibilities also influence the effective stress conditions.

2. Effective stress in unsaturated soils

Numerous 'effective stress' equations are proposed for use in unsaturated soils (Croney et al 1958, Bishop 1959, Aitchison 1960, Jennings 1960 and Richards 1965). All incorporate a parameter, linking together more than one stress state variable. Aitchison suggests that this parameter (X) is related to one set of stress conditions only, and is of limited value. Blight (1965), Jennings and Burland (1962) and others express doubt over the X value and indicate severe limitations of the same.

3. Dependence of volume change upon stress state variables

Coleman (1968), Bishop and Blight (1969), Aitchison (1967), Fredlund (1973) note that unsaturated volume change is highly dependent upon total stress $(\sigma-u_a)$ and suction (u_a-u_w) and formulate relationships based on these components. The uniqueness of these relationships is dependent upon monotonic stress changes i.e. reversals in stress will introduce hysteresis effects and subsequent loss of uniqueness.

4. A general theory for unsaturated soils: Fredlunds proposals

Fredlund(1973) derives the stress state variables and presents constitutive relationships similar to those proposed by Biot(1941) and Coleman(1962) for describing unsaturated soil behaviour.

The theoretical model is consistent with that generally employed for saturated soils, and he claims to have verified it with unsaturated and saturated Kaolinite and Devon silt specimens.

Fredlund assumes that the soil is composed of four phases: soil structure, water, air and contractile skin. The contractile skin

is a means of expressing the surface tension at the air-water interface.

The model has not been experimentally verified for expansive type soils , or a range of soil plasticities.

Fredlund (1980) also presents a practical application of the theory to the constant volume swell pressure test for insitu heave prediction. Once again however, verification appears to be extremely limited - the literature indicating one verification only (Yoshida et al (1983)).

5. Suitability of Fredlund's proposals for expansive soils

Unsaturated soil will generally exhibit a volume increase upon wetting. The swelling will continue until equilibrium is attained. (soil virtually saturated). Expansive soils exhibit the bulk of their volume change due to double diffuse layer considerations at interparticle level. However, this process will only occur when the soil is unsaturated.

Fredlund presents an experimentally verifiable theory for volume change in unsaturated soil. However, this has not been verified for use with expansive soils or medium high plasticity soils.

His theory therefore appears to be the most promising presently available, but requires further examination. The theoretical assumptions and derivations upon which the proposals are based are listed in Appendix E. These are critically appraised in the next section.

4.3 CRITICAL EXAMINATION OF FREDLUND'S WORK

4.3.1 Implications of a discontinuous air phase

The aim of this section is to examine the implications of a discontinuous air phase upon Fredlund's experimental and theoretical proposals. Fredlund assumes that all the constituent phases within an unsaturated soil (i.e. soil particles, air and water) remain continuous until saturation is achieved. At this point the air phase is assumed to abruptly disappear.

However, the literature indicates that the air phase does not always exist in a continuous form, and becomes occluded at some intermediary stage of saturation (85% and above - also at optimum moisture content in remoulded soils). Clearly, the effects of this upon the theoretical and experimental work must be assessed.

4.3.1.1 The wetting process

The effects of the soil microscale mechanisms and a free access to water can be collectively termed the wetting process. The soil may commence the wetting or drying process at any stage of saturation, therefore it should be examined at all stages of moisture intake.

It is well known that clay minerals attract water to their surfaces by electrochemical forces and even in dry soils the clay particles are covered by a thin layer of water known as the adsorbed layer. If sufficient water is present this layer of highly viscous adsorbed water thickens and a gradual transition takes place from

the relatively static viscous state to the free pore water which can move freely under potential gradients.

Where clay particles come into contact with one another, the adsorbed layers coalesce forming curved menisci as shown in Fig. 4.2.

The moisture films are considered continuous for saturations greater than 25% (Hilf, 1956).

These curved menisci and their associated surface tension forces give rise to a pressure difference between the pore air and water pressures. If the air pressure is atmospheric this will give rise to a considerable water pressure deficiency (suction). It is generally implied that soil suction includes the adsorptive and osmotic pressure differences as well as surface tension forces.

Interparticle contact is by no means continuous and 'free' or gravitational water may flow through the pores under potential gradients. Although the adsorbed water cannot flow freely under the action of gravity, it is not static, and considerable quantities may be transferred over long periods.

Upon access to water, the soil grain surfaces are wetted and the capillaries fill until the water is continuous throughout the soil mass.

The water migrates under surface tension forces until all the menisci at the points of grain contact have the same curvature and hence suction (provided the soil mass is small enough for constant gravity effects).

The water will therefore tend to flow from the larger to the smaller pores. Hence there is a tendency for air to occupy the larger pores while the smaller ones are full of water.

For low degrees of saturation, the air is continuous in the larger pores and free to flow through the clay.

Numerous investigations have revealed something of the effects of increasing saturation upon air permeability. Corey, (1957), Matyas, (1963), Madedor (1967) and others have shown that air permeability of an unsaturated soil decreases to essentially zero as the degree of saturation approaches eighty five per cent (85%). In the case of compacted soils, this corresponds to approximately optimum moisture content.

With regard to the process involved, as this critical degree of saturation is approached, the thin sacks of air between the pores tend to fill up with water and the air ceases to be continuous over any distance. At this stage the air is said to be occluded. Madedor (1967) notes the abrupt manner in which the air permeability finally decreases - as the critical degree of saturation is approached, indicating a very rapid occlusion process.

It must be noted that despite the abrupt transition between the inter-connected and occluded air states, there is a definite transition zone in which the pore air is a mixture of inter-connected and occluded states. Subsequently, the behaviour of such a mixture is intermediate between soils of wholly inter-connected and wholly occluded air.

The term 'occluded air' encompasses all pore air held within the water between approximately eighty five per cent and full soil saturation. Occlusion will commence with the air phase being near continuous, the few bubbles being separated by short columns of water.

As the degree of saturation increases, diffused and occluded air predominates. Full saturation is rarely achieved during the wetting process due to the entrapment of bubbles within the soil matrix.

Hilf (1956), Bishop and Henkel (1962), Fredlund (1973) and others debate the value of occluded air pressure and raise the following questions.

(i) what is the value of occluded air pressure, i.e. is it equal to the pore water pressure?

(ii) do the occluded air bubbles reach a common equilibrium pressure?

There appears to be no consensus of opinion regarding these points, and attempts at formulating a compressibility equation for air-water mixtures must make assumptions in this respect. A common assumption after Bishop and Henkel (1962) is that occluded air pressure equals the pore water pressure.

4.3.1.2 Categorising saturation

The previous evidence indicates distinct degress of saturation through which the soil passes.

Aitchison (1956) was one of the first to identify distinct categories of saturation, and indicated four states :
(a) saturated ; (b) quasi saturated ; (c) partially saturated and (d) unsaturated.

where

P'' = water suction ; P_g = pressure in occluded air
S_r = degree of saturation ; Δw = soil moisture deficit
n_t = compressibility of pore fluid relative to water

His categories of saturation (ref. fig. 4.3) are as follows :

(a) Saturated

$S_r = 100\%$; $\Delta w = 0$; $n_t = 1$; $P'' = 0$; $P_g = 0$

Since all the pores are filled with water then there is no suction ($P''= 0$) and there is no occluded air

(b) Quasi saturated

$S_r = 100\%$; $\Delta w = 0$; $P_g = 0$; $0 < P'' < P_d''$; $n_t = 1$
P_d'' = suction at which largest pore drains

All pores are filled with water in which a finite pressure deficiency exists.

This state occurs in the first stage of desiccation of a saturated soil. Although Δw and P'' assume only small values for sands and silts, they may assume very large values in the case of high clay content materials.

(c) Partially saturated

$S_r < 100\%$; $\Delta w = 0$; $P'' \leq 0$; $n_t > 1$; $P_g > 0$

Some of the pore space is occupied by occluded or adsorbed air. The soil will not imbibe further water (at atmospheric pressure) while in its ambient stress system. This condition occurs primarily in remoulded soils such as a rolled-fill earth dam. It is also exhibited by recent geological deposits.

(d) Unsaturated

$S_r < 100\%$; $P'' > 0$; $\Delta w > 0$; $n_t > 1$

The air and water are continuous throughout the specimen with little or no occluded air. This state may be approached in three ways :

(i) the soil is initially quasi-saturated and subjected to increasing desiccation until pore drainage occurs i.e. $P'' > Pd''$; $P_g = 0$ (i.e. atmospheric)

(ii) soil is initially partially saturated, then subjected to desiccation (but insufficient to cause pore drainage) $P' \leq Pd$; $P_g > 0$

(iii) the soil is initially partially saturated, then subjected to desiccation until pore drainage occurs i.e. $P'' > Pd''$

The value of P_g varies : drained pores $P_g = 0$

occluded pores $P_g > 0$

Recognising that certain soils exist in yet a lower band of saturation, the author proposes a further lowest category :

(e) Low-unsaturated

$S_r < 100\%$; $P'' > 0$; $\Delta w > 0$; $n_t > 1$

The air phase is completely continuous, however, the water content is so low that very little 'free' water exists.

A possible boundary for this proposed lower category is the point at which the air phase becomes discontinuous - generally saturation at about 30%.

4.3.1.3 Theoretical implications of a discontinuous air phase

The existence of a continuous air phase is one of Fredlund's fundamental assumptions in his derivation of the air phase equilibrium equation. Conditions of occluded noncontinuous air phase apparently invalidate such equations.

Assumptions in the derivation of equilibrium equations

Fredlund adopts the coincident stress field of a multiphase system approach and assumes that stress fields of all phases (i.e. air, water, solid and contractile skin) can be superimposed upon one another to obtain the overall equilibrium equations.

This can only be achieved if the equilibrium equations for each phase contain linear operations, which in turn is dependent upon each phase being continuous (Malvern, 1969).

Fredlund satisfies the above requirements by considering a model of water with uniform air channels passing through. He states that although uniformly distributed bubbles would be a more realistic assumption, they would in fact be both discontinuous and unstable. The author notes that Fredlund's model apparently does not allow for the occluded air state through which unsaturated soils are considered as passing during the wetting process.

Allowance for occluded air in the equilibrium equations

Since the air phase is not continuous under occluded air conditions, then equilibrium equations taking such conditions into account would contain non-linear operations. As such, the air phase-stress field could not be superimposed upon those of the other phases.

Theoretical modifications to the air phase equilibrium equation do therefore not appear possible.

Limitations of theoretical model

Clearly, the failure of the model to adequately describe the occluded air state will be of importance if the behaviour of a soil operating entirely in this saturation zone (between 85% and approximately 100%) is to be studied. This does not necessarily imply that the model will not work in this range, but it cannot be fully justified theoretically. However, if the specimen is being allowed to saturate i.e. freely absorb water as in swell testing, then the initial unsaturated and final saturated condition will involve continuity of the phases and the basic requirements of the model will be fulfilled.

4.3.1.4 Experimental implications of a discontinuous air phase

The existence of continuous air voids (i.e. no occluded air) throughout testing is imperative for the correct functioning of the axis translation technique employed in the testing of unsaturated soils.

This section examines previous experimental and theoretical considerations of occluded air.

The axis translation technique

Pore water pressure deficiencies of -14.7 psi (-1 atmosphere) are rarely reported in engineering literature and most values usually exceed -100 psi (-6.8 atmospheres). The problem involved in measuring such suctions is that the water in the measuring system will cavitate below -1 atmosphere. This is overcome by using the axis translation technique where the pore air pressure is raised until the pore water pressure increases to a level that can be measured directly. (ref. Ch. 5 for details).

The radius of curvature of the air-water menisci do not appear to change significantly when the air pressure is increased, thus the difference between final air and water pressures equals the initial negative pore water pressure. Several authors : Hilf (1956), Bishop and Donald (1961) and Olsen and Langfelder (1965) have apparently verified the technique by measuring the changes in pore water pressures corresponding to apparently equal pore air pressure changes.

Requirements for technique validity

For the technique to be valid, it must be possible to increase the ambient air pressure around the specimen without producing deformation. To achieve this, the internal pressure increase must equal the external pressure increase and for this the air voids must be inter-connected. However, as indicated earlier, the air in unsaturated soils may well exist in an occluded state, resulting in a compressible air-water mixture. It is thus reasonable to assume that behaviour of the axis translation technique will be altered in some way.

Since the saturation level of some soils used in this study (and in the field) will exceed the moisture level for air occlusion, then the behaviour of the axis translation technique under such conditions must be examined.

The effects of occluded air upon the axis translation technique

The effects of occluded air upon the axis translation technique are primarily related to the change of pore water properties under such conditions (broadly indicated in fig. 4.4).

Although the literature indicates extensive discussion concerning occluded air, little work appears to have been undertaken regarding the effects of occluded air upon the axis translation technique.

Bocking and Fredlund (1980) is one of the few papers to address this problem and presents two mathematical models to simulate the

measurement of negative pore water pressure in a pressure plate apparatus using the axis translation technique. Their models, which separately consider either an interconnected or occluded air phase, are complex, but provide an approximate solution only. Consequently, only general equipment behaviour can be deduced from the results. Their results indicate:

(a) The axis translation technique predicts suction satisfactorily for soils with interconnected air pores. In the case of occluded soil air however, the suction is invariably overestimated, especially in highly compressible soils.

In practice, this means that the actual suction will always be less than the target value.

(b) For test soils with a continuous air phase, the specimen is noted as undergoing a volume change at the ceramic disc - specimen interface following a water pressure change. This remains until equilibrium is achieved throughout the specimen, and the original void ratio restored.

A corresponding increase in saturation occurs which inevitably affects air permeability.

A similar temporary volume change is noted for soils with occluded air bubbles, however the soil element undergoes a further permanent deformation due to compression of the pore fluid.

No increase in base moisture content is noted under occluded air conditions.

There also appears to be a lack of experimental research regarding the effects of occluded air, this probably being connected with the

great difficulties associated with quantifying the volume and pressure of the occluded air in a soil.

4.3.1.5 Observations

1. The axis translation experimental technique has been widely employed and successfully verified for use in unsaturated soils exhibiting a wide range of saturation.

2. For the technique to be theoretically valid however, the air phase must be continuous in order that the increase in ambient air pressure equals the internal air pressure increase thus producing no deformation.

3. The literature clearly indicates the existence of an occluded air state within soils of approximately 85% saturation and above. Since, in such circumstances, the air is most definitely discontinuous, the behaviour of the technique must be monitored very closely.

4. Little experimental evidence is available specifically observing the behaviour of the axis translation technique with soil containing occluded air. Bocking and Fredlund (1980) attempt to mathematically model the above test, and incorporate the effects of occluded air. Their solutions are approximate however, and only general conclusions are possible. They note that suction will be overestimated during the presence of occluded air.

4.3.2 Interparticle forces

Fredlund apparently makes no allowance for the attractive and repulsive forces at interparticle level in his thesis or subsequent publications.

The developments employing this approach for modelling soil are discussed below.

Interparticle forces

The expansive properties of soil (i.e. volume change and swell pressure) occur primarily due to the adsorption of water molecules to the exterior and interior surfaces of the clay mineral to balance the particle charge deficiency. The degree of hydration, hence swell, is influenced by the amount and type of ions adsorbed on the particle and in the pore fluids (ref. Ch. 2 for detailed discussion).

As a result of the above and other processes, there exist attractive and repulsive interparticle forces. In the case of expansive clay the repulsive forces dominate and are primarily attributed to an interaction between the double layers surrounding clay particles (Lambe, 1958; Seed et al,1959).

Lambe and Whitman (1957) state that : "this force can far exceed the externally derived force applied to the particles". Lambe and Whitman also propose that these forces be designated :

R - repulsive ; A - attractive

Lambe (1960) subsequently proposes a modification to the effective stress equation by considering the A and R forces.

$$\sigma = \bar{\sigma} \cdot a_m + u_a + a_a + u_w \cdot a_w + R - A \qquad (4.17)$$

where

$\bar{\sigma}$ = mineral-mineral contact stress

u_w = pore water

a_w = area of water/unit contact area

R = repulsive, A = attractive electrical forces per unit area

u_a = pore air pressure

a_m = area of mineral-mineral contact

a_a = area of air/unit contact area

This is subsequently modified by Sridharan and Venkatappa (1973) to take account of the fact that the intergranular (effective) stress actually increases with attractive force.

where

$$\bar{C} = \sigma - \bar{u}_w - \bar{u}_a - R + A \qquad (4.18)$$

$\bar{C}$ = effective constant stress (total)

The above mentioned researchers conclude that clay volume behaviour is controlled by :

(a) shearing resistance at particle near contact points and

(b) the double layer repulsive forces

However, to the author's knowledge, there is presently no means of quantitatively measuring R and A and thus no way of verifying equation (4.18).

Fredlund apparently makes no mention of these attractive and repulsive forces in his thesis and subsequent publications. However, his linking of volumetric behaviour to changes in stress state variables; in particular suction (u_a-u_w) is believed to encompass these stresses (due to the undoubted relationship between suction and particle charge deficiency).

4.4 FINAL SUMMARISING REMARKS

4.4.1 Choice of theory

1. There are presently three main approaches for modelling soil behaviour - the energy/thermodynamic, electrical charge and the model approach. None of these have apparently provided a major breakthrough with regard to describing unsaturated-expansive soil behaviour. However, the model approach does appear to provide the most promising basis for a workable stress-deformation analysis.

2. With regard to the model approach, the effective stress principle after Terzaghi (1936) is one of the most widely employed stress-deformation type analyses. This has been successfully employed over many years for volume change predictions in saturated soils.

   Numerous 'effective stress' models are proposed for use in unsaturated soils (Croney et al, 1958; Bishop, 1959; Aitchison, 1960; Jennings, 1960 and Richards, 1966) and all incorporate a soil parameter linking more than one stress state variable. Aitchison (1960), Jennings and Burland (1962) and Blight (1965) indicate that this soil parameter X will vary according to the prevailing stress

conditions, and its application is therefore of extremely limited value.

The 'effective stress' approach is therefore considered unsuitable in its original form for application to unsaturated soils.

3. Several authors, including Coleman (1962), Bishop and Blight (1963) and Aitchison (1967) note the limitations of the modified effective stress equations and suggest separating the total σ and suction $(u_a - u_w)$ component stress terms in the consideration of volume change behaviour.

Matyas and Radhakrishna (1968) extend this by relating these terms to void ratio and degree of saturation and verify their proposals by experimentation.

4.4.2 A theory for modelling unsaturated soil behaviour

4. The theoretical work by Fredlund (1973) regarding volume change in unsaturated soils stands out as the most promising development presently available. This is a continuation of the work outlined above and involves two main developments.

The first identifies the independent stress variables required to describe the stress state in an unsaturated soil (total stress: σ, air pressure: u_a, water pressure: u_w). This is achieved by writing the equilibrium equations for the soil, air, water and contractile skin phases. The contractile skin refers to the thin boundary between air and water phases which exhibits surface tension. It constitutes a separate phase because its properties differ from those exhibited by adjoining phases.

Three independent variables are identified and include the two total stress variables $(\sigma-u_a)$, $(\sigma-u_w)$ and the suction variable (u_a-u_w). Any two of these are sufficient to describe unsaturated soil behaviour.

The soil element should exhibit no volume change If these variables remain unchanged (and of course provided they are of the right form).
This criteria forms the basis of Fredlund's Null tests.

The second of Fredlund's developments is an amendment to the constitutive relationships first presented by Biot (1941); these describe the phase volume changes resulting from a stress change within an unsaturated soil.

Fredlund conducts experiments similar to those devised by other researchers which involves subjecting the specimens to three stress paths whilst monitoring water and total volume changes.

The compressibility moduli are then calculated on the basis of two results enabling prediction of the volume change resulting from the third.

The predicted volume change is finally compared with the experimental observations to give an indication of the theories' reliability.

Both the stress state variables and volume change equations were apparently verified by Fredlund during his experimental programme. However, his work only encompassed non expansive Kaolinite and Devon silt.

5. The requirement of continuous phases is central to Fredlund's formulation of his volume change theory. Continuity of the soil, air and water phases are essential if the stress functions are to be combined, thereby yielding the constitutive equation.

   Despite the existence of voids and cracks within in situ soils, Fredlund still believes that a continuity approach provides the most practical analysis. He proposes that the solid air and water phases may be considered continuous throughout the wetting process right up to saturation, at which point the air phase abruptly disappears.

   In reality, the pore air becomes occluded at around 85% saturation, resulting in an air-water mixture.
   Also, for much lower saturation levels (say <25%) the water phase contracts sufficiently to be considered discontinuous.

   The author suggests that the application of the theory might be limited to a certain range of saturation, or, at the very least it might require some modification when used with discontinuous phases.

6. The author notes that the presence of a discontinuous or occluded air phase will also affect the operation of the main testing methods as employed by Fredlund - namely the axis translation technique. This was originally intended by Hilf (1956) for the measurement of suctions below one atmosphere, however, it is now employed (in a modified form) for controlling or measuring the total, air and water stresses.

The presence of occluded air causes the axis translation technique to under-record suction due to the compression of the air-water mixture.

Very little information is available on this problem and the magnitude of the occluded air effects cannot presently be theoretically or experimentally quantified with any measure of accuracy.

However, the axis translation technique continues to be successfully employed for a variety of unsaturated soils worldwide, therefore, the problem of occluded air is not presently introduced into the calculations.

7. Fredlund indicates that soils of liquid limit above 50% require extended periods of time to reach volume change equilibrium. Premature curtailment of testing in such cases will result in an incorrect measurement of volume change, but permit a greater number of tests to be undertaken. These aspects must be carefully considered when planning a test programme.

   It appears that some difficulty may be encountered in this respect when testing expansive clays of high plasticity.

8. Hysteresis is a phenomena associated with numerous materials, where the stress-deformation characteristics are related to the direction of stress change.

   In the case of unsaturated soil, volume change is closely related to the water pressure deficiency (suction), and several authors including Chu and Mou (1973); Barden, Madedor and Sides (1969) and Matyas and Radhakrishna (1968) have clearly

indicated the potential significance of reversals in volume change.

Fredlund broadly uses hysteresis to explain why in some cases, his overloaded specimens do not return to their original volume upon correction of the overburden. However, he does not allow for this in his theoretical model and concentrates experimental effort upon swell behaviour (increasing saturation/decreasing suction) only.

Fredlund's model may therefore require some modifications for application to in situ soils where hysteresis commonly occurs - however, this is outside the scope of the project.

4.4.3 Aspects requiring further investigation

Fredlund's unsaturated soil model provides a suitable base from which to commence development of a theory for volume change in expansive soils. The conclusions have highlighted several aspects requiring further investigation and are listed along with comments regarding feasibility:

(a) applicability of the model to a range of expansive clay types (i.e. testing the chosen stress state variables and volume change constitutive relationships with several clays)

The model should be shown to work for a range of expansive clay types, by conducting a test programme of uniqueness and null tests.

(b) assessment of the theory when used with soils containing discontinuous phases (i.e. very low saturation levels with discontinuous water and medium-high saturations (85%+) containing occluded discontinuous air phase

A complete study of the occluded air phase or of soils at very low saturation is considered beyond the scope of this project. However, since swelling behaviour is to be examined, with soils passing through the occluded stage, then the behaviour of the model under such conditions should be assessed as far as equipment limitations permit.

(c) applicability of the model to hysteretic behaviour

This is an important aspect of in situ soil behaviour, not covered by Fredlund's model. However, the variability of hysteretic effects between soil types is significant, and the formulation of a suitable mathematical model is a study in its own right.

Therefore, because of this, and suitability of the equipment for measuring one dimensional swell only, then the effects of volume change reversal will not be studied in this project.

(d) assessment of the theory for practical application i.e. to a routine geotechnical test

The verification of the theoretical model need not be limited to the involved stress-deformation study as previously indicated. Supporting data could usefully be obtained by application of the theory to the consolidometer swell pressure test as presented by Fredlund (1980).

(e) three-dimensional (isotropic) or one-dimensional (K_o) swell testing system?

Fredlund combines the developments of several researchers to construct isotropic and K_o type testing systems. The author believes that since his testing system must be developed from scratch then

it would be best to initially construct a simplified design such as a K_o type system and then to develop as time limitations permit.

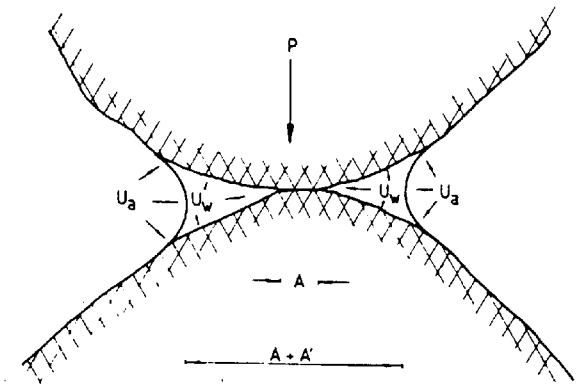

FIGURE 4·1
FORCES AT INTERGRANULAR CONTACT
IN UNSATURATED SOILS

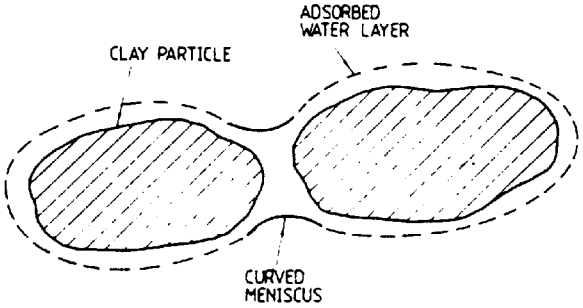

FIGURE 4·2
INTERPARTICLE WATER PHASE

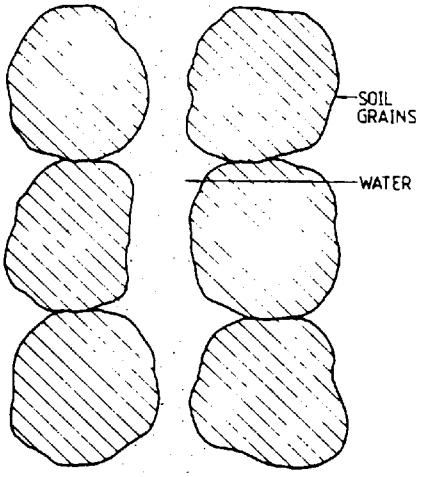

SATURATED

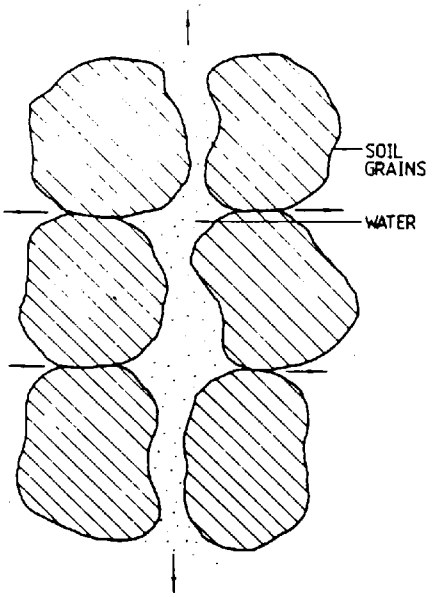

QUASI - SATURATED

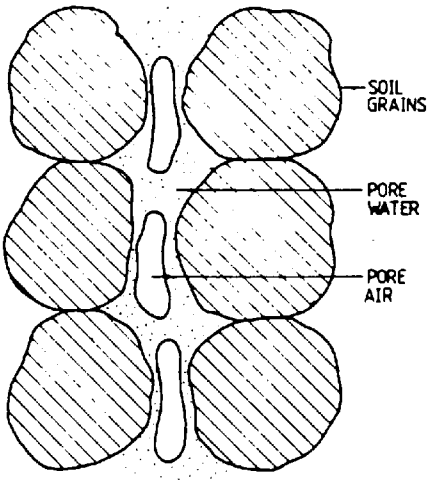

PARTIALLY SATURATED

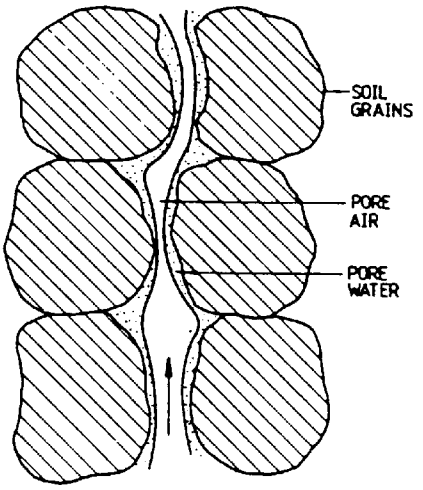

UNSATURATED

FIGURE 4·3
STATES OF SATURATION
(AITCHISON, 1956)

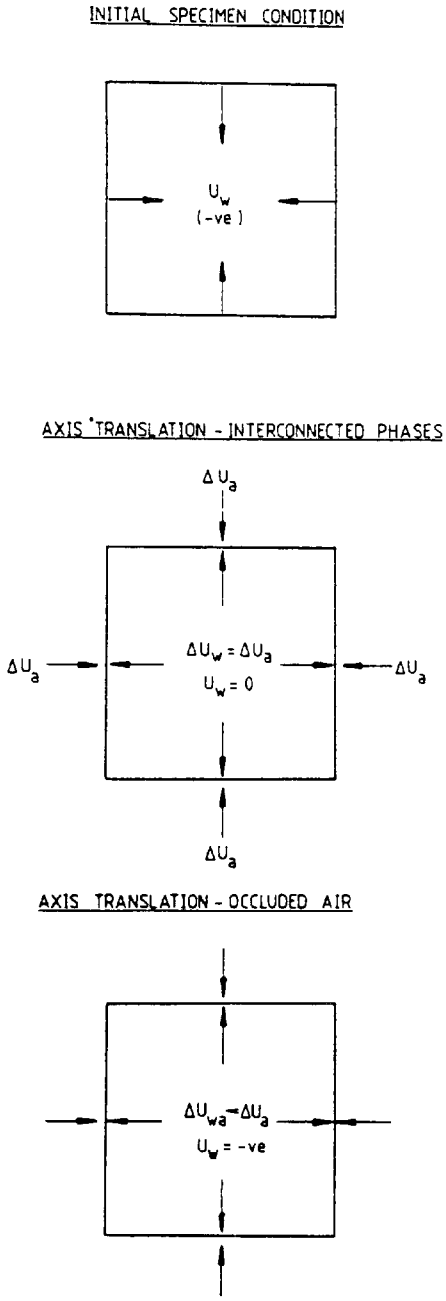

FIGURE 4·4
EFFECTS OF OCCLUDED AIR UPON THE AXIS TRANSLATION TECHNIQUE

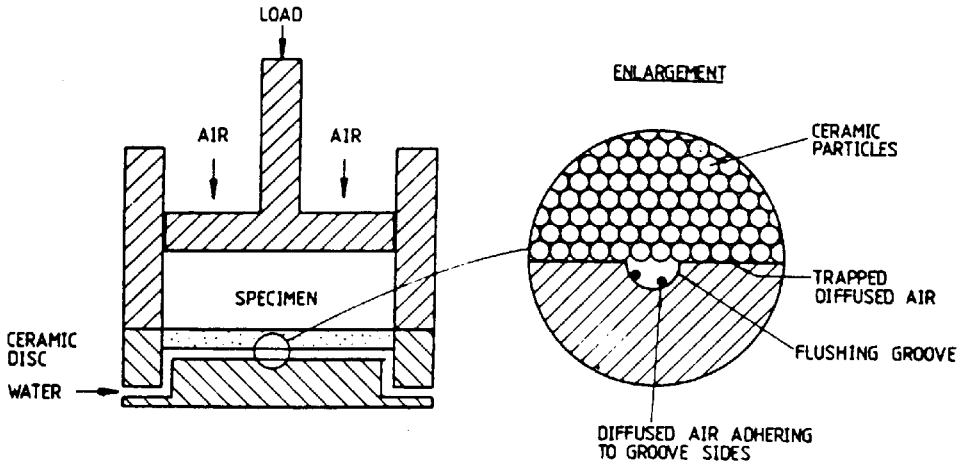

FIGURE 4·5
FLUSHING DIFFUSED AIR FROM
BENEATH THE CERAMIC DISC

CHAPTER 5

APPARATUS AND TECHNIQUES FOR TESTING UNSATURATED EXPANSIVE SOILS

5.1 General

The aim of this chapter is to describe the testing systems and techniques employed in this project for monitoring the stress-deformation behaviour of synthetically produced expansive unsaturated clays.

Experiments are developed to provide data for a rigorous evaluation of the volume change theory and involve the following test methods :

(i) the monitoring of all deformations (total and water volumes) with full control of total stress, air and water pressures

This equipment is developed from the Rowe cell and a conventional triaxial cell for monitoring one dimensional swell behaviour only.

Fredlund, whose volume change theory is to be evaluated, has combined the developments of other researchers to form a test system. The suitability of his equipment for use with unsaturated expansive soils is noted and influences the authors own development.

(ii) the monitoring of total volume change with a varying total stress only

These employ conventional consolidometers with minor modifications to enable the measurement of swell pressure at constant volume in

addition to the compressibility and rebound characteristics of the soil.

Although the consolidometer type tests have been widely employed on a variety of soil types, the more sophisticated systems have only been tested on non-expansive, low-plasticity soils to the authors knowledge.

When applied to medium-high expansive soils, the described equipment is subject to the associated secondary volume change effects, and must therefore be capable of operating for extended periods of time.

The more complex equipment has many potential sources of leakage due to the numerous joints, seals etc. Any leakage however small on a daily basis will assume significant proportions over extended test times and must therefore be curtailed or at least. least, compensated for.

The author acknowledges that the next logical development of the equipment is a three dimensional (isotropic) volume change system. However in view of the numerous additional complications associated with three dimensional volume change measurements, such a system is considered beyond the scope of this project.

5.2 EQUIPMENT DEVELOPED FOR TESTING UNSATURATED EXPANSIVE SOILS

5.2.1 Basic design considerations

The aim of the testing is to verify Fredlund's theoretical proposals for a range of synthetically produced expansive clays.

This is achieved by measuring the flow of fluids and deformation

of the solids. Consequently, the system may operate in either of two modes.

Undrained : no flow of water or air in or out of the specimen

Drained : the air and/or water moves in and out of the specimen against a controlled pressure system.

The measurement and control of air and water pressures

The difficulty of separating the applied air and water pressures has long been recognised by soil scientists and is solved by employing a pressure membrane or pressure plate technique.

The pressure plate is chosen for use in this project since it is more convenient to use. It normally consists of a high air entry ceramic disc, which is highly susceptible to cracking when subjected to an overall uplift pressure greater than 5psi / 34.5 KN/M^2. This condition must therefore be avoided.

The water and air phase are separated from one another by the high air entry ceramic disc located at the base of the specimen. This permits a flow of water but prevents the direct passage of air (up to a pressure deficiency equivalent to the high air entry value of the disc - 5 bar / 72.5 psi / 500 KN/M^2.)

The difficulties associated with measuring high pressure deficiencies in expansive soils, are overcome by elevating the air pressure surrounding the specimen until the'negative pressure' becomes 'positive' relative to atmospheric . This is acceptable since the air-water pressure equilibrium is dependent upon the water pressure deficiency ($u_a - u_w$) regardless of the absolute pressure values.

This procedure is termed the 'axis translation' technique after Hilf (1956) and is verified by Bishop and Henkel (1962), Olsen and Langfelder (1965) and Fredlund (1973) (refer figure E.11).

The technique is of limited value however due to the passage of diffused air through the ceramic disc and subsequent formation of bubbles beneath it.

Water volume change measurements are effectively invalidated in such instances unless adjusted for the diffused air volume.

Displacement measurement

The four component phases of an unsaturated soil and associated measurements are outlined below :

Phase	Measurement
1. total volume/soil structure (s)	vertical movement (with constant cross sectional area)
2. water phase (w)	inflow or outflow
3. air phase (a)	inflow or outflow
4. contractile skin (c)	cannot be measured

by continuity ,

$$\Delta V = \Delta V_a + \Delta V_w + \Delta V_c \qquad (5.1)$$

where V = total volume; V_a = air volume; V_w = water volume;

V_c = contractile skin volume ; Δ = change

Since the contractile skin volume is insignificant by comparison to the other volumes, then (5.1) may be rewritten :

$$\Delta V = \Delta V_a + \Delta V_w \qquad (5.2)$$

The air volume change is susceptible to temperature and pressure change effects, therefore the water and total volumes are considered as being more suitable for measurement purposes. Both must be measured to obtain a complete understanding of the unsaturated soil behaviour.

5.2.2 Literature review of equipment developed

The aim of this review is to trace the development of equipment for the one dimensional volume change testing of unsaturated soils. Relevant developments from three dimensional testing systems are also discussed where appropriate.

Volume change testing of unsaturated soils usually involves either: applying total pressure and monitoring volume change, or applying differential air and water pressures, and monitoring water volume change.

A thorough understanding of unsaturated, expansive soil behaviour requires that all stresses be controlled and (preferably) all deformations monitored. Several authors develop systems which partially fulfil the above requirements, however, Fredlund (1973) is the first to take all requirements into account and fully consider the influence of diffused air upon measured water volume changes.

Hilf (1956)

Using a modified concrete air meter, Hilf measures the change in volume and the induced pore water pressure in remoulded specimens subjected to a change of total stress.

The pore water variation is measured by inserting a high air entry porous tip into the specimen, and nulling a mercury slug within a fine bore capillary tube. The specimen is protected from the surrounding water by coating it with natural latex rubber.

Total volume change is monitored in a capillary tube situated on top of the concrete air meter.

Gibbs (1967) and Gibbs and Coffey (1969) extend Hilf, testing system to accommodate shear strength testing in the triaxial cell. The total volume change is determined by measuring the change in water volume surrounding the specimen;however, the vertical and lateral displacements cannot be measured separately.

The air pressure and air volume change can both be measured at the base of the specimen; the water is similarly controlled from the top of the specimen. There is no facility for flushing diffused air from beneath the base high air entry disc however.

The water volume change measured is subject to errors induced due to expansion of the cell wall.

Bishop and Donald (1961)

Four inch (100mm) triaxial cells are modified for performing shear strength tests on unsaturated Braehead silt.

A high air entry ceramic disc is built into the triaxial pedestal and a closed circuit bubble pump and air trap are also incorporated into the system to permit the removal and measurement of diffused air

from beneath the disc (thus enabling the correct water volume change to be determined).

The water volume change is measured using a Bishop paraffin volume change indicator (described later). This instrument is simple and safe to use and can be back pressured.

It is noted that the air phase diffuses appreciably with time through the rubber membrane around the specimen, thus preventing long term testing. This error is eliminated by surrounding the specimen with a perspex sleeve and filling the intervening space with mercury, in which air exhibits negligible solubility.

Accurate measurements can therefore be made of the vertical and lateral specimen displacements using a cathotometer. The main disadvantages of this setup is the hazard associated with liquid mercury.

MIT (1963)

The one dimensional compression devices utilised by MIT (1963) are designed with differing features to those used on the triaxial apparatus in this research.

High air entry discs are installed at the top and bottom of the specimen - the water volume change being monitored at both points using a closed circuit bubble pump similar to that used by Bishop and Donald (1961). This pump is constructed from glassware, thus the water supply cannot be back pressured. Total volume change is

measured by monitoring the displacement of the loading piston, while the overburden is measured by a stud force transducer located at the base of the specimen.

It is suggested by MIT that the air pressure be adjusted by sensitive reducing valves. Several researchers subsequently employ similar valves for the control of all stresses.

Matyas and Radhakrishna (1968)

The equipment developed by Radhakrishna (1967) is similar in many respects to Bishop and Donald's (1961) apparatus. An electrical lateral strain indicator is also incorporated into the design (utilising strain gauges).

The test system measures, total volume change as well as those of the two fluid phases (water and air). The air volume change (within the specimen) is measured using a Bishop-type two limb water manometer located between the sample and the air source.

No attempt is apparently made to measure, or even flush the diffused air from beneath the high air entry ceramic disc.

Barden,Madedor and Sides (1969)

The apparatus is a modified form of the Rowe and Barden (1966) consolidation cell.

The specimen is 6" (150mm) in diameter by 1" (25mm) thick and is contained within a cell body. The total stress is applied to the rigid top plate by means of hydraulic pressure to a convoluted rubber jack.

The water pressure is controlled by high air entry discs situated on top and below the specimen. The water volume change is monitored by measuring the movement of a mercury plug in a horizontal glass tube.

The diffused air collected at the base of the ceramic discs may be flushed out but not measured.

The total volume change is measured using a dial gauge connected to the settlement rod. The equipment is subject to the same operational problems encountered in the conventional Rowe cell i.e. inadequate de-airing of the water used in the load application system.

Aitchison(1969)

Aitchison uses a conventional consolidometer and encloses it within an airtight pressure vessel. The raising of the ambient air pressure then permits a control of suction and enables corresponding swell to be measured.

Although the system permits the flushing of diffused air from underneath the ceramic disc, no attempt is made to quantify it.

The volume of water taken into the specimen is also apparently not recorded.

Escario (1969)

Escario employs the pressure membrane technique to enable the measurement of very high suction (≈970psi/ 6688 KN/M^2).

Escario realises that a specimen will imbibe water during assembly of the equipment prior to test commencement.

This he allows for by separating the base plate (thus water supply) from the specimen, during routine apparatus assembly. It is then raised into contact immediately upon commencement of the test.

The apparatus does not measure fluid phase volume changes (air and water) or permit control of the water pressure.

Pufahl (1970)

The Anteus consolidometer is intended for the one dimensional consolidation testing of a soil with a water back pressure.

Pufahl modifies this by installing a high air entry ceramic disc in its base, and regulates the specimen air pressure by means of a back pressure regulator.

The equipment lacks a means of measuring the fluid phase volume changes (i.e. water volume change and diffused air volume).

Compton (1970)

A Bishop consolidometer as manufactured by Wykeham Farrance is modified by installing a high air entry disc (75 psi / 517 KN/M^2) in the base.

The pore water pressure is measured using a Bishop's null indicator, and the change in water volume measured using a Bishop's paraffin volume change indicator.

No attempt is made to account for the diffused air beneath the ceramic disc.

Fredlund (1973(a))

Fredlund develops two testing systems for measuring volume change behaviour in unsaturated soils. The first is based upon the 'Anteus' consolidometer design (Testlab Equipment Corp) and measures one dimensional (K_o) swell behaviour.

The second consists of a modified 4" triaxial cell for monitoring three dimensional (isotropic) swell-shrink behaviour.

The following discussion concentrates upon the one dimensional (K_o) testing systems, but incorporates relevant aspects of the isotropic testing system where appropriate.

The 'Anteus' consolidometer is chosen by Fredlund because of its suitability for modification (figure 5.1). The total pressure is applied to the specimen via a rolling rubber diaphragm. The air pressure is applied to the main test chamber and reaches the upper specimen surface through the low air entry porous loading stone.

The main modification entails the installation of a high air entry disc into the consolidometer base. This separates the air and water phase sources thus facilitating their separate control.

The water volume change (entering or leaving the specimen) is recorded using a Bishop's paraffin-type water volume change indicator. Fredlund notes that Bishop's indicator is susceptible to leakage, and suggests that this is due primarily to faulty seals.

The water volume change measurements are influenced by the diffusion of air through the ceramic disc, thus the diffused air volume must be quantified to enable application of a suitable correction. A critical aspect of Fredlund's work is the development of an indicator to measure this air volume. The indicator is connected to the cell base, and the diffused air is periodically flushed into it for quantification.

Since the cross-sectional area is constant, then the vertical uplift of the specimen is directly representative of the volume change. However, this is not the case following an isotropic shrinkage, when the specimen parts from the cell wall. The cell is therefore restricted to the study of swell behaviour. The component stresses are generated using a pneumatic air supply.

The pore air pressure is supplied directly from the pressure source, however, the water pressures must be generated by applying pneumatic pressure to the water surface in a sealed reservoir.

The pressures are controlled using precision pneumatic air regulators (constant bleed type) and quantified using electronic pressure transducers.

In addition to the details indicated above, the author notes that the following equipment features and operating procedures may adversely influence volume change measurements in Fredlund's equipment.

The measurement of diffused air

The importance of correctly quantifying the diffused air penetrating the ceramic disc has been fully discussed previously. The design of the equipment plays the key role in this operation, and it is therefore essential that all the necessary design measures be undertaken to limit erroneous measurement.

However, certain features essential to the operation of Fredlunds equipment, appear to present possible sources of error, and these are discussed below :

(i) Flushing air from beneath disc

The ceramic disc is bedded upon a grid of water flushing grooves as indicated in the generalised diagram (fig.4.5). The diffused air as collected in the grooves is then flushed to the diffused air volume indicator by initiating a pressure imbalance across the base. However as can be seen from the inset (fig. 4.5) diffused bubbles may become lodged in between the ceramic particles themselves, away from one of the flushing grooves. It is unlikely that such air could be consistently flushed away and quantified. The figures also indicate small bubbles adhering to the side of the flushing grooves,although this is less likely.

(ii) Flushing groove geometry

The purpose of the flushing groove is to direct water beneath the ceramic disc and flush away the collected diffused air for measurement. Fredlund adopts a wave type flushing groove geometry; this is a continuous channel design and thus reduces the possibility of air entrapment during the flushing process. However, the groove distributes water over a limited area of the ceramic disc face only, and diffused air would be very difficult to flush from one of the areas not covered by the groove.

An improvement upon this design is to cut a groove in the shape of a spiral, one flushing port at the centre, another at the outer end of the spiral. The design distributes water underneath most of the disc, thus greatly reducing the possibility of air entrapment.

(iii) Insufficient flushing pressure for diffused air

An insufficient flushing pressure can fail to remove all the collected air bubbles from under the ceramic disc.

Fredlund recommends a 5 psi / 35 KN/M^2 pressure, but in the authors opinion a 10 psi / 69 KN/M^2 back pressure is more effective. However care must be taken to avoid creating too high a pressure difference otherwise cavitation will probably occur , resulting in the creation of more air bubbles.

Operating procedures

The accuracy of data is not only dependent upon the equipment design but also upon the nature and consistency of equipment operating procedures.

The following procedures influence the accuracy of data and operation of equipment.

(i) Inconsistent reading of diffused air and water volume changes

The author notes that the optically unaided reading of burettes as undertaken by Fredlund and previous researchers is susceptible to the inconsistent reading of air water interface meniscii. The author suggests the use of a small travelling microscope to observe the meniscii on a constant plane.

(ii) Simultaneous alteration of stress components

Fredlund notes difficulties in achieving an instantaneous stress change at the beginning of each test. This process involves changing the total stress, pore air and pore water pressures.

Two distinct difficulties are encountered :

(a) Due to the large volume of the triaxial cell any change in pressure cannot be instantaneously achieved. Fredlund overcomes this by momentarily opening the air pressure valve in advance of the total and water pressure valves. This he claims,results in near instantaneous 'peaking' of all stresses.

Although not entirely satisfactory, there presently appears to be little alternative to this procedure..

(b) The simultaneous opening of the three valves (one each controlling total, air and water stress) is physically impossible for one operator and difficult to coordinate with more.

The procedure employed is to simultaneously open the total and air stress valve followed by the water stress valve.

The author suggests that the values may be physically linked to ensure simultaneous opening. However this would not necessarily ensure that all stresses build up to the desired values simultaneously.

Observations

A critical examination of the literature yields the following observations :

1. The axis translation technique presented by Hilf (1956) has been shown by several authors to work satisfactorily in unsaturated soils as a means of measuring and/or controlling negative pore water pressures.
2. The importance of collecting the diffused air beneath the ceramic disc was first recognised by Bishop and Donald (1961). They propose a simple constant volume circulating pump for flushing and measuring the diffused air. Unfortunately this design cannot create more than a modest pressure difference accross the cell base (less than 1 psi / 6.9KN/M^2) and will therefore be unable to remove all the air bubbles. In addition, the measuring capacity of the bubble trap (5ml) is insufficient for long term testing. Since there is no provision to reset the trap without terminating the back pressure, the design is somewhat limited in its present form.
3. Fredlund (1973) is the first to develop a diffused air volume indicator capable of being back pressured. The design is straightforward and warrants serious consideration.
4. MIT (1966) and Fredlund (1973) suggest controlling the air and water pressures with sensitive constant bleed air values. This permits very accurate control of the applied stresses.

5. Ideally, it is better to record the water and total volume changes, since the air phase is susceptible to complex variations with temperature and pressure.

6. The Bishop's paraffin volume change indicator is used by many authors and provides a safe and accurate means of measuring water volume changes. Recent developments have modified the device so as to automatically record volume changes on a data logging system; however, this latter device is not available to this project.

7. One dimensional consolidometers such as the Rowe cell and 'Anteus'types have been modified by installing high air entry ceramic discs to permit the measurement of one dimensional swell in expansive unsaturated soils. These units are versatile and ideally suited to modification.

8. Regarding the effects of diffused air upon the apparent water volume change, it is essential that the bubbles be 'completely' flushed from beneath the ceramic disc in order that a true correction be made for them. This is partly achieved by incorporating a flushing groove beneath the ceramic disc.
   Since 'complete' flushing is difficult to achieve, it is important that the groove covers as much of the underside of the disc as possible.
   It is suggested that a groove in the shape of a spiral would be suitable (manufacturing difficulties permitting).

9. The one dimensional volume change testing in the described equipment is limited to observing swelling behaviour, since a three dimensional shrinkage (isotropic) cannot be adequately monitored.

10. Fredlund's system incorporates most of the above observations and is therefore considered as a suitable starting point for the development of equipment for studying the stress - deformation behaviour of unsaturated expansive clays.

5.2.3 Equipment Development

The remainder of this chapter is devoted to the authors equipment development. His test system utilises several aspects of Fredlunds experimental work, some of which are improved or modified to fit in with the available facilities. The overall system controls the total, air and water stresses and permits measurement of the total and water volume changes. In addition, the diffused air collecting under the ceramic disc may be flushed away and quantified. thus enabling the true water volume change to be calculated.

The specimen is contained within one of two test cells developed for the project :

(i) 76mm cell : this employs a 3" (75mm) diameter specimen housed within a modified Rowe consolidation cell.

(ii) 102mm cell : A 4" (100mm) specimen housed within modified 4" triaxial cell components.

It is emphasised that both cells are designed to measure one dimensional swell behaviour only. The terms 'Rowe' and 'Triaxial' are retained so as to facilitate identification of the cell types.

The 102mm cell is a later development, arising from (a) the doubts concerning reliability of the 76mm cell loading system (rubber convoluted jack), and (b) the desire to examine larger specimens.

The increased working space within the 102mm cell was originally considered suitable for incorporating some form of internal pore pressure monitoring system (ref. Section 5.2.3) into the specimen. However, this aspect was discontinued because of the anticipated problems and since the measurement of pore water pressure from the base ceramic disc was considered satisfactory.

Both test cells are noted as being compatible (Chapter 6) and are simultaneously employed to increase data. The operation of the cells differs from previous research in that the loading system is operated from a pneumatic as opposed to hydraulic, source - effectively suppressing the need for a de-airing procedure within loading system fluid.

The entire equipment is located in an environmental chamber thereby minimising the variation in temperature and humidity.

The equipment is discussed under the following headings :

1. One dimensional swell testing cells.
   (a) 76mm cell (modified Rowe type cell)
   (b) 102mm cell (modified 4" triaxial cell components)
2. Plumbing
3. Pressure control and measurement
4. Total volume change measurement
6. Water volume change measurement
7. Measurement of diffused air beneath ceramic discs.
8. Data logging.

5.2.3.1 76mm cell (modified Rowe type cell)

The Rowe cell is chosen for its versatile design with regard to total and water stress application. The original design permits total stress to be applied under plane stress or plane strain conditions. In addition, the specimen may be tested under drained or undrained water conditions.

The cell employed in this project is produced by Armfield Engineering Ltd. after the original design by Rowe and Barden (1966) - refer plate 5.2 and figure 5.2. The specimen is 75mm in diameter by 25mm thick and is contained within a rigid cell body.

The outlet, normally employed for the drainage of water is used to pressurise the air above the specimen and thus regulate the pore air pressure. The load is applied using the convoluted rubber jack assembly with the exception that the jack is operated using pneumatic instead of hydraulic pressure (see later for details). Water is supplied to the specimen through a high air entry ceramic disc located in the base. The water is supplied to the cell from a pressurised reservoir via the Bishop's paraffin volume change indicator which monitors water volume flow. A diffused air volume indicator is connected to the other base tapping.

The vertical movement of the loading piston and hence total volume change is measured on an accurate dial gauge (0.001mm /division).

The design of the Rowe cell permits a simplification of the plumbing and control systems presented by Fredlund, and in this

respect it is considered superior. However, the problem of numerous seals, joints and connections and their ensuing potential leakages persist. In order to ensure precise water volume measurements, these must be eliminated or at least accurately measured and adjusted for.

The 76mm cell consists of essentially three components: Body, cover and base. The last two have been modified to permit the installation of high air entry and low air entry porous discs, details being given below (ref. fig. 5.3 and plate 5.2).

Cell Base

The main alterations to the base are the installation of a high air entry ceramic disc and provision of an additional water point (ref. fig. 5.4, plate 5.2(c)).

A suitable sized recess is machined in the bronze base to accept the ceramic disc - porosities located within the casting being filled with a suitable solder. 1mm deep water flushing grooves are then machined at the bottom of the recess. The grooves are cut in a concentric pattern since a spiral cut is not possible within the available facilities.

Prior to installing the high air entry ceramic disc, an additional water point is machined in the base to provide an inlet and outlet for the flushing water. The 2mm diameter water points emerge at opposite locations beneath the disc to ensure uniform water distribution.

The water ports are finally cleaned with a compressed air jet and tested for water passage. The high air entry ceramic disc is then located in the base. The discs employed in this research are produced by the Soil Moisture Equipment Corporation and have a 72.5 psi / 500 KN/M^2 air entry value (this equals the air pressure required to force air through the plate once it is thoroughly wetted with water).

The high air entry disc is placed in the base recess and clamped in position. Liquid Araldite No. CY 1301/HY 1300 is then injected into the space surrounding the disc to provide a strong watertight seal.

The low viscosity of the Araldite ensures that it flows into and completely fills the recess. In addition, this type of epoxy may be de-aired in a vacuum desicator so as to extract the bubbles introduced during the mixing process (thus preventing a possible leakage path from forming around the ceramic disc).

Finally, once the epoxy is fully set (3-4 days), the clamps are removed and the base is ready for use. Care must be taken not to back pressure an unloaded disc, otherwise cracks may develop rendering it unserviceable.

A Bell and Howell pressure transducer is located at the outlet port in the base. This ensures that the true base water pressure is always recorded. Full details of the transducers employed are given later.

The existing on/off Klinger values are replaced with compact miniature values produced for Soil Instruments Ltd. These values are being increasingly used by equipment manufacturers due to their compact size and equivalent performance compared to the bulkier Klinger types.

Cell Body and Cover

The cell body, which contains the specimen, is not altered in any way except that the inner surface is coated with petroleum jelly prior to testing to reduce friction between it and the rubber loading jack. The cover (Plate 5.2A)requires a few small modifications. In addition to the replacement of on/off values with the smaller "Soil Instruments" type, several porosities have been located. These permit air leakage and must therefore be plugged with conventional (high viscosity) Araldite No. 2001. This process is tested by pressurising the cell with air and immersing it under water to observe leakage. The rubber jack is pressurised with air in place of the original hydraulic pressure because

1. air pressure is easier to control.
2. it dispenses with de-airing procedures required for a hydraulic loading system.
3. the time delay required to de-air (2), would result in an unsaturated specimen imbibing unwanted water prior to test commencement.

The rubber jack is noted as not applying the same pressure to the specimen as is applied to it. This is presumably due to the expansion of the convoluted jack against the cell body, creating friction and thus reducing the actual surcharge applied to the specimen. In order to determine the true overburden being applied to the specimen therefore,a calibration factor must be determined. This is achieved by accurately measuring the difference between the supply air pressure and the load applied by the rubber jack to a load cell. The full procedure and subsequent calculation of the factor are detailed in appendix C7.

The air pressure is fed to the specimen surface via the outlet normally used for water drainage. The air is distributed over the surface of the specimen by placing a highly porous sintered phosphorus bronze disc between the rubber jack and specimen. The disc is fairly rigid and maintains a flat specimen surface, at the same time it is sufficiently flexible to resist mechanical damage (unlike porous stones).

This technique is similar to that originally used by Bishop and Henkel (1962) and subsequently by several other authors.

The air entry value of the porous disc must be less than the pressure deficiency within the specimen to ensure that water is not drawn into the disc during the test, thus creating an apparent increase in water inflow (especially at the commencement of the test).

5.2.3.2 102mm cell (modified triaxial cell components)

This employs a new 4" (100mm) diameter one dimensional swell testing cell housed within a 4" (100mm) triaxial pressure vessel - refer plate 5.4 and figure 5.5. This is developed :

(i) to observe the behaviour of larger specimens

(ii) because of some doubt regarding the loading system in the 76mm cell, and

(iii) to increase the amount of data

It was also intended that the large working space available within the 102mm cell be utilised for incorporating a pore pressure measuring device into the specimen itself. However, this approach was terminated since the tip causes a large disturbance within the specimen and also because the measurement of pore water pressure from the ceramic disc was considered satisfactory.

The triaxial cell is ideal for modifications due to the multiple tappings on the cell base. The specimen is 100mm diameter by 30mm depth, and is housed within a rigid brass cell wall (cylinder). Water is supplied via a modified triaxial pedestal with an incorporated high air entry ceramic disc.

The entire unit is enclosed within a 4" triaxial pressure vessel, thus enabling control of the pore air pressure. The total stress is applied using a specially designed pneumatic loading rig - the entire apparatus being held in a rigid loading frame. The water pressure is generated at a pressurised reservoir, passes through the

Bishop's water volume indicator and finally enters the cell base. The water outlet is connected to a diffused air volume indicator (see later).

As with the 76mm cell, a modified version of Fredlund's plumbing and control system is employed. The equipment is routinely examined for leaks, the procedure used being outlined in Section 5.2.4.

The 102mm test cell consists of two major components : the test cell, and the loading rig. Their construction is examined in detail.

The test cell

As previously mentioned, the unit is a one dimensional testing rig located within a 4" (100mm) triaxial pressure vessel (ref. fig. 5.6 and plate 5.4). The cell is composed of three portions: the base, the body and the loading plate.

The base is machined from brass stock, and is intended as a replacement pedestal to be bolted onto the original 4" (100mm) triaxial base (ref. fig. 5.7). A recess is cut into its surface to hold the high air entry ceramic disc, and 1mm deep water flushing grooves cut below this to facilitate the collection of diffused air.

Two vertical water flushing ports are machined to coincide with the existing ones in the triaxial base.

The high air entry ceramic disc is positioned in the recess and glued around its circumference with a low viscosity epoxy seal (as with the 76mm cell). The pedestal is finally bolted into position using the original fixing. Once again, back pressuring an unloaded disc must be avoided.

The body, which restrains the specimen laterally, is again machined from brass stock. It connects to the pedestal by a very fine LH thread (ref. fig. 5.8). The load is distributed across the upper face of the specimen by a brass loading plate (fig. 5.9). The plate is machined to close tolerances with a 0.5mm all round gap (to BS1377 tolerances for consolidation equipment).

The free access of air pressure to the specimen is facilitated by incorporating a grid of air channels through the loading plate. The distribution of air across the specimen's surface is facilitated by inserting a low air entry disc in between the specimen and loading plate.

The water outlet from the base is connected to a brass transducer junction. This enables measurement of the true base pressure (necessary when correcting the apparent water volume change for measured diffused air).

Only three of the original four tappings to the base are required - the air supply inlet and the water inlet and outlet - the fourth tapping is sealed.

The Klinger on/off values are replaced with the smaller soil instrument type (for the reasons noted in the 76mm cell development).

The pressure vessel which requires no modification, must be carefully sealed to the cell base to prevent air leakage.

A longer loading piston is manufactured from 19mm stainless steel rod. A very close piston bushing fit is achieved by moving the piston in the bushing whilst coated with liquid abrasive.

The loading rig

The loading rig provides the means of applying an overburden/ surcharge to the specimen. It consists of a rigid loading frame and an air cylinder for applying the load.

Loading system (Fig. 5.10)

The loading system comprises of a double acting air cylinder. This is in effect a pneumatic piston, the applied load being proportional to the air pressure supplied to it.

The piston, which is made out of a non-corrosive steel alloy, can be raised or lowered by directing the air flow accordingly (hence the term double acting). The air flow is actually directed using a 3-way, 2 position valve. Both the cylinder and valve are manufactured by Compair Maxam Ltd.

In order that an instant pressure increase/decrease can be accomplished, an on/off valve is located next to the three way valve. This is of the miniature Soil Instruments type as discussed earlier.

Since oil is introduced to the air cylinder via the air supply to facilitate lubrication, an oily mist vents to atmosphere following a reversal in air cylinder movement. This is collected to prevent air pollution.

The load applied by the air cylinder is controlled using a precision air regulator. These are of the constant bleed type and manufactured by Norgren Ltd.

As a result of piston friction, and the difference between specimen and air cylinder piston diameters, then the air pressure applied to the air cylinder does not equal the specimen overburden. In consequence, the air cylinder must be calibrated (ref. App. C6).

The air pressure supplied to the air cylinder is controlled from the supply board (described later).

Loading frame (Fig. 5.11)

The loading frame is a rigid steel assembly, designed to hold the test cell while being subjected to the air cylinder loading. It comprises of upper and lower rectangular 20mm steel plates, separated by four 40mm threaded studs located at the corners.

Where studding passes through a plate, a nut is secured above and below it to form a rigid connection.

The frame is designed for zero deflection under anticipated loading conditions.

Provision must also be made within the design to monitor vertical displacement of the specimen. Two methods are employed : the first involves mounting a magnetic based dial gauge to the upper main plate (see Plate 5.3D), and the second method utilises two 15mm mild steel vertical bars, (mounted on the base only so as not to be susceptible to extension undergone by the rig) to which movable arms bearing linear displacement transducers are connected.

Plumbing

Since accurate verification of the volume change theory depends upon the water volume change measurements, then it is imperative that any system 'leaks' be eradicated. One of the greatest potential leak sources is the plumbing, and the various aspects of this are separately discussed below.

Pipework

Two types of polypropylene tube are employed in this equipment :

water pipe : 5mm OD , 3mm ID

airline : 8mm OD , 6mm ID

Pipe connections

These are essential to ensure an absolute water or air seal. The airline is connected to equipment via non permanent and easily detachable push-in type connectors (manufactured by Compair Ltd.).

The smaller water pipe is connected using brass 'olive' type connectors. A brass washer (olive) is attached to the pipe, against which is tightened a nut, thus effecting a watertight joint. (Manufactured by Simple-fix).

Constant bore pipe and fittings

A variation in bore diameter can result in air being trapped within the system, and may even cause diffused air to come out of solution as a result of a change in fluid pressure. The bore of most fittings varies from manufacturer to manufacturer and steps must therefore be taken to standardise.

This is achieved by fixing a greased section of piano wire (2mm diameter) through the fitting and filling the surrounding space with a low viscosity epoxy resin. Once this has set, the piano wire is removed, resulting in a smooth uniform bore.

Air/watertight-threaded connections

The system employs a large number of threaded connections, most of which are of a permanent nature (although a few are regularly disconnected).

Attempts to seal connections with PTFE plumber's tape result in the tape deteriorating - essentially contaminating the water supply.

However, the tape is apparently not affected by the air supply.

The main advantage of PTFE tape is the ease with which sealed components can be dismantled.

'Lockite' - a semi permanent setting fluid that seals and locks threaded connections is found to provide an effective water/air-tight seal. The main disadvantages of this compund are : the lengthy setting time (> 2 days) and the difficulty encountered in dissassembling sealed threads.

It is decided however to utilise Lockite on all permanent water system connections involving metal to metal contact.

Connections with perspex are sealed using the more flexible PTFE tape (thus preventing cracking).

Pressure control and measurement

The test systems require an easily controlled air pressure source for the total, pore air and air volume indicator back pressures. In addition, the water stress must also be pressurised.

Hilf (1956) and others, show that water will assume the same pressure as the air pressure applied to it, thus the required water pressure can be generated by applying a pneumatic pressure to the surface of a sealed water reservoir.

A total of four separate air pressure outlets are required; three capable of delivering 80 psi / 552 KN/M^2 for the the air pressure, water pressure, and the diffused air volume indicator) and a fourth capable of providing 115 psi / 793 KN/M^2

(total stress). The actual requirements are twice those listed above, due to there being two test systems used concurrently.

Pressure distribution board

The pressure supply for both systems is controlled from the pressure distribution board or 'board' as henceforth referred to (Plate 5.5).

The equipment is designed to withstand 200 psi / 1379 KN/M^2, thereby providing a safety margin well above the maximum working pressure.

The air supply first passes through a dirt/moisture trap and is then fed to the control precision air regulator valve (by Norgren Ltd.). This valve dictates the magnitude of the maximum board pressure. The air flow is then split into four branches leading to the total, pore air, pore water and air volume change indicator back pressure supplies. The output from each branch is controlled by a further Norgren valve, and monitored by a further 2" face diameter pressure gauge. For accurate pressure measurement, a single Bell and Howell pressure transducer is cut into either of the four channels as required (refer figures 5.2 and 5.5) .

The above network of pipes, gauges and valves are mounted on a thin metal sheet, this in turn being reinforced with a wooden frame. (Ref. Plate 5.6). The entire assembly is quite heavy, but successfully mounted on the wall using two bolts. This method of fixing also facilitates rapid inspection of the assembly.

Pressure supply

The basic requirements of the pressure supply are firstly a minimum output of 115 psi/ 793 KN/M^2, and secondly, that it is available for 24 hrs per day.

The 'in house' compressed air supply fails to meet the above specification, however it can be employed for lower pressure ranges (n.e. 80 psi/ 552 KN/M^2) between 0900 and 1630 hrs weekdays.

The above specification is met by a small electric compressor. Only a small size is required since the volume of air used is limited.

Pressure measurement and recording

Pressure measurement

The pressures within the system are measured using electronic pressure transducers. Two types are employed to accommodate the anticipated pressure ranges.

Channels 2, 3 and 4 with an 80 psi/ 552 KN/M^2 maximum requirement utilise 100 psi/ 690 KN/M^2 Bell and Howell pressure transducers. These require a 10v DC excitation voltage and have a maximum output of 200 mV.

Channel 1 requires a maximum 115 psi/ 793KN/M^2 and utilises a 225psi / 1551KN/M^2 pressure transducer by Druck Ltd. The other characteristics are identical to the Bell and Howell type. Calibration information is presented in Appendix C2.

The pressure transducers are 'energised' using a 10 VDC voltage generator. The outputs are connected to sensitive voltmeters and

calibration factors applied to obtain true pressure readings.

The adoption of such a simplified data acquisition system is discussed later.

Measurement of total volume change

The total volume is measured on the 'Rowe' and 'triaxial' systems by mechanical dial gauges capable of recording deflections to at least 0.001mm. These monitor the deflections of the loading pistons in both cases (ref. plates 5.1 and 5.3).

The specimens are restrained laterally, thus the measured swell is fully representative of the total volume change. The volumetric behaviour of an unsaturated soil is determined by the water pressure deficiency (suction). The specimen will swell provided suction is decreasing. Conversely, an increase in suction will result in an isotropic shrinkage of the specimen, causing it to 'pull away' from the test cell body. It is apparent that under such circumstances the measured displacement will not be representative of the total volume change.

The apparatus described in this chapter is therefore restricted to the study of one dimensional (vertical) swell behaviour.

Both systems are subject to compressibility effects, the calibrations being listed in Appendix C3.

The measurement of water volume change

This is achieved using a Bishop's type double tube, double acting water volume change indicator as produced by Farnell Engineering Ltd.

The burettes have a full travel of the water kerosene interface equal to 25 ml, volume changes being recorded to within 0.02ml.

In an effort to reduce leakage, new seals were installed in the indicators used with each system. The inside of the burettes are coated with silicon water repellant to ensure consistent meniscus forms. The back pressuring of the devices over several days indicates that they consistently leak a small quantity of water. these leaks will amount to a significant loss over extended testing periods; the measured water volume changes must be corrected accordingly. The formulation of these corrections are detailed in appendix C.1.

It is noted that volume changes should always be recorded using the interface moving downwards, since this exhibits the best meniscus form and therefore the most consistent reading mark.

Measurement of the diffused air beneath ceramic discs

Although free air cannot pass through the ceramic discs (up to the air entry value pressure), diffused air can and does, pass through and form as bubbles below the ceramic disc. The recorded water volume change is therefore in error, and must be adjusted for the volume of diffused air recorded over the same time period (in accordance with Boyles law - refer Appendix D).

The volume of diffused air is measured using a purpose built indicator. It is flushed with water from beneath the ceramic disc to the indicator by creating a pressure gradient across the cell base.

A diffused air volume indicator designed after Fredlund (1973) is adopted with suitable alterations. (Figures 5.2-5.5 for general layout). The design is centred around an inverted 25ml glass burette, partly filled with water and closed at the top (fig. 5.12).

Water is flushed from the cell base and enters the diffused air volume indicator (DAVCI) into the lower end of the burette. At this point, flushed bubbles float to the air-water interface within the burette. The water cannot fill the burette due to its closed end, and is thus diverted to an exit tube and finally into the main chamber. The amount of diffused air is registered as a change in the meniscus level.

The main chamber may be back pressured to create any desired pressure gradient across the cell base. (see section on operating procedures for further details). The design consists essentially of the base and a housing, both being examined below.

The base

This is the 'heart' of the device and directs the water flow firstly to the burette and secondly to the indicator chamber. It is turned from 125mm perspex stock, all channels subsequently being drilled to 2.0mm diameter. The main entry and exit parts are threaded to $\frac{1}{8}$" BSP to accept the on/off values from Soil Instruments Ltd. The burette is positioned by a threaded brass sleeve - metal to glass contact being prevented by a greased P.V.C. 'O' ring. This 'flexible' joint is found to protect the burette from knock damage, and prevent

build up of excess torque, and subsequent cracking of glass during assembly. Water is directed to the burette via a 5mm OD/ 2.5mm ID perspex tube - which is glued into the base.

The exit tube, originally proposed by Fredlund, was glued directly into the base. This has been modified such that it can be screwed into place, thus facilitating easy replacement.

The base is connected to the indicator housing by a coarse machined thread (60 x 2.5ø). A water/airtight seal between the base and housing is accomplished by countersinking a large P.V.C. 'O' ring into the base.

The indicator housing

This comprises of a perspex chamber which screws to the base. The housing is composed of an 80mm diameter perspex cylinder with 5mm walls, it being capped with a 30mm thick perspex plug. Into the plug are machined a threaded air entry port for the air pressure entry valve and a central locating hole for the burette. The central hole also contains two countersunk 'O' rings to provide an airtight seal at the head of the burette. A small amount of petroleum jelly at the head of the burette prevents the development of excess torque and subsequent cracking of the burette during equipment assembly. All perspex joints are permanently cemented using ICI Tensol cement No 12.

Logging of data

A manual data logging procedure is adopted in this project. Readings to be taken include: water volume, diffused air and specimen

swell, in addition to the digital pressure readings, recorded as a voltage output from the transducers.

The main reason for adopting a manual recording procedure is that the water volume and diffused air must be recorded manually due to the nature of the apparatus. Even if the other quantities were logged automatically, the combination of logging methods is not considered satisfactory due to the potential booking errors. In addition, a manual procedure is adopted for the following reasons :

(i) the electricity supply is prone to very short cuts or power surges overnight - due to the absence of an emergency supply. The adoption of one of the available micro computer based systems would result in a complete loss of data and possible 'corruption' of the floppy disc following any such interruption of supply.

(ii) since the system is still under development, then an unnecessarily complicated logging system is presently considered inappropriate.

(iii) since readings are taken on a once daily basis only, then a continuous 24 hr/day recording system is considered superfluous.

Water supply

For the sake of consistency, double de-aired-deionised water is employed for all testing.

Constant temperature

Temperature is recognised as affecting the swell potential of expansive clays (ref. Chapter 2.7(g)). Krazynski (1973) and more recently Sherif et al (1982) demonstrate this experimentally.

Since it is not the object of this project to examine temperature effects, and in the interests of consistency, all testing is conducted in a temperature/humidity controlled environmental chamber.

Records indicate a mean temperature of 24^{o}C with a standard deviation of 2.4 ^{o}C.

5.2.4 Preparations for testing

The verification of Fredlund's theory requires that all water and volume changes are accounted for, and therefore related either to an equipment deficiency or a soil process. To achieve this, the apparatus must be thoroughly examined in between each test for new leakage.

Bishop and Henkel (1962) indicate that the high air entry disc must be de-aired before every test and the air entry and permeability values be determined so as to highlight cracking of the disc and subsequent inaccuracies in the readings.

Since all water volume change measurements are made with reference to the Bishop's water volume change indicator, then it is imperative that its functioning is fully accountable.

In addition to the above (regular) checks, there are general one-off calibrations which are determined only periodically.

The above are discussed in the following pages.

Saturation of the high air entry disc

The high air entry discs are de-aired by filling the cell with water, and applying an air pressure of 100 psi/ 690KN/M^2. The exit valves from the base are initially closed, thus allowing the pressure to build up within the disc and underlying water chamber. After two hours, the bubbles have dissolved in the water and the exit valve is opened, thus flushing away the diffused air. This process must be repeated for at least one day with a new disc, although pre-saturated discs should be satisfactory. The disc is kept saturated once the above procedure is conducted.

Permeability of disc

The equalisation of the disc permeability indicates that the high air entry disc is saturated. The permeability value should remain constant throughout the disc's life, and a sudden increase is considered indicative of a crack. The permeability is measured by filling the test chamber with water to a depth of 20mm, applying a pressure and monitoring the rate of water outflow to a Bishops' indicator (ref. App. C5 for details).

The pore pressure response time of the disc is not studied in this thesis,since in view of its small magnitude (Robinson,unpublished) it is not considered as significantly influencing the overall system response time.(appendix C5).

Air entry valve

The object of this test is not to determine the actual air-entry valve but more to assess whether the disc can withstand pressure differences in excess of those anticipated during testing. The test involves wiping the disc almost dry and applying the required pressure to its surface. If the port to the Bishop's indicator is opened then the air diffusing through the disc will displace water and be recorded. A sudden increase in air flow indicates either a cracked disc or a leakage within the cell. This aspect is again dealt with in Appendix C5.

Water leakages

All water volume changes recorded during testing must be accounted for.

The large number of joints and connections, create many possible sources of leakage, and a methodical - regular examination of the equipment is essential. The order of assessing equipment is as follows :

(a) Bishops water volume change indicator

Since all subsequent water volume changes are measured using this device it is essential that leakage from it be halted or at least allowed for. The indicator is back pressured through each limb for two days at 50 psi / 345 KN/M^2 and subsequent volume change recorded. It is suggested that the indicator should not leak > 3/100ml over two days - although all leakage must be accounted for during the analysis.

(b) Valves

Both testing systems (based on the 76mm and 102mm cells) employ several on/off valves which must be regularly tested. The back pressured Bishops indicator is attached to the cell, but with the connecting valve closed. Each valve is tested for a minimum of one day in either direction.

(c) Cell leakage

Cell leakage will cause a demise in air pressure when the cell is isolated (as during the changing of stress condition). To identify leakage, the cell is pressurised to a high pressure (100 psi/ 690KN/M^2) all valves closed and any demise of pressure monitored. Losses should be less than 1 psi / 6.9KN/M^2 per day. (ref. App. C4)

The actual point of leakage can be determined by immersing the cell in water and observing any escape of air (see Section 5.2.3.1 on porosities).

5.2.5 Testing procedures

The two procedures employed as the primary means of evaluating the volume change theory are as follows :

(a) Null (undrained) testing

Fredlund (1973) and Barden, Madedor and Sides (1969) employ 'null' tests to validate the proposed stress state variables (refer Chapter 4 and Appendix E), for specimens of comparatively low expansion and

plasticity characteristics (liquid limit < 64%).

Although the author uses null tests primarily for the verification of the stress state variables for medium-high expansive soils, they are also employed for the following purposes :

(a) perfecting specimen production technique

(b) to ensure correct functioning of apparatus (comparing with other research)

(c) development of operating procedures

It is indicated in Chapter 3 that if the stress components, U_a ,U_w and σ are changed, no process should occur in the soil provided the stress state variables : $(\sigma - U_a)$ and $(U_a - U_w)$ or $(\sigma - U_w)$ and $(U_a - U_w)$ remain constant.

This procedure is the basis of null testing and is achieved by increasing σ ,U_a and U_w by equal amount simultaneously. The tests are therefore termed null since their object is <u>not</u> to produce a change within the phase/phases under consideration. This is further discussed in Appendix E3.10.

<u>(b) Drained/Uniqueness tests</u>

The purpose of these tests is to determine whether the proposed constitutive relationships for volume change are unique (i.e. whether there is only one relationship between the stress state variables).

A complete examination of the constitutive surface requires :

(a) small stress deviation about a stress point

(b) larger stress changes to examine the entire surface

(c) reversals of stress to observe hysteretic effects

However, due to time and equipment limitations, this investigation is limited to small stress deviations at a point, and the procedure adopted is as follows :

Small stress deviations about a stress point

The specimen is subjected to small stress increments along three stress paths. Using the deformation from any two of the increments, it is possible to compute two corresponding compressibility moduli. Now the deformation equation can be used to compute the anticipated deformation along any other stress path. The computed deformation is compared with the measured deformation. The constitutive surface at a point is unique if the measured and predicted deformations are essentially equal in all cases.
(Appendix E5.9).

Detailed testing procedures

The overall testing procedures are essentially the same whether operating in the drained or undrained modes. The prime difference occurs in the interpretation of data.

The procedures involve :

1. Specimen preparation
2. Equipment assembly and test initiation
3. Routine measurements
4. End test and equipment disassembly
5. Additional operations

The above are detailed in Appendix A1 and A2.

5.2.6 Data processing

The large quantity of experimental output is typed into a microcomputer and processed using a purpose written program. The program is formulated to : (i) apply the previously determined correction factors for compressibility and known water leakage to the experimental output and (ii) determine the total volume, water volume and pressure histories for each test.

A similar procedure is adopted for the oedometer swell pressure tests, full details and sample calculations being given in Appendix D.

5.3 CONVENTIONAL CONSOLIDOMETER EQUIPMENT USED TO PROVIDE SUPPORTING DATA

Aim

The aim of this section is to describe the consolidometer equipment and procedures employed to provide supporting data for the main tests outlined previously.

5.3.1 Basic Considerations

The full testing of unsaturated soils requires a complex system incorporating control of the air, water and total stresses. Such a system, although essential for the rigorous experimental verification of a theory is probably beyond the means of most soil testing laboratories. A simplified testing system and procedure is therefore desirable for engineering application. Various testing procedures involving the one dimensional consolidation apparatus are used in practice. These include the "constant volume" and free swell testing methods. It is assumed that the soil matrix suction is eliminated by immersing the specimen in water, and that the soil properties and stress values are obtained from the total stress plane.

In the constant volume swell pressure test the specimen is subjected to a token load and submerged in water. As the negative water pressure is released to atmospheric conditions, the specimen tends to swell. The applied load is increased to maintain constant volume until no further tendency to swell is exhibited. This maximum load is termed "the uncorrected swell pressure". The results are normally plotted in a two-dimensional format (void ratio (e) against total stress variable $(\sigma-u_a)$) they are more readily understood in a three dimensional format (refer figure 5.14for example).

Figure 5.14 illustrates the ideal void ratio stress path with a minimum of disturbance. In reality the stress paths are more significantly affected by sampling (fig. 5.15) the swell pressure being reduced from P_s to P'_s. This value must therefore be adjusted to compensate for the sampling disturbance, and a semi empirical technique based upon Casagrande's method for determining preconsolidation pressure in overconsolidated clays is presented by Fredlund (1980).

The freeswell type test involves allowing the immersed specimen to swell freely under a token load only. The load required to bring the specimen back to its original void ratio is termed the swell pressure.

The main criticism of this test is that it incorporates hysteresis into the prediction of swell pressure (the specimen being permitted to swell and then compressed to yield the swell pressure value). Even so, this is found to have a beneficial side effect and tends to compensate for the sampling disturbance. The measured swell pressure is therefore more accurate than that obtained from the constant volume swell pressure test before correction.

Choice of test procedure

The constant volume swell pressure test (CVSP) is one of the 'accepted' swell testing methods in geotechnical practice and is preferred due to it:

(a) already having been employed by Fredlund (1980) and Yoshida et al (1983) for evaluating the volume change theory on a low-expansive soil. This limited success provides scope for further verification of the theory with a range of higher expansive soil types.

(b) being quicker to perform than the free swell test, due to the smaller time required for swell pressure to achieve equilibrium.

The reliability of this method is best gauged by comparing the swell prediction (based on experimental data) with observed insitu behaviour. However, the absence of suitable field data requires that free swell tests be conducted to provide some data for comparison purposes.

Test types

Two types of consolidometer based tests are therefore used:

Constant volume swell pressure test (CVSP)

A standard 'swell' indicating test employed to provide a prediction of potential heave and swell pressure.

Free swell test

A modified free swell type test devised by the author to provide a heave value with which to compare the predictions made from the CVSP test. A specimen is permitted to swell freely under a particular overburden value. The final equilibrium swell (change in height) is

taken as the soil swell, and expressed as a percentage of the original specimen height.

The CVSP test in relation to the volume change theory for unsaturated soil

The data is used to determine the appropriate moduli (compressive and rebound) wrt the insitu stress state.

The swelling exhibited by an unsaturated soil is assumed equivalent to the rebound experienced due to the unloading of a saturated soil (held at constant volume during swell pressure build up). The rebound surface is unique when plotted on the 3D void ratio constitutive surface. (Figure 5.13).

The soil specimen is initially at $(\sigma - u_a)_o$ and $(u_a - u_w)_o$ and then inundated with water - swelling until equilibrium is attained (and $(u_a - u_w) = 0$). Swell can be predicted on the basis of the suction plane rebound modulus, however, this is difficult to measure, thus heave is determined using an alternative stress path. There are an infinite number of stress paths a specimen can take, however, the following is adopted : from the initial point, the specimen proceeds along the constitutive surface until suction equals zero. At this point swell pressure is a maximum, and further increase in load will decrease the voids ratio (Fig. 5.13). This value is said to be equal to the sum of the equivalent matrix suction, and total insitu stress. The equivalent matrix suction (in the total

stress plane Fig. 5.14) does not actually equal the matrix suction, but the dissipation of either results in the same amount of heave.

The stress path finally rebounds to the final void ratio in the total stress plane.

As indicated in figure 5.15, sampling disturbance will result in a reduced swell pressure. When the void ratio versus log pressure curve is plotted for the test, a modification of Casagrande's empirical correction (originally for calculating preconsolidation pressures) is applied to yield a swell pressure value adjusted for sampling disturbance.

In addition, the void ratio versus pressure plot is adjusted for compressibility of the consolidometer.

The adjustment procedures for equipment compressibility and sampling disturbances are fully discussed by Fredlund (1983). Example calculations are presented in Appendix C

Theoretical aspects of the CVSP test

(a) General

Fredlund visualises the behaviour of unsaturated soils in terms of changes in moisture content and loading. He presents a series of constitutive relationships for total and water volume changes (Chapter 4) in terms of $(u_a - u_w)$ and $(\sigma - u_a)$, and also expresses them diagrammatically.

Where the logarithm of the stress state variable is used, the void ratio constitutive surface may be linearised over a wide range of stress such that :

$$\Delta_e = C_t \log \frac{(\sigma-u_a)_f}{(\sigma-u_a)_o} + C_m \log \frac{(u_a-u_w)_f}{(u_a-u_w)_o} \qquad (5.1)$$

where

C_t = compressive index with respect to total stress

C_m = compressive index with respect to matrix suction

'f' subscript designates final conditions

'o' subscript designates initial conditions

The heave (Δh) of a soil layer of thickness (h) is given as

$$\Delta h = \frac{h \cdot \Delta_e}{(1 + e_o)} \qquad (5.2)$$

e_o = initial void ratio

The final degree of saturation is assumed to be in the region of 100% (Fredlund (1979)), thus the change in water content can be calculated, where

$$\Delta W = \frac{S_f \cdot \Delta e}{G_s} + \frac{e_o \cdot \Delta s}{G_s} \qquad (5.3)$$

S_f = final saturation ; G_s = specific gravity

ΔS = change in degree of saturation

Fredlund recommends that an analysis of heave through a soil profile be considered in terms of several layers - the above procedure being applied to each layer in turn; however, in the case of this project, a single layer is assumed.

(b) Initial stress conditions

Since the ambient air pressure is taken as the reference pressure, then the pore water pressure distribution is considered equivalent to the matrix suction distribution which can be measured indirectly using the procedure described later.

(c) Final stress (boundary) conditions

A limited number of field studies are undertaken by Yoshida et al (1983) who conclude that the following assumed final stress conditions result in the best predictions of heave :

(a) final air pressure equals zero (atmospheric)

(b) final pore water pressure assumed constant and equal to atmospheric.

5.3.2 Apparatus

The testing system employed for undertaking constant volume swell pressure tests is based upon a conventional consolidometer linked to a data logging system for continuous readings. (Refer to plate 5.9 and figure 5.17). The system is duplicated to increase data output.

Specimen and test cell

The specimen is compacted to the required specification as detailed in Appendix A. The specimen measures 75mm diameter by 15mm deep, some 5mm shorter than the consolidometer ring height so as to ensure expansion within the confines of the ring only. The ring is placed within the cell body that holds the water supply. Porous plates are located above and below the specimen and the screw-on base 'plate' positioned.

The cell is located on the consolidometer loading frame, which loads the specimen in a lever arm and stirrup type assembly. The load (metal weights) is suspended on a weight hanger located at the end of the 11:1 ratio lever arm.

Data monitoring system

Data monitoring can be achieved manually, however since a continuous record of deformation is desirable, then a linear displacement transducer is located above the specimen and linked to a chart recorder. This provides a complete volume change history for the specimen at every loading stage.
Operation of the chart recorder is straightforward; however, it must be recalibrated prior to each test.

The linear displacement transducers are centrally located above the consolidometer loading pin and are energised using a 2 volt DC electricity supply.

Although the recorder is mains operated, and subject to data loss in the event of power failure, the time base is sufficiently slow that short power failures can be tolerated.

The displacement transducers are actually connected to the chart recorder via a Wheatstone bridge circuit so as to amplify the signal and thus increase the response of the recorder.

5.3.3 Preparation for testing

In order that the equipment will function correctly, and yield consistent data, it is essential that all necessary preparations are made prior to commencement of testing.

These can broadly be grouped into two categories : equipment and calibrations.

(a) Equipment

Specimen preparation

The specimen is produced from synthetically prepared mixtures of Kaolinite and Bentonite (Appendix A).

Moisture content of the porous discs

These are air dried in an environmental chamber for 24 hrs and then weighed immediately prior to testing to determine the moisture content. This is undertaken to ensure a consistent starting point for each test.

Consolidometer ring

The inner face of the consolidometer ring is lubricated with petroleum jelly prior to insertion of the specimen. This should provide a uniform reduction in friction for all specimens.

Cleaning of equipment

Since the specimen is saturated during testing, some clay particles become suspended in the water and contaminate the equipment. Prior to testing therefore, all apparatus must be thoroughly washed then dried.

(b) Calibration

Routine calibration

These include calibrations that must be undertaken prior to each test. Only one calibration of this type is necessary - that of the data recording system.

Periodical calibration

These encompass calibrations made after equipment construction and only periodically conducted thereafter. They involve the calibration of the linear displacement transducers, essential to convert their voltage output into real displacement, and secondly, the compressibility of the equipment. This latter aspect is thoroughly examined in an early paper by Fredlund (1969). This publication highlights the probable causes of compressibility in the consolidometer and proposes a series of corrections to allow for them.

This information is applied to the authors data. Details of these corrections and their formulation are given in Appendix C.

5.3.4 Testing procedures

These include the testing procedures employed for the constant volume swell pressure and free swell tests. Since they involve many steps, they are too long for inclusion in the main text and are therefore described in appendix A3.

5.3.5 Data processing

The data processing procedure involves several stages.

It is less straightforward than for other test methods since the data must be plotted and an empirical correction graphically applied before the main processing can commence.

Initially the paper chart output is taken from the chart recorder then the deflections corresponding to each load scaled off in millimetres. The initial and final specimen dimensions and weights are recorded, all information then being typed into a Commodore Pet microcomputer. This data is processed using the first of two computer programs which calculates the void ratio and corresponding load values after taking the previously determined equipment compressibility values into account.

The data from this computer program enables the void ratio versus load diagram to be plotted, to which a modification of Casagrande's empirical correction (for sampling disturbance) is applied. This yields the 'corrected' swell pressure. (Refer Appendix C).

The data from the above graphical construction is then combined with the original data file and entered into the second and final

program which calculates anticipated phase volume changes (total and water) on the basis of the volume change theory and compares them with measured values.

5.4 EXPERIMENTAL PROGRAMME

Upon the basis of conclusions drawn in chapter 4, and using the preceding equipment development, the proposed scope of experimentation is outlined in figure 5.17.

A full list of tests is given at the start of each results chapter (i.e. ch. 6,7 &8).

The criteria adopted was to conduct as many tests as time would permit; however, as will be seen later, the long equalisation times required by the high plasticity specimens imposed a limit upon the total number.

5.5 NUMBERING SYSTEM

The following numbering system is used for the test programme.

5.5.1 Stress control apparatus(76mm and 102mm cells)

The numbering system is similar irrespective of the type of test conducted (i.e. null or uniqueness).

A typical test number is NR0203 and is decoded in the following manner:

N = null test (U represents uniqueness test).

R = 76mm cell based upon Rowe cell components
(T represents 102mm cell based upon triaxial cell components).

02 = the second specimen

03 = the third stress change

Using the full coding permits immediate identification of each test conducted;however, specimens may be generally referred to using an abbreviated form e.g. NR02.

5.5.2 Consolidometer apparatus

The coding of consolidometer tests consisted of simply assigning an ascending number to each subsequent test.

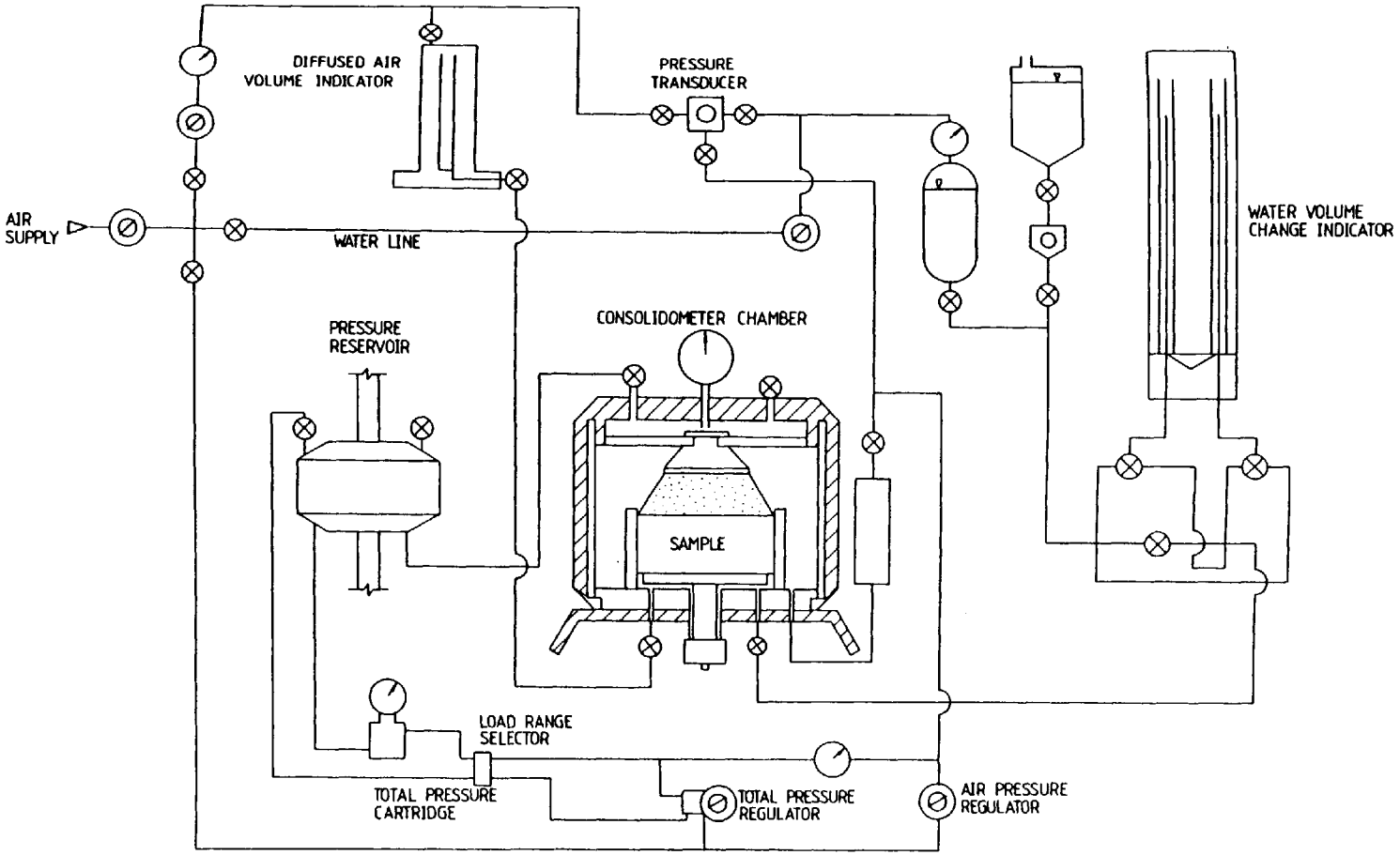

FIGURE 5.1

FREDLUNDS MODIFIED
'ANTEUS' CONSOLIDOMETER

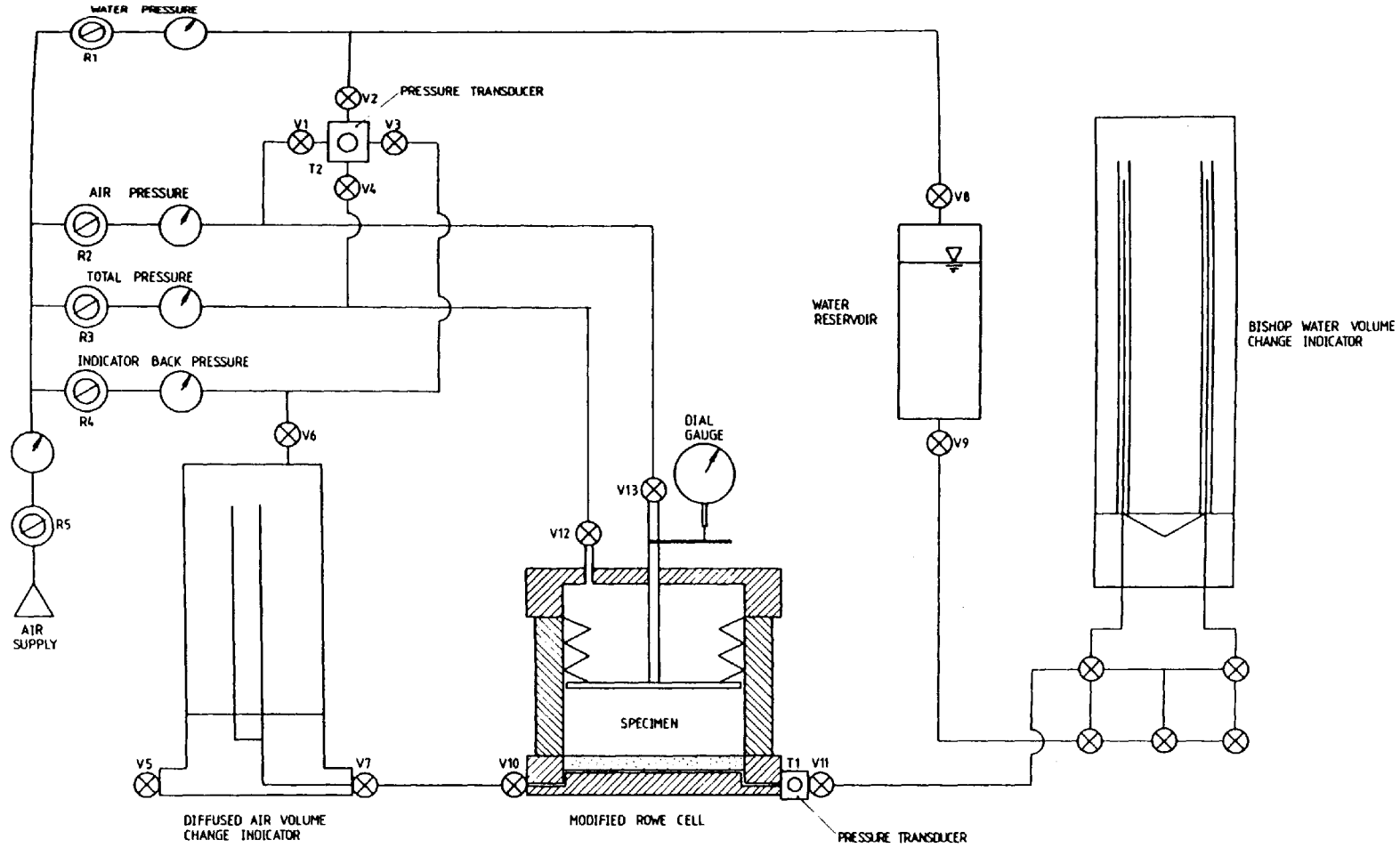

FIGURE 5.2

GENERAL LAYOUT OF ONE DIMENSIONAL SWELL TESTING SYSTEM (USING ROWE - CELL COMPONENTS)

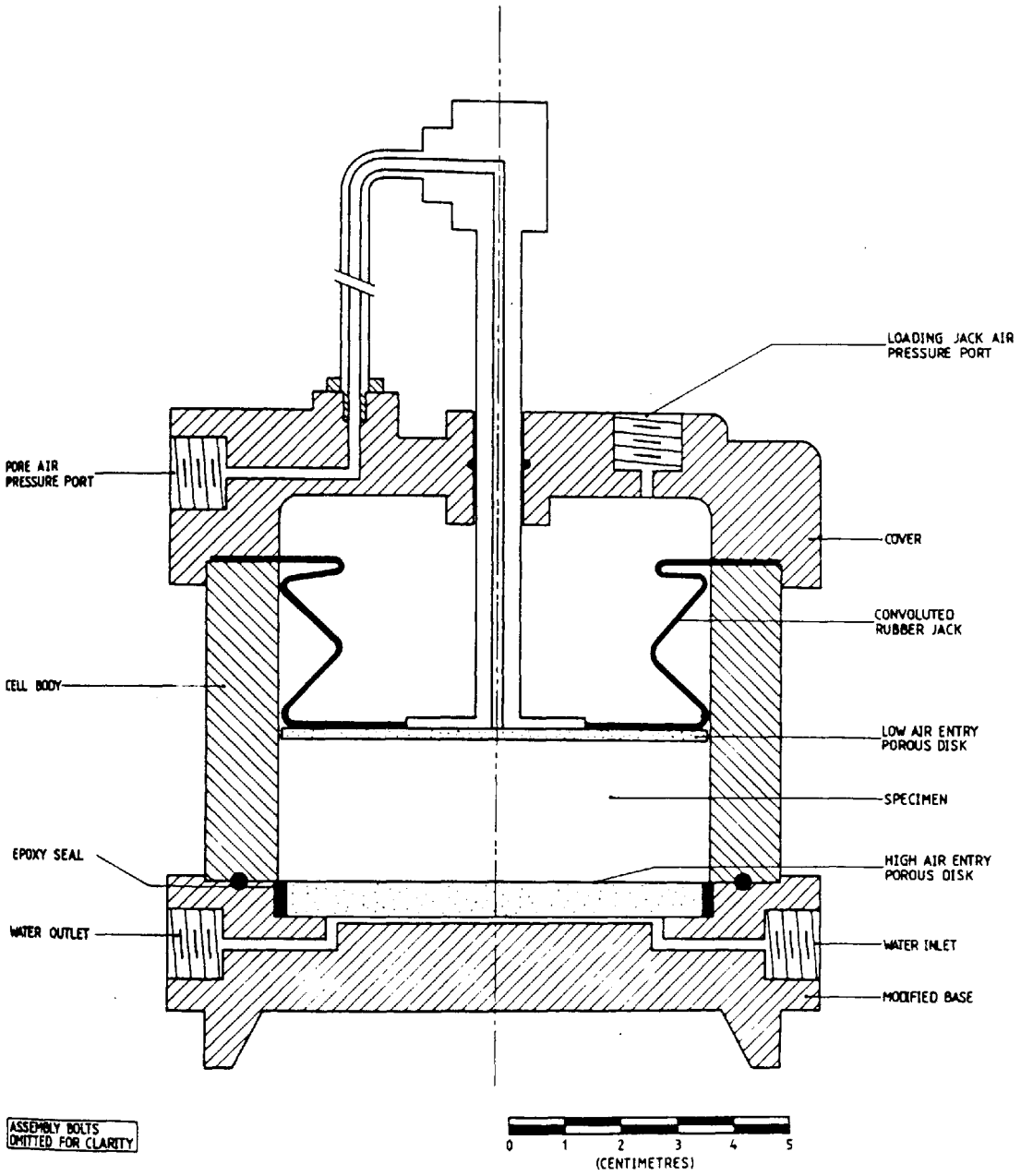

FIGURE 5.3

ONE DIMENSIONAL SWELL TESTING CELL(76 MM DIAMETER X 25 MM HIGH SPECIMENS)

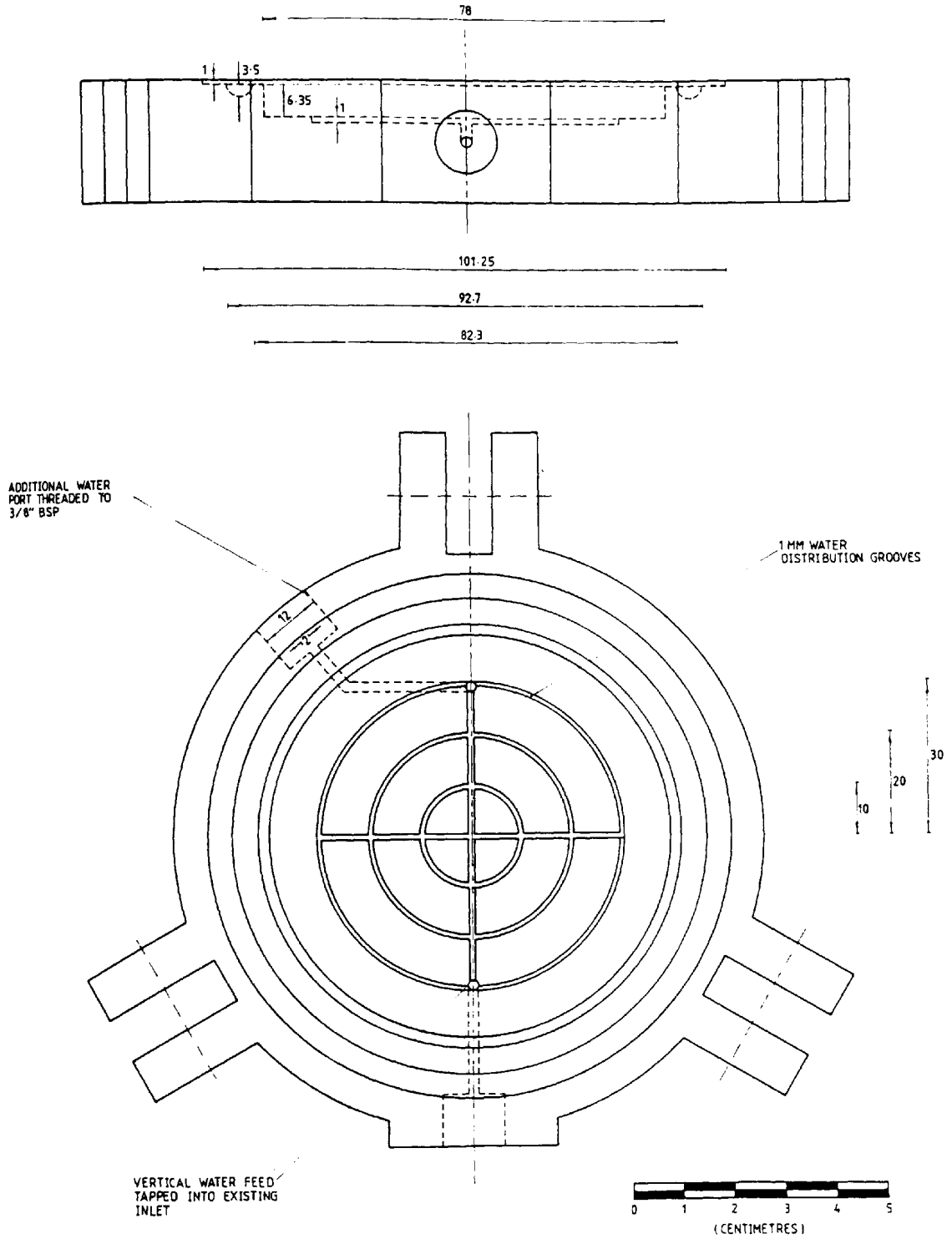

FIGURE 5.4

MODIFIED ROWE CELL BASE

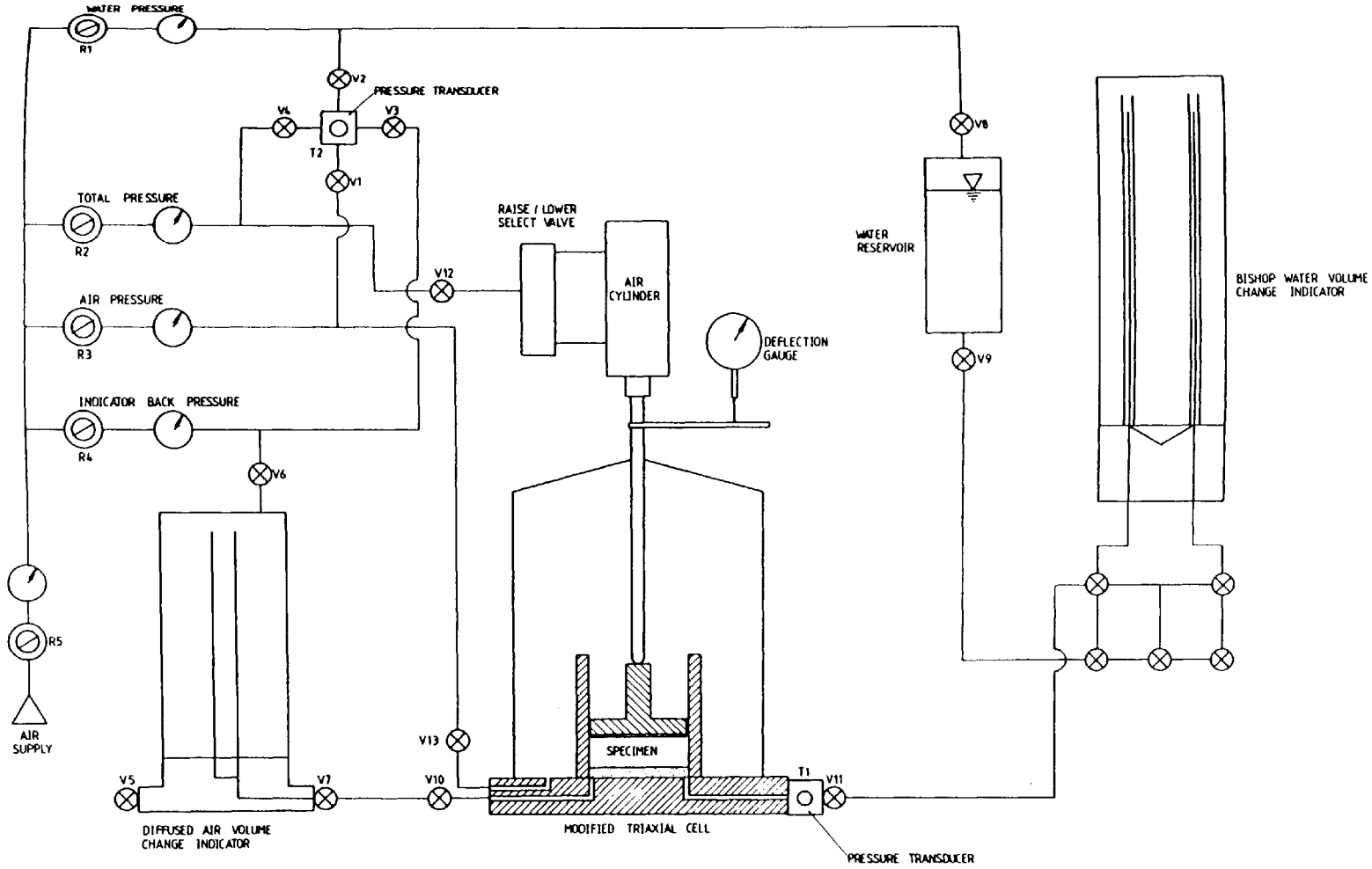

FIGURE 5.5

GENERAL LAYOUT OF ONE DIMENSIONAL SWELL TESTING SYSTEM (USING TRIAXIAL - CELL COMPONENTS)

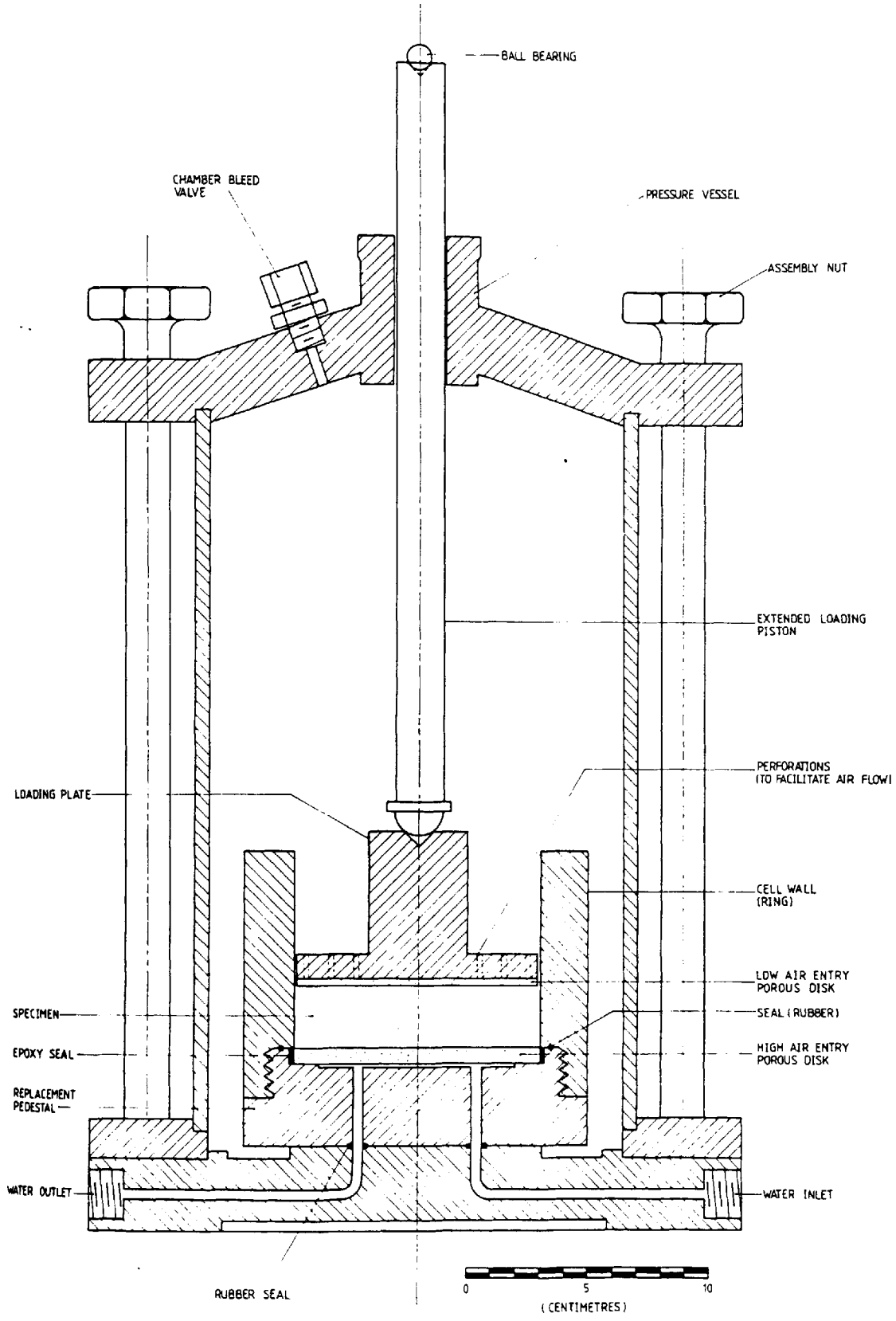

FIGURE 5.6

ONE DIMENSIONAL SWELL TESTING CELL(102 MM DIAMETER X 30 MM HIGH SPECIMENS)

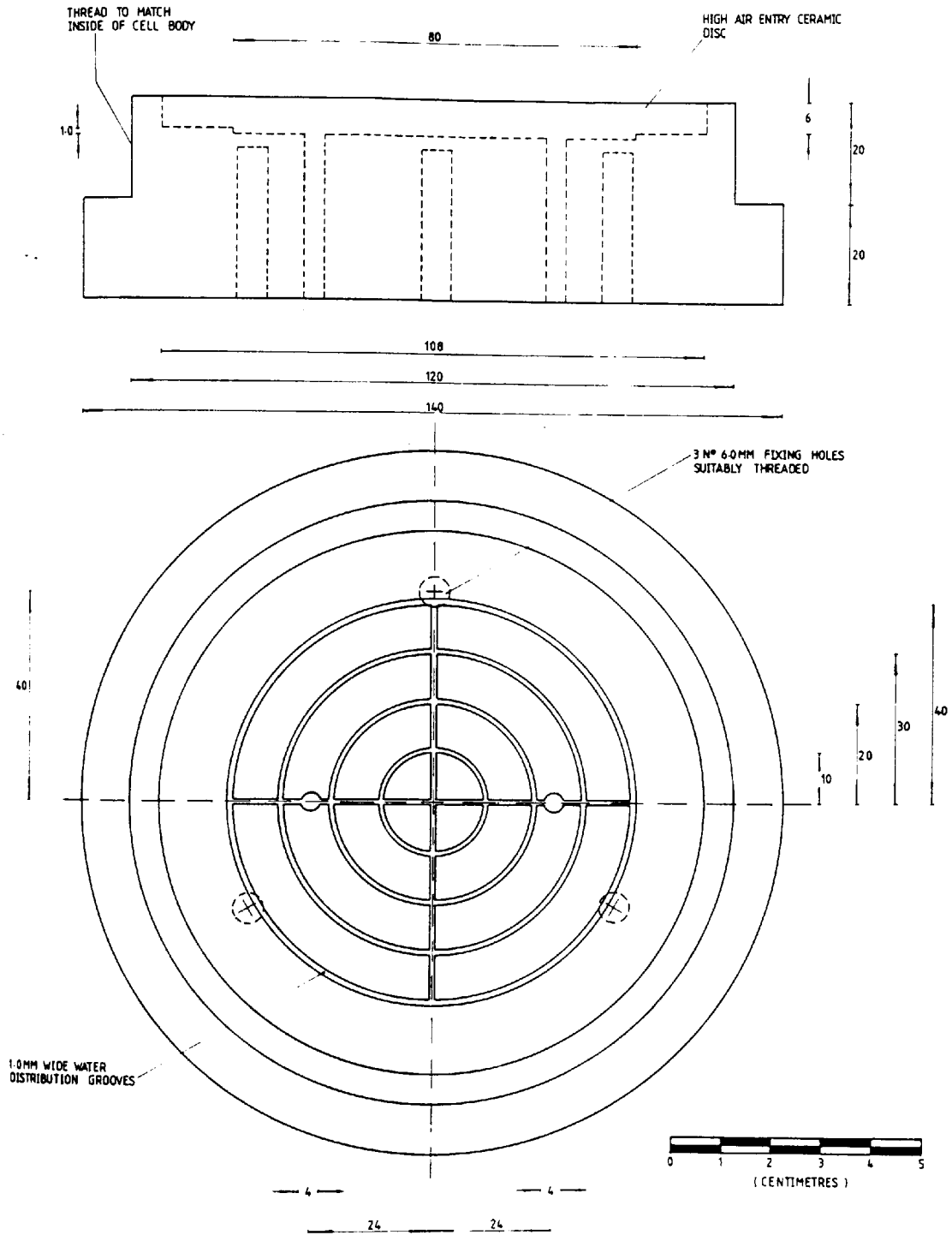

PEDF

FIGURE 5.7

REPLACEMENT PEDASTAL

FIGURE 5.8
CELL BODY

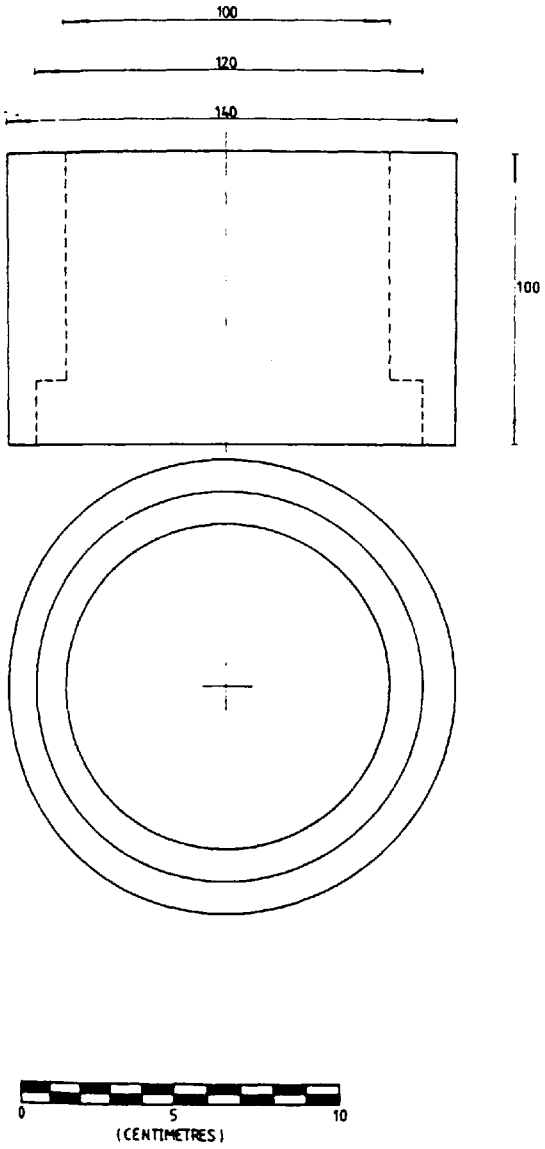

FIGURE 5.9
LOADING PISTON

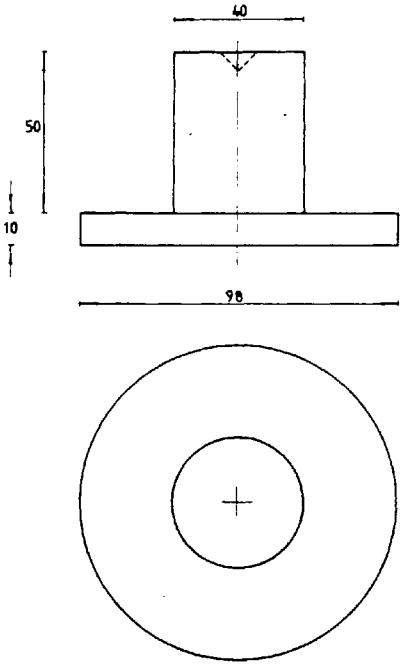

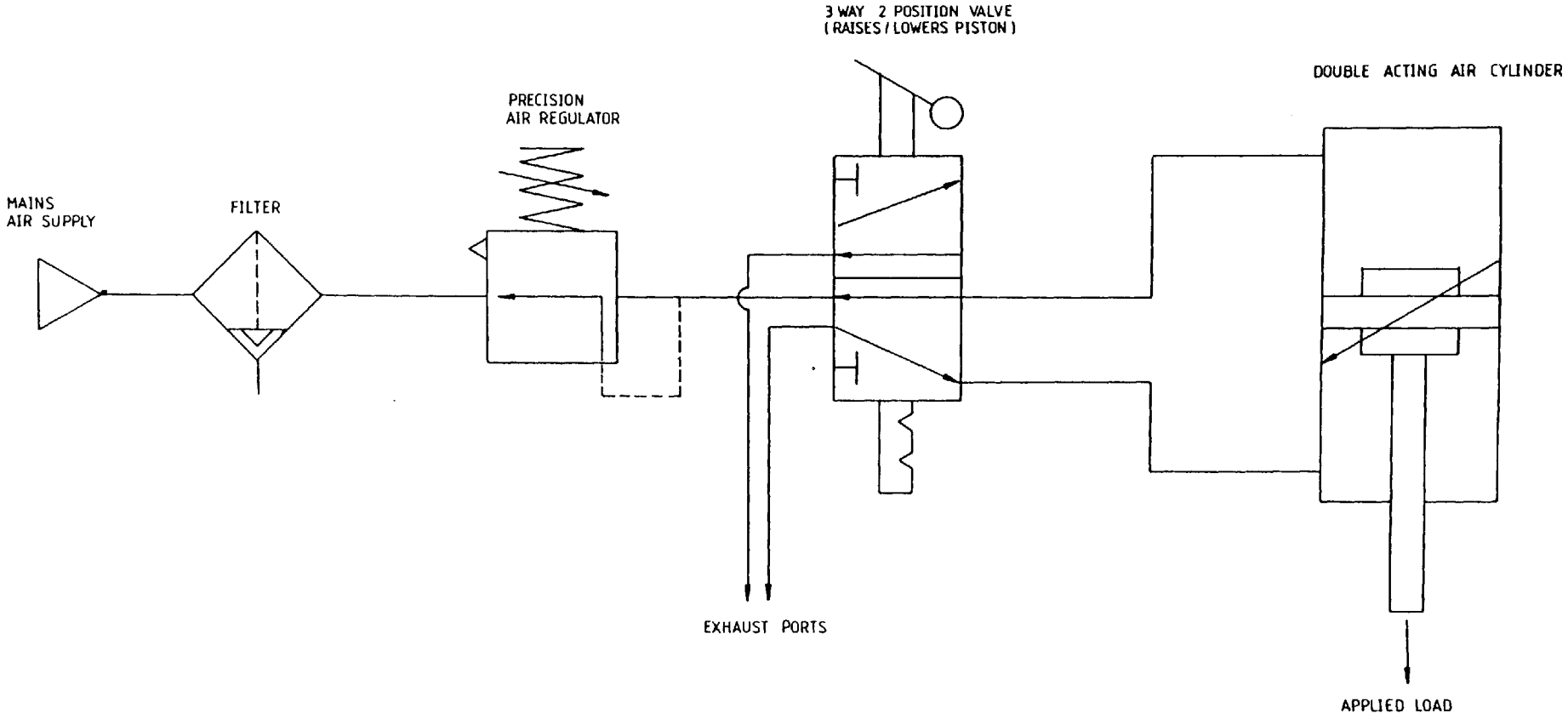

FIGURE 5.10

SCHEMATIC REPRESENTATION OF
LOADING SYSTEM

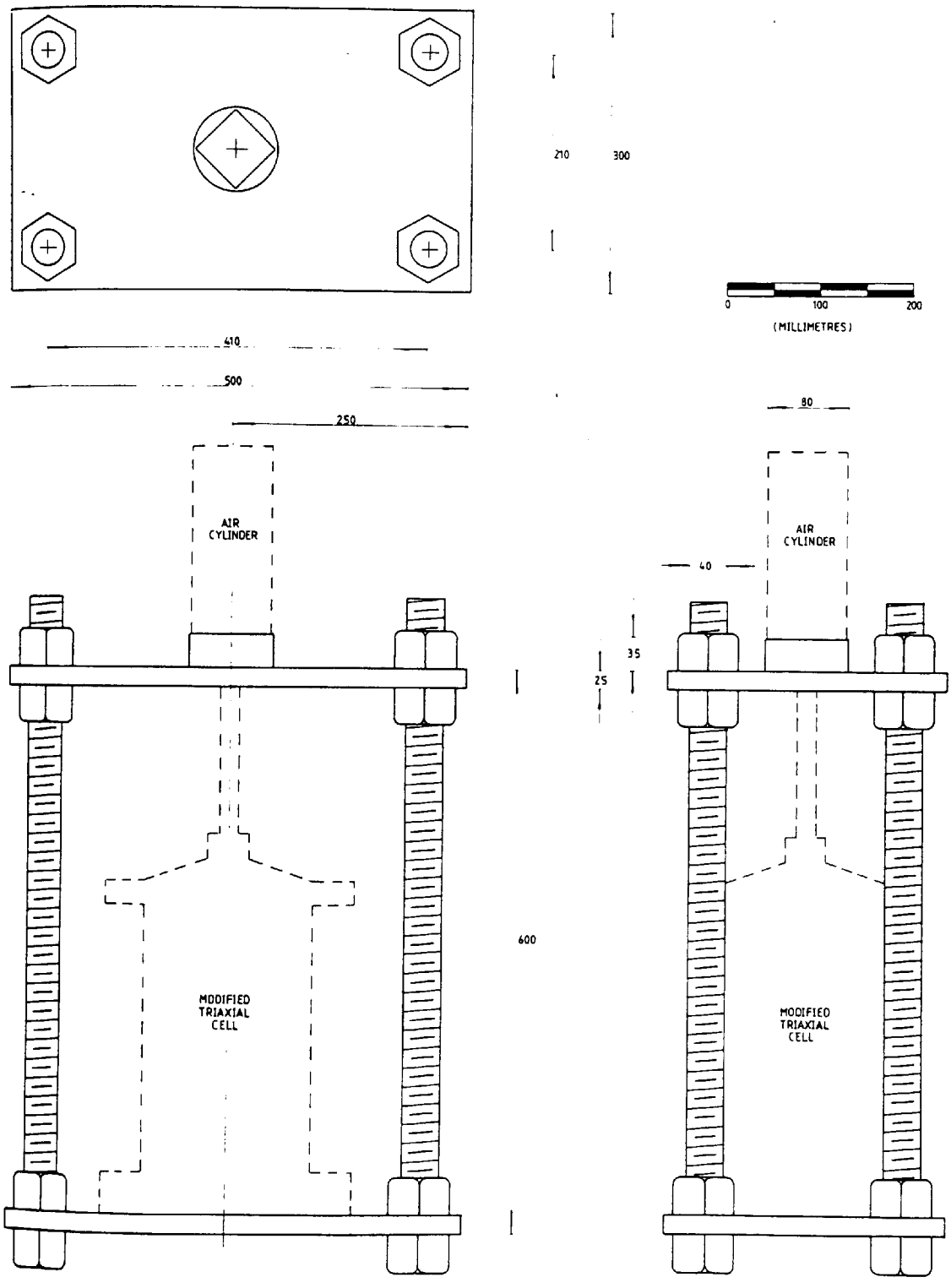

FIGURE 5.11
LOADING FRAME

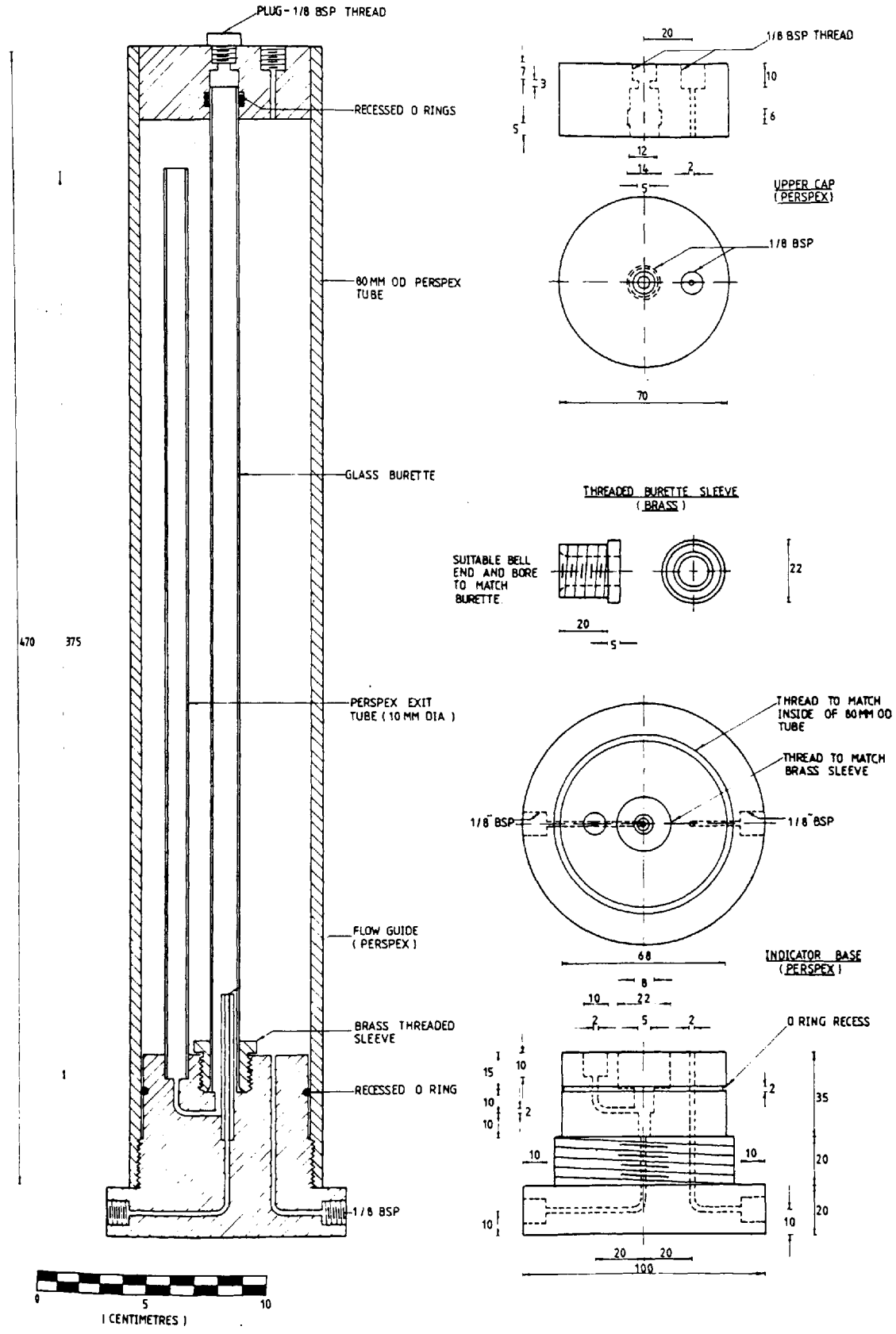

FIGURE 5.12

DIFFUSED AIR VOLUME INDICATOR

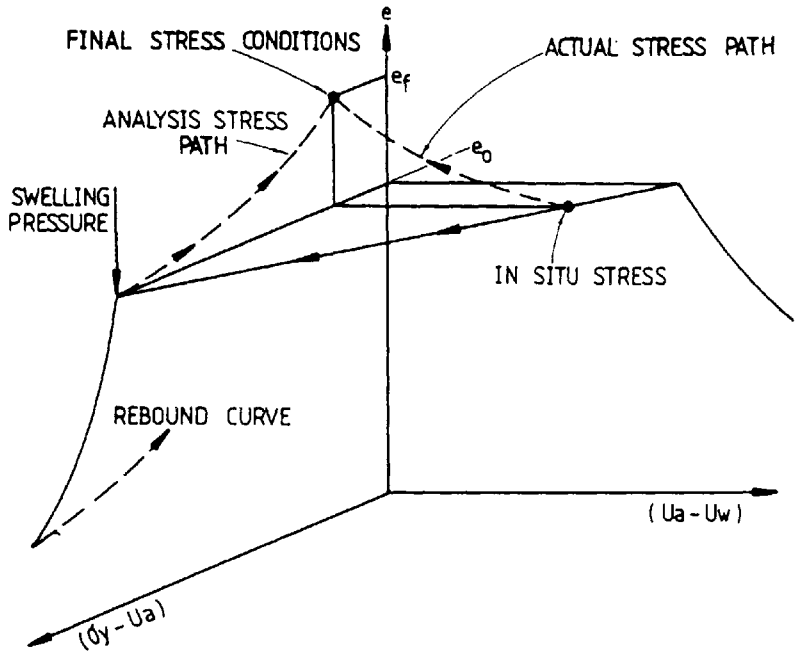

FIGURE 5.13
ACTUAL AND ANALYSIS STRESS PATHS

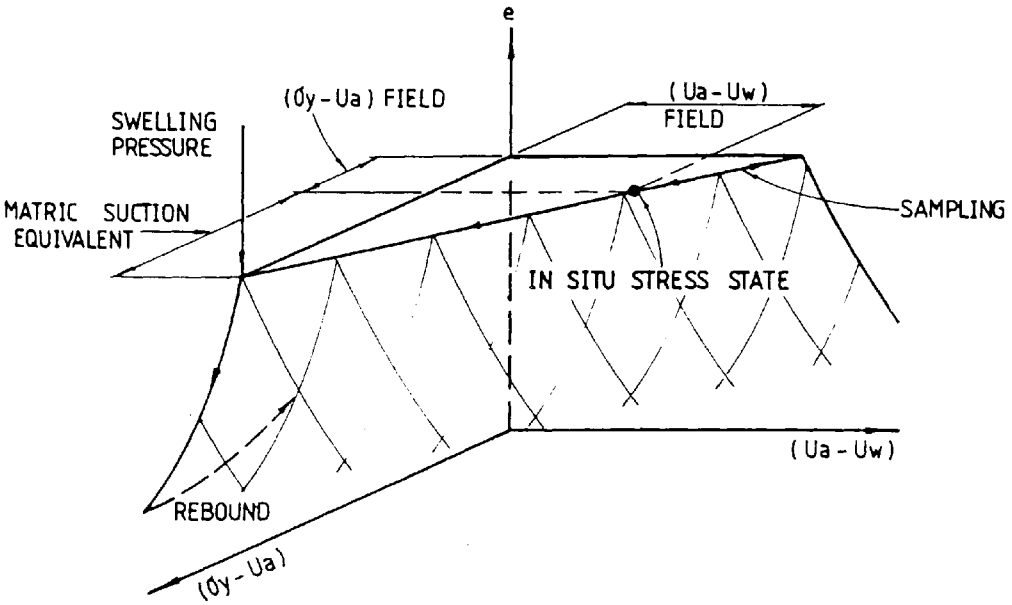

FIGURE 5.14
IDEAL INTERPRETATION OF SAMPLING AND
THE CONSTANT VOLUME SWELL PRESSURE TEST

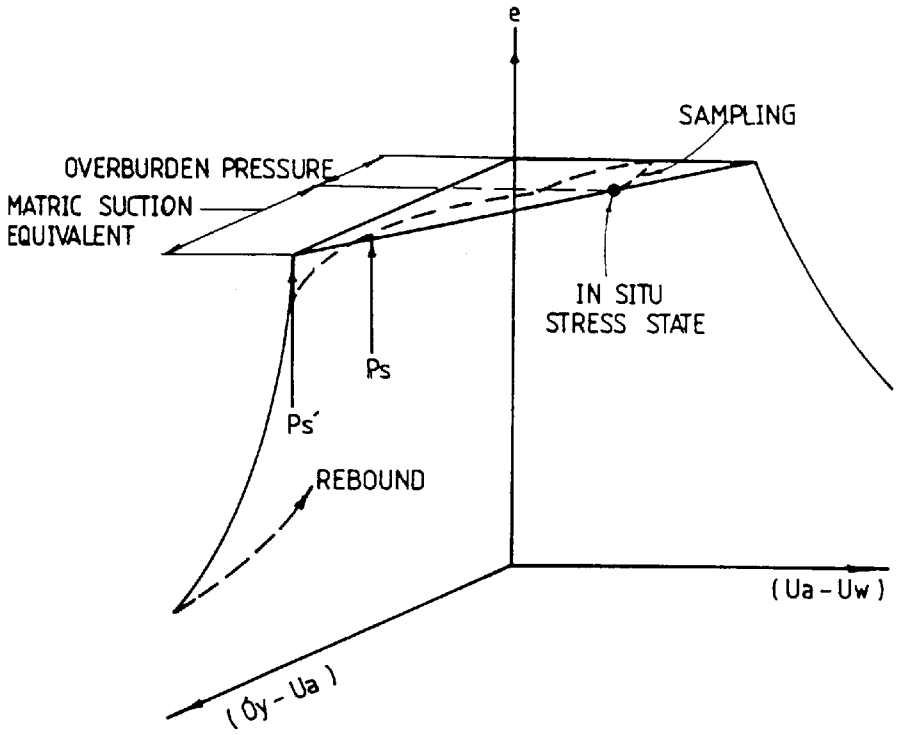

FIGURE 5.15

ACTUAL STRESS PATH DURING SAMPLING AND
THE CONSTANT VOLUME SWELL PRESSURE TEST

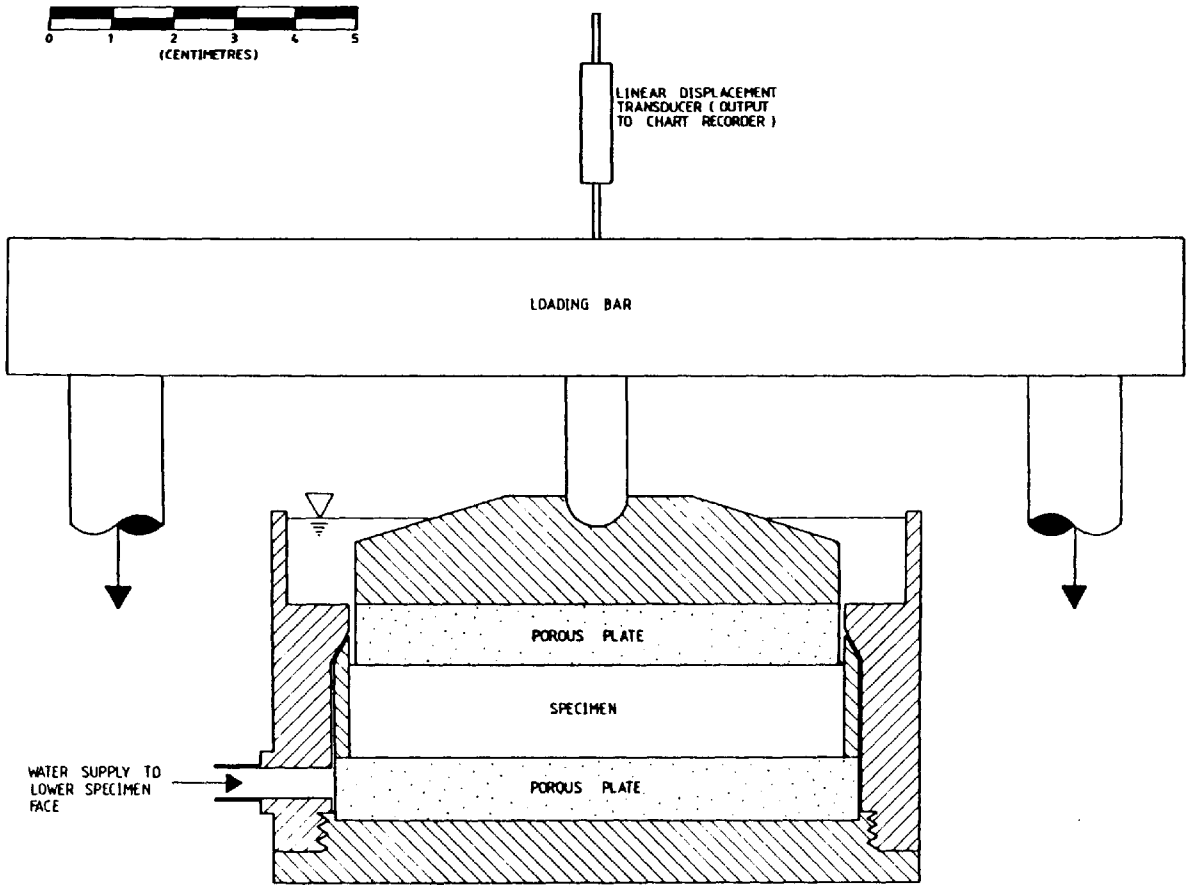

FIGURE 5.16

CONSOLIDOMETER APPARATUS EMPLOYED FOR THE CONSTANT VOLUME SWELL PRESSURE AND UNRESTRAINED VERTICAL SWELL TESTS.

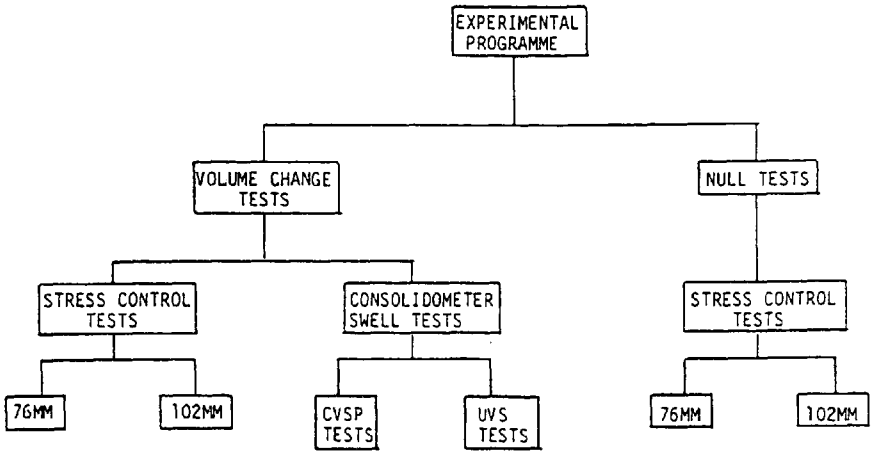

NOTES:

1. 76MM & 102MM REFER TO THE SPECIMEN SIZES USED IN THE STRESS CONTROL APPARATUS
2. CVSP - CONSTANT VOLUME SWELL PRESSURE TEST
3. UVS- UNRESTRAINED VERTICAL SWELL TEST

FIGURE 5.17

TEST PROGRAMME

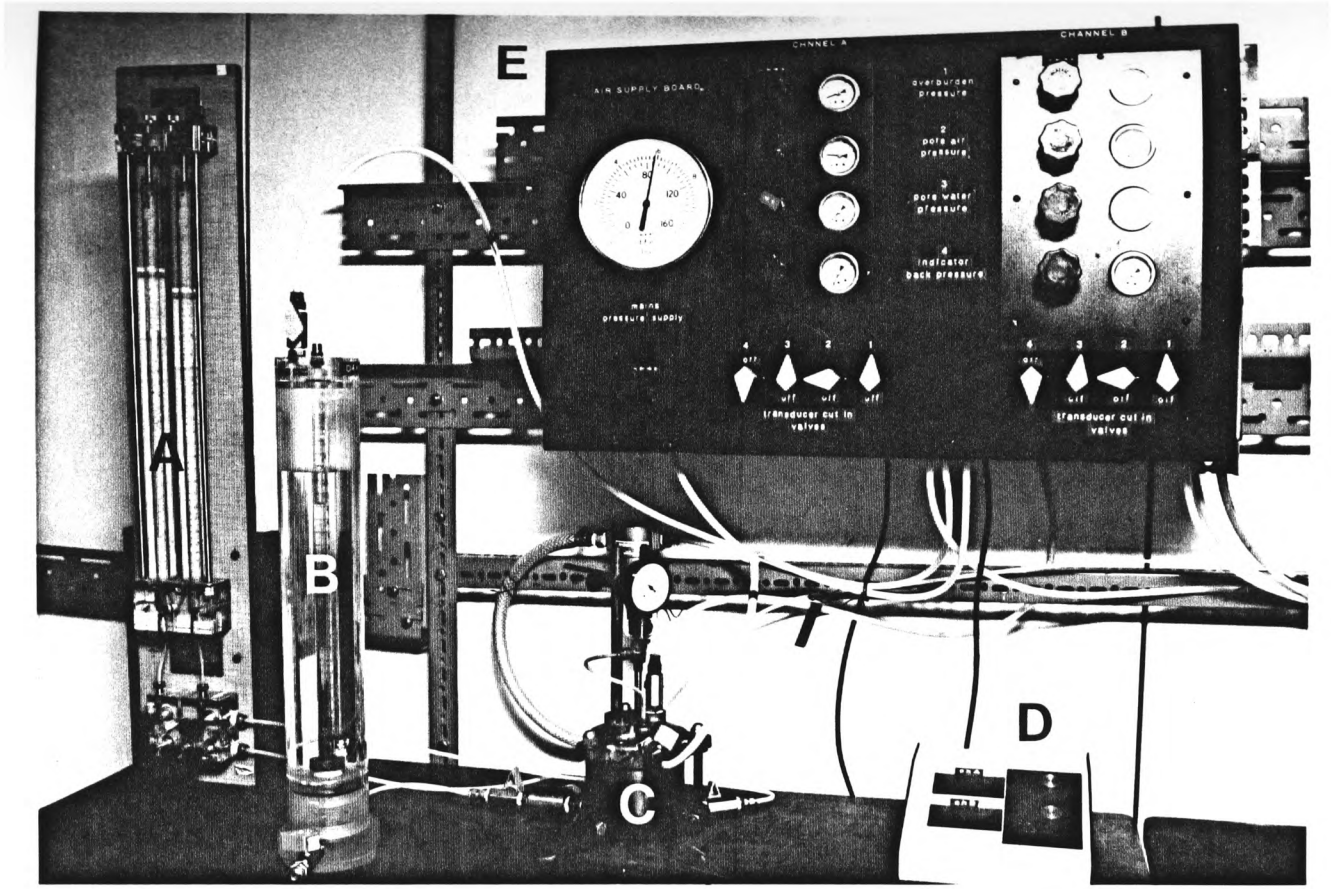

A. Bishops Water Volume Change Indicator
B. Diffused Air Volume Change Indicator
C. Test Cell
D. Transducer Readout Unit
E. Pressure Distribution Board

PLATE 5.1

ONE DIMENSIONAL SWELL TESTING SYSTEM FOR 76MM DIAMETER SPECIMENS

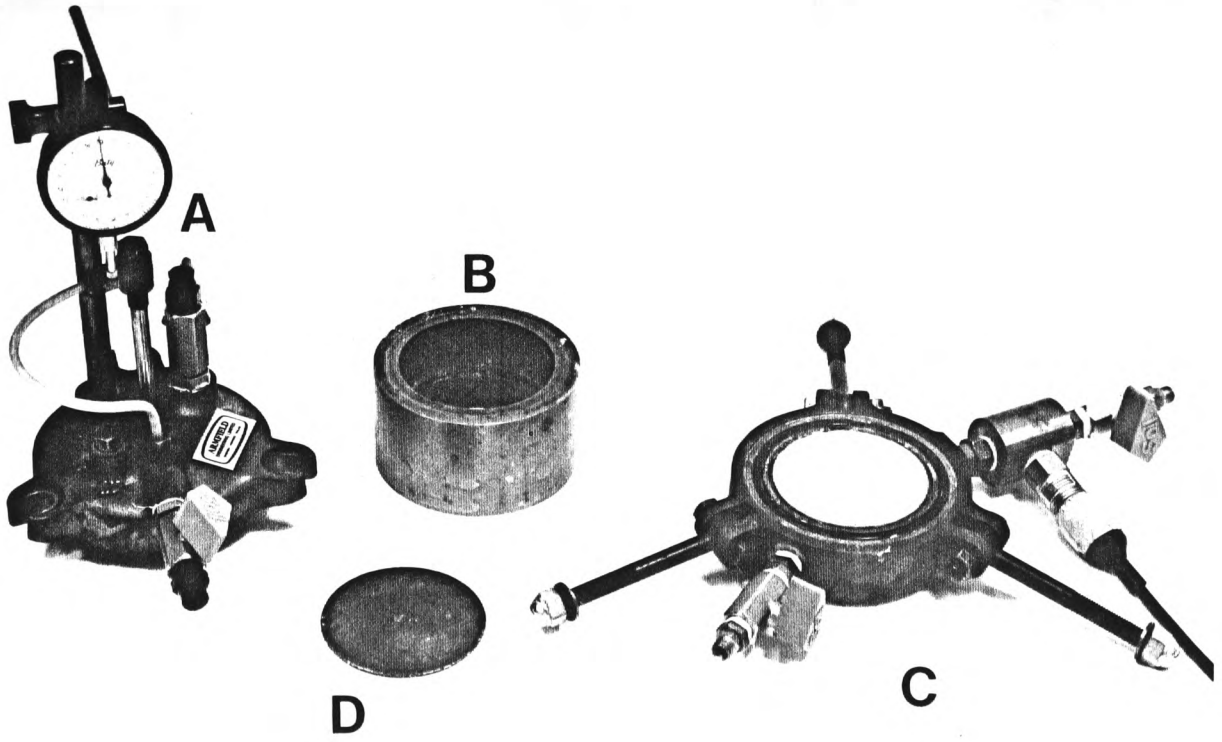

A. Cover
B. Body
C. Base
D. Porous Disc

PLATE 5.2

MODIFIED ROWE CELL FOR TESTING 76MM DIAMETER SPECIMENS

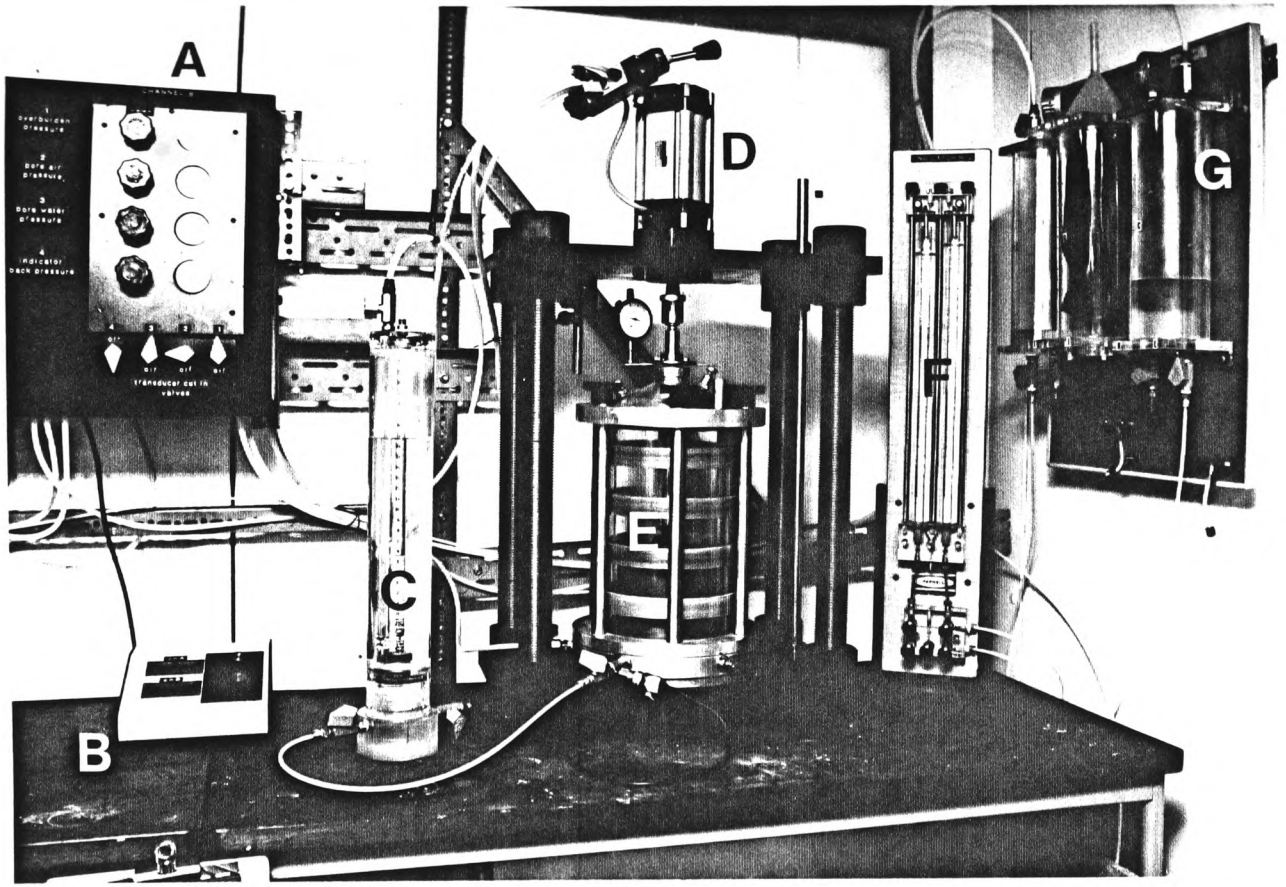

A. Pressure Distribution Board

B. Transducer Readout Unit

C. Diffused Air Volume Change Indicator

D. Loading System

E. Test Cell

F. Bishops Water Volume Change Indicator

G. Water Reservoir

PLATE 5.3

ONE DIMENSIONAL SWELL TESTING SYSTEM
FOR 102MM DIAMETER SPECIMENS

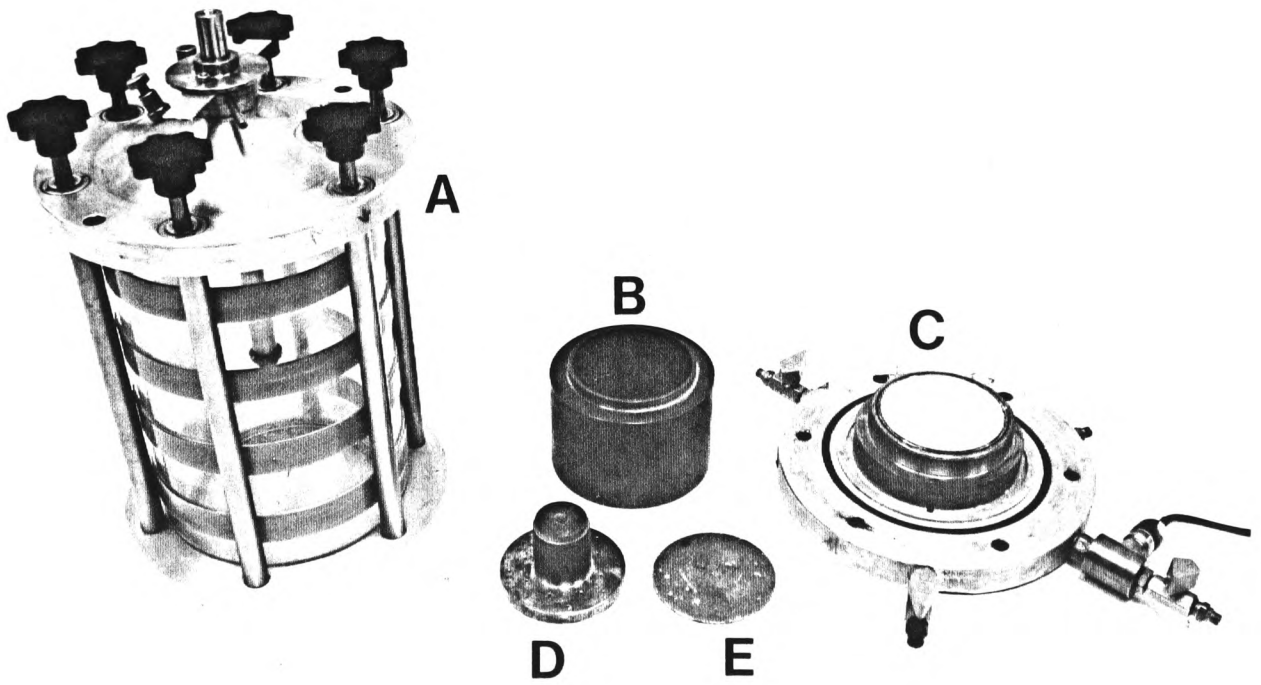

A. Pressure Vessel
B. Cell Body
C. Cell Base
D. Loading Piston
E. Porous Stone

PLATE 5.4

CELL FOR TESTING 102MM DIAMETER SPECIMENS (TRIAXIAL CELL COMPONENTS)

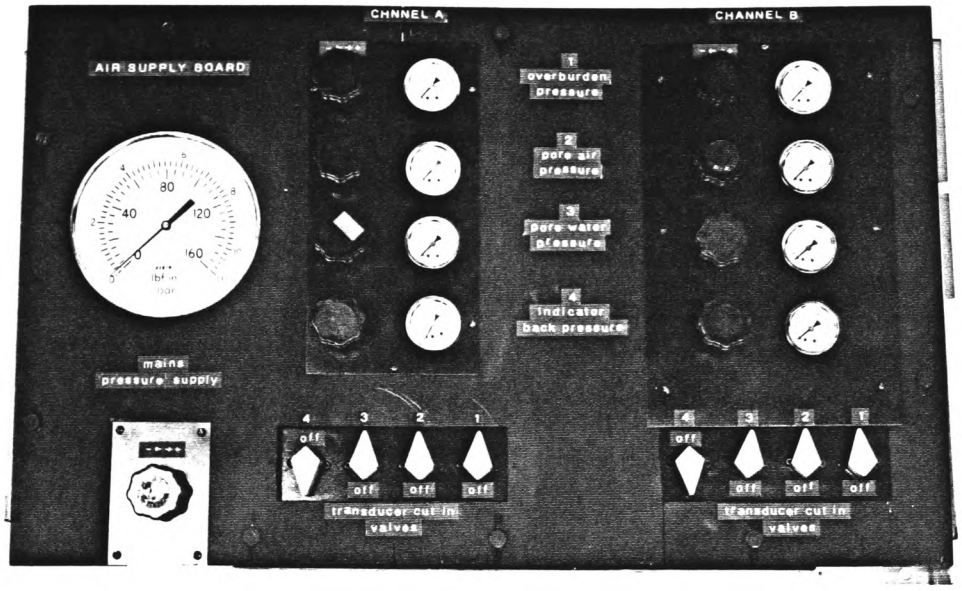

PLATE 5.5

PRESSURE DISTRIBUTION BOARD
(FRONT)

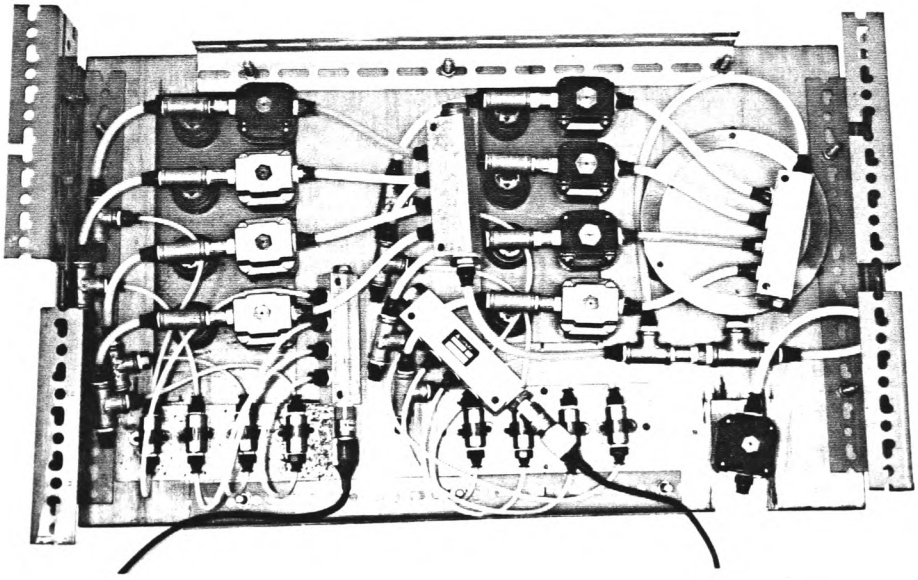

PLATE 5.6

PRESSURE DISTRIBUTION BOARD
(REAR)

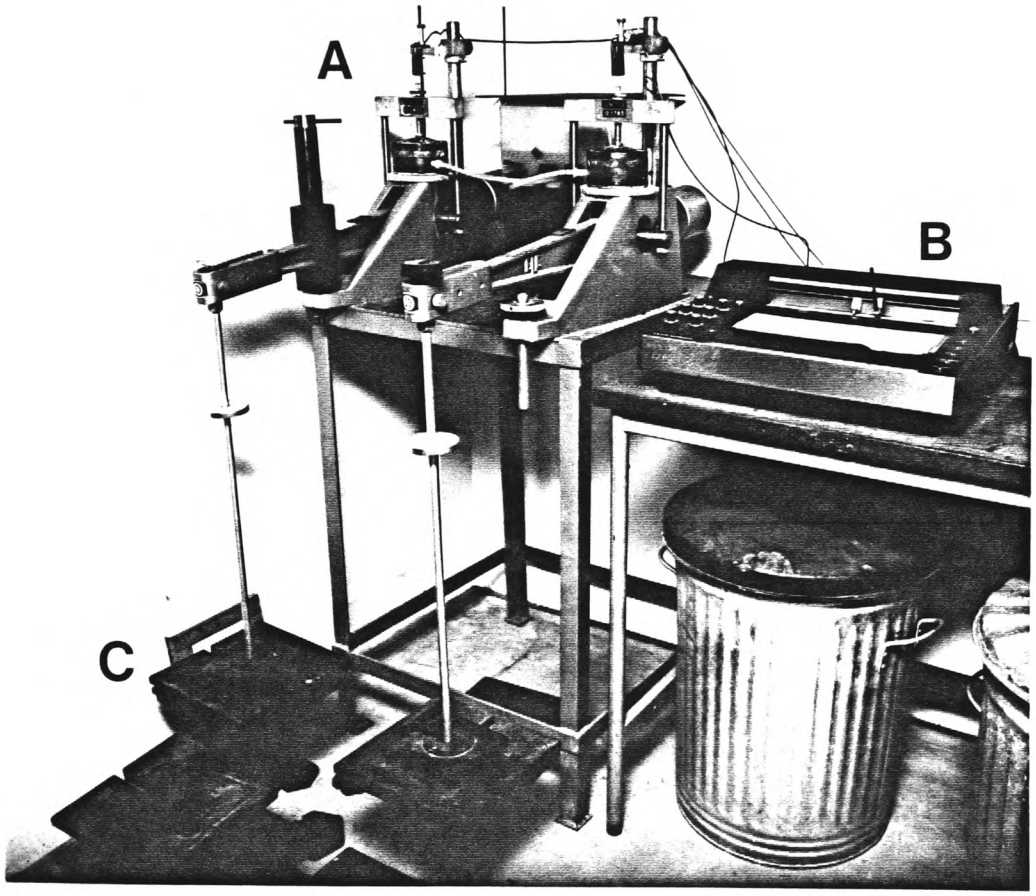

A. CONSOLIDOMETER

B. CHART RECORDER

C. WEIGHTS

PLATE 5.7

CONSOLIDOMETER APPARATUS USED FOR SWELL TESTING

CHAPTER 6

NULL TESTS

6.1 INTRODUCTION

The primary aim of the null test is to verify that the chosen stress state variables (i.e. $(\sigma-u_a)$, $(\sigma-u_w)$ and (u_a-u_w)) are of the correct form, and hence whether or not the volume change theory is valid. The null tests involve simultaneously changing all the stress components (i.e. total stress σ , pore air pressure u_a and pore water pressure u_w) by equal amounts and closely monitoring the total and water volumes for deformation. Since the stress state variables are kept constant then no volume changes should occur (null behaviour); thus, any deviation from equilibrium must be fully explained.

In the context of this project, the null test was employed for assessing the validity of the volume change theory for use with a range of synthetically produced, expansive unsaturated clays. In addition, it provided a means of assessing the compatibility of data from the two equipment types.

To ensure consistent initial conditions, four clay specimens were carefully mixed and statically compacted. (refer Appendix A and B for full procedure and mix properties).

The following mixtures were employed :

(i) 100% Kaolinite

(ii) 10% bentonite + 90% Kaolinite

(iii) 20% bentonite + 80% Kaolinite

(iv) 30% bentonite + 70% Kaolinite

The liquid limits of the above synthetic clay mixtures vary between 47% and 142% , which are considered as covering the majority of plasticity characteristics likely to be encountered in practice.

To the author's knowledge, this is the first time these stress state variables have been systematically assessed for use with a range of unsaturated expansive clays. Each specimen was initially subjected to prescribed stress conditions (conditioning stresses) and allowed to come to equilibrium.

Four null type tests as described previously, were then conducted; each comprised of two increases in stress components and two decreases.

A total of six specimens were tested in this manner yielding thirty tests in total - these were allocated (15 tests each) between the 76mm and 102mm type test cells.
The numbering system used in the null tests is outlined at the end of chapter 5.

6.2 SUMMARY OF SPECIMEN BEHAVIOUR IN THE 76mm CELL

6.2.1 Total volume change

(i) Stress Increase Cycle

The specimens generally exhibited a marked decrease in total volume following the application of the conditioning stress components;

the volume changes at this stage were considerably larger than those resulting from the subsequent null tests (up to ten times greater). The magnitudes of the soil compressibilities (based on these initial volume changes and applied stresses), apparently increased with soil plasticity, although this could not be conclusively ascertained upon the basis of this data alone. The subsequent null tests involved a simultaneous equal increase in the component stresses which resulted in a further decrease of total volume; the magnitude of these compressions increased with increasing plasticity.

The main exception to the above behaviour was specimen NR03 which exhibited an expansion following the application of the conditioning stresses. This was traced to an incorrect application of the component stresses where the total stress (σ) was under applied by 15 psi (103.4kN/m^2). This resulted in the 'total' stress state variables i.e. (σ-u_a) and (σ-u_w) being too low, which in turn caused an immediate expansion. It is noted that the suction stress state variable (u_a-u_w) was unaffected by this error and remained constant throughout testing (10 psi /68.95kN/m^2).

A subsequent partial correction of the total stress had little effect upon the total volume and the specimen equilibrated to 1.03% expansion at the end of the conditioning phase, (i.e. test NR0316).

Subsequent testing of the specimen also yielded some inconsistent behaviour and is further described below. The stresses were fully corrected in test NR0317 to σ = 50 psi (345kN/m^2), u_a = 40 psi (276kN/m^2) and u_w = 30 psi (138kN/m^2) thereby bringing the stress state variables to the required values (refer Table 6.3). However, the specimen continued to expand by another 0.33% which coincided with a simultaneous increase in water volume of 0.38%. It appears that any processes commenced during the previous test remained in operation throughout this test. The specimen subsequently exhibited a near null behaviour for test NR0318.

Although it is acknowledged that the initial test stages of this specimen were incorrectly undertaken, the unloading cycle appeared to exhibit a behaviour consistent with that of the other specimens. For this reason, this portion of the test was included in the following description of the stress decrease cycle.

(ii) Stress Decrease Cycle

The stress decrease cycle consisted of two separate, equal reductions in all stress components. These consistently resulted in an expansion (maximum of 0.41% in NR0305); however, the specimens only partially recovered their original volume.

Swell indices (stress/deformation) were computed from the data (Table 6.5) and indicated an increasing rebound with increased clay plasticity. With regard to the clay mineral mixtures employed, it appeared that the volume change characteristics were not linearly related to the bentonite content, but rather they increased very rapidly

for only a small increase in the bentonite content.

A small exception to the above behaviour was specimen NR01 (100% Kaolinite), which rebounded to a volume greater than it exhibited on the stress increase cycle.

However, the magnitude of this rebound was less than 0.1% and not considered of great significance.

(iii) Phases of Volume Change

The specimens exhibited two distinct phases of total volume change :

(1) immediate - which occurred simultaneously with the stress change

(2) secondary - occurring over a longer period - sometimes as long as the test duration.

The application of conditioning stresses caused the greatest immediate and secondary volume changes; in all cases the specimens compressed immediately upon stress application and then rebounded for the remainder of the test. This behaviour is believed to be due to the over-riding initial influence of the total stress increase upon the volume change, followed by a delayed equalisation of pore air and water pressures - and subsequent rebound of the specimen.

Volume changes also occurred following the stress component changes during the null tests but by a considerably reduced amount.

The immediate behaviour of the total volume was not entirely consistent and seemed to suggest a variation in the experimental procedure.

For instance, consider specimen NR01 (Fig. 6.1); tests NR0102-NR0104 resulted in negligible volume change (< 0.02%) whereas the final stress component reduction - test NR0105 caused a sharp increase in volume followed by a gradual compression, which tended to, but never actually reached the original volume.

The immediate volume change behaviour of specimen NR02 was more random (Figure 6.2), however, its direction at least corresponded with the general volume change behaviour noted previously. (i.e. increase in stress caused a decrease in volume and vice versa).

Specimen NR03 exhibited very little immediate volume change for the null tests conducted upon it. The overall random nature of the immediate volume changes exhibited, suggested an experimental inconsistency, rather than a soil related process.

In view of the fact that null tests were being conducted and that no volume changes should have occurred, it was to be expected that any immediate volume changes would be counteracted by secondary volume change in the opposite direction. In general this was the case for the lower plasticity specimens (NR01 and NR02) which rebounded to approximately their original volume provided the specimen had not undergone an immediate volume change greater than 0.05% .

The same specimens (NR01 and NR02) exhibited volume change equilibrium for all tests within 15000 minutes. This was not the case with specimen NR03 which exhibited a continuous expansion up to 20000

minutes (tests were stopped after this time, primarily because of the early experimental error upon this specimen, thus shedding some doubt over the credibility of the test data).

Since equilibrium was not attained during the tests upon NR03, then the measured volume changes were incorrectly low (0.41%) and had to be adjusted accordingly during analysis of data.

6.2.2 Water Volume Changes

The water phase exhibited a constant increase (i.e. apparent intake to the specimen) during all null tests (figures 6.1-6.6). Although the rate of inflow for all specimen's did not vary by more than 0.07 cc/day, a definite pattern emerged from the data (Fig. 6.9); the rate of inflow decreased with increasing stress components and vice versa. In addition, the rate of inflow behaved in a hysteretic manner, and was consistently less on the stress reduction cycle than on the stress increase cycle.

The inflows to the higher plasticity clays were less susceptible to the effects of a specimen loading and unloading cycle, i.e. the inflows to a low plasticity clay remained substantially reduced following a decrease in stress components, whereas those inflows exhibited by a high plasticity clay rebounded to a value almost equal to the original value.

6.3 SUMMARY OF SPECIMEN BEHAVIOUR IN THE 102mm CELL

6.3.1 Total Volume Change

(i) Stress Increase Cycle

The 102mm specimens exhibited a decrease in total volume following all increases in total stress (fig. 6.8).

The largest compressions occurred following the application of the initial (conditioning) stresses; although the results indicated that the plasticity influenced the initial compressions, firm relationships between the two were not immediately apparent.

Specimen NT02 was initially subjected to component stresses some 10psi greater than the other specimens, thus the initial compression was larger than it should have been. A more representative volume change was estimated by interpolating back to the initial stress conditions as applied to the other specimens.

This procedure reduced the percentage volume change, from 1.92% (for 40 psi/276kN/m^2 total stress) to 1.44% (for 30 psi/207kN/m^2 total stress). However, results still indicated that compression increased with plasticity.

Specimen NT03 possessed the highest plasticity (20% bentonite content), but displayed less compression than either of the two lower plasticity clays. Although the subsequent null test behaviour of this specimen was consistent with that of the other specimens, the

initial deflection is viewed with doubt. The subsequent null tests also exhibited volume decreases following further stress increases,but of smaller magnitudes than those following the initial stress application. The magnitude of the compressions exhibited a marked increase with increasing plasticity, although again firm relationships were not apparent.

(ii) Stress Decrease Cycle

The total volume consistently increased following a reduction in component stresses (fig. 6.8). Although the specimens only partially recovered their original volumes, the magnitude of recovery definitely increased with increasing clay plasticity. The magnitude of the Kaolinite specimen rebound was substantially increased by the addition of only a small proportion of bentonite (for example a reduction in component stresses of 20 psi/138kN/m^2 caused an expansion of just 0.032% in 100% Kaolinite compared with a 0.31% expansion in 10% bentonite + 90% Kaolinite mixture). Overall, the maximum volume change recorded was a compression of the 20% bentonite - 80% Kaolinite clay mixture (specimen NT03 : 0.623%) .

Notably, the high plasticity specimen NT03 (20% B + 80% K) came to volume change equilibrium and did not exhibit the considerable secondary volume change behaviour of specimen NR03 recorded in the 76mm cell.

(iii) Stages of Volume Change

The volume changes associated with the 102mm cell also exhibited distinct phases i.e. immediate and secondary.

The magnitude of both phases, as with the 76mm cell, was greatest following the application of the conditioning stresses; the immediate volume changes were consistently larger than the secondary ones, however both generally occurred in the same direction (as opposed to the 76mm cell where the secondary volume change was usually opposite to the immediate). The one exception to this was high plasticity specimen NT03, which exhibited a moderate (0.18%) secondary expansion following the immediate compression of 0.95% .

The null testing was undertaken once the specimen had equilibrated under the conditioning stress components. In contradiction to the null principle, and in common with the 76mm cell, the specimens displayed volume changes following equal variation in the stress components.

Most tests resulted in an immediate volume change (with the exceptions of NT0102, NT0207, 08), which generally increased with increasing plasticity.

All specimens exhibited a secondary volume change which, in all but one instance (test NT0315) equalled a compression. Notably, the magnitude of these volume changes did not appear to be related to the clay plasticity.

These latter observations seem unusual, since higher plasticity clays normally exhibit an extended secondary volume change behaviour.

6.3.2 Water Volume Changes

The water volume constantly increased in all null tests in such a consistent manner, that it was possible to accurately determine the inflow rates associated with each combination of stress components.

These results were plotted on figure 6.10 which indicated that the inflow decreased with increasing stress components and vice versa.

Unlike the behaviour observed for the 76mm specimens, the rate of inflow associated with a particular stress was generally less during the loading cycle than on the unloading cycle. The one exception to this was specimen NT03 which exhibited the opposite behaviour. This particular difference between the apparatii cannot be readily accounted for.

The overall consistency of the results strongly suggested that the observed trends are correct and in addition, the maximum variation between specimen inflows did not exceed 0.07 mℓ/day; since the accuracy of the measuring system is 0.02mℓ then it was clear that the stress-inflow behaviour (fig. 6.10) may have varied considerably according to the reading procedure employed.

The plotted curves must therefore be used as an approximate guide to the overall behaviour only. The results did not indicate a precise relationship between inflow and plasticity. However, the magnitude of inflow generally increased with increasing plasticity.

6.4 BEHAVIOURAL INCONSISTENCIES AND POSSIBLE CAUSES

6.4.1 Introduction

Having broadly examined the stress-volume change behaviour of specimens during the null test programme, the previous section indicated that volume changes common to both apparatus types do occur, and that absolute null behaviour is not being observed.

The aim of this section is therefore to indicate the common stress related behaviour of the total and water volumes during testing, and also to identify possible causes for the same.

The total and water volume changes noted above, occurred as a result of one of two causes : (i) experimental (ii) theoretical.

This section will examine the experimental aspects only since the theory will be considered in the penultimate chapter.

6.4.2 Total Volume Changes

6.4.2.1 Variation with stress

The specimens tested in both cells generally exhibited the following volume change behaviour with changing stress components (but constant stress state variables) :

(a) total volume decreased with increasing stress components

(b) total volume increased with decreasing stress components

(c) the total volume only partially recovered its original volume upon reduction of the component stresses

The above behaviour was well illustrated in figures 6.7 and 6.8. The maximum volume change following a stress component increase was -0.623% (triaxial cell) and the maximum following a stress component decrease : 0.41% (Rowe cell). The only exception to this behaviour was specimen NR03, which expanded following an increase in stress components (however this has been satisfactorily explained in terms of an inadvertent under-application of total stress).

These total volume changes generally comprised of immediate and secondary phases, each of which may have resulted from a number of causes. These aspects are therefore dealt with separately.

6.4.2.2 Phases of volume change

The volume changes were observed as comprising of an immediate, secondary or a combination of both phases of volume change.

(i) The immediate volume change is believed to be attributable to three causes acting separately or together :

(a) Non-simultaneous changing of stress components at the commencement of each null test

As a result of the equipment designs and the compressible nature of pore air, then the build-up of air pressure will lag behind that of the total stress and water pressure, even if all three are initially changed simultaneously. The result of this is that the total stress state variable $(\sigma-u_a)$ initially increases - thereby causing an immediate compression. The converse is true following a stress decrease when the stress state variable momentarily decreases resulting in an expansion. The observed volume change behaviour appeared to confirm this.

(b) Compression of occluded air within the pore water

Unsaturated soil specimens are prepared containing pore air in the continuous and occluded states; however, there is presently no way of controlling the amount of either air type.

If the specimen contains occluded air then the pore fluid may compress. In such a case, a portion of the total stress will be transferred to the soil structure and result in a volume change.

The precise contribution of each cause to the immediate volume change was uncertain since it was impossible to isolate them during experimentation. This difficulty was compounded by the absence (at the time of writing) of a suitable proven theoretical base; however, estimations of the occluded air-water mixture volume change based on Boyles law indicated a consistently small decrease in volume following a stress increase.

In addition, the recorded magnitudes of immediate volume change sometimes exhibited a random variation. Consideration of points (a) and (b)suggests that a variation in procedure is likely to have been the cause of the larger immediate deformations.

(c) Compliance of the system

The compliance of the system broadly describes the apparent volume changes exhibited by the equipment upon application of the stress components.

The compressibilities of the apparatii were determined (Appendix C) and the measured volume changes adjusted accordingly. However these adjustments did not take into account (i) the initial bedding effects of the specimen into the porous stone or (ii) the possible extrusion of the material around the loading plate (both of which may have caused a hysteretic volume change behaviour).

Although these possible sources of volume change cannot be accurately quantified, it is nevertheless, highly probable that they did contribute to the total volume change. It is noted that since these effects would be constant irrespective of the specimen depth, then their relative influence would decrease with increasing specimen size.

(ii) The secondary volume change occurs over a period of time, and may continue for the duration of each test. It may be related to the following causes :

(a) Clay mineral-water interaction

The clay mineral- water interaction will result in a secondary volume change; generally, a wetting process will manifest itself as an expansion and a drying process as a shrinkage (these aspects being covered in greater depth in Chapters 2 and 4).

Clays initially exhibit a slight delay in swelling upon free access to water, but then rapidly exhibit the larger part of their swell potential within 1440 minutes. Early consolidometer tests by the author (Fig. 2.11) indicated that 80% of maximum swell is usually achieved within 1400-2000 minutes for most soil types. The time for the secondary deformation to equilibrate may increase due to the over wetting of soil at the clay-water interface. In the case of this project, the specimen was supplied with water from one face only. A change in water pressure will cause a change in moisture content in the clay near the interface, and the time required for that moisture to dissipate throughout the specimen is largely dependent upon the clay type. The extreme case is for highly plastic clays (liquid limit > 100%), where the clay at the interface will begin to exhibit thixotropy and present a barrier thereby limiting moisture migration to the remainder of the specimen. Such an occurrence was believed to be a primary factor in the very long equilibration times exhibited by specimen NR03, although the use of thin specimens probably reduced this effect somewhat.

(b) Air permeability of soil

Once the air pressure surrounding the specimens is altered, a further period is required to allow equalisation of the air pressure within the specimen itself. The duration of this equalisation process and (possibly) associated volume change will be related to the air permeability of the clay.

Although no actual measurements of air pressure variations within the specimen were made, it is believed that this process occurs very rapidly by comparison with the clay-water interactions.

6.4.2.3 Summary

The total volume change exhibited a consistent behaviour following equal variations in the stress components.

The volume decreased with increasing stress components and vice versa, although, the specimen only partially recovered its original volume upon stress reduction. This behaviour was accentuated with increasing plasticity. The overall volume change generally exhibited two distinct phases : immediate and secondary.

Both of these phases occurred as a result of several causes; although the precise contribution of each cause to the final deformation could not be determined, it is apparent from the data that an unequal change in stress components usually generated the largest volume change. indeed, the volume change did not exceed 0.05%.

6.4.3 Water-volume change

6.4.3.1 Constant inflow

Every test exhibited a stress dependent constant inflow of water to the specimen after correction for known leakages and diffused air effects. The inflows were very constant (figures 6.9 & 6.10)and were derived from the linear portion of the plotted data, since this is believed to represent inflow that was not related to a soil process.

6.4.3.2 Variation with stress

The water intake also varied following an equal alteration in all stress components.

The specimens tested in both cells generally exhibited the following behaviour :

(a) inflow decreased with increasing stress components

(b) inflow increased with decreasing stress components

(c) the inflow only partly recovered following a decrease in stress components.

The recorded water volume change was therefore behaviouraly analogous to the total volume change. This above behaviour is illustrated in figures 6.9 and 6.10.

The characteristic inflow curves exhibited other common features.

An increase in the plasticity of the clay :

(a) increased the rate of inflow recovery following a stress decrease

(b) increased the overall magnitude of inflow

Although the behaviour observed for the 102mm specimens was not entirely consistent with that of the 76mm specimens , the overall magnitude of the variation was very close to the accuracy of the measuring system.

6.4.3.3 Possible causes of constant inflow

The apparent constant water inflow contradicted the observance of negligible soil structure volume change; this in turn suggested that the water was not remaining within or even reaching the specimen. Possible explanations for this included :

(a) leakage

Although a possibility, constant pressure tests failed to locate leakages within the pipes, valves and connections. Also, the water inflow apparently decreased with increasing stress components, this does not seem consistent with conventional leakages which usually increase following a stress increase. However, an 'O' ring or similar device may cause this type of behaviour.

(b) Evaporation of water from the specimen surface into the cell chamber

Another possible cause of water loss was due to evaporation from the specimen surface into the test cells. This in itself would not account for constant leakage, since in time the air in the cell would become saturated and evaporation cease. However, the triaxial pressure vessel is largely composed of perspex, and the International Critical Tables document cases of moisture transmission through such plastics. The pressure vessel perspex wall cannot therefore be considered impermeable, and may well provide a possible means of escape for moisture vapour.

Using the critical tables and data obtained by Fredlund, (Table 6.11 and Figure 6.15), the maximum projected rate of water loss through the triaxial pressure vessel wall is 0.148mℓ per day. This is considerably larger than the measured constant inflows which were on average less than 0.1mℓ per day; however, since the calculated value is a maximum (assuming 'dry' air outside and saturated air inside the pressure vessel) then the recorded inflows could conceivably be attributed to this cause.

It must be noted however, that the magnitudes of inflows are approximately the same for both apparatii. Also, since the 76mm cell contains no perspex, then the loss of water by this route is doubted.

6.4.3.4 Summary

In conclusion therefore, although the water inflow cannot presently be accounted for, it was sufficiently consistent to be accurately quantified. The lack of any total volume expansion indicates that the water was not remaining within (or even reaching) the specimen.

The stress-inflow behaviour varied according to the plasticity of the soil, however, the recorded variations in inflow were very close to the accuracy of the measuring system.

Finally, the consistent behaviour of water volume change enabled values to be fixed for specific stress component combinations.

6.5 CORRECTIONS FOR CONSTANT WATER VOLUME INFLOW

6.5.1 Basis for Applying Corrections

The water volume change of each specimen assumed a constant inflow; it was dependent upon the soil type and applied stress magnitude, however, its cause is presently uncertain.

The virtual lack of any total volume change suggests that the water was either not remaining within or even reaching the specimen.

On the basis of this evidence, it is suggested that the inflow be accurately measured in each instance, treated as a 'leakage', and subtracted from the measured water volume change. This will yield a corrected water volume and should provide a better indication of the water volume change behaviour.

6.5.2 Determination and Application

The inflows were measured from the linear position of the water volume change graphs (Figures 6.1 - 6.6). This constant flow of water was then subtracted from the measured overall water volume change in each test.

6.5.3 Evaluation

The graphical presentations (Figures 6.11 and 6.12) indicate that the corrections work very well when applied to the original water volume change data; they are noted as varying in a random manner which suggests a null behaviour (further discussed in Section 6.7).

It must be noted that these corrections can only be applied to soil types and stress conditions used in this programme; otherwise, they must be recalculated, or another method used to allow for the constant inflow.

6.6 COMPATIBILITY

6.6.1 Introduction

One of the main objectives of the chapter is to determine whether the two apparatii yield compatible data (for the purpose of increasing the testing capacity of the project). This was undertaken by assessing the similarity between the total and water volume changes of each apparatus. The general behaviour exhibited by the apparati were

found on the whole to be very similar and are summarised in Table 6.9. The detailed aspects of the total and water volume variations are discussed below.

6.6.2 Total Volume Change

A consistent total volume change behaviour was noted in both apparatii during the null test programme, being well illustrated in Figures 6.7 and 6.8.

The application of the conditioning stresses consistently compressed the specimens in both apparatii (with the exception of specimen NR03, although this was discounted due to an experimental error).

The initial volume change behaviour did not indicate a definite pattern in either apparatus, although this is considered to be primarily due to the non-simultaneous changing of the component stresses.

The stress-volume change behaviour following an equal increase or decrease in component stresses (i.e. null tests) was very similar in both apparatii; the volume decreased with increasing stress components and vice versa, although, the specimen only partially recovered its original volume upon stress reduction. The only non-compatible behaviour was that exhibited during the loading cycle of specimen NR03; nevertheless, it did indicate the outcome of a reduction in component stresses.

The overall volume change of each apparatus generally occurred in two distinct phases : immediate and secondary. Both of these phases occurred as the result of several causes, and although their precise contributions are not known, it appears from the data that unequal changes in component stresses induced the largest volume changes in both apparati .

Increasing plasticity consistently accentuated the volume change behaviour of the specimens; the differences between the compression and rebound surfaces consistently increased with increasing plasticity, however the overall values of deformation were not conclusively affected. The magnitudes of volume change are also compatible; the total volume change of the specimens in both apparati was consistently in the order of -2.0% (inclusive of the large compression following the application of conditioning stresses). Actual null test deformations did not exceed 0.623%. In addition, where the specimens underwent an immediate deformation less than 0.05%, they behaved elastically and recovered their original volume.

Finally, in assessing the null behaviour (Table 6.9 and Figures 6.13 and 6.14) it was noted that both apparatus behaved very similarly (see Section 6.7 for fuller details).

The author concludes that despite certain exceptions, the magnitude and pattern of the total volume change behaviour exhibited by both apparatus is satisfactorily compatible.

6.6.3 Water Volume Change

The water volume changes observed in both apparati were generally quite consistent. Both apparatus exhibited steady inflows to all specimens tested (Figures 6.1 - 6.6), the magnitudes of which varied according to the applied stress components.

The stress-inflow data is illustrated in Figures 6.9 and 6.10; however, the results indicate that the overall behaviour was not precisely the same in both cases. Although they displayed a common decrease of inflow with stress increase and vice versa, two of the 'triaxial' specimens NT01 and NT02 departed from this behaviour and exhibited greater overall inflows on stress reduction than on the stress increase cycle.The cause of this variation is uncertain at the present time.

Further examination of the test data indicates that the total variation of inflow for the two specimens did not exceed 0.05mℓ/day. Since the accuracy of the measuring system is 0.02mℓ, then it is apparent that the anomalous behaviour noted for tests NT01 and NT02 may be attributed to this. The stress-inflow behaviour was consistently accentuated with increasing plasticity in both apparati .

Since the inflows were steady, they were accurately measured and applied as corrections to the water volume change data (Section 6.5). The water volume change plots (Figures 6.11 and 6.12) subsequently indicated a very consistent null behaviour for both apparatii.

In conclusion therefore, the overall magnitude and pattern of water volume change behaviour is consistent for both apparatus. More importantly, the correction of the constant inflows indicates a near null behaviour for the water phase in both equipment.

6.7 NULL BEHAVIOUR

6.7.1 General

The primary aim of this chapterwas to assess the validity of the derived stress state variables and hence to validate the volume change theory itself. This was to be undertaken by conducting a series of null tests (Section 6.1) and subsequently, assessing the recorded volume changes.

'Null behaviour' implies that no volume changes occur, thus validating the chosen stress state variables.

The water volume and total volume changes are separately examined below :

6.7.2 Water Volume Changes

The experimental water volume change data indicated constant inflows to all specimens, however, the lack of any total volume expansion suggested that the water was not actually reaching them (Section 6.5). In consequence, the inflows were not considered to constitute the true water volume behaviour and were therefore accurately measured for each test, and subtracted from the original

water volume change data, to facilitate determination of the true water volume behaviour. The revised water volume change graphs (Figures 6.11 and 6.12) indicate that :

(a) The water volume exhibited virtually no change with time. Furthermore, any variations that did occur were randomly distributed about the x-axis.

(b) The main deviations from zero water volume deformation (i.e. null behaviour) were attributed to either an incorrect application of component stresses or the accumulation of a large volume of diffused air beneath the ceramic disc.

The effect of a non-instantaneous change in component stresses was typified by tests NR0102 and NR0105 (fig. 6.11). These volume changes usually cancelled themselves after approximately 4000mins.

The general undulations in the curves were mainly attributed to the diffusion of air through the ceramic disc with time; however, other air may have been present due to inadequately de-aired water.

(c) The variations of water inflow were very small in magnitude and equalled only 0.12% in the worst instance. Generally however, the volume changes did not exceed 0.02% for both apparatus. This corresponds to a real volume change of 0.047mℓ and 0.023mℓ in the 102mm and 76mm cells resepctively.

These values were very close to the accuracy limits of the Bishops parafin volume change indicators (0.02cc), and therefore considered as indicating a near null behaviour.

In conclusion therefore, the author believes that the water volume change data exhibits a near null behaviour for the range of clay types tested.

6.7.3 Total Volume Change

The majority of specimens did not exhibit a precise null behaviour upon an equal increase or decrease in stress components (i.e. $\Delta\sigma = \Delta U_a = \Delta U_w$) , and generally underwent an immediate and secondary volume change. From observations made at the time , the immediate volume changes appeared primarily related to a failure in ensuring a simultaneous change of cell component stresses, although other influences such as compression of occluded air and compliance of the system may also have contributed to the overall volume change.

The effects of increasing plasticity particularly influenced the volume change behaviour.

Most specimens came to equilibrium following the application of component stresses, with the exception of specimen NR03 (30%bentonite + 70% Kaolinite), whose increased plasticity apparently increased the equilibration time beyond 20,000 minutes. This placed an excessive time demand upon the apparatus, and in view of the procedural error incurred at the outset, the tests on this specimen were subsequently

curtailed after 15000 minutes each. The recorded volume changes were therefore almost certainly not the maximum values and were examined for the purpose of indicating general trends only.

The maximum volume change during the null test programme occurred for test NT03 and equalled 0.623% (0.2mm). This is very small considering the difficulties encountered in simultaneously changing the stresses.

In an attempt to further assess the null behaviour, the total measured volume change for every null test was plotted against the volume change calculated on the basis of the consolidometer swell data (Chapter 8). (Figures 6.13 and 6.14, Table 6.10).

The null test volume changes were recorded following an equal change in all stress components, thereby keeping the stress state variables constant. The volume changes based on the consolidometer test data were calculated by assuming a change of the total stress state variable equal to the stress component change employed in the corresponding null test.

Ideally, no volume changes should follow an equal variation of the component stresses (null behaviour) and in such instances, the plotted data will lie on the horizontal line (y=0). In actuality, the gradient $(\frac{y}{x})$ of this line may vary between 0 and 1 and is indicative of the degree of null behaviour (0 : null behaviour; 1 : non null behaviour).

The above procedure was undertaken for the two apparati and the results presented in Figures 6.13 and 6.14. From these, it was apparent that neither apparatus exhibited a true null behaviour; 76mm : $\frac{y}{x}$ = 0.149 , 102mm : $\frac{y}{x}$ = 0.374. However, in both instances the null test volume changes were considerably smaller than those predicted from the consolidometer data and also, the magnitudes of measured volume change were very small in all cases (maximum of -0.623% ≃ 0.2mm in the cell). Clearly, the magnitudes of deformation are many times greater than those claimed by Fredlund, however, it is noted that he employed full size 4" (100mm) diameter triaxial specimens, as compared to the small specimens used in this project. In consequence, the volume changes resulting from system compliance and compressibility effects would appear far greater for the author's specimens when expressed with respect to the smaller specimen size (despite being of similar actual magnitude).

In conclusion therefore, although volume changes do occur, they are considered to be sufficiently small so as to indicate a reasonably null behaviour.

TABLE 6.1

SUMMARY OF NULL TESTS

TEST[1] CODE	DATE ON	SPECIMEN DIAMETER	SOIL MIX[2] MONT/KAOL.	CHANGES[3] IN STRESS	COMMENTS
NR0101	30.04.85	76MM	0/100	0	Initial conditions
NR0102	13.05.85	"	0/100	+69	
NR0103	29.05.85	"	0/100	+69	
NR0104	07.06.85	"	0/100	-69	
NR0105	19.06.85	"	0/100	-69	
NR0206	15.07.85	"	10/90	0	Initial conditions
NR0207	21.07.85	"	10/90	+69	
NR0208	06.08.85	"	10/90	+69	
NR0209	14.08.85	"	10/90	-69	
NR0210	22.08.85	"	10/90	-69	
NR0316	04.09.85	"	30/70	0	Initial conditions
NR0317	01.10.85	"	30/70	+69	
NR0318	18.10.85	"	30/70	+69	
NR0319	30.10.85	"	30/70	-69	
NR0320	12.11.85	"	30/70	-69	
NT0101	02.05.85	102MM	0/100	0	Initial conditions
NT0102	13.05.85	"	0/100	+69	
NT0103	29.05.85	"	0/100	+69	
NT0104	07.06.85	"	0/100	-69	
NT0105	19.06.85	"	0/100	-69	
NT0206	15.07.85	"	10/90	0	Initial conditions
NT0207	31.07.85	"	10/90	+69	
NT0208	14.08.85	"	10/90	+69	
NT0209	22.08.85	"	10/90	-69	
NT0210	28.08.85	"	10/90	-69	
NT0311	04.09.85	"	20/80	0	Initial conditions
NT0312	23.09.85	"	20/80	+69	
NT0313	18.10.85	"	20/80	+69	
NT0314	30.10.85	"	20/80	-69	
NT0315	12.11.85	"	20/80	-69	

Notes :

1. (N) designates null tests, (R) designates 76MM diameter specimens, (T) designates 102MM diameter specimens
2. soil mix denotes relative proportions of constituent minerals - mont : montmorillonite, kaol : kaolinite
3. changes in stress in KN/M^2.

TABLE 6.2(a)

INITIAL VOLUME-WEIGHT RELATIONSHIPS

SPECIMEN	THICKNESS (mm)	TOTAL VOLUME (mm^3)	SOLIDS VOLUME (mm^3)	AIR VOLUME (mm^3)	WATER CONTENT (%)	VOIDS RATIO	DRY DENSITY (kg/m^3)	SATURATION (%)
1	31.72	255176	128391	34757	27.4	.987	1316	72.59
2	31.47	253165	128391	31608	27.74	.972	1327	74.67
3	31.36	252280	128391	30770	27.72	.965	1331	75.16
4	31.22	251154	128391	29609	27.74	.956	1337	75.88
5	31.22	251154	128391	29598	27.74	.956	1337	75.89
6	31.78	255659	126741	33948	29.04	1.017	1279	73.67
7	31.22	251154	126741	23579	30.83	.982	1302	81.05
8	31.13	250430	126741	22584	30.92	.976	1306	81.74
9	31	249384	126741	21548	30.91	.968	1311	82.43
10	31.03	249626	126741	21621	30.96	.97	1310	82.41
11	30.29	243672	126379	24177	28.94	.928	1320	79.39
12	30.08	241983	126379	5135	34.33	.915	1330	95.56
13	30.63	246408	126379	7595	34.94	.95	1306	93.67
14	30.48	245201	126379	6392	34.94	.94	1312	94.62
15	30.48	245201	126379	6351	34.96	.94	1312	94.66

TABLE 6.2(b)

INITIAL VOLUME-WEIGHT RELATIONSHIPS

SPECIMEN	THICKNESS (mm)	TOTAL VOLUME (mm^3)	SOLIDS VOLUME (mm^3)	AIR VOLUME (mm^3)	WATER CONTENT (%)	VOIDS RATIO	DRY DENSITY (kg/m^3)	SATURATION (%)
1	25.84	117268	61797	11888	26.96	.898	1379	78.57
2	25.31	114863	61797	6488	28.81	.859	1407	87.77
3	25.31	114863	61797	6539	28.78	.859	1407	87.68
4	25.31	114863	61797	6536	28.78	.859	1407	87.68
5	25.31	114863	61797	6558	28.77	.859	1407	87.64
6	25.5	115725	61365	9202	28.52	.886	1368	83.07
7	25.22	114454	61365	3320	31.43	.865	1383	93.75
8	25.15	114137	61365	3008	31.43	.86	1387	94.3
9	25.08	113819	61365	2680	31.44	.855	1391	94.89
10	25.08	113819	61365	2669	31.44	.855	1391	94.91
16	26.31	119401	61597	11682	29.82	.938	1295	79.79
17	26.59	120672	61597	4496	35.29	.959	1282	92.39
18	26.67	121035	61597	4783	35.34	.965	1278	91.95
19	26.68	121080	61597	4847	35.32	.966	1277	91.85
20	26.74	121353	61597	5102	35.34	.97	1275	91.46

TABLE 6.3

ACTUAL STRESS CHANGES

	INITIAL CONDITIONS (PSI)						FINAL CONDITIONS (PSI)						STRESS CHANGES (PSI)		
TEST CODE	TOTAL PRESSURE	AIR PRESSURE	WATER PRESSURE	$(\sigma-U_w)$	$(\sigma-U_a)$	(U_a-U_w)	TOTAL PRESSURE	AIR PRESSURE	WATER PRESSURE	$(\sigma-U_w)$	$(\sigma-U_a)$	(U_a-U_w)	σ	U_a	U_w
NR0101	0	0	0	0	0	0	39.93	29.79	20.02	19.91	10.14	9.77	39.93	29.79	20.02
NR0102	39.93	29.79	20.02	19.91	10.14		60.00	50.01	40.03	19.97	9.99	9.98	20.07	20.22	20.01
NR0103	60.00	50.01	40.03	19.97	9.99		70.02	60.00	50.00	20.02	10.02	10.00	10.02	9.99	9.97
NR0104	70.02	60.00	50.00	20.02	10.02		60.05	50.03	40.05	20.00	10.02	9.98	-9.97	-9.97	-9.95
NR0105	60.05	50.03	40.09	20.20	10.02		39.17	30.06	20.07	19.1	9.11	9.99	-20.88	-19.97	-19.98
NR0206	0	0	0	0	0	0	39.99	29.98	20.04	19.95	10.01	9.94	39.99	29.98	20.04
NR0207	39.99	29.98	20.04	19.99	10.01		59.97	49.99	40.00	19.97	9.98	9.99	19.98	20.01	19.96
NR0208	59.97	49.99	40.00	19.97	9.98		69.95	59.98	49.97	19.98	9.97	10.01	9.98	9.99	9.97
NR0209	69.95	59.98	49.97	19.98	9.97		60.07	50.03	40.02	20.05	10.04	10.01	-9.88	-9.95	-9.95
NR0210	60.07	50.03	40.02	20.05	10.04		40.02	30.03	20.05	19.97	9.99	9.98	-20.05	-20.0	-19.97
NR0316	0	0	0	0	0	0	29.27	29.28	19.06	10.21	-0.01	10.22	29.27	29.28	19.06
NR0317	29.27	29.28	19.06	10.21	-0.01		49.95	39.96	30.00	19.95	9.99	9.96	20.68	10.68	10.94
NR0318	49.95	39.90	30.00	19.95	9.99		60.01	50.02	40.02	19.99	9.99	10.00	10.06	10.06	10.02
NR0319	60.01	50.02	40.02	19.99	9.99		50.02	40.00	30.04	19.98	10.02	9.96	-9.99	-10.02	-9.98
NR0320	50.02	40.00	30.04	19.98	10.02		40.04	30.03	20.03	30.01	10.01	10.00	-9.98	-9.97	-10.01
NT0101	0	0	0	0	0	0	29.50	19.32	9.36	20.14	10.18	9.96	29.50	19.32	9.36
NT0102	29.50	19.32	9.36	20.14	10.18		39.56	29.32	19.33	20.23	10.24	9.99	10.06	10.00	9.97
NT0103	39.56	29.32	19.33	20.23	10.24		49.53	39.30	29.31	20.22	10.23	9.99	9.97	9.98	9.98
NT0104	49.53	39.30	29.31	20.22	10.23		39.61	29.37	19.33	20.28	10.24	10.04	-9.92	-9.93	-9.98
NT0105	39.61	29.37	19.33	20.28	10.24		29.63	19.39	9.34	20.29	10.24	10.05	-9.98	-9.98	-9.99
NT0206	0	0	0	0	0	0	39.57	29.37	19.17	20.40	10.20	10.20	39.57	29.37	19.17
NT0207	39.57	29.37	19.17	20.40	10.20		44.57	34.32	24.34	20.23	10.25	9.98	5.00	4.95	5.17
NT0208	44.57	34.32	24.34	20.23	10.25		49.54	39.27	29.27	30.27	10.27	10.00	4.97	4.95	4.93
NT0209	49.54	39.27	29.27	20.27	10.27		39.59	29.30	19.31	20.28	10.29	9.99	-9.95	-9.97	-9.96
NT0210	39.59	29.30	19.31	20.28	10.29		29.60	19.32	9.29	20.31	10.28	10.03	-9.99	-9.98	-10.02
NT0311	0	0	0	0	0	0	29.55	19.30	10.01	19.54	10.25	9.29	29.55	19.30	10.01
NT0312	29.55	19.30	10.01	19.54	10.25		39.56	29.28	19.30	10.26	10.28	9.98	10.01	10.98	9.29
NT0313	39.56	29.28	19.30	20.26	10.28		44.57	34.31	23.93	20.64	10.26	10.38	5.01	5.03	4.03
NT0314	44.57	34.31	23.93	20.64	10.26		39.60	29.31	18.81	20.76	10.29	10.5	-4.97	-5.00	-5.12
NT0315	39.60	29.31	18.81	20.76	10.29		29.60	19.33	9.3	20.3	10.27	10.03	-10.00	-9.98	-9.51

TABLE 6.4

PROPOSED STRESS CHANGES

TEST CODE	INITIAL CONDITIONS						FINAL CONDITIONS						STRESS CHANGES		
	TOTAL PRESSURE	AIR PRESSURE	WATER PRESSURE	$(\sigma-U_w)$	$(\sigma-U_a)$	(U_a-U_w)	TOTAL PRESSURE	AIR PRESSURE	WATER PRESSURE	$(\sigma-U_w)$	$(\sigma-U_a)$	(U_a-U_w)	TOTAL	AIR	WATER
NR0101	0	0	0	0	0	0	40	30	20	20	10	10	40	30	20
NR0102	40	30	20	20	10	10	60	50	40	20	10	10	20	20	20
NR0103	60	50	40	20	10	10	70	60	50	20	10	10	10	10	10
NR0104	70	60	50	20	10	10	60	50	40	20	10	10	-10	-10	-10
NR0105	60	50	40	20	10	10	40	30	20	20	10	10	-20	-20	-20
NR0206	0	0	0	0	0	0	40	30	20	20	10	10	40	30	20
NR0207	40	30	20	20	10	10	60	50	40	20	10	10	20	20	20
NR0208	60	50	40	20	10	10	70	60	50	20	10	10	10	10	10
NR0209	70	60	50	20	10	10	60	50	40	20	10	10	-10	-10	-10
NR0210	60	50	40	20	10	10	40	30	20	10	10	10	-20	-20	-20
NR0316	0	0	0	0	0	0	40	30	20	20	10	10	40	30	20
NR0317	40	30	20	20	10	10	50	40	30	20	10	10	10	10	10
NR0318	50	40	30	20	10	10	70	60	50	20	10	10	20	20	20
NR0319	70	60	50	20	10	10	50	40	30	20	10	10	-20	-20	-20
NR0320	50	40	30	20	10	10	40	30	20	20	10	10	-10	-10	-10
NT0101	0	0	0	0	0	0	30	20	10	20	10	10	30	20	10
NT0102	30	20	10	20	10	10	40	30	20	20	10	10	10	10	10
NT0103	40	30	20	20	10	10	50	40	30	20	10	10	10	10	10
NT0104	50	40	30	20	10	10	40	30	20	20	10	10	-10	-10	-10
NT0105	40	30	20	20	10	10	30	20	10	20	10	10	-10	-10	-10
NT0206	0	0	0	0	0	0	40	30	20	20	10	10	40	30	20
NT0207	40	30	20	20	10	10	45	35	25	20	10	10	5	5	5
NT0208	45	35	25	20	10	10	50	40	30	20	10	10	5	5	5
NT0209	50	40	30	20	10	10	40	30	20	20	10	10	-10	-10	-10
NT0210	40	30	20	20	10	10	30	20	10	20	10	10	-10	-10	-10
NT0311	0	0	0	0	0	0	30	20	10	20	10	10	30	20	10
NT0312	30	20	10	20	10	10	40	30	20	20	10	10	10	10	10
NT0313	40	30	20	20	10	10	45	35	25	20	10	10	5	5	5
NT0314	45	35	25	20	10	10	40	30	20	20	10	10	-5	-5	-5
NT0315	40	30	20	20	10	10	30	20	10	20	10	10	-10	-10	-10

All pressure units lb/in^2

TABLE 6.5

TOTAL VOLUME BEHAVIOUR OF THE 76MM SPECIMENS

SPECIMEN	SOIL TYPE B/K*	TOTAL STRESS (PSI)	TOTAL STRESS (kN/m^2)	PERCENTAGE VOLUME CHANGE TOTAL	PERCENTAGE VOLUME CHANGE IMMEDIATE	PERCENTAGE VOLUME CHANGE SECONDARY	PREDICTED VOLUME CHANGE ON BASIS OF CVSP RESULTS $(\sigma-U_w)$	PREDICTED VOLUME CHANGE ON BASIS OF CVSP RESULTS (U_a-U_w)	MEASURED WATER INFLOW (%)
NR01	0/100	0	0	-	-	-			
	"	39.93	276	-2.05	-2.40	0.35			
	"	60.00	414	0	0	0	-1.28	0	0.28
	"	70.02	483	0	-0.04	0.04	-0.4	0	0.01
	"	60.06	414	0	0	0	0.13	0	0.07
	"	39.17	276	0.12	0.39	-0.27	0.34	3.5	0.26
NR02	10/90	0	0	-	-	-			
	"	39.90	276	-1.15	-1.11	-0.04			
	"	59.97	414	-0.29	-0.37	0.08	-1.41	20.5	0.22
	"	69.95	483	-0.29	-0.41	0.12	-0.42	69.0	0.01
	"	60.07	414	0	0	0	0.32	0	0.01
	"	40.02	276	0.164	0.164	0	-1.07	15.3	0.358
NR03	30/70	0	0	-	-	-			
	"	29.27	201	1.17	-3.04	4.21			0.44
	"	49.95	345	0.33	-0.04	0.37	-2.63	0.13	0
	"	60.01	414	0.04	-0.04	0.0	-1.01	0.04	0
	"	50.02	345	0.25	0.0	0.25	1.01	0.25	0
	"	40.04	276	0.41	0.04	0.37	2.84	0.14	0

* soil type refers to the composition of the test specimens i.e. (B) - Sodium montmorillonite and (K) - Kaolinite/china clay

TABLE 6.6

TOTAL VOLUME BEHAVIOUR OF THE 100MM SPECIMENS

SPECIMEN	SOIL TYPE B/K*	TOTAL STRESS (PSI)	TOTAL STRESS (kN/m^2)	% DEFORMATION TOTAL	% DEFORMATION IMMEDIATE	% DEFORMATION SECONDARY	PREDICTED VOLUME CHANGE ON BASIS OF CVSP RESULTS $(\sigma-U_w)$	PREDICTED VOLUME CHANGE ON BASIS OF CVSP RESULTS (U_a-U_w)	MEASURED WATER INFLOW (%)
NT01	0/100	0		-	-	-	-	-	-
	"	30	201	-0.80	-0.63	-0.17	-	-	-
	"	40	276	-0.35	0	-0.35	-0.81	0.43	0
	"	50	345	-0.44	-0.252	-0.18	-0.74	0.59	0
	"	40	276	0	0.158	-0.158	0.13	0	0.127
	"	30	201	0.032	0.19	-0.158	0.21	0.15	0.20
NT02	10/90	0	0	-	-	-	-	-	-
	"	40	276	-1.92	-1.68	-0.24	-	-	0
	"	45	310	-0.30	0.04	-0.30	-0.4	0.75	0
	"	50	345	-0.44	0	-0.44	-0.37	*1.18	0
	"	40	276	0.10	0.13	-0.03	0.6	0.16	0
	"	30	201	0.17	0.13	-0.04	0.74	0.23	0.13
NT03	20/80	0	0	-	-	-	-	-	-
	"	30	201	-0.77	-0.95	0.18	-	-	-
	"	40	276	-0.623	-0.33	-0.293	-1.14	0.55	0
	"	45	310	-0.55	-0.51	-0.04	-0.47	*1.17	0
	"	40	276	0	0.04	-0.04	0.48	0	0
	"	30	201	0.183	0.256	-0.073	1.01	0.18	0

* soil type refers to the composition of the test specimens i.e. (B) - Sodium montmorillonite and (K) - Kaolinite (china clay)

TABLE 6.7

STRESS RELATED BEHAVIOUR OF WATER INFLOW FOR THE 76MM SPECIMENS

SOIL TYPE	TOTAL STRESS (PSI)								
B/K*	30	40	50	60	70	60	50	40	30
0/100		2.554		0.259	0.00932	0.0289		0.203	y int
		1.801^{-5}		2.599^{-5}	1.821^{-5}	2.182^{-5}		1.232^{-5}	%/min
		0.0259		0.0374	0.0262	0.0314		0.0177	%/day
		0.9		0.043	0.026	0.0312			
10/90		3.984		0.165	0.0735	0.0456		0.271	
		5.331^{-5}		3.961^{-5}	2.127^{-5}	2.301^{-5}		2.144^{-5}	
		0.0768		0.057	0.0306	0.0331		0.0309	
		0.085		0.064	0.034	0.035		0.043	
30/70	7.082		0.372	0.0743			0.0554	0.00054	
	4.475^{-5}		4.586^{-5}	2.501^{-5}			2.889^{-5}	4.743^{-5}	
	0.0645		0.066	0.03601			0.0416	0.0683	
	0.041		0.064	0.037			0.047	0.065	

TABLE 6.8

STRESS RELATED BEHAVIOUR OF WATER INFLOW FOR THE 100MM SPECIMENS

SOIL TYPE	TOTAL STRESS (PSI)					
B/K*	30	40	45	50	40	30
0/100	0.446	-0.0149		-0.0299	0.0479	0.127
	1.214×10^{-4}	1.213^{-5}		9.834^{-6}	1.589^{-5}	1.896^{-5}
	0.175	0.0175		0.0142	0.0229	0.0273
	0.0471	0.0436		0.0354	0.0569	0.069
10/90		2.294	5.478-6	0.0062	0.011	0.0657
		1.16^{-5}	1.126^{-5}	1.445^{-5}	2.259^{-5}	1.405^{-5}
		0.0167	0.01621	0.0208	0.033	0.0202
		0.062	0.0596	0.0484	0.067	0.0476
20/80	7.121	0.0108	-0.0058		-0.16	-0.0039
	1.339^{-5}	4.879^{-5}	2.66^{-5}		2.261^{-5}	2.89^{-5}
	0.0193	0.0703	0.0383		0.0326	0.0416
	0.044	0.146	0.082		0.073	0.089

TABLE 6.9

COMPARISON OF EQUIPMENT BEHAVIOUR

EQUIPMENT BEHAVIOUR	SPECIMEN SIZE	
	76MM	102MM
TOTAL VOLUME CHANGE		
1. decreases following stress increase	X	0
2. increases following stress decrease	0	0
3. deformation occurs in two phases : immediate and secondary	0	0
4. maximum volume change (representative) following stress increase	-0.29 %	-0.623 %
5. maximum volume change (representative) following stress decrease	0.41 %	0.183 %
6. volume only partially recovers following stress reduction	0	0
WATER VOLUME CHANGE		
1. constant inflow registered	0	0
2. rate of inflow decreases with increasing stress	0	0
3. the rate of inflow only partially recovers upon stress reduction	0	X

0 signifies yes ; X signifies 'almost all' tests

TABLE 6.10

VOLUME CHANGES ASSOCIATED WITH A CHANGE IN THE 'TOTAL' STRESS STATE VARIABLE

TEST NO.	SOIL TYPE K/B	STRESS CHANGE (KN/M^2) FROM	TO	Δe	h_s (mm)	Δh_v (mm)	h_o (mm)	$\frac{\Delta h}{h_o} \times 100$ (%)
NR0102	100/0	275.4	416.9	-0.025	7.71	-0.19	14.85	-1.28
NR0103	"	416.9	478.6	-0.008	"	-0.06	"	-0.4
NR0104	"	478.6	416.9	0.002	"	0.02	"	0.13
NR0105	"	416.9	275.4	0.006	"	0.05	"	0.34
NR027	90/10	275.4	416.9	-0.026	7.92	-0.21	14.93	-1.41
NR028	"	416.9	478.6	-0.008	"	-0.063	"	-0.42
NR029	"	478.6	416.9	0.006	"	0.048	"	0.32
NR0210	"	416.9	275.4	0.02	"	0.16	"	1.07
NR0317	70/30	208.9	346.7	-0.05	7.88	-0.39	14.81	-2.63
NR0318	"	346.7	416.9	-0.019	"	-0.15	"	-1.01
NR0319	"	416.9	346.7	0.019	"	0.15	"	1.01
NR0320	"	346.7	275.4	0.053	"	0.42	"	2.84
NT0102	100/0	208.9	275.4	-0.016	7.71	-0.12	14.85	-0.81
NT0103	"	275.4	346.7	-0.014	"	-0.11	"	-0.74
NT0104	"	346.7	275.4	0.003	"	0.02	"	0.13
NT0105	"	275.4	208.9	0.004	"	0.031	"	0.21
NT0207	90/10	275.4	309.0	-0.008	7.92	-0.06	14.93	-0.4
NT0208	"	309.0	346.7	-0.007	"	-0.055	"	-0.37
NT0209	"	346.7	275.4	0.011	"	0.09	"	0.6
NT0210	"	275.4	208.9	0.014	"	0.11	"	0.74
NT0312	80/20	208.9	275.4	-0.021	7.86	-0.17	14.92	-1.14
NT0313	"	275.4	309.0	-0.009		-0.07	"	-0.47
NT0314	"	309.0	275.4	0.009		0.071	"	0.48
NT0315	"	275.4	208.9	0.019		0.15	"	1.01

TABLE 6.11

TRANSMISSION OF WATER THROUGH PERSPEX

CASE NO.	DESCRIPTION	AVERAGE THICKNESS (CM)	RATE OF WATER LOSS ($ML/CM^2/DAY$)
1*	One surface dried by $CaCl_2$ the other exposed to summer atmosphere	0.0762	0.000288
2*	One surface dried by $CaCl_2$ the other exposed to water saturated air	0.16	0.00062
3*	Same as 2	0.0117	0.0117
4	One surface water saturated the other exposed to summer atmosphere	0.6	0.0001
5	Same as 4	0.29	0.000054

*Signifies data from the International Critical Tables

All other cases from Fredlund (1973)

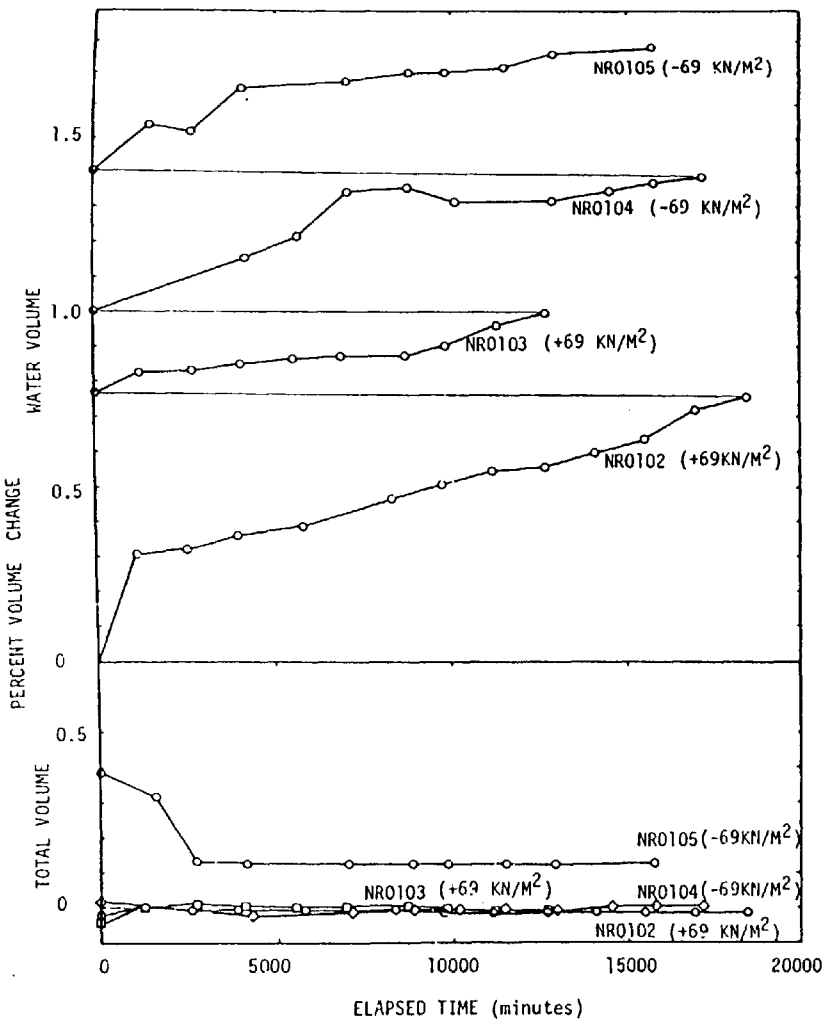

FIGURE 6.1

VOLUME CHANGE HISTORIES OF TESTS
UPON SPECIMEN NR01 (100%K)

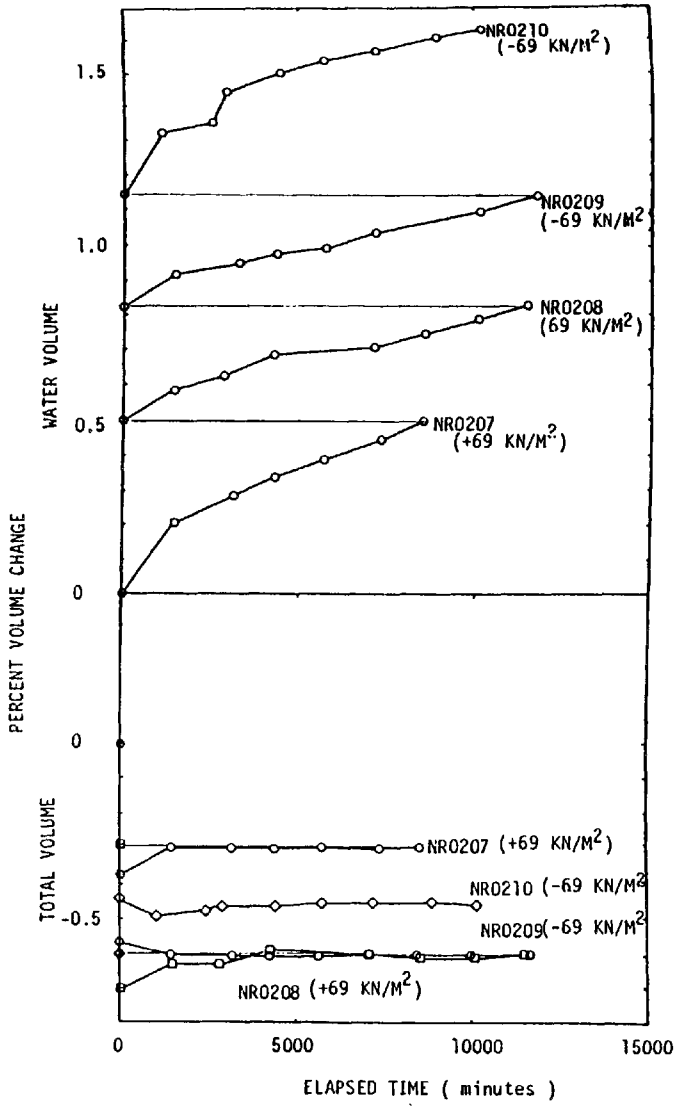

FIGURE 6.2

VOLUME CHANGE HISTORIES OF TESTS
UPON SPECIMEN NR02 (10%B + 90%K)

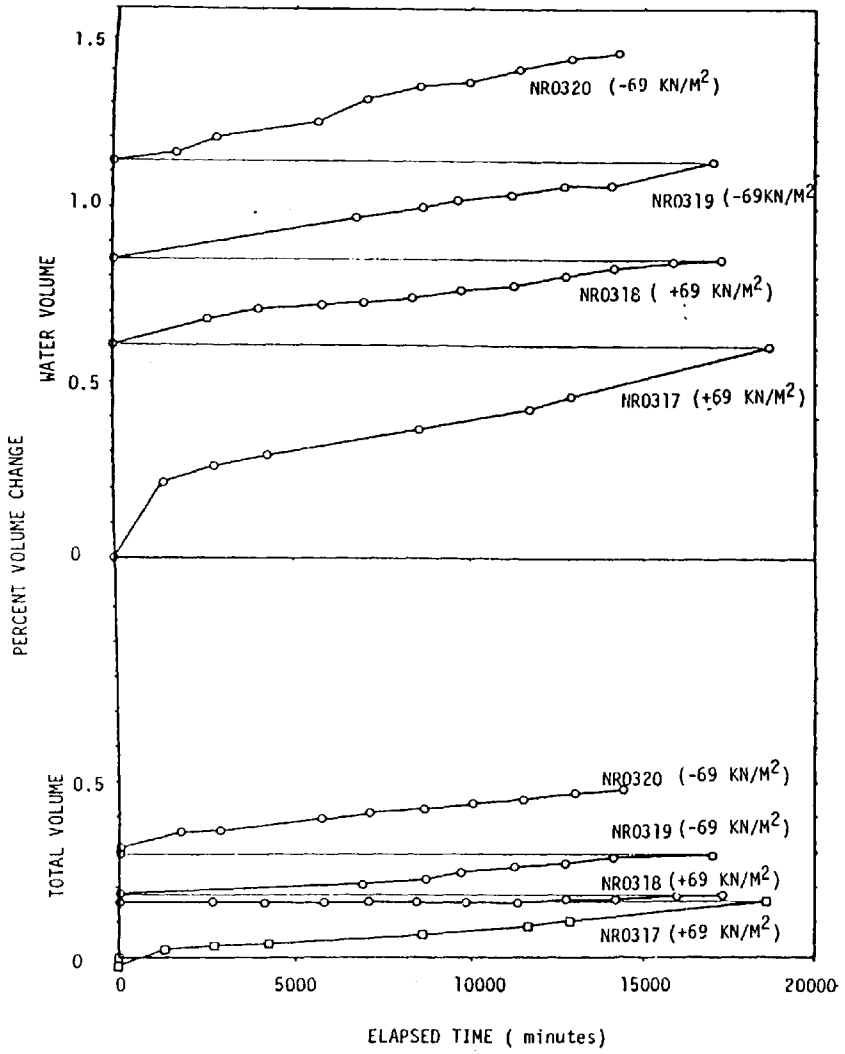

FIGURE 6.3

VOLUME CHANGE HISTORIES OF TESTS
UPON SPECIMEN NR03 (30%B + 70%K)

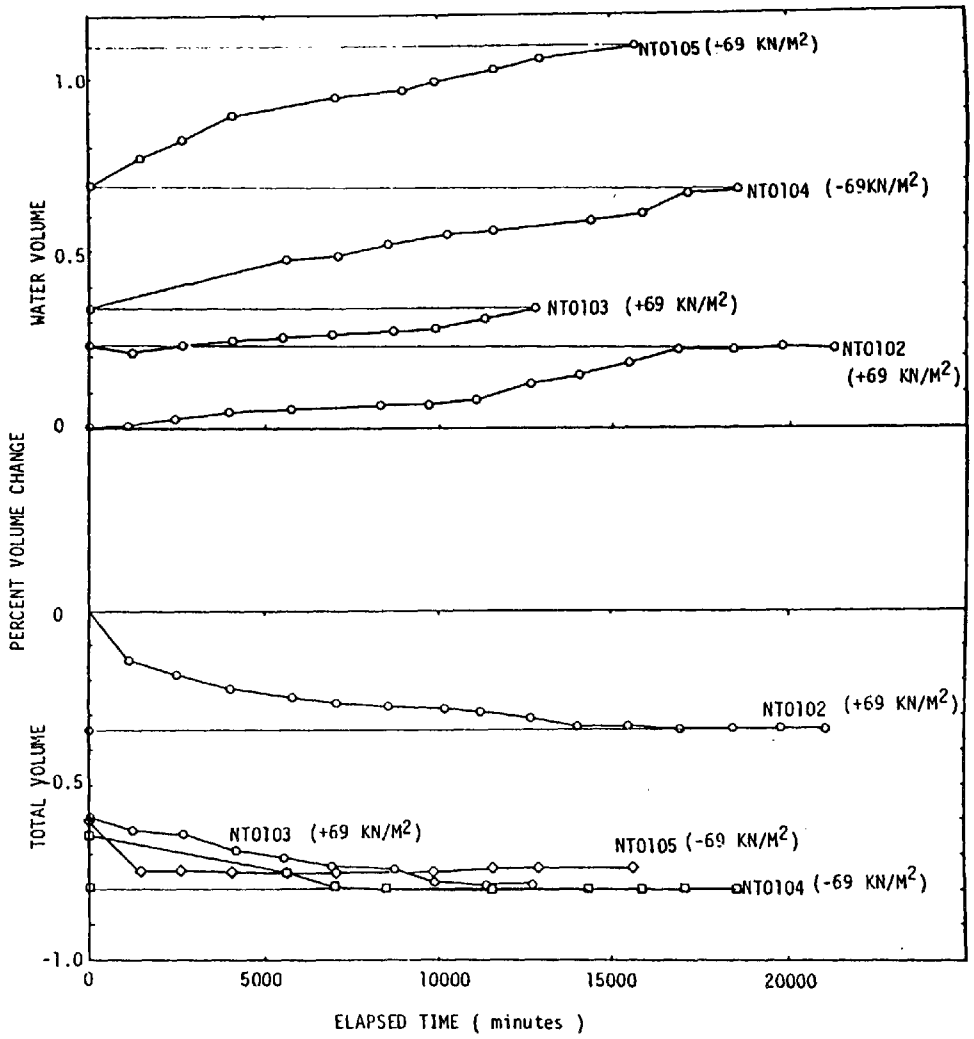

FIGURE 6.4

VOLUME CHANGE HISTORIES OF TESTS
UPON SPECIMEN NT01 (100%K)

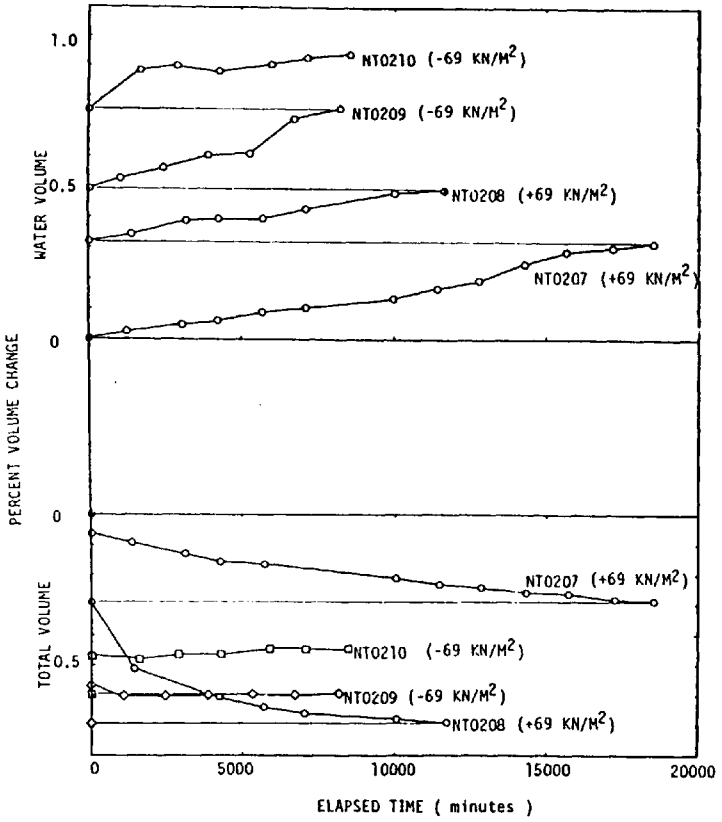

FIGURE 6.5

VOLUME CHANGE HISTORIES OF TESTS
UPON SPECIMEN NT02 (10%B + 90%K)

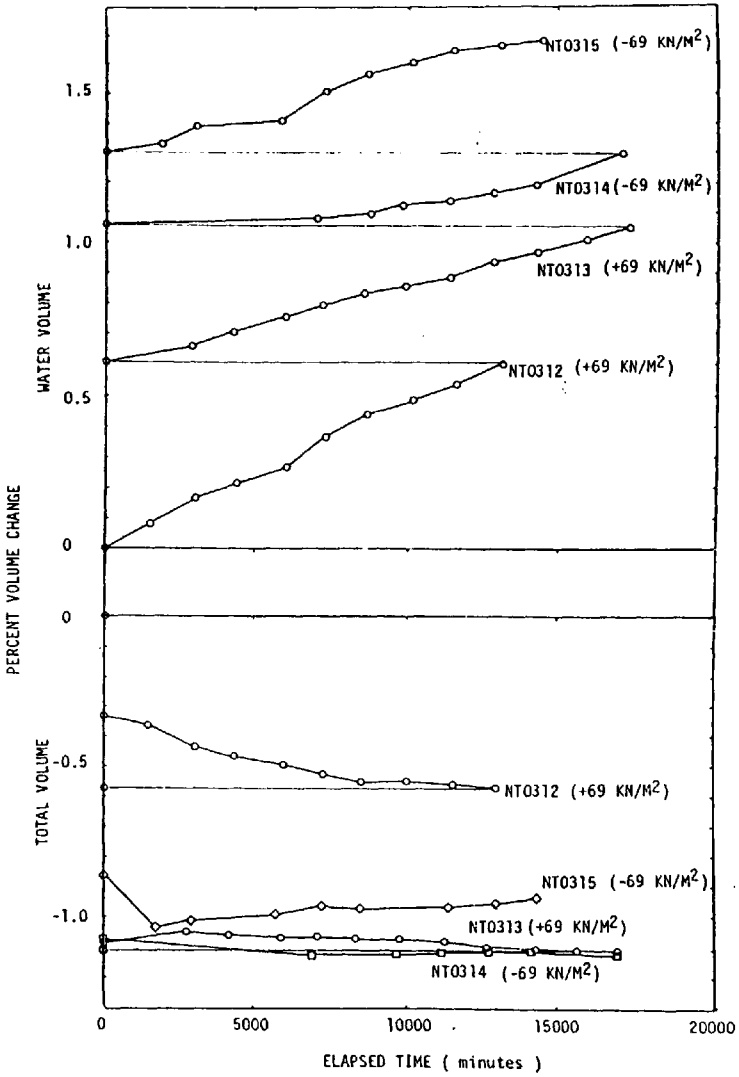

FIGURE 6.6

VOLUME CHANGE HISTORIES OF TESTS
UPON SPECIMEN NT03 (20%B + 80%K)

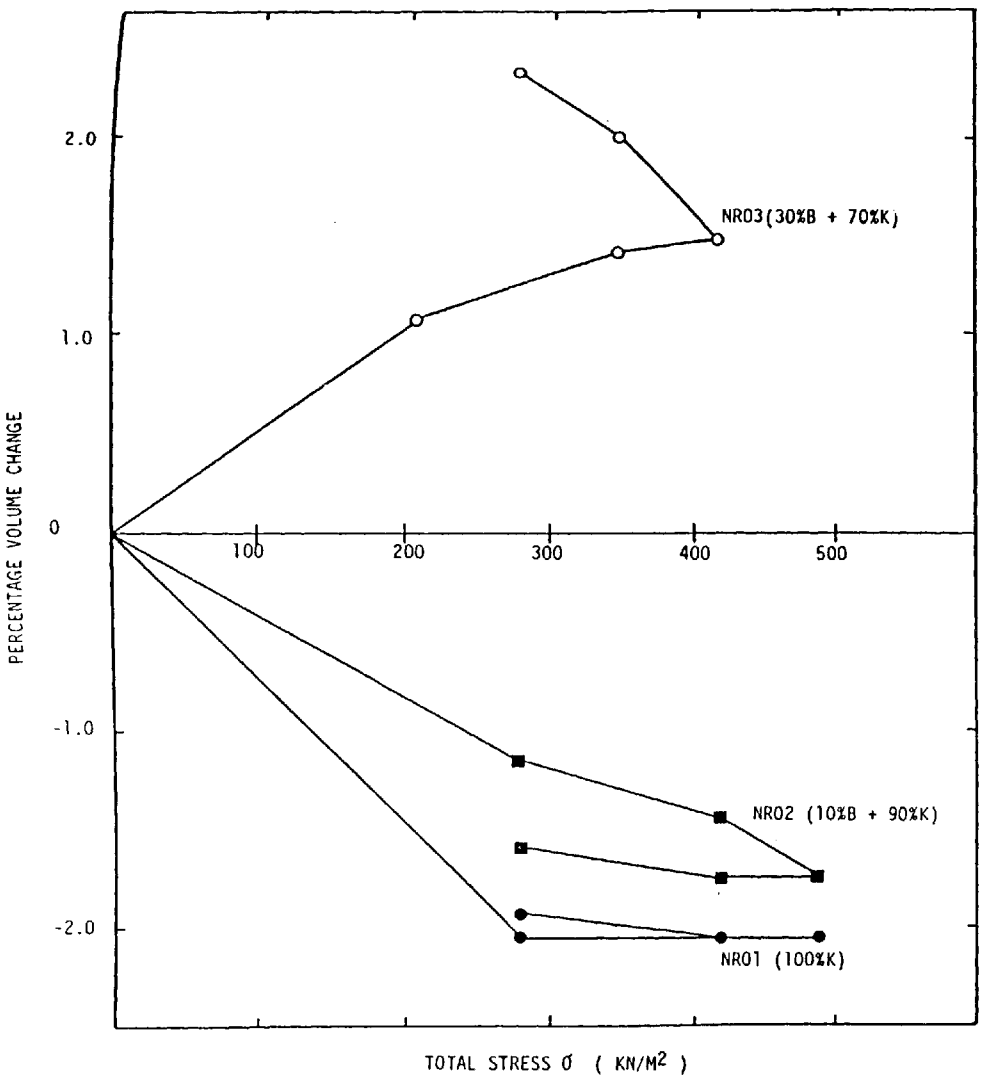

FIGURE 6.7

TOTAL VOLUME CHANGE BEHAVIOUR OF
THE 76MM DIAMETER (ROWE) SPECIMENS

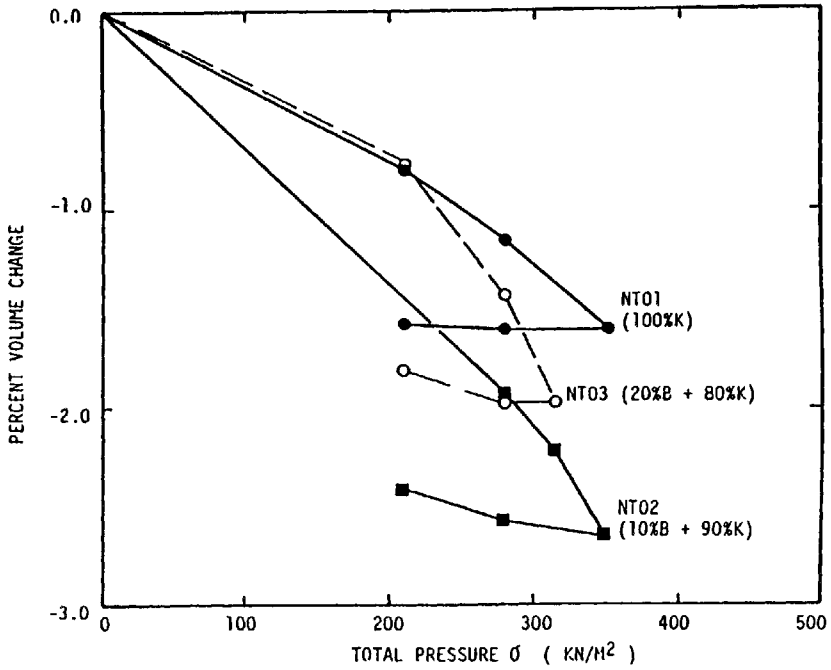

FIGURE 6.8

TOTAL VOLUME CHANGE BEHAVIOUR OF
THE 100MM DIAMTER (TRIAXIAL) SPECIMENS

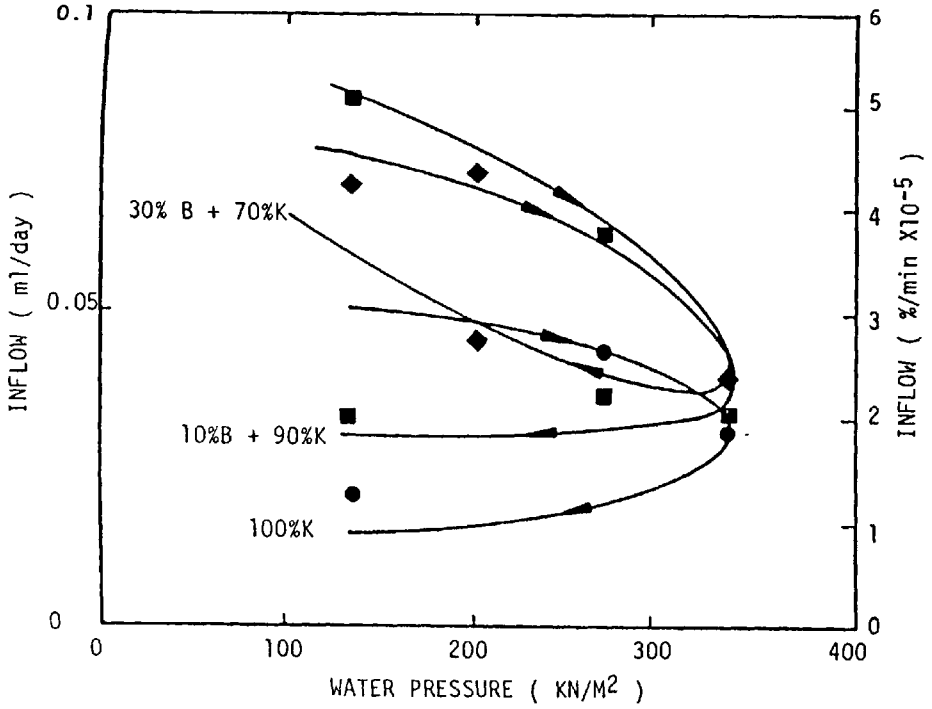

FIGURE 6.9

STRESS RELATED BEHAVIOUR OF THE WATER VOLUME INFLOW FOR 76MM DIAMETER (ROWE) SPECIMENS.

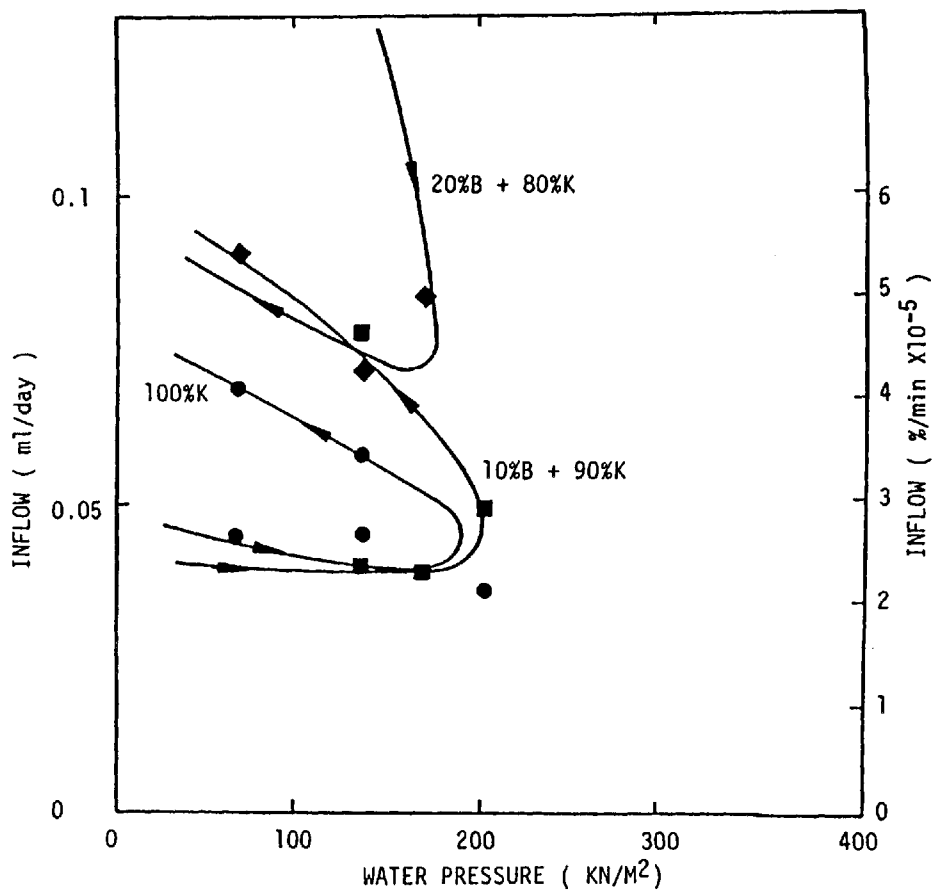

FIGURE 6.10

STRESS RELATED BEHAVIOUR OF THE WATER VOLUME INFLOW FOR 100MM DIAMETER (TRIAXIAL) SPECIMENS

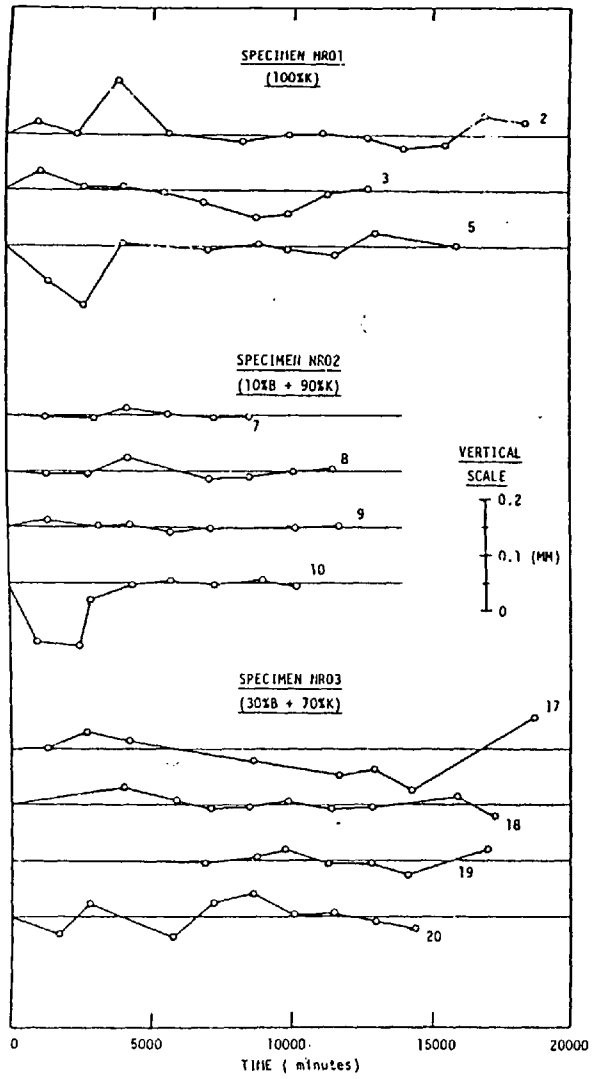

FIGURE 6.11

WATER VOLUME CHANGES-ADJUSTED FOR CONSTANT WATER LOSS (76MM DIA. SPECIMENS)

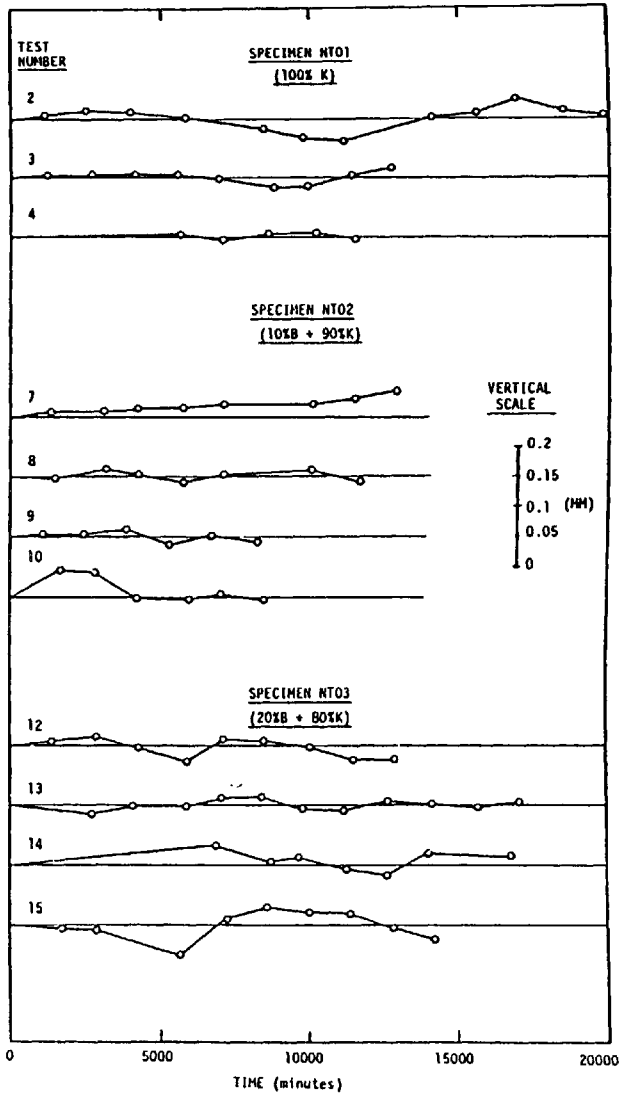

FIGURE 6.12

WATER VOLUME CHANGES-ADJUSTED FOR CONSTANT WATER LOSS (100MM DIA. SPECIMENS)

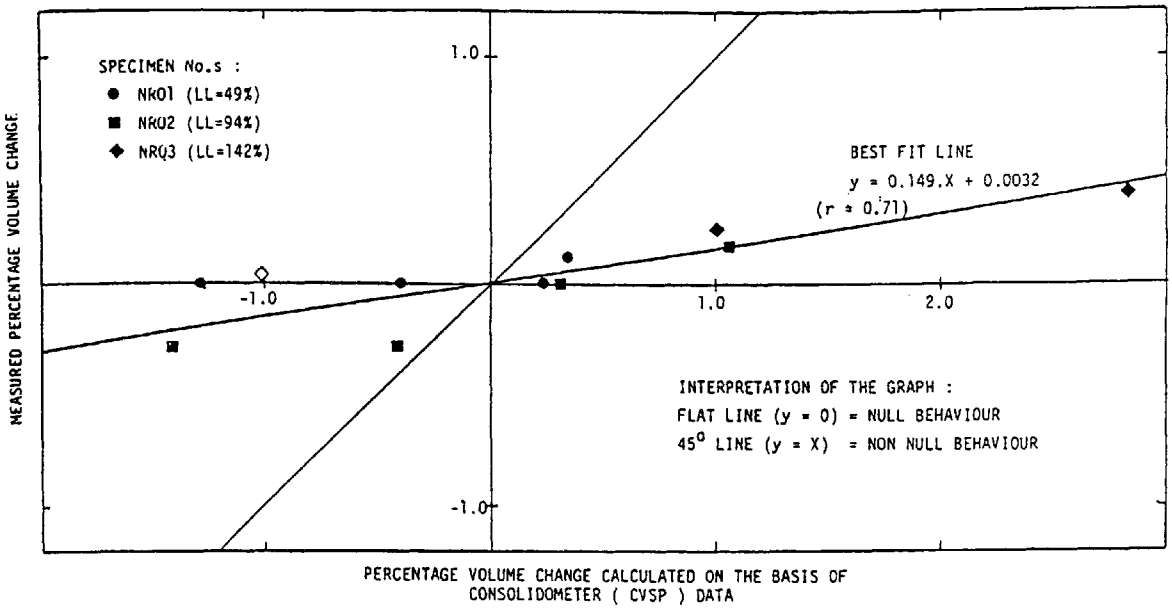

FIGURE 6.13

ASSESSMENT OF NULL TESTS UPON THE 76MM DIA. (ROWE) SPECIMENS.

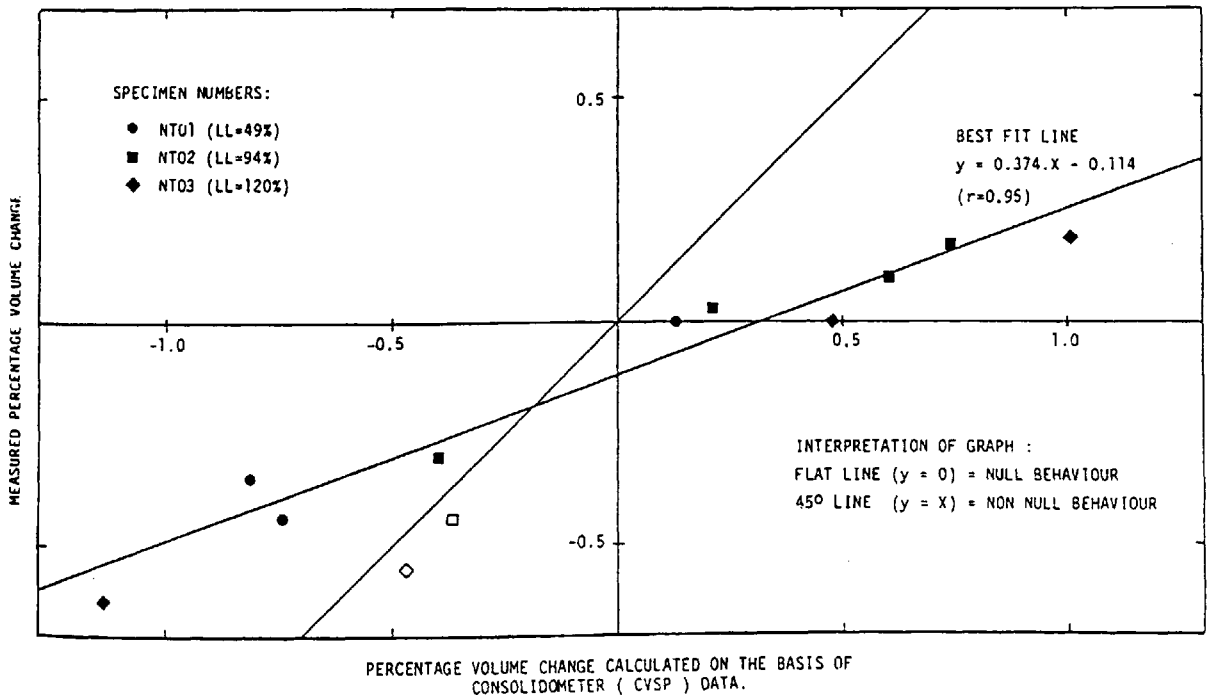

FIGURE 6.14

ASSESSMENT OF NULL TESTS UPON THE 100MM DIA. (TRIAXIAL) SPECIMENS

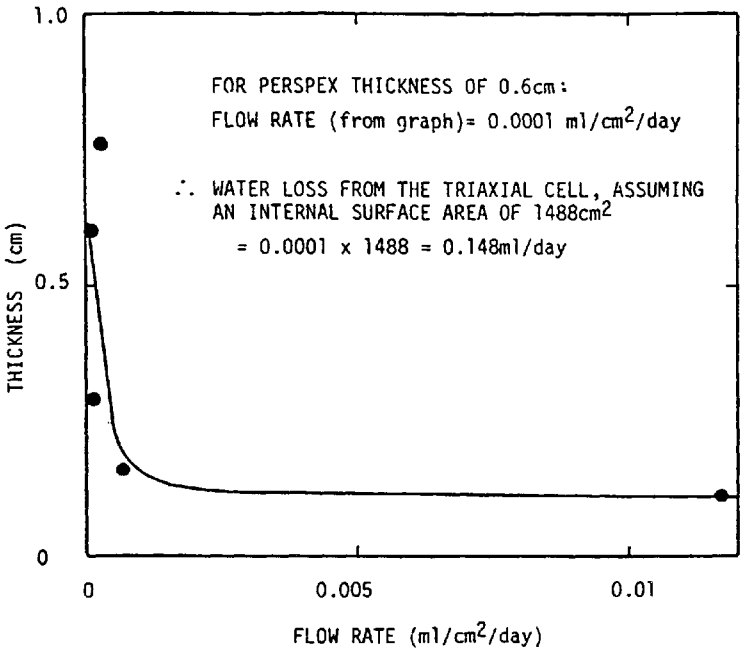

FIGURE 6.15

TRANSMISSION OF WATER THROUGH PERSPEX

CHAPTER 7

VOLUME CHANGE TESTS

7.1 INTRODUCTION

The aim of the volume change testing was to experimentally validate the volume change equations as shown below for use with a range of synthetically produced unsaturated expansive clays.

The volume change equations or constitutive relationships as they are also called, relate the change in total, air or water volume to the stress state variables $(\sigma-u_w)$, $(\sigma-u_a)$, (u_a-u_w). The general form for the volume change equation is :

$$\frac{dv}{v} = C_t \cdot d(\sigma-u_w) + C_a.d(\sigma-u_a) + C_w(u_a-u_w) \qquad (7.1)$$

The equipment and experimental techniques are discussed in Chapter 5 and Appendix A respectively.

Briefly however, the specimens were subjected to small stress increments along three stress paths by individually varying σ , u_a and u_w . The resulting total and water volume changes were recorded, thus enabling the calculation of volume change moduli. (the air volume change was assumed equal to the difference in the total and water volumes). Upon the basis of two such stress changes the corresponding moduli were employed to predict the volume change resulting from a change of the third stress component. The predicted

volume changes were then compared with those measured experimentally, and the volume change equation was considered verified (or the constitutive surface unique) if the predicted and measured volume changes were equal.

In order to assess the results, the predicted and measured volume changes were plotted against one another and the parameters of the best fit line through the data points, used as a measure of the volume change equation validity (the measured volume changes should equal the corresponding prediction i.e. the best fit line should have a gradient of 1 and pass through the origin).

7.2 TESTING PROGRAMME

Each specimen underwent seven 'tests'; the initial one involved application of the conditioning stresses (similar procedure to the null tests), following which the specimen was subjected to two cycles of stress changes (6 tests in total - refer Tables 7.1-7.3).

Since the aim of this study was to measure the volume change properties of expansive clays, then the stress changes were primarily designed to cause a volume increase. This required constantly decreasing suction and total stress state variables and was achieved by conducting the following cycle of stress component changes.

(1) increase in water pressure (u_w)

(2) decrease in air pressure (u_a)

(3) decrease in total stress (σ)

Practically speaking, this involved bringing the specimen to as high a suction as the equipment would permit, and then repeating the above cycle as many times as possible until the suction reduced to zero.

In all, four synthetically produced clay mixtures were tested in the following bentonite:Kaolinite percent ratios : 0:100 , 0:90 , 20:80 and 30:90 ; the testing was then equally allocated between the 76mm and 100 mm cells. To the author's knowledge, this is the first time that these equations have been systematically examined for a range of specimens with controlled plasticity and expansivity.

The testing programme is summarised in Tables 7.1 through 7.3.

The soil related properties at the commencement of each test are listed in Tables 7.4(a) and (b).

The volume change histories for the total and water volumes are illustrated in figures 7.1 through 7.5 and the maximum equilibrium volume changes listed in Table 7.5. The stages of volume change prediction are detailed in Tables 7.5 through 7.7.

Finally, the results of the regression analysis are listed in Tables 7.8 to 7.9 and figures 7.6 to 7.17.

The numbering system used in the volume change tests is outlined at the end of chapter 5.

7.3 EXPERIMENTAL RESULTS

7.3.1 Data Recording and Processing

The data was collected and processed using an identical procedure to that employed with the null test programme. The main difference was in the interpretation of results.

The testing procedure involved separate changes in each of the three stress components; this resulted in a change of total and water volumes. These were considerable at first but came to equilibrium over varying time periods - depending upon the soil type (refer Figs. 7.1-7.5).

The stress-related total and water volume changes employed for the subsequent volume change analysis were then observed to be as follows :

7.3.2 Total Volume Change

The total volume increased at first, then came to equilibrium in virtually every case. Since the equilibration time varied according to the soil type, then the maximum volume changes were recorded at different intervals, thereby providing a consistent criteria by which they could be compared.

7.3.3 Water Volume Change

The water volumes generally exhibited an initially large and rapid increase, and quickly reached equilibrium; at this point a

minute, but constant inflow was recorded and persisted for the remainder of the test. This latter 'constant intake' coincided with that observed during the null tests and is not believed to be actually reaching the specimen. The overall water volume change had therefore to be corrected for this 'base inflow' in order to ascertain the true water volume behaviour.

Two distinct stages of testing were conducted upon each specimen

(a) application of conditioning stress components

and (b) variation of individual stress components

Each of these stages exhibited distinct magnitudes of water inflow.

The application of conditioning stresses led to the largest overall magnitude of water inflow. The inflow curves exhibited the general features described previously, and had also to be adjusted for the-'base inflow'. This was achieved by projecting the linear 'constant inflow' portion of the cuvres back to the y-axis - the intercept of which was taken as the quantity of water entering the specimen. Lower overall magnitudes of water inflow were then recorded following the changing of stress components.

Initially, in order to determine the actual inflow it was envisaged that the recorded water volume change be corrected for the 'constant inflows' recorded during the null test programme. However, this was not undertaken since the stress state variables under which the null test 'inflows' were obtained, were quite different to those applied in the volume change tests.

In any event, it was not necessary to apply these previously determined corrections since the true inflows were adequately calculated by projecting the 'constant inflow' portion of each inflow curve back to the y-axis.

7.4 PREDICTION OF VOLUME CHANGES

The volume change predictions were made upon the basis of moduli derived from the experimentally measured values.

This section details the assumptions and calculations involved in the predictions and describes: the sign conventions employed, the volume change moduli calculated and a worked example of the volume change predictions.

7.4.1 Sign Convention for Volume Changes

The sign convention adopted for all volume changes was :

(+) positive : increase in respective phase volume

(-) negative : decrease in respective phase volume

and this refers to the volume changes within the specimen.

7.4.2 Volume Change Moduli

The changing of each stress component resulted in a corresponding change of both the total and water volumes; from these, the respective phase volume change moduli i.e. for soil, air and water were calculated such that :

$$\text{volume change modulus (total or water or air)} \quad (C) = \left(\frac{\text{measured change in volume with respect to the original volume}}{\text{change in stress state variable under consideration due to a change in the stress component under consideration}} \right)$$

The sign conventions, for these moduli were not straightforward, since the changes in stress components did not necessarily result in the same change in all stress state variables. For example, an increase (+) of the air pressure (u_a) resulted in a decrease (-) of the total stress ($\sigma-u_a$) variable, but an increase (+) in the suction (u_a-u_w) stress variable. The sign conventions associated with the various stress component changes are summarised in Table 7.10.

For example, consider the test UT0102 which involved an increase in water pressure of +4.98 psi (34.34kN/m^2). The total volume change was +0.003%, and the increase in the water pressure caused a decrease in the stress state variables ($\sigma-u_w$) and (u_a-u_w) of -4.98 psi /34.34KN/M^2. Therefore, the volume change modulus was calculated:

$$\frac{0.003}{-4.98} = -0.0006 \text{ in}^2/\text{lb} = 0.000087 \text{ m}^2/\text{kN}$$

7.4.3 Example of Volume Change Prediction

Test UT0203 involved a decrease in the air pressure of 4.97psi/ 34.27 kN/m^2 , and this caused a decrease in total volume of 0.072% . The object was to predict the total volume change that would result from a similar air pressure change.

Tests UT0204 and UT0205 involved a decrease in (σ) and increase in (u_w) of -4.95psi and +5.01 psi respectviely. This resulted in associated total volume changes of 0.046% and -0.017% respectively (Table 7.5). From this information, the volume change moduli were calculated (Table 7.6); since a change in air pressure was being considered then only those moduli associated with (u_a) (i.e. (σ-u_a) and (u_a-u_w)) were required for the calculation of the total volume change. These moduli were -0.0093 : (σ-u_a) and +0.0034 : (u_a-u_w) respectviely.

The total volume change was calculated using the general volume change relationship (equation (7.1)) with the exception of the (σ-u_w) term, which dropped out because ($\Delta\sigma$) and (Δu_w)= 0 .
The volume change was therefore :

$$\frac{dv}{v} = 4.98.- 0.0093 - 4.98.\ 0.0034$$
$$= -0.063\%$$

It must be noted that the signs of the stress changes relate to their effect upon the respective stress state variables (Table 7.10)

7.4.4 Comparison of Measured and Predicted Volume Changes (Uniqueness Tests)

The validation of the volume change equations assumes that all stress changes occur at the same point on the constitutive surface. However, this is not actually the case since the cyclic alteration

of the total, air and water stresses constantly changes the stress state variables. Thus, the number of meaningful comparisons that can be made between the measured and predicted volume changes are limited, if they are not to be made over too wide a stress range.

Suitable combinations of pressure increments for the prediction of volume change are as follows :

where u_i = the pressure increment

i = number of pressure increment

n = total number of increments

then

Combination 1

u_i and u_{i+1} for $i = 1$ to $n - 1$

Combination 2

u_i and u_{i+2} for $i = 1$ to $n - 2$

The first combination of pressure increments may be compared with the previous and subsequent volume changes measured i.e. u_{i-1} and u_{i+2} for $i > 1$ and $i < n + 1$.

The second combination may be compared with the measured volume changes in test u_{i+1} .

In all, a total of twelve such comparisons were made for each specimen in this project.

7.5 REGRESSION ANALYSIS OF THE DATA

7.5.1 Introduction

The comparison of predicted and measured total, air and water volume changes is termed a uniqueness analysis; its purpose is to assess the linearity of the constitutive surface and/or validity of the volume change equation.

The predicted volume changes may be visually assessed by plotting them against the measured values (Figs. 7.6 to 7.17), however it is most desirable that the success of the correlation be quantified.

One method of achieving this is to determine the best fit line through the data by the least squares method; this procedure yields the gradient and y intercept of the best fit line, and also the coefficient of correlation of data points about it.

These results provide a suitable means for quantifying the correlation, provided the data points occur on or very near the perfect correlation (45^{o}) lines. Where the data exhibits some degree of scatter, this approach again determines the best fit line; however, it assumes that only one of the variables are subject to error. This latter assumption as employed by Fredlund, is inappropriate since the predictions are themselves based upon the measured values, thus both variables are subject to error.

A second less frequently used method is to calculate the best fit line for the least perpendicular distances to the data points

(i.e. assuming both variables as subject to error). Although this does not yield a correlation coefficient, it does at least provide a correct indication of the underlying trend in the data.
Both of the above approaches are therefore employed.

7.5.2 Regression to Determine the Best Fit Line Assuming Only One Variable Subject to Error

(a) Theory

This first procedure determines the best fit line through a series of points using the method of least squares. Therefore, where the general equation for a line is $y = mx + C$, then standard tests give us

$$m = \frac{\Sigma xy - \frac{(\Sigma x)(\Sigma y)}{N}}{\Sigma x^2 - \frac{(\Sigma x)^2}{N}} \qquad (7.1)$$

$$C = \frac{(\Sigma x)(\Sigma xy) - (\Sigma y)(\Sigma x^2)}{(\Sigma x)^2 - N(\Sigma x^2)} \qquad (7.2)$$

where

m = gradient of best fit line

C = y intercept of best fit line

x = predicted volume change values

y = measured volume change values

N = number of observations

In the problem under consideration, the slope should equal 1.0 and the y intercept equal zero. The dispersion of the data points about the best fit line may be gauged by using the coefficient of correlation; this is computed from the following equation :

$$r = \frac{N\Sigma xy - \Sigma x \Sigma y}{\sqrt{|N\Sigma x^2-(\Sigma x)^2||N\Sigma y^2-(\Sigma y)^2|}} \qquad (7.3)$$

where

r = coefficient of correlation

The value of r may vary between +1 and -1 , where a value of +1 denotes a perfect relationship between an increasing x and y variable and -1 , a perfect relationship between decreasing x and y variables. An 'r' value of zero indicates no relationship.

The coefficient of correlation may itself be evaluated by comparing it with the value that can be expected at a given level of significance if the observations are drawn by chance (i.e. critical correlation coefficient). If the computed correlation coefficient exceeds the critical value then it can be concluded that a correlation does exist.

(b) Results

Soil Structure (Figures 7.6 to 7.9, Table 7.8)

Three out of four of the specimens exhibited reasonably consistent correlations; however, specimen R1 displayed no discernible

correlation between the measured and predicted volume changes (correlation coefficient = 0.046).

It is noted (Figure 7.7), that the data of this specimen, plots as two discernible groups either side of the 45^{o} line, and it thus appears that an average line drawn through the groups would tend to indicate a 45^{o} line. However, the average best fit line assuming one variable subject to error does not indicate this.

Since the lines are determined on the basis of one variable subject to error, whereas in reality both variables are interrelated and subject to error, then the results from this and the other specimens will be re-evaluated in the next section.

Specimens R2, T1 and T2 exhibited gradients closer to, but still less than one (i.e. the predicted volume change was greater than the measured value). This behaviour was confirmed by the high associated coefficients of correlation (which exceeded the critical correlation coefficient for 5% significance for R2 and T1 and 1% significance for T2). Although the best fit lines were not 45^{o}, a consistent trend was observed.

The results indicated that the magnitude of measured total volume changes did not relate to the specimen plasticity; this is displayed by the random spread of data and axes limits used on figures 7.6 - 7.9.

Notably, the gradient of the best fit line (measured Vs predicted volume changes) tended to unity and the correlative coefficient 'r' tended to increase with increasing plasticity (i.e. the volume change equations apparently performed better for specimens of higher plasticity - refer table 7.8).

This behaviour was more evident upon examining the volume change results of each apparatus (hence specimen size) separately - again refer table 7.8.

This contradicts those observations made during the null tests where reliability of the volume change theory apparently deteriorated with increasing plasticity (chapter 6).

Water phase (Figures 7.10-7.13., Table 7.8)

Three of the four specimens exhibited consistent correlations. Unlike with the soil structure volume changes, the 102mm specimen T1 virtually exhibited no correlation between measured and predicted water volume changes.

As with the soil structure correlation, all of the gradients were less than one, again indicative of the predicted volume change being greater than measured values.

In this instance however, the 76mm specimens indicated far better degrees of correlation than the 102mm specimens their coefficients of correlation exceeded the critical value for 1% significance.

The 102mm specimen on the other hand, exhibited CC^S well below critical value for 5% significance.

The water volume changes generally increased with increasing plasticity and this is clearly displayed by the spread of data and axes limits used in figures 7.10 - 7.13.
The volume changes comprised of immediate and secondary phases, although it is the immediate phase which consistently demonstrated an increase with increasing plasticity (figure 7.1).

The best fit lines and correlative coefficients from each apparatus type were not consistent with one another.
Data emanating from the 102mm cell specimens indicated that the best fit line gradient (measured Vs predicted volume changes) tended

to unity, and the correlative coefficient 'r' increased with increasing plasticity (i.e. accuracy of the predicted volume changes increased with increasing plasticity.)
This conflicted with the 76mm specimen data which indicated the opposite behaviour.

Air phase (Figures 7.14-7.17, Table 7.8)

The air phase volume changes were calculated as the difference between the soil structure and the water phase volume changes; in consequence, the correlation of the air phase volume change data was closely related to that of the soil structure and water phases.

The results confirmed this; specimen T1 whose water phase volume changes exhibited such a poor gradient and correlation coefficient, displayed a similarly poor correlation for the air phase volume changes. The same was noted for specimen R1.

Specimens R2 and T2 both exhibited very good correlations of near identical magnitude. The gradients obtained were 0.69 and 0.72 respectively and the coefficients of correlation were 0.84 and 0.83 respectviely. These coefficients of correlation were well in excess of those required for 1% significance.

(c) Summarising Remarks

1. The 100% kaolinite specimen (T1) exhibited the worst correlation for the water volume change, and the 90% kaolinite + 10% bentonite specimen (R1), the worst correlation for the total volume change. The gradients and correlative coefficients for the two specimens were 0.06 and 0.08, 0.046 and 0.05 respectively.

2. The predicted volume changes were consistently greater than the measured ones for both the total and water volumes.

3. The correlative coefficients for water volume changes in the 76mm specimens were greater than those observed with the 101mm specimens. The former exceeded the critical value for 1% significance whereas no such behaviour was observed with the total volume changes.

4. The overall magnitude of water volume change increased with increasing plasticity whereas no such relationship was observed with the total volume change behaviour.

5. The reliability of the total volume change predictions increased with increasing plasticity. Three of the four specimens exhibited best fit line gradients of between 0.52 and 0.91. Although these values are far short of an ideal value of 1, the corresponding correlative coefficients exceeded the critical value for 5% significance which is considered as at least partly confirming the observed behaviour.

6. The water volume change - plasticity relationship was not consistent between both cell types (specimen sizes); the 105mm specimen predictions improved with increasing plasticity, whereas the 76mm specimen predictions exhibited the opposite behaviour.

7. The results predominantly indicate that the reliability of volume change predictions increases with increasing plasticity. This contradicts the behaviour noted during the null testing programme where reliability deteriorated with increasing plasticity.

7.5.3 Regression to Determine the Best Fit Line Assuming Both Variables Subject to Error

(a) Introduction

The previous approach was suitable in cases where the data correlated well (such as with the soil structure volume changes for specimen T2); the reason for this is that when the measured values are true, then the predicted values (which are based upon them) will also be correct.

Thus, the best fit line, based upon one variable subject to error will probably be satisfactory in such instances. However, where the measured volume changes are subject to error, and the data plots exhibit scatter, then the resulting predictions will also be less consistent. In such instances, the best fit line must take into account that both variables are subject to error.

(b) Theory

This method determines the best fit line through a set of data points assuming the least perpendicular distances between the correlated line and data points (i.e. both variables subject to error). Because this type of problem is not commonly encountered, then neither is this method, however it is recognised as the standard solution (Pedoe, 1967). Therefore, the slope of the best fit line may be determined from :

$$\tan 2\alpha = \frac{2(\Sigma xy - N\bar{x},\bar{y})}{(\Sigma x^2 - N\bar{x}^2)-(\Sigma y^2 - N\bar{y}^2)} \qquad (7.4)$$

where

α = anticlockwise between horizontal and the line being derived

The parameters for the best fit line are then calculated from the following :

$$\text{slope } (m) = \frac{-1}{\tan \alpha} \qquad (7.5)$$

$$y \text{ intercept } (C) = \bar{y} + \frac{\bar{x}}{\tan \alpha} \qquad (7.6)$$

Unfortunately, an indication of the degree of correlation is not readily obtainable for this type of problem, however, the best fit line does give a better indication of the underlying trend in the data.

The line may be assessed by examining (i) the gradient $(\frac{y}{x})$, which should equal (1) , (ii) the y intercept which sould equal (0) and (iii) to some extent, the average x and y values which should equal each other.

(c) Results

Soil structure (Figures 7.6-7.9, Table 7.9)

Specimen R1 exhibited the worse correlation between measured and predicted volume changes with a gradient of 3.417. In addition, the y intercept deviated unacceptably to -0.633%. However, the average x and y values were quite close (0.252 and 0.177 respectively)to the 45^{o} line.

This poor correlation, confirmed that obtained from the application of the previous method to this specimen. Examination of the plotted data (Fig. 7.7) indicates two groups of points (one located either side of the 45^{o} line).

The best fit lines through the upper and lower group of points exhibit gradients of 0.976 and 0.801 respectively and intercepts of +0.38 and -0.4 . Clearly it is not statistically permissible to take the average of these values, however the evidence does indicate that the data is more evenly spread around the 45^{o} line passing through the origin, than the best fit correlation would suggest.

The remaining specimens (R2, T1 and T2), exhibited very consistent best fit lines. The gradients were all in excess of 1 (1.23, 1.343 and 1.06 respectively), which indicated that the predicted volume changes were less than the corresponding measured ones. The average x and y values were very similar in magnitude and plotted very close to the 45^{o} line.

The results (table 7.12) indicate that the total volume change failed to exhibit a definite relationship with the specimen plasticity. The best fit line gradient tended to unity (i.e. predictions were more accurate) with increasing specimen plasticity; this behaviour was more apparent when considering each apparatus (hence specimen size) separately - table 7.12.

Water Volume Change (Figs. 7.10-7.13, Table 7.9)

Specimen T1 exhibited the worse correlation between predicted and measured values. The gradient and y intercept of 4.343 and -0.246%

respectively were unacceptably high, although the average x and y values were very close to each other (0.074 and 0.076).

This poor correlation is consistent with that obtained using the previous method which confirms the questionable nature of this particular result.

The remainder of the specimens exhibited much better correlation between the measured and predicted values; all gradients were greater than 1 (measured values greater than the predicted values), however their overall values were slightly greater (i.e. more in error) than for the soil structure volume changes.

The intercepts were quite large in all instances. (R1 : -0.155 , R2 : -0.327 and T2 : -0.099). However, the average x and y values were again very similar in magnitude (thus lying on the 45^{o} line).

The water volume changes generally increased with increasing specimen plasticity. This was more evident by separately considering the results from each equipment type (hence specimen size) - table 7.12.
The best fit line gradients from each equipment type were not consistent; the 102MM (triaxial cell) specimens results indicated that the gradient tended to unity with increasing plasticity wheras the 76MM (Rowe cell) specimensindicated the opposite behaviour.

Air Volume Change (Figs. 7.14-7.17, Table 7.9)

As previously noted, the air phase volume changes were calculated as the difference between those of the soil structure and water phases; the correlated air volume change lines therefore reflected those separately determined for the solid and water phases.

The most erroneous best fit line (i.e. with the greatest gradient) was obtained primarily from specimen R1 and secondly, specimen T1;

the line gradients were intermediate between those of the solid and water phases - this presumably being due to the averaging effect obtained by combining two data sets of varying quality.

The y intercepts varied considerably, with specimen R1 exhibiting the worst values (-1.014%). Surprisingly specimen T2 (the best data source) also exhibited a large y intercept value of 0.1% .

The average x and y values were again very consistent.

(d) Summarising Remarks

1. The best fit line gradients for the total and water volume changes tend to unity (i.e. the value of measured and predicted volume changes converged) when considering both variables as subject to error.
2. Unlike the previous section, the predicted volume changes were less than the measured values (gradient consistently greater than one).
3. The relative success of the volume change predictions between equipment types remained unchanged upon considering both variables as subject to error.
4. The average measured and predicted volume changes were consistently similar in magnitude (7.18), giving the impression of accurate volume change predictions.
   In practice, the measured and predicted values were more distant from one another, thus the average values can only be employed as a general indicator of volume change behaviour.
5. The relationships between volume change (total and water) and plasticity remained unchanged after considering both variables as subject to error.

7,5.4 Discussion

Two of the specimens (R1 and T1) exhibited particularly poor correlation between their associated measured and predicted volume changes (for total and water volume respectively).

In view of this, and the mediocre correlations obtained in some other cases, it was decided that an attempt be made to isolate and quantify any influences that might adversely affect the results.

The potential influences may have included (a) hysteresis effects (b) apparatus characteristics and (c) procedural factors, and these are separately detailed below :

(a) Hysteretic Effects

Although the stress changes were designed to ensure constantly decreasing suction and total stress state variables, the specimens always underwent a decrease in total volume following the decrease of air pressure. (Refer Table 7.5). Evidently, the increasing influence of the total stress state variable $(\sigma-u_a)$ was greater than that of the decreasing suction (u_a-u_w) stress state variable. This reversal in volume change almost certainly led to the introduction of hysteretic effects, which in turn, adversely affected the correlation between measured and predicted volume changes.

In order to be able to quantitatively assess the influence of hysteresis, it was therefore necessary that a method be devised to compensate the total volume changes for the anticipated effects.

This was achieved by assuming that the predicted volume change associated with a decrease in air pressure, equalled the measured value. It is recognised that this had the automatic effect of increasing the correlation coefficient and improving the best fit line equation parameters;however,this procedure at least produces some indication of hysteresis effects.

Correlations with One Variable Subject to Error (Table 7.11)

All the soil structure gradients increased considerably (with the exception of the already highest value T2) after allowing for hysteretic effects.

In addition, most y intercept values were halved in magnitude, and the coefficients of correlation for specimens R2 and T1 climbed above the critical value for 1% significance (0.66).

Notably, the previously poor, low gradient and correlation coefficient of specimen R1 rose from 0.046 and 0.05 respectively to 0.32 and 0.36 respectively. This is a marked improvement which indicated that hysteresis effects probably accounted for a large measure of data scatter in that specimen.

The application of a correction for hysteresis to the water volume changes did not generally improve the best fit line gradients; this suggests that some other factor was to blame for their low values.

The correction increased all correlation coefficients, such that specimens R1, R2 and T2 exhibited values in excess of the critical value for 1% significance.

The most notable improvement was recorded for specimen T1, whose gradient and correlation coefficient increased from 0.06 and 0.08 respectively to 0.43 and 0.4 respectively; this modified behaviour was then consistent with that of the other specimens.

The air phase correlations were not dramatically improved by correcting for hysteresis effects. The one exception was for specimen T1 where the best fit line gradient and coefficient of correlation increased from 0.14 and 0.16 respectively to 0.41 and 0.46 respectviely.

Correlations with Both Variables Subject to Error (table 7.12)

The soil structure gradients and y intercepts all improved after application of the hysteresis correction. The gradients for R2, T1 and T2 were all then very close to 1 and the intercepts negligible. The greatest improvement occurred for specimen R1, whose gradient and y intercept improved from 3.417 and -0.683% respectviely to 1.368 and -0.063% respectviely.

Although these new parameters for specimen R1 were not perfect (i.e. $\frac{y}{x} = 1$, and $y_{int} = 0$), they were a vast improvement upon the initial values, and indicated that the specimen would have behaved consistently with the others if the effects of hysteresis had not been so pronounced.

The water volume change correlation generally exhibited little improvement following the correction for hysteresis - with the exception

of specimen T1. The improvement in this case was more dramatic than that exhibited for specimen R1 soil structure; the gradient and y intercept improved from 4.348 and -0.246% respectively to 0.943 and 0.167% respectively.

The average x and y (predicted and measured) values exhibited a closer agreementfollowing the hysteresis correction; in fact, most of the above pairs of results for soil structure and water volume changes then indicated a unique behaviour (i.e. they all plotted on a 45^{o} line passing through the origin). The only exception occurred for the air phase volume changes, when the measured and predicted values were -0.041% and -0.082% respectively.

(b) Apparatus Characteristics

In addition to the adverse affects of a reversal in total volume change upon uniqueness of the constitutive surface, the equipment is also considered as having contributed to an inconsistency in measurements on two counts :

(i) The one dimensional test cells are incapable of accurately monitoring isotropic shrinkage since the specimen will tend to come away from the cell walls, thus preventing a true volume measurement to be made.

Even where the specimen does not actually part from the cell wall, the adhesion between the clay and the smooth confining walls will prevent a representative volume change, thus further hampering accurate measurements. Data will therefore tend to be under-recorded.

(ii) friction acting between the specimen sides and the cell wall would reduce the amount of expansion or shrinkage by 'gripping' the specimen around its circumference. In consequence, the specimen would probably bulge or contract at its centre following volume change.

In practice friction was offset as much as possible by coating the inner cell wall with non-reactive petroleum jelly (Vasoline).

This countermeasure appears to have worked since the specimens displayed no evidence of a central volume change.

In addition, any volume changes that may have occurred are not considered to have unduly influenced comparisons of data since :

Firstly, the predicted swell values are based upon experimentally derived moduli, hence both predicted and measured swell will be subject to the same friction influence and

Secondly, the percentage of side wall area to total volume is very similar for both cell types, hence both are considered to have been influenced by friction to the same degree.

Nevertheless, sidewall friction will reduce the volume change moduli measured from one dimensional tests, and this should be taken into account when attempting to correlate such results with field behaviour.

(c) Procedural Factors

These included errors in the testing procedure or other unknown experimental factors, which may have led to unwanted volume changes, thereby reducing the degree of correspondence between measured and predicted values.

An examination of the raw data, indicated that specimen R1 exhibited inconsistent total volume change in test 2 and inconsistent total and water volume changes in tests 5 and 7.

All inconsistencies involved an unexplained volume increase of the respective phases; the most pronounced volume increase occurred for test UR0105, where the total and water volumes exhibited a sharp increase after 11800 minutes. Examination of the stress component record gave no indication as to the precise cause of this. A similar but less pronounced occurrence was noted for test 7.

It is apparent that such an apparently uncontrolled jump in the saturation level and total volume would decrease the volume change behaviour. These volume changes were totally out of character with the majority of results, and coincided with known overnight variations of the pressure supply. In consequence, they were adjusted accordingly for the purpose of this analysis

These modified values were then used throughout the analysis since they were considered as giving a better indication of the volume change trend.

The variation in the water volume change predictions of specimen T1 could not be readily explained, and the volume change history as illustrated in Figure 7.4 exhibited no outstanding irregularities.

Procedural factors are not considered to be of significance in this case.

7.6 Summarising remarks

1. The aim of the volume tests was to validate the general volume change theory in unsaturated soils for use with expansive type unsaturated clays. The tests involved subjecting the specimens to a cyclic variation of the component stresses (σ, u_a and u_w) and monitoring the resulting total and water volume changes. Air volume changes were taken as the difference between the total and water volume changes.

   Stress-related volume change moduli were then calculated upon the basis of the above volume changes and inserted into the general volume change equation for the purpose of making predictions.

2. The theory was assessed by comparing the predicted volume changes of all phases with the measured values. This was achieved visually, by plotting the measured against the predicted values and quantitatively by regression analysis, involving the determination of the best fit line through the data. The volume change relations were considered validated if the gradient, y intercept and correlation coefficient equalled 1 , 0 and 1 respectively. Since the measured volume changes were subject to several sources of error, then it follows that the moduli-based predictions were also erroneous.

   Regression procedures were therefore chosen to take into account both one and two variables subject to error.

3. The initial regression analysis determined the best fit line assuming one variable as subject to error. The gradient of the lines so determined were consistently less than 1 (i.e. predicted greater than measured values). In addition, the majority of specimens exhibited a correlation coefficient for the soil structure and water volume change in excess of the critical value for 5% significance; this indicated the high likelihood of a relationship.

4. The second regression analysis determined the best fit line assuming both variables subject to error. Although the output was limited to gradient, y intercept and average values of x and y, it was considered to provide a better indication of the underlying trend in data.

   All the gradients exceeded 1 (i.e. predicted > measured value), however, in general, they exhibited an improved behaviour (i.e. closer to unity) than for the previous method.

   The average x and y values were examined with a view to using them as an indicator of the prediction reliability for each specimen. However, they were found to be too general for this purpose. Nevertheless, they did display an excellent correlation (Figure 7.18) with a gradient of 1.09 and a coefficient of correlation of 0.99; this evidence indicates that on average the volume change equations work well with most of the soils.

5. Two of the specimens exhibited poor correlations for two different phases : R1:soil structure and T1:water phase. Potential adverse influences upon the results were discussed such as side wall friction within the cell, which reduced the readings, and procedural factors, which allowed specimen R1 to freely imbibe unwanted water.
   Of greater importance were the volume change reversals(expansion) following each decrease in air pressure; these were considered as introducing hysteresis effects into the results.
   Although it was not possible to accurately quantify these effects, an attempt was made to assess their influence upon the phase volume changes;
   this involved assuming that the predicted values equalled the measured values, and then repeating the regression analyses.
   A dramatic improvement was subsequently noted in the correlations for the total volume changes in specimen R1 and the water volume changes in specimen T1. However, considerably less improvement was noted in the other cases.

   In general, the total volume correlations were more susceptible to the hysteresis effects than the water volume change.

6. The observed total volume changes decreased following an increase in saturation and total volume; general behaviour was as follows:

stress component change	change in total volume following an increase in saturation and total volume
$-\Delta\sigma$	increased
$-\Delta u_a$	decreased
$+\Delta u_w$	increased

TABLE 7.1

SUMMARY OF UNIQUENESS TESTS

TEST CODE	DATE ON	STARTING TIME	TEST DURATION (Mins)	SOIL TYPE[1] (%) MONT/KAOL	STRESS CHANGES (PSI)[2] TOTAL (σ)	AIR (U_a)	WATER (U_w)	COMMENTS
UR0101	061285	10:10	15743	10/90	49.99	39.98	9.99	initial
UR0102	171285	9:30	14458	"	-	0.02	5.01	
UR0103	271285	10:58	14306	"	0.02	-5.00	-	
UR0104	070186	9:38	10676	"	-5.00	0.01	0.02	
UR0105	160186	9:13	19031	"	-0.01	0.02	5.03	
UR0106	290186	15:05	11152	"	0.03	-5.01	-0.02	
UR0107	060286	9:10	15958	"	-5.05	-0.01	-0.03	
UR0201	180286	10:55	11395	30/70	49.96	39.95	10.02	initial
UR0202	250286	9:08	11484	"	0.06	0.05	5.05	
UR0203	060386	9:15	12940	"	-0.02	5.00	-0.06	
UR0204	150386	9:02	15958	"	-5.00	-	-	
UR0205	260386	11:18	13169	"	0.01	-	4.99	
UR0206	040486	15:00	14046	"	-	-5.01	-	
UR0207	140486	9:45	17279	"	-4.99	0.03	0.02	
UT0101	061285	10:54	15716	0/100	59.39	34.91	5.55	initial
UT0102	171285	9:15	14456	"	-0.04	-0.07	4.87	
UT0103	271285	11:04	15725	"	-2.01	-4.86	0.07	
UT0104	070186	9:45	12904	"	-17.76	-0.76	-1.21	incorrect
UT0105	160186	9:08	17611	"	13.15	0.77	6.09	incorrect
UT0106	290186	15:11	11134	"	-	-4.88	-0.02	
UT0107	060286	9:15	15963	"	-18.15	-0.85	-1.08	incorrect
UT0201	180286	10:45	11391	20/80	44.51	34.31	4.84	initial
UT0202	260286	9:14	11491	"	0.0	0.06	4.49	
UT0203	060386	9:20	12918	"	0.04	4.97	-0.05	
UT0204	150386	8:40	15955	"	-4.95	0.02	0.03	
UT0205	260886	11:12	13156	"	-0.04	-0.01	5.01	
UT0206	040486	15:05	14035	"	-	-4.98	0.04	
UT0207	140486	9:32	17223	"	-4.99	-0.02	-	

notes :

1. soil type denotes relative proportions of constituent minerals :
   mont : montmorillonite, kaol : kaolinite

2. stress changes listed in psi units since equipment was incremented
   in these

3. test codes; eg UR0103: U:uniqueness test; R:76mm diameter specimen
   (T: 102mm diameter specimens); 01 : specimen No. 01; 03 : test No. 03.

TABLE 7.2

PROPOSED STRESS CHANGES FOR THE UNIQUENESS TESTS

	INITIAL CONDITIONS (PSI)						FINAL CONDITIONS (PSI)						STRESS CHANGES (PS		
TEST CODE	TOTAL PRESSURE	AIR PRESSURE	WATER PRESSURE	$(\sigma-U_w)$	$(\sigma-U_a)$	(U_a-U_w)	TOTAL PRESSURE	AIR PRESSURE	WATER PRESSURE	$(\sigma-U_w)$	$(\sigma-U_w)$	(U_a-U_w)	σ	U_a	U_w
UR0101	0	0	0	0	0	0	50	40	10	40	10	30	50	40	10
UR0102	50	40	10	40	10	30	50	40	15	35	10	25	0	0	+5
UR0103	50	40	15	35	10	25	50	35	15	35	15	20	0	-5	0
UR0104	50	35	15	35	15	20	45	35	15	30	10	20	-5	0	0
UR0105	45	35	15	30	10	20	45	35	20	25	10	15	0	0	+5
UR0106	45	35	20	25	10	15	45	30	20	25	15	10	0	-5	0
UR0107	45	30	20	25	15	10	40	30	20	20	10	10	-5	0	0
UR0201	0	0	0	0	0	0	50	40	10	40	10	30	50	40	10
UR0202	50	40	10	40	10	30	50	40	15	35	10	25	0	0	+5
UR0203	50	40	15	35	10	25	50	35	15	35	15	20	0	-5	0
UR0204	50	35	15	35	15	20	45	35	15	30	10	20	-5	0	0
UR0205	45	35	15	30	10	20	45	35	20	25	10	15	0	0	+5
UR0206	45	35	20	25	10	15	45	30	20	25	15	10	0	-5	0
UR0207	45	30	20	25	15	10	40	30	20	20	10	10	-5	0	0
UT0101	0	0	0	0	0	0	45	35	5	40	10	30	45	35	5
UT0102	45	35	5	40	10	30	45	35	10	35	10	25	0	0	-5
UT0103	45	35	10	35	10	25	45	30	10	35	15	20	0	-5	0
UT0104	45	30	10	35	15	20	40	30	10	30	10	20	-5	0	0
UT0105	40	30	10	30	10	20	40	30	15	25	10	15	0	0	+5
UT0106	40	30	15	25	10	15	40	25	15	25	15	10	0	-5	0
UT0107	40	25	15	25	15	10	35	25	15	20	10	10	-5	0	0
UT0201	0	0	0	0	0	0	45	35	5	40	10	30	45	35	5
UT0202	45	35	5	40	10	30	45	35	10	35	10	25	0	0	+5
UT0203	45	35	10	35	10	25	45	30	10	35	15	20	0	-5	0
UT0204	45	30	10	35	15	20	40	30	10	30	10	20	-5	0	0
UT0205	40	30	10	30	10	20	40	30	15	25	10	15	0	0	+5
UT0206	40	30	15	25	10	15	40	25	15	25	15	10	0	-5	0
UT0207	40	25	15	25	15	10	35	25	15	20	10	10	-5	0	0

TABLE 7.3

ACTUAL STRESS CHANGES DURING THE UNIQUENESS TESTS

	INITIAL CONDITIONS (PSI)						FINAL CONDITIONS (PSI)						STRESS CHANGES (PSI)		
TEST CODE	TOTAL PRESSURE	AIR PRESSURE	WATER PRESSURE	$(\sigma-U_a)$	$(\sigma-U_w)$	(U_a-U_w)	TOTAL PRESSURE	AIR PRESSURE	WATER PRESSURE	$(\sigma-U_a)$	$(\sigma-U_w)$	(U_a-U_w)	σ	U_a	U_w
UR0101	0	0	0	0	0	0	49.99	39.98	9.00	10.01	40.00	29.99	49.99	39.98	9.99
UR0102	49.99	39.98	9.99	10.01	40.00	29.99	49.99	40.0	15.0	9.99	34.99	25.00	0	+ 0.02	+5.01
UR0103	49.99	40.00	15.00	9.99	34.99	25.00	50.01	35.0	15.0	15.01	35.01	20.00	+0.02	-5.00	0
UR0104	50.01	35.00	15.00	15.01	35.01	20.00	45.01	35.01	15.02	10.00	29.99	19.99	-5.00	+0.01	+0.02
UR0105	45.01	35.01	15.02	10.00	29.99	19.99	45.0	35.03	20.05	9.97	25.06	14.98	-0.01	+0.02	+5.03
UR0106	45.00	35.03	20.09	9.97	25.05	14.98	45.03	30.02	20.03	15.01	25.00	9.99	+0.03	-5.01	-0.02
UR0107	45.03	30.02	20.03	15.01	25.00	9.99	39.98	20.01	20.00	9.97	19.98	10.01	-5.05	-0.01	-0.03
UR0201	0	0	0	0	0	0	49.96	39.95	10.02	10.01	39.94	29.93	49.96	39.95	10.02
UR0202	49.96	39.95	10.02	10.01	39.94	29.93	50.02	40.0	15.07	10.02	34.95	24.93	+0.06	+0.05	+5.05
UR0203	50.02	40.00	15.07	10.02	34.95	24.93	50.0	35.0	15.01	15.00	34.99	19.99	-0.02	+5.00	-0.06
UR0204	50.00	35.00	15.01	15.00	34.99	19.99	45.0	35.0	15.01	10.00	29.99	19.99	-5.00	0	0
UR0205	45.00	35.00	15.01	10.00	29.99	19.99	45.01	35.0	20.0	10.01	25.01	15.00	+0.01	0	+4.99
UR0206	45.01	35.00	20.00	10.01	25.01	15.00	45.01	29.99	20.0	15.02	25.01	9.99	0	-5.01	0
UR0207	45.01	29.99	20.00	18.02	25.01	9.99	40.02	30.02	20.02	10.00	20.00	10.00	-4.99	+0.03	+0.02
UT0101	0	0	0	0	0	0	44.51	34.29	4.28	10.22	40.23	30.01			
UT0102	44.51	34.29	4.28	10.22	40.23	30.01	44.49	34.22	9.28	10.27	35.23	24.90	-0.02	-0.07	+4.98
UT0103	44.49	34.22	9.26	10.27	25.23	24.96	42.99	29.30	9.33	13.69	33.66	19.97	-1.5	-4.02	+0.07
UT0104	42.99	29.30	9.33	13.69	33.66	19.97	39.58	29.26	9.28	10.32	30.30	19.98	-3.11	-0.04	-0.05
UT0105	39.58	29.26	9.28	10.32	30.30	19.98	39.57	29.30	14.32	10.27	25.25	14.98	-0.01	+0.04	+5.04
UT0106	39.57	29.30	14.32	10.27	25.25	14.98	39.57	24.32	14.30	15.25	25.27	10.02	0	-4.98	-0.02
UT0107	39.57	24.32	14.30	15.25	25.27	10.02	34.58	24.3	14.27	10.28	20.31	10.03	-4.99	-0.02	-0.03
UT0201	0	0	0	0	0	0	44.51	34.81	4.84	10.20	39.67	29.47	44.51	34.31	4.34
UT0202	44.51	34.31	4.84	10.20	39.67	29.47	44.51	34.25	9.33	10.26	35.18	24.92	0	-0.06	+4.49
UT0203	44.51	34.25	9.33	10.26	35.18	24.92	44.55	29.28	9.28	15.27	35.27	20.00	+0.04	+4.97	-0.05
UT0204	44.55	29.28	9.28	15.27	35.27	20.00	39.60	29.3	9.31	10.30	30.29	19.99	-4.95	+0.02	+0.03
UT0205	39.60	29.30	9.31	10.30	30.29	19.99	39.56	29.29	14.32	10.27	25.24	14.97	-0.04	-0.01	+5.01
UT0206	39.56	29.29	14.32	10.27	25.24	14.97	39.56	24.31	14.36	15.25	25.20	9.95	0	-4.98	+0.04
UT0207	39.56	24.31	14.36	15.25	25.20	9.95	34.57	24.29	14.36	10.28	20.21	9.93	-4.99	-0.02	0

TABLE 7.4(a)

INITIAL VOLUME-WEIGHT RELATIONSHIPS
FOR THE 76MM (ROWE) SPECIMENS

TEST	THICKNESS (mm)	TOTAL VOLUME (mm^3)	SOLIDS VOLUME (mm^3)	AIR VOLUME (mm^3)	WATER CONTENT (%)	VOIDS RATIO	DRY DENSITY (Kg/m^3)	SATURATION (%)
0101	26.1	118448	62679	9029	28.9	.89	1365	83.81
0102	25.34	114999	62679	4299	29.69	.835	1406	91.78
0103	25.47	115589	62679	4656	29.84	.844	1399	91.2
0104	25.46	115544	62679	4332	30.01	.843	1400	91.81
0105	25.48	115634	62679	4598	29.9	.845	1399	91.32
0106	25.57	116043	62679	2898	31.2	.851	1394	94.57
0107	25.55	115952	62679	1593	31.95	.85	1395	97.01
0201	26.01	118040	60366	12502	29.8	.955	1284	78.32
0202	25.87	117404	60366	4409	34.72	.945	1291	92.27
0203	25.87	117404	60366	3454	35.35	.945	1291	93.94
0204	25.82	117177	60366	-1683	38.59	.941	1294	102.
0205	25.86	117359	60366	-1667	38.7	.944	1292	102.93
0206	25.92	117631	60366	-3675	40.2	.949	1289	106.42
0207	25.89	117495	60366	-5731	41.47	.946	1290	110.

TABLE 7.4(b)

INITIAL VOLUME-WEIGHT RELATIONSHIPS
FOR THE 100MM (TRIAXIAL) SPECIMENS

TEST	THICKNESS (mm)	TOTAL VOLUME (mm^3)	SOLIDS VOLUME (mm^3)	AIR VOLUME (mm^3)	WATER CONTENT (%)	VOIDS RATIO	DRY DENSITY (Kg/m^3)	SATURATION (%)
0101	31.46	253085	132171	19675	29.28	.915	1366	83.73
0102	30.8	247775	132171	14112	29.35	.875	1395	87.79
0103	30.8	247775	132171	13820	29.44	.875	1395	88.05
0104	30.79	247695	132171	12770	29.72	.874	1396	88.95
0105	30.78	247614	132171	12972	29.64	.873	1396	88.76
0106	30.8	247775	132171	12027	29.96	.875	1395	89.6
0107	30.8	247775	132171	11154	30.21	.875	1395	90.35
0201	30.38	244397	123016	28579	29.63	.987	1282	76.46
0202	29.5	237317	123016	15132	31.66	.929	1320	86.76
0203	29.49	237237	123016	14621	31.8	.928	1320	87.2
0204	29.47	237076	123016	12067	32.56	.927	1321	89.42
0205	29.46	236995	123016	12319	32.46	.927	1322	89.19
0206	29.45	236915	123016	8421	33.68	.926	1322	92.61
0207	29.43	236754	123016	3095	35.33	.925	1323	97.28

TABLE 7.5

STRESS CHANGES AND CORRESPONDING EQUILIBRIUM VOLUME CHANGES

TEST	ELAPSED TIME (Mins)	STRESS COMPONENT * CHANGES (PSI) $\Delta\sigma$	ΔU_a	ΔU_w	PERCENT VOLUME CHANGE TOTAL	AIR	WATER	
UR0101	15000	40.99	39.98	9.99	-2.930	-4.012	1.082	**
UR0102	"	0	0	5.01	0.448	0.068	0.38	
UR0103	"	0	-5.00	0	-0.115	-0.78	0.665	
UR0104	"	-5.00	0	0	0.096	-0.064	0.1596	
UR0105	"	0	0	5.03	0.358	-0.437	0.793	
UR0106	"	0	-5.01	0	-0.069	-0.95	0.881	
UR0107	"	-5.05	0	0	0.682	0.672	0.01	
UR0201	"	49.96	39.95	10.02	-0.540	-6.859	6.319	**
UR0202	"	0	0	5.05	-0.015	-0.545	0.53	
UR0203	"	0	-5.00	0	-0.204	-0.694	0.49	
UR0204	"	-5.00	0	0	0.196	-0.114	0.31	
UR0205	"	0	0	4.99	0.188	-0.962	1.15	
UR0206	"	0	-5.01	0	-0.099	-1.439	1.34	
UR0207	"	-4.99	0	0	0.638	0.278	0.36	
UT0101	"	44.51	34.29	4.28	-2.110	-2.210	0.1	**
UT0102	"	0	0	+4.98	0.003	-0.177	0.18	
UT0103	"	0	-4.92	0	-0.028	-0.128	0.1	
UT0104	"	-3.11	0	0	0.045	0.085	0.02	
UT0105	"	0	0	+5.04	0.067	0.037	0.03	
UT0106	"	0	-4.98	0	-0.0064	-0.364	0.13	
UT0107	"	-4.99	0	0	0.15	0.02	0.13	
UT0201	"	44.51	34.31	4.84	-2.890	-5.496	2.606	**
UT0202	"	0	0	4.49	-0.013	-0.343	0.33	
UT0203	"	0	-4.97	0	-0.072	-1.122	1.05	
UT0204	"	-4.95	0	0	0.046	0.006	0.04	
UT0205	"	0	0	5.01	-0.017	-1.617	1.60	
UT0206	"	0	-4.98	0	-0.069	-1.889	1.82	
UT0807	"	-4.99	0	0	0.072	-0.008	0.08	

* stress component changes quoted in p.s.i. units since original experimentation was conducted using equipment calibrated in these units.

** represent the volume changes recorded during the conditioning phase

TABLE 7.6

SUMMARY OF VOLUME CHANGE MODULI WITH RESPECT TO SOIL, AIR , AND WATER PHASES

TEST	SOIL STRUCTURE COMPRES. $\Delta(\sigma-U_w)$	$\Delta(\sigma-U_a)$	$\Delta(U_a-U_w)$	COMPRESSIBILITY W.R.T AIR PHASE $\Delta(\sigma-U_w)$	$\Delta(\sigma-U_a)$	$\Delta(U_a-U_w)$	COMPRESSIBILITY W.R.T WATER PHASE $\Delta(\sigma-U_w)$	$\Delta(\sigma-U_a)$	$\Delta(U_a-U_w)$
UR0102	-0.089	*	-0.089	-0.014	*	-0.014	-0.076	*	-0.076
UR0103	*	-0.023	+0.023	*	-0.156	+0.156	*	+0.133	-0.133
UR0104	-0.0192	-0.0192	*	+.0128	+.0128	*	-0.032	-0.032	*
UR0105	-0.071	*	-0.071	+.087	*	+.087	-0.158	*	-0.158
UR0106	*	-0.0188	+0.0188	*	-0.189	+0.189	*	+0.176	-0.176
UR0107	-0.135	-0.132	*	-0.133	-0.133	*	-0.002	-0.002	*
UR0202	+0.0029	*	+0.0020	+0.108	*	+0.108	-0.105	*	-0.105
UR0203	*	-0.041	+0.041	*	-0.139	+0.139	*	+0.098	-0.098
UR0204	-0.0392	-0.0392	*	+0.023	+0.023	*	-0.062	-0.062	*
UR0205	-0.0377	*	-0.0377	+0.193	*	+0.193	-0.23	*	-0.23
UR0206	*	-0.0198	+0.0198	*	-0.287	+0.287	*	+0.267	-0.267
UR0207	-0.128	-0.128	*	-0.056	-0.056	*	-0.072	-0.072	*
UT0102	-0.0006	*	-0.0006	+0.036	*	+0.036	-0.036	*	-0.036
UT0103	*	-0.0056	+0.0056	*	-0.026	+0.026	*	+0.02	-0.02
UT0104	- .015	- .015	*	-0.008	-0.008	*	-0.0064	-0.0064	*
UT0105	-0.0134	*	-0.0134	-0.0073	*	-0.0073	-0.006	*	-0.006
UT0106	*	-0.0013	+0.0013	*	-0.027	+0.027	*	+0.026	-0.026
UT0107	-0.03	-0.03	*	-0.004	-0.004	*	-0.026	-0.026	*
UT0202	+0.0029		+0.0029	+0.076		+0.076	-0.073	*	-0.073
UT0203	*	-0.015	+0.015		-0.226	+0.226	*	+0.211	-0.211
UT0204	-0.0093	-0.0093	*	-0.0012	-0.0012		-0.0081	-0.0081	*
UT0205	+0.0034	*	+0.0034	+0.323		+0.323	-0.32	*	-0.32
UT0206	*	-0.014	+0.014		-0.379	+0.379	*	+0.365	-0.366
UT0207	-0.014	-0.014	*	+1.603+			-0.016	-0.016	*

TABLE 7.7

COMPARISON OF PREDICTED AND MEASURED VOLUME CHANGES

COMPRESSIBILITIES FROM TESTS	STRESS CHANGE (PSI)	SOIL STRUCTURE VOLUME CHANGE (%)		AIR PHASE VOLUME CHANGE (%)		WATER PHASE VOLUME CHANGE (%)	
		MEASURED	PREDICTED	MEASURED	PREDICTED	MEASURED	PREDICTED
UR0102-UR0103	$\Delta\sigma$ = -5	0.096	0.56	-0.064	0.85	0.1596	-0.29
UR0103-UR0104	ΔU_w = -5	0.448 0.356	-0.019	0.068 -0.437	-0.72	0.38	0.83
UR0104-UR0105	ΔU_a = -5	-0.115 -0.069	0.250	-0.78 -0.95	0.37	0.793 0.665	0.63
UR0105-UR0106	$\Delta\sigma$ = -5	0.006 0.682	0.424	-0.084 0.672	1.39	0.881 0.1896	-0.09
UR0106-UR0107	ΔU_w = 5	0.356	0.606	-0.437	-0.28	0.01 0.793	0.89
UR0102-UR0104	ΔU_a = -5	-0.115	0.349	-0.78	0	0.665	0.22
UR0103-UR0105	$\Delta\sigma$ = -5	0.096	0.470	-0.064	1.21	0.1596	0.12
UR0104-UR0106	ΔU_w = 5	0.356	0.027	-0.437	-0.89	0.793	1.05
UR0105-UR0107	ΔU_a = -5	-0.069	-0.32	-0.95	-0.23	0.881	0.78
UR0202-UR0203	$\Delta\sigma$ = -5	0.196	0.1905	-0.114	0.15	0.31	0.03
UR0203-UR0204	ΔU_w = +5	-0.015 0.188	-0.009	-0.445 -0.962	-0.81	0.83 1.15	+0.8
UR0204-UR0205	ΔU_a = -5	-0.204 -0.099	-0.0075	-0.694 -1.439	-0.85	0.49 1.34	0.84
UR0205-UR0206	$\Delta\sigma$ = -5	0.196 0.638	0.288	-0.114 0.278	+0.47	0.31 0.36	-0.18
UR0206-UR0207	ΔU_w = 5	0.138	0.541	-0.962	-1.160	1.15	1.69
UR0202-UR0204	ΔU_a = -5	-0.204	-0.213	-0.694	-0.43	0.49	0.21
UR0203-UR0205	$\Delta\sigma$ = -5	0.196	0.394	-0.114	-0.27	0.31	0.66
UR0204-UR0206	ΔU_w = +5	0.168	0.097	-0.962	-1.55	1.15	1.64
UR0205-UR0207	ΔU_a = -5	-0.099	-0.452	-1.439	-1.24	1.34	0.79
UT0102-UT0103	$\Delta\sigma$ = -5	0.045	0.0192	0.025	-0.03	0.02	0.05
UT0103-UT0104	ΔU_w = 5	0.003 0.067	0.047	-0.177 0.037	-0.17	0.18 0.030	0.13
UT0104-UT0105	ΔU_a = -5	-0.028 -0.0064	-0.008	-0.128 -0.1364	0	0.1 0.13	0.0
UT0105-UT0106	$\Delta\sigma$ = -5	0.045 0.15	0.046	0.025 0.02	0.08	0.02 0.13	+0.08
UT0106-UT0107	ΔU_w = 5	0.067	0.145	0.037	-0.12	0.030	0.26
UT0102-UT0104	ΔU_a = -5	-0.028	-0.071	-0.128	-0.14	0.1	0.15
UT0103-UT0105	$\Delta\sigma$ = -5	0.045	0.0591	0.025	0.06	0.02	-0.04
UT0104-UT0106	ΔU_w = 5	0.067	0.0691	0.037	-0.18	0.030	0.16
UT0105-UT0107	ΔU_a = -5	-0.0064	-0.083	-0.1364	-0.06	0.13	-0.1
UT0202-UT0203	$\Delta\sigma$ = -5	0.046	0.0605	0.006	0.74	0.04	-0.68
UT0203-UT0204	ΔU_w = 5	-0.013 -0.017	-0.0285	-0.343 -1.617	-1.08	0.33 1.6	1.04
UT0204-UT0205	ΔU_a = -5	-0.072 -0.069	-0.064	-1.122 -1.889	-1.6	1.05 1.82	1.55
UT0205-UT0206	$\Delta\sigma$ = -5	0.046 0.072	0.053	0.006 -0.008	0.28	0.04 0.08	-0.23
UT0206-UT0207	ΔU_w = 5	-0.017	0	-1.617	-1.89	1.6	1.91
UT0202-UT0204	ΔU_a = -5	-0.072	-0.12	-1.122	-0.37	1.05	0.33
UT0203-UT0205	$\Delta\sigma$ = -5	0.046	0.058	0.006	-0.48	0.04	0.54
UT0204-UT0205	ΔU_w = 5	-0.017	-0.024	-1.617	-1.91	1.6	1.87
UT0205-UT0207	ΔU_a = -5	-0.069	-0.087	-1.889	-1.62	1.82	1.51

TABLE 7.8

LINEAR REGRESSION TO FIND THE BEST FIT LINES, ONE VARIABLE SUBJECT TO ERROR

	SOIL STRUCTURE			AIR PHASE			WATER PHASE		
	$\frac{Y}{X}$	Y int	r	$\frac{Y}{X}$	Y int	r	$\frac{Y}{X}$	Y int	r
R1	0.046	0.16	0.05	0.26	-0.42	0.45	0.59	0.25	0.82
R2	0.56	0.046	0.64	0.69	-0.25	0.84	0.49	0.41	0.69
T1	0.52	0.02	0.63	0.14	-0.04	0.16	0.06	0.07	0.08
T2	0.91	0.0	0.95	0.72	-0.31	0.83	0.7	0.32	0.32

Key : X = predicted volume changes
Y = measured volume changes
Y/X = gradient
Y int = Y intercept
r = correlation coefficient

Critical 'r' values :
5% significance : 0.49
1% significance : 0.66

TABLE 7.9

LINEAR REGRESSION TO FIND THE BEST FIT LINES, BOTH VARIABLES SUBJECT TO ERROR.

SPECIMEN* NUMBER	GRADIENT (y/x)	Y INTERCEPT (%)	AVERAGE PREDICTED (X) VOLUME CHANGE (%)	AVERAGE MEASURED (Y) VOLUME CHANGE (%)	tanα (α = ANTICLOCKWISE ANGLE FROM X-AXIS)
R1S	3.417	-0.683	0.252	0.177	-0.293
R1A	2.867	-1.014	0.231	-0.352	-0.349
R1W	1.487	-0.155	0.459	0.528	-0.672
R2S	1.230	-0.016	0.092	0.097	-0.813
R2A	1.256	0.073	-0.573	-0.647	-0.796
R2W	1.619	-0.327	0.662	0.744	-0.618
T1S	1.343	0.001	0.026	0.035	-0.745
T1A	1.469	0.048	-0.053	-0.03	-0.681
T1W	4.348	-0.246	0.074	0.076	-0.23
T2S	1.06	0.001	-0.007	-0.006	-0.943
T2A	1.198	0.105	-0.861	-0.926	-0.835
T2W	1.202	-0.099	0.85	0.923	-0.832

* specimen numbering code : R - Rowe cell (76mm dia specimens)
T - Triaxial cell (100mm dia specimens)
S - solid phase
A - air phase
W- water phase

TABLE 7.10

SUMMARY OF SIGN CONVENTIONS

STRESS COMPONENT CHANGE	STRESS STATE VARIABLE		
	$(\sigma-U_w)$	$(\sigma-U_a)$	(U_a-U_w)
$+\Delta\sigma$	+	+	0
$-\Delta\sigma$	-	-	0
$+\Delta U_a$	0	-	+
$-\Delta U_a$	0	+	-
$+\Delta U_w$	-	0	-
$-\Delta U_w$	+	0	+

TABLE 7.11

LINEAR REGRESSION TO FIND THE BEST FIT LINE THROUGH THE VOLUME CHANGE DATA - ONE VARIABLE SUBJECT TO ERROR (ALLOWING FOR HYSTERETIC EFFECTS)

SPECIMEN	SOIL STRUCTURE			AIR PHASE			WATER PHASE		
	$\frac{y}{x}$	Y int	r	$\frac{y}{x}$	Y int	r	$\frac{y}{x}$	Y int	r
R1	0.32	0.11	0.36	0.38	-0.3	0.71	0.62	0.2	0.89
R2	0.71	0.02	0.72	0.69	-0.2	0.88	0.53	0.34	0.77
T1	0.67	0.01	0.63	0.41	-0.01	0.46	0.43	0.03	0.4
T2	0.94	-0.01	0.97	0.75	-0.23	0.87	0.74	0.24	0.86

Key : X = predicted volume changes
Y = measured volum 'changes
Y/X = gradient
Y int = Y intercept of best fit line
r = correlation coefficient

Critical 'r' values :
5 % significance : 0.49
1 % significance : 0.66
(for 12 observations)

TABLE 7.12

LINEAR REGRESSION TO FIND THE BEST FIT LINE THROUGH THE VOLUME CHANGE DATA - BOTH VARIABLES SUBJECT TO ERROR (ALLOWING FOR HYSTERETIC EFFECTS)

SPECIMEN* NUMBER	GRADIENT (y/x)	Y INTERCEPT (%)	AVERAGE PREDICTED (X) VOLUME CHANGE (%)	AVERAGE MEASURED (Y) VOLUME CHANGE (%)	TANα *
R1S	1.368	-0.063	0.175	0.177	-0.731
R1A	2.252	-0.027	-0.145	-0.352	-0.444
R1W	1.479	-0.243	0.521	0.528	-0.676
R2S	1.026	-0.003	0.098	0.097	-0.975
R2A	1.323	0.211	-0.648	-0.647	-0.756
R2W	1.611	-0.455	0.744	0.744	-0.621
T1S	0.903	0.073	0.034	0.035	-1.107
T1A	1.285	0.063	-0.082	-0.041	-0.778
T1W	0.943	0.167	0.088	0.074	-1.06
T2S	1.038	0.001	-0.012	-0.011	-0.963
T2A	1.19	0.193	-0.948	-0.934	-0.84
T12W	1.187	-0.167	0.918	0.923	-0.842

* specimen number code : R - Rowe cell (76mm dia specimens)
T - Triaxial cell (100mm dia specimens)
S - solid phase
A - Air phase
W - Water phase

α = anticlockwise angle taken from X axis

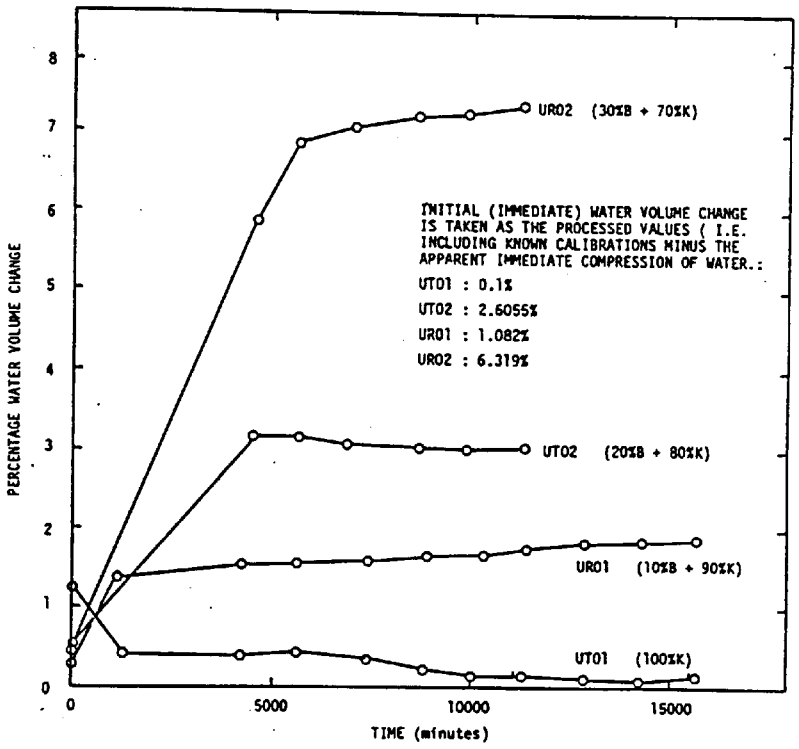

FIGURE 7.1

INITIAL WATER FLOW TO ALL SPECIMENS

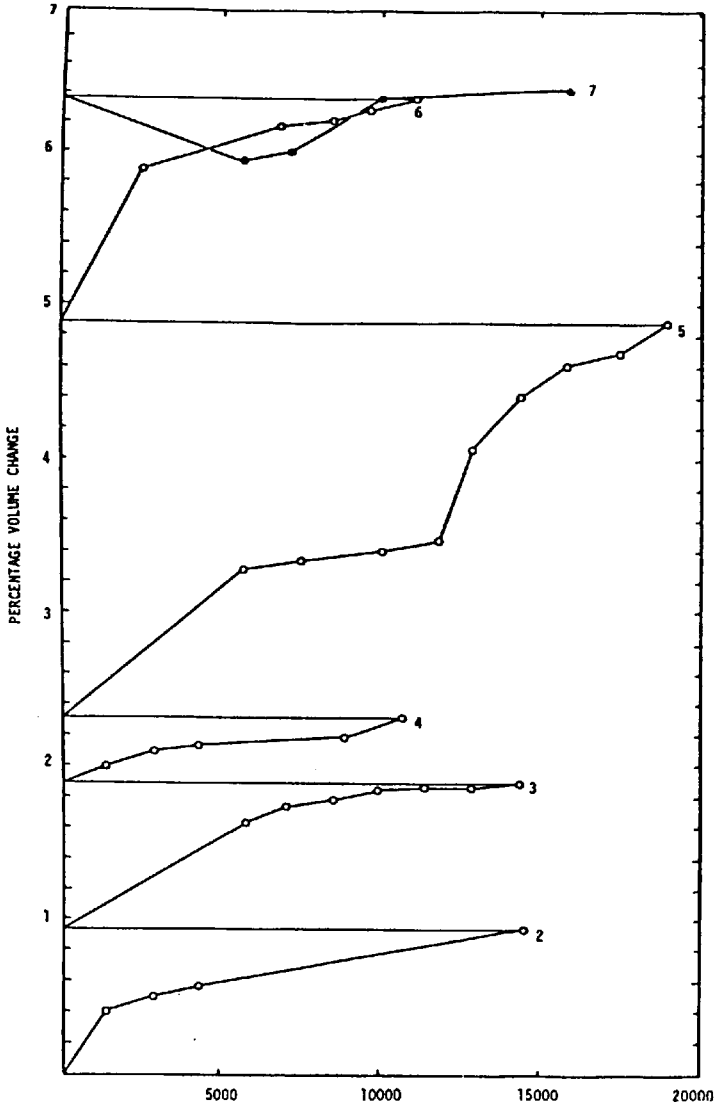

FIGURE 7.2 (a)
WATER VOLUME CHANGES OF SPECIMEN UR01

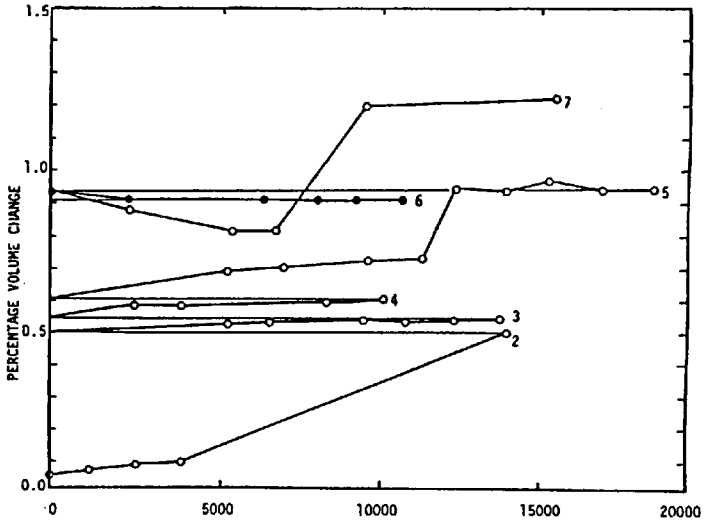

FIGURE 7.2 (b)
TOTAL VOLUME CHANGES OF SPECIMEN UR01

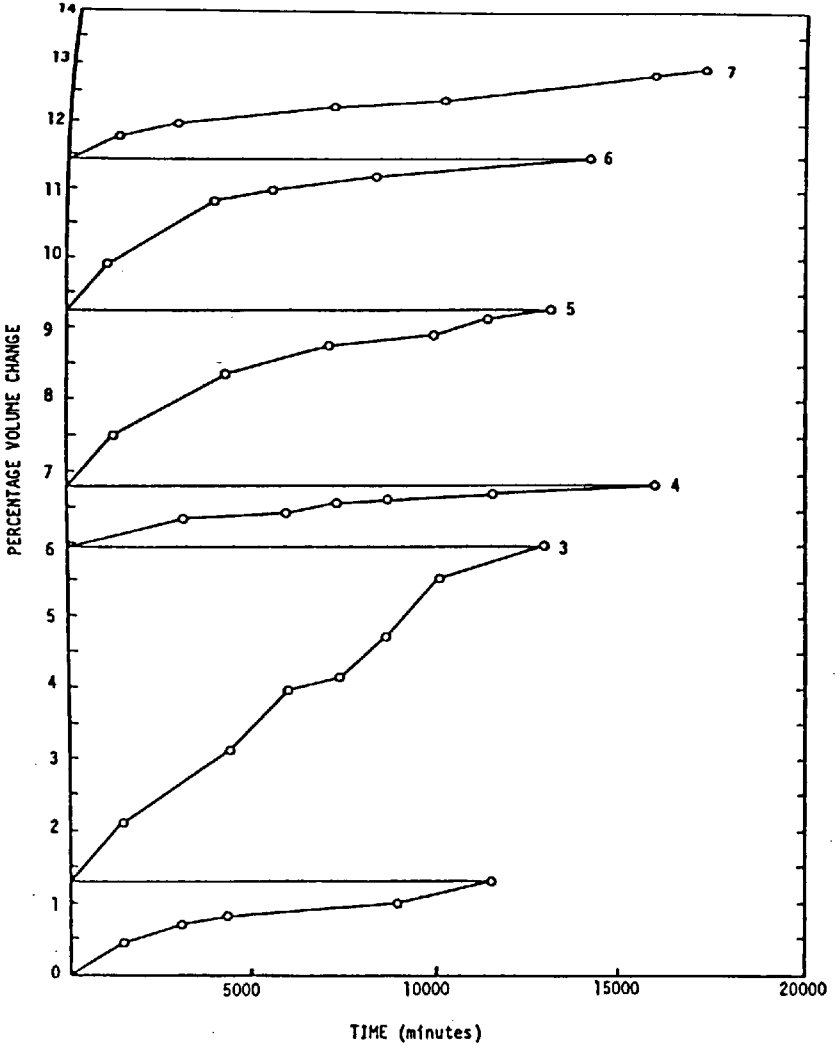

FIGURE 7.3 (a)
WATER VOLUME CHANGES OF SPECIMEN UR02

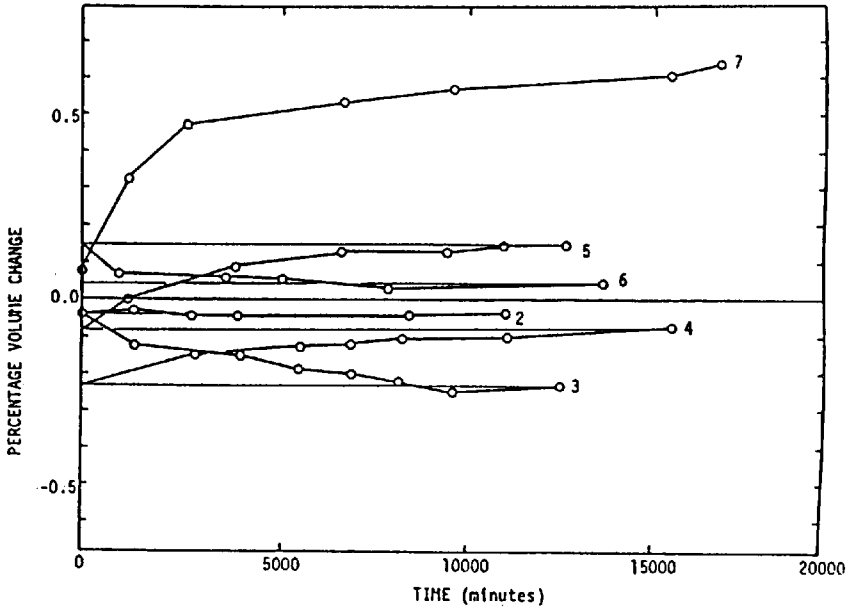

FIGURE 7.3 (b)
TOTAL VOLUME CHANGES OF SPECIMEN UR02

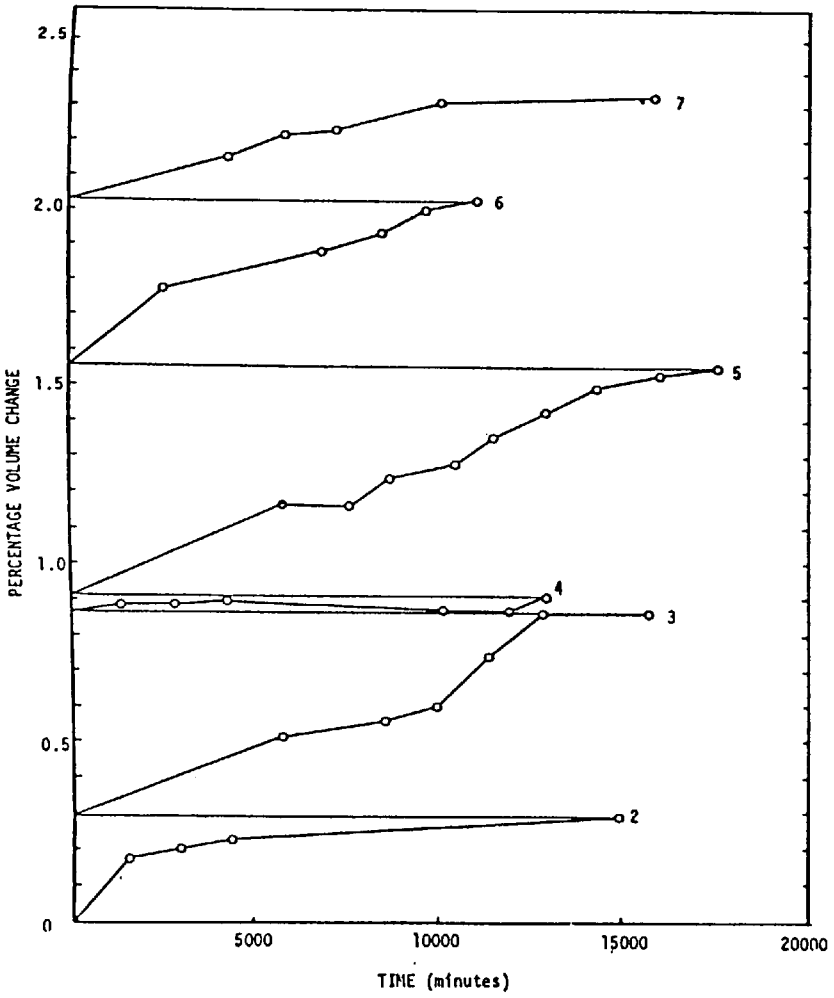

FIGURE 7.4 (a)
WATER VOLUME CHANGES OF SPECIMEN UT01

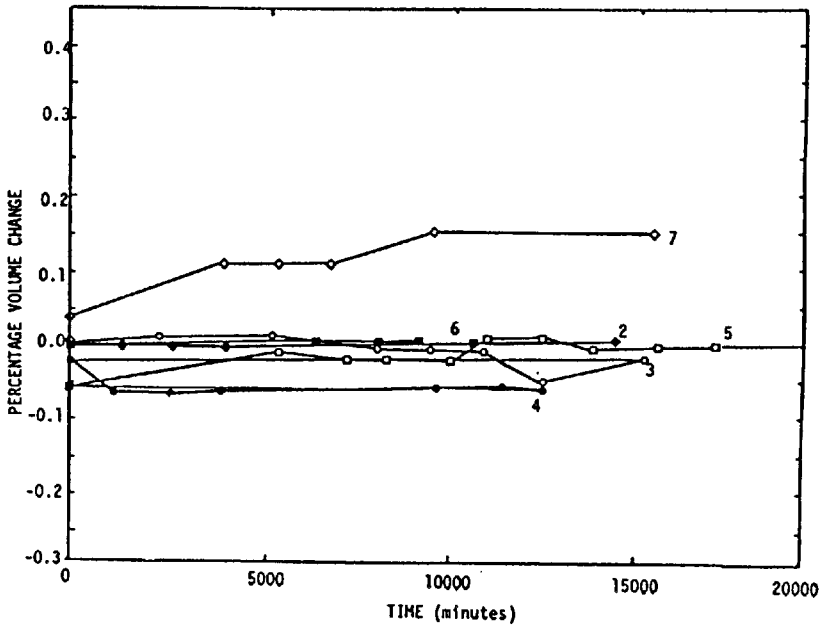

FIGURE 7.4 (b)
TOTAL VOLUME CHANGES OF SPECIMEN UT01

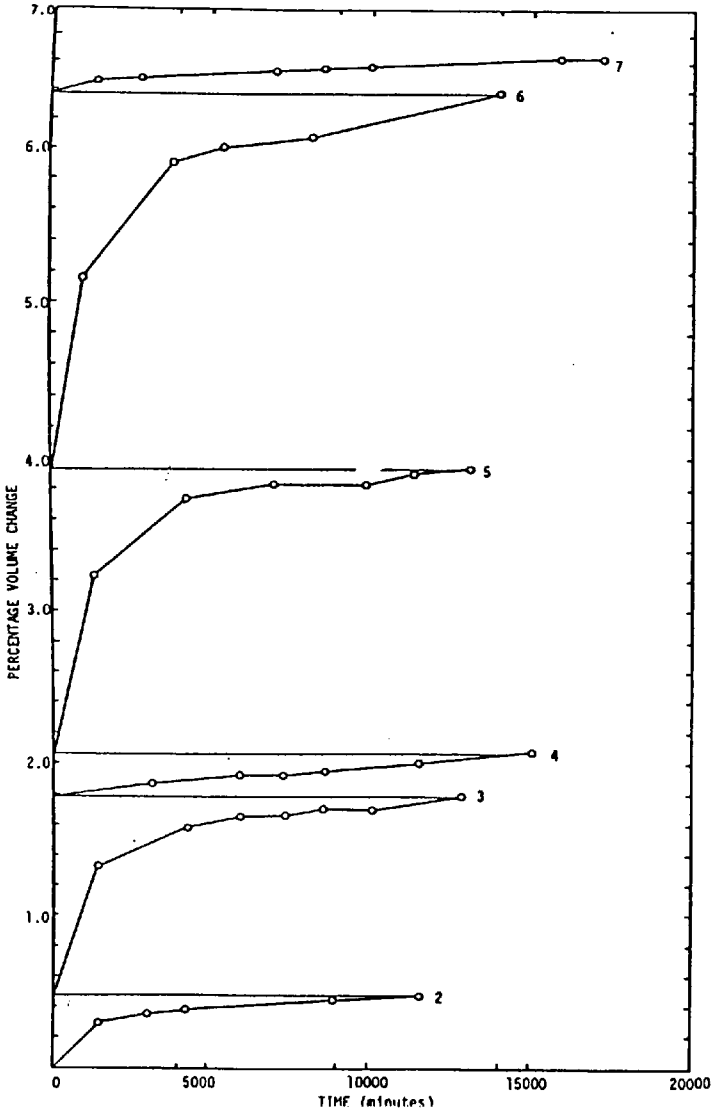

FIGURE 7.5 (a)
WATER VOLUME CHANGES OF SPECIMEN UTO2

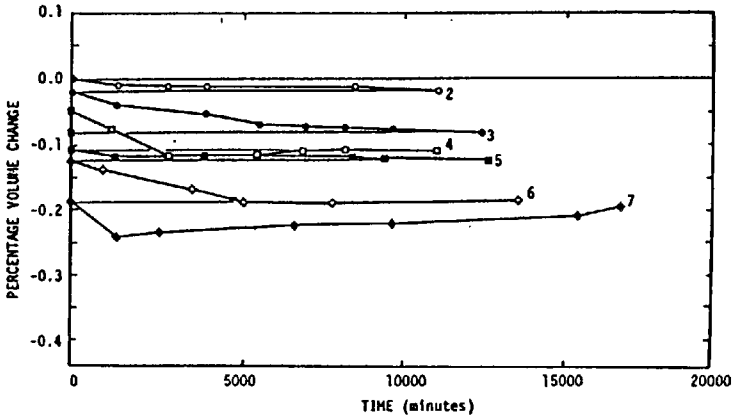

FIGURE 7.5 (b)
TOTAL VOLUME CHANGES OF SPECIMEN UTO2

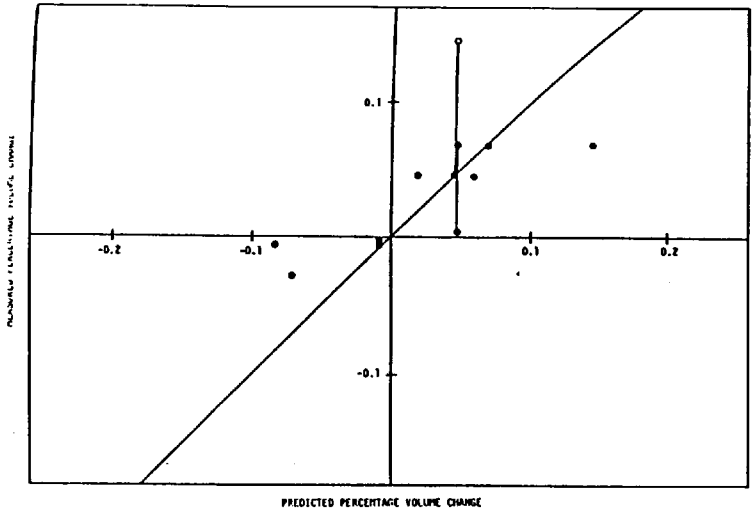

FIGURE 7.6

COMPARISON OF MEASURED AGAINST PREDICTED
SOIL STRUCTURE VOLUME CHANGES (UT01)

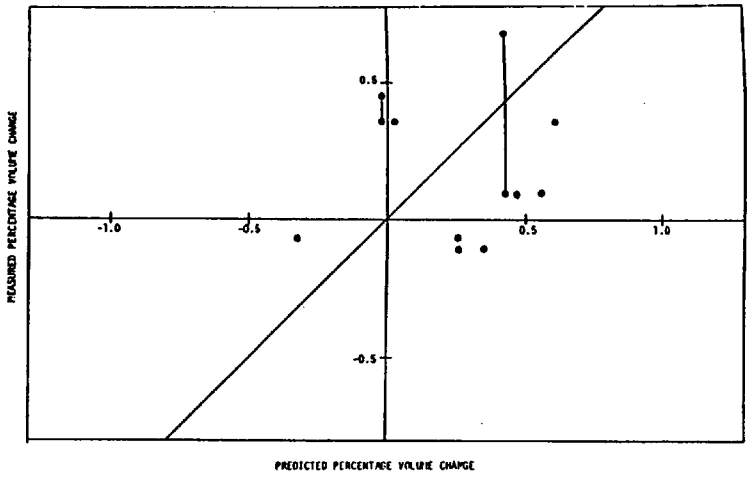

FIGURE 7.7

COMPARISON OF MEASURED AGAINST PREDICTED
SOIL STRUCTURE VOLUME CHANGES (UR01)

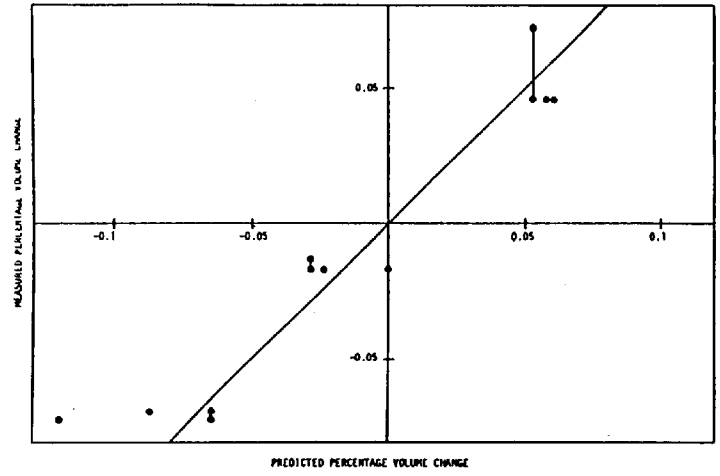

FIGURE 7.8

COMPARISON OF MEASURED AGAINST PREDICTED
SOIL STRUCTURE VOLUME CHANGES (UT02)

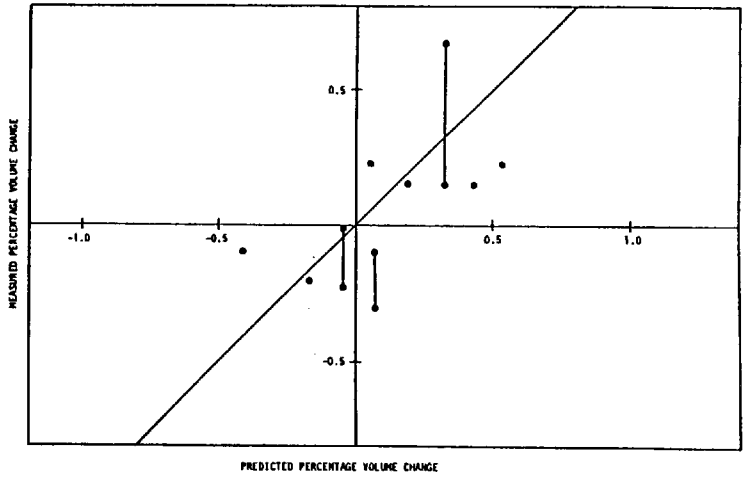

FIGURE 7.9

COMPARISON OF MEASURED AGAINST PREDICTED
SOIL STRUCTURE VOLUME CHANGES (UR02)

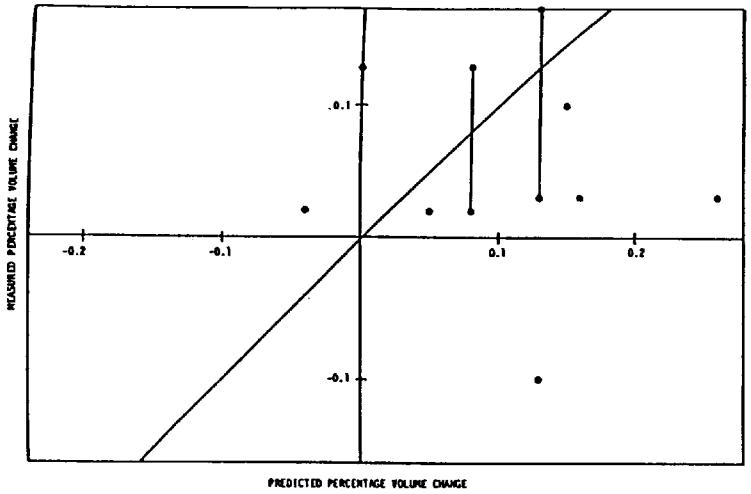

FIGURE 7.10

COMPARISON OF MEASURED AGAINST PREDICTED WATER PHASE VOLUME CHANGES (UTO1)

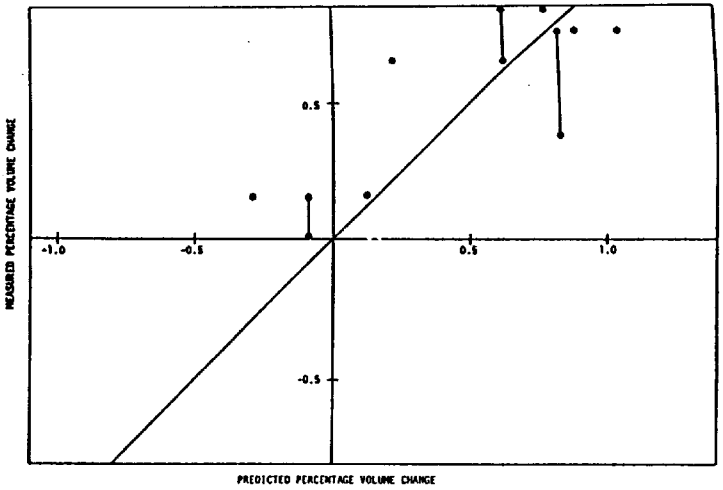

FIGURE 7.11

COMPARISON OF MEASURED AGAINST PREDICTED WATER PHASE VOLUME CHANGES (URO1)

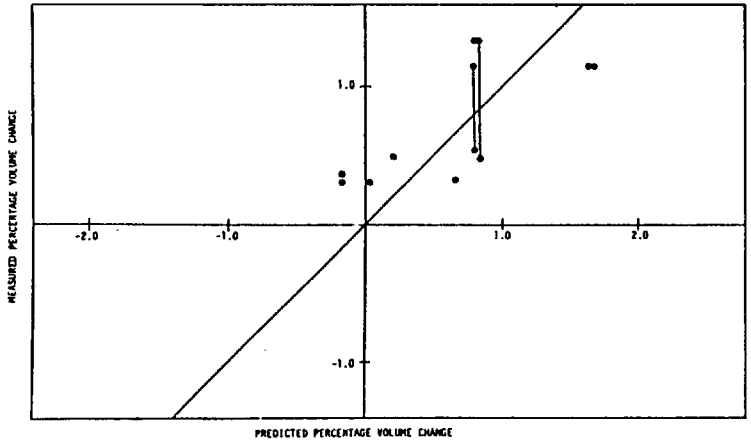

FIGURE 7.12

COMPARISON OF MEASURED AGAINST PREDICTED WATER PHASE VOLUME CHANGES (UTO2)

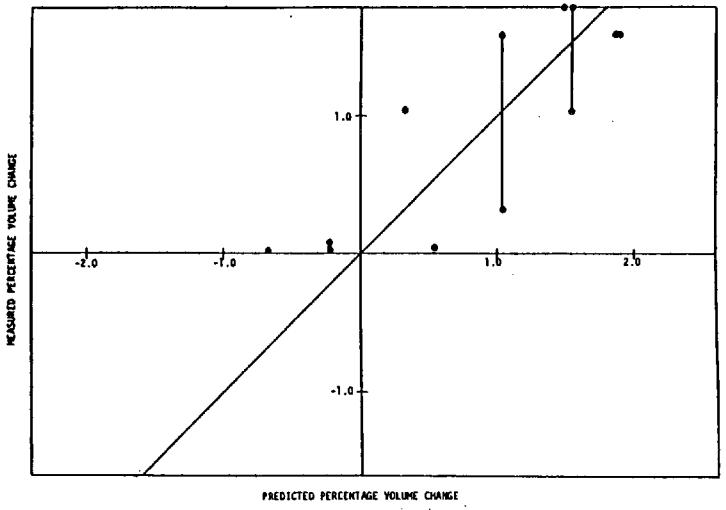

FIGURE 7.13

COMPARISON OF MEASURED AGAINST PREDICTED WATER PHASE VOLUME CHANGES (URO2)

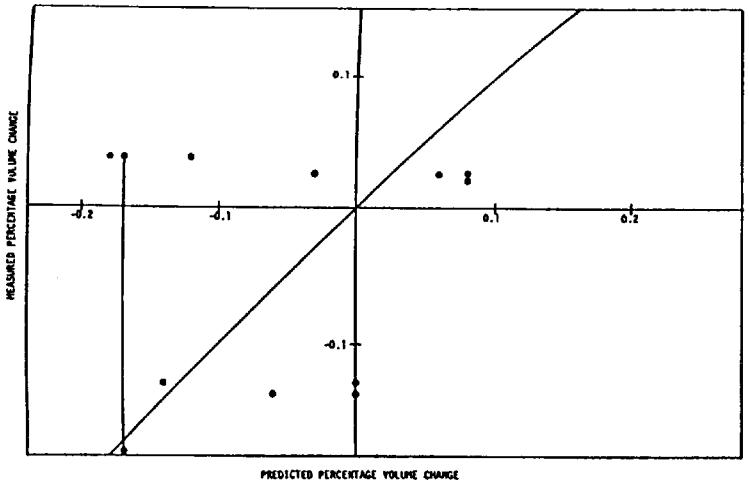

FIGURE 7.14

COMPARISON OF MEASURED AGAINST PREDICTED AIR PHASE VOLUME CHANGES (UT01)

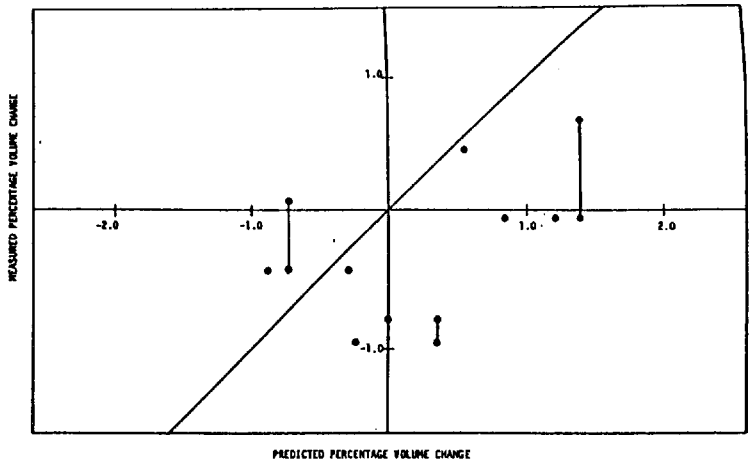

FIGURE 7.15

COMPARISON OF MEASURED AGAINST PREDICTED AIR PHASE VOLUME CHANGES (UR01)

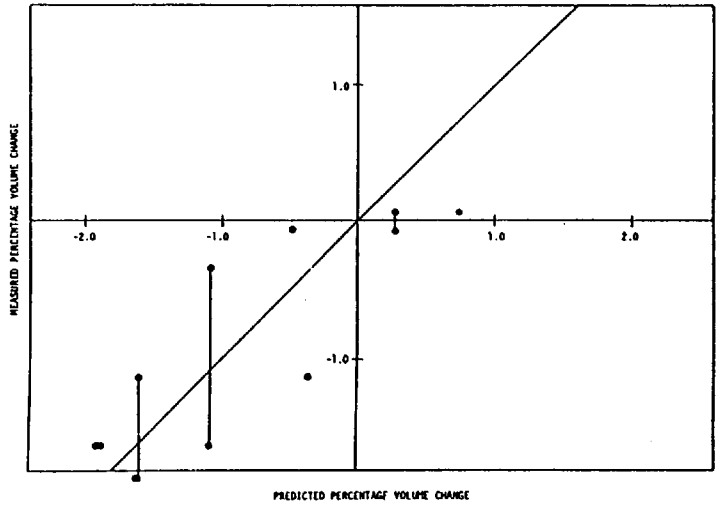

FIGURE 7.16

COMPARISON OF MEASURED AGAINST PREDICTED AIR PHASE VOLUME CHANGES (UT02)

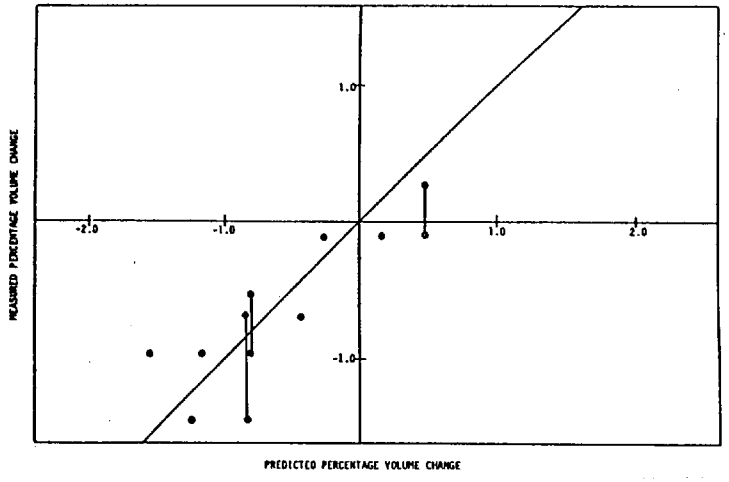

FIGURE 7.17

COMPARISON OF MEASURED AGAINST PREDICTED AIR PHASE VOLUME CHANGES (UR02)

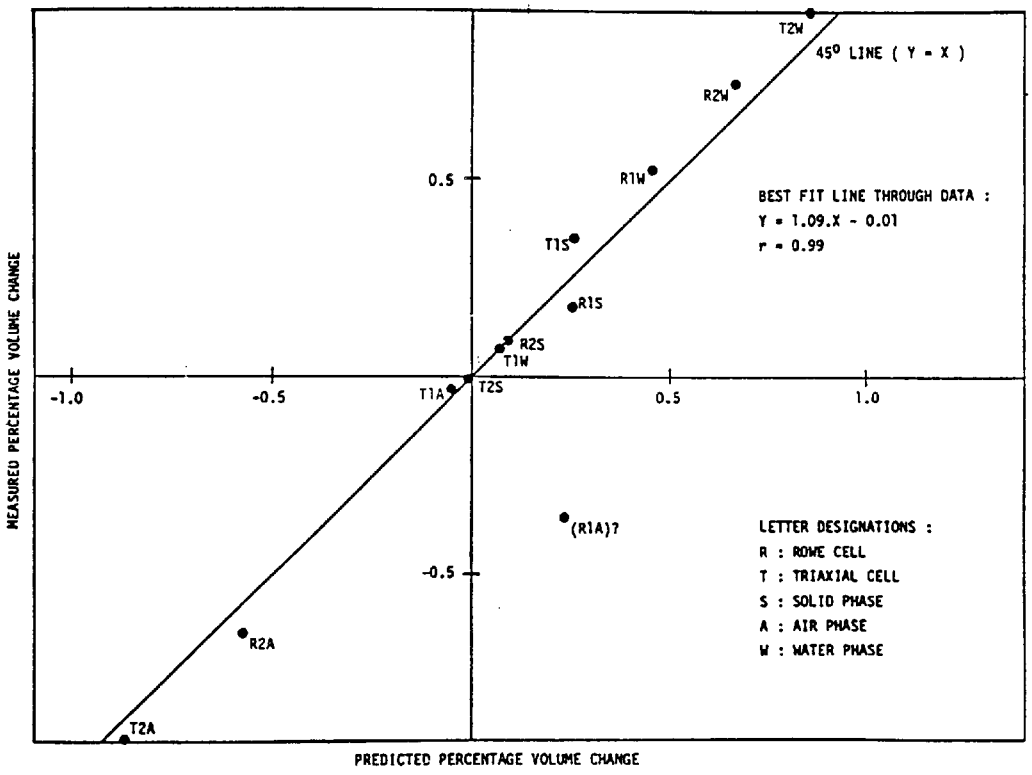

FIGURE 7.18

COMPARISON OF MEASURED AGAINST PREDICTED AVERAGE VOLUME CHANGES FOR ALL PHASES AND ALL SPECIMENS.

CHAPTER 8

CONSOLIDOMETER SWELL TESTS

8.1 INTRODUCTION

The primary aim of the consolidometer tests was to provide supporting data for the main tests described in Chapters 6 and 7.

Two series of tests were carried out; an initial series of constant volume swell pressure (CVSP) tests yielded the swell pressure value, compressibility and swelling indices and also provided sufficient data upon which to make a swell prediction (utilising the volume change theory). A smaller second series of unrestrained vertical swell (UVS) tests yielded swell values by which the previous swell prediction method would be evaluated.

It was decided at an early stage to examine a wide range of soil types (i.e. clay mineral mixtures) e.g.

Soil type	China Clay (Kaolinite)	Wyoming Bentonite (Sodium montmorillonite)
1	100	0
2	90	10
3	80	20
4	75	25
5	70	30
6	50	50

The specimens were produced to initial moisture contents of 25, 30 and 35% , and initial air voids of 3% , 5% and 8% (i.e. straddling the optimum moisture content line.)

A total of forty nine consolidometer tests were conducted, thirty three of which were the (CVSP) type with the remaining (16) being of the (UVS) type.

The results of the above are summarised in Tables 8.1, 8.2 and 8.3.

8.2 CONSTANT VOLUME SWELL PRESSURE (CVSP) TESTS

The standard (CVSP) test initially involves loading the specimen to its original insitu overburden conditions.

The specimen is then flooded with water, but prevented from swelling by continually increasing the load (hence the term constant volume); a point is reached where no further tendency to swell is exhibited, and the balancing pressure at that time is known as the swell pressure.

The specimen is then further loaded thereby compressing it, and finally unloaded to obtain the compressibility and rebound characteristics respectively.

Although the test programme does not utilise insitu soils, the influence of a varying initial loading is examined.
The specimen is subjected to disturbance between removal from the mould and initiation of the test; this induces a hysteretic effect which reduces the -

measured swell and swell pressure. A modification of Casagrande's empirical determination of the preconsolidation pressure in an over-consolidated clay is employed to estimate the 'true' swell pressure (Appendix D).

The processing of the experimental data is also discussed in Appendix D, however a typical experimental output is indicated in figure 8.1; the main measurements (as shown) include the initial and corrected swell pressures, and the compressibility and rebound moduli. The test results are summarised in Tables 8.1 and 8.2.

8.2.1 The prediction of volume change using the unsaturated soil volume change theory

The application of the volume change theory to the constant volume swell pressure test in the consolidometer is detailed in Chapter 5; the main assumptions made during these predictions are :

(a) zero overburden change during test : $\Delta\sigma = 0$

(b) final degree of saturation $(Sr)_f$ = 100%

(c) final pore water pressure $(U_w)_f$ = 0

(d) pore air pressure (U_a) = 0 (atmospheric)

8.2.2 Presentation of data

The results summarised in table 8.1 are examined graphically for interrelationships between the various parameters. They are split into two categories which are separately examined; these include (a) experimental data (as obtained directly from the test) and (b) predicted data (as calculated using the volume change theory).

The parameters include : (experimental) : swell pressure, liquid limits, compressibility and swell moduli, change in moisture content and
(theoretical) : swell pressure, percent swell, change in moisture content.

The graphical results are then discussed, and possible engineering applications highlighted.

8.2.3 Experimental data

(i) Adjusted swell pressure calculation using modified Casagrande's method

As previously noted, the specimen undergoes a measure of disturbance during the production phase. This in turn influences (decreases) the measured swell and swell pressure.

Fredlund (1983) suggests applying a modification of the graphical technique by Casagrande (1936) as a means of estimating the true swell pressure; this method has been successfully employed for many years in determining the preconsolidation pressure in overconsolidated clays.

Fredlund contends that Casagrande's graphical technique for determining the point where the void ratio curve bends downwards, is sufficiently similar to the problem of fixing the compression branch on the constant volume swell pressure test curve to justify its application.

The author notes that the technique is still relatively unproven in the expansive soil context, and examines its performance.

Application of the technique to the measured swell pressures consistently increased their values (for the soils tested) and it is these 'corrected' values that are utilised in subsequent graphical presentations.

(ii) Measured swell pressure Vs corrected swell pressure.

The measured and corrected swell pressures are plotted against each other in figure 8.2.

The corrected swell pressure was consistently greater than the experimentally measured value; the figure generally indicates that the swell pressure increased with plasticity.

The low expansive clay mixtures exhibited corrected and experimental SP values of similar magnitude, however, by increasing the liquid limits (and hence expansiveness) the corrected swell pressure increased such that for measured swell pressures above 140 kN/m^2 the corrected swell pressure was consistently in the order of 123 kN/m^2 greater.

The correction for sampling disturbance is considered to be relevant to these tests because the specimens are believed to have undergone a disturbance following removal from the mould and insertion into the consolidometer equipment; the relative consistency of the

corrections suggests a uniform production and experimental procedure.

Since the volume change predictions are directly related to the swell pressure (initial stress state), then the increased 'corrected' swell pressure will consequently increase the swell prediction; however this is further discussed in Section 8.4.

The author believes that the magnitude of swell pressure variation will be directly related to the type of sampling disturbance.

(iii) Swell pressure V^s volume change moduli

The plot of measured swell pressure versus the swell and compressibility volume change moduli (figire 8.3) exhibits an unusual relationship; the moduli generally remain constant for soils of increasing swell pressure however, they do increase temporarily for swell pressures of around $300kN/m^2$ in this test series. The cause of this localised increase in the moduli is unclear. The relatively constant moduli, suggests that they are not very suitable for predicting the swell pressure.

(iv) Volume change moduli versus liquid limit

Both the compressibility and swell moduli appear well related to the liquid limit (Figures 8.5 and 8.4 respectively) for the soils tested. The swell modulus exhibits the greatest variation in magnitude, the largest variation occurring up to a LL of 300%. (Since the

data above this LL is limited, then it is difficult to accurately assess the trend beyond this).

The compressibility modulus exhibits considerably less variation than the swell index over the initial range of liquid limit up to 300% ; above this however they both vary only slightly.

The relationships plot as curves, and these will be displaced when considering different moisture contents; this is exhibited by the curves plotted for 25% and 30% initial moisture content.

The same appears to be true for variations in density, however, the lack of experimental data prevents a thorough investigation of this aspect (refer liquid limit V^S swell pressure, figure 8.7a for available data). Since both the compressibility and swell moduli are related to the liquid limit, the latter may be used to link them. In this way, a knowledge of either the liquid limit of compressibility modulus may be employed to predict swell modulus.

In engineering terms this will permit an approximate estimation of the swell properties from the compressibility output of a conventional consolidation test.

The apparently successful relationship between the volume change indices and swell pressure has led the author to plot the swell modular ratio (C_s/C_c , after Yong and Warkentin, 1969) - refer figure 8.6. The figure indicates a general trend, whereby the swell pressure increases very slowly for a rapid increase in modular ratio. The figure illustrates varying initial conditions (moisture content

and air voids) and is thus considered as giving an indication of the data scatter and hence overall trend in behaviour.

Although the swell modular ratio (C_s/C_c) relates to swell pressure, the relationship is not as decisive as those between the individual moduli and swell pressure. C_s/C_c is therefore not considered as suitable for the prediction of swell pressure.

(v) Swell pressure V^s liquid limit

The swell pressure (SP) was plotted against liquid limit (LL) for various combinations of initial conditions i.e. moisture content, air voids and overburden. The initial graph (fig. 8.7a) shows the relationship between (SP) and (LL) with a constant air voids and overburden but varying moisture content.

Although the data is limited for the higher plasticity soils, sufficient points are available to establish an unmistakable relationship for the 25% moisture level. The curves for other moisture contents are drawn by interpolating between the available data points. As anticipated, the swell pressure reduced with increasing initial moisture content.

The second figure (8.7b) illustrates the relationship between liquid limit and swell pressure with a varying initial air voids.

Although the curves are not entirely smooth, they do exhibit a definite trend whereby the swell pressure increases with a decreasing air voids (i.e. increasing density).

The third figure (8.7c) also exhibits a trend whereby the swell pressure increases with increasing initial overburden.

(vi) Swell and compressibility moduli V^S change in moisture content

Both the swell (C_s) and compressibility (C_c) moduli appear related to the change in moisture content (Δw) (Figures 8.8 and 8.9 respectively).

(C_s) plots as a smooth curve against (Δw) for any particular initial moisture content. A series of such curves are formed by considering varying moisture contents such that for a fixed value of (C_s) , the change in moisture will increase with decreasing initial moisture content.

(C_c) also plots as a smooth curve against (Δw) although the curves for varying initial moisture content appear to bell outwards around a central axis (the 30% moisture content curve). The change in moisture again increases with decreasing initial moisture content.

In both instances, the 25% initial moisture specimens yielded the most consistent curves. Examination of Table 8.1 indicates that the initial moisture contents of these specimens were very close to their target value of 25% whereas the other specimen moisture contents deviated to varying extents from their targets.

Although the swell modulus provides a more consistent indication of the likely change in moisture content, it is worthwhile noting

that the compressibility modulus also provides a usable indication of the same.

This relationship is of particular value since it may be used in conjunction with previous consolidometer data.

(vii) Moisture content change V^S liquid limit

The change in moisture content relates quite well to the liquid limit (Figure 8.10) although attempts to separate the results according to initial moisture content have not worked due to the scatter of data points.

8.2.4 Predicted data.

(i) Predicted swell V^S liquid limit

The predicted swell exhibits a limited relationship with liquid limit values up to 140%; above this, there is a lack of data thereby preventing an adequate assessment (Figure 8.11).

Since reconstituted materials are used, observed relationships cannot be generally applied (quantitatively) to other soils; however, the result does indicate that the volume change theory may be used to develop similar relationships for other soil types.

(ii) Predicted swell V^S compressibility (C_c) and swell (C_s) moduli

Both the swell and compressibility moduli relate to the predicted swell (%) (Figures 8.13 and 8.12) respectively); however the swell modulus yields the most consistent prediction by far. This is to be expected since the prediction is itself based upon the C_s value .

The predicted swell V^S compressibility modulus graph (Fig. 8.12) exhibits a considerable scatter, and this leads to the conclusion that it cannot be satisfactorily employed for the purpose of predicting swell.

(iii) Predicted moisture content change V^S liquid limit

The predicted moisture content change does not relate very well to the liquid limit and the plotted results exhibit a scatter about the best-fit line (Figure 8.14). However, ignoring the two 'displaced' results (35% moisture content specimens of LL = 49% and 141%) the graph is vastly improved, although there remains a distinct lack of data for specimens above LL = 235% , (however in practice this is itself an acceptable upper limit).

(iv) Predicted change in moisture contents V^S compressibility (C_c) and swell (C_s) moduli

As with the predicted percent swell, the predicted moisture change relates very well to the swell modulus (C_s) (Fig. 8.16); this is considered to be due to the same reason i.e. both the moisture content and swell predictions are based upon the swell modulus.

On the other hand, the predicted moisture change (Figure 8.15) does not relate well to the compressibility index. The predicted moisture changes generally increase with increasing (C_c) and (C_s) values although this behaviour is difficult to relate to the liquid limits due to the large scatter of data.

8.2.5 Summaries

The results of the (CVSP) tests are summarised below :

Summary of experimental data

1. Tests were carried out on reconstituted specimens, and a modification of Casagrande's method applied to estimate the true swell pressure; however, this method may not be applicable to relatively undisturbed preconsolidated samples from the field.

   The test results seem to be in reasonable agreement with the predictions, however, the predicted swell pressure is consistently 123 kN/m^2 greater than the measured value when the latter excees 140 kN/m^2 and the liquid limit exceeds 124%.

2. The recorded volume change moduli vary by only a small amount with changes in swell pressure (Fig. 8.3); on this basis, therefore, they are not considered suitable for basing swell pressure predictions.

3. Attempts to correlate the swell modulus (C_s/C_c after Yong and Warkentin, 1969) with swell pressure (Fig. 8.6) have indicated a general trend in behaviour only. In particular, those soil mixtures with liquid limit > 94% exhibit a considerable over-lapping of behaviour which renders this approach of little value for accurately predicting swell pressure.

4. The swell pressure relates very well to liquid limit (Figure 8.7(a)), and despite the limited variety of testing conditions(i.e. initial moisture content and air voids)it was possible to make certain observations (Figures 8.7(a)-8.7(c)) :

(a) The swell pressure increases for a decreased initial moisture content.

(b) The swell pressure decreases with increasing initial air voids.

(c) The swell pressure tends to increase with increasing initial loading.

These general relationships also hold true for the swell related volumetric changes (total and water volume changes).

5. Both the swell and compressibility moduli appear well related to the liquid limit (Figures 8.4 and 8.5 respectively); as a result, the swell modulus and to some extent swell behaviour may be approximated from only conventional consolidation data. This relationship has a potentially great practical application and its examination for other soil types is recommended.

6. The moisture content change relates well to the liquid limit for the soils tested (Figure 8.10); however, the relationship has previously been shown to vary considerably, even for specimens of the same soil type. This observation confirms those made in Chapter 3 in that the liquid limit is at least of value in the qualitative prediction of swell characteristics (pressure and vertical movement)

7. The change in moisture content relates well to both the swell and compressibility moduli (Figures 8.8 and 8.9). Although the relationship with the swell modulus is better, the association of moisture content change with the compressibility modulus has

considerable potential application for use with existing consolidation test data.

8. The 25% initial moisture content specimens exhibited the most consistent behaviour (note linearity of the curve drawn through these data points in most graphs).

   Examination of the original data (Table 8.1) indicates that this is probably due to the specimens having been produced to a more consistent initial moisture value.

9. Finally it is recognised that the interrelationships are numerically applicable to those soils employed in this project only; but , the trends should apply universally to most swelling soils.

Summary of predicted data

1. The predicted swell exhibits a relationship with the liquid limit (Figure 8.11) for the range of soils tested (up to a liquid limit of 142%). Although the results diverge with increasing liquid limit, they do appear uniformly distributed about the best fit line; more importantly, the volume change theory appears to predict the swell of different soils by consistent relative proportions.

2. Both the predicted swell (total volume) and predicted moisture content change (water volume) exhibit very good relationships with the swell (C_s) modulus (Figures 8.13 and 8.16

respectively). This is primarily due to the predictions being based upon the swell modulus. The value of these relationships for the purpose of swell prediction is therefore limited.

3. The compressibility modulus (C_c) does not relate well to the predicted swell or moisture content changes (Figures 8.12 and 8.15 respectively). The various soil types do not exhibit any sort of pattern within the data plots, thus, the modulus is considered of little value for the prediction of the total and water volume changes.

4. The relationship between moisture content change and liquid limit is reasonable if the two outermost (questionable) data points are ignored.

   Consideration of the two outriding points make little or no difference to the best fit line.

5. Overall therefore the predicted swell is the only parameter which successfully relates to a simple test (in this case liquid limit); this relationship is also limited in its application to soil types similar to those tested.

8.3 UNRESTRAINED VERTICAL SWELL (UVS) TESTS

8.3.1 Introduction

The (UVS) test is introduced in Chapter 5, for continuity, however, it is briefly described below; the procedure involves flooding the specimen with water and permitting it to swell freely.

The resulting change in specimen depth is expressed with respect to its original total depth and recorded as a percentage.

This value is subsequently compared with the predicted swell for a similar specimen in the CVSP test, thus providing a basis for evaluating the CVSP test based predictions.

The test data is described in this section, however, the processing required to obtain usable data from raw experimental output is described in Appendix D.3. The experimental output is summarised in Figure 8.17 and Tables 8.4 and 8.5.

8.3.2 Experimental output

The experimental output for this test records the volume change history for several swelling clay specimens.

Patterns of behaviour are evident from the data and although these have been widely documented by other researchers, they are briefly discussed below.

8.3.3 General volumetric behaviour

Since only a comparatively small range of specimens were tested here, the main variable that can be evaluated is initial moisture content. Figure 8.8 illustrates the influence of varying moisture content upon the percent swell, and it can be clearly seen that swell decreases with increasing initial moisture content.

Since only one specimen type of a different density was tested trends were not discernable, although the swell apparently increased, with increasing density (decreasing air voids).

The swell also increased for increasing liquid limit (Montmorillonite content). The consistency of this behaviour is well illustrated in Figure 8.18. One unusual feature of the wholly Kaolinite specimen was that of collapsing, whereby the specimens decreased in volume upon wetting. This is consistent with that noted by Burland (1961) and several other authors since.

The swelling time is also well illustrated in Figure 8.7; 75% of the speicmens exhibit greater than 80% of their final swell within 2500 minutes (51 hours) of wetting. However, the average swell at this time is 75.5% maximum value.

It was also noted that the higher plasticity soils (30% Montmorillonite) exhibited swell for the entire duration of the test. Thus the recorded swell values were almost certainly lower than the absolute maximum.

The curved relationships recorded on Figure 8.18 will therefore tend to curve upwards i.e. become convex in shape.

8.4 EVALUATION OF THE CVSP SWELL PREDICTION PROCEDURE

8.4.1 Introduction

The aims of this chapter, apart from providing additional information regarding the nature of the test soils, are to evaluate the (CVSP) test method (in conjunction with the volume change theory) for the purpose of predicting swell characteristics.

The latter aim is pursued in this chapter by comparing the volume change characteristics (total and water) as measured during

the (UVS) test with those predicted upon the basis of the CVSP test results.

This section (8.4) also discusses the empirical correction for specimen disturbance, and also the general factors influencing the test and hence heave prediction.

8.4.2 Comparison between predicted and measured phase volume changes

(a) Predicted V^S measured swell

With the exception of one result, the predicted swell is increasingly lower than the measured value as the liquid limit increases (Figure 8.19).

Since the object of this section was to determine the overall predictive reliability of the test, all specimens, irrespective of initial moisture content and air voids were plotted on the same graph.

The different soil types, which composed of varying proportion of Montmorillonite,are indicated in terms of their liquid limits; as expected, the higher plasticity soils exhibit a higher overall swell value. Although the results for each soil type are scattered, an overall trend in behaviour is observed.

(b) Predicted $\bar{V}s$ measured change in moisture content

The predicted change in moisture content exhibits little variation for soils of liquid limits up to 120% (figure 8.20). The results exhibit some scatter, although this is attributed to the initial variation of specimen properties.

(c) Predicted final Vs measured final moisture contents

The graphical presentation (figure 8.21) is based upon the same results used for (b), but expressed as a total moisture content. In consequence, the figure does not appear to indicate any new discoveries.

8.4.3 Swell pressure

(a) Corrections for disturbance effects

It is widely acknowledged that sampling disturbance will effectively reduce the observed swell characteristics. In examining the three dimensional projection of the problem (Figure 5.15) it can be seen that the plane of a disturbed specimen will bend downwards prematurely; if this is viewed on the total stress $(\sigma-U_a)$ plane then the problem is seen to be one of predicting what the 'undisturbed' curve should have looked like or more importantly, by how much would the swell pressure be greater for the undisturbed case.

This problem is very similar to that of trying to predict the preconsolidation pressure in an overconsolidated clay, and the author considers the use of Casagrande's (1936) construction to be a logical answer.

This method has been suitably modified by Fredlund (1983), and subsequently chosen by the author for application to the consolidometer tests conducted during the course of this project. Both Casagrande and Fredlund's proposals are detailed in Appendix D3.4.

Fredlund's method differs from Casagrande's original proposals in that a line parallel to the rebound curve (rather than the compression curve) is drawn to intersect the bisector line. This

procedure yields a lower 'pressure' value than Casagrande's method; the reason for using this approach is not clear from his publications, although it would appear to be a logical approach since it is the swell properties that are being sought.

(b) Implications of applying disturbance corrections

The sampling disturbance corrections consistently resulted in an increased swell pressure.

An examination of the swell prediction procedure using the volume change theory (chapter 5.3), indicates that an increase in swell pressure will increase the predicted total and water volume changes. Therefore, the correction for disturbance consistently increases all apparent swell related behaviour.

8.4.4 Experimental influence

(a) Scale effects

Both test types i.e. (UVS) and (CVSP) are conducted using the same sized specimens. This should offset the scale differences that might ensue through employing different specimen sizes.

(b) Side wall friction

The side wall friction generated between the test cell wall and the specimen undoubtedly exerts a restraining influence upon all swell behaviour - especially so for the smaller specimens. However, the identical size of specimens used in both test types will result in similar friction effects; thus for the purpose of the comparisons of swell behaviour made between the (UVS) and (CVSP) test specimens, the friction effects were the same and have been ignored.

(c) Environmental variation

The environmental factors such as temperature, humidity, grade of water were all controlled to the same rigid standards as employed for the null and volume change tests (Chapters 6 and 7).

(d) Final saturation levels

It is noted that many of the final saturation levels exceed 100%; these are only considered to be approximate however, since additional water was probably absorbed during dissassembly of the equipment.

8.4.5 Summary of swell prediction evaluation

1. The predicted swell (from CVSP results) is approximately equal to the measured value (UWS test results) for soils of liquid limits up to 94% (Figure 8.19).

   As the liquid limits increase, so the predicted swell becomes increasingly lower than the measured value. This behaviour is observed on test materials of liquid limits up to 142%; beyond this, the trend in behaviour is uncertain due to the lack of data.

   The best fit line through the data has a gradient (Predicted swell ÷ measured swell) of 0.477; this is considerably less than would occur for a 100% prediction success i.e. gradient = 1).

2. The predicted water volume change behaviour is similar (in trend) to that of the predicted swell (Figure 8.20).

   The predicted water volume change approximately equals the measured value for the lowest liquid limits (49%); however, the predicted value becomes increasingly less than the measured

value as the liquid limit increases up to 120%. Beyond this, the gap between predicted and measured swell apparently reduces although once again, the absence of samples with a (LL) above 142% prevents a detailed assessment of this.

Since the graph for final moisture content (Figure 8.21) is based on the water content change data of figure 8.20, then it is not surprising that their form is very similar. The main difference between the two, is the superior relationship between the final measured and predicted moisture contents- giving the impression of an increased accuracy of prediction.

3. Notably, the gradient of the best fit line through the final moisture content and swell graphs exhibit a very similar trend (0.305 and 0.477 respectively). This is not unexpected since both gradients were predicted from the same theory and therefore subject to the same errors. These gradients, represent an average behaviour, and are suitable for comparison purposes only. The varying trend in behaviour between soil types should be considered when formulating corrections.

TABLE 8.1

CVSP TESTING ITINERARY

TEST NO.	APPARATUS NO.	INITIAL CONDITIONS			SOIL TYPE	TEST TIME		
		AIR VOIDS (%)	MOISTURE (%)	SURCHARGE (kN/m^2)	B/K	FROM	TO	DURATION (DAYS)
3	F	5	30	64.8	25/75	28.10.84	15.11.84	10
4	G	5	30	"	25/75	28.10.84	15.11.84	19
5	F	5	30	"	0/100	18.11.84	5.12.84	20
6	G	5	30	"	50/50	18.11.84	23.12.84	34
7	F	5	30	"	75/25	24.12.84	21.01.85	28
8	G	5	30	"	100/0	26.12.84	21.01.85	28
9	F	5	25	"	100/0	28.01.85	04.03.85	35
10	G	5	25	"	75/25	28.01.85	04.03.85	35
11	F	5	25	"	50/50	07.03.85	29.03.85	22
12	G	5	25	"	25/75	07.03.85	29.03.85	22
13	F	5	25	"	0/100	31.03.85	24.04.85	24
14	G	5	35	"	0/100	31.03.85	24.04.85	24
15	F	5	25	"	10/90	27.04.85	17.05.85	20
16	G	5	25	"	20/80	27.04.85	17.05.85	20
17	F	5	25	"	30 /70	17.05.85	11.06.85	25
18	G	5	30	"	30/70	17.05.85	11.06.85	25
19	F	5	30	"	10/90	12.06.85	08.07.85	26
20	G	5	30	"	20/80	12.06.85	08.07.85	26
21	F	5	35	"	10/90	08.07.85	07.08.85	30
22	G	5	35	"	20/80	08.07.85	07.08.85	30
23	F	3	30	"	30/70	08.08.85	02.09.85	25
24	G	5	35	"	30/70	08.08.85	02.09.85	25
25	F	3	30	"	10/90	04.09.85	28.09.85	24
26	G	3	30	"	20/80	04.09.85	28.09.85	24
27	F	3	30	"	0/100	28.09.85	18.10.85	20
28	G	8	30	"	0/100	28.09.85	18.10.85	20
29	F	8	30	"	10/90	18.10.85	10.11.85	22
30	G	8	30	"	20/80	18.10.85	10.11.85	22
31	F	8	30	"	30/70	16.11.85	02.12.85	16
32	G	5	30	"	30/70	16.11.85	02.12.85	16
33	F	5	30	194.2	0/100	03.12.85	26.12.85	20
34	G	5	30	"	10/90	03.12.85	26.12.85	20
35	F	5	30	"	20/80	28.12.85	20.01.86	23
36	G	5	30	"	30/70	28.12.85	20.01.86	23

TABLE 8.2

CVSP EXPERIMENTAL DATA

TEST NO.	INITIAL CONDITIONS				FINAL CONDITIONS					C_s ($\frac{\Delta e}{\Delta \log p}$)	C_c ($\frac{\Delta e}{\Delta \log p}$)	$\frac{C_s}{C_c}$	MEASURED SWELL PRESSURE (kN/m^2)
	DEPTH (mm)	MC_o (%)	e_o	Sr_o (%)	MC_F (%)	e_F	* Sr_F (%)	Δe	ΔW (%)				
3	14.85	34.13	0.97	89.15	49.62	1.01	124.82	0.04	15.49	0.108	0.217	0.49	151.04
4	14.85	33.77	0.97	88.31	50.77	1.01	126.59	0.04	17.0	0.109	0.221	0.49	151.04
5	14.85	28.44	0.92	81.19	32.63	0.84	101.28	0	4.19	0.032	0.137	0.23	64.73
6	14.85	38.31	0.98	95.73	56.00	1.0	139.15	0.02	18.68	0.178	0.276	0.65	215.78
7	14.85	43.19	0.94	102.0	-	-	-	-	-	0.211	0.432	0.49	409.98
8	14.79	45.74	0.89	-	-	-	-	-	-	0.141	0.147	0.96	388.40
9	14.97	25.31	0.69	86.89	73.26	0.98	176.03	0.294	47.95	0.140	0.140	1.0	-
10	14.99	26.39	0.67	-	-	0.89	-	-	-	0.175	0.103	0.128	-
11	14.85	24.02	0.68	86.14	50.23	0.89	137.82	0.21	26.21	0.091	0.138	0.660	1059
12	14.89	24.10	0.71	85.93	47.55	0.87	138.65	0.16	23.45	0.097	0.141	0.69	646
13	15.198	23.97	0.77	81.68	33.09	0.80	107.97	0.03	9.12	0.042	0.112	0.36	437
14	14.41	35.00	0.94	96.94	33.75	0.87	101.37	0.07	-	0.033	0.150	0.22	64.57
15	14.85	24.75	0.74	86.52	39.77	0.83	123.65	0.09	15.02	0.070	0.087	0.81	501.20
16	14.85	25.57	0.74	88.58	46.78	0.86	138.49	0.13	21.21	0.062	0.130	0.47	478.63
17	15.12	28.05	0.79	89.62	56.39	1.01	140.05	0.23	28.38	0.162	0.177	0.92	389.04
18	14.81	32.64	0.87	93.88	62.17	1.14	136.45	0.27	29.53	0.236	0.223	1.06	239.90
19	14.92	31.71	0.90	89.6	48.20	1.07	114.48	0.17	16.49	0.158	0.168	0.94	237.39
20	14.98	30.00	0.91	85.6	39.33	0.99	103.3	0.08	9.33	0.161	0.144	1.12	151.04
21	14.85	24.5	0.99	89.73	40.22	1.02	101.84	0.03	5.72	0.165	0.198	0.83	87.02
22	14.76	34.35	0.95	91.6	51.14	1.15	113.22	0.20	16.79	0.243	0.239	1.02	215.78
23	14.86	31.06	0.83	94.41	60.37	1.08	140.37	0.25	29.31	0.185	0.164	1.12	323
24	14.78	36.77	0.99	93.17	63.67	1.57	101.70	0.58	26.90	0.525	0.457	1.15	214
25	14.91	30.13	0.84	92.88	40.50	0.93	112.25	0.09	10.37	0.149	0.161	0.93	151.4
26	15.03	30.89	0.85	93.06	52.03	0.92	144.46	0.07	21.14	0.101	0.122	0.83	151.4
27	14.90	29.27	0.83	91.92	32.68	0.85	100.94	0.014	3.41	0.066	0.118	0.56	125.9
28	14.85	29.21	0.92	83.05	33.48	0.85	102.68	-0.07	4.27	0.004	0.137	0.003	-
29	14.80	-	-	-	-	-	-	-	-	-	-	-	-
30	14.80	-	-	-	-	-	-	-	-	-	-	-	-
31	15.01	29.77	0.94	79.69	53.03	1.19	112.38	0.25	23.26	0.233	0.281	1.01	240
32	14.94	29.53	0.85	87.23	53.57	1.09	123.50	0.24	24.04	0.199	0.182	1.09	288.4
33	15.60	28.92	0.97	78.40	39.00	0.97	105.16	0.01	10.08	0.044	0.110	0.40	-
34	14.93	30.07	0.88	88.48	36.84	0.97	97.6	0.09	6.77	0.111	0.141	0.79	194.2
35	14.87	26.62	0.82	83.05	44.63	0.96	118.36	0.14	18.01	0.141	0.166	0.85	194.2
36	14.88	28.57	0.84	85.41	48.47	0.80	151.39	-0.36	19.9	0.131	0.149	0.88	194.2

* these are only approximate values, since additional water was probably absorbed following unloading and dissassembly procedure.

TABLE 8.3

CVSP THEORETICAL CALCULATIONS

TEST NO.	CORRECTED SWELL PRESSURE (kN/m^2)	PREDICTED CHANGES					
		MC_F (%)	e_F	Sr_F (%)	Δe_{th}	ΔMC_{th} (%)	$(\frac{\Delta h}{h} \times 100)$ (%)
3	188.20	40.25	1.02	100	0.05	6.12	2.6
4	190.54	40.27	1.02	"	0.05	6.50	2.6
5	87.09	35.19	0.93	"	0.01	6.75	1.1
6	309.03	44.96	1.10	"	0.03	6.65	6.1
7	524.81	-	-	"	-	-	9.9
8	548.30	-	-	"	-	-	6.9
9	1445.40	37.13	0.87	"	0.19	11.82	27.1
10	1402.55	-	-	"	-	-	13.9
11	1216.19	32.63	0.79	"	0.11	8.61	6.9
12	776.20	32.17	0.82	"	0.11	8.07	6.1
13	562.30	30.84	0.81	"	0.04	6.87	2.4
14	131.83	36.49	0.96	"	0.016	1.49	0.8
15	588.80	31.21	0.81	"	0.072	6.46	4.1
16	602.60	31.22	0.79	"	0.06	5.65	3.2
17	512.70	37.11	0.93	"	0.15	9.06	8.2
18	371.53	41.89	1.06	"	0.19	9.25	9.9
19	416.90	40.41	1.03	"	0.13	8.70	6.8
20	288.40	39.13	1.01	"	0.10	9.13	5.2
21	169.82	41.12	1.06	"	0.07	6.62	3.5
22	309.03	43.82	1.12	"	0.17	9.47	8.7
23	662.00	39.82	1.00	"	0.17	8.76	9.3
24	288.00	53.02	1.33	"	0.34	16.25	17.1
25	288.4	36.18	0.93	"	0.09	6.05	4.9
26	263.00	35.60	0.91	"	0.06	4.71	3.2
27	204.17	44.40	1.16	"	0.33	15.13	1.8
28	37.15	34.78	0.91	"	-0.01	5.57	0.1
29	-	-	-	"	-	-	-
30	-	-	-	"	-	-	-
31	354.80	44.23	1.11	"	0.17	14.46	8.9
32	457.1	36.20	0.92	"	0.07	6.67	9.1
33	177.8	36.24	0.95	"	-0.02	7.32	0.9
34	346.7	35.07	0.91	"	0.03	5.00	4.3
35	380.2	33.66	0.86	"	0.04	7.04	5.9
36	426.78	35.24	0.88	"	0.04	6.67	5.8

TABLE 8.4

UNRESTRAINED VERTICAL SWELL (UVS) TEST PROGRAMME

TEST NO.	TARGET MC (%)	TARGET AV (%)	SOIL COMPOSITION B (%)	K(%)	SURCHARGE (kN/m^2)	DATE ON	DATE OFF	DURATION (days)	APPARATUS IDENTIFICATION CODE
01	30	5	0	100	64.73	21.08.85	29.08.85	8	A
02	30	5	10	90	"	"	"	8	B
03	30	5	20	80	"	"	"	8	C
04	30	5	30	70	"	"	"	8	D
05	35	5	0	100	"	01.09.85	10.09.85	9	A
06	35	5	10	90	"	"	"	9	B
07	35	5	20	80	"	"	"	9	C
08	35	5	30	70	"	"	"	9	D
09	25	5	0	100	"	11.09.85	19.09.85	8	A
10	25	5	10	90	"	"	"	8	B
11	25	5	20	80	"	"	"	8	C
12	25	5	30	70	"	"	"	8	D
13	30	3	00	100	"	19.09.85	27.09.85	8	A
14	30	3	10	90	"	"	"	8	B
15	30	3	20	80	"	"	"	8	C
16	30	3	30	70	"	"	"	8	D

TABLE 8.5

UVS TEST DATA

TEST NO.	HEIGHT (mm)	MC_o (%)	e_o	Sr_o (%)	σ (kN/m^2)	e_F	Sr_f (%)	MC_f (%)	Δe	FINAL SWELL (%)	PROPORTION OF FINAL SWELL AT 40 MINS. (%)
01	14.84	29.4	0.84	91.53	64.73	0.895	102.47	35.07	0.055		
02	14.77	30.12	0.865	89.85	"	0.965	111.41	41.28	0.100	5	80
03	14.77	29.92	1.026	74.26	"	1.258	91.7	45.31	0.232	10.93	84
04	14.71	30.18	1.005	75.40	"	1.424	92.92	52.69	0.419	20.3	83
05	14.92	35.11	0.974	94.26	"	0.964	102.29	37.71	-0.010	- 3.77	95
06	14.86	36.6	1.007	93.78	"	1.019	108.48	42.92	0.012	0.92	100
07	14.82	36.44	1.193	77.77	"	1.295	90.2	45.88	0.102	3.89	62
08	14.85	36.39	1.172	77.96	"	1.4	94.47	52.67	0.228	9.19	76
09	15.04	23.4	1.344	45.52	"	1.286	67.7	33.29	-0.058	3.27	100
10	15.01	23.54	0.753	80.67	"	0.878	117.42	39.95	0.125	7.11	90
11	15.02	24.32	0.92	67.30	"	1.199	93.31	43.94	0.279	14.51	88
12	15.05	24.6	0.914	67.59	"	3.025	42.18	50.81	2.111	22.05	88
13	14.83	29.72	0.851	91.33	"	0.865	153.84	50.89	0.014	0.802	87
14	14.88	32.29	0.872	95.55	"	0.95	111.28	40.97	0.078	4.17	73
15	14.95	30.24	1.023	75.25	"	1.245	89.47	43.75	0.222	10.97	82
16	14.83	45.2	1.225	92.66	"	1.49	96.99	57.55	0.265	11.94	89

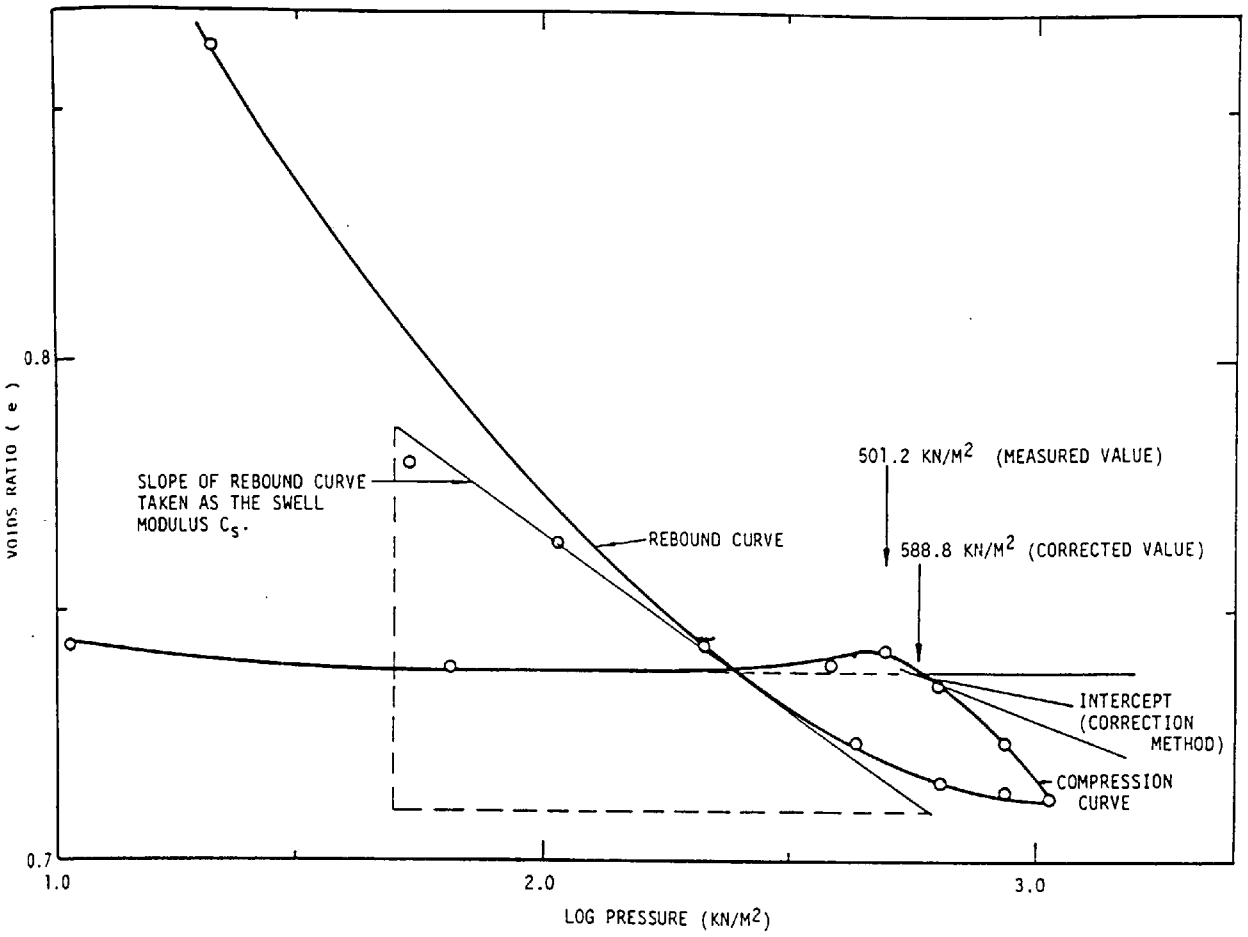

FIGURE 8.1

TYPICAL (e - LOG(P)) GRAPH
(TEST 15)

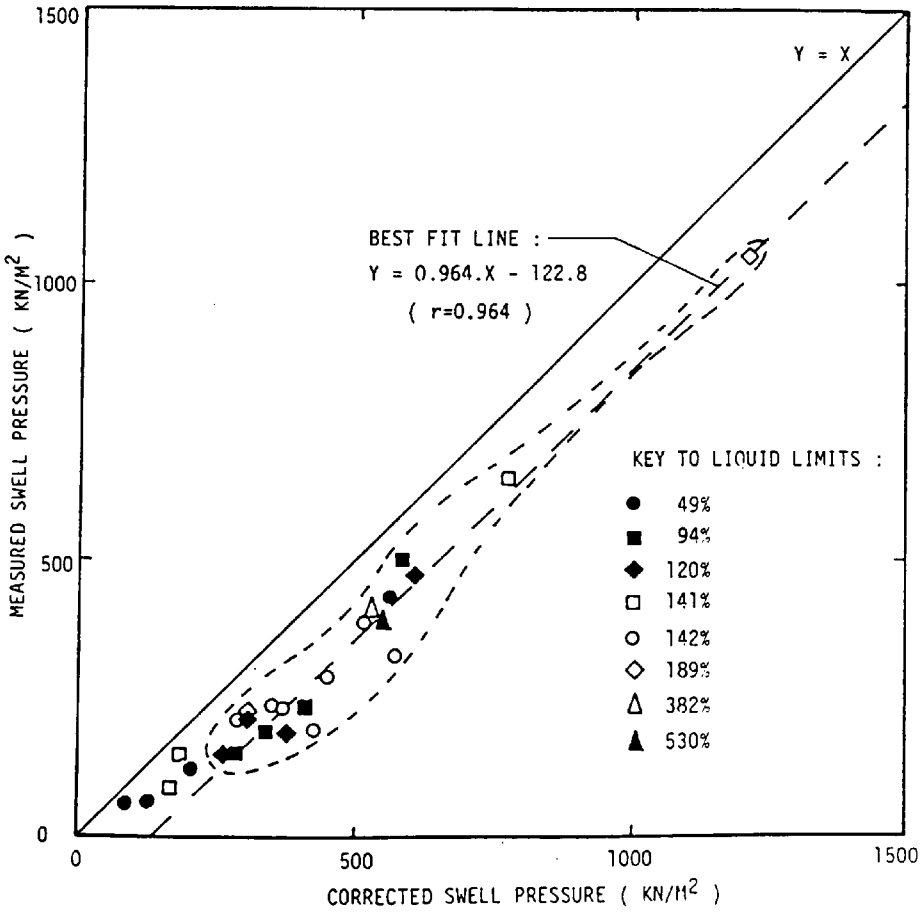

FIGURE 8.2

MEASURED VERSUS CORRECTED
SWELL PRESSURE

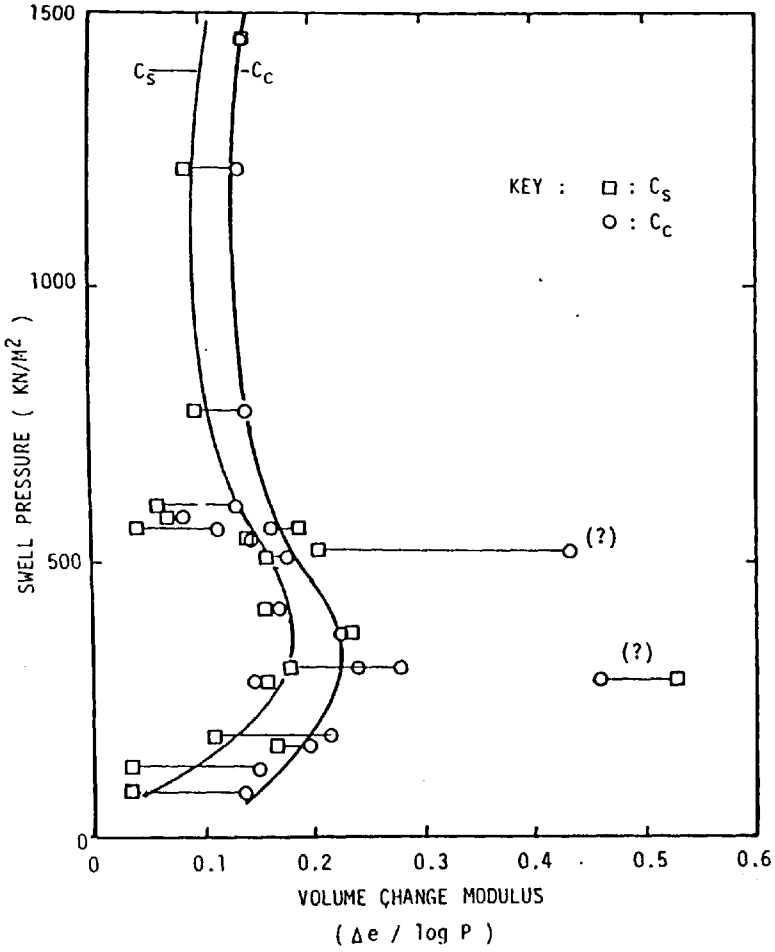

FIGURE 8.3

SWELL PRESSURE VERSUS
VOLUME CHANGE MODULI

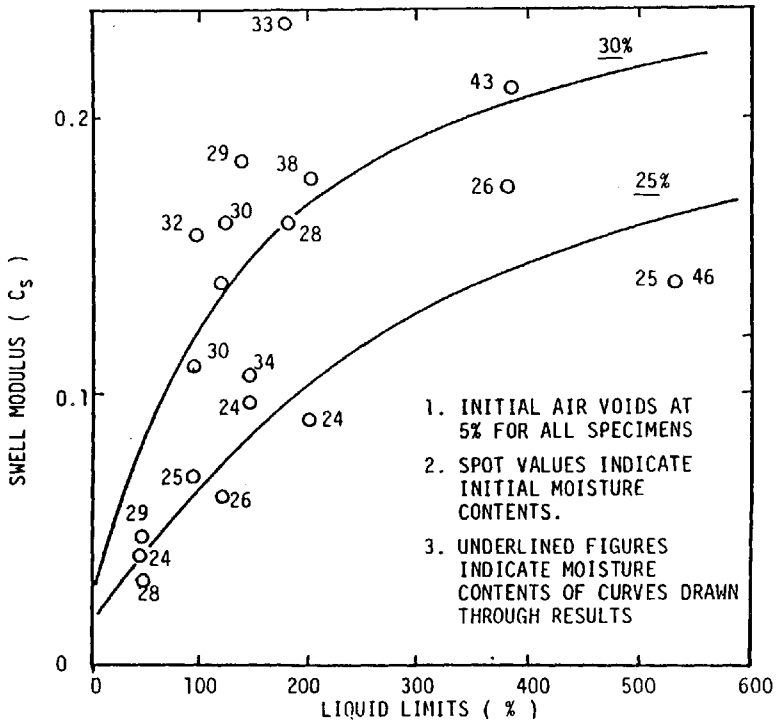

FIGURE 8.4

SWELL MODULUS VERSUS
LIQUID LIMIT

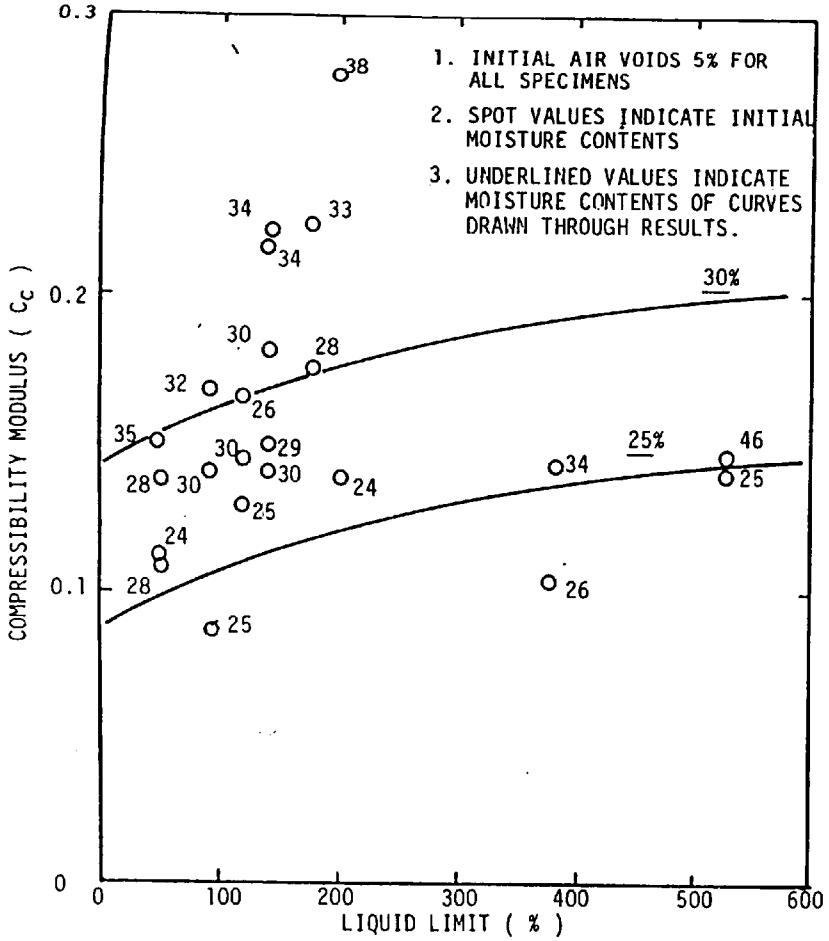

FIGURE 8.5

COMPRESSIBILITY MODULUS VERSUS
LIQUID LIMIT

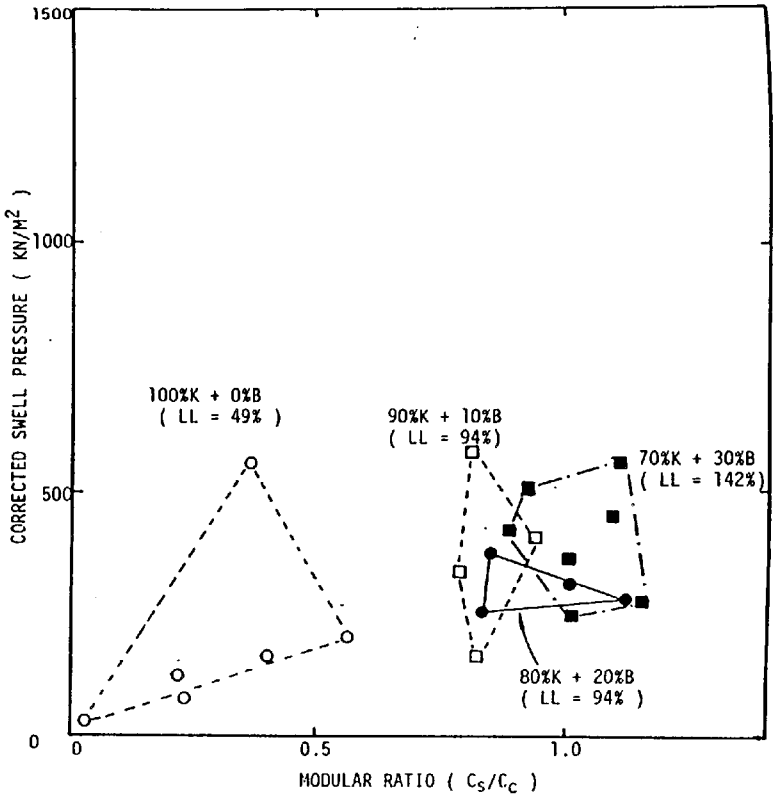

FIGURE 8.6

SWELL PRESSURE VERSUS
SWELL MODULAR RATIO

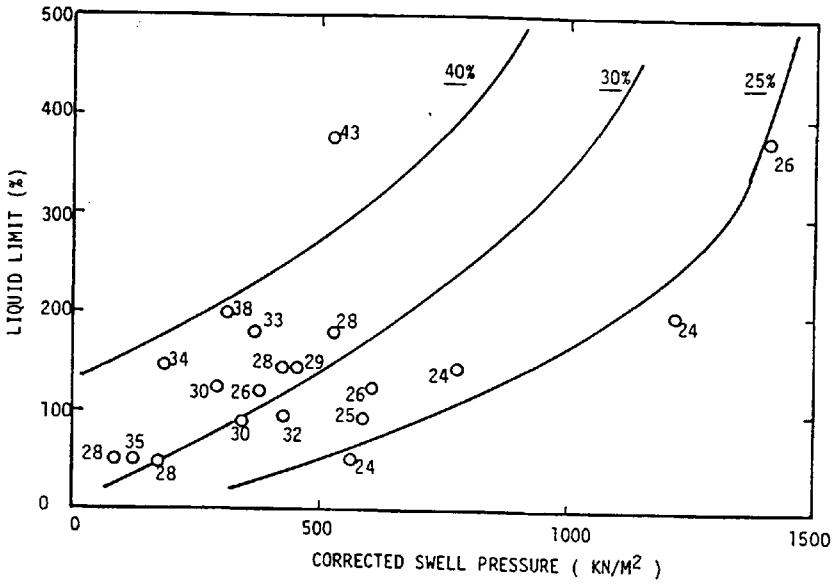

NOTES :

1. INITIAL AIR VOIDS OF ALL SPECIMENS = 5%
2. SPOT VALUES INDICATE INITIAL MOISTURE CONTENTS.

FIGURE 8.7(a)

LIQUID LIMIT VERSUS
SWELL PRESSURE

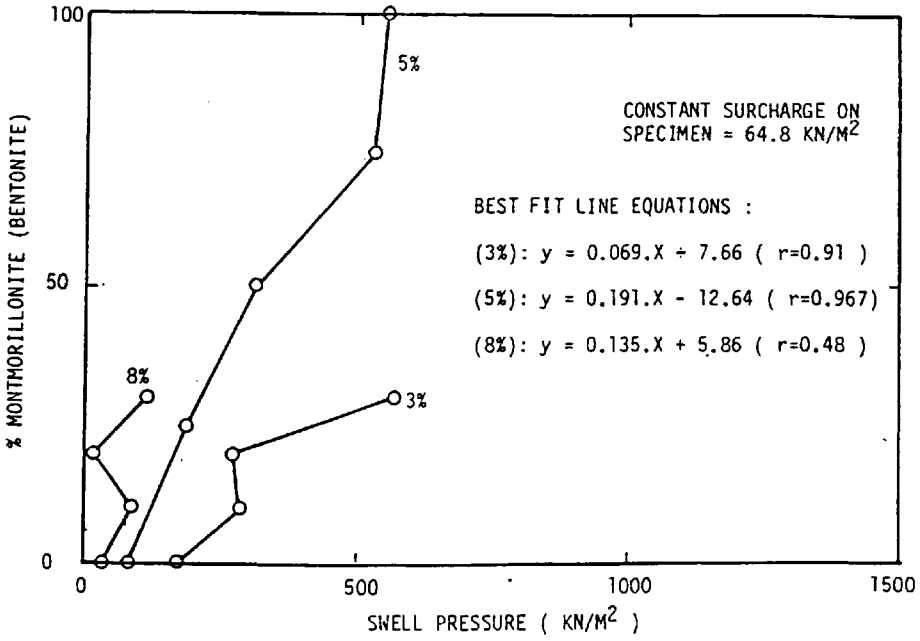

FIGURE 8.7(b)

LIQUID LIMIT VERSUS SWELL
PRESSURE(VARYING AIR VOIDS)

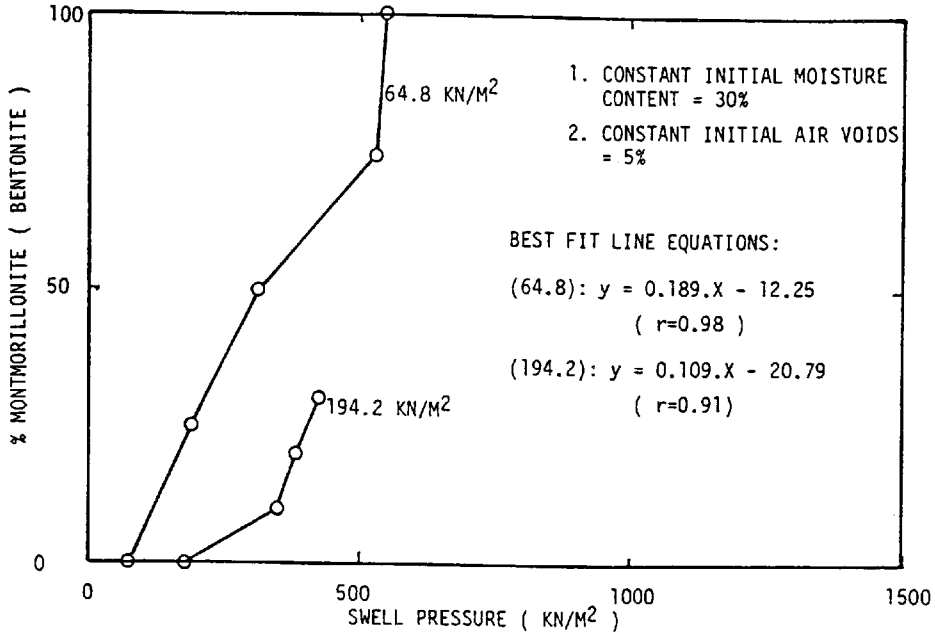

FIGURE 8.7(c)

LIQUID LIMIT VERSUS SWELL PRESSURE(VARYING OVERBURDEN)

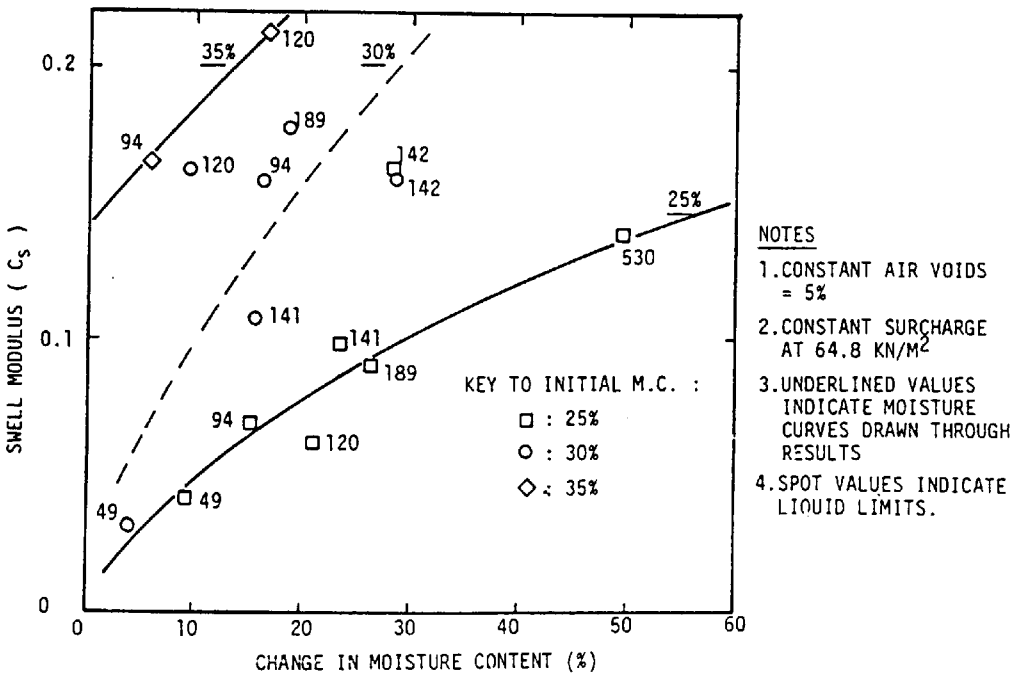

FIGURE 8.8

SWELL MODULUS VERSUS CHANGE IN MOISTURE CONTENT

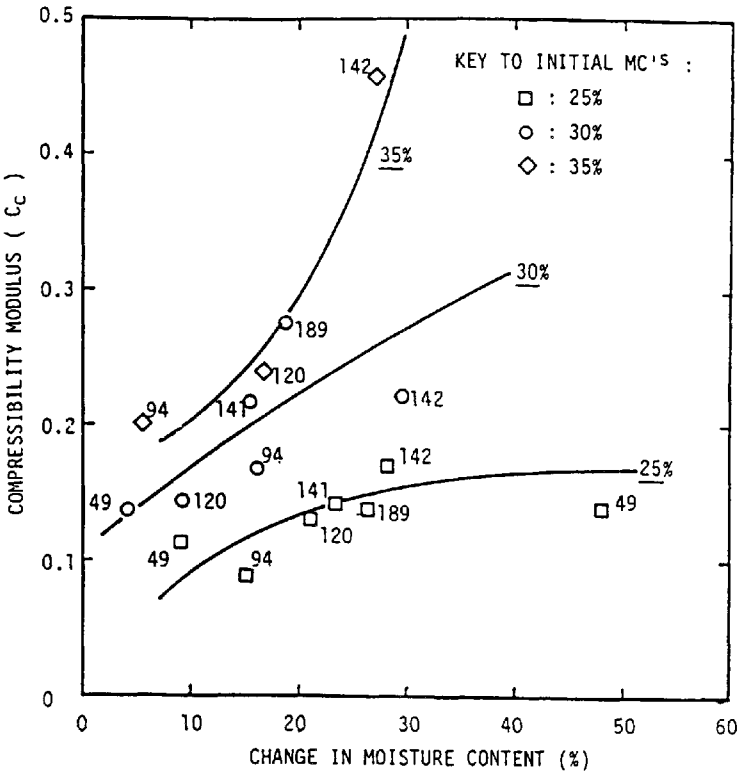

FIGURE 8.9

COMPRESSIBILITY MODULUS VERSUS
CHANGE IN MOISTURE CONTENT

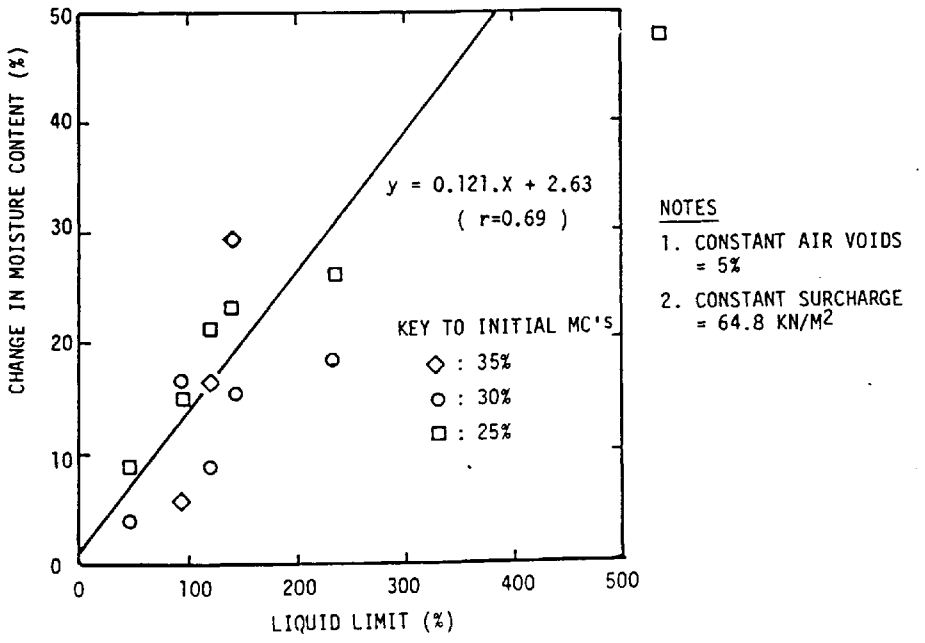

FIGURE 8.10

CHANGE IN MOISTURE CONTENT
VERSUS LIQUID LIMIT

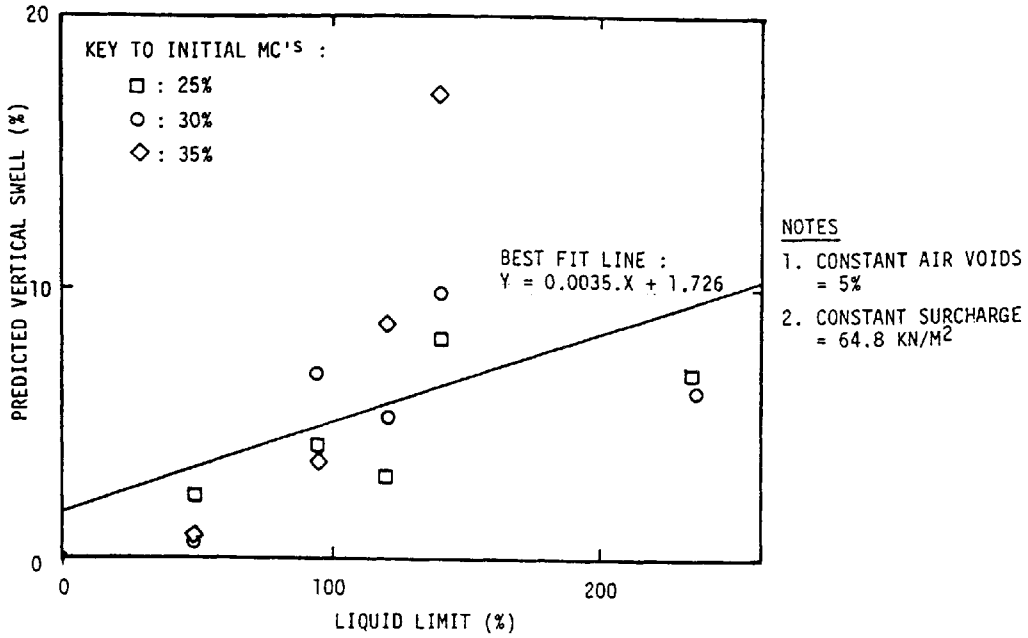

FIGURE 8.11

PREDICTED SWELL VERSUS
LIQUID LIMIT

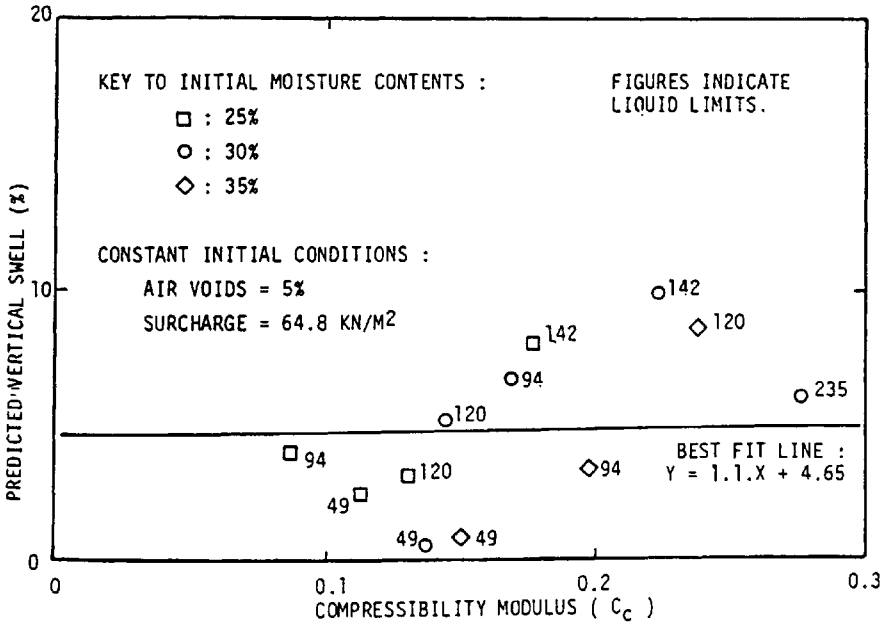

FIGURE 8.12

PREDICTED SWELL VERSUS
COMPRESSIBILITY MODULUS

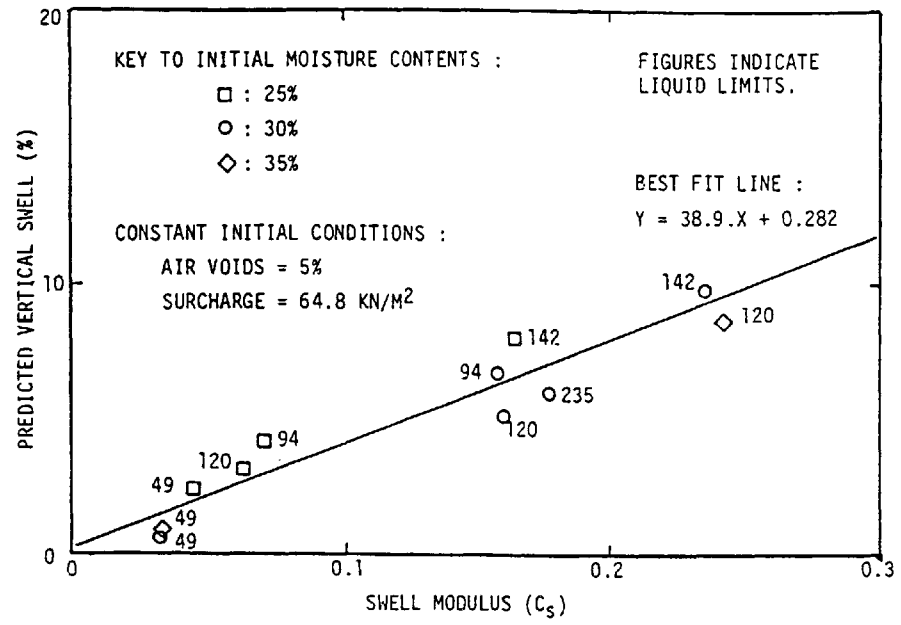

FIGURE 8.13

PREDICTED SWELL VERSUS
SWELL MODULUS

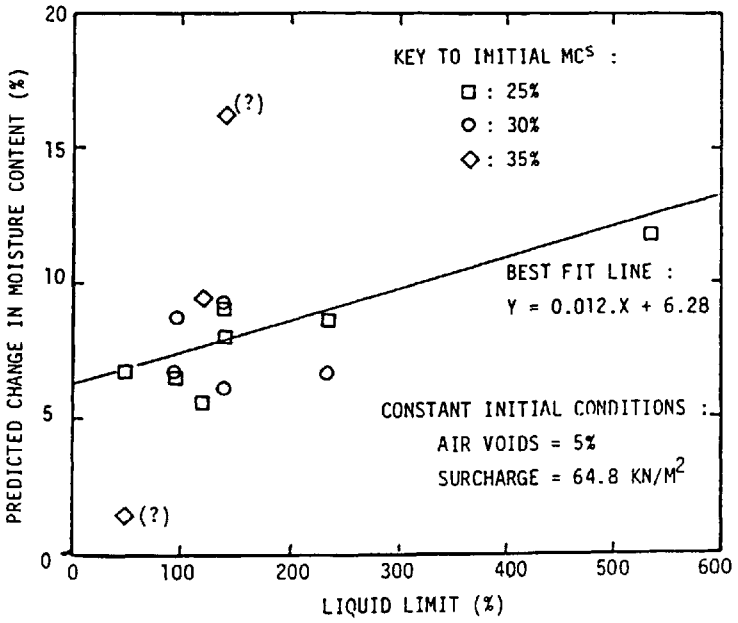

FIGURE 8.14

PREDICTED MOISTURE CONTENT CHANGE
VERSUS LIQUID LIMIT

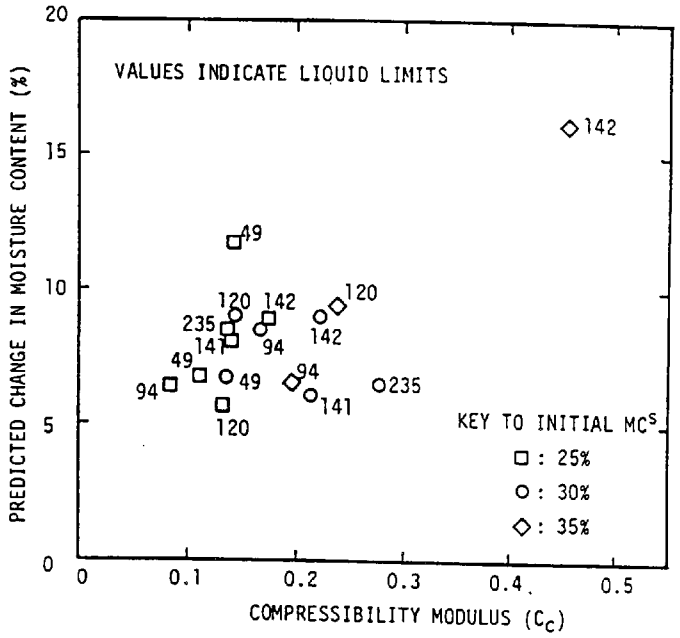

FIGURE 8.15

PREDICTED MOISTURE CONTENT CHANGE
VERSUS COMPRESSIBILITY MODULUS

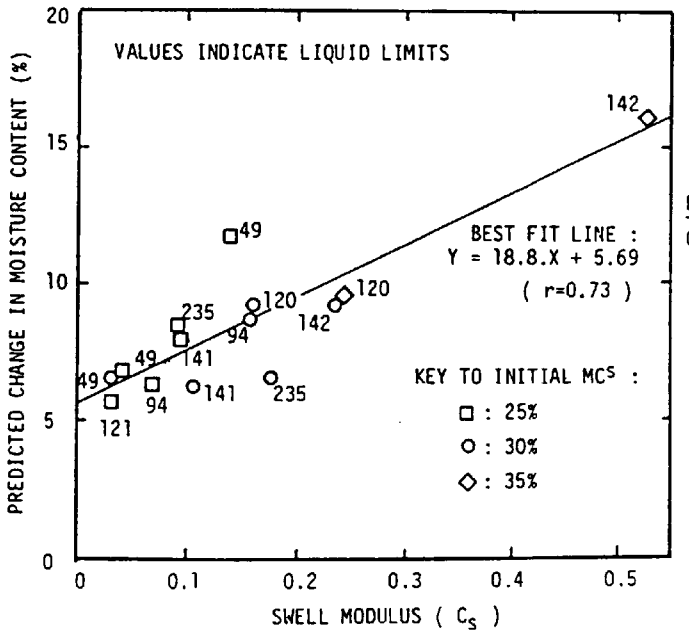

FIGURE 8.16

PREDICTED MOISTURE CONTENT CHANGE
VERSUS SWELL MODULUS

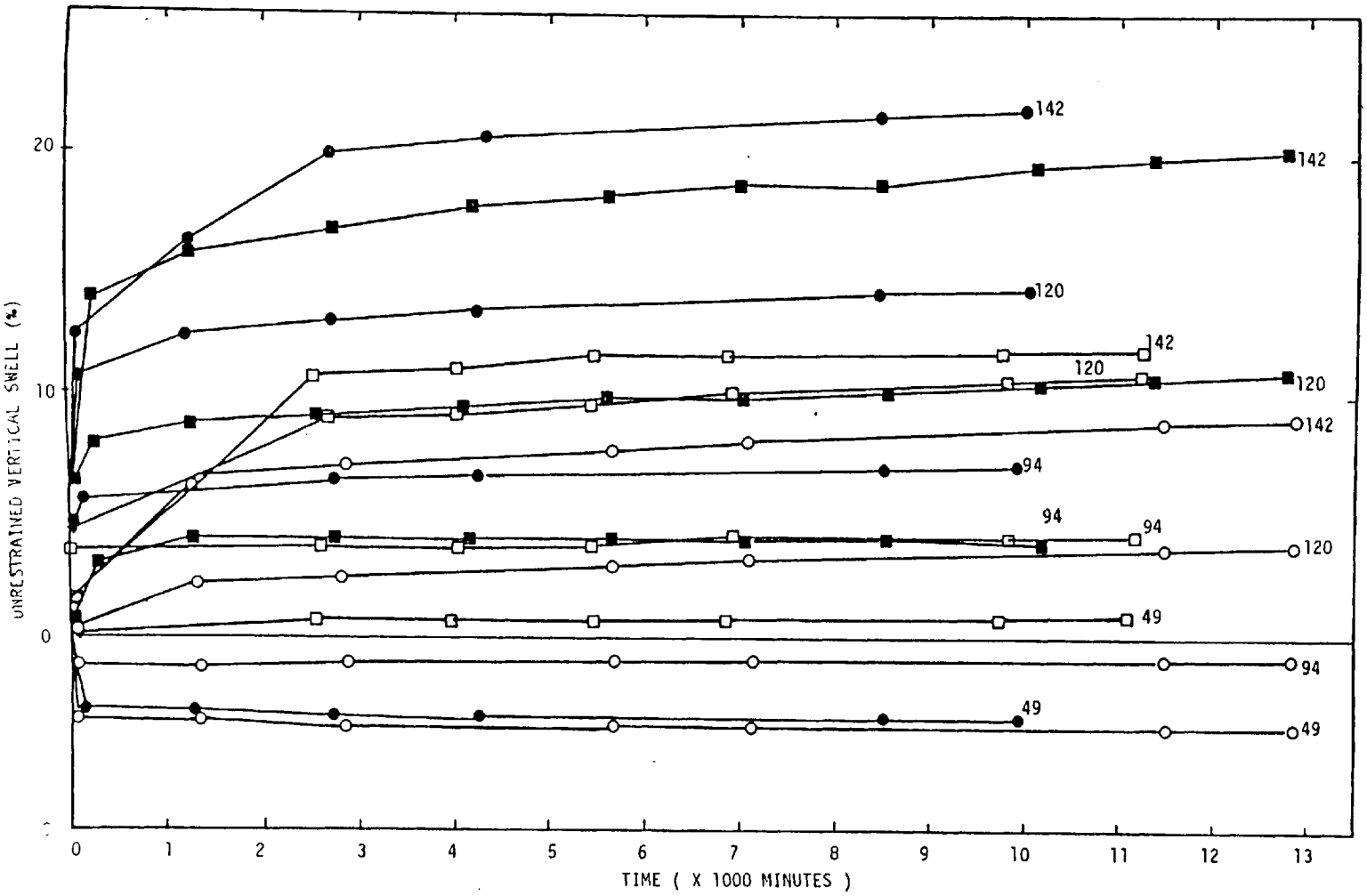

* KEY TO SWELL CURVES :

	MOISTURE CONTENT	AIR VOIDS
■ :	30	5
○ :	35	5
● :	25	5
□ :	30	3

* CONSTANT INITIAL SURCHARGE = 64.8 KN/M^2

* NUMBERS ON GRAPH REPRESENT LIQUID LIMITS.

FIGURE 8.17

SUMMARY OF UNRESTRAINED
VERTICAL SWELL TESTS

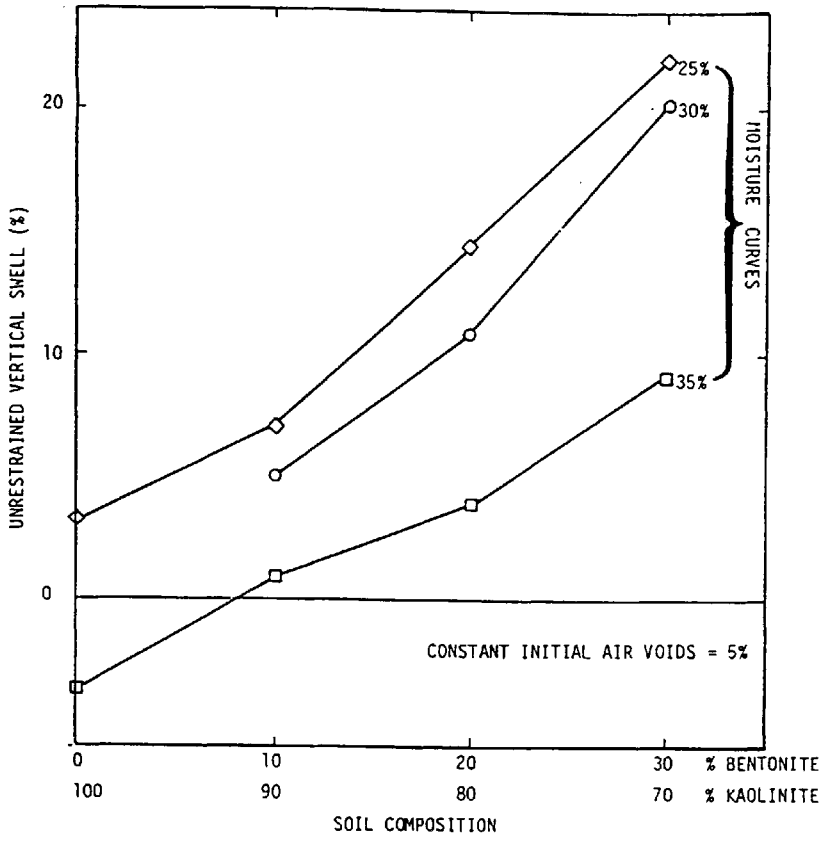

FIGURE 8.18

PERCENT SWELL VERSUS
SOIL COMPOSITION

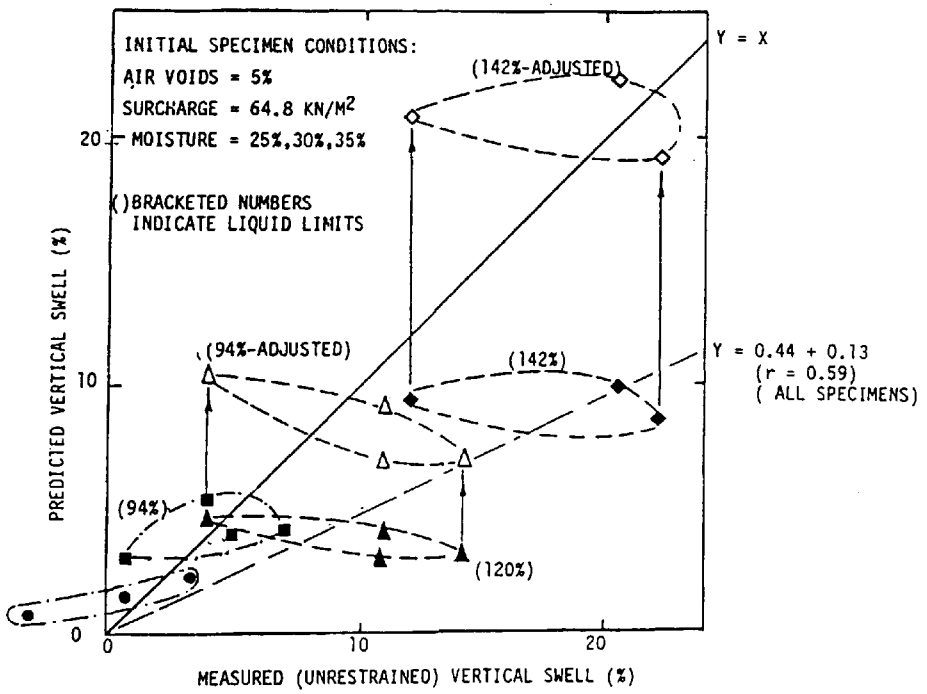

FIGURE 8.19

PREDICTED SWELL VERSUS
MEASURED SWELL

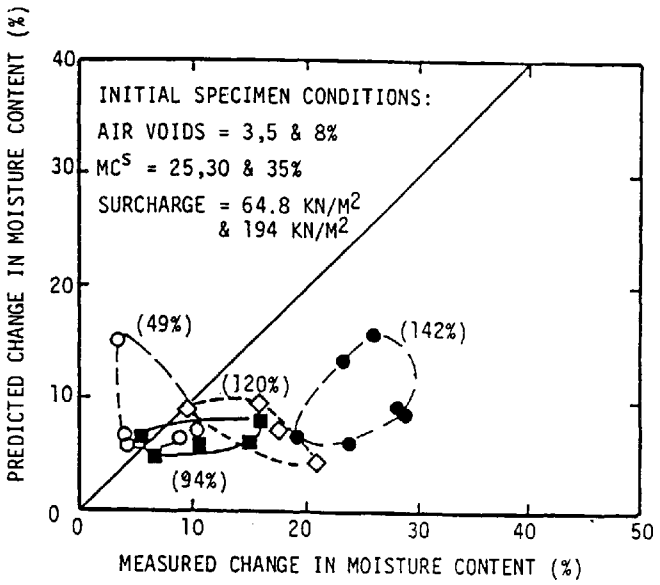

FIGURE 8.20

PREDICTED VERSUS MEASURED
CHANGE IN MOISTURE CONTENT

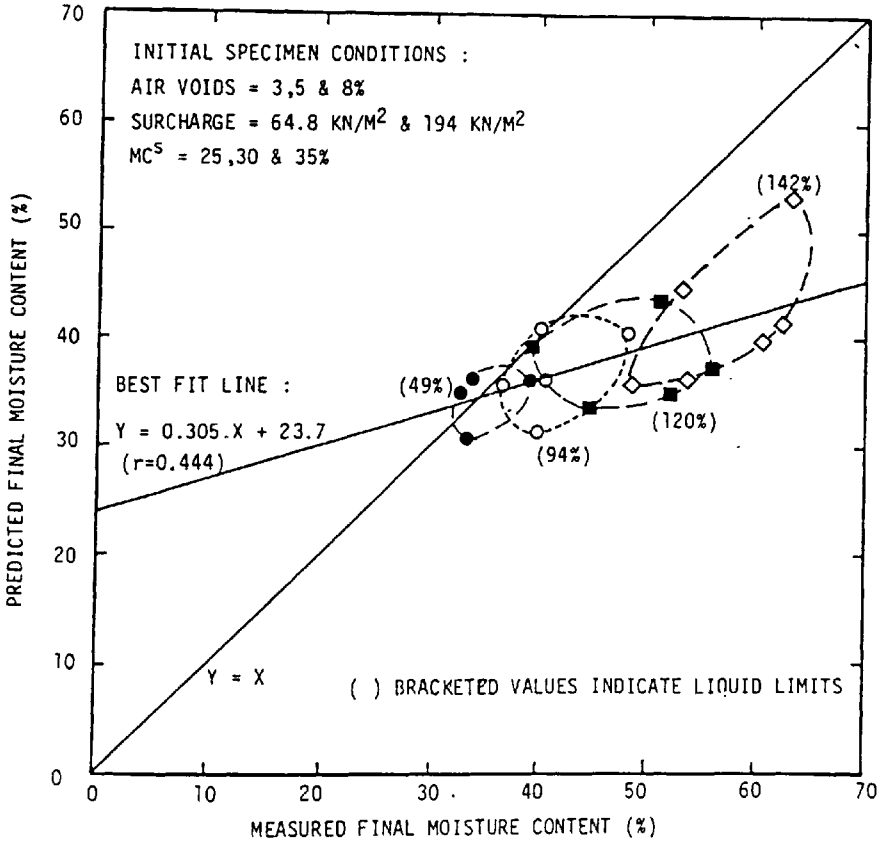

FIGURE 8.21

PREDICTED MOISTURE CONTENT VERSUS
MEASURED MOISTURE CONTENT

CHAPTER 9

EVALUATION OF FREDLUND'S VOLUME CHANGE THEORY

9.1 INTRODUCTION

9.1.1 Background

In the literature review (Chapter 4) it was shown that Fredlund's theory for unsaturated soil might be suitable for predicting volume changes in expansive unsaturated clay soils.

An experimental programme was then formulated to provide data for checking this statement.

The soils used in the programme were, in the main, artificially constituted mixtures of sodium montmorillonite (Bentonite) and kaolinite (china clay); these were mixed in a Kenwood blender and conditioned in sealed containers for 24 hours. The consistencies of these samples are listed in Table 9.5, with liquid limits varying between 49% and 142% (refer also to Appendices A and B).

The programme itself involved two approaches for one-dimensional swell testing.

The first entailed the development of a comprehensive test system (termed stress control apparatus) for controlling the total air and water stresses; the system also provided for measuring the total and water volume changes.

Two specimen sizes were employed; 76mm diameter x 15mm high specimens were housed in a modified 'Rowe' type cell and the 102mm diameter x 30mm high specimens within a cell utilizing four inch triaxial apparatus components. These specimens will be referred to as the

'76mm specimens' and '102 specimens' respectively for the remainder of this chapter.

The stress control apparatus was used to test two aspects of Fredlund's theory :

(a) Null tests : to determine the validity of the stress state variables.

(b) Volume change (uniqueness) tests : to assess the volume change equations.

The second test system was a conventional consolidometer apparatus linked to a chart recorder for continuous data monitoring. This was employed to assess the application of the volume change theory to routine soil tests. Two procedures were undertaken :

(a) Constant volume swell pressure (CVSP) test was used to provide results from which the maximum vertical swell and swell pressure could be predicted upon the basis of the theory.

(b) Unrestrained vertical swell (UVS) test : in the absence of suitable field data, this test was used to generate unrestrained vertical swell data from which the predictions in (a) could be assessed.

The foregoing experimental programme was successfully completed, and the results are presented in Chapters 6, 7 and 8.

Finally, throughout the testing programme, several instances were recorded where a reversal in volume change occurred. The unsaturated soils subsequently exhibited a consistent tendency not to return to their original volume and this is henceforth termed a hysteretic behaviour for the remainder of this chapter.

9.1.2 Aim

The aim of this chapter is to make a 'global' assessment of Fredlund's

theory primarily upon the author's experimental results. This is achieved by :

(a) undertaking a separate critical appraisal of the null, volume change and consolidometer tests.

(b) highlighting the experimental influences and suggesting corrective procedures where feasible.

(c) discussing theoretical aspects where appropriate, and finally

(d) presenting the overall assessment.

9.2 NULL TESTS

9.2.1 General

The aim of null testing was to assess the validity of the stress state variables $(\sigma - u_w)$, $(\sigma - u_a)$ and $(u_a - u_w)$ for describing volume change in expansive unsaturated soils.

This involved simultaneously changing the stress components σ , u_a and u_w by equal amounts (thereby keeping the stress state variables $(\sigma - u_a)$, $(\sigma - u_w)$ and $(u_a - u_w)$ constant) and closely monitoring the total and water volumes.

Since volume change should directly relate to variations of the stress state variables, then a no volume change or 'null' situation was interpreted as validation of the chosen variables.

Several such stress changes were implemented (as far as equipment limitations would permit) with an equalisation period allowed in between each one.

The results were assessed by plotting the measured volume change (resulting from a zero variation of stress state variables) against predicted

volume change (assuming a change in the 'effective stress' state variable equal in magnitude to the previous stress component changes , refer to Figs. 6.13 and 6.14).

A linear regression was then undertaken to determine the best fit line through these data points. The gradient and correlation coefficient of this indicated the extent to which swell behaviour was being observed whereby 0 represents total null behaviour and 1 , zero null behaviour.

The experimental results are separately examined from the point of view of total volume and water volume changes; they are discussed with due regard to the following aspects :

(a) observed null behaviour

(b) reasons for volume change

(c) incompatible behaviour of different specimen sizes

(d) comparison of the author's results with other (published research data)

(e) influence of plasticity upon volume change.

However, the reader is referred in the first instance to the summarising remarks given in Section 9.2.4 to gain an overview of the null tests.

9.2.2 Total Volume Change

The total volume change is the experimentally measured change in volume of a laterally confined specimen. The quoted volume changes are referenced to the initial specimen volume and expressed as a percentage.

The lateral confinement of specimens in this apparatus will inevitably create some boundary effects and may influence total volume changes.

However, since only minimal changes were induced during null testing, then this aspect is not considered to have greatly influenced the results. The influence of boundary effect is considered to be more relevant to volume change testing however, and is therefore further examined in that section.

9.2.2.1 Experimental Observations

The pattern of stress change - volume change behaviour was very consistent for most specimens (Figs. 6.7 and 6.8).

The volume consistently decreased with increasing stress components and vice versa; however, the behaviour was mostly non elastic, and the total volume only returned to its original value following an initial change of less than 0.05%.

The maximum compression and expansion recorded for the total volume change was 0.373% and 0.31% respectively; the compilation of maximum values recorded for each test is given in Table 9.1. The magnitude of these changes tended to increase with liquid limits (Fig. 9.1).

The total volume changes comprised of two distinct phases :

(i) immediate (following stress changes), and

(ii) secondary (time related).

These are discussed together with contributing influences in the following sections.

9.2.2.2 Immediate Volume Change

The immediate volume change was mainly attributed to a combination of non-simultaneous stress changes, compression of occluded air and compliance effects; however, these pose quite different problems and are examined separately.

(a) Non-simultaneous stress component changes

This is believed to have been the main cause of non-null behaviour; the effects were instantaneous and are attributed to the limitations of the present apparatus design. This was evident from the longer time taken by the 102mm cell to achieve a target air pressure compared with the smaller 76mm cells.

This is understandable however, when comparing the relative size of a 4" triaxial pressure vessel with the small air space above the 75mm specimen.

In consequence even presuming an instantaneous change of stress components, the air pressure change in the larger cell always lagged behind that of the smaller one and induced a temporary imbalance of the stress state variables $(\sigma - u_a)$ and $(u_a - u_w)$. The exact influence over volume change depended upon the direction of component stress changes :

(i) following an increase in component stresses, the $(\sigma - u_a)$ stress state variable for the 102mm specimens temporarily increased above that of the 76mm specimens, resulting in a larger percent compression of the former.

(ii) following a decrease in component stresses, the $(\sigma - u_a)$ stress state variable for the 76mm specimens temporarily decreased below that of the 102mm specimens, resulting in the larger percent expansion of the former in the air pressure change upon total volume behaviour, it is not presently possible to make a meaningful correction due to the inconsistent nature of the volume changes so induced.

(b) Compression of occluded air

During the wetting of an unsaturated soil, a certain degree of saturation is reached where the air phase becomes discontinuous; at this point the air is said to be occluded.

The presence of occluded air will cause the water to exhibit increased compressibility and the literature indicates that this occurs between a saturation level of about 85% and 100%.

It is therefore desirable that the influence of occluded air upon the water volume change characteristics be assessed.

Towards this goal two compressibility equations were discussed and applied to the author's results.

The theoretical modelling and experimental measurement of such behaviour has proven very difficult, and few authors have tackled the additional problems associated with volume change in unsaturated soils.

Two approaches were applied to the author's results for the purpose of estimating the air-water mixture volume changes.

The first method is modification of the triaxial test correction proposed by Bishop and Henkel (1962); this accounts for the volume change of the pore air (including that trapped between the rubber membrane and specimen). However, this makes no allowance for the compressibility of water and the stiffening influence of the soil structure.

$$\therefore \quad \frac{\Delta V_v}{V_v} = \left(\frac{u_{ao}}{u_a} - 1\right)(1 - S_o + S_o.H) \qquad (9.1)$$

where ΔV_v = change in voids volume ie $(\Delta V_a + \Delta V_w)$

V_v = volume of voids

u_{ao} = absolute initial air pressure

u_a = absolute current air pressure

S_o = initial degree of saturation

H = Henry's coefficient of solubility $(24.62 \times 10^{-6}$ at 20°C)

The equation accounts for (i) the application of Boyle's law to the air phase and (ii) the solubility of air into the water; examination of results (Table 9.1) indicated that the volume change predicted from each component of equation 9.1 generally exceeded the measured total volume change (Table 9.2).

It was therefore decided to assess another relationship.

A second expression was proposed by Fredlund (1980). The author has examined the derivation of this, and ascertained its close similarity to Bishop and Henkel's expression with the exception that an additional allowance is made for water compressibility :

$$\frac{(\Delta V_w + \Delta V_a)}{V_T} = S_o.n.\beta_w.\Delta u_w + \left[\frac{(1 - S_o) + H.S_o}{(u_a + u_{atm})}\right] . \Delta u_a.n \qquad (9.2)$$

where :

$(\Delta V_w + \Delta V_a)$ = change in water and air volume

n = porosity

β_w = water compressibility = 3.158×10^{-4} in²/lb

= 4.58×10^{-5} m²/kN

The additional allowance for water compressibility further increases the predictions (Table 9.2) above those obtained by Bishop and Henkel's equation (9.1).

All predictions for air-water multiphase volume changes therefore significantly exceeded the corresponding measured total volume changes.

Since both equations (9.1 and 9.2) encompass the effects of air and water only, then it is suggested that they be amended to include the 'stiffening' effect of the soil structure, in order that they can be meaningfully applied to an unsaturated soil (soil-water-air combination).

Further investigation is recommended to ascertain this.

In conclusion, it does not appear possible to make a meaningful correction for the effects of occluded air using the theory at its present stage of development.

Further research on this aspect is highly recommended.

(c) Compliance

System compliance is a non-reversible behaviour, and comprises the extrusion of soil around the loading piston, and the bedding of soil into the porous disc(s) (upper and lower) following specimen loading. The bedding was impossible to measure and despite several attempts, the extrusion also proved difficult to consistently quantify, due to material loss during dissassembly of the equipment. However, it was possible to make an estimate of the amount of material extruded upon the basis of experimental observations. These indicated that clay filled the space between the loading plate and confining ring (thickness of 2mm) and was extruded to a minimum length of at least 2mm.

Estimations can therefore be made upon the basis of these observations for each equipment type (specimen size).

Rowe cell (76.1mmø specimen) :

Confining ring diameter = 76.1mm

Outer loading piston diameter = 75.1mm

Depth extruded = 2mm

$\therefore$ Volume extruded $= \frac{(76.1^2 - 75.1^2)\pi .2}{4} = 237.5mm^3$

$= 0.208\%$ (WRT total volume).

Triaxial cell (104mmø specimen) :

Confining ring diameter = 104mm

Outer loading piston diameter = 102mm

Depth extruded = 2mm

$\therefore$ Volume extruded = $\frac{(104^2 - 102^2)\pi.2}{4}$ = 647.2mm^3

= 0.25%

These estimations represent minimum values, since extrusion was probably a creep related process and continued with time.

The overall effects of extrusion upon volume change were considered to have manifested themselves as follows :

(i) exaggerated compression upon initial loading due to the extrusion of soil out of the cell

(ii) a reduced subsequent expansive behaviour as a result of there being less material within the test cell.

It is suggested therefore, that any corrections be applied to decrease the measured compressions and increase expansions.

Table 9.1 (columns 7 and 8) indicate that compliance is a major contributor to volume changes during null tests. However, despite the remaining volume change exceeding the measuring accuracy of the equipment, the overall magnitude is considered to be below that of engineering significance (maximum values, compression : 0.373%, expansion : 0.31%).

9.2.2.3 Secondary Volume Change

This section assesses the secondary long-term volume changes

observed during null testing; these were mainly attributed to :

(i) the partial recovery of earlier instantaneous volume changes,

and

(ii) time related soil processes such as wetting, diffusion of air through the soil and soil water.

The results indicate that both the magnitude and duration of the secondary effects increased with increasing plasticity.

In the extreme case, the highest plasticity soil mixture (LL = 142%) continued to expand for extended test times up to 19000 minutes (13 days). These tests were curtailed due to practical difficulties and in consequence the volume changes were underrecorded and must be treated with caution. On the other hand, the non expansive, 76mm and 102mm kaolinite specimens (LL = 49%) exhibited a volume decrease for most of the test duration although equilibrium was achieved before 15000 minutes (10.5 days).

The magnitude of volume change (both compression and expansion) increased with increasing liquid limit (Fig. 9.2); however, in consequence of the different percentage magnitudes of volume change from each specimen size, it was only possible to examine the general trends in behaviour.

Finally, the possibility of long term chemical interaction between soil specimen and its confining ring could not be discounted, and was considered during the equipment design phase; this resulted in the apparatus being machined from a corrosion resisting brass stock.

A subsequent examination of the specimens indicated only a slight surface discolouration after testing; upon the basis of this observation therefore, the matter was not further pursued.

9.2.2.4 Compatibility of Volume Change Magnitudes

It must be clearly stated that the overall magnitude of all volume change was minimal; nevertheless, the 102mm specimen volume changes were 20% to 50% greater than those of the 76mm specimens (Fig. 9.1).

This difference is attributed to a combination of : loading system designs, specimen sizes, volumes of the air pressure vessels, difference in compliance effects and sidewall friction.

Some of these have been discussed previously, however, they are all covered below for continuity.

(a) Different loading systems

The 102mm specimen was loaded vertically using a pneumatically driven piston (air cylinder).

Initial evaluation of this unit indicated that provided sufficient lubication (oil) was injected into the cylinder, then friction effects would be minimised, and the piston operate without hindrance; routine maintenance was therefore undertaken in between tests.

Despite minimising friction, the piston was observed as sticking for variations in stress less than 5 psi; overall, however, it must be noted that the results from both cell types were compatible during null testing.

As a final comment, the loading system used in the 76mm diameter (modified Rowe) cell, exhibited no such tendency to stick.

(b) Specimen size

The use of two specimen sizes may induce incompatible data in several ways, however, not all causes would necessarily induce consistently higher volume changes in the 102mm specimens.

For instance, the larger specimens are potentially more susceptible

to variations in preparation quality; resulting variations would be erratic and not consistent as observed.

A more likely explanation is the different equalisation times required by each specimen following a stress change; the equalisation of stresses throughout the 102mm specimens would consistently take longer than in the 76mm specimens. In consequence, stress imbalances and hence volume change would also be greater and continue for longer periods.

(c) Volume of air pressure vessels

The 102mm specimens were enclosed in a very large pressure vessel; in consequence, the air pressure surrounding the specimen took much longer than with the smaller specimens to reach a target pressure.

This resulted in a temporary imbalance of the stress variables and hence a volume change. The erratic nature of this behaviour, prevented the derivation of any meaningful corrections. This is fully discussed in Section 9.2.2.3.

(d) Compliance effects

The earlier estimations of compliance effects indicated that the 102mm specimens exhibited 20% more volume change than the smaller 76mm specimens.

However, the subsequent adjustment of experimental data for these effects failed to eliminate the incompatibility of volume change magnitudes.

(e) Sidewall friction

The author acknowledges that sidewall friction occurs within the apparatus; however, it has little influence over the null test results since the procedure primarily involves 'zero' volume change. (Sidewall friction only affecting movement).

9.2.2.5 Published Data

The objective of the section is to conduct an additional assessment of the author's results by comparing them (where possible) with the limited published data.

Hilf (1956) claimed to have observed minimal volume change following several equal variations of all stress components. Unfortunately, his results are not available for inspection.

Bishop and Donald (1961) conducted a well documented series of 'null' type triaxial tests upon 105mmø specimens of Braehead silt. The pattern of volume change behaviour recorded by them corresponded very closely to that measured by the author; i.e. the specimens compressed upon increasing stress components and vice versa.

Notably, the author's data exhibited a much higher degree of null behaviour than Bishop and Donald; this observation is reinforced by the fact that the author's maximum volume changes were recorded for a much higher plasticity soil than Bishop and Donald's Braehead silt.

Fredlund (1973) conducted a series of null tests on kaolinite and claimed null behaviour for both total and water volumes.

Within the limitations of the experimental technique, his results correspond to the overall pattern and magnitude of behaviour observed by the author for total volume change (Fig. 6.1); his (Fredlund's) maximum compression and expansion values were 0.22% and 0.05% respectively, as compared to 0.19% and 0.04% respectively, recorded by the author.

Fredlund's results are comparable to the author's because they have been adjusted to account for his larger specimen size (200mm high as opposed to 30mm) .

This correlation was undertaken since both Fredlund and the author, referred volume changes to their respective specimen sizes; it is clear from this that a similar (real) volume change occurring in both will appear

much smaller in Fredlund's equipment, and the correction is intended to take this into account.

In conclusion, the author's results indicate that the stress state variable for unsaturated soils (as tested by other researchers) are equally applicable to expansive unsaturated soils.

9.2.2.6 Range of Soil Types

In addition to the kaolinite specimens, three other synthetic soil mixtures were tested, with the aim of establishing the influence of plasticity and expansivity upon the validity of the stress state variables.

The results indicated that despite the volume change magnitude (hence non null behaviour) rapidly increasing above liquid limit values of 100%, the overall magnitude of volume change was still sufficiently small to be termed null (in the context of engineering behaviour).

9.2.2.7 Saturation

As noted previously, it was not originally intended to test a range of saturations. However, as a result of variations in the initial values, it was possible to conduct a limited assessment of the influence of the initial degree of saturation upon volume changes.

The initial saturation values varied from 72% to 95%; the total volume change was clearly influenced by initial saturation (Fig. 9.3) and significantly increased for $S_r > 80\%$.

This level of saturation approximates to that suggested by Aitchison, 1960 ($\cong$ 85%) as marking the lower boundary above which occluded air bubbles begin to form in unsaturated soils.

The above correspondence in behaviour is important, and this aspect should be pursued in conjunction with further experimentation for the

purpose of accurately fixing the saturation ranges to which the theory can be applied.

9.2.3 Water Volume Change

This section covers the water volume changes recorded during null testing; the quoted values represent the actual readings when referenced to the initial total volume of the specimen (expressed as a percentage).

9.2.3.1 Experimental Observations

The author's results indicated a smaller overall water volume change (i.e. higher degree of null behaviour) than that recorded by Bishop and Donald (1961) and Fredlund (1973) (see Fig. 9.4).

Initial experimental data indicated a continuous inflow of water to all specimens (Figs. 6.11 and 6.12), the rates of which were well related to the stress components (Figs. 6.9 and 6.10).

Notably, however, the total volume exhibited no change (relatively) during the same periods; this in turn suggests that the observed water volume behaviour was due to an experimental influence resembling leakage rather than due to a soil related process.

Bishop and Donald (1961) and Fredlund (1973) noted similar difficulties although it is not clear from their work how these were resolved.

In consequence, the author's continuous water volume changes were quantified and used as 'correction' factors to give a truer indication of the phase behaviour.

The corrected water volume records exhibited a maximum variation of only 0.025%; this can be considered below the level for engineering significance, and would appear to validate the stress state variables for unsaturated expansive clays.

9.2.3.2 Range of Soil Types

Despite the magnitude of water volume change increasing with liquid limits (Fig. 9.4) the overall values are still much smaller than the total volume changes.

The author therefore considers that null behaviour is being observed for all specimen types.

9.2.3.3 Saturation

The water volume changes exhibit little relation to the degree of saturation (Fig. 9.5) and neither conflicts nor corroborates those observations made for the total volume.

9.2.4 Concluding Remarks

The stress state variables were adequately verified by the results despite limitations of the test system.

The observed total and water volume changes for all specimens (liquid limits between 50% and 142%) were minimum; however, it must be noted that the observed total volume changes were up to ten times greater than the water volume change results.

Despite testing only a limited range of saturations, the author notes that the magnitude of volume change significantly increased with saturations above 80%. It is suggested that this may be due to the formation and increase in the amount of occluded air, although further work upon this aspect is recommended.

Total volume changes were mainly attributed to (i) non simultaneous changing of stress components, (ii) compression of occluded air and (iii) compliance effects ('bedding in' of apparatus and specimen at outset of test).

Efforts were made to ascertain the individual contribution of the above effects; however, the correction for compliance appears to presently provide the only realistic adjustment.

Initial readings of water volume change indicated a constant stress related increase, resembling leakage. The application of a correction proved very successful, indicating a minimal overall variation in volume.

On the basis of the above evidence therefore, it is suggested that the stress state variables $(\sigma - u_a)$, $(\sigma - u_w)$ and $(u_a - u_w)$ (as employed in Fredlund's volume change theory) are suitable for describing volume changes in expansive unsaturated soils of liquid limits up to 142%.

9.3 VOLUME CHANGE TESTS

9.3.1 General

The second test procedure conducted in the complex stress control apparatus was the volume change test. The primary aim of this was to provide data by which Fredlund's volume change equations could be assessed for use with unsaturated expansive clays.

The procedure is also called the 'uniqueness' test since it is basically used to indicate whether there is one and only one relationship between the chosen stress state variables.

The experimental procedure involves subjecting a specimen to small stress increments along three stress paths and allowing equalisation after each pressure change. Using the volume change from any two of the increments, it is possible to compute two corresponding volume change moduli. Fredlund's equations can subsequently be used to compute the volume change along any other stress path.

This is then compared with the measured value, although an overall assessment of the volume change equation is only made after considering all results from several stress sequences upon the specimen.

For this purpose, the predicted volume changes (described above) were plotted against the measured values.

Invariably the results did not plot exactly on the 45° line (perfect correspondence), and a best fit line was determined by regression analysis through the points.

This section initially contains an assessment of the observed behaviour and encompasses such aspects as the regression analysis of data, plasticity influence, test system compatibility and reversals in volume change.

Unlike the null test discussions, the section is primarily concerned with assessing total volume change predictive capability; in consequence the discussions are biased towards total volume change although water volume behaviour is discussed for continuity.

Finally, the apparatus and test procedures are again examined due to inconsistencies within the test results.

9.3.2 Observed Behaviour

9.3.2.1 Linear Regression Analysis

This was intended to aid assessment of the volume change predictions and involved plotting the predicted volume changes against the measured values. Invariably, the results did not plot exactly on the 45° line (perfect correspondence) and a best fit line was determined by regression analysis through the points (refer to Fig. 9.6 for typical example).

This yielded a gradient and correlation coefficient which can be thought of as a guide to prediction accuracy and consistency respectively, whereby the closer to unity they are, the better the prediction and accuracy is considered to be.

Since the predicted volume changes were based upon coefficients derived from experimental results, then the author assumed that both predicted and measured volume changes were subject to (the same in this case) influences. The comparison of these results was therefore considered justifiable since both sets of variables should be affected to the same extent thereby not affecting the validity of the measured versus predicted plots.

The results indicate that the predicted total volume change varied between 81% and 94% of measured value with corresponding correlation coefficients of 0.64 to 0.67 (Fig. 9.7).

The water volume change mirrored this behaviour but displayed a wider variation of results :

predicted = 62% - 106% measured values (correlation coefficients 0.32 - 0.89, Fig. 9.8) .

Despite these promising observations, the magnitudes of recorded volume changes in the two test cells (Fig. 9.9) were clearly different and this aspect is discussed in the following sections.

In an attempt to be consistent with Fredlund's work, the results were also examined assuming only the measured volume change as subject to influence.

Notably, the predicted volume changes were then calculated as being between 6% and 23% greater than the measured values. This behaviour was apparently confirmed with relatively high associated coefficients of correlation (between 0.64 and 0.97) (refer to Figs. 9.10).

The water volume change correlations again reflected the total

volume behaviour, (refer to fig. 9.11)

9.3.2.2 Sidewall Friction

The Problem :

As noted earlier, some interaction will inevitably occur between the specimen and its laterally confining brass ring.

During the volume change tests, this influence is thought to have manifested itself as a restraining force or 'friction' at the specimen boundary (sidewall) and hindered vertical volume changes of the specimen.

Previous Work :

Sidewall friction was first highlighted as a problem on one-dimensional testing by Taylor (1942). More recently Madhare (1970) amended this work to encompass cohesive as well as granular soil types. He suggested that the coefficient of friction is dependent upon : (1) soil type, (2) applied pressure, (3) degree of consolidation and (4) lubricant type.

Clearly, implementation of the friction coefficient is a lengthy process because of these numerous considerations.

Notably, however, Madhare (1970) recorded a 50% minimum decrease in the coefficient after coating the cell wall with silicone grease.

Discussion

Despite the undoubted existence of sidewall friction, the author does not believe that this will prevent volume change; however, the reaction time of the soil specimens to stress changes will probably increase as a result.

This difficulty is considered to be offset somewhat as a result of the extended time periods allowed between stress changes.

In the 'classical' example of side friction, the specimen tends to bulge at its central point, with the degree of bulging being largely dependent upon the specimen width/depth ratio.

The width/depth ratios of both specimens were approximately 4:1 and not therefore considered immune to bulging; however, a close examination of the specimens immediately after testing indicated no signs of this behaviour.

The problem of sidewall friction is not considered as unduly affecting the assessment procedure, because both the measured moduli and subsequent predictions were subject to the same influences; in consequence, both values are affected to the same extent and are justifiably compared provided that the specimens are subjected to comparable ranges of stress change and directions of volume change. The question of compatibility between specimen sizes in relation to side wall friction is also not considered to be significant; this is because the proportion of sidewall area to specimen size is the same for the smaller and larger specimen sizes - the proportion of friction induced compared with the specimen volume and hence expansive potential is also constant.

Conclusions

The assessment of volume change equations can proceed despite the influence of sidewall friction. This may include a comparison between predicted and measured values since both will be subject to the same errors; however, the actual magnitude of these values will be low. Although such 'under measurements' should not affect this assessment procedure, they will have a direct influence upon the consolidometer results used for the prediction of insitu behaviour.

9.3.2.3 Compatibility of Test Systems

The 76mm specimens exhibited approximately ten times the volume change (%) observed for the larger 102mm specimen (Fig. 9.9).

This conflicts with the earlier evidence of compatibility observed during null testing, and has necessitated that the results be separately examined upon the basis of specimen size.

The influence causing incompatibility are considered to be the same as those outlined for null testing (9.2.2.4); they include : (1) loading systems, (2) specimen dimensions, (3) pressure vessel volume, (4) sidewall friction, and (5) compliance effects.

However, in consequence of changes in the stress state variables, greater percent volume changes resulted and the loading system, pressure vessel volume and sidewall friction effects (i.e. factors influencing movement in the system) are considered to have contributed much more to the overall behaviour.

9.3.2.4 Plasticity Influence

The incompatibility of volume change magnitudes prevented the direct comparison of results from the small and large test cells for plasticity influence.

In consequence, it was not possible to assess the 'global' influence of specimen plasticity upon the effectiveness of the volume change equations.

However, certain common characteristics were identified through separately considering the behaviour of each specimen size, and these are indicated below :

(a) the overall accuracy of total volume change predictions increased with increasing specimens plasticity (Fig. 9.7). (The only exception being the specimen with LL = 94%). Notably, this conflicts with

earlier observations made during null testing.

(b) The accuracy of water volume change prediction also increased with specimen plasticity in the case of both 102mm specimens, and one of the 76mm specimens (Fig. 9.8). The only exception (LL = 94%) exhibited the opposite behaviour; however, this confirms earlier observations of inconsistency noted for this specimen.

9.3.2.5 Reversals in Total Volume Change

The volume change test comprised of repeating a sequence of changes in total (σ), air (u_a) and water pressures (u_w); the intention of this was to induce (as far as possible) a continuous increase in the total and water volumes.

However, earlier work by Fredlund (1973) indicated that the total volume decreased following an air pressure decrease. The author recognised that this must have induced some hysteretic effects into the volume behaviour (see later); however, an examination of alternative testing procedures indicated that they would require a considerably increased number of specimens to cover the same range of stresses.

In view also of the time limitations of the research project, the test procedure after Fredlund (1973) was therefore adopted, and the observed effects of hysteretic behaviour are discussed below.

Firstly, it must be noted that, the total volume change reversal was also recorded by the author, for all specimens tested (LL = 49% - 142%); the results (Fig. 9.9) indicate that the degree of hysteretic behaviour increased with the number of volume change reversals experienced.

An examination of the influence of an air pressure (u_a) reduction upon the stress state variables gives a better insight into the hysteretic

effects experienced in these soils.

A reduction in the air pressure (u_a) simultaneously :

(a) increased the 'total' stress state variable $(\sigma - u_a)$ and

(b) decreased the 'suction' stress state variable $(u_a - u_w)$.

These changes are normally associated with a decrease and increase in total volume respectively; however, the specimen actually underwent a volume decrease.

It is suggested therefore, that the total stress variable $(\sigma - u_a)$ exerts more influence over total volume than the suction stress variable $(u_a - u_w)$.

This observation was verified by another assessment procedure which indicated the same behaviour (Section 7.5.4(a)).

Finally, the author acknowledges that the magnitude of volume change reversals will not only depend upon an experimental influence, but also be closely related to the soil type.

This is another aspect of hysteretic behaviour that requires further investigation.

In conclusion therefore, it is not possible to presently make a meaningful adjustment to the tests results for reversals in volume change. Despite this, the volume change test procedure was adopted for practical reasons.

The lack of provision for hysteretic effects, appears to be one of the main limitations of Fredlunds theory; in consequence, the cyclic loading/unloading of soils cannot be adequately modelled. Nevertheless, the theory does appear suitable for situations not involving a stress change reversal.

9.3.2.6 The Stress Sequence

Figure 9.12 illustrates a typical stress-total volume change path as followed by one of the specimens during volume change testing. It is noted that the degree of agreement between the measured and predicted values increased as the stress sequence progressed. It is suggested that this may have been due to an averaging of various influences occurring over each stress change sequence.

The same general behaviour was noted for all specimens tested (see Fig. 9.13 for final volume change comparison).

9.3.2.7 Saturation

The specimens were tested with an initial saturation range of between 70% and 90%.

However, upon the basis of the results, it appears that the correspondence between measured and predicted volume changes is unaffected by variations in the initial degree of specimen saturation. (Refer to Figs. 9.14 (total volume) and 9.15 (water volume)).

9.3.3 Equipment Related Influences

The general operating characteristics and behaviour of the two test cells during volume change testing were very similar (Figs. 7.1 to 7.5); however, the magnitudes of volume change measured in each cell were distinctly different (Fig. 9.9), and this observation has required that the output from each test cell be examined separately in order to make a meaningful overall assessment of the results.

Initially, it was intended that the effects of differing specimen size be evaluated, in addition to the other volume change properties. In consequence of this requirement, and general equipment availability

at that time, two cell designs (although similar in principle) were adopted, and were therefore subject to slightly varying influences.

In hindsight, for the purpose of consistency, it would have been better to use one specimen size and cell type only, thereby facilitating the cross-checking of all data.

Despite the near compatibility of test cells indicated by Table 6.11, it is recommended that the 76mm diameter cell be duplicated for this purpose (instead of the modified triaxial cell) because :

(1) the cell design is more responsive to changes in total volume,

(2) the air pressure vessel is smaller and will therefore respond to pressure changes much faster,

(3) the loading system contains fewer moving parts, and will therefore experience minimal seating problems.

However, it is also suggested that the rubber jack (bellows type) loading systems be replaced with a rolling diaphragm assembly as developed by Bellofram Corp. (USA). This will alleviate the possibility of any friction within the loading system.

The incompatible magnitudes of volume change exhibited by the two specimen sizes are believed to be primarily attributable to the following varying design factors : (i) loading systems, (ii) specimen sizes, and (iii) non-instantaneous changes in air pressure.

All of the abcve are discussed earlier.

9.3.4 Operating Procedures

Operating procedures are not considered as significantly influencing the volume change behaviour; any influences which did occur are believed

to have been very consistent for both cell types due to the near identical control systems employed.

9.3.5 Concluding Remarks

The objective of these tests was to experimentally measure the volume change moduli of a range of unsaturated expansive clays (Table 7.6) from which Fredlund's volume change equations could be assessed.

The results indicated that the 76mm specimens exhibited up to ten times greater percent volume change than the 102mm specimens (Fig. 9.9); in consequence, it was necessary to assess the volume change behaviour of both specimen sizes upon the basis of common trends in behaviour as opposed to a direct comparison of volume change magnitudes. This was justifiable since the assessment of Fredlund's constitutive equations was primarily concerned with comparing measured and predicted values as opposed to determining absolute values.

Several causes of incompatibility had previously been identified during null testing; these were reconsidered in view of the increased volume change; notably, the significance of sidewall friction is considered to have increased due to its close relationship with volume change. However, since predictions were made using the same measured values (and hence subject to the same adverse influences), then the plotting of one against the other was considered justifiable.

Another cause of unwanted effects was volume change reversal.

In consequence of the air pressure reductions during stress sequencing, the total volume change reversed from expansion to consolidation.

The result of this was to reduce all subsequent volume changes below what would otherwise have occurred (Fig. 9.9).

However, the effects of this influence were not uniform, and a

meaningful correction cannot presently be devised.

In conclusion, the results indicate that after applying available corrections, the predicted total volume changes varied between 81% and 94% of the measured values.

The water volume change behaviour generally mirrored this, although a greater spread of data was apparent; predicted volume change varying between 62% to 106% of the measured value.

The degree of correspondence between measured and predicted total volume changes consistently decreased with increasing liquid limits (Fig. 9.7); however, no clear patterns emerged from the associated water volume change behaviour (Fig. 9.8). In addition, the degree of initial saturation also exhibited little noticeable influence upon the above degree of correspondence.

The volume change tests have therefore indicated that Fredlund's volume change equations, 'near uniquely' describe the behaviour for expansive unsaturated soils of the plasticity range LL = 49% to 142% .

9.4 CONSOLIDOMETER SWELL TESTS

9.4.1 General

The consolidation tests were conducted to provide data by which the application of Fredlund's theory to a 'routine' geotechnical test could be assessed. For this purpose, the constant volume swell pressure (CVSP) test was chosen since (a) it has already seen limited use with the theory on low-expansion soils and (b) a more representative value of swell pressure is obtained since it is measured at the original specimen condition prior to consolidation and expansion procedures. The test therefore involves the measurement of swell pressure and total volume change

moduli and is conducted in two stages.

The first stage involves flooding the specimen, then preventing expansion by increasing the vertical load; the maximum surcharge required to maintain constant volume is considered to equal the swell pressure (hence the test name).

The second stage involves incrementally loading the specimen beyond the 'swell pressure' value, and finally unloading (in increments) to obtain the consolidation and rebound curves respectively.

The data (typically plotted in Fig. 8.1) is then used to determine the compressibility and swell moduli respectively.

The swell potential was subsequently predicted by inserting the swell pressure and swell modulus into the volume change equation. To the author's knowledge, however, the (CVSP) test had not been employed for laboratory produced expansive specimens, in consequence there was a lack of suitable data by which the accuracy of the predictions could be assessed.

This problem was resolved by conducting a series of unrestrained vertical swell (UVS) tests (using the same apparatus and identical soil types) to provide suitable data for comparison purposes.

As the name implies, the (UVS) test involves flooding the specimen and permitting it to expand freely to its maximum volume.

As with the other test procedures discussed earlier, the (CVSP) test has not, to the author's knowledge, been employed with highly expansive soils.

This deficiency was exploited by preparing a range of artificially reconstituted clay mixtures to examine the range of plasticity/ expansivity likely to be encountered in the field.

9.4.2 Swell Pressure

9.4.2.1 Purpose

The swell pressure is measured for two purposes during CVSP testing.

The first is to give the engineer an idea of the uplift pressure that can be expected; the practical value of knowing this is not doubted, and the results are discussed later.

The second and most important reason from the point of view of this project is to use the swell pressure value in conjunction with Fredlund's constitutive equations for predicting volume change. In this respect, the swell pressure value (after correction for disturbance effects - see later) is assumed for analysis purposes to exert an equivalent influence to the initial stress state or matric suction. This has been discussed at length in Chapter 8 and 5.

The literature indicates that the measured swell pressure value is most susceptible to disturbance effects and these are discussed in the next Section.

9.4.2.2 Production Disturbance

Fredlund (1983) and others have shown that the effects of sampling disturbance reduce the swelling potential of expansive clays.

Although the author's specimens were not obtained from the field, they were subject to a loading/unloading cycle during laboratory preparation; in consequence, there is some justification in adjusting for the disturbance effects.

(a) Correction to swell pressure

Most of the developments for predicting the influence of sampling disturbance have tended to be empirically or semiempirically derived (Nagaraj and Srinivasamurthy, 1985).

One such technique by Casagrande (1948) for predicting the over-

consolidated clays, was modified by Fredlund (1983) for correcting the measured swell pressure value. This was subsequently chosen by the author in view of its previously successful record.

The author's results indicate that the corrected swell pressure was greater than the measured value by a constant amount, such that :

$$\text{(measured swell pressure)} = 0.964\ \text{(corrected swell pressure)} - 123$$

$$r = 0.964$$

The consistent results (Fig. 8.2) indicate :

(i) consistent experimental and correction procedures

(ii) sampling disturbance correction appears independent of the soil type and more related to the type and amount of disturbance.

However, the rebound moduli of specimens with high liquid limits (> 200%) were too large to enable application of the correction technique; therefore, the technique is considered to presently be limited in its use to the primary range of soil types (LL = 50 - 142%). This aspect is further discussed later.

Despite this, the correction technique worked consistently for the bentonite/kaolinite soil mixtures used; this is largely attributed to the consistent disturbance effects experienced by the specimens during laboratory preparation.

The author believes that the method will be less consistent when applied to field soils due to the variations in sampling technique. This aspect requires further examination.

(b) Correction for predicted swell

Another way of presenting the sampling disturbance correction is to illustrate its influence upon swell predictions.

This was undertaken in Fig. 9.16, and the pattern of behaviour is seen to mirror that of the swell pressure correction in Fig. 8.2.

In view of the common specimen production technique employed for all consolidometer testing it is suggested that this correction could be used for all consolidometer test samples - including the UVS tests.

It is noted however, that such a correction to the UVS results would not improve the overall assessment (i.e. the theory underpredicting swell).

Finally, since the swell pressure and swell correction graphs (Figs. 8.2 and 9.16) were derived from the consolidometer equipment, then the results should not be applied to the more complex stress-controlled criteria employed for the null and volume change testing.

9.4.2.3 Predicting Swell Pressure

Fredlund's theory does not presently encompass the prediction of swell pressure.

His volume change equations utilise experimentally measured moduli and it is suggested that a similar approach might be possible for swell pressure predictions.

However, efforts to relate his volume change moduli to the swell pressure (Figs. 8.3 and 8.6) have not proven fruitful with the author's data.

This aspect is nevertheless important, and warrants further investigation.

9.4.3 Total Volume

The results indicated that the volume change was accurately predicted

for specimens of liquid limits up to 94% (correlation coefficient = 0.78). Above this value, (and up to LL = 142%) the predicted swell was lower than the measured value by a constant ratio (Fig. 8.19), such that :

(predicted swell) = 0.44 (measured swell)
(correlation coefficient = 0.6).

However, a similar comparison between the initial degree of saturation and difference between measured and predicted total volumes does not exhibit any clear relationship. (ref. Fig 9.19)

9.4.4 Water Volume Change

Unlike with the earlier stress control apparatus, the water volume change moduli were not measured during consolidometer testing. Instead, the water volume changes were calculated upon the basis of the predicted total volume change and classical soil relationships (assuming a 100% final degree of saturation).

The final specimen moisture contents were measured and provided a means of assessing the 'predicted' changes.

The results indicated that the moisture changes were predicted with some accuracy for the kaolinite specimens (LL = 49%); however, for higher plasticity specimens (i.e. up to LL = 142%) the final moisture content was underpredicted by a constant ratio (Fig. 8.21) :

(predicted' final moisture content) = 0.305 (measured final moisture content) + 0.24

(correlation coefficient) = 0.444)

The underprediction in water volume change is largely attributed to the excessively high final moisture contents of high plasticity specimens; this was largely caused by additional water being absorbed following the unloading and dissassembly of equipment, and reflected in some (impossibly) high final saturation levels(table 8.2).

9.4.5 Factors Affecting Volume Change

The three main aspects of the CVSP testing procedure are considered to be (i) theoretical, (ii) experimental, and (iii) data interpretation. These are separately discussed in the following Sections.

9.4.5.1 Theoretical

Fredlund's equations are a modification of earlier work by Biot (1946) and Coleman (1962); these were derived upon the basis of continuum mechanics, and do not therefore justifiably describe volume change behaviour for cases of discontinuous water and air phases (<25% and 85% to 100% saturation respectively).

However, during the CVSP test, the specimens are flooded with water, and usually pass straight fron one continuous phase state (25% to 85% saturation) to another (approximately 100% saturation).

In consequence, the inherent saturation restrictions of the theory although limiting, should not prevent its use with the CVSP test.

9.4.5.2 Experimental Procedure

This Section refers to those aspects of experimental procedure (within the CVSP test) which may have contributed to the volume change being underpredicted by a constant ratio.

(a) Rebound branch (CD) of the CVSP test results (Fig. 9.17)

One of the main assumptions made during Fredlund's swell prediction method is that the measured rebound branch (CD) is parallel with that of the assumed analysis branch (BF). If this were correct, then it would imply that the same swell could be anticipated irrespective of the initial voids ratio.

However this seems unlikely,since the results (fig 9.18) clearly indicate that the swell(rebound) modulus decreased with increasing initial volume.

This implies that the measured rebound moduli were too large and should be reduced; however, since the predicted swell values were already too small then correction of the results for this effect would only further increase the difference between measured and predicted values.

9.4.5.3 Data Interpretation

Data interpretation is the final aspect of the CVSP test which may have influenced the volume change predictions.

This encompassed extracting the swell pressure and swell modulus values from the experimental data; and these were subsequently used as the main variables in the volume change equation.

$$e = - C_s . \log \left(\frac{FST}{IST}\right)$$

e = change in void ratio

C_s = swell modulus

FST = final stress state

= overburden + change in total stress and final water pressure

IST = initial stress state = corrected swell pressure.

The potential of these values for influencing swell prediction cannot therefore be over-emphasised and they are individually discussed below.

(a) Swell modulus

The final operation of the CVSP test involves the incremental unloading of the specimen to obtain the rebound curve; the swell modulus is determined by drawing a tangent to this.

This is standard procedure for most CVSP tests, however in the case

(i) the specimens may require many weeks to reach maximum swell and clearly, such a timescale is unrealistic for a 'routine' type test.

(ii) a high maximum swell may exceed the measuring capacity of the apparatus, thereby resulting in a loss of specimen and associated measurements.

In consequence, the swell modulus was obtained by ensuring that the tangent drawn to the rebound curve, also passed through a point corresponding to the original voids ratio (after Fredlund, 1983).

This proved to be a consistent approach, and answered the above criticisms; however, initial analysis of the data has indicated that the swell is being underpredicted by a constant ratio for the test soils with liquid limits between 94% and 142%.

This is considered to be primarily due to the swell modulus measuring threshold (i.e. e_o) being too low.

It is suggested that this problem might be offset by drawing the tangent at a higher voids ratio value.

However, verification of this proposal is not presently possible, since most CVSP test specimens were only rebounded above their initial void ratios by a relatively small amount. In view of this, and as an interim solution, the author suggests predicting the swell of the high plasticity soils (LL = 94% to 142%) by using the regression equation devised earlier (Fig. 8.19). The corrected results are indicated upon the same diagram and appear to work well. The successful measurement of the swell modulus is of great practical importance, and further work to examine the 'full' extent of the rebound curve for high swell soils is recommended.

(b) Swell pressure

The 'measured' swell pressure can be consistently determined from the

experimental graph (typically Fig. 8.1); however, as shown earlier, it must be corrected for disturbance effects.

The author notes that the correction procedure cannot be meaningfully applied where the swell modulus (for high plasticity soils) exceeds the compressibility modulus.

This is an inherent deficiency of the correction method which would only be aggravated by the earlier suggested increases in swell modulus. It is therefore suggested that when the swell modulus exceeds the compressibility modulus, the measured swell pressure value of high plasticity soils (LL = 94% to 142%) should be corrected using the regression information derived from earlier plotted data (Fig. 8.2).

9.4.6 Summarising Remarks

The results indicated that the total volume change was accurately predicted for specimens with liquid limits up to 94% (cc = 0.78). Above this, volume change was underpredicted by a constant ratio (0.44 times measured value, cc = 0.6). The water volume changes were also underpredicted but by a larger ratio (predicted final water content = 33% measured value + 24%,correlation coefficient = 0.444).

The application of Fredlund's theory to the constant volume swell pressure test still does not encompass the prediction of swell pressure. Rather, the measured value is used in combination with the swell (rebound) modulus for predicting volume change.

The swell pressure was noted as being susceptible to disturbance effects during preparation, and Fredlund's modification of Casagrande's correction method was adopted. This worked well with specimens of liquid limits up to approximately 200%, and it is suggested that the regression

equation derived from Fig. 8.2 presently be employed to change measured volume changes from specimens of higher liquid limits.

In view of the close relationship between swell pressure and predicted swell, a similar graph is proposed, for predicting the influence of sampling disturbance upon the predicted swell (Fig. 9.16).

It is suggested that this will be applicable to all tests conducted in the same consolidometer using the test soil types.

Various aspects of the CVSP test concept and procedure were examined in an effort to determine the cause of underpredictions; however, the results did not indicate a firm reason for this behaviour.

An examination of the data interpretation procedure indicated that the underpredictions could at least be attributed in part to an incorrect measuring of the swell modulus. However, this observation could not be fully tested due to limitations of the available data, hence further work on this aspect is recommended.

The influence of the degree of initial saturation upon the correspondence between measured and predicted volume changes was not clear from the results (Figs. 9.14 and 9.15). However, this is not considered significant, since the difficulties relating to occluded air (as outlined earlier) are thought to have played only a limited effect upon the CVSP results since the specimens are totally immersed in water and therefore assumed 'saturated' within the bounds of engineering practice.

9.5 DISCONTINUOUS PHASES

9.5.1 Theoretical Aspects

One of the fundamental assumptions of the theoretical model is that all phases (solid, water and air) are continuous - i.e. interconnected.

This permits the stress fields of each phase to be superimposed and the subsequent derivation of stress state variables and constitutive equations (refer to Appendix E)

In practice, the phases are very often not continuous; in such instances, Fredlund's theory is not applicable in its present form and further work is necessary to examine such aspects.

A critical appraisal of the literature has indicated the following limitations :

(i) The theory is applicable (on the basis of a continuum) for soils with saturation levels between 25% and 85%.

Below 25% the soil dries such that the water phase is discontinuous; between 85% and close to 100%, the air phase becomes occluded and hence discontinuous.

(ii) The theoretical model also applies to the free swelling condition where the specimen passes from the (25% to 85%) saturation zone to near 100% saturation; this is because both stages comprise of continuous phases. However, the intervening zone (85% to 100% saturation) cannot be justifiably modelled using the current theory.

(iii)The test specimens were not cracked or fissured, however, field specimens may be damaged, and in such instances all phases will be disrupted and the theory not applicable until water is imbibed to generate sufficient swell to close the cracks.

9.5.2 Experimental Aspects

9.5.2.1 Stress Control Apparatus

This apparatus was fundamentally based upon the axis translation

technique after Hilf (1956) which has been widely employed for use with a variety of unsaturated soils exhibiting varying saturation levels.

The technique assumes that a change in air pressure (u_a) will induce a similar change in the water pressure (i.e. $\Delta u_a = \Delta u_w$) ; this behaviour has been shown to specifically work for deaired water only (Hilf, 1956; Bishop and Donald, 1961; Olsen and Langfelder, 1965).

However, in the case of unsaturated soils, the air may exist in a free or occluded state; the combination of air bubbles and water will then behave as a compressible mixture, and the actual water pressure will be less than the amount applied by the control system.

This was almost certainly the case for most test specimens to some extent in view of their close proximity to the occluded zone.

This behaviour appears to have been verified by observed total volume changes which increased considerably above saturation level of approximately 80%.

In conclusion, the accurate prediction of occluded air effects appears to be beyond current theoretical and technological developments. However, this is a crucial aspect of unsaturated soil testing and deserves further development.

9.5.2.2 Consolidometer Apparatus

One of the main assumptions during consolidometer testing is that the flooded specimens eventually reach 100% saturation.

The author very much doubts that this actually occurs, and believes that small air pockets will remain within the sample for some considerable time.

However, the recorded swell pressure is still considered to represent the maximum value within a very small tolerance.

Following measurement of swell pressure, the specimen is further loaded in increments to obtain the compression curve.

The author believes that these high loadings will drive most of the remaining free air into solution, thereby ensuring that the rebound curve will be measured for a relatively saturated soil.

9.6 FINAL DISCUSSIONS

The individual aspects of different test procedures were discussed in the previous Sections, and are now combined for the purpose of assessing Fredlund's theory.

9.6.1 Validity of the Stress State Variables

The 'building blocks' of Fredlund's theory are the stress state variables, to which, the engineering behaviour (in this case volume change) is related. Fredlund derived these variables (i.e. $(\sigma - u_a)$, $(\sigma - u_w)$ and $(u_a - u_w)$) in a similar manner to Terzaghi (1936) for saturated soils, by considering the stress equilibrium across a cube element.

Since the engineering behaviour is controlled by the stress state variables, then no volume change should occur provided they remain constant.

This principle was used to assess the variables, by subjecting the specimens to equal variations of the component stresses and thereafter closely monitoring the phase volumes.

The results indicate that despite limitations of the test system, the total and water volume changes were minimal for the soils tested.

Total volume change varied from -0.373% to + 0.31% and the water volume change from -0.02% to +0.02%, for the range of bentonite/kaolinite mixtures tested (LL = 49% to 142%).

The initial saturation levels varied from 72% to 95%.

The magnitude of total volume change considerably increased for initial saturation levels above 85% (Fig. 9.3); this is consistent with the behaviour of the occluded air/water mixture anticipated in this range (see later for further discussion).

The water volume change behaviour on the other hand was not as clear with the plotted data exhibiting considerable scatter (Fig. 9.5).

Despite this, the total volume behaviour was sufficiently promising to recommend further work on this range of saturations.

The total volume change behaviour was clearly accentuated with increasing liquid limits (Fig. 9.1); however, the overall magnitude of change remained minimal.

The author suggests that from a theoretical viewpoint, Fredlund's assumptions of continuous soil air and water phases over the entire saturation range have been oversimplified, and this is supported by other authors observations.

Aitchison (1961) and others have indicated that an unsaturated soil will pass through several distinct stages of saturation during the wetting and drying process; some of these stages encompass discontinuous phases during which the basic assumptions of continuity will not prevail.

The author therefore suggests that the theoretical model is not presently universally applicable and must be restricted in use to those saturation stages involving continuous phases.

Although the project did not involve studying the full range of saturation, the literature indicated that continuous phases (soil, water and air) can be expected between approximately 25% and 85% saturation.

The fully saturated condition is also considered to consist of continuous phases, i.e. soil and water.

However, a special case arose during the author's consolidometer swell testing when the specimens were flooded and changed from an unsaturated condition (25% to 85% saturation) to near fully saturated conditions.

This was special because, although the theory does not apply to the intervening saturation range, (85% to 100%), the swell predictions were acceptable since they were based upon volume change moduli measured after complete saturation of the specimen (and therefore related to continuous phase condition).

In conclusion therefore, the 'null' test results infer that Fredlund's stress state variables do work for the range of expansive unsaturated soils tested (LL = 49% to 142%) .

However, the author suggests that since the stress state variables were derived assuming a continuum, then application of the theory must (presently) be restricted to saturation states involving continuous phases (25% to 85% saturation - and also 100% saturation).

9.6.2 Volume Changes

Fredlunds work was assessed by comparing the volume change predictions made using his constitutive equations with corresponding experimentally measured values; in consequence, the correct measuring of the volume change moduli for the equations cannot be overstated.

Despite the test methods having been previously employed to assess volume changes in unsaturated soils, this is the first time they have been directly applied to a range of expansive clays. Experimentation was divided into consolidometer, and the more involved stress control testing using 102mm and 76mm diameter specimens.

(a) Total volume

The results indicate that the total volume change was consistently under predicted irrespective of the test procedure for all soils

to the predicted total volume change, and assuming a final saturation of 100%.

In consequence, it was not surprising that water volume change predictions resembled (in behaviour) the corresponding total volume values.

These particular results are therefore not considered significant and are ignored for the remainder of this discussion.

(c) Plasticity

The correspondence between predicted and measured total volume changes consistently decreased with increasing liquid limits for all results.

This trend is illustrated for the volume change (stress control) test results in Fig. 9.7, and supported by similar observations in the consolidometer swell tests (Fig. 8.19).

However, in the case of the (CVSP) testing there were indications that swell could be predicted with reasonable accuracy with specimens of liquid limits up to 94%.

The water volume predictions derived from volume change (stress control) testing did not indicate any clear pattern of behaviour and remained relatively constant, irrespective of liquid limits.

(d) Saturation

The range of initial specimen saturation levels was limited to (70% - 90%) since the main emphasis of the test programme was to investigate ranges in liquid limits.

In consequence, it was not surprising that the examination of the effects of saturation levels upon volume change (Figs. 9.14 and 9.19) should not reveal definite trends in behaviour.

(e) Volume change reversals

A change in one or more of the component stresses may cause the direction of volume change to reverse. The result of this behaviour upon unsaturated soil is to cause a permanent volume change irrespective of whether the original stress conditions are restored.

This behaviour (termed hysteretic in the context of this investigation) is not covered by Fredlund's theory; however, he has presented a 'correction procedure' for estimating the influence of stress reversal (sampling disturbance) upon the swell pressure measured during the CVSP tests.

This was applied to the author's results and found to exert little influence over the final degree of correspondence between measured and predicted swell values.

The author notes that such procedures have little or no theoretical basis, and the correction factors once determined are limited in application to specific soil types and stress conditions.

It is therefore suggested that the theory be ideally applied to situations not involving a reversal in the direction of stress change. However, the author recognises that this situation cannot always be avoided (e.g. consolidometer testing of field and laboratory produced specimens); in such instances, underpredictions should be expected and comparison tests (such as those described in Chapter 8) conducted, if at all possible.

(f) Swell pressure

Fredlund's theory can certainly be used to represent most stress states within unsaturated soils, including the swell pressure. However, the use of the constitutive volume change equations and associated experimentally derived moduli are presently considered

unsuitable for predicting the swell pressure (refer to poor correlations between volume change moduli and swell pressure, Figs. 8.3 and 8.6). Nevertheless, the prediction of swell pressure is a potentially important practical application of Fredlund's work, and further investigation of this aspect is recommended.

(g) Discontinuous phases

In view of situations involving discontinuous phases, Fredlund's theory is not presently suitable for modelling the volume change behaviour of unsaturated soils in this condition (since one of the basic assumptions of the theory is the existence of a continuum).

The author suggests that the approximate saturation range (25% - 85%) noted by many authors' as comprising continuous phases be provisionally taken as the operational limits; although not intended to cover this aspect, the author's null test results apparently verified this by indicating a more erratic behaviour of the theory above saturation levels of approximately 80% (Fig. 9.3). However, comparable observations made during the volume change (stress control) tests were inconclusive.

Further work is therefore required to examine this aspect.

TABLE 9.1

MAXIMUM TOTAL VOLUME CHANGES RECORDED DURING NULL TESTING (INCLUDING CORRECTIONS FOR COMPLIANCE EFFECTS)

SPECIMEN	LIQUID LIMIT (%)	MAX COMPRESSION (%)	STRESS CHANGE psi	MAXIMUM EXPANSION (%)	STRESS CHANGE (p.s.i/KN/M^2)	COMPLIANCE ADJUSTED (%) COMPRESSION	EXPANSION
NR01	49	0	-	0.14	-20 /-138	-	0.04
NR02	94	-0.29	20	0.164	-20 /-138	-0.04	0.064
NR03	142	0	-	0.41*	-10 /-69	-	0.31*
NT01	49	-0.44	10	0.032	-10 /-69	-0.19	0
NT02	94	-0.44	5	0.17	-10 /-69	-0.19	0.07
NT03	120	-0.623*	10	0.183	-10 /-69	-0.373*	0.083

1. VOLUME CHANGE CONVENTION : EXPANSION +ve
   COMPRESSION -ve
2. * SIGNIFIES MAXIMUM RECORDED VALUES

TABLE 9.2

COMPARISON OF ACTUAL AND PREDICTED VOLUME CHANGES OF THE AIR-WATER MIXTURE.

SPECIMEN	MEASURED VOLUME CHANGE(%) (total)	BISHOP & HENKEL (%)	FREDLUND
NR0101	-2.05	-4.1	-4.4
	0	-1.8	-2.1
	0	-0.8	-0.91
	0	0.9	1.02
	0.12	2.5	2.74
NR0201	-1.15	-4.9	-5.12
	-0.29	-0.8	-1.1
	-0.29	-0.35	-0.5
	0	0.35	0.5
	0.164	1.0	1.2
NR0301*	1.17	-6.0	-6.3
*	0.33	-0.7	-0.8
*	0.04	-5.9	-0.7
	0.25	0.7	0.8
	0.41	0.9	0.9
NT0101	-0.80	-7.6	-8.0
	-0.35	-2.8	-3.0
	-0.44	-2.3	-2.0
	0	2.7	3.0
	0.032	3.5	4.0
NT0201	-1.92	-8.1	-8.0
	-0.30	-0.4	-0.9
	-0.44	-0.8	-0.8
	0.10	1.8	1.9
	0.17	2.4	3.0
NT0301	-0.77	-4.9	-5.0
	-0.623	-4.1	-0.55
	-0.55	-0.3	-0.33
	0	0.3	0.31
	0.183	0.5	0.79

TABLE 9.3

PREDICTED SWELL AND SAMPLING DISTURBANCE

SPECIMEN N°.	LIQUID LIMIT (%)	SWELL PREDICTED (%)	SWELL CORRECTED (%)
3	141	2.0	2.6
4	141	2.0	2.6
5	49	0	1.1
6	235	4.7	6.1
7	382	8.7	9.9
8	530	5.8	6.9
9	530	-	27.1
10	382	-	13.9
11	235	16.2	6.9
12	141	5.7	6.1
13	49	1.9	2.4
14	49	0	0.8
15	94	3.6	4.1
16	120	3.1	3.2
17	120	7.1	8.2
18	142	7.2	9.9
19	94	4.7	6.8
20	120	3.1	5.2
21	94	1.1	3.5
22	120	6.51	8.7
23	142	7.1	9.3
24	142	13.7	17.1
25	94	2.9	4.9
26	120	2.0	3.2
27	49	1.1	1.8
28	49	-	0.1
29	94	-	-
30	120	-	-
31	142	6.8	8.9
32	142	6.9	9.1
33	49	-	0.9
34	94	-	4.3"
35	120	-	5.9
36	142	-	5.8

TABLE 9.4

(CVSP) AND (UVS) DATA USED FOR THE ASSESSMENT PROCEDURE

(UVS)				(CVSP)					
SPECIMEN	e_o	s_{ro}	PREDICTED SWELL	SPECIMEN	e_o	s_{ro}	SWELL	DIFFERENCE Δ SWELL	LL
1	0.84	91.53	-	5	0.92	81.19	1.1	1.1	49
2	0.865	89.85	5	19	0.9	89.60	6.8	1.6	94
3	1.026	74.26	20.93	20	0.91	85.6	5.20	-5.75	20
4	1.005	75.40	20.3	18	0.87	93.88	9.98	-10.32	142
5	0.974	94.26	-3.77	14	0.94	96.94	0.82	4.59	49
6	1.007	93.78	0.92	21	0.99	89.73	3.50	2.58	94
7	1.193	77.77	3.89	22	0.95	91.6	8.72	4.83	120
8	1.172	77.96	9.19	24	0.99	93.17	17.1	7.91	142
9	1.344	45.52	3.27	13	0.77	81.68	2.4	-1.3	49
10	0.753	20.67	7.11	15	0.74	86.52	4.12	-2.99	94
11	0.92	67.30	14.51	16	0.74	88.58	3.2	-11.31	120
12	0.914	67.59	22.05	17	0.79	89.62	8.1	-13.95	142
13	0.851	91.33	0.8	27	0.83	91.92	-	-	49
14	0.872	95.55	4.2	25	0.84	92.88	4.9	0.7	94
15	1.023	75.25	10.9	26	0.85	93.06	3.2	-7.7	120
16	1.225	92.66	11.9	23	0.83	94.41	9.3	-2.6	142

TABLE 9.5

SUMMARY OF SPECIMEN SOIL TYPES

	SOIL MIXTURES MONTMOR. (%)	SOIL MIXTURES KAOLINITE (%)	LIQUID LIMIT (%)	PLASTIC INDEX (%)	TEST CODES: STRESS CONTROL APPARATUS: VOLUME CHANGE TESTS 102mm SPECIMENS	VOLUME CHANGE TESTS 76mm SPECIMENS	NULL TESTS 102mm SPECIMENS	NULL TESTS 76mm SPECIMENS	CONSOLIDOMETER: CVSP TESTS	CONSOLIDOMETER: UVS TESTS
*	0	100	49	22	UT01	-	NT01	NR01	5,13,14 27,28,33	1,5,9,13
*	10	90	94	64	-	URQ1	NT02	NR02	15,19,21 25,29,34	2,6,10,14
*	20	80	120	87	UT02	-	NT03	-	16,17,20 22,26,30,35	3,7,11,15
	25	75	141	105	-	-	-	-	3,4,12	
*	30	70	142	99	-	UR02	-	NR03	18,23,24 31,32,36	4,8,12,16
	50	50	235	207	-	-	-	-	6,11	
	75	25	382	343	-	-	-	-	7,10	
	100	0	530	487	-	-	-	-	8,9	

Notes: 1. Refer to Tables: 6.1, 7.1, 8.1, 8.4 and 83

2. '*' denotes principal soil mixtures

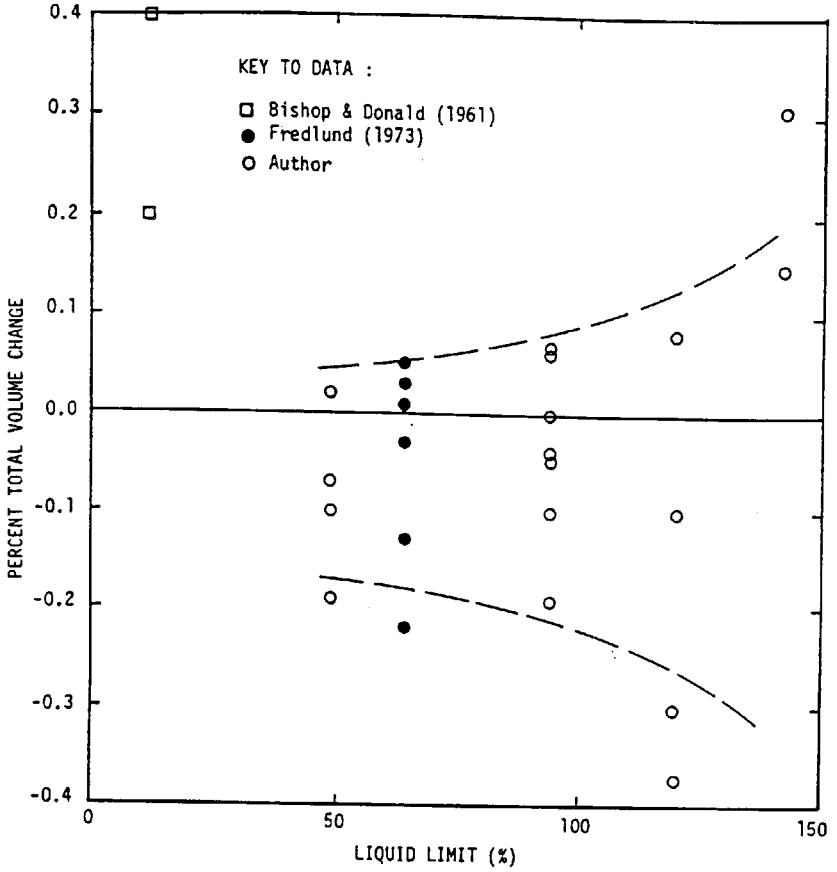

FIGURE 9.1

TOTAL VOLUME CHANGE
Vs LIQUID LIMITS

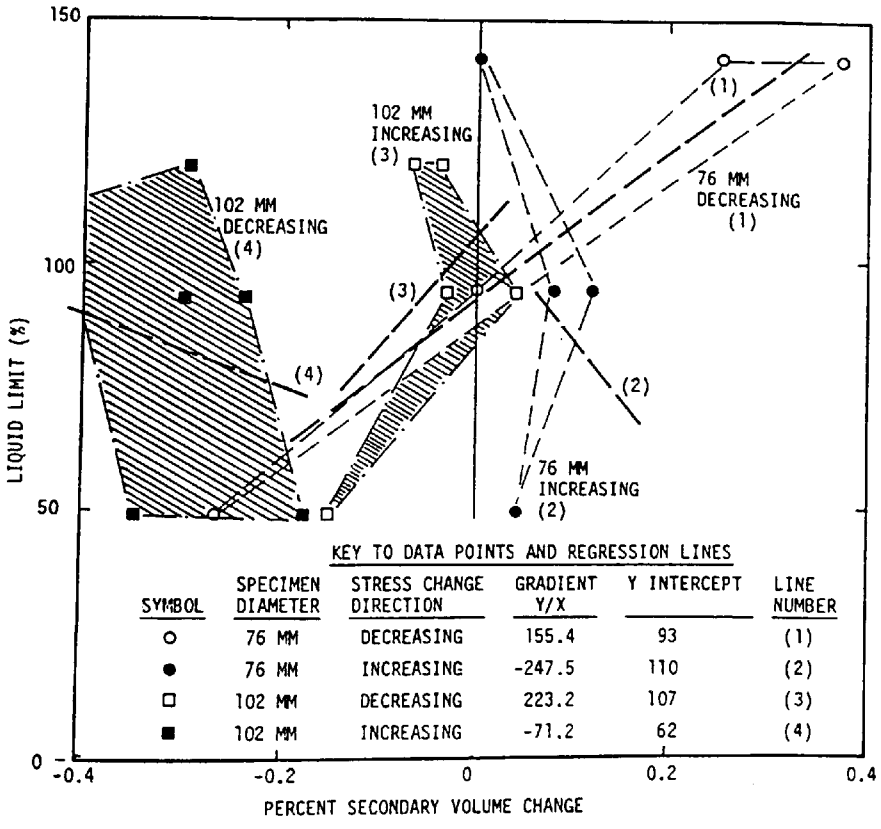

KEY TO DATA POINTS AND REGRESSION LINES

SYMBOL	SPECIMEN DIAMETER	STRESS CHANGE DIRECTION	GRADIENT Y/X	Y INTERCEPT	LINE NUMBER
○	76 MM	DECREASING	155.4	93	(1)
●	76 MM	INCREASING	-247.5	110	(2)
□	102 MM	DECREASING	223.2	107	(3)
■	102 MM	INCREASING	-71.2	62	(4)

FIGURE 9.2

SECONDARY TOTAL VOLUME
CHANGE Vs LIQUID LIMITS
(NULL TESTS)

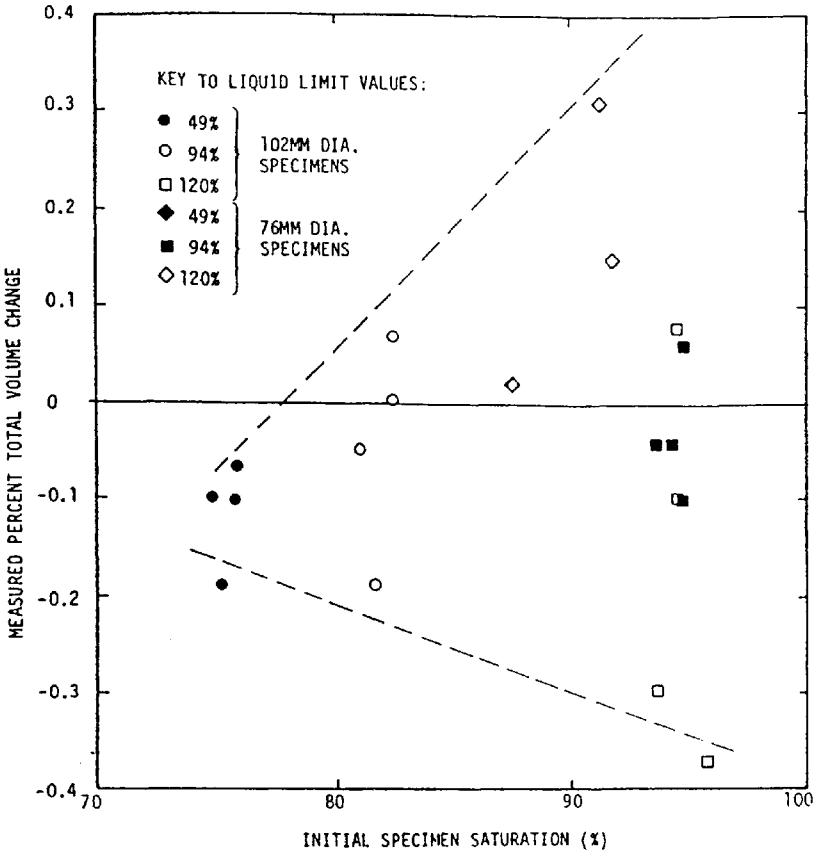

FIGURE 9.3

TOTAL VOLUME CHANGE
Vs INITIAL SATURATION
(NULL TESTS)

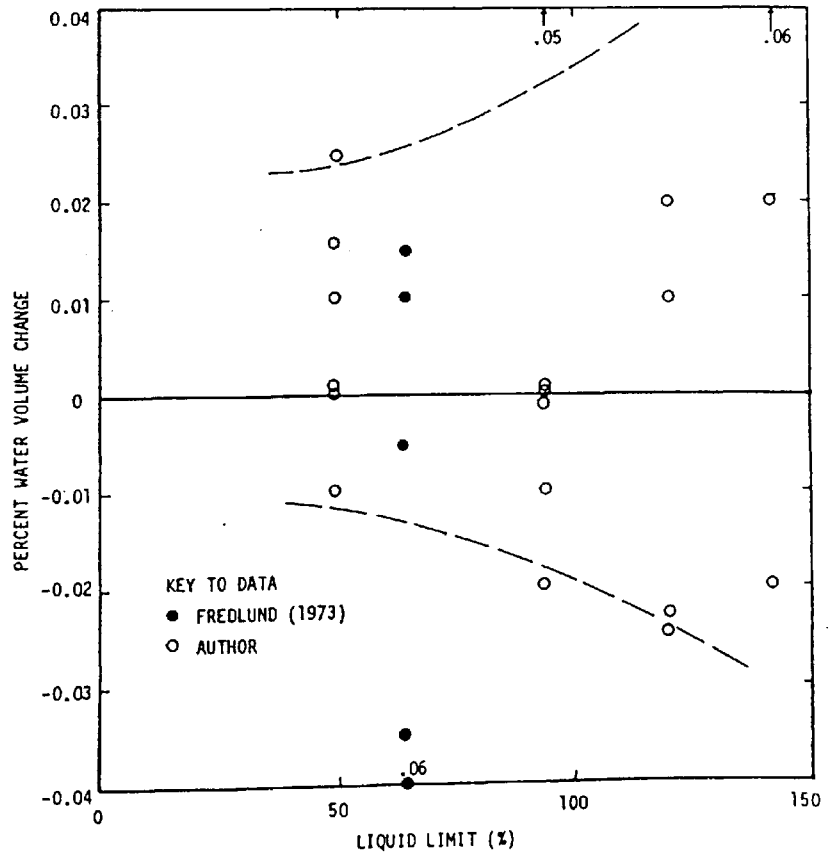

FIGURE 9.4

WATER VOLUME CHANGE
Vs LIQUID LIMIT

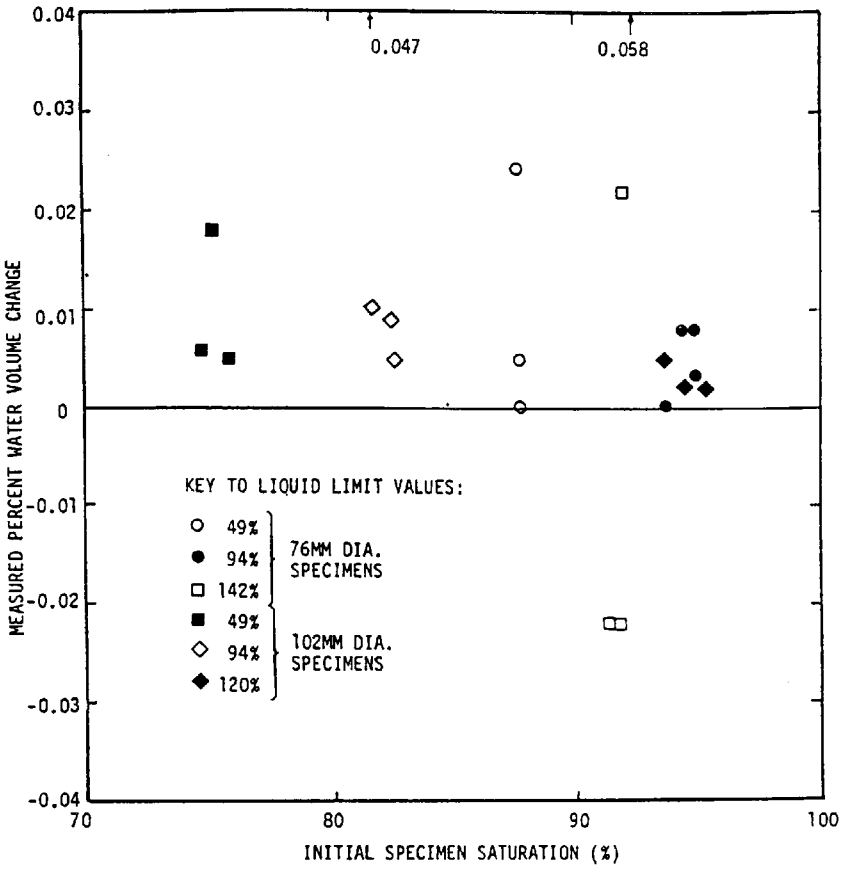

FIGURE 9.5

WATER VOLUME CHANGE
Vs INITIAL SATURATION

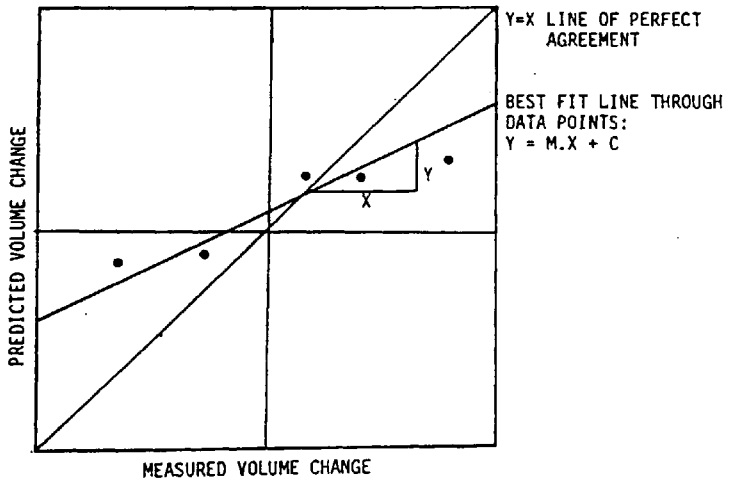

NOTES :

1. GRADIENT REPRESENTS ACCURACY OF PREDICTION; THE CLOSER THE VALUE TO UNITY, THE BETTER THE PREDICTION
2. CORELLATION COEFFICIENT (WHEN QUOTED) IS A MEASURE OF THE CLOSENESS OF THE DATA SET AS A WHOLE TO THE BEST FIT LINE.

FIGURE 9.6

TYPICAL ASSESSMENT OF
VOLUME CHANGE DATA

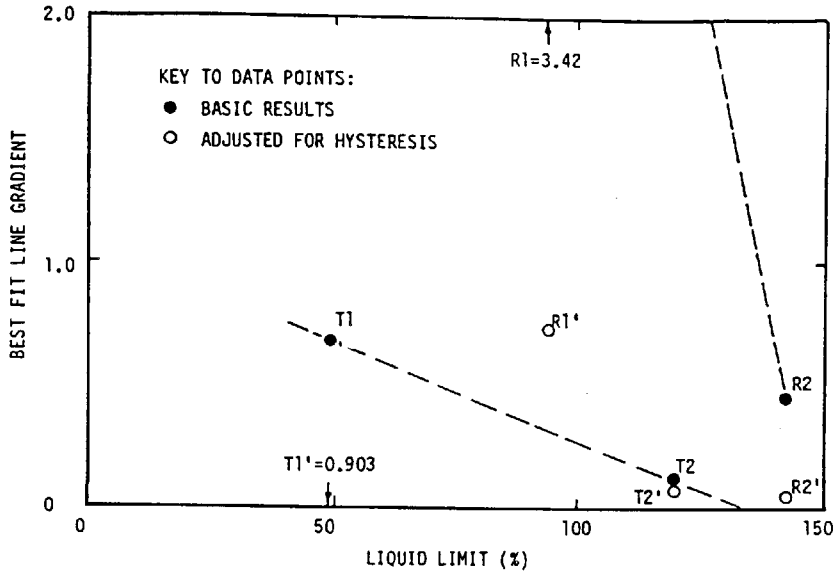

FIGURE 9.7

TOTAL VOLUME CHANGES;
BEST FIT LINE GRADIENT Vs LIQUID LIMIT
(MEASURED AND PREDICTED VALUES SUBJECT TO ERROR)

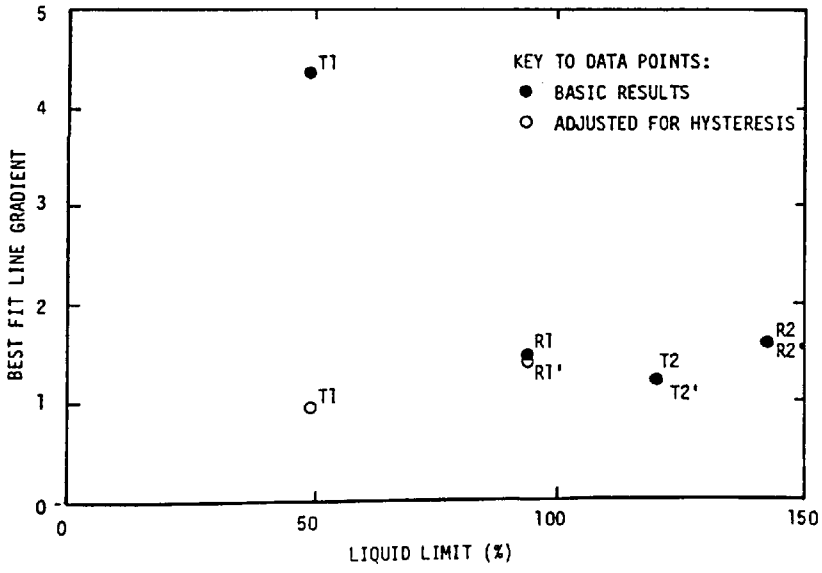

FIGURE 9.8

WATER VOLUME CHANGES;
BEST FIT LINE GRADIENT Vs LIQUID LIMIT

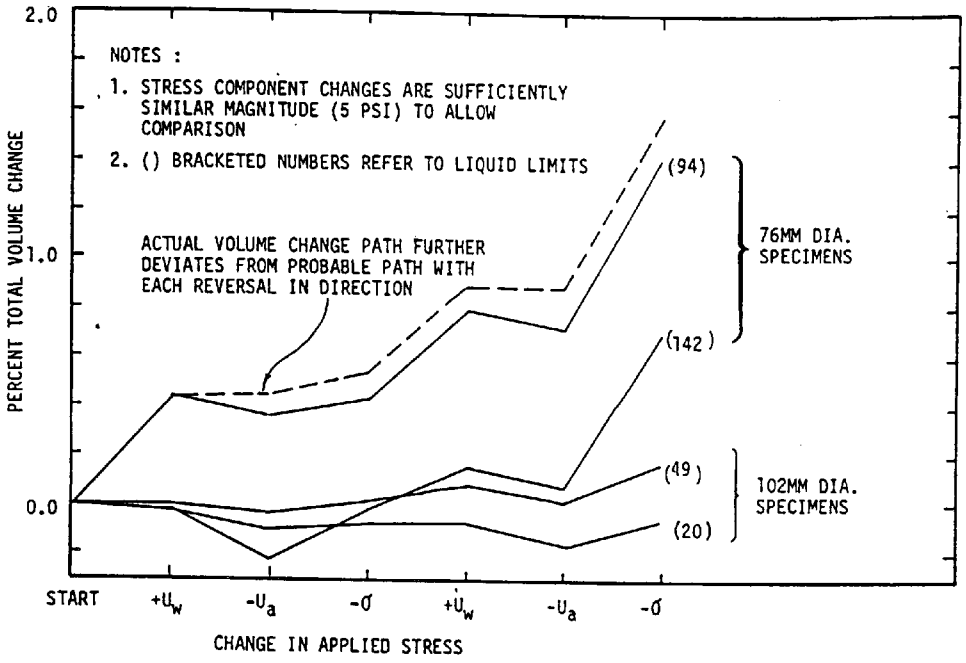

FIGURE 9.9

TOTAL VOLUME CHANGES CORRESPONDING
TO COMPONENT STRESS CHANGES

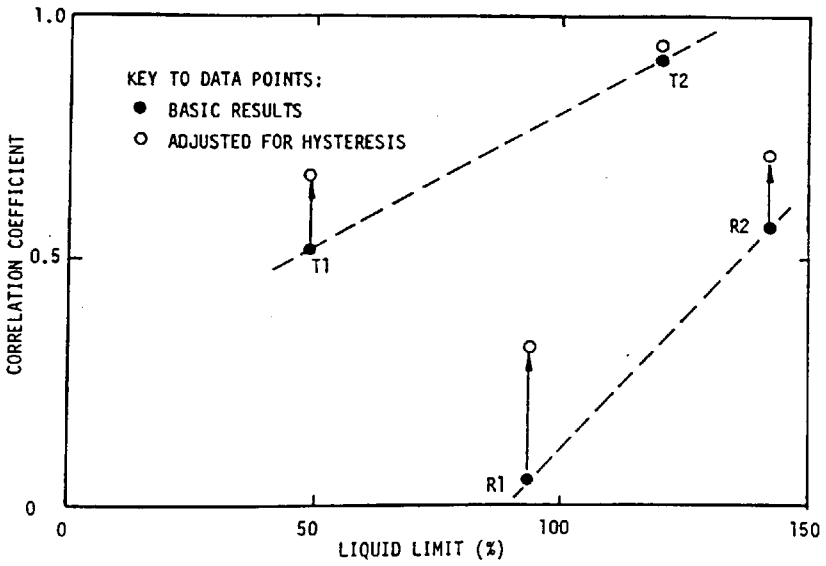

FIGURE 9.10

TOTAL VOLUME CHANGES;
BEST FIT LINE GRADIENT Vs LIQUID LIMIT
(MEASURED VALUE ONLY SUBJECT TO ERROR)

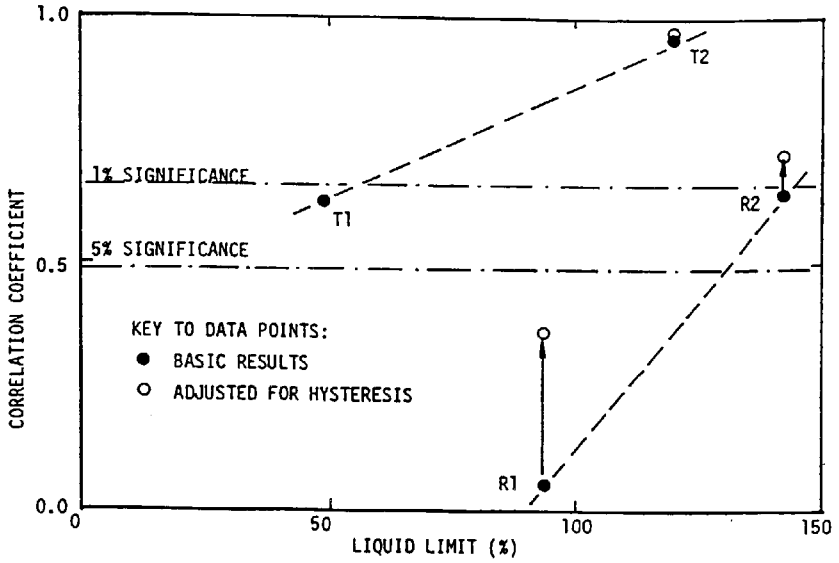

FIGURE 9.11
WATER VOLUME CHANGES;
BEST FIT LINE GRADIENT Vs LIQUID LIMITS
(MEASURED VALUE ONLY SUBJECT TO ERROR)

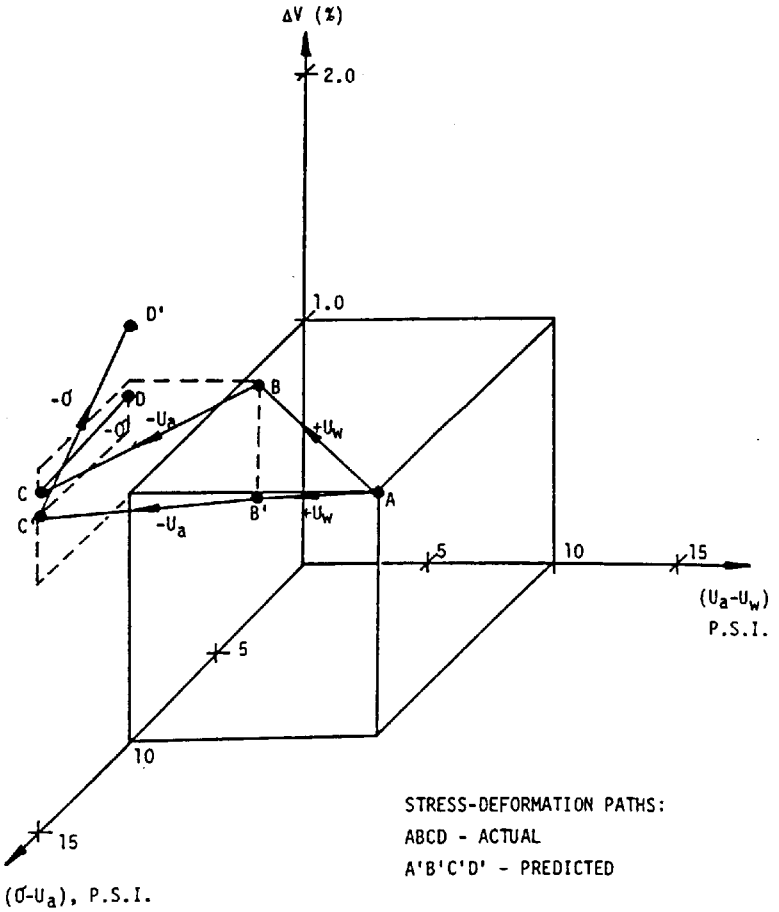

FIGURE 9.12

TYPICAL STRESS - VOLUME CHANGE PATHS
FOR 76MM DIA. SPECIMEN (LL = 94%).

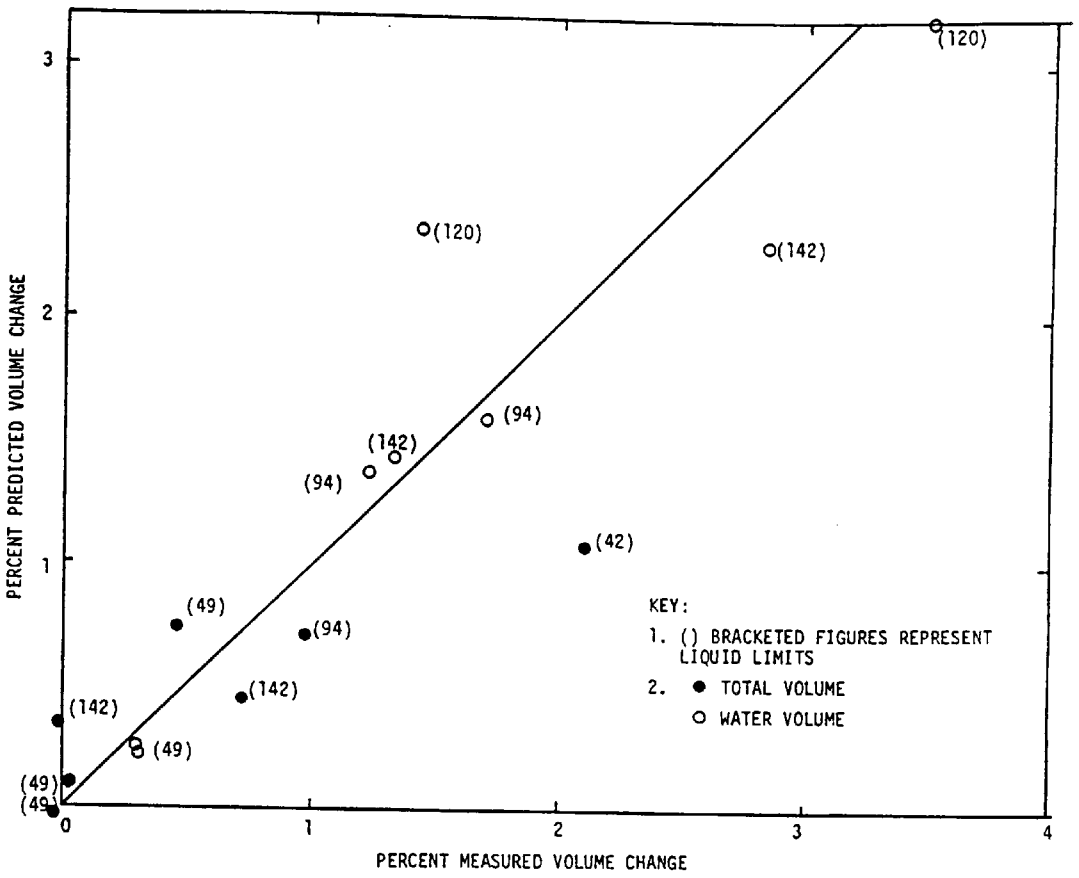

FIGURE 9.13

ACTUAL Vs PREDICTED TOTAL VOLUME CHANGE
FOLLOWING EACH STRESS CHANGE SEQUENCE

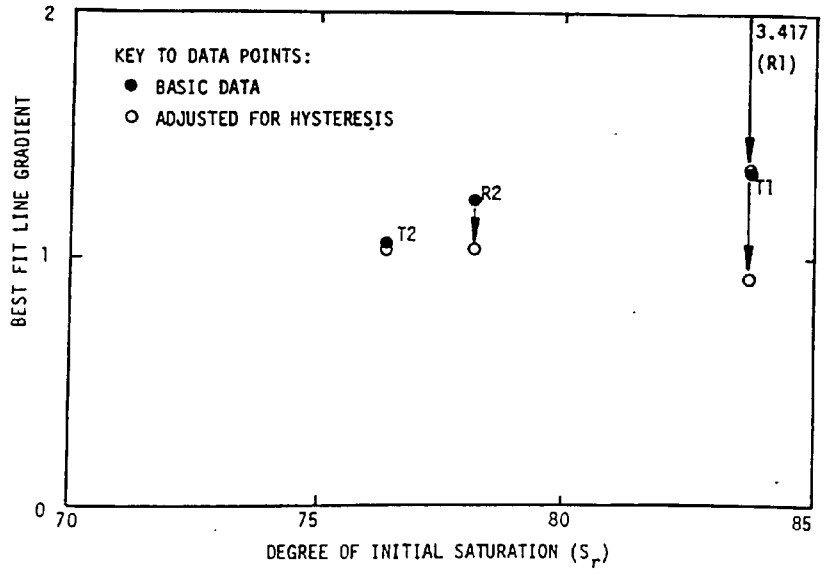

FIGURE 9.14

TOTAL VOLUME CHANGES;
BEST FIT LINE GRADIENT Vs INITIAL SATURATION
(MEASURED AND PREDICTED VALUES SUBJECT TO ERROR)

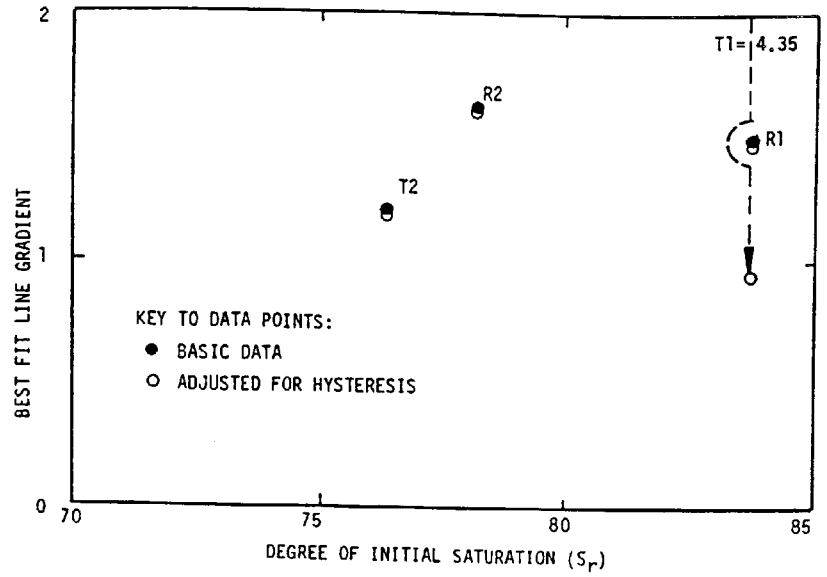

FIGURE 9.15

WATER VOLUME CHANGES;
BEST FIT LINE GRADIENT Vs INITIAL SATURATION
(MEASURED AND PREDICTED VALUES SUBJECT TO ERROR)

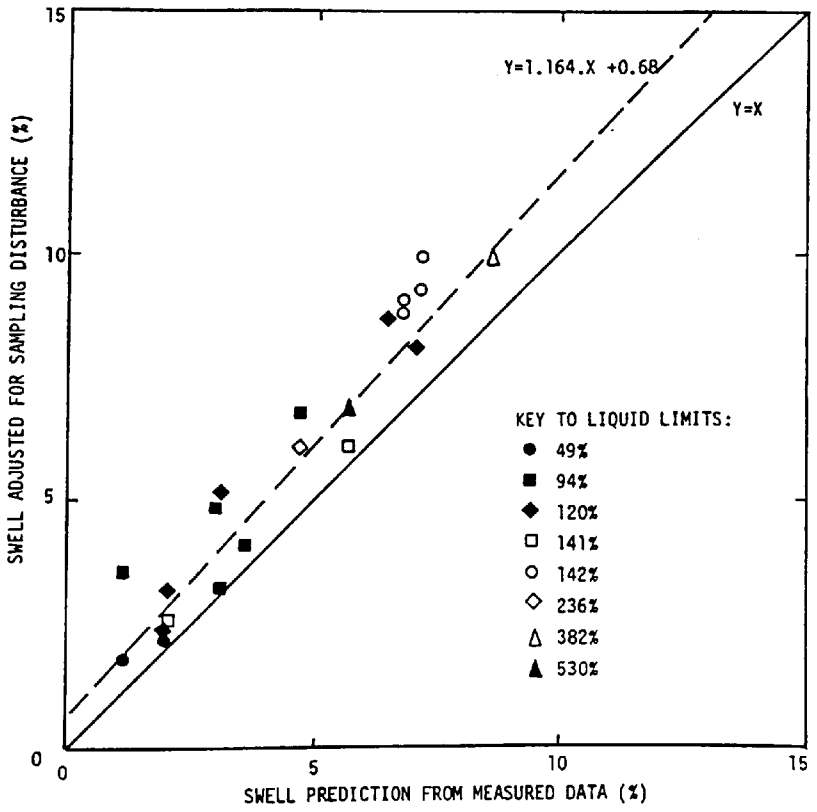

* MAJORITY OF RESULTS OCCUR BETWEEN 0% AND 10% SWELL; AVERAGE DIFFERENCE BETWEEN CORRECTED AND UNCORRECTED SWELL = 1.15%

SUGGESTED CORRECTION (PRELIMINARY) = 1.15 . (MEASURED EXPANSION)

FIGURE 9.16

EFFECTS OF DISTURBANCE UPON
PREDICTED VERTICAL SWELL

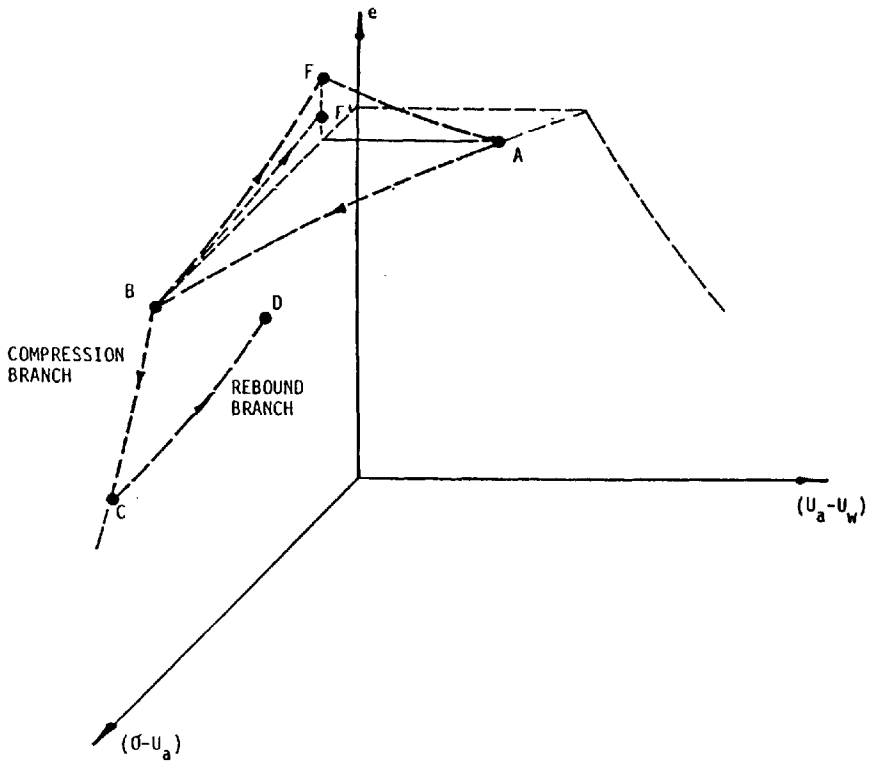

NOTES:

1. 'FREE' SWELL PATH (UNRESTRAINED VERTICAL SWELL-UVS) : AF
2. CONSTANT VOLUME SWELL PRESSURE (CVSP) TEST PATH : ABCD
3. THEORETICAL FREE SWELL (UVS) PATH : ABF
4. PREDICTIONS BASED UPON CVSP RESULTS : ABF'
5. BF AND CD ASSUMED PARALLEL FOR CVSP TEST PROCEDURE

FIGURE 9.17

ACTUAL AND THEORETICAL STRESS PATHS DURING (CVSP) AND (UVS) TESTING

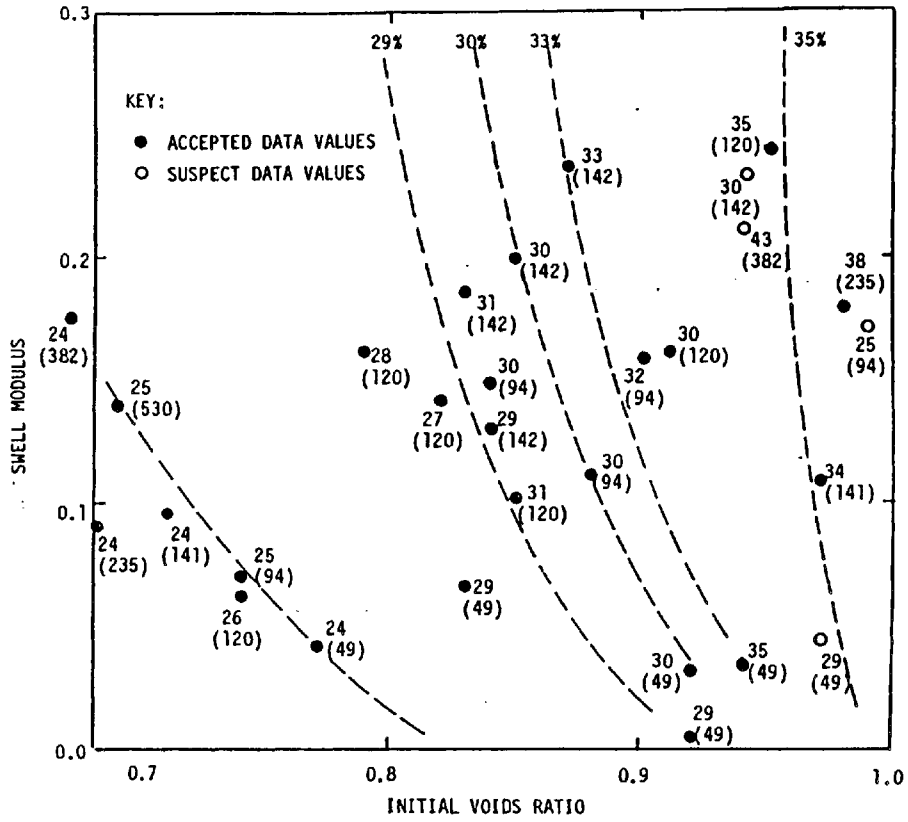

NOTES:

1. () BRACKETED FIGURES REPRESENT LIQUID LIMITS (%)
2. OTHER FIGURES REPRESENT MOISTURE CONTENTS
3. FIGURES FOLLOWED BY '%' REPRESENT CURVES DRAWN THROUGH SPOT MOISTURE VALUES.

FIGURE 9.18

SWELL MODULUS Vs INITIAL VOIDS RATIO (CVSP TEST DATA)

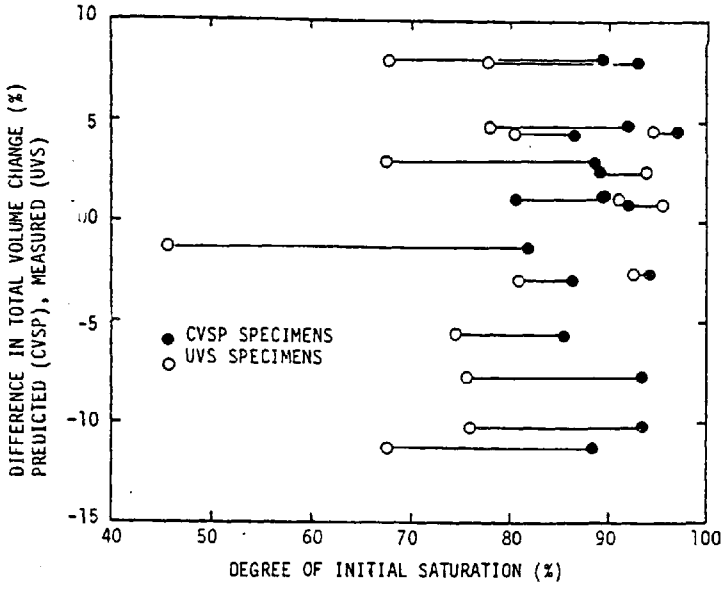

FIGURE 9.19

TOTAL VOLUME CHANGE Vs INITIAL SATURATION (CVSP AND UVS TESTS)

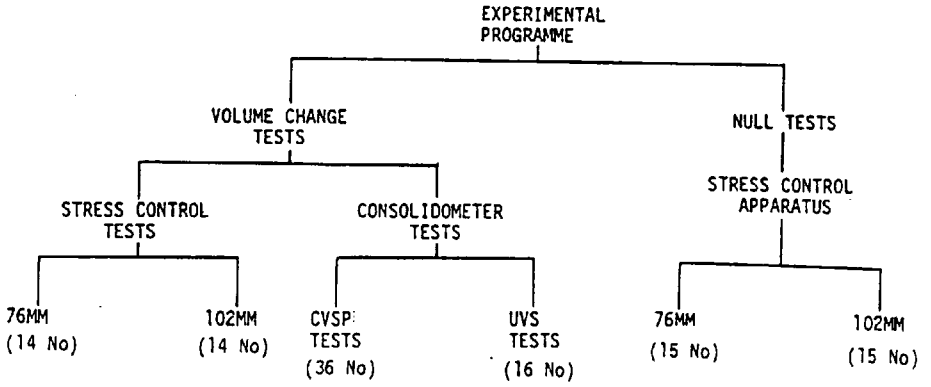

NOTES:

1. 76MM & 102MM REFER TO THE SPECIMEN SIZES USED IN THE STRESS CONTROL APPARATUS
2. CVSP - CONSTANT VOLUME SWELL PRESSURE TEST
3. UVS- UNRESTRAINED VERTICAL SWELL TEST

FIGURE 9.20

EXPERIMENTAL PROGRAMME

CHAPTER 10

CONCLUSIONS AND FUTURE WORK

10.1 OVERVIEW

The underlying motivation for this investigation was the need to provide the Engineer with improved techniques for predicting the swelling behaviour encountered in many unsaturated soils.

The initial phase of the work involved a survey of existing swell prediction methods. Besides providing a useful insight into expansive behaviour through the examination of considerable published data, two suggested swell predicting amendments for two national soil classification systems were presented.

The second and main part of the work was to verify Fredlund's volume change theory for use with swelling (expansive) unsaturated soils.

After developing suitable laboratory equipment, an experimental programme of three test series was undertaken to verify this theory. The conclusions drawn from this work are discussed in the following sections.

10.2 IDENTIFICATION AND CLASSIFICATION TECHNIQUES

10.2.1 General

National soil classification systems currently make little or no provision for the prediction of swell behaviour. A survey was conducted of available swell prediction techniques and current soil classification systems to assess if they could be related and whether swelling behaviour could be incorporated into a national soil classification system.

10.2.2 Assessment of existing techniques

Initially, published swell prediction methods (quantitative and qualitative) were assessed by applying them to available data sources.

The quantitative methods (including two developed by the author from Casagrande's plasticity chart - figures 3.8 and 3.18) worked well when used with the data source from which they were derived; however, their reliability becomes questionable when applied to different soils and environments.

The four most successful qualitative methods were based upon varying functions of plasticity index, clay content and shrinkage limit. Out of these, only the method after the Building Research Establishment (1980) does not include the shrinkage limit; since this variable was earlier shown not to relate to expansion (Chapter 3) then it was considered that this method was currently the most suitable for qualitatively classifying swell potential.

swell classification

BRE (1980)

Plasticity Index %	Clay Fraction %	Shrinkage/Expansion potential
>35	>95	V. high
22-48	60-95	high
12-32	30-60	medium
<18	<30	low

10.2.3 Parameter Significance

The order of soil parameter significance with regard to swelling potential and swell pressure was determined for the available data by

stepwise linear regression analysis. Consideration of the four most widely quoted parameters indicated the following order of significance : liquid limit, plasticity index, initial dry density and finally, initial moisture content. Liquid limit still featured strongly even when many more parameters were considered, however, the field suction value (although not widely quoted) exhibits the best correlation with percent swell.

As with the quantitative swell prediction methods discussed earlier, the derived relationships are applicable to specific soil types and environments; in consequence they differ from one another, and the reader is referred to Table 3.23 for a complete listing.

It is suggested that future work examines the swell suction relationship for as many soils as possible since it would prove of great value to the engineer, particularly with the advent of reliable field suction measurement equipment.

10.2.4 New prediction methods

A new method for assessing the probable degree of swell behaviour (qualitative) from the AASHTO group index is suggested :

AASHTO group index	Degree of potential swell
0-1	low
1-5	medium
5-12	high
> 12	very high

In addition, upon the basis of the earlier assessment of published swell prediction methods, it is suggested that the BRE (1980) method (based upon Atterberg limits, see 10.2.2) may be incorporated into the British soil classification system to account for swelling soils.

In both the above systems, the degree of probable (qualitative) swell is consistently predicted; however, the investigation indicated that the more specific relationships for predicting percentage swell (quantitatively) were limited in application to the soil types and localities from which they were derived.

10.3 DEVELOPMENT OF APPARATUS

Generally, the apparatus worked well despite the long duration of some tests. However, since the development of apparatus and testing techniques was one of the primary functions of the project, a detailed review is given of the performance/limitations of the equipment.

10.3.1 Consolidometer

The conventional consolidometer was successfully used to measure the swell pressure, volume change modulii (swell and consolidation) and unrestrained vertical swell characteristics of laboratory constituted expansive clays.

The main drawback of this equipment was that the standard consolidometer rings were not deep enough to accommodate the unrestrained swell of the few very high plasticity specimens (LL > 230%); in consequence the measured values for these particular samples were unreliable and too low due to the 'mushrooming' effect of the soil once the specimen height exceeded that of the consolidometer ring.

10.3.2 Stress control apparatus

This equipment was successful in permitting the control of total, air and water pressures for the unsaturated soil specimens, and a good level of confidence is placed in the results.

However, this was only achieveable due to the establishment of correct testing procedures and technique.

10.3.3 Test cells

Two test cells were constructed, one from a Rowe cell and the other from Triaxial cell components, with specimen sizes of (76mm ø x 25mm) and (102mm ø x 30mm) respectively.

The main development encompassed installing high air entry ceramic discs by Soil Moisture Equipment (USA) into the cell bases to provide an interface between the air and water phases; this was based upon the axis translation technique presented by Hilf (1957).

A facility for measuring and flushing the amount of diffused gases beneath the ceramic disc was incorporated into the water volume change measuring system. It is suggested that the system could be improved by cutting the flushing groove in the shape of a spiral. Air pressure was applied to the specimens via the inlet ports normally used for applying cell pressure in the Triaxial cell, and water pressure in the Rowe cell.

The need for automatic data logging system did not arise due to the nature of the testing procedures; nevertheless, it could easily be incorporated into the system if required.

The following observations are made with regard to the performance of the apparatus :

(a) The high air entry ceramic disc proved more rugged than expected, with no breakages being recorded during the test period.

(b) The experimental observations and analysis of final data indicated that the flushing system was not removing all the diffused air beneath the cell base. This is mainly attributed to the flushing groove design which could be improved by manufacturing another in a spiral configuration.

Whatever course of action is adopted this aspect should be further considered prior to further testing.

(c) The diffused air indicator (after Fredlund, (1973)) worked well for the most part; however, the device requires regular removal of diffused air bubbles from the main chamber, and cleaning of the burette for accurate reading of the diffused air volume.

(d) Minute continuous water losses from the Bishops 'paraffin' water volume change indicators were identified, and corrections successfully applied.

Despite the renewal of all seals, the losses are thought to have primarily originated from the flow valves.

(e) The primary limitation of the pore air pressure system was its inability to produce an 'instantaneous' change of pressure due to the compressibility of the air phase. This influenced the null tests by causing temporary imbalance of the stress equilibrium which in turn led to small immediate volume changes.

However, these varied in magnitude and could not be allowed for. The volume change (uniqueness) tests on the other hand were unaffected since simultaneous instantaneous stress changes were not essential to the tests.

(f) Although the total volume changes of the 102mm diameter specimens were much lower than those recorded for the 76mm specimens under their respective testing condition, the predicted volume changes were close to the measured values in each case.

A detailed examination of the test system indicated that this behaviour was probably attributable to the differences in specimen sizes, loading systems, air pressure vessel volumes, sidewall friction and compliance.

A correction was successfully applied for compliance by measuring the volume of soil extruded around the loading plates, nevertheless, despite every effort, the individual contribution of the other noted factors could not be quantified.

10.3.4 Loading systems

(a) 76mm cell

It was noted that the 76mm cell bellows loading device appeared to expand against the cell wall during loading, thereby reducing the apparent specimen surcharge. These effects were sufficiently consistent to enable a calibration of the device and a subsequently successful correction applied to all measurements.

(b) 102mm cell

The pneumatic piston and loading frame assembly proved to be very successful for the stress ranges employed (40 psi to 70 psi)/276 to 483 kN/m^2). However, the piston exhibited a slight tendency to stick at very low seating pressures (< 1 psi/7 kN/m^2); although this behaviour was not serious during this project, it should be borne in mind prior to future testing.

10.3.5 Stress control system

The following difficulties were encountered during use of the stress control system.

(a) Simultaneous stress change

During null testing it was physically very difficult for a single person to manually change all three component stresses simultaneously. Although this was overcome by employing additional labour, it is suggested that incorporation of a linkage between the control valves or

a purpose built 3 source/outlet valve into the design would be a more satisfactory solution.

(b) Air purity

The available in-house air pressure supply was found to contain contaminants such as water and rust particles. These were successfully removed by the use of special traps in the airline. Nevertheless, these devices required regular cleaning to maintain their efficiency.

10.3.6 Preparation of test specimens

To ensure specimen consistency involved careful control of clay mineral storage (dry), mineral blending (dry) addition of water, conditioning of prepared mixes and finally specimen forming (compaction and trimming). Nevertheless, slight departures of the final moisture content and density from the target values did occur, and were attributed to evaporation effects and the specimen forming process respectively. The variation in density and moisture content throughout each specimen are thought to have been minimal; and this was corroborated by the careful examination of selected specimens.

Of greater importance, were the small variations of initial moisture content, and voids ratio between specimens. These should be reduced as far as possible, and suggestions are made under the section on future work.

10.4 CHOICE OF THEORY FOR PREDICTING VOLUME CHANGE

10.4.1 General Approach

The physical constitutive model approach was adopted in this study in preference to the energy (thermodynamic) and electrical charge approaches since it was considered more appropriate for determining the magnitude of soil movement resulting from swelling and shrinkage.

10.4.2 Fredlund's Theory

Fredlund's theory was chosen for use with swelling soils in this project on account of its :

(a) improvement over other modified effective stress equations by describing volume change in terms of two independent stress state variables, namely $(\sigma-U_a)$ and (U_a-U_w)

(b) proven record with low-swell soils

(c) logical development from Terzaghi's accepted effective stress principle

(d) suitability for verification by experimental means.

(e) incorporation of useful volume change equations of the general form

$$\frac{\Delta V}{V} = C_t.d(\sigma-U_w) + C_m.d\ (U_a-U_w)$$

On a more fundamental basis, Fredlund's unsaturated soil element is new and consists of four phases, namely soil, air, water and an air-water interphase or contractile skin.

Although he considers the contractile skin to be the principal conductor of suction throughout the soil mass, it may be ignored for the purpose of volume weight relationships by virtue of its negligible weight and it is considered as part of the water.

10.4.3 Discontinuous phases : Theory

Fredlund's theory is based upon the assumption of continuous phases at all degrees of saturation. However, this is questioned upon the basis of previous research (Aitchison, 1961, Madedor, 1967) which indicates that the continuity of all phases can only be anticipated between 25% and 85% saturation. However, it is appreciated that swelling soils will unavoidably pass outside this range at some point in the wetting/drying cycle and that the performance of the theory should therefore be carefully assessed in such instances.

10.4.4 Discontinuous phases : Axis translation technique

The axis translation technique was chosen for controlling and measuring the suction within the test specimens upon the basis of its widespread application to unsaturated soils. However, for correct functioning, the technique is dependent upon an incompressible water phase, which will clearly not exist when $85\% < S_r < 100\%$ and the air and water phases act as a compressible mixture.

Every effort was made therefore, using current theories to calculate the effects of occluded air upon the experimentally measured volume changes; however, meaningful corrections could not be determined. Nevertheless, upon the basis of observed behaviour, the effects of the compressible air water mixture were considered to have manifested themselves in the following general ways :

In the null tests where $\Delta\sigma = \Delta U_a > \Delta U_w$, then $(\sigma - U_w)$ and $(U_a - U_w)$ will effectively increase. Since $\Delta(\sigma - U_w)$ was observed to exert a greater influence over total volume than $\Delta(U_a - U_w)$ during testing, then the total volume is expected to be comparatively less than would result with an incompressible water phase.

In the volume change tests :

$$\Delta U_{w(actual)} < \Delta U_{w(applied)}$$

In consequence the induced volume changes were probably less than would have occurred with an incompressible water phase.

10.4.5 Volume change reversals

Despite universal recognition of a non elastic behaviour in unsaturated soils following a reversal in stress change, Fredlund's theory makes no provision for this effect.

A modification of Casagrande's sampling disturbance correction technique was applied to the consolidometer swell test results with only limited success. So far as the stress control apparatus is concerned however, the practicality of such a correction is restricted in view of its dependence upon so many related factors.

10.5 EVALUATION OF THEORY BY EXPERIMENT

10.5.1 Stress State Variables.

Null type tests were performed in the stress control apparatus to assess validity of the stress state variables. The results indicated that despite limitations of the apparatus, minimal changes were observed for the total and water volumes of all soils tested.

(a) The maximum total volume compression and expansion was 0.37% and 0.31% respectively, the maximum water volume changes were even smaller with a compression and expansion of 0.021 and 0.028% respectively.

These results are an improvement over comparable work by other authors and are considered as validating the chosen stress state variables for expansive clays with liquid limits up to 142%.

(b) Despite the observance of minimal volume changes, the magnitude of 'volume change' significantly increased for specimens with liquid limits above 100%.

(c) Fredlund's theory is based upon the assumption of (i) phase continuity and (ii) that a soil will pass smoothly from the unsaturated to the saturated state during the wetting process. However, the author notes that the published evidence suggests that the continuity of soil, air and water phases is only likely to occur between 25% and 85% saturation, and, he is in agreement

with the distinct zones of saturation presented by Aitchison, 1961 (Section 4). Furthermore, published evidence indicates that the transition between unsaturated and saturated zones is abrupt.

These observations are apparently confirmed by the author's results which indicate an increased compressibility of the specimens (presumably due to increased occluded air content) for saturation values above 80%.

In consequence, despite present limitations of Fredlund's work with regard to certain saturation ranges, his theory does appear suitable for describing the stress equilibrium within expansive unsaturated soils.

10.5.2 Volume change equations

(a) Fredlund's volume change equations were assessed upon the basis of the agreement between experimentally measured volume changes and those predicted using his general form equation :

$$\frac{dV}{V} = \frac{\partial v}{\partial(\sigma-U_w)} \cdot d(\sigma-U_w) + \frac{\partial v}{\partial(U_a-U_w)} \cdot d(U_a-U_w)$$

Two series of volume change tests were conducted; the primary series involved producing small stress changes from a stress point (stress control apparatus), whilst the other series involved much greater stress changes in the consolidometer.

The total volume was consistently under predicted irrespective of the test procedure or soil type. However, the agreement between measured and predicted values was apparently unrelated to the liquid limits; despite every effort, no firm reason could be determined for this.

The stress control data indicated a good agreement between the measured and predicted values, such that :

predicted swell = 75%-95% measured swell

(correlation coefficients between 0.64 and 0.97)

The agreement of values consistently increased for specimens of higher liquid limits.

The consolidometer results also led to an under-prediction of swell, however, the agreement between values decreased with increasing specimen liquid limit. The results indicated :

Specimen liquid limits 50-94%

predicted swell = 98% measured swell

(correlation coefficient = 0.78)

Specimen liquid limits 94%-142%

predicted swell = 44% measured value

(correlation coefficient = 0.6)

(b) The agreement between measured and predicted water volume changes (stress control apparatus) was less convincing; whereby the predicted water volume change = 62-106% measured value. With correlation coefficients between 0.32 and 0.89.

(c) The swell pressure was measured as part of the consolidometer tests and the results indicate that the measured values are unrelated to the corresponding compression and swelling moduli.

In consequence, it appears that Fredlund's work cannot be used in the present form to predict swell pressure.

(d) The agreement between measured and predicted volume changes did not appear to be influenced by the degree of initial saturation.

(f) During the course of testing, it was not always possible as a result of limitations in procedure, to ensure the continuous expansion of the specimens.

The results indicated that reversals in the direction of volume change influenced all subsequent volume change behaviour. This behaviour was termed hysteretic, and is not accounted for by Fredlund's work; furthermore an adaptation of a published empirical correction procedure (Casagrande's technique for the consolidometer) was shown to be of limited value in offsetting these effects.

In view of the theory not allowing for reversals in stress and volume change, then it should ideally be restricted at present to non reversal situations. However, since reversals are common in the field, then it was felt prudent to at least estimate the resultant effects.

In consequence, since volume change reversals are recognised as reducing the subsequent magnitude of volume change then the resulting swell or compressibility moduli will be under-measured, thereby causing the constitutive equations to under-predict volume change.

10.6 CONSTANT VOLUME SWELL PRESSURE TEST (CONDUCTED IN CONVENTIONAL CONSOLIDOMETER APPARATUS)

Fredlund's proposals for combining his theory with an established soils laboratory test were successfully implemented in this project to measure the rebound modulus and swell pressure for a wide range of reconstituted expansive clay mineral mixtures. However, the resulting swell was underpredicted for soils with liquid limits exceeding 100%. This was attributed to the volume change moduli being measured before the specimens had expanded to their maximum volume.

Although the criteria for measuring the moduli at the original voids ratio worked well for soils of low liquid limit, the long term secondary effects of the higher liquid limit soils - (LL > 100%) meant that expansion could in extreme cases continue far beyond the original voids ratio.

In conclusion therefore, the accuracy of swell predictions is directly related to that of the rebound modulus. In the case of soils up to LL = 94%, the modulus can be satisfactorily measured at the point corresponding to the original voids ratio. However, for soils of higher liquid limits, the specimens should be rebounded for as long as practicable and the rebound modulus measured at that point if any greater reliance is to be placed in the result.

Since the water volume change predictions were made upon the basis of the total volume changes then the patterns of behaviour are identical and hence there was little value in repeating the analysis procedure. Of greater benefit would be an independent measure of the water volume actually taken into the specimen.

10.7 FINAL APPRAISAL

This project is the first to investigate unsaturated or expansive soils at The Polytechnic and was reasonably successful despite some difficulties.

The initial phase of the work on identification and classification of swelling soils, isolated the limitations of several existing swell prediction methods.

Besides providing a useful insight into expansive soil behaviour, this also led to amendments being suggested for the AASHTO and British soil classification systems to identify potentially expansive soils.

The second and most important phase of the work encompassed an experimental investigation to determine the suitability of Fredlund's constitutive model approach (for unsaturated soils) to expansive clays.

The results were sufficiently convincing to suggest that Fredlund's volume change theory is suitable for application to expansive clays of a liquid limit range typically found in the field (up to 142%).

Indeed, the main limitations were associated with Fredlund's approach as opposed to expansive soils; notably his work does not provide for discontinuous phases(ie very high or very low degrees of saturation) or the hysteretic effects resulting from a reversal in volume change. In consequence, it is highly recommended that future work be directed towards these areas.

Another important contribution of the work was the considerable development of equipment and associated procedures for measuring total, pore air and pore water volume changes. A critical evaluation before and during the test programme identified the main limitations, and every effort was made to meaningfully adjust the data for associated effects. Nevertheless, some trends in behaviour could not be fully explained, and it was only possible to identify the probable causes in such instances.

It is suggested that future development be directed towards a triaxial testing system. Finally, in view of the author being the first to investigate this subject at The Polytechnic, it was necessary to cover considerable ground as part of the familiarisation process. However, in consequence of the knowledge gained, it will be possible for future projects to concentrate on the specific areas noted in the final section.

10.8 SUGGESTIONS FOR FUTURE WORK

The two primary aspects of the theory requiring further study are :

(a) applicability of the theory to soils composed of discontinuous phases and

(b) the effects of stress reversals upon the volume change behaviour.

The following suggestions are therefore made with the above overall aims in mind.

10.8.1 Identification and Classification

(a) The proposed relationships and classification systems should be tested with a variety of soils

(b) The reliability of available instruments for measuring field suction should be assessed with a view to relating suction suction to insitu swell for a variety of soil types and environments.

10.8.2 Equipment development

In addition to the suggested developments detailed in Conclusion 10.3, the following suggestions are made :

(a) Development of a triaxial swell testing cell for conducting stress path testing from the technology developed during the course of the investigation.

(b) The specimen size and test cells for the stress control system should be standardised.

(c) The cell base flushing groove design should be improved - possibly cut as a spiral.

(d) The ceramic disc could be mounted in an easily removable collar to obviate the need for a complete overhaul in the event of a disc breakage.

(e) Incorporation of automatic data logging system.

(f) Re-evaluation of specimen production techniques.

10.8.3 Constant volume swell pressure test procedure :
a routine soils laboratory test for measuring the swell parameters

(a) Evaluate the technique in conjunction with insitu case study records

(b) Investigate the effects of differing types of disturbance upon swell pressure and swell pressure correction technique

(c) Re-evaluate the criteria adopted for measuring the rebound modulus in view of the earlier observations

(d) Evaluate the influence of cell wall - specimen friction upon the measured volume change moduli.

10.8.4 Hysteresis Effects

(a) Stress path testing should be employed so as to avoid hysteresis effects.

(b) Future work should seek to extend Fredlund's theory so as to account for reversals in volume change.

(c) A study of the types of sampling disturbance and their effects upon volume changes.

10.8.5 Occluded Air

(a) The transition zones between saturation ranges containing continuous and discontinuous phases need to be investigated and the applicability of Fredlund's theory to these conditions assessed.

(b) There is a need for technological and theoretical development for the prediction of occluded air effects upon volume change in unsaturated soils.

(c) The effect of occluded air upon the axis translation technique has not yet been conclusively demonstrated.

REFERENCES

AITCHISON G.D. (1956). " Some preliminary studies of unsaturated soils: (a) The circumsatance of unsaturation in soils with particular reference to the Australian environment " . Proceedings . 2nd Australia - N.Z. Conference on soil mechanics and foundation engineering. N.Z ICE .

AITCHISON G.D. (1960) . " Relationship of moisture stress & Effective stress functions in unsaturated soils" . Pore pressure & Suction in soils. Butterworth, London 1961 .

AITCHISON G.D. (1965). " Engineeing concepts of moisture equilibria and moisture changes in soils" . Statement of the review panel for the symposium in print - moisture equilibria and moisture changes in soils beneath covered areas . Butterworth, Australia.

AITCHISON G.D. (1967) . "Separate of site investigation, Quantification of soil properties and selection of operational environment in the determination of foundation design on expansive soils". Proceedings. 3rd Asian regional conference . On soil mechanics . And foundations. Engineering. Haifa Israel . Vol 2.

AITCHISON G.D. (1969). " Soil suction in foundation design ". Proceedings 7th international . Conference . Soil mechanics and foundation engineering. Vol 2 , Mexico . pp 1-8

ALTMEYER W.T. (1955) . " Discussion of engineering properties of expansive clays " . Proceedings . ASCE, Vol 1 , No 658, 1955, pp 17-18 .

ANDERSON K.O. & THOMPSON S . (1969). " Modification of expansive of western Canada with lime ". Proceedings 2nd International research & Engineering conference on expansive soils. Texas A&M university , College station , Texas Aug 1969 pp i.75-182 .

ATTERBERG A. (1911). " Die plastizitat tone " (German?). International mitt. Boden 1, 4-37 .

BARDEN . L. , MADEDOR A.O. , SIDES G.R. (1969) . " Volume change characteristics of unsaturated clay " . Journal of soil mechanics foundations division . ASCE (JAN) . pp 33-51

BIKERMAN J.J. (1958) . " Surface chemistry , Theory and applications ". 2nd , Academic PR . INC . NewYork .

BIOT M.A. (1955) . " Theory of elasticity and consolidation for a porous anisotropic solid " . Journal of applied physics, Vol 26, No 2 . pp 182-185

BISHOP A.W. (1956) . " Lecture delivered in oslo, Norway in 1955 The principle of effective stress " . Prinied in tek . Ukeflad . No39 .

BISHOP A.W. & ELDIN A.K.G. (1950). " Undrained triaxial tests on saturated sands and their significance in the general theory of shear strength " . Geotechnique , 2 . pp 13-32

BISHOP A.W. & HENKEL D.J. (1962) . " The measurement of soil properties in the triaxial test " Edward Arnold (Publishing) LTD, London 2nd edition.

BISHOP A.W. & BLIGHT G.E. (1963) . " Some aspects of effective stress in saturated & Unsaturated soils " Geotechnique , Vol 13 . pp 177-197

BISHOP A.W , WEBB D.T. , SKINNER A.E.(1965) ." Triaxial tests on soil at elevated cell pressures " 6th International conference on soil mechanics and foundation engineering .

BLIGHT G.E.(1965)." A study of effective stresses for volume change " Moisture eguilibria and moisture changes in soils beneath covered areas" Butterworth , Australia .

BOCKING K. & FREDLUND D.G. (1980) . " Limitations of the axis translation technique " 4th International conference on expansive soils, Denver Colorado . pp 117-136

BRACKLEY I.J.A.(1971). " Particle collapse in unsaturated expansive clay" 5th regional conference for Africa. On soil mechanics and foundation engineering, Luanda, Angola .

BRINK A.B.A , PARTRIDGE T.C. , WILLIAMS A.A.B. (1982). " Soil survey for engineering " Clarenden press, Oxford, 1982. pp 23-30

BRITISH STANDARDS INSTITUTUION. " Site investigations " : BS 5930 : 1981 code of practice.

BUILDING RESEARCH ESTABLISHMENT (1980) " Low - Rise buildings on shrinkable clay soils : Pt 1. " Building research digest No 240/1, 1980.

BURLAND J.B. (1961) " The concept of effective stress in partly saturated soils " Msc thesis , University Witwatersrand.

BURLAND J.B. (1965) . " Some aspects of the mechanical behaviour of partly saturated soils " Moisture equilibria and moisture changes in soils beneath covered areas, Butterworth, Australia.

CASAGRANDE A. (1948). "Classification and Identification of Soils". Trans ASCE, Vol. 113, pp 783-810.

CHEN F.H.(1975). " Foundation on expansive soils " Elsevier. Scientific Puplishing . Co. NewYork .

CHU, T , MOU C.H. (1973). " Volume change characteristics of expansive soils determind by controlled suction tests" . Proceedings . 3rd international conference on expansive soils, Haifa, Israel .

COATSWORTH A.M. (1980). " Summary of panel discussion on testing and prediction methods ". 4th international conference on expansive soils. Denver, Colorado .

COLEMAN J.D. (1962). Correspondence to geotechnique " Stress / Strain relations in partly saturated soils". Vol 12, NO4, pp. 348 to 350 .

COMPTON P.V.(1970) . " A study of the swelling behaviour of an expansive soil as in influenced by the clay microstructure, Soil suction & external loading". Technical report No afwl- tr. 70 -26 Airforce weapons laboratory, New Mexico.

COREY A.T.(1957). " Measurement of air & Water permeability in unsaturated soil " Soil science society of America proceedings .p 21 : 7-10 .

CRONEY D. (1952) . " The movement & distribution of water in soils " . Geotechniqu, Vol 3 . pp 1

CRONEY D, COLEMAN J.D. BLACK W.P.M. (1958) . " The movement & Distribution of water in soil in reletion to highway design and performance " . Highway research board special report No 40 Washington. D.C.

DAKSHANANMURTHY V. & RAMAN V. (1973). " A simple method for identifying an expansive soil" . Soils & Foundations, Japanese society of soil mechanics and foundations engineering . pp 97-104

DAVIES J.T & RIDEAL E.K. (1963) . " Interfacial phenomena " 2nd edition Academic press. NewYork .

DEFAY R., PRIGOGINE I (1966) . " Surface tension and adsorption" Longmans, G . B.

DERJAGUIN B.V. (1965) . " Recent research in to the properties of water in thin films and in micro capillaries " Society for experimental biology symposia xlx . The state and movement of water in living organisms .

DONALDSON G.W. (1969) . " The occurrence of problems of heave and the factors affecting its nature " . 2nd international research & Engineering conference . on expansive clay soils , Texas A&M, 1969 . pp 25-36

DRISCOLL R (1983) . " The influence of vegetation on the swelling and shrinkage of clay soils in Britain " . Geotechnique , Vol 33, June 1983. pp 93-105

DUMBLETON,M.J , WEST G (1966). " The influence of the coarse fraction on the plastic properties of clay soils " . Trrl report No 36, crowthorne .

ESCARIO .V (1969) . " Swelling soils in contact with water at a negative pressure " 2nd international conference on expansive Soils, Texas A&M . pp 207-217

FABRYCKY W.J. & MIZE J.H. (1974) . " Introductory statistics and probability for engineering science and technology " . Prentice HALL INC , USA ISBN 0 - 13 - 501627 - A .

FAIZULLAEV D.F. (1969). " Linear motion of multiphase media in conducts" Special research report , Translated from Russian by consultants Bureau NewYork.

FREDLUND D.G (1969). " Consolidometer test procedural factors affecting swell properties " . Proceedings 2nd conference on expansive clay soils, Texas A&M, pp 435 - 456 .

FREDLUND D.G.(1973). " Volume change behaviour of unsaturated soils " . PHD dissertation, University of Alberta , Edmonton , Alta .

FREDLUND D.G.(1975). " A diffused air volume indicator for unsaturated soils". Canadian geotechnical journal, Vol 12, No4, 1975, pp 533 - 539 .

FREDLUND D.G. & MORGENSTERN N.R. (1979). " Constitutive relations for volume change in unsaturated soils" . Canadian geotechnical journal, Vol 13, No 3, 1976 pp 261 - 276 .

FREDLUND D.G. & MORGENSTERN N.A. (1977). " Stress state variables for unsaturated soils" . Geotechnical journal, ASCE, No GT5 MAY 1977, pp 447 - 466 .

FREDLUND, HASAN, FILSON . (1980) . " The prediction of total heave " . 4th International conference on expanaive soils pp 1 - 7 , Denver , Colorado, 1980 .

FREDLUND D.G. (1983) . " The prediction of ground movements in swelling clays". 31st soil mechanics and foundation engineering conference , Minnesota University, Minneapolis, Minnesota .

FREDLUND D.G. RAHARDJO. H . (1985) . " Theoretical context for understanding unsaturated residual soil behaviour " 1st International Conference on Geomechanice in tropical lateritic and saprolitic soils, Brazil .

FUNG Y.C. (1965) . " Foundations of solid mechanics " prentice Hall inc, Englewood cliffs N. J.

FUNG Y.C. (1969) . " A first course in continuum mechanics " Prentice Hall INC , Englewood cliffs, N. J. USA .

GIBBS N.J., COFFEY C.T. (1969). "Techniques for pore pressure measurements and shear testing of soil" proc. 7th ICSMFE, Mexico.

GIL A.C. (1969) ." Contribution to the study of expansive clays of Peru" 2nd international on expansive soils, Texas A & M university . pp 183-193

GOODRICH F.C. (1969) . " The thermodynamics of fluid interfaces " Surface & & Colloid science , Vol I, Wiley interscience , Toronto .

GREEN A.E., NAGHDI P.M (1965) . " A dynamical theory of interactive continua" International . journal pp 231-241

GRIM R.E. (1953). " Clay mineralogy " Mcgraw - Hill book company INC, NewYork.

GROMKO G.J. (1974) . " Review of expansive soils " . ASCE journal geotechnical division . GT6, JUNE 1974 . pp 667-687

HEAD K.A.(1982) . " Manual of soil laboratory testing Vol 2 : Permeability, Shearstrength and compressibility tests " . Pentech press. ISBN 07273 1305 .

HILF J.W. (1956) . " An investigation of pore water pressures in compacted cohesive soils " . Technical memorandum. 654, US dept of Interior , Bureau of Reclamation, Denver, Colorado .

HOLTZ W.G.(1959). " Expansive clays : Properties & Problems" . Quarterly , Colorado school of mines , Vol 54, No4, OCT 1959, pp 89 - 125 .

HOLTZ W.G. & GIBBS H.J. (1956) . " Engineering properties of expansive clays " ASCE trans , Paper 2813 , Vol 121 . pp 658 (17-19)

HUBBERT M.K. & W.W. RUBEY (1959) . " Role of fluid pressure in mechanics of overthrust faulting " Bulletin of the geolechnical . Society of America FEB. Vol 70 , pp 115 - 166

JENNINGS J.E. (1960) . " A revised effective stress law for use in the prediction ofthe behaviour of unsaturated soils . " Pore pressure & Suction in soils Butterworth , London , 1961 .

JENNINGS J.E. (1969) " The engineering problems of expansive soils" . 2nd International conference on expansive . Clay soils .

JENNINGS J.E. & BURLAND J.B. (1962) . Limitations to the use of effective stresses in partly saturated soils " . Geotechnique 12 : 2 .

JONES D.E..(1979) ." The expansive soil problem " Underground space Vol 3, No s ,pp. 221 - 226 .

KANTEY B.A. (1980). " Some secrets to building structures on expansive " Civil engineering - ASCE , December 1980 .

LORD KELVIN (SIR W. THOMSON). (1871). "Hydrokinetic Solutions and Observations" Phil Mag Nov 1877

KEZDI A. (1974) . " Handbook of soil mechanics part 1 : Soil physics " Elsevier , 1974 .

KOMORNIK A. & LIVNEH M . (1969). " Influence of graunlar constituents on the swelling characteristics of expansive clays " 2nd International conference on expansive clay soils , Texas A & M University.

KONING H. L. (1963). " Some observations on the modulus of compressibility of water " . Conference settlement & Compressibility of soils , Wiesbaden.

KRAZYNSKI L.M. (1973) " The need for uniformity in testing of expansive clays". Proceedings, Workshop on expansive clays & Shales in Highway design & Construction. Dr Lambe & S.J . Hanna Editor , Prepared for FHWA (Washington) , Vol 1, pp98 - 128 .

LADD C.C. & LAMBE T.W. (1961). " The identification and behaviour of compacted expansive clays " . Proceedings 5th ICSMFE , Paris 1961 .

LAMBE T. W. (1958) . " The engineering behaviour of compacted clay ". Proceedings ASCE 84 SM2 , 1655- 1 to 1655 - 35 .

LAMDE T. W. (1960) . " A mechanistic picture of shear strength in clay ". Conference on soil shear strength , Colorado pp 503 - 532 .

LAMBE T.W. WHITMAN R.V. (1959) . " The role of effective stress in the behaviour of expansive soils " . Quarterly , Colorado sch . of mines, Vol 54 , No 4 pp 33 - 61 .

LAMBE T.W , WHITMAN R.V. (1969) . " Soil mechanics " . John Wiley & Sons INC . NewYork .

LAUGHTON A.S. (1955) . " The compaction of ocean sediments " . PHD Thesis, University . Cambridge .

LEE I. K. (1969) . " Soil mechanics selected topics . " Butterworths , London.

LI, WEN - HSIUNG , LAM SAU - HAI (1964). " Principles of fluid mechanics " Addison Wesley Publishing CO Internstionsl , Reading , MASS . USA .

LOWE J , JOHNSON T. C. (1960) " Use of back pressure to increase degree of saturation of triaxial test specimens " Research Conference On shear Strength of cohesive soils , ASCE , Boulder Colorado .

LOWE J , ZACCHEO P.F, FELDMAN H.S. (1964) . " Consolidation testing with back pressure " Journal of soil mechanics & Foundations engineering division ASCE Vol90 , No SM 5 , Paper 4058 sept , pp 69 - 86 .

MADEDOR A.O. (1967) . " Consolidation characteristics of compacted clay ." PHD thesis , VMIST , 1967 .

MADHAV M.R. (1970). "Side friction in consolidation tests". Acta Technica Academiae, Scientiarum Hungaricae, Tomus 69, (3-4), pp 467-475.

MALVERN L.E. (1969) . " Introduction to the mechanics of a continuous medium " . Prentice Hall series in engineering of the physical sciences .

MATYAS E.L. (1963) . " Compressibility & Shear strength of compacted soils " . PHD thesis University of London .

MATYAS E.L. , RADHAKRISHNA H.S. (1968) ." Volume change characteristics of Partially saturated soils " . Geotechinque , Vol xvlll, No 4 , December . pp 432-448

METSIK M.S. (1964) ." Research in the field of surface forces " P138 , Moscow Nauka P.R. (In Russian) .

MIT (1963) . " Engineering behaviour of partially saturated soils " . Soil Engineering , Division , Massachusetts institute of technology . DA Paoj 1 -T- 0 - 2i701 - A - 046 - 05 With US army waterways STN .

NAYAK N.V. & CHRISTENSEN R.W. (1974) ." Swelling charecteristics of compacted expansive clays " Clay minerals, Vol 19, No 4 , 1974, pp 251 .

NUR A , BYERLEE J.D. (1972) ." An exact effective stress for elastic Deformation of rock with fluids " . Journal of geophysical research, SEPT, Vol 76 , No 26 , PP 6414 to 6419 .

OLSEN R.E. & LANGFELDER L.J. (1965) ." Pore water pressures in unsaturated soils " Proceedings , ASCE, Vol 91 , No SM4 , PT 1 , PP 127 - 150 .

PADDAY J.F(1969) ." Theory of surface tension " . Surface & Colloid ,Vol 1, Vol 1, Wiley - Interscience, Toronto , PA .

PEDOE .J (1967) ." Advanced national certificate mathematics " . English University Press , P 310 - 312

PUFAHL D.E. (1970). " Evaluation of effective stress componets in non saturated soils " . MSC Thesis, university saskatchewan , Saskatoon SASK. PA

RAMAN V. (1967) ." Identification of expansive soils from the plasticity index and the shrinkage index data". The Indian engineer , Calcutta, Vol 11, No 1, 1967 , pp 17-22 .

RADHAKRISHNA M.S. (1967) ." Compressibility of partially saturated soils". PHD Thesis, University Waterloo, Canada.

RANGANATHAM B.V. & SATYANARAYANA B. (1965)." A rational method of predicting swell potential for compacted expansive clays" . Proceedings 6th International Conference on soil mechanics and foundation engineering , Vol 1 , 1965 .pp 92-96

RENDULIC L (1936) . "Relation between void ratio and effective principle stresses for a remolded silty clay " . Proceedings 1st International conference soil mechanics . p 3

RICHARDS B. G. (1966) ." The significance of moisture flow and equilibria in unsaturated soils in relation to the design of engineering structures built on shallow foundations in Australia ". Symposium on permeability & Capillarity ASTM, Atlantic , city , NewYork , USA .

RING G.W. (1965) "Shrink-swell potential of soils" Public Roads, Vol 33, pp 97-105.

ROWLANDS G.O. (1984) ." The casagrande A and U - lines in soil classification ". Proceedings 8th regional conference . For Africa on Soil mechanics and foundation engineering , Harare . pp 93-98

SALAS J.A.J. & SERRATOSA J.M. (1957) " Foundations on swelling clays " . Proceedings 4th ICSMFE , London . pp 424-428

SAMUELS S.G. (1967) . " The uplift of buildings on swelling clays ". International note 40/67, Building research station .

SCHOFIELD R.K. (1935). "The pF of the water in soil". Trans. 3rd Int. Congr. Soil Sei. 2, 37 - 48.

SCHUURMAN E. (1966) . " The comprssibility of an air water mixture and a theoretical relation between the air and water pressures " . Geotechnigue Vol 16, No 4. pp 269-281

SCOTT R.F (1963). " Principles of soil mechanics ". Addison - Wesley publishing Co INC, Reading , MASS, . USA .

SEED H.B. , CHAN C.K. (1959). " Structure and strength characteristics of compacted clays" . Proceedings ASCE 85 , SM 5 , 87 -128 .

SEED , WOODWARD, LUNDGREN (1962) . " Prediction of swelling potential of compacted clays - for compacted clays" . Journal ASCE , Geotechnical engineering division , Vol 88 , 1962 . pp 53-87

SHERIF M.A , ISHBASHI I , MEDHIN B.W. (1982) ." Swell of wyoming montmorillonite and sand mixtures " . Journal of geotechical Engineering division , Proceedings ASCE . Vol 108 , No GT1 , JAN 1982 . pp 33-45

SHROEDER W.L. (1984) ." Soils in construction " Journal Wiley & Sons , Third edition . 1984 .

SISLER H.H., VANDERWERF C.A. , DAVIDSON A.W. (1953) ." General chemistry ; A systematic approach " . Macmillan Co, NewYork .

SKEMPTON A.W. (1961) ." Effective stress in soils , Concrete & Rocks " . Pore pressure & Suction in soils conference, London , Butterworths .

SNETHEN D.R. (1979) ." An evaluation of methodology for prediction and mininization of detrimental volume change of expansive soils in highway subgrades " . FHWA research peport No FHWA RD 79 49 .

SNETHEN D.R, TOWNSEND F.C, JOHNSON .D, PATRICK D.M , VEDROS P.J. (1975) "A review of engineering experiences with expansive soils in highway subgrades " . FHWA Interim report , FHWA RD 75 48 .

SRIDHARAN A , VENKATAPPA R. (1973) . " Mechanisms controlling the volume change of saturated clays and the role of the effective stress principle". Geotechinque 23 , No 3 , pp 359 - 382 .

TAYLOR D.W. (1942). "Research on consolidation of clays". Dept. of Civil and San. Engg. MIT, Rep No. 82.

TERZAGHI K. (1936) ." The shearing resistance of saturated soils " . Proceedings 1st International , Conference , Soil Mechanics . Vol 1 .

TILLER F.M. (1953) ." Chemical engneering progress" . 49 , 467.

TRUESDELL C. (1966) ." Continuum mechanics 1 - the mechanical foundations of elasticity and fluid dynamics " . International SCI review series 8, Gordon and Breach SCI . Publs International , NewYork .

APPENDIX A

SPECIMEN PRODUCTION TECHNIQUES

A1.1 Introduction

Synthetically prepared soils are employed so as to provide consistent test specimens. It is noted however that in addition to the nature of blend constituents, the method of preparation can significantly effect the soil properties.

Thus, a fixed procedure is presented that repeatedly yields specimens of the required properties.

The following specimen production technique is applicable to all testing systems up to the static compaction procedure, where variations in equipment design require the adoption of differing procedures.

The moulding procedures involve placing the soil in one layer only. This is considered acceptable due to the small overall specimen thicknesses (30mm max.). Larger specimens generally exhibit a density gradient when statically compacted in a single layer. However, no variation has been noted in the author's specimens.

The laboratory facilities at the Polytechnic have a variety of equipment for statically compacting different materials, thus existing equipment is utilised where possible.

A1.2 Equipment required (General)

The required equipment can be separated into two categories : soil preparation and specimen production.

Soil preparation

(a) Kenwood Chef electric mix with bowl and mixing paddle

(b) Suitable steel spatula with flexible blade

(c) Agricultural water spray (hand held) with adjustable nozzle.

(d) Electronic balance (4200g capacity)

(e) Soil container of known mass

(f) Soil constituents, including deaired, deionised water.

(g) Fume cupboard (to minimise dust during dry mixing)

The equipment required for specimen production is described separately for each testing system.

A1.3 Calculation of mix quantities

From fundamental soil mechanics it can be shown that :

$$\rho_d = \frac{\rho_w(1-A_r)}{\frac{1}{G_s} + w} = \frac{\rho_b}{1 + w} \qquad (A.1)$$

where

ρ_d = dry density ; ρ_w = water density ; G_s specific gravity

w = moisture content ; A_r = air voids ; ρ_b = bulk density

and $$\rho_b = \frac{M_s + M_w}{V_s + V_v} \qquad (A.2)$$

M_s = mass of solids ; M_w = mass of water ; V_s = volume solids ;

V_v = volume of voids

Combining (A.1) and (A.2) gives :

$$\frac{\rho_w (1 - A_r)}{\frac{1}{G_s} + w} = \frac{M_s + w M_s}{(V_s + V_w)} \cdot \frac{1}{(1 + w)} = \qquad (A.3)$$

$$= \frac{M_s}{V_T}$$

V_T = total volume

Finally, (A.3) is modified to account for two soil constituent types :

$$\frac{\rho_w (1 - A_r)}{\frac{1}{nG_{s1} + (n-1) G_{s2}} + w} = \frac{M_{s1} + M_{s2}}{V_t} \qquad (A.4)$$

n = percentage of first soil of specific gravity G_{s1}

Thus, knowing all the other parameters, the mass for each constituent (including moisture required) can be calculated.

The above relationships are written into a simple computer program in Basic language for use on the 'Pet' microcomputer thus facilitating rapid calculation of quantities.

Examples of mix quantity calculation

Water density = 10^{-3} g/mm^3

air voids required = 5%

required moisture content = 30%

percentage of soil 1 = 25%

specific gravity soil 1 = 2.24

specific gravity soil 2 = 2.615

total volume = 119448 mm^3

$$\therefore \text{ Total mass of soil } = \frac{10^3 (1 - 0.05)}{\frac{1}{0.25.2.24 + 0.75.2.615} + 0.3} \cdot 119448$$

$$= 162.89\text{g}$$

$\therefore$ Mass of soil 1 = 0.25.162.89 = 40.72 g

Mass of soil 2 = 162.89-40.72 = 122.17 g

A1.4 Mixing procedure

The mixing of material is undertaken in two stages; firstly the constituents are dry mixed, then the required amount of moisture added and wet mixing of the synthetic mix undertaken. The procedure is as follows :

Dry mixing

(a) weigh the correct amount(s) of constituent soil(s).

(b) place constituents into the Kenwood mixing bowl, and mix the constituents using the metal paddle attachment at speed setting 1 for ten (10) minutes.

(c) switch off mixer, remove bowl and check to see that the constituents are thoroughly blended.

The addition of moisture

(a) the mixing bowl is returned to the mixer and approximately a third of the required moisture added to the mix from an agricultural hand-powered water spray. The mixer is then engaged at speed setting 1 until the water is reasonably dissipated throughout the mix.
This procedure is repeated until all the water has been added.

(b) Prior to adding water, wet soil is scraped from the sides of the bowl so as to inhibit caking of the mix. Soil from the bowl is brushed over any water droplets located on the bowl, in order that all water added enters the soil.

(c) The synthetic soil is mixed for one minute at speed setting 3.

(d) Remove the bowl and hand mix soil for two minutes ensuring that all soil is removed from the bowl sides and around the mixing blade.

(e) Repeat steps (c) and (d) until 21 minutes have elapsed (7 times).

In the case of the high plastic or high water content soil mixtures, serious caking of the mixture will occur after about ten minutes in the mixer. Further mixing should only be continued by hand under such circumstances.

(f) The soil mixture is placed in metal foil, the entire package being sealed with clingfilm. This is then placed within a sealable polythene container and allowed to cure for 24 hours.

(g) Prior to curing, a sample is taken from the soil for moisture content determination. This will indicate whether the mixture has been correctly prepared and is suitable for use.

A1.5 Compaction of specimen

The specimens are formed to the required specifications by static compaction. This is achieved by compressing a previously prepared clay mix into a mould using the hydraulic jack.

This basic procedure is common to all specimens, although the varying requirements of the different equipment result in some slight differences between the mould assemblies employed.

The general compaction procedure is therefore listed along with the various mould assemblies required. Further procedural details have been made available in the Polytechnic Geotechnics

Laboratory for future research.

Consolidometer specimens (75mm diameter x 15.0mm depth)

Equipment required : (Refer Figure A.1)

(a) loading frame and hydraulic jack

(b) mould body with upper and lower caps

(c) loading piston

(d) polythene discs (prevents specimen adhering to mould)

(e) block and cylinder for aiding disassembly

(f) stop clock

The soil is compacted using the above equipment into a mould larger than the required diameter. It is then removed from the mould and the consolidometer ring pressed into it to form the final specimen. Finally, excess clay is trimmed away.

76mm and 102mm specimens

These specimens are compacted directly into the test cell bodies employing the same procedure as above.

76mm cell (75mm diameter X 25mm depth)

Equipment required. (Refer Figure A.3)

(a) loading frame and hydraulic loading jack

(b) mould assembly consisting: Rowe cell body; upper collar; loading piston; base plate (steel); two polythene discs.

(c) stop clock

102mm specimen (100mm diameter X 30mm depth)

Equipment required (Refer Figure A.2)

(a) loading frame and hydraulic jack

(b) mould assembly: cell body; base plate; loading piston; two polythene discs; spacing collar

(c) stop clock

A.2 DETAILED 76mm AND 102mm TESTING PROCEDURES

The following information is applicable to both the drained and undrained testing modes, the differences occurring primarily in the interpretation of data which is discussed in Chapters 6 and 7. Procedural differences are noted where appropriate. The test procedure involves five basic steps :

(1) specimen preparation

(2) equipment assembly and test initiation

(3) routine measurements

(4) end test and equipment disassembly

(5) additional operations

A2.1 Specimen preparation

This is fully discussed in Appendix A1.

A2.2 Equipment assembly

(i) 76mm cell assembly (Figs. 5.3; plates 5.1-5.4)

(a) wipe base dry with paper towel

(b) locate cell body containing specimen

(c) place coarse porous disc on top of specimen

(d) locate cell cover and tighten assembly nuts

(e) hand push the piston until slack taken out of system

(ii) 102mm cell assembly (Figs. 5.6,; plates 5.5,5.6)

This differs slightly to that of the 76mm type cell

(a) wipe base dry with paper towel

(b) screw on the ring containing the specimen until hand tight

(c) place coarse porous disc on to specimen, then lower the loading plate over this

(d) attach the triaxial pressure vessel, tighten the assembly nuts - opposite pairs at a time

(e) place cell assembly inside loading frame

(f) engage air cylinder under 2 psi and lower to contact with triaxial plunger

Precise centralising of the cell is achieved by moving the cylinder until secure fit is achieved.

A2.3 Test initiation

The test initiation procedure is common to both test cells :

(a) read initial dial gauge deflection, Bishop's indicator water level and diffused air volume indicator values

(b) isolate cell by closing valves V10, V11 and V12, V13.

(c) apply the required pressure to the respective phases by adjusting the precision regulators 'on the board'. Each pressure is individually checked using the cut in valves provided for each channel (V1 → V4).

(d) ensure that the Bishop's indicator is in operational mode (i.e. volume change mechanism engaged).

(e) open total and air pressure valves V12 and V13 simultaneously followed by valve V11 (water pressure)

Refer to figures 5.2 and 5.5.

A2.4 Routine measurements

These include the flushing and measurement of diffused air from the ceramic disc and monitoring the water volume and total volume changes. They should be made on a daily basis, the general procedure being as follows :

(a) record present value on water volume indicator and diffused air volume indicator using the travelling microscope (discussed later). Artificial illumination is employed for improving visibility, however, the light source is positioned sufficiently distant from the apparatus to prevent heating effects. A low powered, hand held torch was employed, since this had a negligible effect upon the conditions within the environmental chamber.

The vertical deflection and time are also noted.

(b) The Bishop's indicator is switched to the by-pass mode, valves V10 and V7 opened and water flushed from beneath the base into the diffused air indicator. The flushing technique adopted by the author involves several sudden operations of flushing. tap V10, this being very effective at removing trapped bubbles and also resulting in a smaller momentary drop in base pressure. (It is noted that during 'flushing' the base pressure reduces, and remains lowered during continuous flushing). It is advised that a back pressure be applied to the DAVC1 in order that not more than a 10 psi pressure differential occurs across the base plate (so as to avoid cavitation of the water). This pressure is controlled from the 'board'. The procedure is reversed once flushing is complete.

(c) Valve V10 is closed, the Bishop's indicator switched again to the operational mode (engaged), and new readings taken from the Bishop's paraffin and diffused air volume indicators, dial gauge and clock.

A2.5 End test and disassembly

After taking the final set of readings, the equipment is disassembled and the specimen removed for weighing. It is important that the equipment be dismantled as rapidly as possible to prevent ingress of water to the specimen. The following procedure is recommended :

(a) reduce pressures to zero in the following order

(i) isolate cell by closing valves V11, V12 and V13 (V10 is closed).

(ii) adjust pressures (on the board) to zero.

(iii) open valves V11, V12 and V13 in that order.

(b) uncouple airlines to the total and air pressures.

(c) unscrew assembly bolts (on both 76mm and 102mm cells ,remove specimen and ring from the equipment, and dry any water droplets.

(d) weigh the ring and soil and take a specimen for moisture content determination

When the cells are not in use, they are filled with unpressurised de-aired water so as to maintain the disc saturation.

A2.6 Additional operations

(a) Implementation of stress changes

In order to accomplish 'instantaneous' stress changes, the cell valves must first be closed, the pressures raised or lowered and the valves again opened. Some air leakage will inevitably occur at this stage; in order that the stress state will remain constant therefore, it is imperative that leakage is minimised and that the stress change procedure is accomplished as rapidly as possible.

(i) close valves V11, V12 and V13.

(ii) adjust pressures on 'the board' as required.

(iii) open valves V12 and V13 simultaneously, closely followed by V11.

(b) Replenishment of the water reservoir

Due to minute system leaks, this operation must also be completed as soon as possible.

(i) close valves V11 and V9.

(ii) reduce water supply pressure (on the board) to zero.

(iii) remove reservoir, pressure dial.

(iv) refill reservoir with de-aired deionised water.

(v) reseal reservoir, repressurise the water supply.

(vi) engage valves V11 and V9.

(c) Emptying diffused air volume indicators

Following three or four flushings of the cell base, the diffused air indicator chamber will require emptying. This is achieved by simply attaching a pipe to valve T5 and opening it to permit drainage until the desired indicator water level is achieved.

(d) Reading the diffused air volume indicators

The diffused air volume indicator is used daily following the flushing of bubbles from under the high air entry ceramic disc. The operating procedure is as follows :

The initial burettes reading is taken when the indicator chamber is at atmospheric pressure. The chamber is then pressurised so as to create a pressure differential ≒ 10psi across the cell base, and the diffused air flushed to the indicator. Finally, the chamber is depressurised and the burette reading taken.

The lower edge of the meniscus is always taken as the reading point.

Condensation is noted as sometimes forming on the inside of the indicator. This prevents reading of the burette, thus it is suggested that the water level in the indicator chamber always be maintained above the level of the burette air-water interface.

It must be noted that readings made through water will be susceptible to refraction of light in the water. Thus it is imperative that the water level is read on a level plane.

(e) The travelling microscope for measuring the water volume changes in the Bishops (paraffin) indicator

Although primarily designed for making accurate determination of height differential using an in built vernier, this instrument is utilised by the author, for making consistent readings of the burette meniscus levels. It achieves this in two ways :

1. level viewing of the burette is consistently achieved
2. magnification of the meniscus permits a superior judgement of divisions, thus increasing accuracy.

This aspect has apparently not been covered by previous researchers in this field and the above procedure is believed to considerably increase the degree of reading accuracy of the employed indicator.

(g) Use of the Bishops (paraffin) water volume change indicator

The Bishop's water volume change indicator is designed to measure the water flow into or out of a specimen, whilst maintaining a back pressure. The pressurised water supply enters the indicator through a 'junction box' and may be directed in any one of the following ways :

(i) into the left hand burette, out the right or

(ii) into the right hand burette, out of the left or

(iii) by pass the indicator completely, when flushing required

The direction of flow is governed by the position of the select valves in the junction box.

The indicator should be back pressured for one day minimum prior to operation, to ensure that all air is in the diffused state and may be flushed out. The indicator is always read by recording the interface moving downwards. The lowest part of the meniscus is taken as the reading point.

(h) Maintaining ceramic disc saturation

When not in use, the disc is kept flooded by placing a rubber collar around the pedestal to form a reservoir.

A3 CONSOLIDOMETER TESTING PROCEDURES

A3.1 The constant volume swell pressure (CVSP) test

As implied by the title, this test measures the swell pressure of an unsaturated soil generated following innundation with water, by preventing all expansion. The test procedure can be outlined as follows :

Preliminary stage

(a) production of the specimen : the test soil is prepared and the specimen produced as detailed in Appendix A.

(b) the equipment is assembled (ref. Section 5.3.2) care being taken to ensure that all slack is taken out of the system. A clingfilm seal is placed over the test chamber to restrict water evaporation during testing.

(c) a nominal seating pressure of 1 psi is applied to the specimen.

(d) the chart recorder is calibrated and the pen markers set to the start position.

Test stage

(a) The specimen is loaded to the desired conditioning overburden pressure and allowed to come to equilibrium volume; subsequent testing must not proceed until this is achieved, however, this will be clearly indicated on the chart recorder.

(b) The specimen is innundated with de-aired, deionised water by feeding water to the upper and lower specimen faces.

(c) As the specimen imbibes water. and attempts to swell, the consolidometer is loaded, thereby increasing the restraining pressure so as to maintain constant volume. Once the tendency to swell ceases, this pressure is termed the apparent swell pressure..

(d) The load is then incrementally increased in order to obtain sufficient data for plotting the load-deflection curve. Successive increments are not applied until the specimen has achieved equilibrium under the previous loading conditions.

(e) Once the specimen has been loaded to a maximum value, the load is then reduced incrementally (rebounded) back to the original seating load (0.5 Kg).

(f) The test procedure is concluded by dismantling the cell as rapidly as possible, and removing the specimen for moisture content determination.

A3.2 The Unrestrained Vertical Swell (UVS) test

This test method is devised by the author as a means for verifying the constant volume swell pressure (CVSP) test. It is not one of the earlier described free swell tests.

The possibility of using a case study data for verification purposes was quickly ruled out due to the lack of suitably documented sites within the U.K. This led to the development of a procedure that would provide a swell value by which the CVSP predictions could be assessed.

The new test involves inundating the specimen with water and permitting it to swell freely to equilibrium, under the in situ overburden.

The measured swell is then compared with that calculated using the constant volume swell pressure data, an assessment of the latter made on that basis. The testing procedure is as follows :

Preliminary stage

The same as the constant volume swell pressure test.

Testing stage

(a) The specimen is loaded to the required overburden as before.

(b) The specimen is innundated with de-aired, deionised water and permitted to swell freely until equilibrium is achieved.

(c) The equipment is dismantled as rapidly as possible and the specimen removed for moisture content determination.

The chart recorder

The chart recorder plots the deformation history of each specimen. However, it is necessary to indicate on the output which loading conditions correspond to each deformation.

The possibility of using a case study data for verification purposes was quickly ruled out due to the lack of suitably documented sites within the U.K. This led to the development of a procedure that would provide a swell value by which the CVSP predictions could be assessed. The new test involves inundating the specimen with water

This value of 'free swell' is then compared with that calculated using the constant volume swell pressure test data an assessment of the latter made on that basis. The testing procedure is as follows ;

Preliminary stage

The same as the constant volume swell pressure test.

Testing stage

(a) The specimen is loaded to the insitu overburden as before.

(b) The specimen is inundated with de-aired, deionised water and permitted to swell freely until equilibrium is achieved.

(c) The equipment is dismantled as rapidly as possible and the specimen removed for moisture content determination.

The chart recorder

The chart recorder plots the deformation history of each specimen, but requires recalibration in between each test.

CONSOLIDOMETER SPECIMEN
COMPACTION APPARATUS

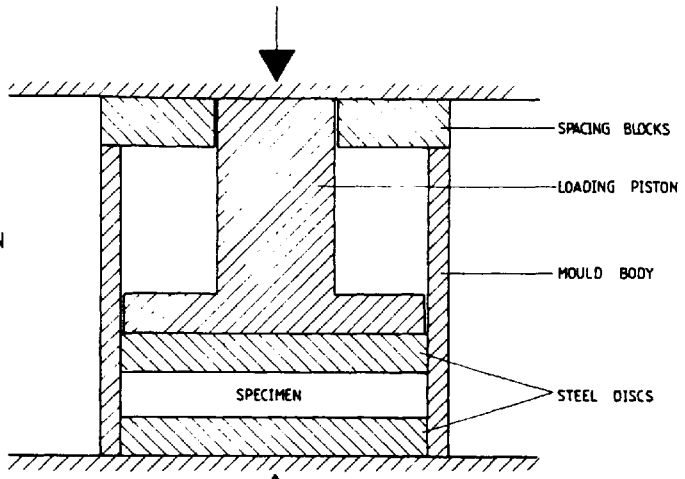

FIGURE A·1

'TRIAXIAL' SYSTEM SPECIMEN
COMPACTION APPARATUS

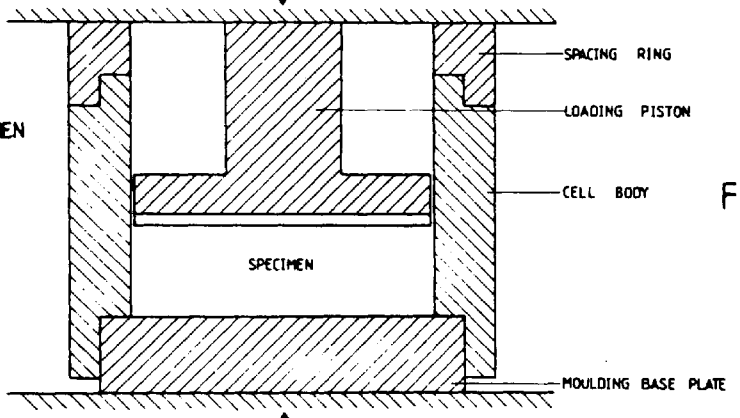

FIGURE A·2

'ROWE' SYSTEM SPECIMEN
COMPACTION APPARATUS

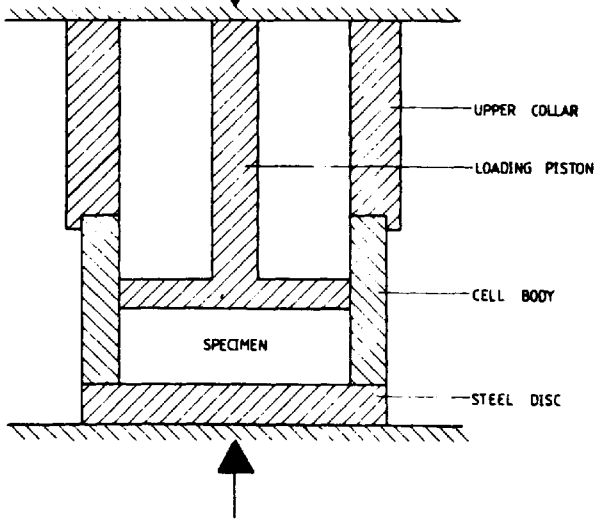

FIGURE A·3

APPENDIX B

B.1 CHOICE OF SUITABLE TEST CLAYS

In order to gain an understanding into the volume change behaviour of expansive clays, it was considered imperative that

(i) several soils be tested, exhibiting a range of swell properties, and

(ii) the swell properties could be consistently controlled.

The above criterion was fulfilled by employing artificially reconstituted clay mineral mixtures, which comprised of the following components :

(a) Expansive component (Sodium Montmorillonite)

This was chosen as the expansive component since it is probably the most expansive clay mineral available (LL $\simeq$ 530%); it will therefore (when combined with an inert material) permit production of all expansive soil types likely to be required for the purpose of this project.

In addition, the mineral may be readily procured from the larger suppliers.

(b) Non expansive - inert component (Kaolinite)

Since the emphasis of this study was to examine expansive clays, it was decided that a clay should be used as the second non expansive component (granular and other inert materials have been employed by several authors). Kaolinite was chosen since it is

known to exhibit minimal expansion behaviour although the liquid limit of 49% is slightly higher than ideally required.

This mineral is also readily available from the larger suppliers.

The refined quality of the minerals ensured that the reconstituted 'test soils' would repeatedly exhibit constant swell properties; the mixing procedure, also crucial to specimen consistency is detailed in Appendix A.

It was recognised that the properties of the minerals might vary between supply batches, thus sufficient quantitites were procured for the anticipated test programme.

B.2 TEST MATERIALS

B.2.1 Sodium Montmorillonite

The mineral used in this project (trade name : Wyoming Bentonite) originated from the Wyoming, South Dakota area of the United States. It has a very high liquid limit (600%:Steetley, 530%:author) and is widely acknowledged as exhibiting extreme swell characteristics.

It was supplied by Steetley Mineral Ltd. in the form of a light greyish, finely ground powder (72% passing the 300BSS), and came packed in 50Kg bags.

The mineral is extremely hydroscopic, and although 'dry' when supplied, it does in fact contain up to 3% moisture when stored in the atmosphere; it was therefore dried and effectively sealed in

moisture proof containers for 24 hours prior to testing. The properties of the mineral as provided by the suppliers are listed in Table B.1. The author disputes the liquid limit and specific gravity values given and has determined the following values

LL = 530% as opposed to 600%
SG = 2.27 as opposed to 2.5

It is acknowledged that the liquid limit test is very difficult to successfully conduct upon such a high swelling (and thixotropic) mineral; for this reason, the variation between the author's and Steetley's values are considered inevitable.

Of greater importance (with regard to the mix quantity calculations) is the specific gravity value; the author has consistently determined the specific gravity to be in the order of 2.27. Due to the mineral's thixotropic nature, the sample could not be thoroughly wetted with water; the test was therefore conducted with paraffin and the result adjusted accordingly.

The difference in results cannot be readily explained however. The author's results are preferred since they are known to relate to the material as used.

B.2.2 Kaolinite

This whiteish coloured mineral originated from Cornwall, UK where it is hydraulically mined and sold to the ceramics industry under the trade name of 'China Clay'. It has an intermediate plasticity (LL = 49%), although it is widely acknowledged as

exhibiting minimal expansive behaviour.

The mineral was supplied by Steetley Minerals Ltd. in a partially crushed and dried form (maximum lump size of 20mm, average moisture content = 12%); it had therefore to be dried, crushed and its moisture content conditioned prior to laboratory use. However, once dried, it retained a low moisture value for a considerably longer period than Montmorillonite (due presumably to its lower hydroscopic nature).

The suppliers technical information regarding this mineral is given in Table B.2.

B.2.3 General

The technical data provided by the supplier, apart from being insufficient, was considered of marginal accuracy only. The policy was therefore to repeat the more important (and any missing) tests, which were carried out according to BS 1377. The results of these are listed in Table B.3.

B.3 RANGE OF CLAY MIXTURES

The maximum possible range of liquid limit was between 49% (Kaolinite) and 530% (Sodium Montmorillonite). However, it was decided that a more modest range would be employed for the main test programme, thereby coinciding with the liquid limit and swell properties likely to be encountered in practice.

Four main mineral mixtures were produced (Table B.3) the Montmorillonite content varying between 0 and 30% ; this yielded a maximum liquid limit of 142%. Other mix proportions were employed during the consolidometer testing in an attempt to determine trends in extreme expansive behaviour; these are also detailed in the same table.

B.4 CLAY MINERAL COMPOSITION

In addition to the chemical analysis data provided by the suppliers (Tables B.1 and B.2), a qualitative analysis of the clay mineral composition by XRD indicated small amounts of impurities in both the Wyoming Bentonite and China Clay.

(a) Wyoming Bentonite = Sodium Montmorillonite + Quartz + Feldspar

(b) China Clay = Kaolinite + Illite + Feldspar

The above impurities were anticipated due to the minerals having been obtained'straight from the ground'; however, it is likely that the relative proportions of these would vary between supply batches - which validates the policy of procuring sufficient raw materials for the entire programme.

B.5 CAPILLARY-MOISTURE RELATIONSHIPS

B.5.1 Description

One of the main distinguishing features of an unsaturated expansive soil is its varying moisture deficiency (suction) with

changes in the overall moisture content; this is known as the capillary moisture relationship.

Since all experimentation in this project involved the wetting of specimens, it was considered appropriate that the suction-moisture content relationships be determined for the employed clay mineral mixtures.

B.5.2 Test procedure

The relationships (figure B.1) were determined by using the main testing equipments detailed in Chapter 5 and a test procedure very similar to Hilf's axis translation technique (1957). Specimens were produced (Appendix A) and the apparatus assembled as quickly as possible; the air pressure was then increased until the specimen exhibited no moisture deficiency - this was termed the initial suction value.

The specimen was then allowed to stand for 48 hours until it was positively ascertained that no moisture intake would occur.

The air pressure was then reduced, the specimen again allowed to equilibrate and the moisture content and corresponding suction values recorded. This procedure was repeated until sufficient data points could be obtained to plot the capillary moisture relationships.

B.5.3 Comments

Figure B.1 illustrates the capillary moisture relationships for the main clay mineral mixtures employed during the project.

Notably there are comparatively few data points below a suction value of 100kN/m^2 ; this is due to the extremely long equilibrium times required for the specimens at that stress condition (in excess of a week following each stress change for the higher plasticity soils).

The figure clearly indicates a dramatic reduction in pressure deficiency (suction) for a comparatively small increase in moisture content - down to suction values of between 100-150 kN/m^2. Below this value, the opposite tends to occur i.e. a large increase in the moisture content is required to effect a small change in suction. Also, increasing plasticity appears to slightly decrease the influence of moisture content change upon the suction value i.e. by increasing the liquid limit, a larger increase in moisture content is required to effect the same decrease in swell pressure.

The above relationships were observed during the wetting cycle of the soils only; it is anticipated that they would exhibit hysteretic behaviour were the drying cycle also examined. The drying cycle could not be instigated due to equipment limitations.

B.6 CLAY MINERAL MIXTURE STRUCTURES

B.6.1 Introduction

It was not intended that an investigation be conducted into the structures of the clay mineral mixtures employed - that would require a study in its own right.

However, a series of scanning electron miscrocope (SEM) photographs (plates B.1 to B.5) were obtained of the basic mineral constituents and subsequent mixtures. This was undertaken in an attempt to usually gauge the influence of an increasing proportion of expansive minerals (in this case sodium Montmorillonite) upon the structure. The photographs are also provided to facilitate future development of this aspect.

B.6.2 Basic constituents

(a) Sodium Montmorillonite

Plates B.1(a,b) illustrates two views of the sodium Montmorillonite employed in this project.

Plate B.1(a) indicates the characteristically 'crinkled' end on view and plate B.1(b) , the apparently flatter surface resulting from looking down on several layers.

(b) Kaolinite

Plate B.2(a) provides a 'low' magnification (x 50) view of the soil grains as produced.

The higher magnitifcation view in plate B.2(b) clearly indicates the hexagonal plate type structure of Kaolinite.

(c) Comments

Section B.4 indicated the small quantity of impurities present in the mineral constituents. These appeared to exhibit themselves in many of the photographs in the form of unidentifiable nodules etc.

B.6.3 Clay mineral mixtures

It was not possible to quantify the relative proportions of Montmorillonite and Kaolinite from the photographs (plates B.1-B.5) ; however the qualitative effects were clearly observable in the form of the various clay mineral structures.

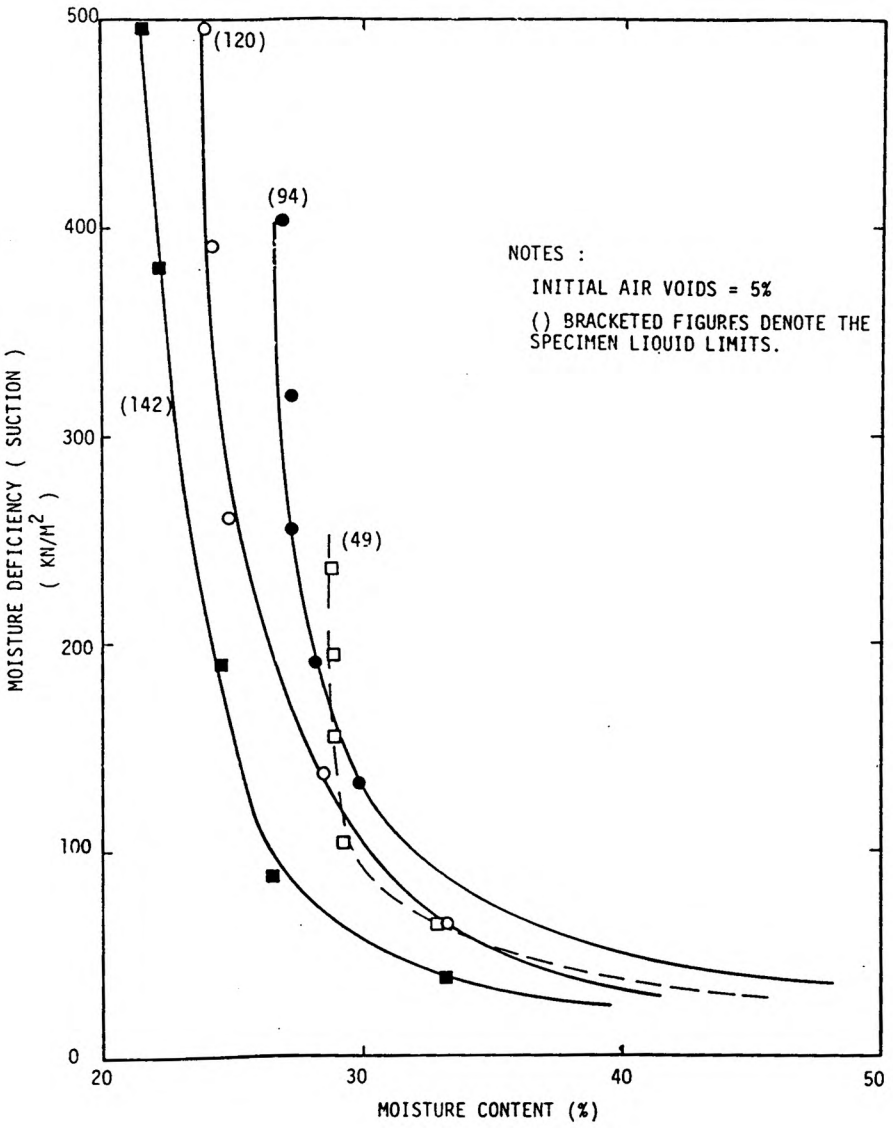

FIGURE B.1

CAPILLARY - MOISTURE RELATIONSHIPS
FOR THE CLAY MINERAL MIXTURES

NAME	: SODIUM MONTMORILLONITE
TRADE NAME	: WYOMING BENTONITE
ORIGIN	: WYOMING, SOUTH DAKOTA AREA OF THE UNITED STATES
COLOUR	: YELLOWISH - GREY

CHEMICAL ANALYSIS :

	%
SiO_2	55.6
TiO_3	0.1
Al_2O_3	16.5
Fe_2O_3	5.1
Ca O	1.9
Mg O	2.0
Na_2O	1.2
K_2O	0.6
Mn_3O_4	0.1
LOSS AT 105°C	11.5
LOSS AT 1000°C	5.7

SPECIFIC GRAVITY = 2.5

pH (5% SUSPENSION IN DISTILLED WATER) = 9.3

SWELLING VOLUME = 20-25 mls/2gms

LIQUID LIMIT = 630% (BS 1377)

CATION EXCHANGE CAPACITY (AMMONIUM EXCHANGE) = 70 Meqs/100g

BULK DENSITY = 800-950 Kg/M^3 (LOOSE)

PARTICLE SIZE (PASSING 200 MESH BS MINIMUM) = 99.95%

TABLE B.1

SODIUM MONTMORILLONITE : SUPPLIERS TECHNICAL DATA

NAME	: KAOLINITE
TRADE NAME	: CHINA CLAY (TYPE 5 PAPER FILLER CLAY)
ORIGIN	: PAR, CORNWALL, UNITED KINGDOM
COLOUR	: WHITE

CHEMICAL ANALYSIS :

	%
SiO_2	47.4
Al_2O_3	37.2
Fe_2O_3	0.65
TiO_3	0.04
Ca O	0.05
Mg O	0.22
K_2O	1.6
Na_2O	0.06

MOISTURE CONTENT = 10 ± 2 %

pH = 5 ± 0.5

PARTICLE SIZE DISTRIBUTION :

+300 BSS MESH = 0.03% MAX

10mM = 15.0%

2mM = 45.0%

(SEE BELOW)

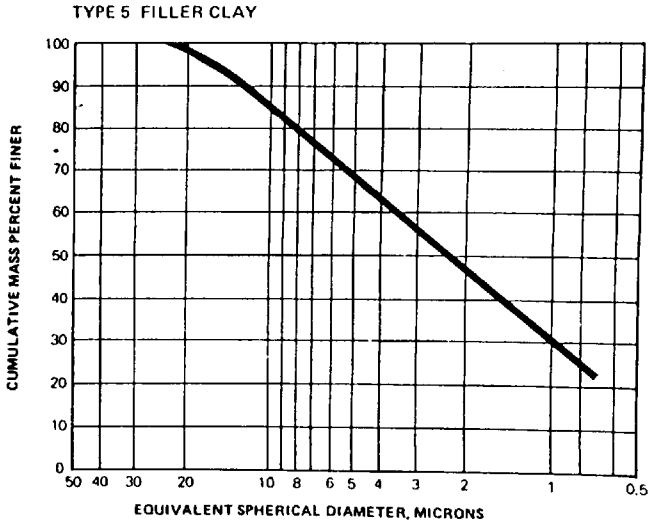

TABLE B.2

KAOLINITE : SUPPLIERS -TECHNICAL DATA

SOIL TYPE			LIQUID LIMIT	PLASTIC LIMIT	PLASTIC INDEX	LINEAR SHRINK.	SPECIFIC GRAVITY
MONTMOR. (%)		KAOLINITE (%)	(%)	(%)	(%)	(%)	
0	*	100	49	27	22	5	2.616
10	*	90	94	30	64	14	2.580
20	*	80	120	33	87	18	2.546
25		75	141	36	105	NA	NA
30	*	70	142	43	99	19	2.511
50		50	235	27	207	NA	2.442
75		25	382	39	343	NA	NA
100		0	530	43	487	NA	NA

* DENOTES MINERAL MIXTURES USED IN THE MAIN TESTING PROGRAMME

TABLE B.3

GENERAL PROPERTIES OF THE CLAY MINERALS AND THEIR MIXTURES

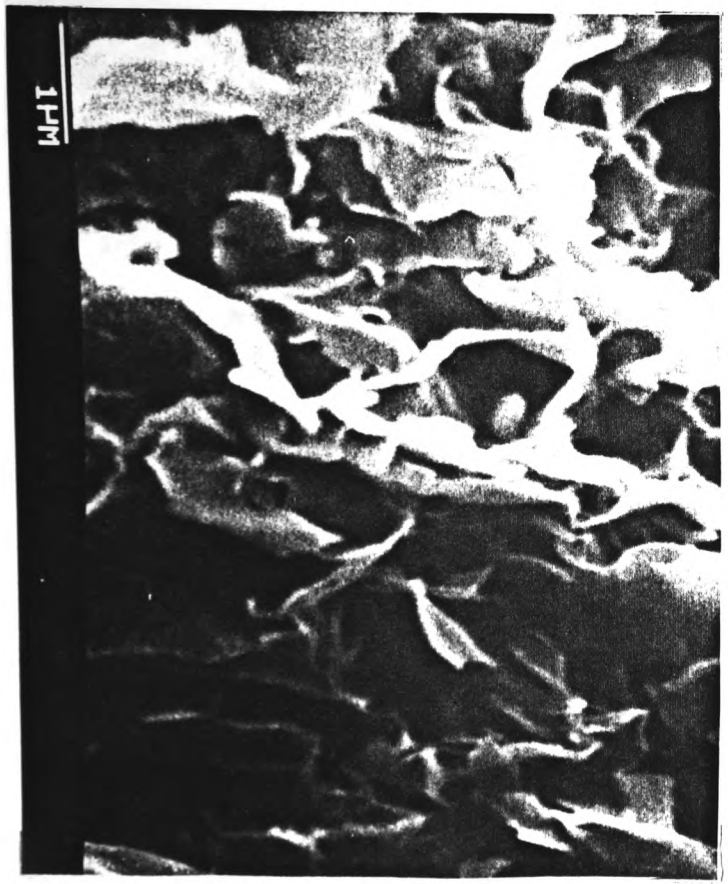

PLATE B.1(a)

SODIUM MONTMORILLONITE (VIEW No 1)
MAGNIFICATION OF 20000X

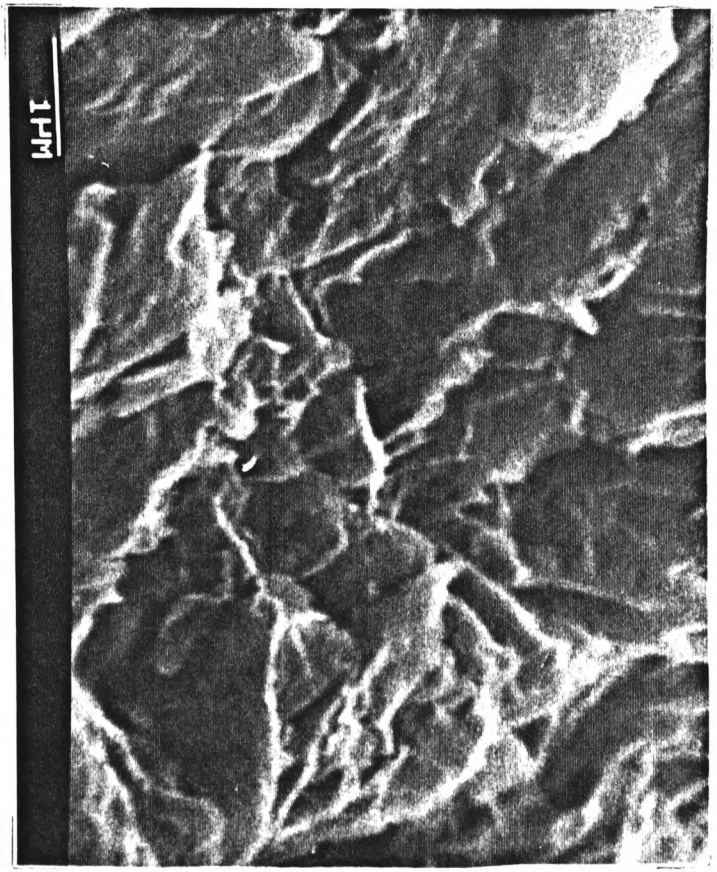

PLATE B.1(b)

SODIUM MONTMORILLONITE (VIEW No 2)
MAGNIFICATION OF 20000X

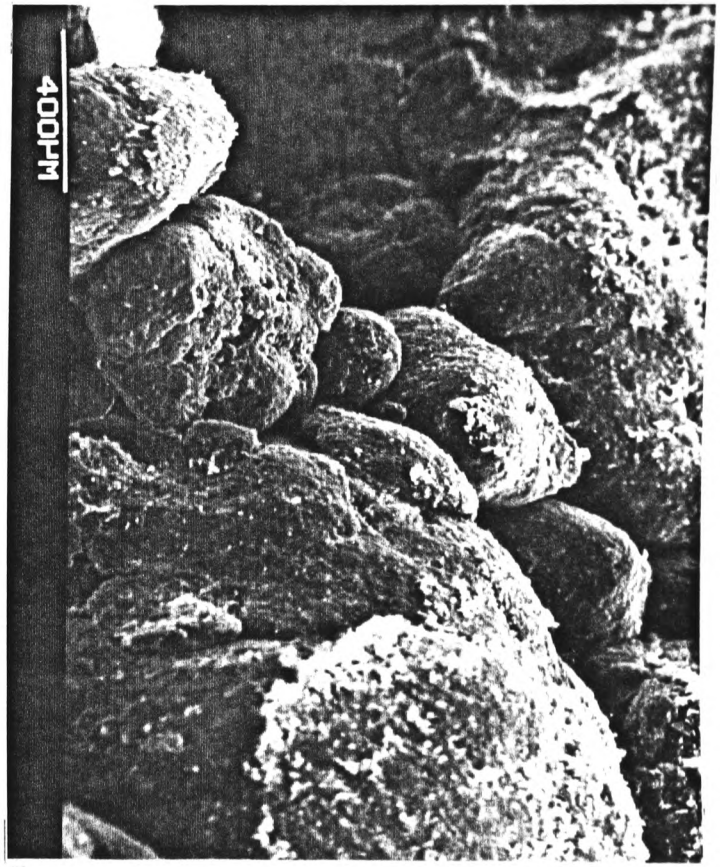

PLATE B.2(a)

KAOLINITE (VIEW No 1)
MAGNIFICATION OF 50X

PLATE B.2(b)

KAOLINITE (VIEW No 2)
MAGNIFICATION OF 20000X

PLATE B.3

10% MONTMORILLONITE + 90% KAOLINITE
MAGNIFICATION OF 5000X

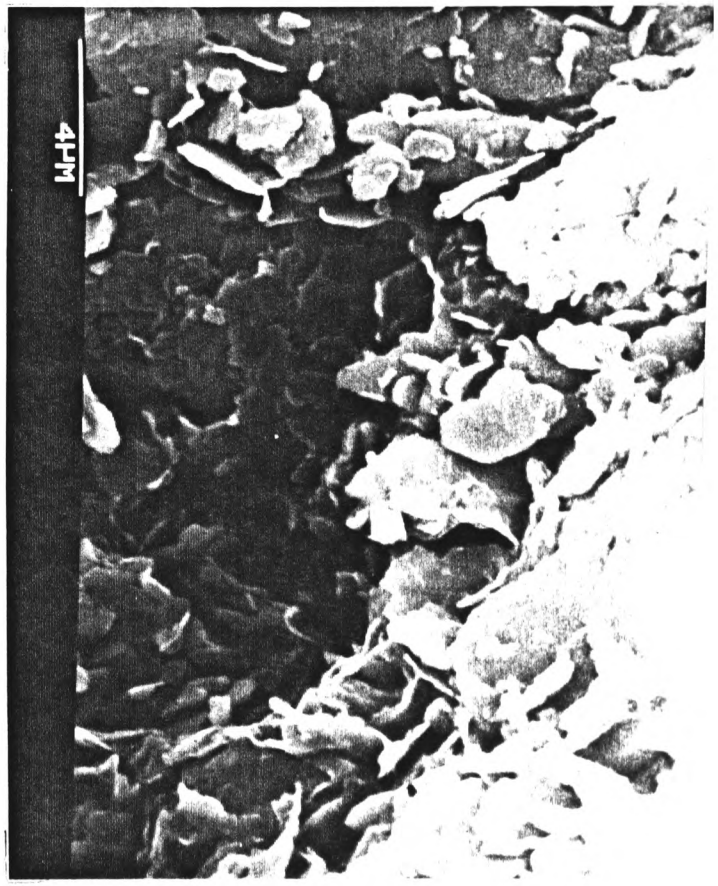

PLATE B.4

20% MONTMORILLONITE + 80% KAOLINITE
MAGNIFICATION OF 5000X

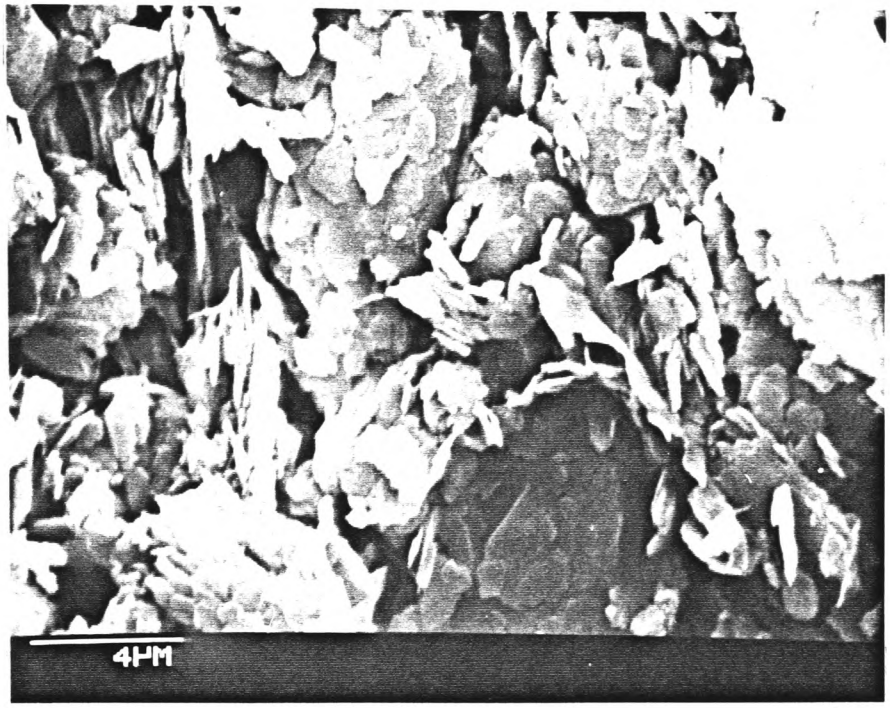

PLATE B.5

30% MONTMORILLONITE + 70% KAOLINITE
MAGNIFICATION OF 5000X

APPENDIX C

CALIBRATIONS

INTRODUCTION

Most of the equipment employed in this project was either constructed 'in house' or obtained direct from the manufacturers. In either case, calibration factors were not available and had to be accurately determined before testing could proceed.

This Appendix outlines the calibration procedure and presents the calibration either in graphical, tabular or both forms.

C.1 MEASUREMENT DEVICES

C.1.1 Linear displacement transducers

Continuous displacement monitoring of the consolidometer tests was accomplished using linear displacement transducers linked to a chart recorder.

The transducers have a 12mm maximum travel and require a 2 VDC energising supply; the ones used in this project were produced by the Sakai Equipment Corporation (Japan).

The transducers were calibrated by mounting them with a micrometer to a sturdy base and energising with 2.0VDC (figure C.1). The voltage output was then recorded as the micrometer was adjusted. The results and calibration line are presented in figure C.2.

C.1.2 Pressure Transducers

Electronic pressure transducers were employed for the purpose of monitoring hydraulic (water) and pneumatic (air) pressures. The types employed, consisted of a strain gauge bridge mounted onto a silicon diaphragm; these were then energised using a 10VDC voltage supply, and yielded a maximum output of 200mV.

Two pressure ranges were monitored, and required the use of two transducer models. The first range exhibited a ceiling of 80 psi/552kN/m^2 and was easily handled by those produced by Bell and Howell Ltd. (up to 100 psi/690kN/m^2). The second range (up to a maximum of 115 psi/793kN/m^2) required the use of 'Druck Ltd' transducers with a ceiling of 225 psi/1551kN/m^2.

The transducers were calibrated by pressurising them with a reference pressure source (in this case a G.D.S. pressure controller; the corresponding electronic output was then recorded and a calibration line constructed.

The calibrations for all transducers are listed in Table C.1 and a typical calibration line illustrated in figure C.3.

C.1.3 Water volume change indicators

The Bishop's paraffin volume change indicators were employed for monitoring the water volume intake to the specimens. Since the volume changes encountered were to be very slight in some instances (i.e. null testing) then it was imperative that any leaks be plugged or at least quantified with some accuracy.

The indicators were tested for leakage by back pressuring them to a value equal to the maximum anticipated operating pressure. The water-paraffin (Kerosene) interface was then monitored over a period of days.

The calibration results are presented in figure C.4.

C.1.4 Diffused air volume change indicator

Since the diffused air volume change indicator is actually employed for only a very short period each day (less than a few minutes) then the minute long term leakages so relevant to the water volume change indicators are of secondary importance only.

Of primary importance therefore is the ability to accurately measure the total volume of diffused air bubbles collecting beneath the ceramic disc.

This can be ascertained by pressurising an empty test cell and leaving the valve open to the water volume change indicator. As the air diffuses through the ceramic disc, so the water will be displaced in the indicator; if the diffused air is now flushed from beneath the base (refer flushing procedure, Appendix A2.4(b)) then the volume of air recorded in the indicator should equal the previously recorded apparent change in water volume. Non equivalence of the measured values indicates malfunctioning of the equipment.

Both diffused air volume change indicators were subject to the above testing procedure and exhibited a satisfactory calibration curve. (Figure C.5).

C.2 LOADING SYSTEMS

C.2.1 Air cylinder

As a result of piston friction, and the difference between the specimen and air cylinder piston diameters, the air pressure applied to the air cylinder did not equal the specimen overburden. It was therefore necessary to determine a calibration factor before testing could proceed.

This was achieved by bolting the air cylinder into a rigid loading frame and pressurising it,thereby causing a load to be applied to an accurately pre-calibrated load cell. The corresponding voltage readout from the load cell was recorded and thus permitted the calculation of a voltage/air cylinder thrust calibration.

By applying the load cell calibration it was then possible to calculate the air cylinder-specimen surcharge calibration curve (figure C.6).

C.2.2 76mm cell convoluted rubber jack

As a result of the expansion of the convoluted rubber jack against the Rowe cell body, the apparatus does not apply the same pressure to the specimen, as is applied to it.

A correction factor was determined by comparing the difference between the applied pneumatic pressure and the pressure applied by the rubber jack to a load cell (figure C.7).

The load cell employed was energised using a 2VDC supply and the output monitored using a Bruel and Kjaer strain bridge.

C.3 EQUIPMENT COMPRESSIBILITIES

C.3.1 76mm cell

The 76mm cell loading system was noted as undergoing a load related compression during use. It was therefore essential that such behaviour be quantified in order that the true specimen volume change could be determined. The calibration data was obtained by replacing the soil specimen with a near identically sized rigid steel plug and then incrementally increasing the load (simultaneously recording both the deflection and applied load) - refer figure C.3. The figure is employed by subtracting the correction value (corresponding to the surcharge on the specimen) from the measured deflection during a test.

C.3.2 102mm cell

A similar equipment compressibility related problem was encountered with the 102mm cell.

As before, a specimen sized steel plug was inserted in the apparatus, and the loading mechanism operated in increments to determine its compressibility behaviour.

The data is presented in figure C.9, and as with the 76mm cell, the compression value (obtained from the curve at a surcharge value corresponding to test surcharge) is subtracted from the measured deflection.

C.3.3 Consolidometers

Consolidometers have long been recognised as undergoing compression during loading, and Fredlund (1969) suggests computing the mean deflection over the anticipated loading range. This provides a correction factor by which measured volume changes may be adjusted to indicate the true value. These suggestions have been implemented and the compressibility values for the repeated cyclic loading of all consolidometers used presented in Tables C.2 and C.3. The correction values are employed by subtracting from the measured deflection at a corresponding applied load.

C.4 LEAKAGES

C.4.1 On/off valves

The on/off valves employed throughout the equipment were of a sub miniature type produced by Soil Instruments Ltd.

Each valve was tested for leakage by back pressuring one side up to 60 psi and connecting the other to a water (paraffin type) volume change indicator. None of the accepted valves exhibited any observable leakage over a period of one week. The connections were then reversed.

It is noted that approximately a fifth of all valves leaked unacceptably and were therefore rejected.

C.4.2 76mm cell leakage

The main pressure housing of this test cell was required to maintain an internal air pressure whilst isolated (i.e. all incoming

valves closed). This aspect was tested by connecting a pressure transducer to one of the upper cell ports, pressurising the cell to the maximum anticipated cell pressure (60 psi) and then monitoring the pressure over a period of a few days.

Initial efforts (by immersing the pressurised cell in water) quickly isolated the main leaks, and final monitoring indicated a linear air pressure demise of approximately 5 psi in 30 minutes. This was considered satisfactory in view of the fact that the cell would be operated in this mode for less than 5 minutes at a time.

C.4.3 102mm cell

As with the 76mm cell, 102mm cell (100mm specimen) was pressurised, and monitored for pressure variation. The immersion procedure was again repeated and resulted in the location of the major leakages; having undertaken this procedure, the cell leakage was reduced to 1 psi/8 minutes.

Subsequent remedial action failed to improve upon this loss; however, its use was justified since the cell was to be operated in this mode (isolated) for no more than 5 minutes, and the loss of such a small pressure was considered having minimum influence over the soil stress state.

C.5 CERAMIC DISCS

C.5.1 General

The ceramic discs were purchased over sized and had to be turned on a lathe to the correct dimensions; the final measurements are given in Table C.3.

C.5.2 Hydraulic conductivity

The hydraulic conductivity (permeability) should remain relatively constant throughout the disc's life; a sudden increase is considered indicative of a crack, which effectively renders it unserviceable (as a barrier to direct air flow).

The permeability was measured by filling the test chamber with water to a depth of 20mm, applying an air pressure to its surface, and monitoring the rate of water outflow to a Bishop's paraffin indicator. The conductivity readings taken intermittently during the testing are presented in figure C.10; these indicate a gradual reduction in the conductivity with time, and this is considered to be due to the contamination of the disc's upper surfaces with the fine clay particles.

MANUFACTURER	MAXIMUM PRESSURE (KN/M^2)	NUMBER	CALIBRATION [3]
BELL & HOWELL	690	L60435	V = 2.867.P + 0.441
"	"	L61978	V = 3.747.P - 0.973
"	"	L61977	V = 3.700.P - 0.038
"	"	L61979	V = 3.639.P + 0.035
"	"	L61976	V = 3.7199.P + 0.059
DRUCK Ltd.	1551	95692	V = -6.67.P - 0.319
"	"	95651	V = -6.67.P - 0.619

NOTES

1. PRESSURE SOURCE : GDS HYDRAULIC PRESSURE CONTROLLER
2. EXCITATION VOLTAGE : 10 V DC
3. CALIBRATION UNITS : VOLTAGE OUTPUT (V)= mV ; PRESSURE (P)= KN/M^2

TABLE C.1

CALIBRATION DATA FOR
PRESSURE TRANSDUCERS

EQUIPMENT IDENTIFICATION	NUMBER OF OBSERVATIONS	PRESSURE RANGE (KN/M^2)	MEAN DEFLECTION (MM)
F	20	10.79 - 107.91	0.0281
		107.91 - 1079.1	0.0862
		1079.1 - 107.91	0.0835
		107.91 - 10.79	0.0304
G	20	10.79 - 107.91	0.0261
		107.91 - 1079.1	0.0653
		1079.1 - 107.91	0.0622
		107.91 - 10.79	0.0288

TABLE C.2

COMPRESSIBILITY OF CONSOLIDOMETERS
(CVSP TESTING)

EQUIPMENT IDENTIFICATION	NUMBER OF OBSERVATIONS	PRESSURE RANGE (KN/M^2)	MEAN DEFLECTION (MM)
A	20	10.79 - 107.9	0.0199
		107.91 - 1079.1	0.0516
		1079.1 - 107.9	0.0473
		107.91 - 10.79	0.0129
B	20	10.79 - 107.91	0.0319
		107.91 - 1079.1	0.0597
		1079.1 - 107.91	0.0567
		107.91 - 10.79	0.0345
C	20	10.79 - 107.91	0.0197
		107.91 - 1079.1	0.0318
		1079.1 - 107.9	0.0301
		107.91 - 10.79	0.0209
D	20	10.79 - 107.91	0.0203
		107.91 - 1079.1	0.0408
		1079.1 - 107.91	0.0373
		107.91 - 10.79	0.0234

TABLE C.3

COMPRESSIBILITY OF CONSOLIDOMETERS
(UVS TESTING)

DISC NUMBER	EQUIPMENT TYPE	DIAMETER (MM)	AVERAGE THICKNESS (MM)	MASS (g)
2	ROWE	73.8	6.97	53.63
3	"	79.3	7.33	65.26
4	TRIAXIAL	99.12	7.60	110.13
5	"	100.38	7.51	104.10
6	"	100.54	7.83	110.48
7	"	99.71	7.51	111.00
8	"	108.39	7.53	120.95

TABLE C.4

CERAMIC DISC MEASUREMENTS

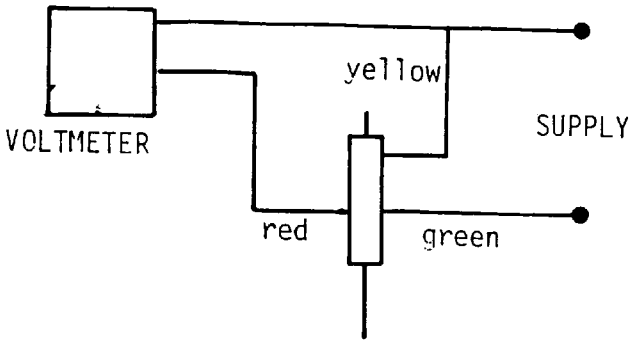

FIGURE C.1
WIRING DIAGRAM FOR LDT CALIBRATION

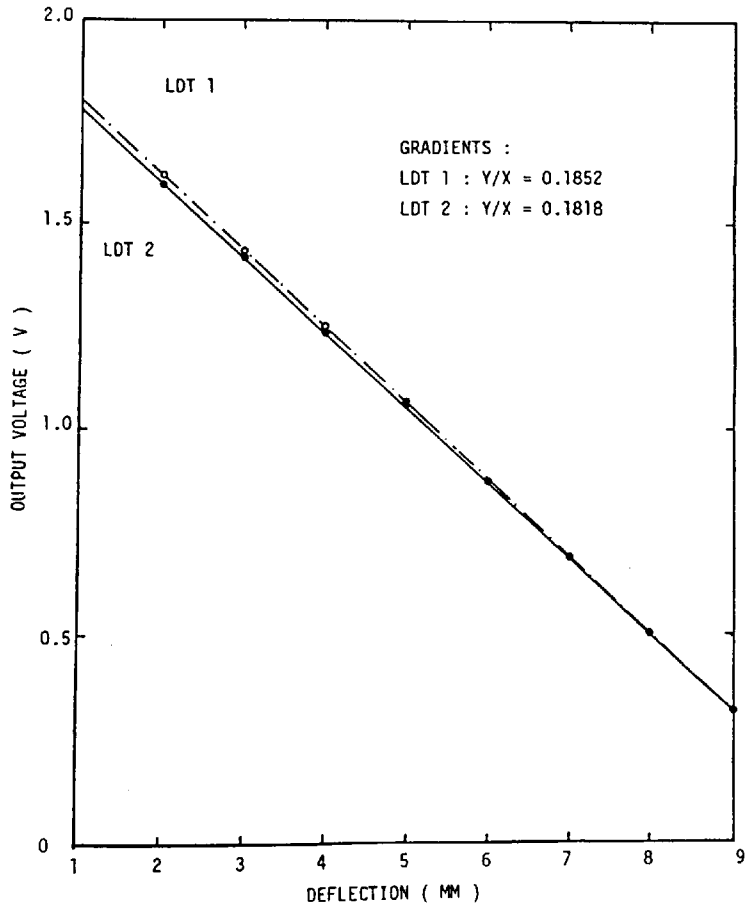

FIGURE C.2
LDT CALIBRATION LINES

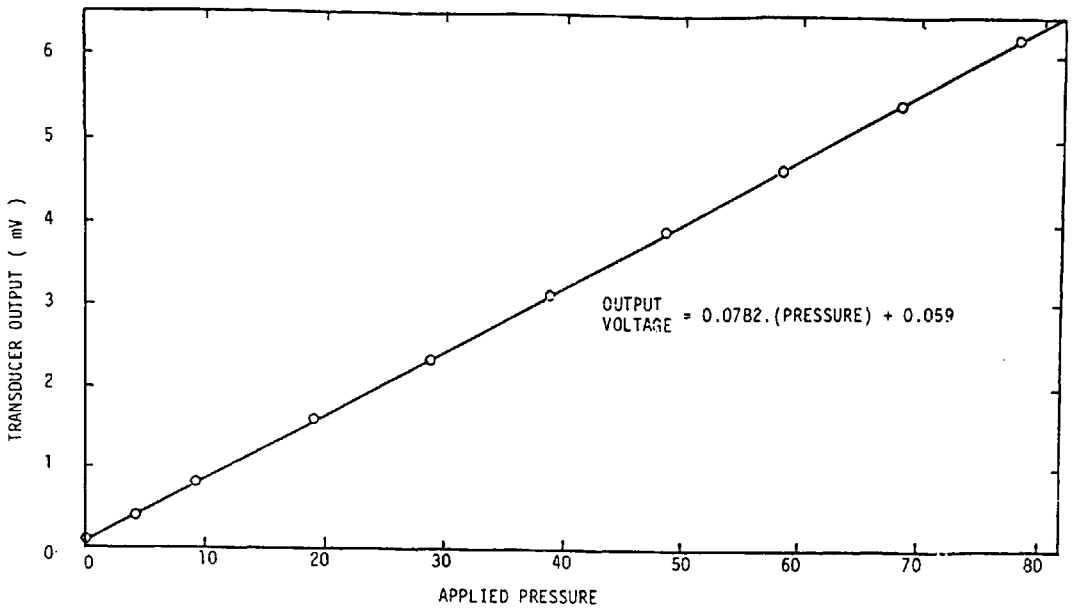

FIGURE C.3

TYPICAL CALIBRATION LINE FOR A PRESSURE TRANSDUCER (No L61976)

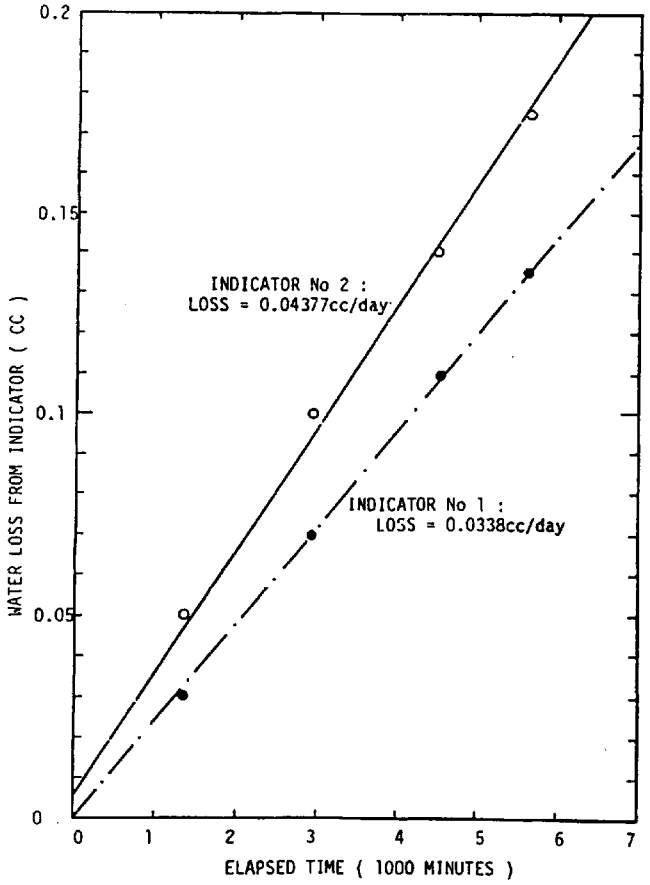

FIGURE C.4

WATER LEAKAGE DATA FOR THE PARAFIN (BISHOPS) WATER VOLUME CHANGE INDICATORS.

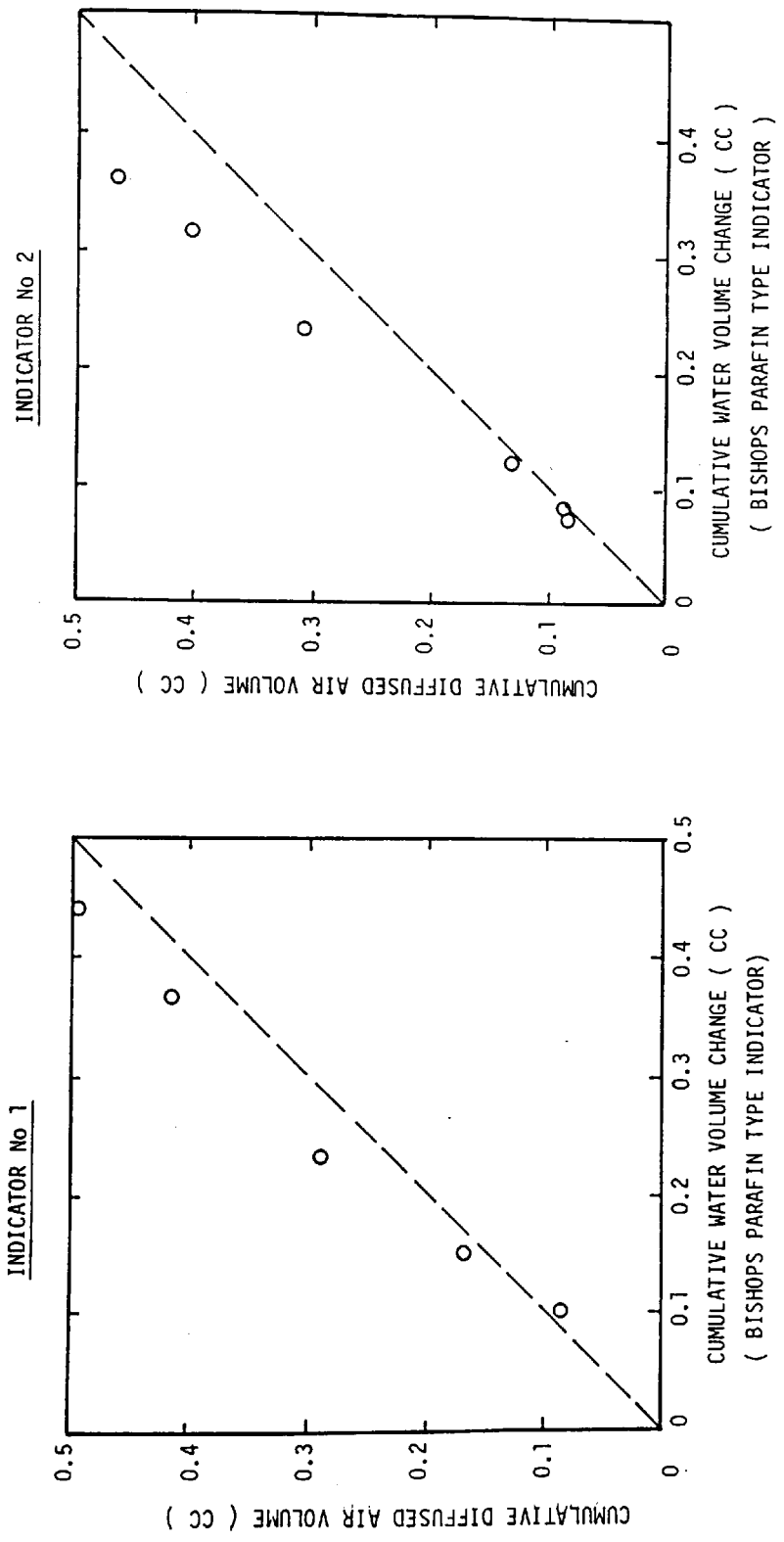

FIGURE C.5

PERFORMANCE OF THE DIFFUSED AIR
VOLUME CHANGE INDICATORS.

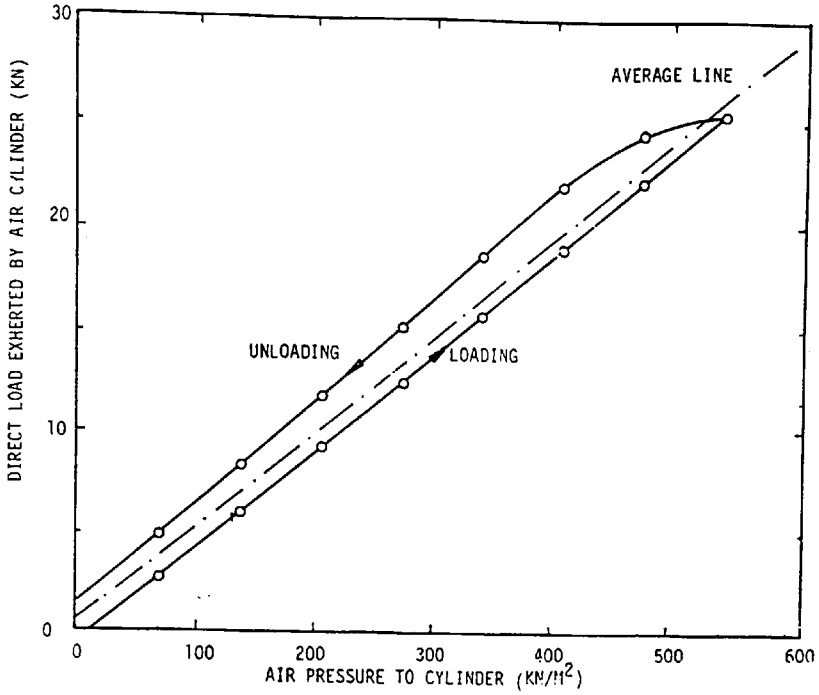

FIGURE C.6

AIR CYLINDER PERFORMANCE CALIBRATION CURVE

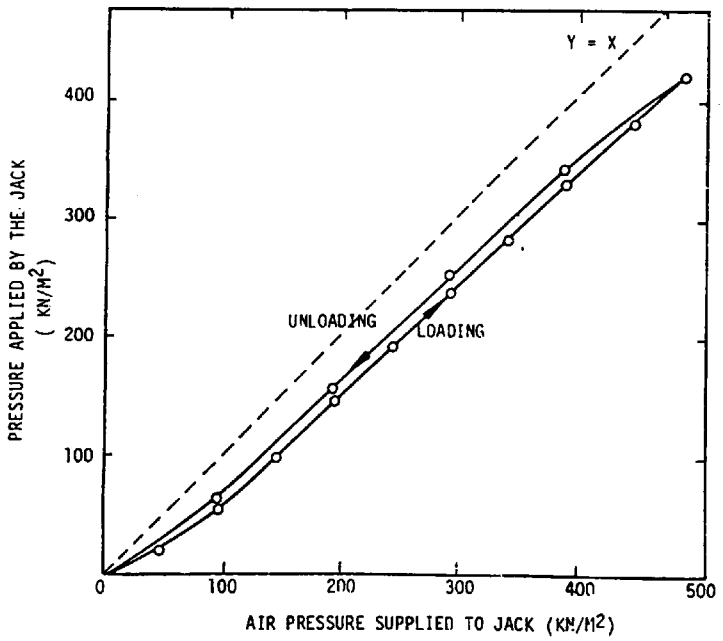

FIGURE C.7

ROWE CELL LOADING JACK PERFORMANCE CALIBRATION CURVE

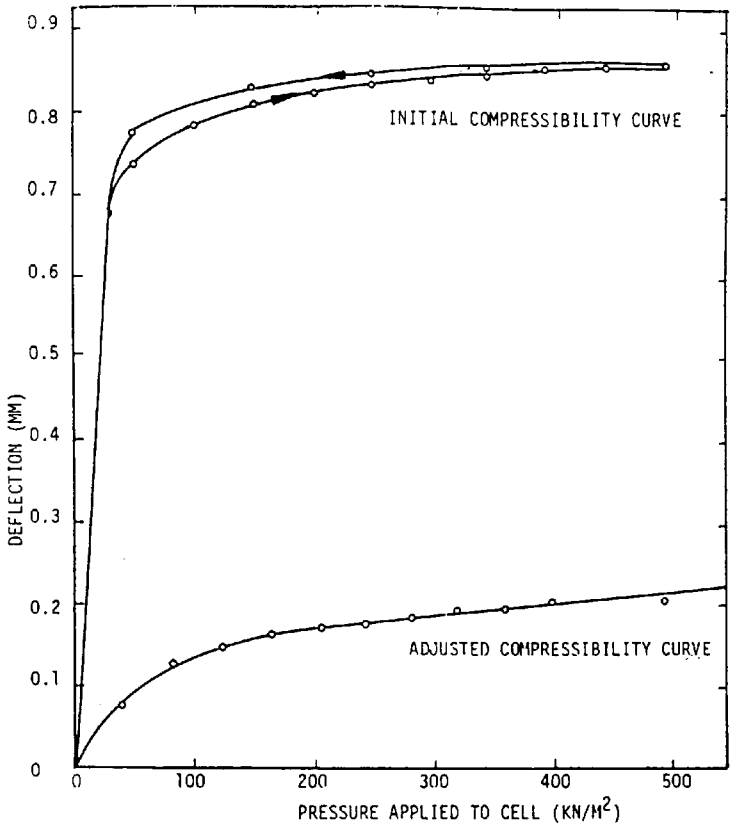

FIGURE C.8

COMPRESSIBILITY CURVE FOR
THE ROWE CELL.

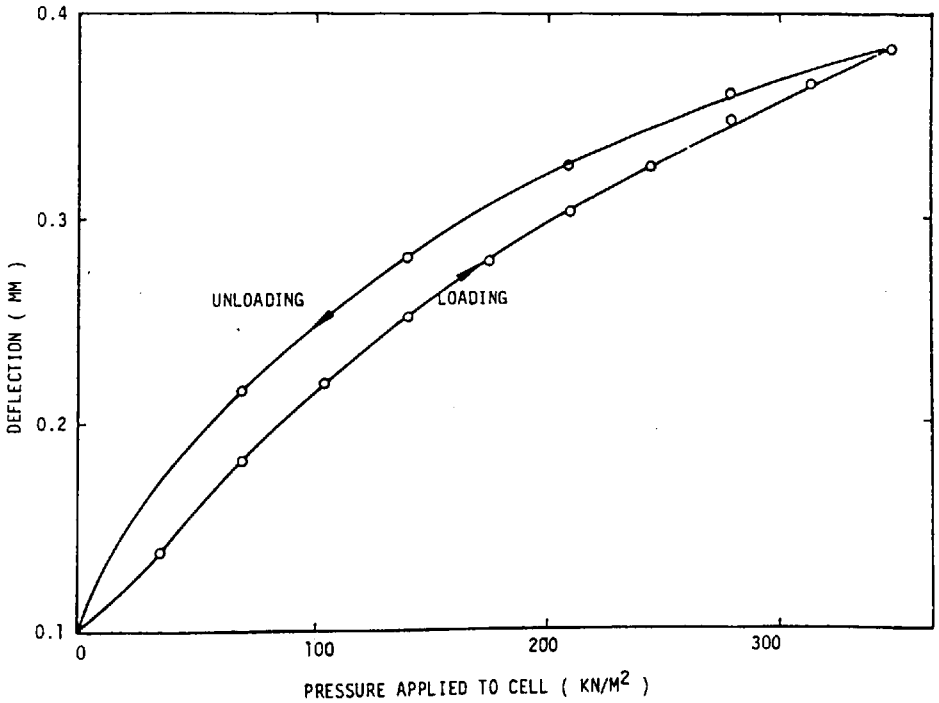

FIGURE C.9

COMPRESSIBILITY CURVE FOR
THE TRIAXIAL CELL

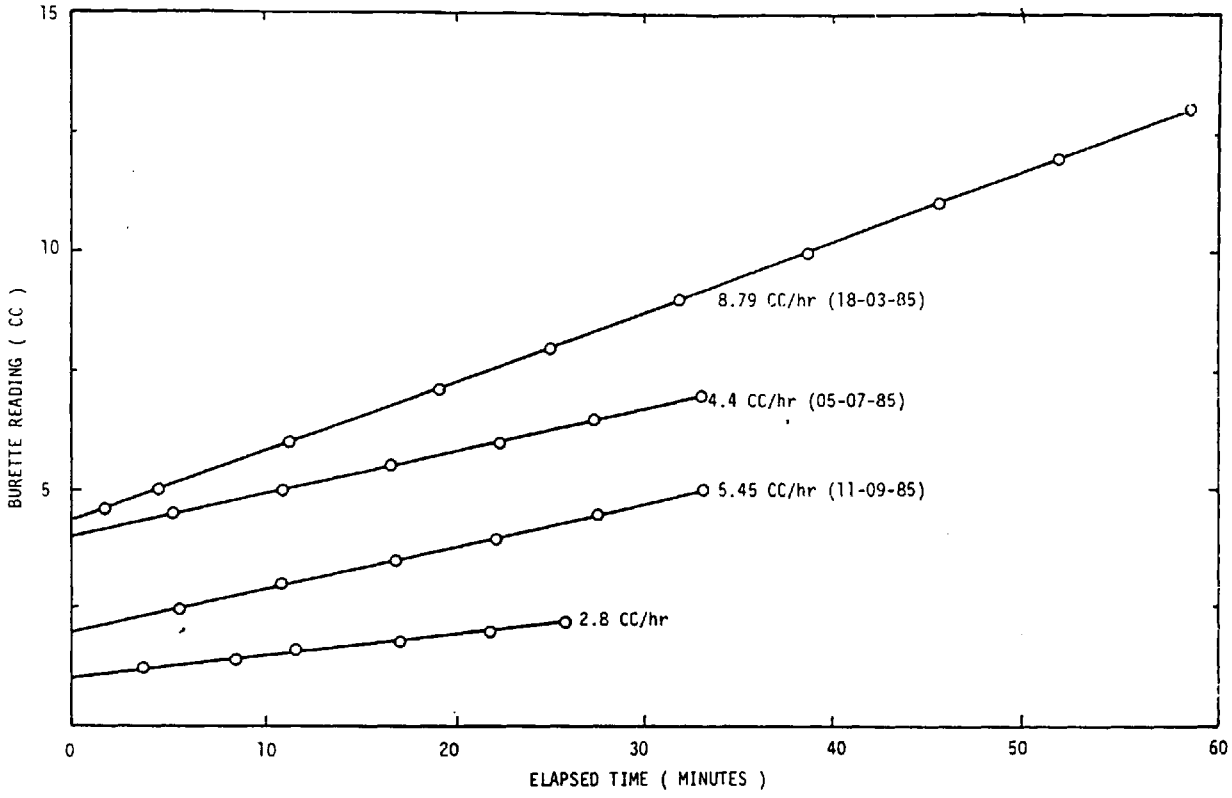

FIGURE C.10

HYDRAULIC CONDUCTIVITY OF THE
ROWE CELL CERAMIC DISC.

APPENDIX D

DATA PROCESSING

D1 INTRODUCTION

The overall procedure of reducing data to a usable form is termed data processing.

This project has generated a large quantity of raw experimental data, and with few exceptions, the results have required correction before they could be analysed. Corrections were applied to account for equipment compressibility and/or water and air leakages.

This Appendix details the implementation of the corrections listed in Appendix C and the subsequent calculations of volume change using the unsaturated soil theory. The repetitive nature of many calculations has necessitated the development of small programmes for use on a microcomputer; these permitted the rapid preliminary analysis of data during the course of testing.

D2 CONTROLLED ONE-DIMENSIONAL SWELL TESTING

D2.1 General

This program involved the one dimensional swell testing of 76mm and102mm diameter specimens.

Although the overall aim of testing was to monitor swelling, the tests were divided into two distinct types, the uniqueness tests (volume change) and null tests (no volume change). Despite this, it

was possible to employ the same data processing procedure in both instances, which led to considerable savings in time.

D2.2 Overall Procedure

The nature of the equipment led to a manual data recording procedure (Chapter 5). The data was logged into a preformatted data sheet and then typed into a computerised data base on a weekly basis.

The results were then processed by running them through the main data processing computer program (Section D2.5). The output format is listed in Table D.1 and displays the correction-calculations for the measured diffused air. Also included in the program (but not displayed in the output) are corrections for known water leakages and equipment compressibilities. The individual corrections are detailed in the following sections.

D2.3 Water Volume Changes

The water volume change is monitored using the Bishop paraffin type volume change indicator. In order that a true representation of volume change is obtained, the measured value must be corrected for known influences. These include direct leakage from the apparatus and, the influence of diffused air collecting beneath the ceramic disc within the test cell.

(a) Leakage

The water volume change indicators were calibrated for leakage (Section C1.3). The rates of leakge are uniformly added to the measured water volume changes since they are considered as occurring continually.

(b) Correction for diffused air

The water supply is fed to the specimen via a high air entry ceramic disc; this allows free movement of water but prevents the direct passage of air. Unfortunately, diffused air within the water can and does pan down through the ceramic discs and collects as bubbles beneath it. These are then flushed to the diffused air volume change indicator to be volumetrically quantified. These bubbles displace water, effectively reducing the apparent specimen water intake (Figure D.1); it follows that the measured diffused air effects must be added to the measured water volume change. The correction must take into account the two mediums involved i.e. gas and a fluid, and this is achieved by applying Boyles law for gases. The correction procedure is outlined in Figure D.2.

D2.4 Total volume change

The measured total volume change (normally swell) will be too great because of equipment compressibility. This is adjusted for by subtracting the correction value (Section C3.2 and C3.3) from the measured volume change (for corresponding stress conditions).

D2.5 Computer programs for data processing

The repetitive nature of the above outlined corrections has necessitated the development of computer programs to expedite the processing procedure. Two programs have been written for the Commodore PET microcomputer in BASIC; they are cellular in design i.e. sub-routines linked by a compiling program and are therefore easily modified.

The two main programs include :

(a) data storage and retrieval (DATST01)

This program is used to format, store and update data on floppy discs.

(b) processing of data (DATPR01)

This is the main processing program and undertakes all necessary corrections to the measured total and water volume changes.

A typical data output is displayed in Table D.1.

D3 CONSOLIDOMETER CONSTANT VOLUME SWELL PRESSURE TEST

D3.1 General

The processing of consolidometer data is less straightforward than for the controlled one dimensional swell tests; this is due to the fact that the data must be plotted and an empirical correction applied before the main processing can proceed.

The overall procedure is as follows :

(a) transfer chart recorder out put and specimen details to computerised data base (using DATST02)

(b) calculation of (e-log p) data from experimental results (using DATVOID)

(c) plot the (e-log p) graph and implement Casagrande's empirical correction for sampling disturbance

(d) undertake volume change prediction using the volume change theory (employing DATVOL)

As seen, the processing involves the use of computer programs to expedite the procedure.

The above steps are detailed in the following sections.

D3.2 Extraction of data from the chart output

The consolidometer deflections are recorded for extended time periods to ensure that equilibrium values are being recorded.

Upon completion of the test, the deflections are scaled off the chart output and transferred onto the computerised data base whilst employing the program DATST02.

The data is then suitably formatted for subsequent processing.

D3.3 Calculation of data for the (e-log p) graph

The e-log p graph yields all the data for subsequent swell predictions and must therefore be carefully constructed.

The change in voids ratio is determined from the recorded deflections and initial specimen conditions as follows :

where

H_1 = initial specimen depth (mm)

M_d = dry mass of soil (g)

G_s = specific gravity

ρ_w = density of water (kg/m^3)

A = cross sectional area of specimen (mm^2)

ΔH = change in specimen depth (mm)

H = current depth of specimen (mm)

then height of solid constituent (H_s) :

$$H_s = \frac{M_d}{G_s . \rho_w . A} \qquad D.1$$

and height of voids (H_v) :

$$H_v = H - H_s \qquad D.2$$

$\therefore$ voids ratio (e) :

$$e = \frac{H_v}{H_s} \qquad D.3$$

The measured deflections were subject to the compressibility of the equipment and were too large; these were therefore reduced using the correction values listed in Appendix C3.1 .

The above calculations were very repetitive and all undertaken using the computer program DATVOID. A typical printout of data is illustrated in Table D.2.

D3.4 (E-log p) graph and Casagrande's empirical corrections for sampling disturbance

A typical (e-log p) graph is indicated in figure 8.1. This type of plot yields the compressibility and swell (rebound) moduli in addition to the apparent swell pressure. Also indicated on the plot is the empirical correction procedure; however, for clarity, this is further discussed below in some detail.

The effect of sampling disturbance upon swell pressure has been previously discussed in Chapters 5 and 8, and is well illustrated in figure 5.15.

The empirical method after Casagrande (and subsequently modified by Fredlund) is employed to estimate a correction for the sampling disturbance.

Casagrande based his correction upon the observed effect of cyclic loading on the void ratio of undisturbed clay samples; his final correction was closely related to the compression curve, whereas Fredlund's modification quite logically employs the swell curve instead.

The procedure is as follows (refer figure D.3)

(a) the (e-log p) graph is plotted as previously indicated

(b) a horizontal line is projected through the initial void ratio value to the extreme right hand side of the graph (line A-B)

(c) mark the point of maximum curvature on the compression curve (C), and through it draw two lines : one horizontal (C-D) and the other at a tangent to the compression curve at point C. (C-E).

(d) bisect lines CD and CE through C (line CF)

(e) draw a line, parallel to the rebound curve so that it tangentially touches the compression curve (GH)

(f) the intersection between GH and CF is considered as indicating the corrected swell pressure ·

In practice, great difficulty has been encountered in determining the precise slope of the rebound curve for highly plastic soils. The criteria adopted was to position the tangent at a point where the voids ratio equalled its original value prior to testing. Notably, this approach has yielded consistent results between specimens.

D3.5 Volume change predictions using the unsaturated soil theory

A typical application of the volume change theory is presented in Chapter 8.2.2.

This has been written in the form of a computer program to expedite the calculation procedure (see table D.1 for typical output)

D3.6 Computer programs for processing data

A total of three separate programs were written to handle the data processing procedure.

(a) Data storage (DATST02)

This program stores, and permits the updating of the test records.

(b) Calculation of void ratio (DATVOID)

Utilising the data originally stored using (DATST02), this program calculates the stress related variation in voids ratio whilst taking into account the effects of consolidometer compressibility.

A typical output is listed in Table D.2.

(c) Volume change predictions (DATVOL)

This program predicts the volume change of a soil (originally at the specified conditions) following free access to water.

The program accepts data formatted by DATST02.
A typical output is presented in Table D.3.

TEST NO : 1
TEST TYPE :UNIQ
SPECIMEN : 1
APPARATUS :TRIAX

TABLE 1: ADJUSTED TEST DATA

CUM TIME (MINS)	DELTA BISHOPS (CC)	DELTA AVCI (CC)	AVCI CORR (CC)	TRUE BISHOPS (CC)	CUM BISHOPS (CC)	TRUE THICKN (MM)	CUM BISHOPS (%)	CUM VOL (%)
0	0	0	0	0	0	31.46	0	0
1	1.8	0	0	1.8	1.8	29.91	1.2609	-4.9205
1296	-1.53	.43	.31	-1.22	.58	30.82	.4059	-2.0197
4205	-.09	.09	.06	-.02	.56	30.81	.3894	-2.0515
5619	-.03	.18	.13	.1	.65	30.81	.4566	-2.0623
7429	-.15	.07	.05	-.1	.55	30.81	.3847	-2.0668
8867	-.03	-.28	-.2	-.23	.32	30.81	.2228	-2.0718
10305	-.08	0	0	-.08	.23	30.8	.1642	-2.0966
11377	-.07	.1	.07	.01	.24	30.8	.1679	-2.0966
12831	-.13	.07	.05	-.08	.15	30.8	.1085	-2.0966
14255	-.1	.12	.08	-.02	.14	30.8	.0954	-2.0966
15716	-.03	.18	.13	.09	.23	30.8	.1607	-2.1017

TABLE 2: TRUE PRESSURES

CUM TIME (MINS)	PRESSURES (PSI) TOTAL	AIR	WATER	BASE
0	.29	-1.47	-1.47	-2.84
1	44.57	34.28	4.29	4.11
1296	43.95	34.3	4.27	4.04
4205	44.54	34.28	4.27	4.14
5619	44.58	34.28	4.31	4.16
7429	44.59	34.28	4.27	4.33
8867	44.59	34.3	4.27	4.64
10305	44.49	34.26	4.22	4.54
11377	44.62	34.34	4.33	4.66
12831	44.55	34.26	4.29	4.62
14255	44.58	34.26	4.27	4.62
15716	44.58	34.28	4.29	4.52
AVERAGE PRESSURES	44.51	34.29	4.28	4.4

TABLE D.1

TYPICAL PROCESSED COMPUTER
OUTPUT FOR MAIN TEST PROGRAMME

CVSP TEST:P1625052QG

PRESSURE (KN/M12)	LOG PRESSURE	ADJ VOIDS RATIO	COMMENTS
10.79	1.03	.74	
64.73	1.81	.735	
474.71	2.68	.74	
625.75	2.8	.731	
755.22	2.88	.722	
971	2.99	.708	
1186.77	3.07	.696	
863.11	2.94	.699	
647.33	2.81	.705	
431.55	2.64	.716	
215.78	2.33	.745	
107.89	2.03	.785	
53.94	1.73	.849	
21.58	1.33	.958	

TABLE D.2

TYPICAL (e - LOG(P)) DATA
PROCESSED ON THE COMPUTER

STATE CHANGE CALCULATIONS

R20300510G

SOIL PROPERTIES

TEST CODE :R20300510G
SOIL MIX : 10 % BENTONITE + 90 % KAOLINITE TE
SPECIFIC GRAVITY : 2.5803

INITIAL DATA

INITIAL HEIGHT	: 14.98 MM
IN. MOISTURE CONTENT	: 30 %
IN. DENSITY	
IN. VOID RATIO	: .91
IN. SATURATION	: 85.55 %
FIN. WATER PRESSURE	: 0 KN/M2
SWELL PRESSURE	: 288.4 KN/M2
OVERBURDEN	: 64.73 KN/M2
LOADING CHANGE	: 0 KN/M2.
PREDICTED VOIDS CHANGE	: .1 KN/M2

STATE CHANGE DATA

	EXPERIMENTAL	FREDLUND PREDICTION (FINAL SAT=100%)
FINAL VOID RATIO	.99	1.01
FINAL SATURATION	103.03 %	100%
FINAL MOISTURE CONTENT	39.33 %	39.13 %

TABLE D.3

TYPICAL VOLUME CHANGE PREDICTIONS
MADE FROM CONSOLIDOMETER DATA
(PROCESSED ON COMPUTER)

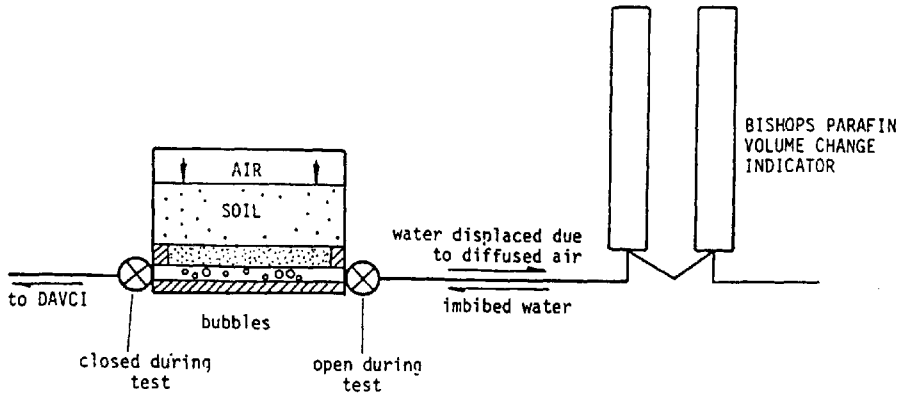

FIGURE D.1

THE EFFECTS OF DIFFUSED AIR UPON WATER VOLUME CHANGE READINGS

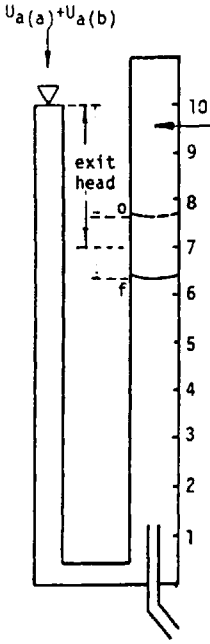

$$\text{ABSOLUTE INDICATOR PRESSURE} = \left[\text{BAROMETRIC PRESSURE}\right] + \left[\text{INDICATOR PRESSURE}\right] + \left[\text{EXIT TUBE HEAD}\right]$$

$$= U_{a(a)} + U_{a(b)} + U_{w(h)}$$

$$\text{AIR VOLUME IN BASE} = \frac{\left[\text{INDICATOR VOLUME CHANGE}\right] \times \left[\text{ABSOLUTE INDICATOR PRESSURE}\right]}{\left[\text{ABSOLUTE BASE PRESSURE}\right]}$$

$$\text{i.e.} \quad V_w = \frac{V_a \cdot P_a}{P_w}$$

FIGURE D.2

CORRECTION PROCEDURE FOR DIFFUSED AIR EFFECTS.

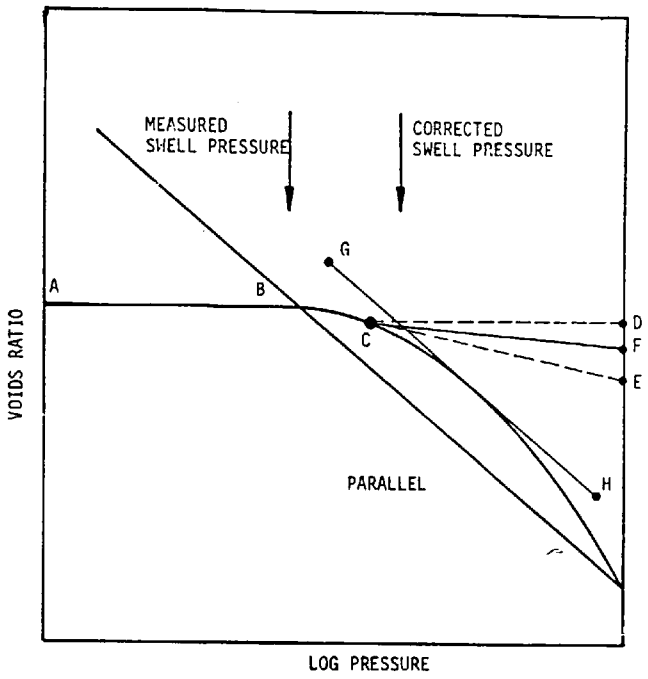

FIGURE D.3

MODIFIED CASAGRANDES CORRECTION
FOR SAMPLING DISTURBANCE EFFECTS
UPON THE SWELL PRESSURE

APPENDIX E

A THEORY FOR UNSATURATED SOILS : FREDLUND'S PROPOSALS

E.1 INTRODUCTION

The success of the effective stress concept in describing the behaviour of saturated soils has led research workers into a search for a similar statement for unsaturated soils.

Numerous equations are proposed in the literature. Common to all is theincorporation of a soil parameter (χ) characteristic of the soil behaviour in the description of the stress state. This parameter has proven essentially impossible to evaluate uniquely and is difficult to apply to practical problems.

The literature indicates a trend towards uncoupling the effective stress equation and treating the stress variables independently.

Fredlund (1973) considers an unsaturated soil to be composed of four (4) phases : soil solids; air; water and the air-water interphase or contractile skin (this being examined in detail later).

On the basis of this, and the literature, he proposes a general theory relating the stress state to the volumetric behaviour of unsaturated soils in terms of continuum mechanics.

This chapter describes the key points of Fredlund's derivations, it being divided into the following sections :

(a) Nature of unsaturated soils : describes Fredlund's interpretation of the physical nature of unsaturated soils with emphasis on the air-water interphase.

(b) Identification of stress state variables : Equilibrium equations are written for each phase of an unsaturated soil in terms of measurable quantities. On the basis of these equations, it is possible to identify the independent variables required to describe the stress state of an unsaturated soil. These variables are verified by Fredlund using 'null' type tests on two soils.

(c) Constitutive equations for use with unsaturated soils : Suitable constitutive relationships are proposed from a semi-empirical stand point which combine the stress and deformation state variables. One equation describes the deformation of soil structure and the second equation defines the water volume present in the element.

Experimental verification entails measuring the volume changes resulting from stress changes in two orthogonal directions and comparing predicted and measured volume changes resulting from a stress change in a third direction. This is termed uniqueness testing.

E.2 NATURE OF AN UNSATURATED SOIL

A soil mass consists of a particular assemblage of solids; the voids being filled with one or more compressible or incompressible fluids. Classical soil mechanics has primarily considered the case in which the voids are filled with water (saturated), however, the

general unsaturated case involves pores that contain varying portions of gas.

Although Fredlund employs the term 'unsaturated' for all soils containing an air phase, his approach makes no allowance for the various stages of saturation, through which a soil passes during the wetting process (Aitchison, 1956). Fredlund considers a simplified unsaturated soil case where the voids are filled with varying portions of air (with/without water vapour) and water (with/without dissolved air).

Unsaturated soil is generally considered to be a three phase system (Lambe and Whitman, 1969) fig. E.2 containing solid particles, gas and liquid. In considering the definition of the word phase, Sisler, Vanderwerf and Davidson (1953) state that "many mixtures are heterogenous, consisting of two or more physically distinct portions, differing in properties and composition and separated from each other by definite bounding surfaces". This definition appears consistent throughout the fields of chemistry and physics.

Embracing the above definition, Fredlund proposes an unsaturated soil system containing a fourth phase (fig. E.2). This would be the air water interface, often referred to as the 'contractile skin', in surface chemistry literature.

Since the surface tension concept is used for the first time with regard to engineering behaviour, the evidence of its existence and application to Fredlund's proposals are examined.

E.2.1 The surface tension concept

The conditions at the air water interphase are widely discussed in the literature.

Davies and Rideal (1963) state : "The boundary between two homogenous phases is not to be regarded as a simple geometrical plane, upon either side of which extends the homogenous phases, but rather as a lamina or film of which a characteristic thickness . The material in this surface phase shows properties differing from those of the materials in the adjoining homogenous phases".

They continue, "liquid behaves as if it were surrounded by an elastic skin with a tendency to contract". This latter statement explains why a drop tends to a spherical shape when uninfluenced by external forces, and that any liquid surface area will tend to decrease spontaneously.

Researchers have been unable to directly measure this tendency to contract (surface tension), but several experimental observations (Padday, 1969), indicate the existence of a boundary phase :

1. hydrostatic pressure below a curved surface is different from that below a flat surface.
2. The liquid assumes a shape of minimum area when there is no influence of gravity.
3. The vapour pressure of a liquid with a curved surface is different to that of a flat surface.
4. A thin film of liquid stretched on a wire frame pulls in, and thereby tends to distort the wire frame.

Defay (1966) observes that the contractile skin has a pressure deficit that manifests itself macroscopically as a tension. The magnitude of the integral of this tension across the contractile skin is known as the surface tension.

E.2.2 Physical properties of the contractile skin

The existence of the proposed surface tension concept is indicated by experimentally verifying that the contractile skin exhibits different physical properties than the bulk of either phase in contact with it.

Bikerman, (1968) presents clear evidence that the tensile pull is observed in the surface layer of a liquid only.

Derjaguin (1965) notes that the viscosity of the surface layer is very sensitive to change from the bulk of the liquid. The surface viscosity is some three times greater than that of the bulk liquid, and is believed to be an indication of the soil structure.

Padday (1969) notes that the surface water molecules are strongly oriented due to their polar nature. The surface molecules are therefore attracted to one side and allowed to relax on the other - thus reducing the surface density.

Metsik (1964) indicated an increase in heat conductance as the surface layer thickness decreased.

With regard to the transition between liquid and gas phases, Derjaguin (1965) states "the absence of a pronounced drop in these peculiarities in water layers as the distance from the interface increases up to a certain thickness gives grounds for assuming that the specific structure of water in boundary layers is uniform and changes abruptly at a certain small distance from the interface into the normal structure of the bulk liquid phase."

"Theoretically, it is natural to assume a jumpwise change as this is observed in liquid crystals. Thus, there are grounds to speak of boundary phases separated from the bulk liquid by a sharp interface, but differing from conventional phases in that their thickness is definite under given conditions and they depend upon the nature of the substratum".

By assuming the existence of a contractile skin 4th phase , an unsaturated soil is considered as a composite mixture of four phases - two fluid phases that flow under the application of stress, and two solid phases that come to equilibrium under a stress application.

Since the thickness of the contractile skin is believed in the order of a few molecular layers only, then its physical subdivision is considered unfeasible and unnecessary from the standpoint of volume weight relationships.

By considering the contractile skin as part of the water phase then the four phase system reverts to a three phase system WRT the volume-weight relationships.

E.3 STRESS STATE VARIABLES FOR UNSATURATED SOILS

E.3.1 Introduction

This section describes the procedure employed by Fredlund (1973) to propose suitable stress state variables for an unsaturated soil based on multiphase continuum mechanics.

The theory of three dimensional elasticity is initially outlined since the developments described are based upon this.

The equilibrium equations for each phase of an unsaturated soil are written in terms of measurable variables. On the basis of these equations, the independent variables necessary to describe the stress state in an unsaturated soil are identified and an experimental verification undertaken.

E.3.2 Three dimensional elasticity

Fredlund derives his theory for unsaturated soil behaviour from the equation of three dimensional elasticity. The full theory therefore provides a useful starting point and is described below.

For internal equilibrium of a body in three-dimensional space the following equations must be satisfied (ref. fig. E.3).

$$\left.\begin{aligned}
\frac{\partial \sigma_{xx}}{\partial x} + \frac{\partial \tau_{xy}}{\partial y} + \frac{\partial \tau_{xz}}{\partial z} + F_1 &= 0 \\
\frac{\partial \tau_{xy}}{\partial x} + \frac{\partial \sigma_{yy}}{\partial y} + \frac{\partial \tau_{yz}}{\partial z} + F_2 &= 0 \\
\frac{\partial \tau_{xz}}{\partial z} + \frac{\partial \tau_{yz}}{\partial y} + \frac{\partial \sigma_{zz}}{\partial z} + F_3 &= 0
\end{aligned}\right\} \qquad \text{(E.1)}$$

where

(a) $\{F_1,F_2,F_3\} = 0$ if there are no body forces

(b) $\{F_1,F_2,F_3\} = -\rho\{u,v,w\}$ for free vibration

(c) $\{F_1,F_2,F_3\} = F\{u,v,w\}$ for general applied stresses on the edges of the body. F is a function of local stresses in the initial state and second order partial differential operators.

$$f = -\left\{\frac{P_x \partial^2}{\partial x^2} + \frac{P_y \partial^2}{\partial y^2} + 2\,\frac{P_{xy} \partial^2}{\partial x \partial y}\right\}$$

For uniform applied normal edge stresses P_x on x=0, and P_y on y=0, b and for shear stresses P_{xy} on x=0, a and y=0, b.

In the above expressions, u , v and w are the displacements of the body in the x , y and z directions repsectively. The body is of length a in the x direction and length b in the y direction and has thickness H in the z direction.

At the surface of the body, the stresses in equation (E.1) must be such as to be in equilibrium with external forces (surface traction) acting on the surface of the body. In problems involving a body subjected to external forces, any solutions to equation (E.1) must also satisfy the following conditions.

$$\left.\begin{aligned} x &= \sigma_{xx}\,\ell + \tau_{xy}\,m + \tau_{xz}\,n \\ y &= \tau_{xy}\,\ell + \sigma_{yy}\,m + \tau_{yz}\,n \\ z &= \tau_{xz}\,\ell + \tau_{yz}\,m + \sigma_{zz}\,n \end{aligned}\right\} \qquad (E.2)$$

x , y and z are components of the external forces per unit area at the point under consideration. ℓ , m and n are the direction cosines of the external normal to the surface of the body at the point under consideration.

The strain displacement relationships of three dimensional linear elasticity are :

$$\varepsilon_{xx} = \frac{\partial u}{\partial x} \;,\; \varepsilon_{yy} = \frac{\partial v}{\partial y} \;,\; \varepsilon_{zz} = \frac{\partial w}{\partial z} \qquad (E.3(a))$$

$$\left.\begin{aligned} \gamma_{yz} &= \frac{\partial v}{\partial z} + \frac{\partial w}{\partial y} \\ \gamma_{xz} &= \frac{\partial w}{\partial x} + \frac{\partial u}{\partial z} \\ \gamma &= \frac{\partial v}{\partial z} + \frac{\partial u}{\partial y} \end{aligned}\right\} \qquad (E.3(b))$$

E.3.3 Stress analysis of a continuum

Fredlund assumes force equilibrium to be the most fundamental physical statement available. The employed analysis applies to any continuum.

A continuum material is defined by Fung (1969) as that for which density of mass, momentum and energy exist in the mathematical sense. The material is assumed to have no gaps or empty spaces.

Although potential discontinuities within a soil present the greatest problem when considering a continuum material, the method still yields the most practical analysis.

Malvern (1969) proposed the concept of a continuous material to define point stresses. In considering an element of area on an imaginary rigid internal continuum plane, it is assumed that as area tends to zero then force/area tends to a limit.

i.e. limiting vector $T_v = \frac{dF}{ds} = \frac{\text{Force}}{\text{Area}}$ (E.4)

The concept may be extended to the three dimensional case, three perpendicular surfaces merging at a point τ_x, τ_y, τ_z.

Resolving the stress vectors into components gives 9 stress vectors or 1 stress tensor (Fig. E.3). The chosen cube element must contain a large enough number of particles to qualify as a continuum.

Although the tensor applies to any continuous medium, and is generally independent of the continuum nature - solids have all 9 components, but non viscous fluids have no shear components.

The equilibrium which is governed by Newton's law of statics and dynamics (ref. fig. E.4) may be expressed as follows :

$$\left(\sigma_y + \frac{\partial\sigma_y dy}{\partial y}\right)dxdz - \sigma_y\, dxdz + \left(\tau_{xy} + \frac{\partial\,\tau_{xy}dx}{\partial x}\right)dydz - \tau_{xy}dydz$$

$$+\left(\tau_{zy} + \frac{\partial\,\tau_{zy}}{\partial z}\,dy\right)dxdy + F_y dxdydz \qquad \text{(E.5)}$$

where F_y = body forces in y direction.

Assuming elemental acceleration = 0, the right hand side of the expression = 0 and the equation reduces to :

$$\frac{\partial\sigma_y}{\partial y} + \frac{\partial\,\tau_{xy}}{\partial x} + \frac{\partial\,\tau_{zy}}{\partial z} + F_y = 0 \qquad \text{similar in x and y direction} \qquad \text{(E.6)}$$

all applying to any material qualifying as a continuum. These linear equilibrium equations assume that the stress components and derivatives are continuous.

E.3.4 Element for a multiphase system

Biot (1955) indicates that the most suitable element for the equilibrium analysis of a multiphase system is a cube, completely enclosed by imaginary unbiased boundaries.

In order to consider each phase as a continuum, the concept of reduced unit weight is introduced.

Reduced unit weight is defined as the uniform distribution of true mass over the whole volume (assuming absence of porous media) thus :

$$\rho_n = n_n \cdot \gamma_n \qquad (n\text{-}n^{th}\ \text{phase}) \qquad \text{(E.7)}$$

where

ρ_n = reduced unit weight of the n^{th} phase

n_n = porosity of the n^{th} phase

γ_n = true unit weight of the n^{th} phase

This is applicable to both water and solid phases.

Since by definition sum of porosity terms :

$$n_1 + n_2 + n_3 + \ldots\ldots + n_N = 1 \qquad \text{(E.8)}$$

then by inserting (E.7) in (E.8)

$$\frac{\gamma_1}{\rho_1} + \frac{\gamma_2}{\rho_2} + \ldots\ldots \frac{\gamma_N}{\rho_N} = 1 \qquad \text{(E.9)}$$

E.3.5 Theoretical approach to multiphase systems

The 'equilibrium of a multiphase systems' approach (consistent with that employed by Green and Naghdi (1965), Truesdell (1966) and Faizullaev (1969) is adopted in view of the assemblage of an unsaturated soil. This assumes that stress fields of a multiphase system are coincident and that the stress field of one phase can be superimposed upon the stress field of another. The principle of superposition applies, provided the equilibrium equation contains only linear operations. The principle can be applied to stresses as well as displacements (Westergaard (1952)).

E.3.5 A general theory of equilibrium for multiphase systems

This requires the consideration of surface traction forces acting upon an elemental volume and the interaction force associated with each phase.

A. Fluids : these include the drag forces associated with relative medium velocities and also the forces associated with the cross-sectional variability of the 'tube' through which flow is occurring.

B. Solids : a further drag/friction force and gravity body force can be added to the body forces described above in the event of two solid phase interactions.

The equations of motion are then written for each phase of the element (water, air, soil particles and contractile skin), it being assumed that each phase has an independent continuous stress field associated with each of the cartesian coordinate directions.

The principle of superposition of coincident stress fields is used in writing the equations of motion. In addition to the stress fields for each phase, an overall or total stress field can be assumed. The number of independent equations is equal to the number of phases involved.

Since our only interest is in the equation of equilibrium and not the equation of motion, the right hand side of the equations of motion (diffusor effect) may be neglected.

The derivations are considered such that all surface tractions are physically measurable quantities.

The above procedure is undertaken for the fluid-solid interphase, air-water interphase and finally, the combined unsaturated soil case.

E.3.7 Fluid-Solid Multiphase

Terzaghi (1936) presented his effective stress hypothesis but without theoretical evidence.

Bishop and Eldin (1950) proposed the superposition of two equivalent force systems.

Hubbart and Rubey (1959) showed by an involved analysis that fluid stress fields are continuous through soil.

Considering an element of soil with all voids filled with water (fig. E.5), the equilibrium equation for the solid phase may be written - the body force being expressed as two components : the gravity body force and the drag force of water on the particles.

where :

$$\frac{\partial \tau_{xy}^{P}}{\partial x} = \frac{\partial \sigma_{y}^{P}}{\partial y} + \frac{\partial \tau_{zy}^{P}}{\partial z} + \gamma_{p} + \frac{F_{pwy}}{n_{p}} = 0 \qquad \text{(E.10)}$$

σ_y^P = normal particle stress

τ_{xy}^P = shear particle stress on x plane

τ_{zy}^P = shear particle stress on z plane

F_{pwy} = drag force of water on particles

n_p = particle porosity or percentage of the element composed of solids $(1-n_w)$

γ_p = unit weight of soil particles

$$= \frac{\text{gravity body force}}{\text{particle porosity}}$$

Similarly the gravity body force of water and seepage force can be substituted into the water phase equilibrium equations to give :

$$\frac{\partial u_w}{\partial y} + \gamma_w - \frac{F_{pwy}}{n_w} = 0 \qquad \text{(y direction only)} \qquad \text{(E.11)}$$

u_w = pore water pressure

γ_w = unit weight of water

n_w = water porosity

All equations assume that the stress field is continuous throughout the element.

It is further shown that the forces acting on a body equal to zero when integrated around the body (assumption of continuous stress fields).

Although the soil structure equilibrium equations show that particle stresses can be used to describe the solids behaviour, usable stress state variables are not immediately apparent. However, the linear nature of the equilibrium equations enables a third equation to be written by combining those of the water and solid phases.

With only two out of three equilibrium equations (water and total) and two stresses being measurable (σ and u_w), then the total and water equilibrium equations are chosen as the independent variables. Since the sum of the phase equilibrium equations equals the total equilibrium equation, then the soil structure equilibrium equation may be written as the difference (total-water) phase equilibrium equations (see Fig. E.5). Thus the soil solids equilibrium equation in the y direction :

$$\frac{\partial \tau_{xy}}{\partial x} + \frac{\partial (\sigma_y - u_w)}{\partial y} + \frac{\partial \tau_{zy}}{\partial z} + \gamma_p + \frac{F'_{py}}{n_p} = 0 \qquad \text{(E.12)}$$

where F'_{py} = body forces on the soil particles in the y direction and similarly in the x and y directions. These equations can then be expressed as a stress tensor :

$$\begin{bmatrix} \sigma_x - u_w & \tau_{yx} & \tau_{zx} \\ \tau_{xy} & \sigma_y - u_w & \tau_{zy} \\ \tau_{xz} & \tau_{yz} & \sigma_z - u_w \end{bmatrix} \qquad \text{(E.13(a))}$$

The normal stress component comprises of the conventionally defined effective stress - thus indicating that the effective stress law is actually a stress-state variable and only part of the tensor required to describe the stress state within a saturated soil.

The preceding analysis may be conducted with a pore fluid of compressible nature such as air (u_a = air pressure). The equilibrium

equations are of a similar form to equation (E.12), the stress tensor becoming :

$$\begin{bmatrix} (\sigma_x - u_a) & \tau_{yx} & \tau_{zx} \\ \tau_{xy} & (\sigma_y - u_a) & \tau_{zy} \\ \tau_{xz} & \tau_{yz} & (\sigma_z - u_a) \end{bmatrix} \qquad \text{(E.13(b))}$$

It is noted that the tensors, (E.13(a)) and (E.13(b)) do not contain an air-compressibility term as do the modified stress variables proposed by Skempton (1961) (ref. equ. (4.1)).

E.3.8 Air-Water Multiphase

The literature indicates the existence of an independent boundary phase between air and water phases. As a result, Fredlund considers the element to be composed of a liquid, air, and a contractile skin phase. He considers a model of water with uniformly spaced air channels passing through.

The element can have a net shear component (net force in the directions parallel to the element surface due to resolution of surface tension forces parallel to contractile skin). The air and water stress fields are assumed to act in opposite directions (ref. fig. E.6). Thus the equilibrium equation in the y direction for the air phase :

$$-\frac{\partial u_a}{\partial y} + \frac{F_{cay}}{n_a} + \gamma_a = 0 \qquad \text{(E.15)}$$

where

F_{cay} = interaction or drag forces of the air with respect to the contractile skin

γ_a = unit weight of air

The equilibrium equation in the y direction for the water phase is :

$$\frac{\partial u_w}{\partial y} - \frac{F_{cwy}}{n_w} + \gamma_w = 0 \qquad \text{(E.16)}$$

F_{cwy} = interaction or drag force of the water WRT contractile skin.

The equilibrium equation in the y direction for the contractile skin is :

$$\frac{\partial \tau^c_{xy}}{\partial x} + \frac{\partial \sigma^c_y}{\partial y} + \frac{\partial \tau^c_{zy}}{\partial z} + \frac{F_{cwy}}{n_c} - \frac{F_{cay}}{n_c} + \gamma_w = 0 \qquad \text{(E.17)}$$

σ^c_y = normal stress component of contractile skin

τ^c_{xy} and τ^c_{zy} = shear components parallel to surface of element

n_c = porosity with respect to the contractile skin

Contractile skin stresses are components of the real stresses in the contractile skin. The normal and shear stresses can be written in terms of surface tension. Thus we are left with three independent equations for a 3-phase air-water multiphase system. The air and water stresses can be measured however the contractile skin stresses are unknown.

Since the phase stress fields are linear, they can be combined to form an overall equilibrium equation :

$$\frac{\partial \tau_{xy}}{\partial x} + \frac{\partial \sigma_y}{\sigma y} + \frac{\partial \tau_{zy}}{\partial z} + F' + \gamma = 0 \qquad \text{(E.18)}$$

where

$$F' = - \frac{F_{cay}}{n_a} - \frac{F_{cwy}}{n_w} + \frac{F_{awy}}{n_c} + \frac{F_{cay}}{n_c}$$

and

$$\gamma = \gamma_w + \gamma_p + \gamma_a$$

Each phase stress field produces a resultant force on each phase. These may be represented by F_a , F_c and F_w for air, contractile skin and water phases respectively.

Referring to equation (E.15), F_A can be written as :

$$F_A = - \frac{\partial u_a}{\partial y} = - \frac{F_{cay}}{n_a} - \gamma_a \qquad \text{(E.19(a))}$$

contractile skin : (equation (E.17))

$$F_c = \frac{\partial \tau^c_{xy}}{\partial x} + \frac{\partial \sigma^c_y}{\partial y} + \frac{\partial \tau^c_{zy}}{\partial z} = - \frac{F_{cwy}}{n_c} + \frac{F_{cay}}{n_c} - \gamma_w \qquad \text{(E.19(b))}$$

water phase : (equation (E.16))

$$F_w = \frac{\partial u_w}{\partial y} = \frac{F_{cwy}}{n_w} - \gamma_w \qquad \text{(E.19(c))}$$

The total stress field exhibits a resultant force F_T.

where

$$F_T = F_A + F_c + F_w = 0 \qquad \text{(E.19(d))}$$

The resultant forces produced on each phase are derived from the respective phase equilibrium equations (Nos. 15, 16 and 17), thus the total stress field force F_T may be described :

$$F_T = \frac{\partial \tau_{xy}}{\partial x} + \frac{\partial \sigma_y}{\partial y} + \frac{\partial \tau_{zy}}{\partial_z} = 0 = \underbrace{\left(- \frac{F_{cay}}{na} - \gamma_a \right)}_{(F_A)} \underbrace{\left(- \frac{F_{cwy}}{n_a} - \gamma_w \right)}_{(F_c)} \underbrace{\left(+ \frac{F_{cwy}}{n_w} - \gamma_w \right)}_{(F_w)} \qquad (E.20)$$

However, only three of the above four force equilibrium equations are independent, thus the air, water and total stress equations are chosen due to their measurability. By rearranging equation (E.19(d)) the contractile skin equation can be expressed :

$$F_c = F_T - F_A - F_w \qquad (E.21)$$

thus

$$\partial\left(\frac{u_a - u_w}{\partial y}\right) + \frac{F_{cwy}}{n_c} - \frac{F_{cay}}{n_c} + \gamma_w = 0 \quad \text{(y direction)} \qquad (E.21)$$

this being the equilibrium equation for the contractile skin in terms of air and water pressures.

The stress state variables can be extracted to form the isotropic stress tensor :

$$\begin{bmatrix} (u_a - u_w) & 0 & 0 \\ 0 & (u_a - u_w) & 0 \\ 0 & 0 & (u_a - u_w) \end{bmatrix}$$

E.3.9 Unsaturated soil case

The unsaturated cubical soil element may be treated as a combination of the air-water and water-solid multiphase systems. Since a linear independent equilibrium equation may be written for each of the four phases, the overall system also has a linear stress field.

The equilibrium equations for the system may be written in terms of the water phase, air, contractile skin and solid phases - there being an equation in the x , y and z directions in each case.

From figure E.7, the equilibrium of the water phase in the y direction is :

$$(n_w \frac{\partial u_w}{\partial y} + n_w \cdot \gamma_w + F_{cwy} + F_{pwy})\ dxdydz = 0 \qquad (E.23)$$

$n_w \cdot \gamma_w$ = gravity body force for the water phase.

Similarly, the equilibrium equation for the air phase is obtained from fig. E7 where :

$$(n_a\ (\frac{\partial u_a}{\partial y}) + n_a \cdot \gamma_a + F_{cay})\ dxdydz = 0 \qquad (E.24)$$

where

$n_a\ \gamma_a$ = gravity body force for the air phase.

The contractile skin and soil particle equilibrium equations can also be written by assuming a general state of stress. However, the associated stresses cannot be physically measured (thus permitting

verification). This difficulty is resolved by uncoupling the soil element into a water-soil multiphase and air-contractile skin multiphase.

The soil structure and contactile skin equilibrium equations are then re-written in terms of the body force F_{cpy}, interaction between the contractile skin and soil particles, and also the air and contractile skin gravity forces.

The y direction equilibrium equations are therefore :

soil particles :

$$\frac{\partial \tau_{xy}}{\partial x} + \frac{\partial(\sigma_y - u_w)}{\partial y} + \frac{\partial \tau_{zy}}{\partial z} + (\gamma' - n_w \gamma_w) + (n_p + n_a + n_c) \frac{\partial u_w}{\partial y}$$

$$- F_{cwy} - F_{pwy} - F_{cpy} + (n_a + n_c) \frac{\partial T}{\partial y} + \gamma_{ac} = 0 \qquad \text{(E.25)}$$

γ_{ac} = unit weight accounting for air and contractile skin gravity force.

where

n_p = % of element that is soil particles

n_c = % of element that is contractile skin

T = relates to the net normal effect of the air and contractile skin stress fields

γp = total unit weight of saturated soil

contractile skin :

$$F_{cpy} + (n_a + n_a) \frac{\partial T_y}{\partial y} + \gamma_{ac} - n_a \frac{\partial u_a}{\partial y} - n_a \gamma_a - F_{cay} = 0 \qquad \text{(E.26)}$$

Now substituting (E.26) into (E.25) gives an equilbrium equation that applies for both the soil particles and contractile skin :

$$\frac{\partial \tau_{xy}}{\partial x} + \frac{\partial(\sigma_y - u_w)}{\partial y} + \frac{\partial \tau_{xy}}{\partial z} + (\gamma - n_w \gamma_w - n_a \gamma_a)$$

$$+ (n_p + n_c) \cdot \frac{\partial u_w}{\partial y} - F_{cwy} - F_{pwy} - F_{cay} - n_a \frac{\partial(u_a - u_w)}{\partial y} = 0 \qquad \text{(E.27)}$$

An examination of the equilibrium equation (E.27) reveals that it contains three independent sets of surface tractions (i.e. $(\sigma - u_a)$, $(u_a - u_w)$ and (u_w)). The u_a term can be eliminated when soil particles are assumed incompressible. Any two out of the three may be used for the analysis of volume change problems. The surface tractions in each of the above equations can be extracted and written in the form of stress matrices - each surface traction is referred to as a 'stress state variable'. All extracted stress state variables cannot be placed in one matrix, since they are linked by differing porosity terms outside the partial differential. Also, the inclusion of a porosity term (i.e. soil property) in the description of the state of stress is not in keeping with continuum mechanics.

Two independent stress matrices can be extracted from the equilibrium equations for the soil particles and the contractile skin (ref. Fig. E.8), they are :

$$\begin{bmatrix} (\sigma-u_w) & \tau_{yx} & \tau_{zx} \\ \tau_{xy} & (\sigma_y-u_w) & \tau_{zy} \\ \tau_{xz} & \tau_{yz} & (\sigma_z-u_w) \end{bmatrix} \text{and} \begin{bmatrix} (u_a-u_w) & 0 & 0 \\ 0 & (u_a-u_w) & 0 \\ 0 & 0 & (u_a-u_w) \end{bmatrix}$$

(E.28)

E.3.10 Experimental verification of the proposed stress state variables

Before Fredlund (1973), it appears that little work is performed to directly prove that stress state variables satisfy equilibrium at a stress state point. The stress state variable for saturated soils $(\sigma-u_w)$ is derived by intuition and the observation of constitutive and shear strength behaviour.

Tiller (1953), while testing the compressibility of Kaolin, demonstrates the dependence of porosity on total and pore water stresses. All curves coincide when plotted against $(\sigma-u_w)$ (Fig. E.9).

Laughton (1965), shows that the area of contact between particles does not effect the stress state variable for a saturated uniform material (lead shot).

In performing two ID consolidation tests on a saturated organic silt, one with, the other without water back pressure, Lowe III et al (1964) notes essentially identical e - logP plots, where p = effective stress.

Bishop et al (1965) varies the total stress on a series of lead shot, aand and calcite specimens. The effective stress is kept constant however by varying water pressure, the resulting shear strengths are

found to remain unchanged. The shear strength is therefore clearly related to the effective stress variable i.e. $(\sigma - u_w)$.

Hilf (1956) proposes the axis translation technique for measuring pressure deficiencies greater than one atmosphere. The technique involves raising the air pressure until the specimen water pressure equals to zero. Since suction is the difference between air and water pressure, it is simply determined by noting the applied air pressure. (Fig. E.11).

Hilf varies total, air and water pressures by equal amounts thus maintaining constant differences. Although he notes no volume change which, in turn, infers correct functioning of the axis translation technique, no water/total volume measurements are available for examination.

Lowe and Johnson (1960) back pressure a sandy clay with an initial saturation of 88%. Total and water volume changes are monitored for increases in cell and water pressures.

It can be seen (fig. E.10) that the total volume decreases, but tends essentially to its original value. Although water volume increases rapidly at first, it eventually equilibrates.

Bishop and Donald (1961) conduct the first known attempt to define the stress state variables controlling the behaviour of an unsaturated soil.

The tests involve a special triaxial test on Braehead silt, and the results indicate that an equal change in total, air and water stress results in a monotonic stress strain relationship.

There are three possible combinations of variables each of which remain constant.

Although no volume change is noted following stress changes, the published data is insufficiently accurate and complete to verify this with assurance.

Fredlund (1973) conducts an experimental verification of stress state variables by running null type tests in specially modified consolidation and triaxial apparatus. Specimens of Kaolinite and Devon silt are statically or dynamically compacted to saturation between 75% and 95%. This is an important step, since the stress state variables form the basis for the subsequent volume change analysis.

Fredlund defines stress state variables as "those that produce no distortion in volume change of an element when their component stresses are equally varied - thus maintaining a constant overall variable". Considering this definition, he conducts a series of 'null' tests whereby specimens are subjected to equal changes in the compressed stresses, the water and total volumes being carefully monitored.

Fredlund defines the stress state variables as those 'that produce no volume change of an element when their component stresses are equally changed thus maintaining a constant overall value'.

The two stress tensors for the unsaturated soil case are :

$$\begin{bmatrix} \sigma_x - u_w & \tau_{yx} & \tau_{zx} \\ \tau_{xy} & \sigma_y - u_w & \tau_{zy} \\ \tau_{xz} & \tau_{yz} & \sigma_z - u_w \end{bmatrix} \text{and} \begin{bmatrix} u_a - u_w & 0 & 0 \\ 0 & u_a - u_w & 0 \\ 0 & 0 & u_a - u_w \end{bmatrix} \qquad \text{(E.29)}$$

In order to maintain equilibrium of both tensors, equal stress changes must be undertaken i.e. $\Delta\sigma = u_a = \Delta u_w$.

The main aim of the null tests therefore is to determine whether any process or volume changes occur as a result of stress changes, this is achieved by considering such factors as testing procedure; air diffusion; water loss from the sample; secondary consolidation. The null test programm consists of three parts :

(i) saturated soils - total of water stress control. These initial tests involve monitoring total and water volume changes for equal changes in total and water stresses. (constant σ-u_w). They are used largely to assess equipment reliability by comparing soil behaviour with a known saturated case.
The measured volumetric changes resulting from stress changes are in close agreement with corresponding changes in effective stress.

(ii) saturated soils - total, air and water stress control. The second test series monitors total and water volume changes but for equal changes in total, air and water stresses. Difficulty is encountered in applying all three pressures simultaneously, resulting in an immediate specimen compression due to a delayed air pressure build-up. Air is also noted as diffusing through the water phase resulting in an apparent decrease in the specimen water phase. Measured volume changes are again in close agreement with a corresponding change in effective stress. (Fig. E12).

iii) unsaturated soils - total, air and water stress control (Fig. E13). Very low volume changes are observed following variations in stress. The initial tendency is for water to flow into the specimen, but reversing with time. Fredlund explains this phenomena in terms of two secondary processes following stress applications: (i) air diffuses through the water, apparently reducing the water phase and

(ii) the compression of occluded air bubbles thereby increasing the water phase. The stress state variable for unsaturated soils are proven at least as conclusively as the effective stress variable in saturated soils. Initial tests are conducted on a modified oedometer produced by the Anteus Equipment Corporation. Later tests utilise a modified 4" triaxial rig. The latter equipment permits isotropic shrinkage/swelling of the specimen to be monitored.

Both equipments yield encouraging results which demonstrate the applicability of the chosen stress state variables for modelling the mechanical behaviour for unsaturated low-plasticity soils.

Fredlund statistically examines all volume changes - calculating mean and standard deviations. His findings indicate that although the spread of data masks any precise processes that may be occurring. It does appear that total volume change is occurring randomly thus suggesting a true null behaviour.

Fredlund's testing programme indicates several unaccountable volume changes, and he suggests the following cases.

1. The largest volume changes experienced follow each large (20 psi) pressure increment change, These are apparently due to some disturbance of the soil structure. Partial recovery is noted with time. Such volume changes are apparently avoided when using small pressure changes.

2. Immédiate volume changes are thought to be related primarily to entrapped air and measuring system compliance.

3. Long term volume changes are related to slight amounts of secondary compression of the soil structure and pore fluid compression.

4. Since measurements (i.e. volume change) are made at the limits of equipment accuracy then a null behaviour (upon magnification) can be expected to exhibit random variation.

5. Fredlund claims that moisture leaks are all but eliminated however this is very difficult to achieve entirely.

E.4 DEFORMATION ANALYSIS OF A MULTIPHASE SYSTEM

This section outlines Fredlund's attempt to provide a complex deformation-displacement formulation applicable to unsaturated soils.

He is apparently the first author to incorporate the contractile skin into a deformation analysis, and adopts the assumption after Fung (1969) and Goodrich (1969) that the contractile skin behaves as a solid.

This assumption is primarily justified by the fact that forces applied to solids cause deformation that come to equilibrium, whereas forces applied to liquids cause continuous deformation or flow. Since the contractile skin in an unsaturated soil comes to equilibrium under the application of forces, it is assumed to behave as a solid, with fluid and air phases at each side.

E.4.1 Deformation analysis literature review

Biot (1941) analyses the three dimensional consolidation of an unsaturated soil. His presentation assumes

(i) isotropy of the material

(ii) infinitesimal deformations

(iii) pore water is incompressible

(iv) the water may contain air bubbles

The deformation of the soil structure is assumed to correspond to a linear elastic solid.

Biot recognises that this does not completely describe the macroscopic unsaturated soil element, and suggests an additional deformation variable to account for the pore water.

Bishop (1957) considers the compression of an unsaturated soil in an undrained test and concludes that volume change is the result of air compression and diffusion into the water. Changes in volume are expressed with respect to the total volume.

Coleman (1962) uses two deformation variables to represent volume change behaviour in unsaturated soils :

(a) water volume change wrt total volume and

(b) total volume change wrt total volume.

Radhakrishna (1967) analyses the deformation state in an unsaturated soil. He proposes volumetric and deviatoric deformation increments to the deformation tensor which must then be indexed to some initial soil properties.

He proposes that volume weight relationships be used to map the state of an element.

Fredlund (1973) considers Radhakrishna's concepts as useful when considering unsaturated soil. The void ratio change is viewed as representing total volume change and water volume/water phases/saturation change as representing contractile skin deformation.

E.4.2 Multiphase element for the deformation analysis

In continuum mechanics, a deformation analysis involves the mapping of movement with respect to a material phase.

Deformation state variables : are evaluated on the basis of the change in relative position of points or particles in a body. They should be such that when integrated over the whole considered body they yield the body displacements.

Deformation as opposed to strain : the term 'deformation' is considered more suitable than 'strain' for describing the volume changes associated with a multiphase system, since such changes may not necessarily be stress related. Strain is normally associated with stress.

Li and Lam (1964) identify two types of movement applicable to multiphase behaviour in the field of kinematics of continuum mechanics :

Referential/Lagrangian description : the position of a fixed element of mass is specified as a function of its initial coordinates and time.

Spatial/Eularian description : attention is fixed upon a given region of space, which is expressed in terms of its current position vector and time. This is usually employed in fluid mechanics.

In order to maintain control over the large number of deformation and displacement terms induced in the complete deformation analysis of a multiphase system subscripts are used to designate each phase.

soil particle P

contractile skin c

air phase a

water phase w

overall soil structure element - s

E.4.3 Theoretical deformation ananlysis of a multiphase system

Basic to the deformation analysis is that discontinuities such as cracks do not occur.

In the deformation analysis of a multiphase system, an independent referential element should not be used since elements would not coincide after deformation.

Two types of multiphase element are functional. Either one consistent spatial element may be used for all phases (Lee 1969) or a referential element can be used for one phase which becomes spatial with respect to other phases.

A consequence of the consistent element approach is that the sum of the deformations of component phases must equal deformation of

the overall element. This is referred to as the 'continuity requirement of multiphase systems' and is a volumetric restriction that prevents 'gaps' between the phases of a deformed multiphase system. Mathematically it may be expressed in terms of volumetric or void ratio changes. Where deformation in each direction are a change in length reference to overall element length :

$$\frac{\Delta V}{V} = \sum_{i=1}^{N} \frac{\Delta V_i}{V} \quad \text{or} \quad \varepsilon = \sum_{i=1}^{N} \varepsilon_i$$

where

ΔV = change in volume of overall element

ΔV_i = change in volume of each phase

V = total volume of element

e = deformation of overall element

ei = deformation of each phase

N = number of phases

Now, in considering the application of continuity requirement to the deformation analysis and assuming that a two phase multiphase system can resist shear and compression, then independent deformation tensors are devised for each phase in the 3D case; phase I assumed referential, phase II spatial wrt phase I.

$$\text{tensors} \begin{bmatrix} \varepsilon_x' & \varepsilon_{yx}' & \varepsilon_{zx}' \\ \varepsilon_{xy}' & \varepsilon_y' & \varepsilon_{z'y} \\ \varepsilon_{xz}' & \varepsilon_{yz}' & \varepsilon_z' \end{bmatrix} \text{ and } \begin{bmatrix} \varepsilon_x^{II} & \varepsilon_{yx}^{II} & \varepsilon_{zx}^{II} \\ \varepsilon_{xy}^{II} & \varepsilon_y^{II} & \varepsilon_{zy}^{II} \\ \varepsilon_{xz}^{II} & \varepsilon_{yz}^{II} & \varepsilon_z^{II} \end{bmatrix}$$

Since each phase displacement is described by a linear displacement field, then a third set of deformation relationships may be written for the overall element. The individual phase equations may therefore be summed :

i.e.

$$\varepsilon = \varepsilon^{I} + \varepsilon^{II} \qquad \text{(E.30)}$$

E.4.4 Fluid-solid multiphase

The fluid solid multiphase system adopted is a particulate solid system, the interstitial spaces being filled with water. The soil particles can resist compression and shear stresses, and the fluid normal stresses only (under undrained state).

Fredlund selects a referential element of soil particles which becomes a spatial element wrt the water phase. The volumetric continuity requirement is :

$$\frac{\Delta V^{S}}{V} = \frac{\Delta V^{P}}{V} + \frac{\Delta V^{W}}{V} \qquad \text{(E.31)}$$

V^{S} = overall volume

V^{P} = volume of soil particles

V^{W} = volume of water

Deformation tensors

The soil particle deformation tensor is written in terms of displacements :

$$\begin{bmatrix} \frac{\partial u^P}{\partial x} & \frac{1}{2}\left(\frac{\partial u^P}{\partial y} + \frac{\partial v^P}{\partial x}\right) & \frac{1}{2}\left(\frac{\partial w^P}{\partial x} + \frac{\partial u^P}{\partial z}\right) \\ \frac{1}{2}\left(\frac{\partial u^P}{\partial y} + \frac{\partial u^P}{\partial x}\right) & \frac{\partial v^P}{\partial y} & \frac{1}{2}\left(\frac{\partial w^P}{\partial y} + \frac{\partial v^P}{\partial z}\right) \\ \frac{1}{2}\left(\frac{\partial u^P}{\partial z} + \frac{\partial w^P}{\partial z}\right) & \frac{1}{2}\left(\frac{\partial v^P}{\partial z} + \frac{\partial w^P}{\partial y}\right) & \left(\frac{\partial w^P}{\partial z}\right) \end{bmatrix}$$

The deformation of the soil particles is considered due to the compression of the solids only.

Assuming incompressible soil particles, then the respective particle deformation components are zero, i.e.

$$\frac{\partial u^P}{\partial x} = \frac{\partial v^P}{\partial y} = \frac{\partial w^P}{\partial x} = 0$$

The water phase has an isotropic deformation tensor.

$$\begin{bmatrix} \frac{\partial u^W}{\partial x} & 0 & 0 \\ 0 & \frac{\partial v^W}{\partial x} & 0 \\ 0 & 0 & \frac{\partial w^W}{\partial z} \end{bmatrix}$$

In the case of the fluid-solid multiphase, since the particle deformation is assumed negligible then the water phase deformation must equal the overall element deformation.

E.4.5 Air water multiphase

Fredlund considers a three phase multiphase system which includes the air-water interphase or contractile skin. The model comprises a spatial element containing uniform air cavities and channels through

a water matrix. This is somewhat fictitious since the contractile skin is unstable in the absence of a solid phase.

The volumetric continuity states :

$$\frac{\Delta v}{v} = \frac{\Delta}{v} + \frac{\Delta v^a}{v} + \frac{\Delta v^c}{v} \qquad (E.32)$$

thus

$$\varepsilon^o = \varepsilon^w + \varepsilon^a + \varepsilon^c \qquad (E.33)$$

where

ε^o = overall deformation of air phase.

Deformation tensors

The deformation tensors for the air, water and contractile skin phases can be written directly. The air and water phases cannot resist shear and therefore have isotropic deformation tensors. The contractile skin, being considered on the macroscopic scale has shear deformation components related to stress components parallel to the element surfaces.

contractile skin deformation tensor

$$\begin{bmatrix} \frac{\partial u^c}{\partial x} & \frac{1}{2}(\frac{\partial u^c}{\partial y} + \frac{\partial v^c}{\partial x}) & \frac{1}{2}(\frac{\partial w^c}{\partial x} + \frac{\partial u^c}{\partial z}) \\ \frac{1}{2}(\frac{\partial u^c}{\partial y} + \frac{\partial v^c}{\partial x}) & \frac{\partial v^c}{\partial y} & \frac{1}{2}(\frac{\partial w^c}{\partial y} + \frac{\partial v^c}{\partial z}) \\ \frac{1}{2}(\frac{\partial u^c}{\partial z} + \frac{\partial w^c}{\partial x}) & \frac{1}{2}(\frac{\partial v^c}{\partial z} + \frac{\partial w^c}{\partial y}) & \frac{\partial w^c}{\partial z} \end{bmatrix}$$

An overall deformation tensor can also be written.

The volumetric deformation is equal to zero since we are considering a spatial element.

There are two physical interpretations of the continuity requirement indicated by equation (E.32) :

(1) the volumetric deformation of the contractile skin is sufficiently small to be included with that of the water phase :

$$\frac{\Delta v}{v} = \frac{\Delta w}{v} + \frac{\Delta v^a}{v} \qquad \text{(E.34(a))}$$

and

(2) the volumetric deformation of the contractile skin is considered equal to that of the air phase. (see below for explanation).

$$\frac{\Delta v}{v} = \frac{\Delta v_w}{v} + \frac{\Delta v_c}{v} \qquad \text{(E.34(b))}$$

The second interpretation is new and demonstrated for the case of a spherical 'air bubble' and a long cylinder (duplicating pore effects):

Consider the case of an expanding soap bubble in air. The additional air is added using a syringe, and sufficient water is added to maintain a constant contractile skin thickness following expansion.

The selected element of contractile skin illustrated in fig. E.14 undergoes a deformation; $\partial u_c/\partial x$ and $\partial V_c/\partial y$ in the x and y directions respectively.

The translation and deformation of the element along the z axis maps two similar triangles (fig. E15) and is best expressed in terms of radius R for the sphere.

$\therefore$ in the x direction

$$\frac{(dx + \frac{\partial u^c}{\partial x})}{R + \Delta R} = \frac{dx}{R} \quad \text{i.e.} \quad 1 + \frac{\partial u^c}{\partial x} = 1 + \frac{\Delta R}{R} \tag{E.35}$$

or

$$\varepsilon_x = \frac{\partial u^c}{\partial x} = \frac{\Delta R}{R} \tag{E.36}$$

and in the y direction

$$\varepsilon_y = \frac{\partial v^c}{\partial y} = \frac{\Delta R}{R} \tag{E.37}$$

Since the z direction deformation is zero then the volumetric deformation of the bubble is

$$\varepsilon_c = \frac{2.\Delta R}{R} \tag{E.38}$$

Fredlund obtains the same relationship by differentiating the surface area of a sphere and then dividing it by the original surface area. In this way, he shows that the volumetric deformation of the contractile skin is equivalent to the increase in surface area.

As indicated above, the dimensionless surface area deformation of a sphere is $2dR/R$. The volume change of a similar sphere is defined $3dR/R$, which demonstrates that the volumetric deformation of a phase

contained within a contractile skin can be used as a measure of the contractile skin deformation.

Fredlund concludes that the air phase volumetric deformation is equivalent to that of the contractile skin, but this is disputed by the author. However, since he concludes that the volumetric deformation of the contractile skin is sufficiently small to include with that of the water phase (refer equation (E.34(a)), then this apparent inconsistency does not influence subsequent theoretical development.

E.4.6 Unsaturated soil case

The unsaturated soil is visualised as a combination of the water-solid and air-water multiphase.

A referential element of soil particles is chosen and used as a spatial element wrt air, water and contractile skin phases.

Each phase displacement is continuously written over the entire element; then the continuous element and linear displacement fields allow all phase displacements to be superimposed. The mapping of the displacements is illustrated in figure E16.

The deformation tensors for all phases are identical to those previously outlined for the water solid and air-water multiphases. The partial differential equations for each phase volumetric deformation are of the general form :

$$\varepsilon = \frac{\partial u}{\partial x} + \frac{\partial v}{\partial y} + \frac{\partial w}{\partial z} \qquad \text{(E.39)}$$

The continuity requirement states $\varepsilon^S = \varepsilon^p + \varepsilon^c + \varepsilon^a + \varepsilon^w$ and may be physically interpreted in two ways :

1. Contractile skin included with water phase and soil particle deformation assumed negligible thus : $\varepsilon^s = \varepsilon^w + \varepsilon^a$.
2. Air phase deformation is used as a measure of contractile skin deformation thus $\varepsilon^S = \varepsilon^w = \varepsilon^c$ (soil particle deformation again assumed = 0).

Therefore, although there is only one continuity equation, there is the possibility of applying more than one physical restriction on the continuity requirement.

Other volume-weight relationships

Deformation with respect to each phase can be presented in terms of conventional soil properties :

void ratio $$e = e_o + \varepsilon^s \frac{V_T}{V_s} \qquad \text{(E.40)}$$

water content $$w = w_o + \varepsilon^w \frac{V_T}{W_s} \qquad \text{(E.41)}$$

saturation $$S = S_o + \varepsilon^a \frac{V_T}{V_v} \qquad \text{(E.42)}$$

where

e = void ratio

w = moisture content

S = degree of saturation

ε = volumetric deformation

W_s = weight of solids

V = volume (s = soil ; v = voids ; T = total)

E.5 CONSTITUTIVE RELATIONSHIPS FOR UNSATURATED SOILS

The independently derived stress and deformation state variables are linked by suitable constitutive relations. In the case of unsaturated soils, these are generally proposed from a semi empirical standpoint and must be checked experimentally for uniqueness.

E.5.1 Constitutive relationship review

Biot (1940), in considering the 3-D consolidation of unsaturated soil, assumes (1) isotropic material (2) reversibility of stress-strain relations (3) linearity of stress-strain relations (4) small strains (5) incompressible pore water (6) pore water may contain air bubbles (7) water flows through porous skeleton according to Darcy's law.

Surface tension effects are apparently not considered and the pore pressure is considered as an independent stress state variable. Re-writing Hook's law for an isotropic elastic body in terms of Fredlund's notation then, the soil structure deformation is :

$$\varepsilon_x = \frac{(\sigma_x - u_w)}{E} - \frac{\nu}{E}(\sigma_y + \sigma_z - 2u_w) + \frac{u_w}{3.H} \qquad (E.43)$$

$$\varepsilon_{xy} = \frac{1}{G} \cdot \tau_{xy} \qquad (E.44)$$

similar in y and z directions, where

E = elastic mod. wrt change in total stress

ν = Poisson's ratio

G = modulus of rigidity

τ = shear stress

H = soil coefficient - a measure of soil compressibility for a change in water pressure

In order to completely describe the unsaturated soil deformation state, Biot proposes a general constitutive relationship to describe the effect of incremental water change on the above stress state variables.

$$\Theta = a_1(\sigma_x - u_w) + a_2(\sigma_y - u_w) + a_3(\sigma_z - u_w) + a_4 \cdot \tau_{xy} + a_5 \cdot \tau_{yz} + a_6 \cdot \tau_{zx} + a_7 \cdot u_w \qquad \text{(E.45)}$$

where

Θ = increment of volumetric water content

$a_1 \rightarrow a_7$ = soil parameters

If the soil is isotropic, then a change in the shear stresses cannot affect the water content therefore $a_4 = a_5 = a_6 = 0$. Furthermore, equivalent properties in the x , y , z directions imply that $a_1 = a_2 = a_3$. Re-writing (E.45) :

$$\Theta = \frac{1}{3H_1}(\sigma_x + \sigma_y + \sigma_z - 3u_w) + \frac{u_w}{R} \qquad \text{(E.46)}$$

where :

$\frac{1}{R}$ measures the change in water content for a given change in water pressure

Although Kelvin (1871) examines surface tension behaviour, this work had not been applied to soil behaviour at the time of Biot's work, who made no mention of surface tension effects. Kelvin relates the pressure difference across an air-water interace (u_a-u_w) with its radius of curvature.

$$d(u_a-u_w) = 2.T_s.d(r^{-1}) \qquad (E.47)$$

where

r = radius of curvature

T_s = surface tension force

Croney and Coleman (1948) are the first to direct soils engineers to the importance of the soil suction term (u_a-u_w). Croney (1952) proposes a constitutive equation to account for suction due to overburden.

$$\alpha.p-s = u_w \qquad (E.48)$$

P = over burden pressure

s = suction-unloaded specimen + atmospheric pressure

α = proportion of overburden effective in changing the suction

Fredlund (1973) re-writes Croney's equation :

$$\alpha.d(\sigma_y-u_a)-(u_a-u_w)_o = (u_a-u_w) \qquad (E.49)$$

α is slope of relationship between $(u_a - u_w)$ and $(\sigma_y - u_a)$.

Although Croney's suction data is linearised when plotted using Schofield's (1935) pF scale (logarithm of water head in centimetres), his equation (E.48) is limited in application due to the α term being a material related property which varies except under constant test conditions. The modification to Terzaghi's effective stress equation can be considered constitutive since they link stress state variables with a soil property. This applies to Bishop (1959); Aitchison (1956); Croney, Coleman and Black (1958); Jennings (1960) and Richards (1966) equations. Physically, they represent the relationship between stress state variables at a stress point.

Hilf (1956) and Bishop (1957) examine the relationship between volume and air pressure changes for a closed unsaturated soil system. Both researchers assume that the soil solids and water are incompressible (i.e. $\varepsilon^p = \varepsilon^w = 0$) , thus the total deformation and air phase deformation are equal.

Bishops equation is :

$$\frac{\Delta P}{P_o} = \frac{\frac{\Delta v}{v}}{\frac{\Delta v}{v} + (1 - S_o + S_o . h)} \qquad \text{(E.50(a))}$$

P = air pressure

$\frac{\Delta v}{v}$ = volumetric deformation

S_o = initial saturation

n_o = initial porosity

h = Henry's coefficient of solubility

Fredlund re-writes this equation in the form of a constitutive equation using terminology consistent with his proposals, where :

$$\Delta u_a = \left(- \frac{u_{ao}}{1 + (1-S_o+S_o.h).\frac{n_o}{\varepsilon^a}} \right).\varepsilon^a \qquad \text{(E.50(b))}$$

ε^a = deformation of the air phase

bracketted terms = stiffness coefficient

Since the stiffness coefficient contains the deformation state variable e^a , the constitutive relationship is non linear.

Jennings and Burland (1962) are apparently the first to question the uniqueness between void ratio and Bishop's effective stress equation.

Bishop and Blight (1963) also recognise this and conclude that the stress paths of the two stress state variables (i.e. (u_a-u_w) and $(\sigma-u_a)$) should be considered in the description of volume change behaviour. They suggest plotting volume change against both these variables as a three dimensional plot to facilitate interpretation. Fredlund summarised his thoughts regarding Bishop's equation for unsaturated soils (equation 4.6) as follows :

(a) the equation is a constitutive relationship and not a stress state variable since it incorporates a soil parameter (X).

(b) the equation does not exhibit a unique relationship with deformation - the X parameter restricting it for use to a particular set of stress conditions.

For these reasons, Fredlund considers the equation unsuitable for general application to unsaturated soils.

Coleman (1962) in uncoupling the components of Bishop's equation proposes a set of constitutive relationships for soil structure and water phase. He considers the volumetric deformations of a triaxial specimen with respect to the overall sample volume. where :

mean stress = $\sigma = \frac{1}{3}(\sigma_1 + 2\sigma_3)$

(σ_1 = vertical stress ; σ_3 = lateral stress)

and water volumetric deformation :

$$\frac{dV_w}{v} = C_{11}(du_w - du_a) + C_{12}(d\sigma - du_a) + C_{13}(d\sigma_1 - d\sigma_3) \qquad (E.51)$$

total volume deformation :

$$-\frac{dV}{v} = -C_{21}(du_w - du_a) + C_{22}(d\sigma - du_a) + C_{23}(d\sigma_1 - d\sigma_3) \qquad (E.52)$$

shear strain :

$$-d(d\varepsilon_1 - d\varepsilon_3) = -C_{31}(du_w - du_a) + C_{32}(d\sigma - u_a) + C_{33}(d\sigma_1 - d\sigma_3) \qquad (E.53)$$

where :

C = soil compressibility parameters, depending upon current stress values and stress history of the soil

V_w = volume of water

e = strain (ε_1 = vertical ; ε_3 = lateral)

Coleman states that 'for elastic behaviour of soil the only coefficients needed are C_{22} and C_{33} which are proportional to the reciprocal of the bulk and shear moduli respectively'. For drained isotropic swelling and shrinkage, the coefficients needed are C_{11} , C_{12} , C_{21} and C_{22} , all other terms being zero.

Aitchison (1967,1969) indicates the importance of describing volume change with respect to independent stress state variables. He subsequently presents experimentally obtained volume change curves, obtained by independently following $(\sigma-u_a)$ and (u_a-u_w) stress paths.

Matyas and Radhakrishna (1968) perform similar tests, but plot the variation in voids ratio and secondly degree of saturation against the stress state variables $(\sigma-u_a)$ and (u_a-u_w) . The void ratio constitutive surface is similar to the volume change constitutive surface indicated by Aitchison.

Their low swell, Kaolin-flint powder mix soil exhibits a collapsing phenomenon upon wetting. This involves a reduction in suction which influences the soil structure by reducing its intergranular stress and rigidity. Above a critical stress $(\sigma-u_a)$ the volume decrease due to rigidity exceeds the volume increase due to the decrease in intergranular stress and this constitutes a collapse.

Radhakrishna (1967) in his thesis, conducts a few tests under constant water content conditions with an increasing degree of saturation. His results apparently confirm the uniqueness of the volume

change constitutive surface with respect to the stress paths followed.

He does however, indicate certain non-unique characteristics regarding volume change behaviour. These are attributed to the hysteresis effects resulting from loading and unloading, wetting and drying.

The wetting paths are noted as not lying exactly on the saturation-constitutive surface, and this is attributed to incomplete saturation during the wetting process.

Barden, Madedor and Sides (1969) experimentally assess the C parameters given in Coleman's equations (E.51 - E.53) by observing the volume change of a small range of synthetically produced clay mixtures of plasticities between 20% and 60% . The specimens are subjected to a variety of stress paths by controlling the total, air and water pressures, and they suggest that the main cause of stress path dependency is due to the direction of saturation.

The author notes that suction is increased in some of Barden et al's tests which would undoubtedly result in isotropic (three dimensional) shrinkage. This is considered incompatible with the one dimensional nature of the equipment, and therefore sheds some doubt upon their results.

E.5.2 Constitutive relationships for a multiphase system

The 'semi empirical' approach is a frequently used method for establishing stress deformation relationships and is the method employed by Fredlund. This involves checking the constitutive surface by experimental means to assure uniqueness.

It is shown in Section E.4 that the mapping of soil structure and contractile skin permits the deformation of an unsaturated soil to be completely described. Therefore, the relationships linking the deformation state variables of the two phases are of primary interest.

The relationships must be studied experimentally, and if shown to be unique, permit the prediction of phase deformations from a knowledge of the stress state variables and soil parameters.

E.5.3 Constitutive relationships for the water solid and and air water multiphases

Considering briefly the water-solid multiphase or saturated soil, then assuming that the soil behaves isotropically and in a linear elastic manner, then the constitutive relationship for the soil structure in the y direction is

$$\varepsilon_y^s = \frac{(\sigma_z - u_w)}{E'} - \frac{\nu'}{E'}(\sigma_x + \sigma_z - 2u_w) \qquad (E.54)$$

E' = Young's modulus for soil structure corresponding to $\Delta\sigma'$

ν' = Poisson's ratio wrt $\Delta\sigma'$.

ε_y^s = soil structure deformation

Similar relationships apply in the x and z directions.

For the air-water multiphase, the contractile skin is assumed to behave as an elastic, isotropic solid that cannot withstand shear. Thus, the deformation of the contractile skin in the y direction is :

$$\varepsilon_y^c = \frac{u_a - u_w}{H'} \qquad (E.55)$$

H' = elasticity parameter for the contractile skin

Similarly in the x and z directions.

The air-water multiphase is somewhat fictitious in the absence of a solid phase.

E.5.4 Soil structure

The unsaturated soil element is considered as a combination of water-solid and air-water multiphase systems. The assumptions of linearity, reversibility and infinitesimal deformations allow the effects of several stress state variables to be added thus forming constitutive relationships within the context of a simple linear elastic model.

As shown in Section E.3, the soil structure and contractile skin equilibrium may be described using any two out of three stress state variables i.e. $(u_a - u_w)$, $(\sigma - u_a)$ and $(\sigma - u_w)$.

Considering $(\sigma - u_w)$ and $(u_a - u_w)$, then the soil structure deformation in elasticity form is :

$$\varepsilon_y^s = \frac{(\sigma_x - u_w)}{E_t^s} - \frac{\nu_t^s}{E_t^s}(\sigma_x + \sigma_z - 2.u_w) + \frac{(u_a - u_w)}{H_a^s} \qquad (E.56)$$

E_t = elasticity modulus associated with the $(\sigma - u_w)$ stress state variable

H_a^s = elasticity modulus for the soil structure defined by changing u_a .

Similar relationships apply in the x and z directions.

The shear constitutive equation in the y direction is :

$$\varepsilon^s_{yz} = \frac{1}{G^s} \cdot \tau_{yz} \qquad (E.57)$$

ε^s_y = shear deformation of soil structure

G = shear modulus

τ = shear stress

The volumetric deformation of soil structure is equal to the sum of deformations in the x , y and z directions. In addition, the soil properties and total stress conditions are assumed isotropic such that :

$$\varepsilon^s = 3\left[\frac{1-2.\nu^s_t}{E^s_b}\right].(\sigma-u_w) + \frac{3}{H^s_a}.(u_a-u_w) \qquad (E.58)$$

This equation may be written in terms of the compressibility modulii. Where $C^s_t = 3(1-2\nu^s_t)/E^s_t$ and $C^s_a = 3/H^s_a$

then :

$$\varepsilon^s = C^s_t\,(\sigma-u_w) + C^s_a.(u_a-u_w) \qquad (E.59)$$

This may be re-written to account for non linear properties such that

$$\varepsilon^s = \frac{dV^s}{V} = \frac{\partial V^s}{\partial(\sigma-u_w)}.\ d(\sigma-u_w) + \frac{\partial V^s}{\partial(u_a-u_w)}.d(u_a-u_w) \qquad (E.60)$$

where

$\frac{\partial V^s}{\partial(\sigma-u_w)}$ = compressibility of soil structure when $d(u_a-u_w)$ is zero

$\frac{\partial V^s}{\partial(u_a-u_w)}$ = compressibility of soil structure when $d(\sigma-u_w)$ is zero

A similar analysis may be conducted using the other combination of stress state variables i.e. $(\sigma-u_a)$ and (u_a-u_w) .

E.5.5 Contractile skin

To the author's knowledge, Fredlund is the first to present a constitutive relationship of this form for the contractile skin. Assuming a linear, reversible model, he writes the constitutive equation as a linear combination of the stress state variables (a procedure similar to Biot (1940)'s assumption with respect to the water phase).

The contractile skin constitutive relationship reduces to the same form as that for the soil structure, since the stress state variables associated with each are the same.

The volumetric deformation of the contractile skin with respect to the $(\sigma-u_w)$ and (u_a-u_w) stress state variables may therefore be written :

$$\varepsilon_y^c = \frac{(\sigma_y-u_w)}{E_t^c} - \frac{\nu_t^c}{E_t}(\sigma_x+\sigma_z-2u_w) + \frac{(u_a-u_w)}{H_a^c} \qquad (E.61)$$

and similarly in the x and z directions.

There are also deformation equations with respect to shear stress such that :

$$\varepsilon^{c}_{yz} = \frac{1}{G^{c}} \cdot \tau_{yz} \qquad (E.62)$$

there being similar relationships in the x and z directions.

The moduli associated with the contractile skin are independent of those for soil structure.

The dependence of contractile skin behaviour upon the same stress state variables as employed to describe soil structure behaviour permits the deformation equation (E.61) to be re-written in the compressibility and partial differential forms as equations (E.59) and (E.60).

E.5.6 Water phase

The water phase constitutive equation describes the volume of water present in the referential element, and accounts for the net inflow and outflow. The water is assumed incompressible.

Presenting the equation as a linear combination of stress state variables therefore, the water volume deformation may be written :

$$\Theta^{w} = \frac{(\sigma_x + \sigma_y + \sigma_z - 3.u_w)}{3H_1} + \frac{(u_a - u_w)}{R_1} \qquad (E.63)$$

where

Θ^{w} = inflow/outflow of water

R_1 = water volumetric modulus associated with a change in $(\sigma - u_w)$

H_1 = water volumetric modulus associated with a change in $(\sigma-u_w)$.

The equation may be re-written to account for non linear properties where

$$\Theta^w = \frac{dV^w}{V} = \frac{1}{D}\frac{\partial V^w}{\partial(\sigma-u_w)}.d(\sigma-u_w) + \frac{1}{\nu}\frac{\partial V^w}{\partial(u_a-u_w)}.d(u_a-u_w) \qquad (E.64)$$

where

V^w = volume of water in element

These equations may also be expressed in a similar manner but using the other two stress state variable combinations.

The graphical representation of the previous constitutive equations is illustrated in figure E.17.

E.5.7 Air phase

The change in air phase may be written from the continuity requirement such that it equals the difference between the change in soil structure and water volumes.

E.5.8 Sign convention for compressibility modulii

A sign convention for the compressibility modulii in unsaturated soils is imperative since an increase in stress state variable will not always produce the same direction of volume change. Once the sign of the moduli is known, it can be incorporated into the differential equation.

The signs are not fixed and depend to some extent upon the soil type under consideration.

The general sign convention for phase deformations following a stress state variable (ssv) variation is:

INCREASE in ssv produces phase volume DECREASE : Moduli is POSITIVE

INCREASE in ssv produces phase volume INCREASE : Moduli is NEGATIVE

and is applicable to the contractile skin, air , soil structure and water phases. Stress state variables can be changed by varying one or other of the components. It is found that the moduli sign will depend upon which component is changed.

E.5.9 Experimental verification of the constitutive equations (uniqueness of the constitutive surface at a point)

Uniqueness requires that there is one and only one relationship between the stress state variables. Even where it does not completely exist, stress path restrictions can at least be imposed upon the constitutive relationship.

Fredlund (1973) proposes a simple procedure for gauging uniqueness. A specimen is subjected to small stress increments along three stress paths (Fig. E18). Using the deformations resulting from any two of the increments, it is possible to compute two corresponding compressibility modulii.

The deformation equation can now be used to compute anticipated deformation along the third stress path. The computed and measured deformations are compared, and the constitutive relationship regarded as unique when they equal each other.

Three stress paths of equal spacing are obtained by changing the total air and water pressure,then allowing equalisation after each

pressure change. Volume changes are measured after two different equalisation times. Fredlund indicates a distortion of the constitutive surface with time,due it is thought, to the secondary behaviour of the tested clay type (Regina clay).

As a result of changing one stress component, six compressibility values may be calculated. However, the values are computed with respect to the stress state variables and not the stress changes. Thus the compressibilities that can be computed are :

soil structure: $C^s(\sigma-u_w)$ = soil structure compressibility wrt $\Delta(\sigma-u_w)$

$C^s(u_a-u_w)$= soil structure compressibility wrt $\Delta(u_a-u_w)$

air phase: $C^a(\sigma-u_w)$ = air phase compressibility wrt $\Delta(\sigma-u_w)$

$C^a(u_a-u_w)$= air phase compressibility wrt $\Delta(u_a-u_w)$

water phase: $C^w(\sigma-u_w)$ = water phase compressibility wrt $\Delta(\sigma-u_w)$

$C^w(u_a-u_w)$= water phase compressibility wrt $\Delta(u_a-u_w)$

The sign of any stress state variable changes must be observed when computing compressibilities, since changes in stress components will yield differing changes in stress state variables i.e. a decrease in u_w will increase the (u_a-u_w) variable whereas an increase in u_a will decrease the same stress state variable.

Fredlund (1973) calculates the compressibility values corresponding to stress changes thus :

$$\text{compressibility} = \frac{\Delta V^{(\text{phase})}}{\Delta(\text{stress state variable})} \qquad \text{(E.65)}$$

His analysis continues, by calculating the anticipated volume changes of each phase using the above calculated compressibilities, these calculated values are compared with those actually measured by experiment.

The data is plotted: experimental vs. theoretical and a best fit line drawn. The coefficient of correlation is determined-thus gauging the dispersion of data about the best fit line. A high coefficient of determination thus implies the existence of a reliable mathematical model of the constitutive surface.

Generally the correlations observed are better with an increased equilibrium time, although Fredlund suggests that this will probably not be the case with high expansion soils.

The statistical data for air phase uniqueness is less encouraging than that for either the soil structure or water phase. This is anticipated since air phase deformations are computed from the soil structure and water phase deformations, thus any inaccuracies tend to be amplified.

A comparison of the measured and predicted volumetric changes (water phase and soil structure), indicates that the constitutive surfaces are unique provided the direction of the volume change is not reversed - thereby introducing hysteresis effects.

E.5.10 Hysteresis

The variation in volume changes resulting from stress reversals is generally known as hysteresis.

Fredlund notes the above soil behaviour in his main testing programme and conducts three tests to briefly examine this aspect further. His findings broadly indicate that the hysteretic properties of a soil are not directly related to the stress component or stress state variable changes but more to the direction of soil structure and/or contractile skin deformation.

Although recognising the magnitude of hysteretic effects upon unsaturated soil behaviour, the limitations of his research programme result in his primarily examining swell behaviour (increasing saturation/decreasing suction).

In addition, the author notes that a comprehensive study of hysteretic effects would require a project in its own right. It is apparent that a theoretical model not considering hysteresis is of limited application to in situ soils where moisture content variation will change with the seasons, and further development is necessary to account for this behaviour.

The hysteretic effects of a stress reduction resulting from sampling disturbance is discussed in Chapter 5.

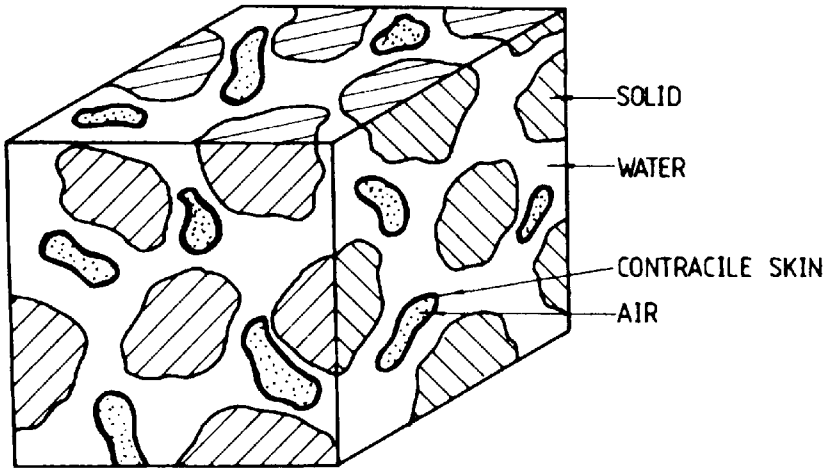

FIGURE E·1
ELEMENT OF AN UNSATURATED SOIL

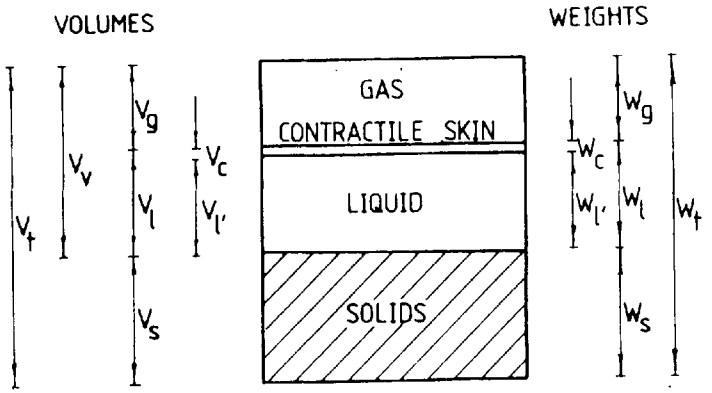

FOUR PHASE UNSATURATED SOIL SYSTEM
- FREDLUND (1973)

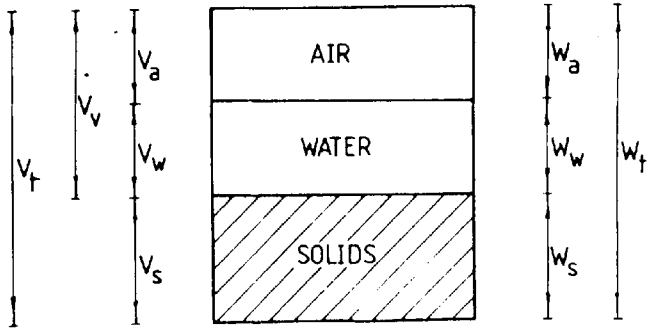

THREE PHASE UNSATURATED SOIL SYSTEM
- LADD & LAMBE (1969)

FIGURE E·2
UNSATURATED SOIL SYSTEMS

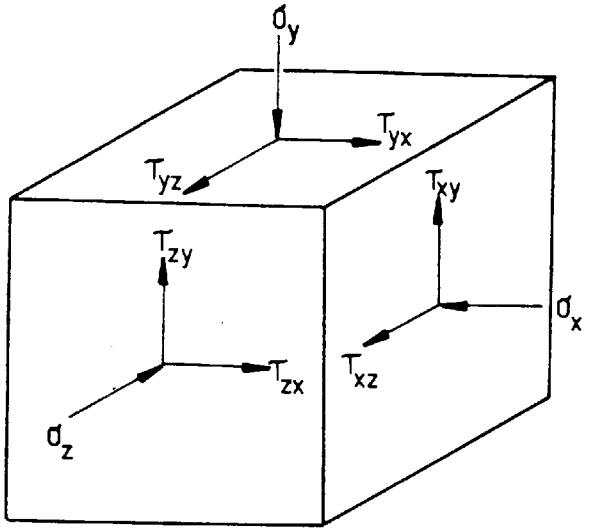

FIGURE E·3
THREE DIMENSIONAL STRESS COMPONENTS AT A POINT.

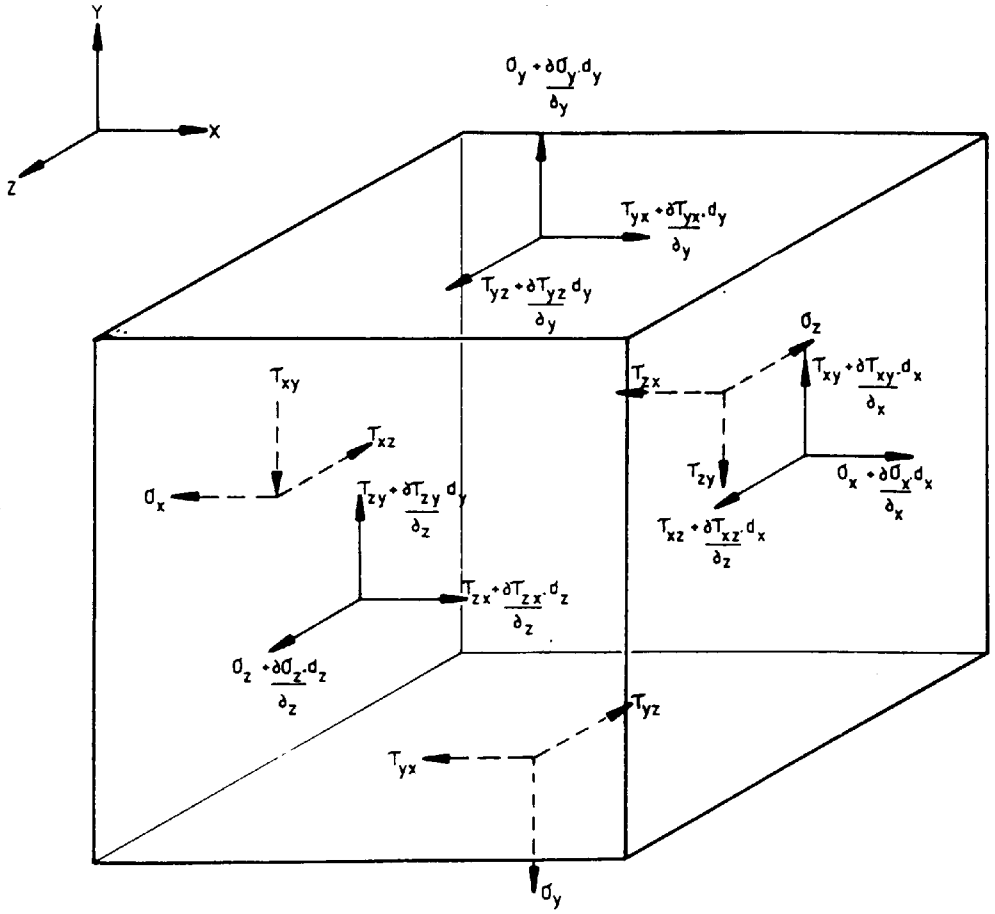

FIGURE E·4
EQUILIBRIUM STRESS FIELDS ACCROSS A CUBE ELEMENT.

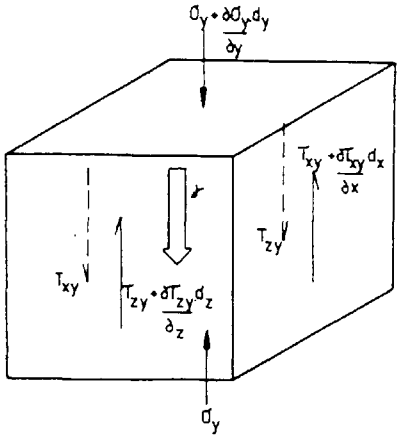

TOTAL STRESS EQUILIBRIUM OF AN ELEMENT OF SATURATED SOIL

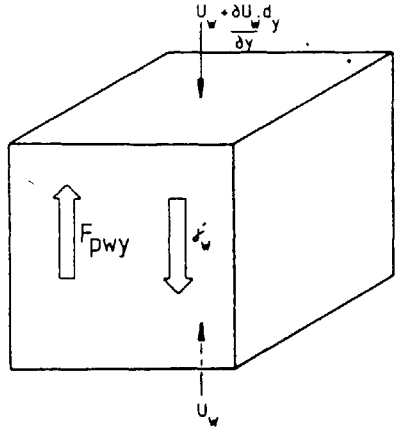

PRESSURE EQUILIBRIUM OF THE WATER PHASE

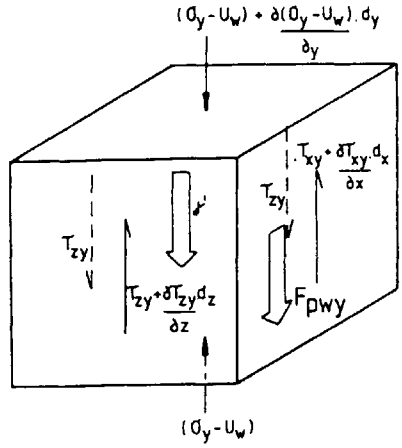

STRESS EQUILIBRIUM OF THE SOIL STRUCTURE

FIGURE E·5
STRESS EQUILIBRIUM OF A WATER SATURATED PARTICULATE SYSTEM.

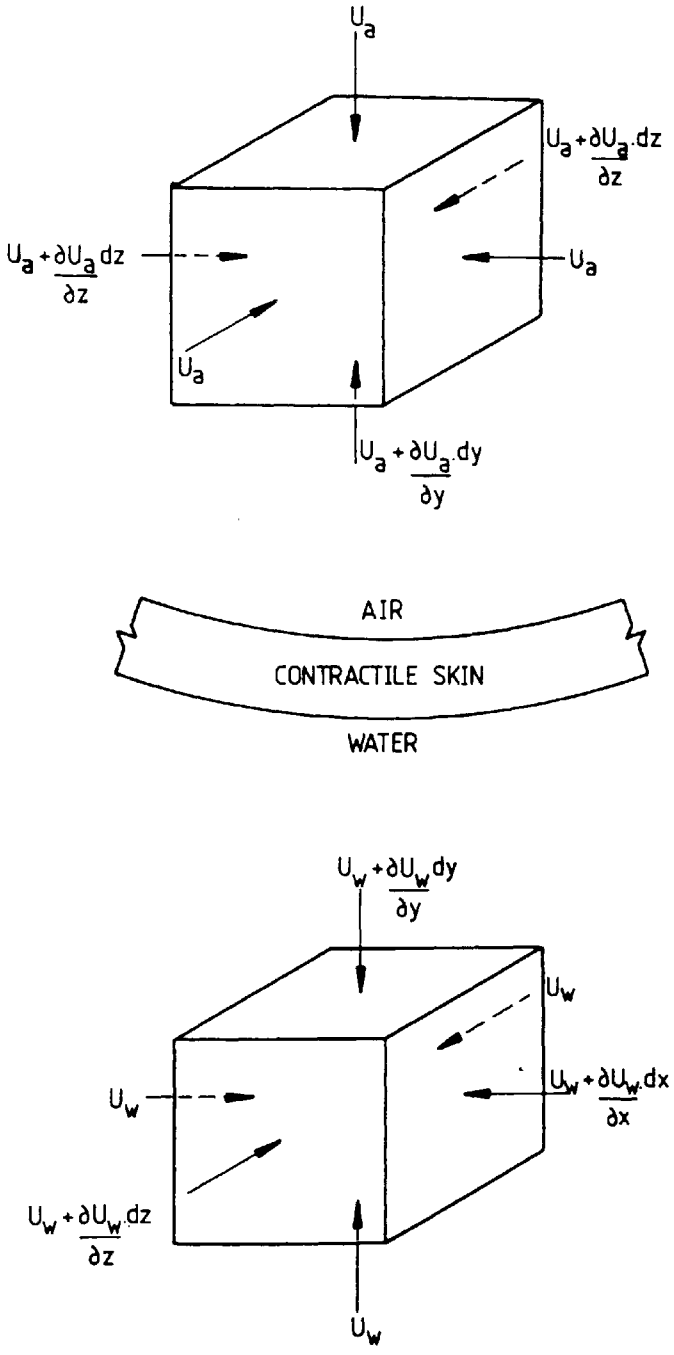

FIGURE E·6
EQUILIBRIUM IN AN AIR - WATER MULTIPHASE

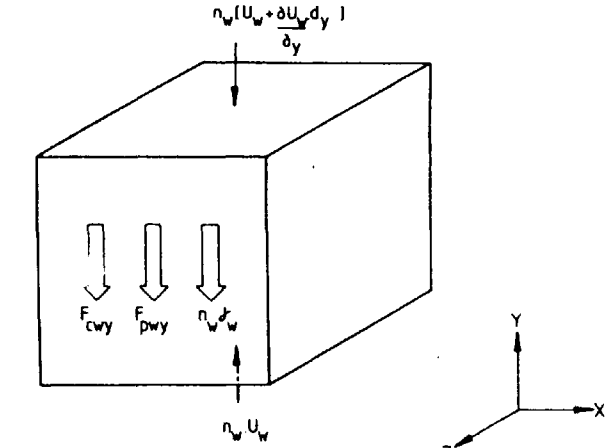

Y-DIRECTION EQUILIBRIUM FOR PORE WATER PHASE OF UNSATURATED SOILS

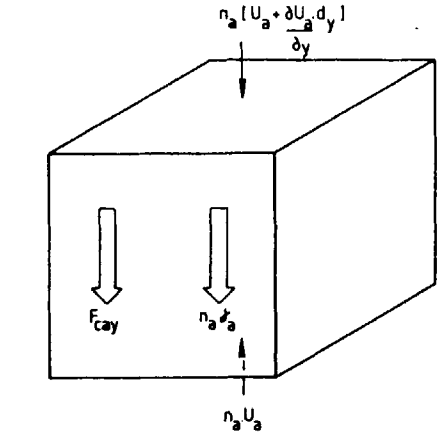

Y-DIRECTION EQUILIBRIUM FOR PORE AIR PHASE OF UNSATURATED SOIL

FIGURE E·7
EQUILIBRIUM OF PORE WATER AND AIR PHASES IN AN UNSATURATED SOIL

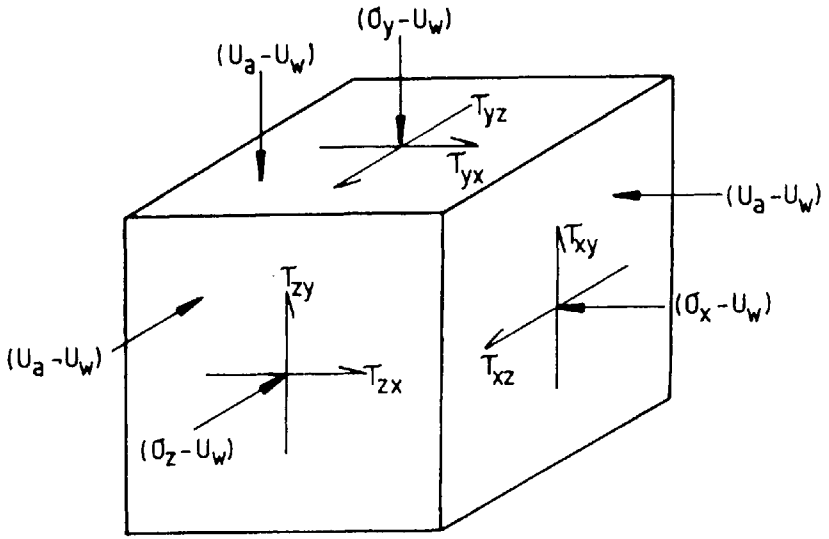

FIGURE E·8
STRESSES AT A POINT IN THE SOIL STRUCTURE.

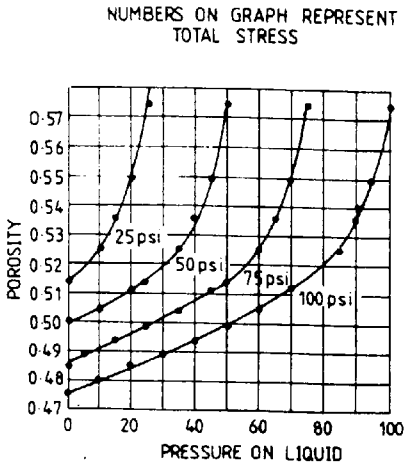

A SET OF CURVES DEMONSTRATING THE DEPENDENCE OF POROSITY ON TOTAL STRESS AND ON THE PORE WATER STRESS, IN THE CASE OF KAOLIN (TILLER, 1953)

FIGURE E·9

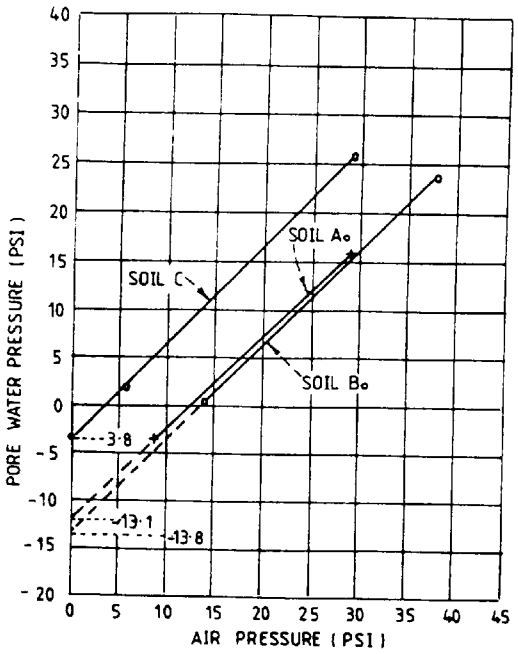

DETERMINATION OF CAPILLARY PRESSURE BY TRANSLATION OF THE ORIGIN (HILF, 1956)

FIGURE E·11

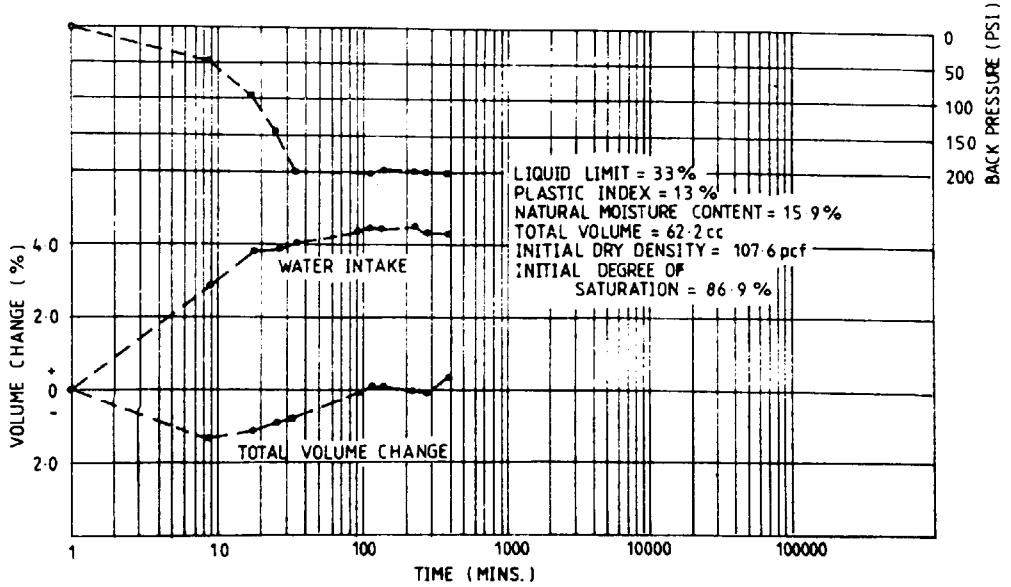

EFFECT OF EQUAL INCREASE IN CELL PRESSURE AND PORE PRESSURE ON THE VOLUME OF A SANDY CLAY (LOWE & JOHNSON, 1960)

FIGURE E·10

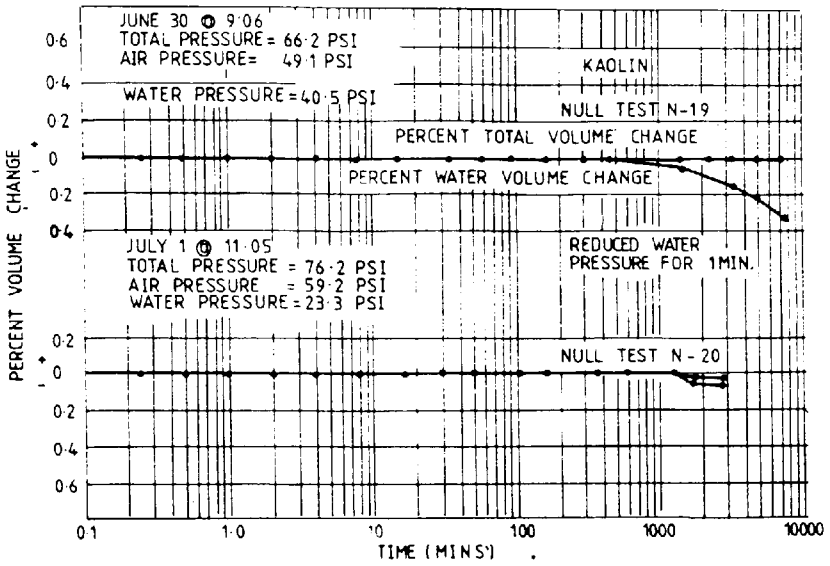

NULL TESTS N-19 AND N-20 ON SAMPLE Nº 6.
SATURATED SPECIMENS WITH TOTAL, AIR AND
WATER PRESSURE CONTROL. (FREDLUND, 1973)

FIGURE E·12

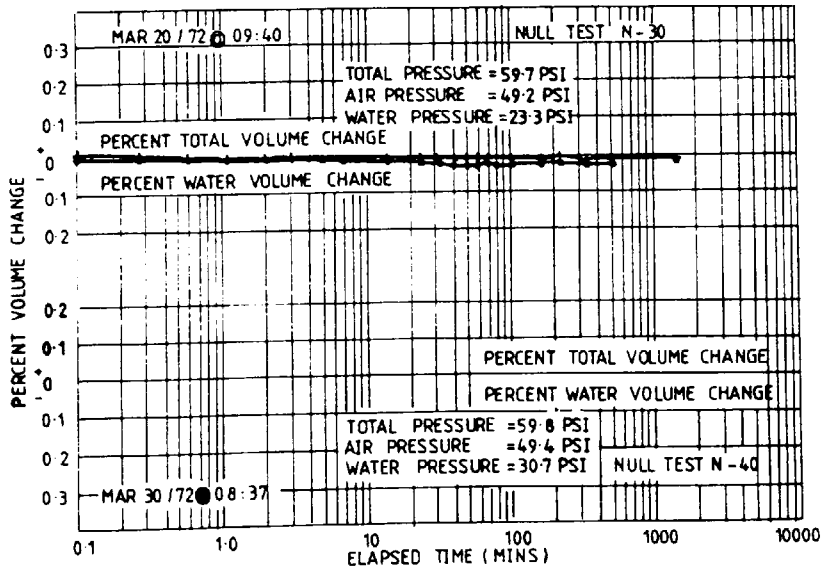

NULL TESTS N-39 AND N-40 ON SAMPLE Nº 31
UNSATURATED SPECIMENS - TOTAL, AIR AND WATER
PRESSURE CONTROL (FREDLUND 1973)

FIGURE E·13

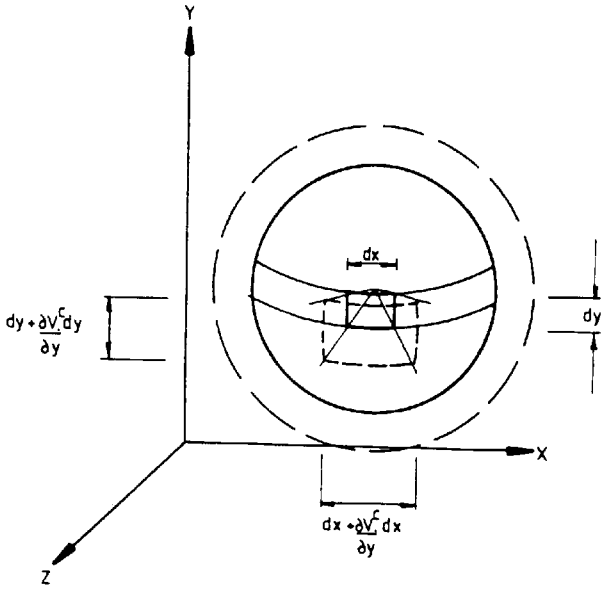

FIGURE E·14
TRANSLATION AND DEFORMATION OF AN ELEMENT FROM A SOAP BUBBLE.

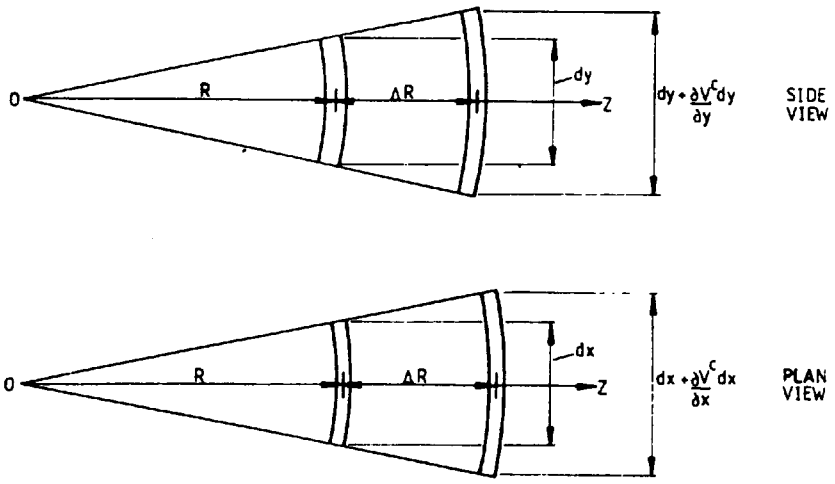

FIGURE E·15
DIMENSIONS AND DISPLACEMENT FOR AN ELEMENT OF THE BUBBLE ALONG Z-AXIS

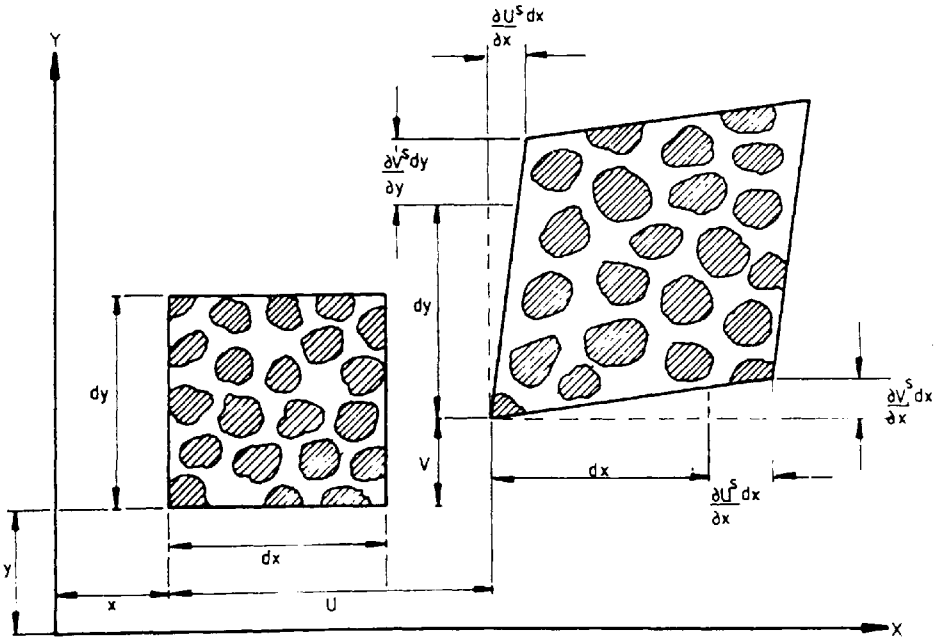

FIGURE E·16
TRANSLATION AND DEFORMATION OF A TWO DIMENSIONAL ELEMENT OF UNSATURATED SOIL

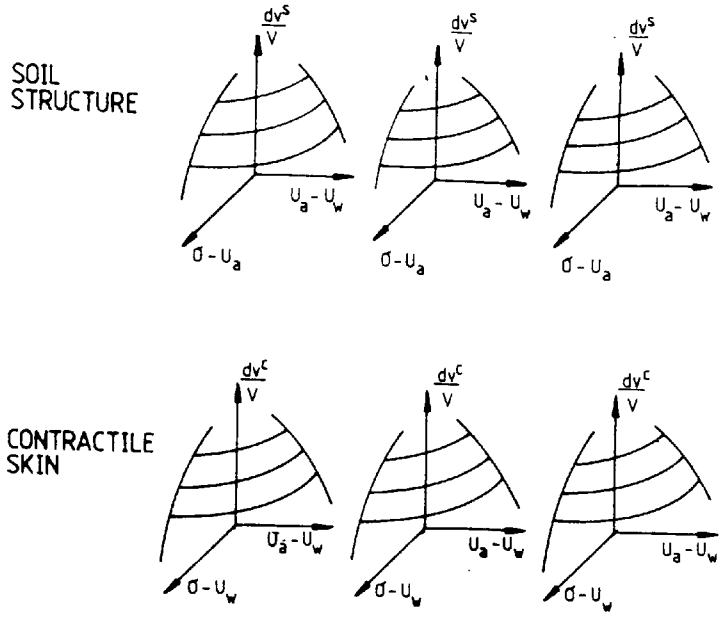

FIGURE E-17
GRAPHICAL REPRESENTATION OF THE CONSTITUTIVE SURFACES

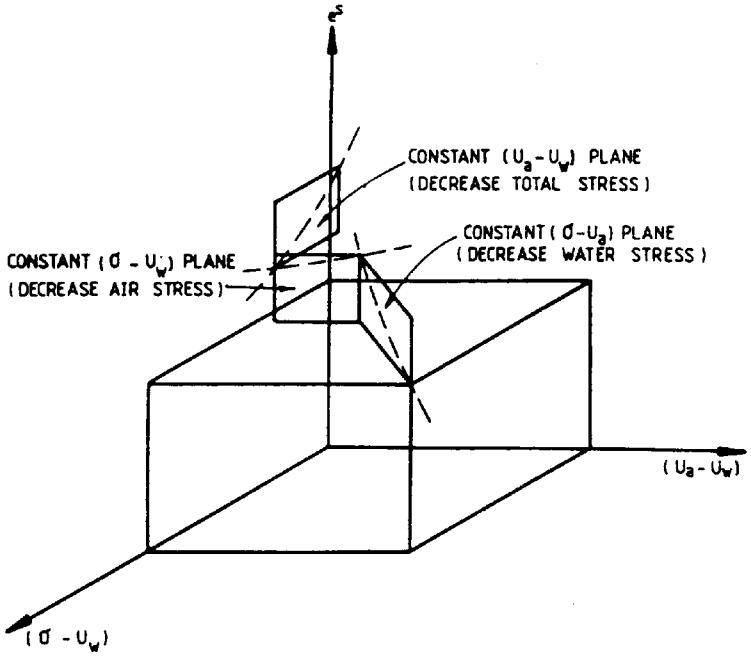

FIGURE E-18
UNIQUENESS TEST STRESS PATH

APPENDIX F

PUBLISHED SWELL DATA USED IN CHAPTER 3

Soil No.	Location: Feature	Location: State	Sample No.	Identification Data: Class	Identification Data: Colloids % -.001 mm	Identification Data: L.L.	Identification Data: P.I.	Identification Data: S.L.	Estimated degree expansiveness	Free swell	Spec. gravity	Mineral
1	Gila Proj., W.M. Canals	Ariz.	14J-217	CH		110	82	9	V. High		2.77	Mo-Mont.
2			-234	CH		142	119	8	V. high		(2.77)	Mo-Mont.
3			-238	CH		89	61	10	V. high		2.77	Mo-Mont.
4			-X249	(1) CH		137	112	7	V. high		2.78	Mo-Mont.
			-X249	(2) CH		137	112	7			2.78	Mo-Mont.
			-X249	(3) CH		137	112	7			2.78	Mo-Mont.
			-X249	(4) CH		137	112	7			2.78	
5	Gila Proj., W.M. P.]	Ariz.	14J-211	CH	57	81	54	11	V. High		2.77	
6			-212	CH	61	68	45	14	High		2.72	
7			-214	CH	31	76	52	13	High		2.76	
8	Casitas Canal	Calif.	22B-168	CL	30	37	22	8	Med.	50	2.71	
9	Ojai Val. Pump	Calif.	26Z-14	CL	25	36	20	12	Med.-low	30	2.73	
10	Putah S. C[illegible]	Calif.	21C-11	CL	17	40	20	13	Med.-low	30	2.71	
			11	CL	17	40	20	13	Med.-low	30	2.71	
11			14	CL-CH	26	50	28	11	Med.	70	2.75	
			14	CL-CH	26	50	28	11	Med.	70	2.75	
12			15	CL		49	31	9	High		2.70	
			15	CL		49	31	9	High		2.70	
13			18	CL		29	11	17	Low		2.69	
			18	CL		29	11	17	Low		2.69	
14	Lind-Strath. Res.	Calif.	17C-4	CL		46	25	8	High		2.81	
15	Lindmore Res.	Calif.	15F-4	CH		54	34	11	Med.-High		2.75	
			15F-4	CH		54	34	11			2.75	
			15F-4	CH		54	34	11			2.75	
16	Ortega Res.	Calif.	16L-2	CH	55	68	35	21	Med.-low		2.69	
17	Delta-Mendota Canal	Calif.	7M-X241	CH	31	64	44	14	Med.-High		2.70	
			7M-X241	CH	31	64	44	14	Med.-High		2.70	
18			7M-103	CL	18	31	14	13	Med.	60	2.66	
19			7M-106	CL	18	40	18	10	Med.	70	2.70	
20	Contra Costa Canal	Calif.	3M-64	CH	44	54	26	8	High-V. High	110	2.71	
21			3M-65	CH	49	76	39	9	V. High	170	2.73	
22	Friant Kern Canal	Calif.	3T-102	CL-CH	23	50	25	9	High	100	2.85	60% Co-Beidellite
23			104	CH	30	59	30	6	High	130	2.76	"
24			106	CL-CH	28	51	23	14	Med.	80	2.72	"
25			130	CH	35	77	50	12	V. High		2.76	"
26			98	CH	30	59	30	6	High-V. High		2.76	"
			98	CH	30	59	30	6			2.76	"
27	Vega Dam Spy.	Colo.	SV-2	CL		42	23	--	Med.		2.74	
28			3	CL		45	24	11	Med.		2.71	
29			4	CL		40	17	--	"		2.73	
30	Horsetooth Canal	Colo.	JW-367	CL	16	29	12	10	Low	10-15	2.70	
31			368	CL	12	32	14	19	Low	10-15	2.69	
32			369	CL	8	36	18	18	Low	10-15	2.68	
33	E.R., Denver	Colo.	RR-1	CH		59	39	8	High-V. High	90	--	
34			4	CH		55	30	11	High	85		
35			5	CH		51	25	8	High			
36			7	CH		55	29	14	Med.	60		
37			9	CH		53	28	11	Med.	100		
			9	CH		53	28	11	Med.	100		
			9	CH		53	28	11	Med.	100		
38	E.I., Colo. Spgs.	Colo.	30G-1	CL-CH	21	48	28	13-16	Med.	70	2.62	
39	E.I., Colo. Spgs.	Colo.	81-4	CH	--	57	30	10	High			
40	Westminster	Colo.	We-A	CL-CH		49	23	13	Med.			
41	Westminster	Colo.	We-B	CL-CH		46	18	11	Med.-low			
42	Wheatridge	Colo.	Wh-1	CL		43	26	13	Med.	50		
43			Wh-2	CH		54	35	10	High	100		
44	Fire Mt. Canal	Colo.	26B-1	CL		43	21	12	Med.		2.68	
45	Navajo Dam Spy.	Colo.	77T-36	CL		30	13	13	Med.-low		2.76	
46	Denver S.E. Ry.	Colo.	A-958	CL-CH		48	23	14	Med.	60	2.69	
47	Boulder-Denver T.P.	Colo.	B-132	CL		43	19	8	Med.	74	2.68	
48	Kirwin Dam	Kans.	7N-830	CL-CH		50	29	--	High		2.73	
49	Emigrant Dam	Ore.	18P-156	CH		69	48	8	V. High		--	60-70% Ca-Bent.
50	Tiber Dam Spy.	Mont.	11P-264	CH	54	227	179	9	V. High	230	2.75	80-90% Na - Mont.
51			263	CH		171	138	6	V. High	510	2.72	80-90% Na - Mont.
52	Sherburne Dam	Mont.	30C-1	CH		63	45	13	Med.-High		2.71	
53	BLM-Collins Dam	Mont.	24Q-34	CH		56	36	10	High		2.71	
54	Little Porcupine Plant	Mont.	15T-135	CH		123	92	--	V. High	170	2.75	70% Mont.
55	Courtland Canal	Neb.	15L-157	CH	37	57	30	16	Med.	80	2.70	
56	Courtland Canal	Neb.	15L-167	CL to		35 to 75	18 to 54	--			2.70 to	
			to 200	CH							2.74	
57	Courtland Pump No. 1	Neb.	29Q-11	CL-CH		49	30	15	Med.		2.73	
58			14	CL		37	17	20	Low		2.74	
59	Lovewell Dam	Neb.	6K-255	CL-CH		49	30	12	Med.		2.70	
60	Watasheemu Dam	Nev.	20N-1, 2,]	CH		65-58	41-36				2.77	
61	Garage-Boulder Cty.	Nev.	25N-1	CH		60	36	12	High		2.73	35% Na-Ca - Mont.
62	McMillan Res.	N. Mex.	30F-3	CH	32	67	41	15	Med.-high	90	--	
63	McCleary Canal	N. D.	22T-130	CH	41	68	40	17	Med.-High	90		
64			123	CL	18	39	17	16	Med.	30		
65	Oahe Pump	S. D.	17D-1	CH					Med.	80	2.78	80% Na-Ca -Mont.
66	Gulf Coast Canal	Texas	28B-71	CH	48	67	47	11	V. High	100	2.80	30% Illite-Beid (Ca)
			71	CH	48	67	47	11	V. High	100	2.80	"
67			67	CH	37	54	35	10	High	100	2.70	"
			67	CH	37	54	35	10	High	100	2.70	"
68			10	CH	54	72	53	9	V. High		2.75	"
69			93	CH	62	72	48	8	V. High		2.77	"
70			4	CH	56	88	71	7	V. High		2.68	"
71			50	CH	46	61	47	8	V. High		2.69	"
72			5	CH	52	73	53	5	V. High		2.73	"
73			43	CH	53	75	56	9	V. High		2.68	"
74	Gateway Canal	Utah	21F-37	CH	37	59	38	11	High	70	2.71	55% Na-Ca - Mont.
			21F-57	CH	37	59	38	11	High	70		
75			1	CH	30	51	28	8	Med.-High	90	2.70	
76			1	CH		59	34	10	High		2.72	
77			36	CH		60	37	11	High		2.72	
			36	CH		60	37	11	High		2.72	

NOTE: ( ) interpolated from other loadings
+ Heavier load released.
++ Total volume changes are computed on basis of dry unit weights of air-dry specimens. Expansion and shrinkage, from natural to saturated and air-dry conditions, are computed on basis of dry unit weights of natural specimens.

TABLE F.1 (part 1)

Soil No.	% expan. nat. to sat. 1 psi load	% shrink. nat. to air dry	** Total vol. change %	Load for 0 expan. psi	Natural Conditions Dry den. pcf	Moist. %	Deg. sat %	Remarks
1	7.0			8	85.3	25.5	94.0	Undisturbed
2	(15)				104.1	24.6	100.0	Undistur
3	(2.5)							
4	(13)			5	82.2	34.8	87.0	Undistu,
	(54)			90	104.0	26.8	87.0	Remolded 1
	(35)			76	103.3	18.4	69.0	Remolded 2
	(33)			65	99.2	21.0	78.0	Remolded 3
					98.6	16.2	59.0	Remolded 4
5	9.6			73	98.5	26.7	97.9	Undisturbed
6	8.4			110	103.1	23.8	100.0	Undisturbed
7	11.8			100	101.8	23.9	95.1	Undisturbed
8	1.9			10+	111.0	13.3	69	Remolded
9	(1.9)			19	108.3	12.0	57	Undisturbed
10	(0)				91.9	26.1	84	Undisturbed
	0.5				Air dried			
11	0.4				98.1	23.7	87	Undisturbed
	7.2				Air dried			
12	1.8				98.1	25.3	95	Undisturbed
	2.6				Air dried			
13	0				104.7	18.4	82	Undisturbed
	1.7				Air dried			
14	(3.4)			(16)	98.0	21.1	75.3	Remolded
15	3.6				95.7	19.1	66.3	Remolded
	1.0				90.7	18.7	57.6	Remolded
	-2.0				86.0	18.9	52.3	Remolded
16	2.0*				80.3	28.8	71.1	Remolded
17	11.7				97.5	13.2	--	Remolded
	1.8				78.0	25.0	--	Remolded
18	5.9	5.1	13.6	11	108.5	10.7	--	Remolded
19	7.7	4.1	10.5	41	107.6	11.1	--	Remolded
20	12.5	17.7	31.6	27	86.9	19.5	--	Remolded
21	21.5	18.3	50.1	68	82.4	29.2	--	Remolded
22	19.3	8.4	27.9	147	113.7	12.9	--	Remolded
23	7.1	21.2	35.0	7	89.9	27.2	--	Remolded
24	3.0	12.5	13.4	24	90.9	23.6	--	Remolded
25	9.9	27.5	48.6	--	86.5	33.8	--	Remolded
26	8.9				97.5	20.5	--	Remolded
	3.0				81.0	25.5	--	Remolded
27	4.3*			95	110.3	15.0	75	Undisturbed
28	0.9			18	107.0	18.8	88	Undisturbed
29	(0.6)*			11	105.8	15.5	--	Undisturbed
30	0.9	6.3	6.9	3	90.4	10.7	--	Undisturbed
31	2.5	7.4	11.0	8	100.9	9.8	--	Undisturbed
32	2.7	7.2	10.7	7	101.2	8.1	--	Undisturbed
33	1.9				103.5	18.1	--	Undisturbed, soil
34	6.3				99.7	18.5	--	Undisturbed, Denver shale
35	7.3				105.8	16.8	--	Undisturbed, Denver shale
36	4.9*				109.2	14.2	--	Undisturbed, Denver shale
37	13.5				101.0	12.0	--	Remolded, Denver shale
	11.6				103.0	17.0	--	Remolded, Denver shale
	1.8				103.0	22.0	--	Remolded, Denver shale
38	14.7	3.4	18.7	68	105.3	11.7	--	Remolded to natural conditions--3311
39	(1.0)			4	87.2	35.6	--	derived from Laramie shale--Undisturbed
40	(5.0)				101.7	11.8	--	Undisturbed
41	(2.0)				101.4	11.0	--	Undisturbed
42								Shale
43								Soil
44	0.4				100.7	18.3	--	Remolded--Soil from weathered Fenece shale
45	(4.0)				113.5	12.0	85	undisturbed, moie
46								Denver shale
47								Laramie shale
48	(2.0)			8	84.1	35.6	94.8	Undisturbed Cella shale
49	96% rebound from 200 psi load				96.1	24.5	86.4	Remolded
50	16.4				109.3	19.8	97.1	Undisturbed, Colorado shale--Bentonite layers
51	25.6				101.6	24.5	97.7	
52								
53	0.5*				98.8	20.3	77	Remolded--Soil derived from Benton shale
54	123% rebound from 300 psi load				113.8	17.7	95.8	Undisturbed, Benton shale
55	(4.8)			(14)	87.4	27.0	--	Remolded
56								
57	1.9			20	96.6	14.0	50	Undisturbed
58	0.9			5	106.7	20.3	92	Undisturbed
59	(3.5)	9.0	13.7	(24)	98.2	18.8	71.0	Remolded
60								
61	8.5				90.1	19.9	--	Remolded
62								Undisturbed
63								Glacial Till
64								Glacial Till
65	12.5			33	81.6	37.2	92	Undisturbed, Pierre shale
66	2.0			8	94.3	29.2	--	Undisturbed, Red Beaumont clay
	6.0			22	94.0	28.9	--	Remolded, Red Beaumont clay
67	1.1	16.1	20.5	5	106.0	19.9	--	Undisturbed, Gray Beaumont clay
	5.4	15.3	24.2	32	106.0	19.9	--	Remolded, Gray Beaumont clay
68	6.7	22.9	36.4	15	97.2	19.2	69.0	Remolded, Red Beaumont clay
69	2.9	21.9	31.6	17	99.0	25.0	92.4	Undisturbed, Red Beaumont clay
70	5.0	26.0	42.0	10+	85.5	26.8	75.0	Remolded, Black Beaumont clay
71	-0.3	28.3	39.0	2	84.1	33.0	89.2	Undisturbed, Black Beaumont clay
72	6.6	16.8	28.2	19	92.0	21.8	69.9	Remolded, Gray Beaumont clay
73	4.5	19.3	29.5	13	94.2	27.3	92.0	Undisturbed, Gray Beaumont clay
74	2.7				105.6	18.2	82	Undisturbed, weathered volcanic ash
	(8.7)				Air dried			Undisturbed, weathered volcanic ash
75	(13.4)				109.6	12.2	60	Remolded, weathered volcanic ash
76	(13.2)				102.9	15.4	64	Remolded, weathered volcanic ash
77	1.3				97.3	24.8	90	Undist... weathered volca.
	(10.2)				Air dried			Undist. weathered volcanic ash

NOTE: ( ) interpolated from other loadings.
* Heavier load released.
** Total volume changes are computed on basis of dry unit weights of air-dry specimens. Expansion and shrinkage from natural to saturated and air-dry conditions are computed on basis of dry unit weights of natural air-dry ...

TABLE F.1 (part 2)

HOLTZ (1959)

Site No.	w_N %	γ_d pcf[4]	% -#200	% -2 μm	LL %	PL %	SL %	BLS[1] %	τ_{nat}[2] tsf[5]	%[3] Swell
1	40.3	80.3	98	82	104	36	9.8	23.2	4.8	12.7
2	25.6	93.8	84	38	61	20	14.5	19.2	1.9	1.3
3	39.5	81.8	96	57	96	38	20.5	19.5	0.3	1.0
4	20.6	105.6	82	37	56	17	12.4	17.7	0.8	0.8
5	24.0	95.4	97	36	58	27	16.2	18.8	1.7	0.6
6	13.8	119.7	89	38	34	21	14.8	20.0	3.2	0.1
7	15.4	117.9	98	43	48	21	20.3	12.1	0.7	0.4
8	12.5	124.9	98	57	47	23	18.9	14.4	1.5	0.1
9	9.4	111.5	69	23	34	18	14.5	13.4	17.4	1.3
10	19.3	101.5	84	13	54	29	16.8	12.8	34.9	3.7
11	9.4	107.8	97	42	46	20	19.8	26.2	23.4	0.3
12	26.1	97.2	98	61	75	24	17.6	20.2	1.8	1.0
13	16.7	112.8	91	32	49	28	23.6	13.6	3.2	0.4
14	26.4	98.2	98	44	56	25	20.2	14.4	7.8	0.9
15	38.2	78.8	98	64	63	24	18.3	15.6	1.6	0.1
16	16.0	103.9	63	33	38	19	15.5	11.0	19.5	3.2
17	26.4	97.5	91	24	55	25	19.1	12.0	2.7	0.8
18	15.7	97.5	97	45	50	28	19.0	12.6	25.8	2.7
19	17.6	110.8	97	44	69	24	12.8	19.6	1.6	0.4
20	34.5	83.4	94	61	80	34	27.3	16.0	2.0	1.9

Notation: 1 - BLS = Bar Linear Shrinkage
2 - τ_{nat} = Natural Soil Suction
3 - % Swell is taken from overburden swell test.
4 - pcf x 0.157 = kN/m^3
5 - tsf x 107.252 = kPa

TABLE F.2

SNETHEN (1984)

No.	Name	Location	A Atterberg Limits (%) LL	SL[1]	PI	B Activity[2]	C F.M.E. (%)[3]	D Free[4] Swell (%)	E Water Contents vs. Rel. Humidity w_{50}	w_{100}	F $V_{F.M.E.-SL}$ (%)[6]	G H_{100} (%) Dry	Moist	Wet	H S.P. (lb./sq.ft.) Dry	Moist	Wet	I PVC Rating
1.	Iredell Clay	Fairfax County, Virginia, U.S.A.	81	14·5	47	1·3	47	95	9·5	~ 17	40	25	22·5	7	~ 10,500	11,600	2,400	7·8
2.	Houston Black Clay	Temple, Texas, U.S.A.	71	18	44	0·65	47	—	8	19	35	~ 20	15	5·5	~ 8,000	—	—	6·8
3.	Enon Loam	Fairfax County, Virginia, U.S.A.	69	17	42	0·95	46	—	5	~ 17	36	14·5	13	4	—	—	1,400	6·1
4.	Vicksburg Buckshot Clay	Vicksburg, Mississippi, U.S.A.	65	16	38	1·1	48	75 (50-100)	7	~ 14	38	24	13	6·5	~ 8,000	7,000	2,800	6·4
5.	Texas Black Clay	Temple, Texas U.S.A.	58	—	34	0·7	38	75	7	14	30 (Estimated)	—	~ 17	4	—	5,400	1,900	5·7
6.	Siburua Shale	Siburua, Venezuela	62	15	30	0·4	34	135 (110-160)	—	~ 16	28	—	17	4	—	10,000?	650	5·6
7.	Keyport Soil	Norfolk County, Virginia, U.S.A.	44	17	21	0·7	33	43	3	9	23	7	8	~ 1	—	7,600	~ 400	3·2
8.	Boston Blue Clay	Cambridge, Mass. U.S.A.	35	18·5	13	0·25	29	15 (10-25)	1·5	~ 5	16	—	4·5	0·1	—	1,800	~ 200	1·8
9.	Vicksburg Loess	Vicksburg, Miss. U.S.A.	33·5	21·5	10	0·65	29	—	2·5	~ 7	11·5	~ 0	2·5	— 1	~ 200	900	< 200	1·2
10.	Guelph Sandy Loam	Sanilac County Michigan, U.S.A.	21	13 ?	7	0·7	16	35 (30-40)	—	~ .5	6	—	0·5	— 0·4	—	500	< 200	0·6

[1] Remolded shrinkage limit.
[2] Activity = $PI/\%$ clay size.
[3] F.M.E. = Field Moisture Equivalent.
[4] Free Swell = $\frac{\text{(Final Volume - Initial Dry Volume)} \times 100}{\text{Initial Dry Volume}}$
[6] $V_{F.M.E.-SL}(\%) = \frac{F.M.E. - SL}{\frac{F.M.E.}{100} + \frac{1}{G_S}}$

TABLE F.3

LADD & LAMBE (1961)

APPENDIX G

LIST OF PRINCIPAL SUPPLIERS

	Components	Company
1.	. High Air entry ceramic discs	Soil Moisture Equipment Corp. PO Box 30025 Santa Barbara CA 93105, USA.
2.	. Pore Pressure Transducers	Druck Engineering Ltd Firtree Lane Groby Leics, LE6 OFH.
3.	. Sub Miniature On/Off ball valves . Water Reservoirs	Soil Instrumentation Ltd Bell Lane Uckfield E. Sussex, TN22 1QL.
4.	. Air cylinder and associated pneumatic control devices, . Nylon tubing . Brass Tubing connectors . Norgren pneumatic control valves	Control Gear Heol Groeswen Treforest Industrial Estate Pontypridd, CF37 5YF.
5.	. Epoxy resins	CIBA GEIGY Ducksford Cambridge, CB2 4QA.
6.	. Kaolinite (china clay) . Montmorillonite (Wyoming Bentonite)	Steetley Minerals Ltd PO Box 1 Par, Cornwall, PL24 2AF.